S.D. Attri
L.S. Rathore
M.V.K. Sivakumar
S.K. Dash
*Editors*

# Challenges and Opportunities in Agrometeorology

Springer

# Challenges and Opportunities in Agrometeorology

S.D. Attri · L.S. Rathore · M.V.K. Sivakumar · S.K. Dash
Editors

# Challenges and Opportunities in Agrometeorology

Springer

*Editors*
Dr. S.D. Attri
India Meteorological Department
Ministry of Earth Sciences
Lodi Road
New Delhi-110003
India
sdattri@gmail.com

Dr. L.S. Rathore
India Meteorological Department
Ministry of Earth Sciences
Lodi Road
New Delhi-110003
India
lsrathore@ncmrwf.gov.in

Dr. M.V.K. Sivakumar
World Meteorological
Organization Climate
and Water Programme Climate
Prediction and Adaptation Branch
7bis, Avenue de la Paix
1211 Geneva
Switzerland
msivakumar@wmo.int

Prof. S.K. Dash
Centre for Atmospheric Sciences
Indian Institute of Technology Delhi
New Delhi-110016
India
skdash@cas.iitd.ac.in

ISBN 978-3-642-19359-0 e-ISBN 978-3-642-19360-6
DOI 10.1007/978-3-642-19360-6
Springer Heidelberg Dordrecht London New York

Library of Congress Control Number: 2011934440



*Cover design:* deblik

Printed on acid-free paper

Springer is part of Springer Science+Business Media (www.springer.com)

सत्यमेव जयते

डॉ. शैलेश नायक
DR. SHAILESH NAYAK

सचिव
भारत सरकार
पृथ्वी विज्ञान मंत्रालय
महासागर भवन, ब्लाक–12, सी.जी.ओ. कॉम्पलेक्स,
लोदी रोड, नई दिल्ली–110 003
SECRETARY
GOVERNMENT OF INDIA
MINISTRY OF EARTH SCIENCES
'MAHASAGAR BHAVAN' BLOCK-12, C.G.O. COMPLEX,
LODHI ROAD, NEW DELHI-110 003

## FOREWORD

In the era of increased climate variability, the challenges and expectations from Agro-meteorological services have increased tremendously. It is well known that intense rainfall, floods, drought etc. have caused damage to the tune of approximately 100 billion dollars in Asia and Pacific regions. The extreme weather events are cause of concern owing to physical destruction potential to crop, at times leading to large scale devastation. The crops need certain threshold values of different meteorological parameters. Hence, large scale variations beyond their tolerance may hamper growth, development and reproduction processes. These ranges of congenial meteorological conditions are specific to crop, varieties and also phenological stages. There is a need to understand crop-weather relationship and accordingly develop crop management strategy. The farming community is interested to get timely information on weather conditions and management advisories to minimize the losses caused by extreme weather conditions. While generating such advisories, the alternate management options should be spelt out unambiguously to enable user to choose the viable and cost effective practice.

There are increasing demands for timely and effective agrometeorological information for non-farm applications. The growing interest in the possible impact of natural and human induced climate variability and climate change on agriculture and forestry have opened up new dimensions and have created new demands for information. The need of the hour is to effectively integrate the skills we have developed in operational, experimental and theoretical aspects of agricultural meteorology and deploy them for agricultural production system to make it more weather and climate resilient.

Risk proofing through weather based crop insurance is aiming to minimize farmers vulnerability. Agrometeorologists should evaluate for the various regions, seasons and crops, the inter annual variability in crop outturns so as to assist in fixing up of premium in a more realistic and rational manner. Also the system must rise to the need for providing fault free reference meteorological observation to determine the payback based on unfavorable weather conditions. There is need for combined use of expertise in meteorological and agricultural sciences in assisting the farmers to cope with and/or counteract the direct and indirect effects of weather anomalies. The book focuses on the important issues dealing with improving, identifying, assessing and managing the agrometeorological risks for enhancing sustainable food production, particularly in marginal and rain-fed areas. I strongly feel that some of the methods discussed in the book will render assistance to operational agrometeorologists to generate more meaningful advisories in an objective form. I hope that the papers presented will serve as a significant source of information to the scientific community, farming community and other stakeholders involved in providing agrometeorological services to farmers.

SR Nayak

(SHAILESH NAYAK)

Tel. : 00-91-11-24360874, 24362548 ▫ E-mail : secretary@moes.gov.in ▫ Fax No. : 00-91-11-24362644/24360336

# Preface

The global food security and sustainable agriculture are the key challenges before the scientific community in the present era of enhanced climate variability, rapidly rising population and dwindling resources. Agriculture is intimately tied to weather and climate influencing every aspect from long term planning to tactical decisions in day-to-day management operations. Agrometeorology has a vital role to play in increasing agricultural production in a sustainable manner using state-of-art technology and resources efficiently. It is the responsibility of the meteorologists to advise the farming community well in advance to take full advantage of benevolent weather and precautions against malevolent weather to minimize losses. Uncertainties of weather and climate pose a major threat to food security of the world in general and developing countries, in particular. Asia in recent years has made considerable progress in the field of agriculture. However, in order to keep pace with the increasing population, the growth in agricultural production should be sustainable. The problem, therefore, has to be addressed collectively by scientists, planners and the society as a whole.

In view of need for increasing agricultural productivity to meet the demand of rapidly growing population and coping with enhanced uncertainties and risks in agriculture, Agrometeorology is facing lot of challenges as well as opportunities for achieving the path of sustainability. Indian Meteorological Society in association with World Meteorological Organization, India Meteorological Department, Ministry of Earth Sciences, Department of Science and Technology and Department of Space, Government of India organized and International Conference (INTROMET 2009) on "Challenges and Opportunities in Agrometeorology" during 23–25 February 2009 in New Delhi, India. The conference was participated by about 300 experts from India and 20 from abroad (USA, Korea, Egypt, Ukraine, Italy, Philippines, South Africa, China and Switzerland) including International organization like WMO.

The INTROMET-2009 was organized with the specific objectives to focus on the above issues and draw attention of global agrometeorological community, administrators and policy makers to debate and devise improved methods and

techniques for better prediction, preparedness and mitigation of the adverse weather impacts and aware of the possible impact, consequences and mitigation measures to sustain food security. The scientific programme was deliberated through following eight sub-themes in addition to opening and closing session wherein 45 oral presentations were made:

- Weather Forecasting
- Monsoon Variability and Crop Production
- Operational Agrometeorology
- Agromet. Information System
- Adaptation to Climate Change
- Risk Evaluation and Management
- Crop Weather Relationship
- Extreme Weather Events

Further, 63 short oral presentations were also made on above themes along with poster display. A special session was organized to share the wisdom of Veteran Scientists on "Role of IMS in addressing Challenges in Weather and Climate Service".

All the participants in the conference took part actively in discussion on these papers and to develop several useful recommendations for all organizations involved in providing agrometeorological services to farmers to cope up with agrometeorological risk management, particularly the National Meteorological and Hydrological Services. The main recommendations emerged from the Conference are summarized as under:

- Set up a comprehensive meteorological observation system ranging surface including Agromet., upper air, radar, satellite etc. for weather forecast up to district/taluka level and possibly at village level.
- Development user oriented meteorological information system keeping in view region-specific requirements of varied users including farming community.
- Establishment of mechanism for greater collaboration/feedback between the providers of information and users and also between meteorologists and agriculture scientists.
- Develop action plan at district level for climate change, identity hot spots and promote inter-disciplinary collaboration to enable effective mitigation of impacts in all sectors of economy.
- Greater role in International arena through the establishment of Regional Climate Centre with association of WMO and other International Organization.
- Review of Agromet curriculum in Agricultural Universities with emphasis on Agromet services, Outreach and Human Resource Development.

Selected papers have been edited and compiled in form of this book. As Editors of this volume, we are highly thankful to all the authors for their efforts and cooperation in bringing out this publication. We are also grateful to the World Meteorological Organization and various Ministries/Departments of the Government of India like Ministry of Earth Sciences, Ministry of Science and Technology,

India Meteorological Department, and Department of Space for providing financial support and encouragement. Our special thanks are to the Springer for this publication and Mr Subhash Khurana and Mr Dinesh Khanna for the assistance.

SD Attri
LS Rathore
MVK Sivakumar
SK Dash
Editors

## Indian Meteorological Society

The Indian Meteorological Society (IMS) established in 1956 has more than 2,000 members at present. The society has been able to reach not only to meteorological community but also amongst a wide spectrum of scientists of allied fields from more than 50 national and international organizations. It carries out its activities from HQ office in Delhi as well as through its 17 Chapters located at different places in India viz. Ahmedabad, Pune, Mumbai, Kolkata, Chennai, Nagpur, Visakhapatnam, Bhopal, Bhubaneswar, Bangalore, Hyderabad, Cochin, Thiruvananthapuram, Guwahati, Noida, Varanasi and Other Places.

The IMS activities are related to encouragement and expansion of R&D in atmospheric, oceanic and allied sciences, sponsored research in meteorology, publication of its biennial Journal – Vayu Mandal (since 1970), IMS News, News letters, scientific books etc. It also organizes annual series of national conference named "TROPMET" since 1992 supplemented with international conference called "INTROMET" every 4 year. Awareness programmes about meteorology and allied sciences are regularly organized in the country. It is co-founder of International Forum of Meteorological Societies. It also felicitates the outstanding scientists by conferring on them the Fellowships and has constituted five national and one international awards in the field of meteorology and atmospheric sciences.

The details of the Society are available on http://www.indianmetsoc.com.

**National Council of IMS (2009–2011)**

**President**
Dr L S Rathore
Tel: 91-11-24619844
lrathore@gmail.com

**Vice-Presidents**
Dr. R. K. Datta
Tel : 09811213169
rkdatta_in@yahoo.com
Dr. S. D. Attri
Tel: 91-11- 24620701
sdattri@gmail.com

**Secretary**
Shri. D. K. Malik
Tel.: 09810618585
dk_malik@hotmail.com

**Jt. Secretary**
Dr. D. R. Pattanaik
Tel:09868554029
pattanaik_dr@vyahoo.co.in

**Treasurer:**
Sh. Virendra Singh
Tel: 09899213832
vsvsingh69@gmail.com

**Immediate Past President**
Sh. R. C. Bhatia
rcbhatia1912@gmail.com

**Council Members:**
Dr V U M Rao
Dr (Mrs) Parvinder Maini
Dr K K Singh
Dr. D. P. Dubey
Sh. B. P. Yadav
Sh N. Nigam
Dr. M. Ravichandran
Sh. Utpal Bhattacherjee

# Contents

# Contributors

**K. K. Agrawal** Department of Physics and Agrometeorology, College of Agricultural Engineering, JNKVV, Jabalpur, MP 482004, India, kkagrawal59@yahoo.co.in

**B. Athiyaman** National Center for Medium Range Weather Forecasting, NOIDA 201 307, India, athiya@ncmrwf.gov.in

**S. D. Attri** India Meteorological Department, New Delhi-110003, India, sdattri@gmail.com

**G. S. Bains** Department of Agricultural Meteorology, Punjab Agricultural University, Ludhiana, India

**U. P. S. Bhadauria** Department of Physics and Agrometeorology, College of Agricultural Engineering, JNKVV, Jabalpur, MP 482004, India, upsb2007@rediffmail.com

**Goutam Bhagavati** Division of Agricultural Physics, Indian Agricultural Research Institute, New Delhi 110012, India, goutombhagawati@gmail.com

**S. C. Bhan** India Meteorological Department, Lodi Road, New Delhi 110 003, India, scbhan@gmail.com

**Venkatesh Bharadwaj** Department of Agrometeorology, College of Agriculture, G.B. Pant University of Agriculture and Technology, U.S. Nagar, Pantnagar, Uttarakhand 263145, India, dr.venkatbh@rediffmail.com

**B. K. Bhattacharya** Space Applications Centre (ISRO), Ahmedabad 380 015, India, bkbhattacharya@sac.isro.gov.in

**S.K. Roy Bhowmik** India Meteorological Department, New Delhi 110 003, India, skrb.imd@gmail.com

**Ryan P. Boyles** State Climate Office of North Carolina, NC State University, Box 7236, Raleigh, NC 27695-7236, USA, ryan_boyles@ncsu.edu

**Mark S. Brooks** State Climate Office of North Carolina, NC State University, Box 7236, Raleigh, NC 27695-7236, USA, mark_brooks@ncsu.edu

**Anca Brookshaw** Met Office, Exeter, United Kingdom, anca.brookshaw@metoffice.gov.uk

**N.V.K. Chakravarty** Division of Agricultural Physics, Indian Agricultural Research Institute, New Delhi 110012, India, nvkchak@iari.res.in

**Xue Changying** Henan Institute of Meteorological Sciences, Zhengzhou 450003, China, xuecy9@163.com

**N. Chattopadhyay** Agricultural Meteorology Division, India Meteorological Department, Pune, India, n.chattopadhyay@imd.gov.in

**J.L. Chaudhary** S.G. College of Agriculture and Research Station, Kumhrawand, Jagdalpur, Chhattisgarh 494 005, India, zars_igau@rediffmail.com

**B. Chintamanie** Department of Water Resources Development and Management, Indian Institute of Technology Roorkee, Roorkee, India, bcrchintamanie@gmail.com

**I.M. L. Das** M. N. Saha Centre of Space Studies, University of Allahabad, Allahabad 211 002, India, profimldas@yahoo.com

**S.K. Dash** Centre for Atmospheric Sciences, Indian Institute of Technology Delhi, Hauz Khas, New Delhi-110016, India, skdash@cas.iitd.ac.in

**Somenath Dutta** India Meteorological Department, Pune, India, dutta.drsomenath@gmail.com

**Ashley N. Frazier** State Climate Office of North Carolina, NC State University, Box 7236, Raleigh, NC 27695-7236, USA, anfrazier@gmail.com

**K.K. Gill** Department of Agricultural Meteorology, Punjab Agricultural University, Ludhiana, India, kgill2002@gmail.com

**R.K. Giri** India Meteorological Department, Lodi Road, New Delhi 110003, India, rkgiri_ccs@rediffmail.com

**Archana P. Hage** Agricultural Meteorology Division, India Meteorological Department, Pune, India

**Zhang Hongwei** Henan Institute of Meteorological Sciences, Zhengzhou 450003, China, xxqxjzhw1966@163.com

**Chen Huailiang** Henan Institute of Meteorological Sciences, 110 Jinshuilu Rd, Zhengzhou, Henan, PR 450003, China, chenhl@cam.gov.ch

**Sanjay Jain** Department of Physics and Agrometeorology, College of Agricultural Engineering, JNKVV, Jabalpur, MP 482004, India, genomics_san@hotmail.com

**Manish K. Joshi** K. Banerjee Centre of Atmospheric & Ocean Studies, Institute of Interdisciplinary Studies, University of Allahabad, Allahabad 211 002, India, manishkumarjoshi@gmail.com

**P.C. Joshi** Space Applications Centre (ISRO), Ahmedabad 380 015, India, pcjoshi35@hotmail.com

**N. Kale** Anand Agricultural University, Anand, Gujarat 388110, India, yogirajvedashram@gmail.com

**M.V. Kamble** Agricultural Meteorology Division, India Meteorological Department, Pune, India, mdhr_kmbl@yahoo.com

**Sarat C. Kar** National Centre for Medium Range Weather Forecasting, Ministry of Earth Sciences, A-50, Sector-62, NOIDA, UP, India, sckar@ncmrwf.gov.in

**B.I. Karande** Anand Agricultural University, Anand, Gujarat 388110, India, babankarande@yahoo.co.in

**A. Kashyapi** Agricultural Meteorology Division, India Meteorological Department, Pune, India, kashyapi_a@yahoo.co.in

**S. Korsakova** Center for Hydrometeorology of the Autonomous Republic of the Crimea, Agrometeorological Station of the Ukraine, State Committee for Hydrometeorology, Nikitskij Sad, Yalta, Ukraine, korsakova@i.ua

**O. Krishna Kishore** Centre for Atmospheric Sciences, Indian Institute of Technology, Delhi, Hauz Khas, New Delhi 110016, India, osurikishore@gmail.com

**S. Raj Kumar** Natural Plant Products & Biodiversity Divisions, Institute of Himalayan Bioresource Technology (CSIR), Palampur, HP 176061, India, ramechek@yahoo.co.in

**Dr. H.S. Kushwaha** Department of Soil Science, College of Agriculture, G. B. Pant University of Agriculture & Technology, Pantnagar, Uttarakhand 263145, India, kushwahahs@yahoo.co.in

**A.J. Litta** Centre for Atmospheric Sciences, Indian Institute of Technology, Delhi, Hauz Khas, New Delhi 110016, India, ajlitta@gmail.com

**R.K. Mall** India Meteorological Department, National Institute of Disaster Management, New Delhi, India, mall_raj@rediffmail.com

**Ashu Mamgain** Center for Atmospheric Sciences, IIT Delhi, Hauz Khas, New Delhi 110016, India, ashumam@gmail.com

**N. Manikandan** Central Research Institute for Dryland Agriculture, Hyderabad, AP 500 059, India

**E.A.R. Mellaart** EcoLink, 83, Karino 1204, South Africa, mellaart.e@soft.co.za

**A.K. Mishra** Department of Agrometeorology, College of Agriculture, G.B. Pant University of Agriculture and Technology, U.S. Nagar, Pantnagar, Uttarakhand 263145, India, ashueinstein@gmail.com

**M.E. Moeletsi** ARC-Institute for Soil, Climate and Water, Private Bag X79, Pretoria 0001, South Africa, moeletsie@arc.agric.za

**U.C. Mohanty** Centre for Atmospheric Sciences, Indian Institute of Technology, Delhi, Hauz Khas, New Delhi 110016, India, mohanty@cas.iitd.ernet.in

**M. Mohapatra** India Meteorological Department, Lodi Road, New Delhi 110 003, India, mohapatra_imd@yahoo.com

**Raymond P. Motha** U.S. Department of Agriculture, Office of the Chief Economist, World Agricultural Outlook Board, 1400 Independence Avenue, Room 4441 South Building, Washington, DC 20250-3812, USA, rmotha@oce.usda.gov

**N.S. Mpandeli** ARC-Institute for Soil, Climate and Water, Private Bag X79, Pretoria 0001, South Africa, SMpandeli@deat.gov.za

**Sandipan Mukherjee** K Banerjee Center of Atmospheric & Ocean Studies, University of Allahabad, Allahabad 211002, India, mukherjee.sandipan@rediffmail.com

**K.P.R. Vittal Murthy** Department of Meteorology and Oceanography, Andhra University, Visakhapatnam, AP, India, kprvm@yahoo.com

**A.S. Nain** Department of Agrometeorology, Indira Gandhi Krishi Vishwavidyalya, Raipur 492006 (C.G.), India

**G.O. Odhiambo** Department of Geography and Urban Planning, College of Humanities and Social Sciences, United Arab Emirates University, 17771, Al Ain, United Arab Emirates, godhiambo@uaeu.ac.ae

**Kavita Pabreja** Research Scholar-BITS, Pilani, C-3A / 39C, DDA Flats, Janak Puri, New Delhi 110058, India, kavita_pabreja@rediffmail.com

**S.P. Pachauri** Department of Agrometeorology, College of Agriculture, G.B. Pant University of Agriculture and Technology, U.S. Nagar, Pantnagar, Uttarakhand 263145, India

**S.K. Panda** Centre for Atmospheric Sciences, Indian Institute of Technology Delhi, Hauz Khas, New Delhi 110 016, India, sampadpanda@gmail.com

**Avinash C. Pandey** Department of Physics, University of Allahabad, Allahabad 211 002, India; M. N. Saha Center of Space Studies, IIDS, University of Allahabad, Allahabad 211002, India, avinashcpandey@rediffmail.com

**Vyas Pandey** Department of Agricultural Meteorology, Anand Agricultural University, Anand, Gujarat 388110, India, pandey04@yahoo.com

**H.R. Patel** Department of Agricultural Meteorology, Anand Agricultural University, Anand, Gujarat 388 110, India, hrpatel410@yahoo.com

**S.R. Patel** Department of Agrometeorology, Indira Gandhi Krishi Vishwavidyalya, Raipur 492006 (C.G.), India, srpatelsr@yahoo.com

**D.R. Pattanaik** India Meteorological Department, New Delhi, India, drpattanaik@gmail.com

**S. Pattanayak** Centre for Atmospheric Sciences, Indian Institute of Technology, Delhi, Hauz Khas, New Delhi 110016, India, sujata05@gmail.com

**Anand Patwardhan** Shailesh J. Mehta School of Management, Indian Institute of Technology Bombay, Powai, Mumbai, MH 400076, India, anand@iitb.ac.in

**Vinayak S. Phadke** 2/17 Dnyanayog Society, Vazira Naka, Lokmanya Tilak Road, Borivli (W), Mumbai, MH 400091, India, vinayakphadke@hotmail.com

**Savita Rai** Centre for Atmospheric Sciences, Indian Institute of Technology Delhi, Hauz Khas, New Delhi 110 016, India, savita1559@gmail.com

**Sethu Raman** State Climate Office of North Carolina, NC State University, Box 7236, Raleigh, NC 27695-7236, USA, sethu_raman@ncsu.edu

**K. Ramesh** Natural Plant Products & Biodiversity Divisions, Institute of Himalayan Bioresource Technology (CSIR), Palampur, HP 176061, India, kramesh@iiss.ernet.in

**A.V.M.S. Rao** Central Research Institute for Dryland Agriculture, Hyderabad, AP 500 059, India, avmsrao@crida.ernet.in

**G.G.S.N. Rao** Central Research Institute for Dryland Agriculture, Hyderabad, AP 500 059, India, ggsnrao@crida.ernet.in

**V.U.M. Rao** Central Research Institute for Dryland Agriculture, Hyderabad, AP 500 059, India, vumrao54@yahoo.com

**L.S. Rathore** India Meteorological Department, New Delhi 110 003, India, lsrathore@ncmrwf.gov.in

**Ritu** Department of Agricultural Meteorology, Punjab Agricultural University, Ludhiana, India, waliadimpy@rediffmail.com

**Federica Rossi** Consiglio Nazionale delle Ricerche, Institute of Biometeorology, Via P. Gobetti 101, Bologna 40129, Italy, f.rossi@ibimet.cnr.it

**A. Routray** Centre for Atmospheric Sciences, Indian Institute of Technology, Delhi, Hauz Khas, New Delhi 110016, India, ashishroutray.iitd@gmail.com

**Dipak K. Sahu** Centre for Atmospheric Sciences, Indian Institute of Technology Delhi, Hauz Khas, New Delhi 110 016, India, dipakmath@gmail.com

**R.P. Samui** Agricultural Meteorology Division, India Meteorological Department, Pune, India, rsamui@yahoo.com

**P. Parth Sarthi** Centre for Global Environmental Research, TERI, Darbari Seth Block, India Habitat Centre, Lodhi Road, New Delhi 110 003, India, drpps@hotmail.com, ppsarthi@teri.res.in

**A.S.R.A.S. Sastri** Department of Agrometeorology, Indira Gandhi Krishi Vishwavidyalya, Raipur 492006 (C.G.), India, asastri@yahoo.com

**G. U. Satpute** SWCE, Department of Soil and Water Conservation Engineering, Dr. Panjabrao Deshmukh Krishi Vidyapeeth, PO Krishi Nagar, Akola (MS) 444 104, India, gusatpute@rediffmail.com

**T. Satyanarayana** South China Sea Institute of Oceanology, Chinese Academy of Science, Beijing, China; Central Research Institute for Dryland Agriculture, Hyderabad 500 059, India, satya_1006@yahoo.co.in

**M.J. Savage** SPAC Research Unit, Agrometeorology discipline, School of Environmental Sciences, University of KwaZulu-Natal, P/Bag X01, Scottsville, Pietermaritzburg 3209, Republic of South Africa

**P.K. Sharma** Division of Agricultural Physics, Indian Agricultural Research Institute, New Delhi 110012, India

**Ravi P. Shukla** Department of Physics, University of Allahabad, Allahabad 211002, India, ravishukla72@gmail.com

**B. Simon** Space Applications Centre (ISRO), Ahmedabad 380 015, India, babysimon@gmail.com

**Aaron P. Sims** State Climate Office of North Carolina, NC State University, Box 7236, Raleigh, NC 27695-7236, USA, aaron_sims@ncsu.edu

**Ajay Singh** Shailesh J. Mehta School of Management, Indian Institute of Technology Bombay, Powai, Mumbai, MH 400076, India, ajayvisen@yahoo.co.in

**Guriqbal Singh** Department of Plant Breeding and Genetics, Punjab Agricultural University, Ludhiana, India, singhguriqbal@rediffmail.com

**Jagadish Singh** Mausam Apartments, West Enclave, Pitampura, Delhi 110 034, India

**K.K. Singh** India Meteorological Department, New Delhi 110 003, India, kksingh2022@gmail.com

**R. Singh** Department of Agrometeorology, Indira Gandhi Krishi Vishwavidyalya, Raipur 492006 (C.G.), India

**S.K. Singh** Department of Agrometeorology, College of Agriculture, G.B. Pant University of Agriculture and Technology, U.S. Nagar, Pantnagar, Uttarakhand 263145, India, sskumar_1983@rediffmail.com

**P.K. Singh** India Meteorological Department, Agromet Service Cell, Mausam Bhavan, New Delhi, India, pksingh@ncmrwf.gov.in

**P.P. Singh** Department of Agrometeorology, College of Agriculture, G.B. Pant University of Agriculture and Technology, U.S. Nagar, Pantnagar, Uttarakhand 263145, India

**Virendra Singh** Natural Plant Products & Biodiversity Divisions, Institute of Himalayan Bioresource Technology (CSIR), Palampur, HP 176061, India, vsgahlan@gmail.com

**M.V.K. Sivakumar** World Meteorological Organization, Geneva, Switzerland, msivakumar@wmo.int

**Robert Stefanski** World Meteorological Organization, Geneva, Switzerland, rstefanski@wmo.int

**M.V. Subrahmanyam** South China Sea Institute of Oceanology, Chinese Academy of Science, Beijing, China, mvsm.au@gmail.com

**Ameenulla Syed** State Climate Office of North Carolina, NC State University, Box 7236, Raleigh, NC 27695-7236, USA, asyed@ncsu.edu

**S. Tabasum** Department of Agrometeorology, Indira Gandhi Krishi Vishwavidyalya, Raipur 492006 (C.G.), India, shabana.tbsm@gmail.com

**K.C. Tripathi** K. Banerjee Centre of Atmospheric & Ocean Studies, Institute of Interdisciplinary Studies, University of Allahabad, Allahabad 211 002, India, kctripathi@gmail.com

**S.K. Tripathi** Department of Water Resources Development and Management, Indian Institute of Technology Roorkee, Roorkee, India, sankufwt@iitr.ernet.in

**Ajit Tyagi** India Meteorological Department, New Delhi 110 003, India, ajit.tyagi@gmail.com

**V.B. Vaidya** Anand Agricultural University, Anand, Gujarat 388110, India, vaidya.vidyadhar@gmail.com

**S.S. Vanjari** Department of Agronomy, Dr. Panjabrao Deshmukh Krishi Vidyapeeth, PO Krishi Nagar, Akola (MS) 444 104, India, wanjari.sanjay@rediffmail.com

**M.C. Varshneya** Anand Agricultural University, Anand, Gujarat 388110, India, mcvarshneya@gmail.com

**Ananta Vashisth** Division of Agricultural Physics, Indian Agricultural Research Institute, New Delhi 110012, India, anantavashisth@iari.res.in

**B. Venkateshwarlu** Central Research Institute for Dryland Agriculture, Hyderabad, AP 500 059, India, Vbandi_1953@yahoo.com

**Lt. Vishwarajashree** INS Goruda, Cochin, India

# Chapter 1
# Modernization of Observation and Forecasting System in IMD in Support of Agromet Services

**Ajit Tyagi**

**Abstract** India Meteorological department has added many data and research networks during the 135 years for climate-dependent sectors, such as agriculture, forestry, and hydrology, rendering a modern scientific background to atmospheric science in India. The inclusion of the latest data from satellites and other modern observation platforms, such as Automated Weather Stations (AWS), and ground-based remote-sensing techniques in recent years has strengthened India's long-term strategy of building up a self-reliant climate data bank for specific requirements, and also to fulfill international commitments of data exchange for weather forecasting and allied research activities. It has augmented forecasting capabilities to meet the operational requirements of day to day seamless weather forecasts in various ranges.

## 1.1 Introduction

Agriculture in India is the means of livelihood of almost two thirds of the work force in the country and needs accurate weather forecasts to plan when to sow seeds, irrigate and fertilise their fields, and harvest their crops. Since most of the area used for agricultural activity is rain fed, agricultural output is influenced by overall seasonal rainfall as well as by intra-seasonal rainfall variations. The dependence of agriculture on weather information and forecasts is going to increase in future on two counts. First is due to increase in extreme weather events and climate variability caused by global warming and second is from increase in demand of food products from growing population having higher quality of life. In addition to

A. Tyagi (✉)
India Meteorological Department, New Delhi 110003, India
e-mail: ajit.tyagi@gmail.com

S.D. Attri et al. (eds.), *Challenges and Opportunities in Agrometeorology*,
DOI 10.1007/978-3-642-19360-6_1, 

general forecast being provided by IMD to agriculture sector at macro scale, there is increasing demand from horticulture, floriculture, and crop specific sectors for location specific forecasts on different time scales.

In view of growing operational requirements from various user agencies, there is a need for a seamless forecasting system covering short range to extended range and long range forecasts, particularly for the agricultural requirements. Such forecasting system is to be based on hierarchy of Numerical Weather Prediction (NWP) models. For a tropical country like India where high impact mesoscale convective events are very common weather phenomena, it is necessary to have good quality high density observations both in spatial and temporal scale to ingest into assimilation cycle of a very high resolution non-hydrostatic mesoscale model. A major problem related to skill of NWP models in the tropics is due to sparse data over many parts of the country and near absence of data from oceanic region.

## 1.2 Augmentation of Observational System

In view of the importance of data in the tropical numerical weather prediction, IMD has been in the process of implementing a massive modernization programme for upgrading and enhancing its observation system. In the first phase of modernisation 550 additional AWS out of which about 125 will have extra agricultural sensors like solar radiation, soil moisture and soil temperature and 1,350 Automatic Rain Gauge (ARG) stations will be installed in the current year. In addition to this, a network of 55 Doppler Weather Radar has been planned of which 12 are to be commissioned in the first phase. DWR with the help of algorithms can detect and diagnose weather phenomena, which can be hazardous for agriculture, such as hail, downbursts and squall. Normalized Difference Vegetation Index (NVDI) derived from the CCD payload of presently available INSAT-3A satellite is useful for agriculture for monitoring the vegetation on a broad scale. NOAA/MODIS/Metop polar orbiting satellite data receiving and processing system will be installed at New Delhi, Chennai and Guwahati. This will enable availability of real time products from these satellites for use in forecasting by conventional means and by assimilating in NWP models in turn improving the Agro meteorological forecasts also. A new satellite INSAT-3D is scheduled to be launched during third quarter of the year. INSAT-3D will usher a quantum improvement in satellite derived data from multi spectral high resolution imagers and vertical sounder. In addition to above, IMD is also planning to install wind profilers and radiometer to get upper wind and temperature data. Data from AWSs, ARGs, DWRs, INSAT-3D, NOAA/MODIS/ Metop and wind profilers will available in real time for assimilation in NWP models. A High Power Computing (HPC) system with 300 terabyte storage is being installed at NWP Centre at Mausam Bhawan. It will greatly enhance our capability to run global and regional models and produce indigenous forecast products in different time scales.

## 1.3 Forecasting System

Currently, IMD runs a number of regional NWP models in the operational mode. IMD also makes use of NWP global model forecast products of other operational centres, like NCMRWF T-254, ECMWF, JMA, NCEP and UKMO to meet the operational requirements of day to day weather forecasts.

Recently, IMD implemented a multimodel ensemble (MME) based district level 5 days quantitative forecast system as required for the Integrated Agro-advisory Service of India. The technique makes use of model outputs of state of the art global models from the five leading global NWP centres (Krishnamurti et al. 1999). The Pre-assigned grid point weights on the basis of anomaly correlation coefficients (CC) between the observed values and forecast values are determined for each constituent model at the resolution of $0.25° \times 0.25°$ and the multimodel ensemble forecasts (day 1 to day 5 forecasts) are generated at the same resolution on a real-time basis. The ensemble forecast fields are then used to prepare forecasts for each district taking the average value of all grid points falling in a particular district. An inter-comparison of spatial co-relation co-efficient (CC) between observed and forecasts rainfall on the basis of the MME technique and the member models is

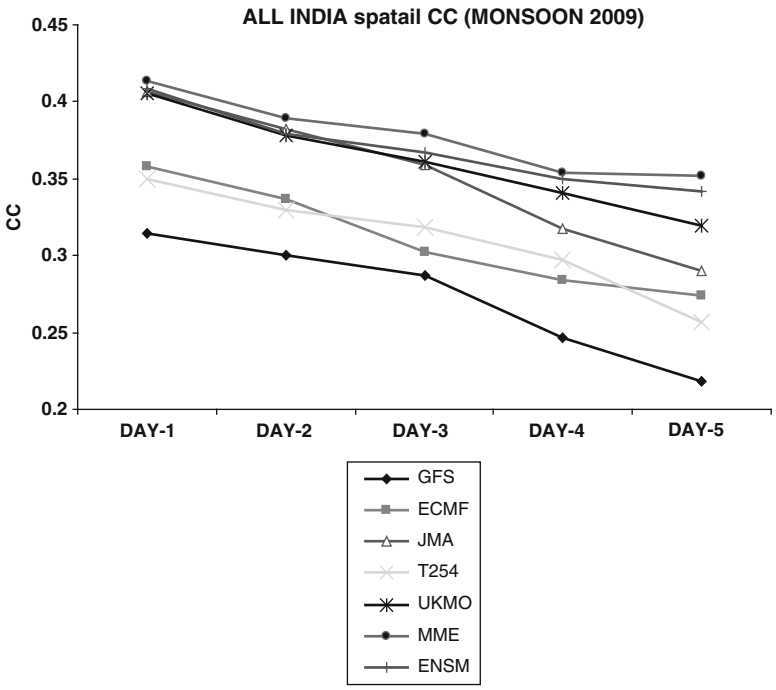


**Fig. 1.1** An inter-comparison of country mean spatial CC of day 1 to day 5 forecasts of rainfall by NCEP, *ECMWF*, *JMA*, NCMRWF, *UKMO*, mean ensemble and *MME* for summer monsoon 2009

illustrated in Fig. 1.1. The results show that MME is superior to each member model at all the forecasts (day 1 to day 5).

In order to evaluate the performance of district level forecasts, skill score – Probability of Detection (POD) is considered. POD is defined as:

$$\mathrm{POD} = \frac{\mathrm{H}}{\mathrm{H} + \mathrm{M}}$$

Where H indicates hits and M for missing events for the following rainfall categories:

1. Rain or no rain
2. Light Rain: 0–10 mm
3. Moderate Rain: >10 mm and <65 mm
4. Heavy Rain: >65 mm

State-wise performance of district level rainfall forecasts for day 1 and day 5 forecasts for some selected states like Orissa, Rajasthan, Maharashtra, Gujarat and Kerala, which represent east central India – the domain of monsoon low; northwest India – region of less monsoon rainfall; west India; region of mid-troposphere circulation and extreme south east Peninsula are illustrated in Figs. 1.2 and 1.3. For the day 5 forecasts, results of Madhya Pradesh (central India) is also included

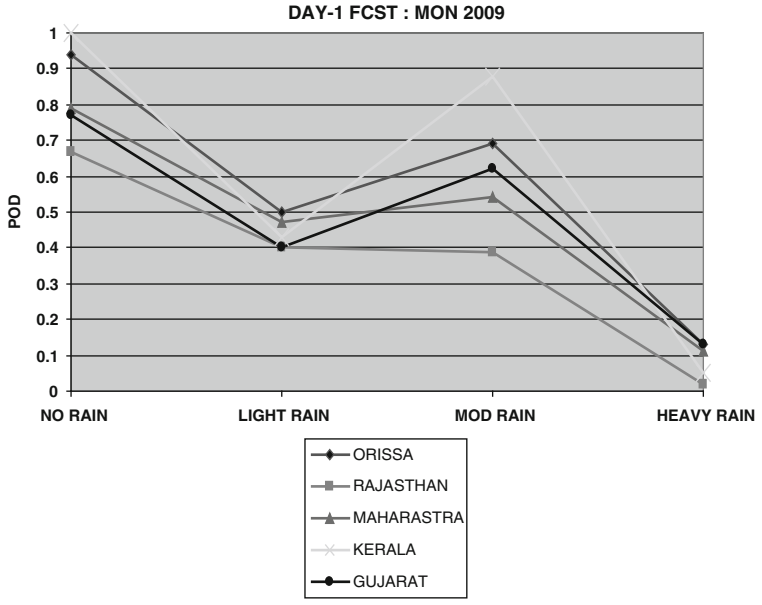


**Fig. 1.2** State-wise performance of district level day 1 forecasts for some selective states

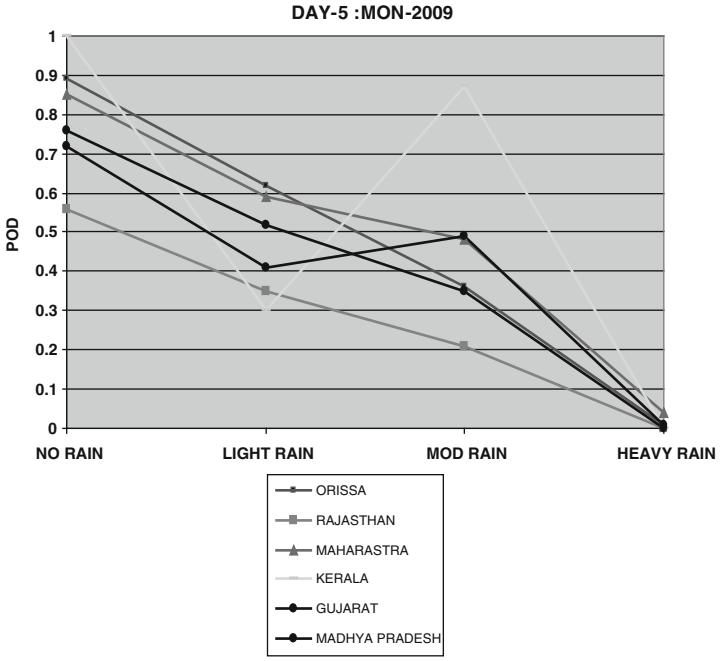


**Fig. 1.3** State-wise performance of district level day 5 forecasts for some selective states

(Roy Bhowmik et al. 2009; Roy Bhowmik and Durai 2010). The results show that performance skill of forecast of the district level rainfall for the rainfall amount of moderate range is reasonably good for all these states, where POD is more than 0.4. District-wise performance of day 1 to day 5 rainfall forecasts for the districts of Orissa is shown in Fig. 1.4. For Orissa, POD for rain/no rain case has been above 0.8 at all the districts, for light rain it is around 0.6, for moderate rainfall it is between 0.3 and 0.4 and for heavy rainfall it is close to 0.

A dynamical statistical technique is developed and implemented for the real-time cyclone genesis and intensity prediction. Numbers of experiments are carried out for the processing of DWR observations to use in nowcasting and mesoscale applications. The procedure is expected to be available in operational mode soon. Impact of INSAT CMV in the NWP models has been reported in various studies. Various multi-institutional collaborative forecast demonstration projects such as, Dedicated Weather Channel, Weather Forecast for Commonwealth Games 2010, Land falling Cyclone, Fog Prediction etc. are initiated to strengthen the forecasting capabilities of IMD.

With the availability of new observations and infrastructure from the modernization programme of IMD, future Weather Forecasting System of IMD would be as briefly given below:

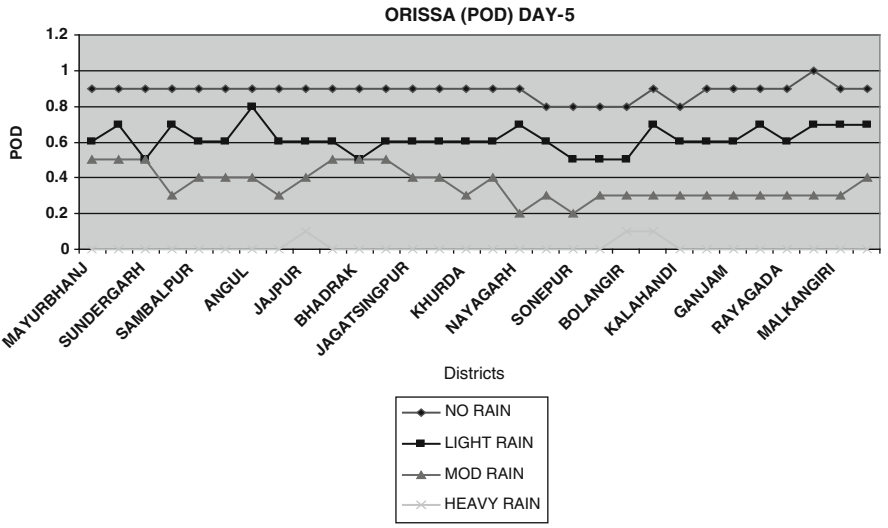


**Fig. 1.4** District-wise performance of day 5 forecasts for the Orissa state

### *1.3.1 Now-Casting and Mesoscale Forecasting System (Valid for Half Hour to 24 h)*

- Processing of Doppler Weather Radar (DWR) observations at a central location (NHAC) to generate 3 D mosaic and other graphics products for nowcasting applications.
- Enhancing mesoscale forecasting capability of local severe weather by providing 3 hourly area specific rainfall and wind forecasts (up to 24 h) at the resolution of 3 km from ARPS with the assimilation (hourly intermittent cycle) of DWR, AWS, wind profilers and other conventional and non-conventional observations.
- Implementation of dynamical Fog prediction model for visibility forecasting at the major airports of India.
- Implementation and customization of the Delhi PP model (based on the UKPP model of UKMO) for the Delhi Commonwealth Games, 2010. This model will give forecasts of precipitation, fog, cloud cover and visibility at 15 min resolution up to 6 h ahead.

India Meteorological Department (IMD) installed four S-Band Doppler Weather Radars (DWR) manufactured by GEMATRONIK GmbH (Model: METEOR 1500S) at Chennai (2002), Kolkata (2003), Machilipatnam (2004) and Visakhapatnam (2006), replacing the old generation S – Band cyclone detection radars at these stations. Very recently two more S-Band DWRs (manufactured by Beijing METSTAR) have been installed at Delhi (Palam) and at Hyderabad.

In addition to the current deployment of DWRs, there are plans to install more such radars for use in severe storm forecasting and airport weather warning. Radars provide detailed information of reflectivity, radial velocity and spectrum width at high spatial and temporal resolution. Recently IMD has initiated research into processing of Indian DWR data for nowcasting and meso-scale modeling. The Nowcasting Application software – "Warning Decision Support System – Integrated Information (WDSS-II)" is used for real-time analyzing and visualizing remotely sensed weather radar data. The quality controlled radar data is assimilated into the Advanced Regional Prediction System (ARPS) model.

A reflectivity field snapshot of the tropical cyclone Khaimuk at 5 km height at 1,410 UTC of 14 November 2008 created from data of the three radars at Chennai, Machilipatnam and Visakhapatnam, when the cyclone was located close to Tamilnadu coast is depicted in Fig. 1.5.

The ARPS model (at 9 km horizontal resolution) simulated reflectivity fields by various experiments against the observed reflectivity valid at 0600 UTC of 27 November 2008 are presented in Figs. 1.6a–c. Three main cells are detected in each experiment and these are marked as A, B and C respectively. An inter-comparison of these results reveal that the cells and the spiral rain band structure is clearly seen in the experimental run (with DWR data) and the pattern is close to observed reflectivity as produced by DWR Chennai in the panel (c). The corresponding maximum intensity of these three cells in experiment (with DWR data) is found to be well matched with the observed one as shown in panel (c). In the experiment (with DWR data), all the three cells and rain band structure appeared similar to the observed pattern.

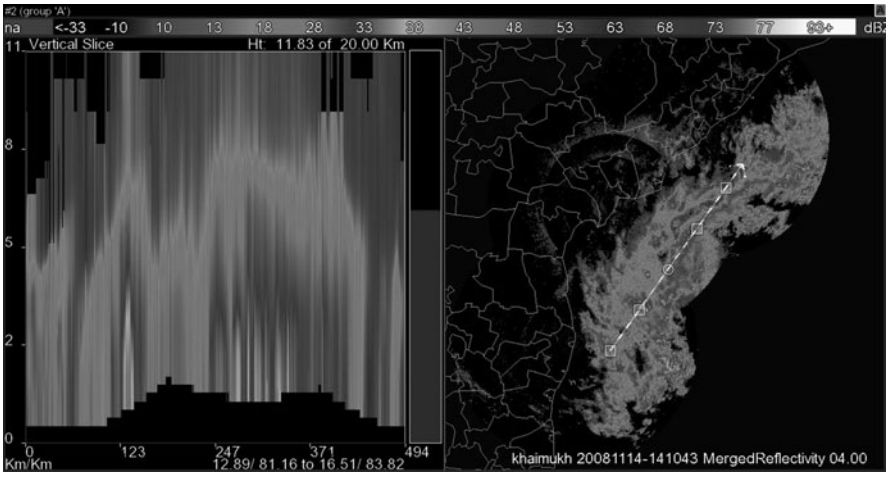


**Fig. 1.5** Snapshot of the mosaic reflectivity field at 4.0 km during the tropical cyclone Khaimukh of at 14 November 2008, which was tracked by the three Doppler radars at Chennai, Machilipatnam and Visakhapatnam

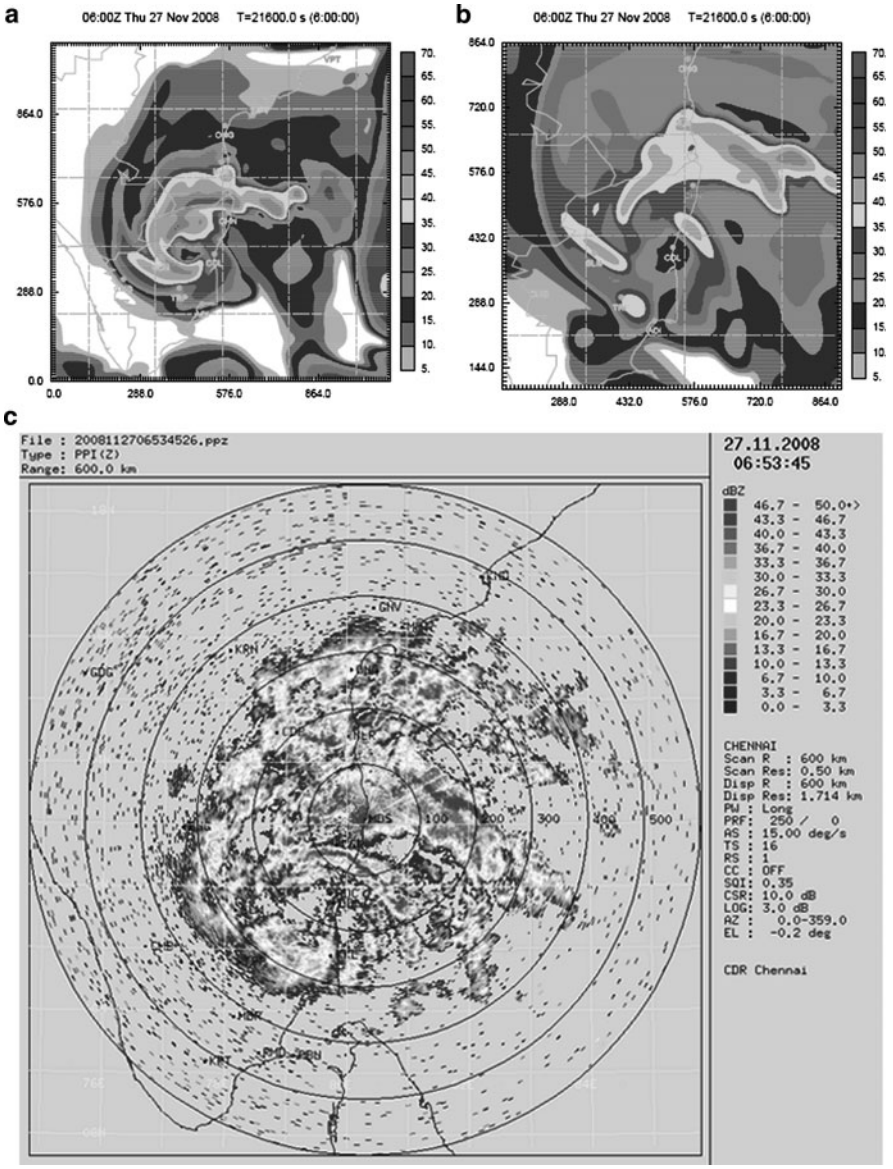


**Fig. 1.6** (**a–c**) Inter-comparison of reflectivity fields (dBZ) of various simulation experiments against the observed field valid at 0600 UTC of 27 November 2008: reflectivity by DWR experiment (using both radial wind and reflectivity), (**b**) Experiment without DWR observations and (**c**) Observed reflectivity

### 1.3.2 Regional Models for Short Range Forecasting System (Valid Up to 3 days)

- Seventy-two hours forecasts from WRF model with three nested domains (at the resolution of 27, 9 and 3 km). The nested model at the 3 km resolution is being operated at the Regional/State Met Centres at 12 h interval with 3 DVAR data assimilation.
- Seventy-two hours forecasts from MM5 model.
- For Cyclone Track Prediction, 72 h forecast from Quasi Lagrangian Model (QLM) at 40 km resolution at 6 h interval; WRF (NMM) at 9 km resolution with assimilation package of Grid Statistical Interpolation (GSI).
- For Cyclone track and intensity prediction: multimodel ensemble technique and application of dynamical statistical approach for 72 h forecasts; forecast would be updated at 12 h interval.
- Development of multimodel ensemble technique for probabilistic forecasts of district level heavy rainfall events.

### 1.3.3 Global Model for Medium Range Forecasting (Valid Up to 7 days)

- NCEP Decoding System.
- Global Data Assimilation System (GDAS), 6 hourly cycles with GSI (Grid Statistical Interpolation).
- Global Forecast System (GFS) T-382/L64.

The regional and global forecast products are routinely made available in the IMD web site: www.imd.gov.in

### 1.3.4 Extended Range Forecast for Rainfall and Temperature

- Statistical downscaling studies using historical GCM data sets (for predictor variables) and IMD's observational data sets of rainfall and temperature as predictands.
- Customization of RCMs for dynamical downscaling studies.
- Multi-model super ensemble approach: based on dynamical and statistical predictions for rainfall and temperature of monthly and seasonal time scales.
- Development of probabilistic forecast models for categorical forecasts of rainfall and temperature in terms of monthly and seasonal time scales for meteorologically homogeneous zones/major agro-climatic zones.
- To implement a dynamical model in conjunction with the statistical model.

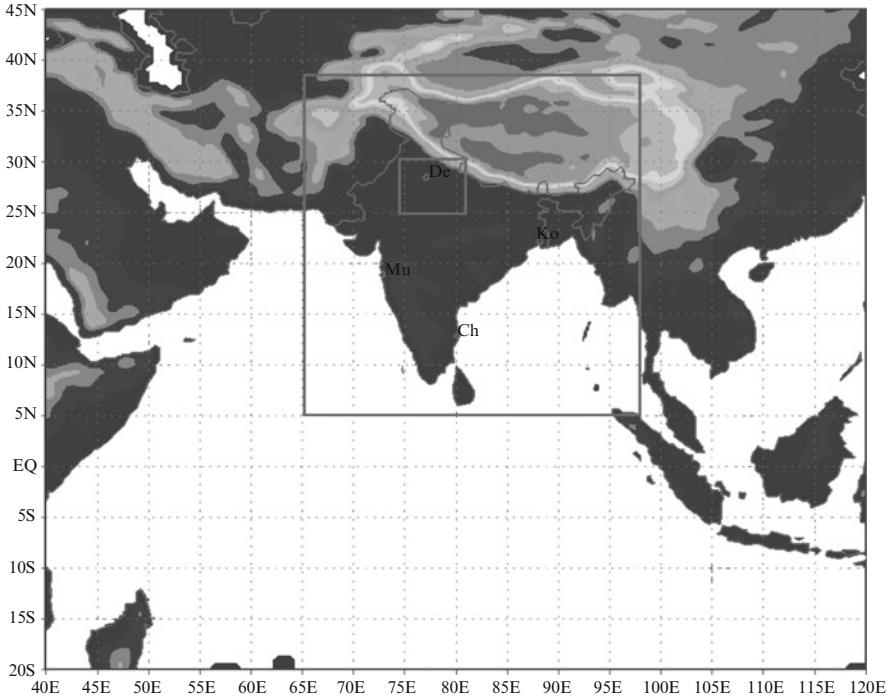


**Fig. 1.7** Short-range forecasting (WRF) strategy at IMD HQ

### *1.3.5 Long Range Forecast for Summer and North-East Monsoon*

Short-range forecasting (WRF) strategy at the New Delhi is presented in Fig. 1.7. Mesoscale data assimilation and generation of high-resolution analysis for RSMC (Regional Specialized Meteorological Centre, Delhi as recognized by WMO) domain at the horizontal grid-spacing of 27 km and vertical resolution 50 Eta levels. Time interval would be 6 hourly cycling. Resolution of the forecast fields would be 27 km for RSMC and 9 km for Indian domain. Triple nested (27, 9 and 3 km) model forecast would be made for specific events or expeditions (e.g. Commonwealth Game 2010). Fig. 1.8 depicts the short-range forecasting (WRF) strategy at the State Meteorological Centres.

## 1.4 Agromet Advisory Services

IMD started issuing district level weather forecast since 1st June 2008. District level agromet advisory meant for farmers are made based on the quantitative district level (612 districts) weather forecast for seven weather parameters viz.,

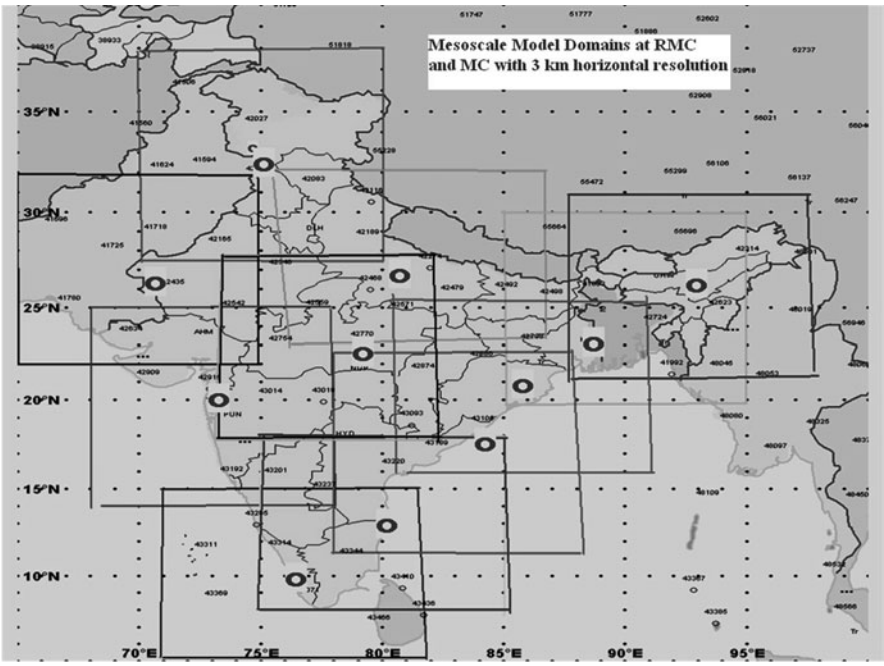


**Fig. 1.8** Short-range forecasting (WRF) strategy at state met centre

rainfall, maximum and minimum temperatures, wind speed and direction, relative humidity and cloudiness up to 5 days. NWP products for the district level forecast generated from NHAC, New Delhi using multimodel ensemble is disseminated to Regional Meteorological Centres and Meteorological Centres of IMD located in different states. These offices undertake value addition to these products and communicate to 130 AgroMet Field Units (AMFUs) located at State Agriculture Universities (SAUs), institutes of Indian Council of Agriculture Research (ICAR) etc who prepare Agro-meteorological advisories for State and Central agricultural authorities as well to individual farmers based on the district specific meteorological information containing observed data, reported phenomena, specially derived weather forecasts for small domains, coupled with information on crop stage, state and diseases. The agro- meteorological advisories prepared by the AMFUs are communicated back to respective Regional Meteorological Centres and Meteorological Centres of IMD to prepare composite bulletin for the state. The dissemination of advisories is made through various modes of mass media (including All India Radio (AIR) and Doordarshan, Private TV and radio channels, news papers, Internet), extension centres of agriculture and rural development related agencies (NGOs, Kisan Call Centres/ICAR and other related Institutes/Agricultural Universities/KVKs etc.) and directly to different Government offices. The purpose or such advisories is to enable farmers to take remedial measures and prevent weather induced losses and to mobilize resources at more organized levels to counter detrimental conditions (Rathore and Maini 2008; Rathore et al. 2009).

## References

Krishnamurti TN, Kishtawal CM, Larow T, Bachiochi D, Zhang Z, Willford EC, Gadgil S, Surendran S (1999) Improved weather and seasonal climate forecasts from multimodel super ensemble. Science 285:1548–1550

Roy Bhowmik SK, Durai VR, Das Ananda K, Mukhopadhaya B (2009) Performance of IMD Multi-model ensemble based district level forecast system during summer monsoon 2008, IMD Met Monograph No. 8/2009

Roy Bhowmik SK, Durai VR (2010) Application of multi-model ensemble technique for real-time district level forecasts over Indian region in short range time scale. Meteorl Atmos Phy 106:19–35

Rathore LS, Parvinder Maini (2008) Economic Impact Assessment of Agro-Meteorological Advisory Service of NCMRWF. Report no. NMRF/PR/01/2008, 104pp, Published by NCMRWF, Ministry of Earth Sciences, Government of India, A-50 Institutional Area, Sector-62, NOIDA, UP, INDIA 201 307

Rathore LS, Singh KK, Baxla AK (2009) Agromet services for ePachayats. Information for Development VII(4):14–16

# Chapter 2
# Monthly and Seasonal Indian Summer Monsoon Simulated by RegCM3 at High Resolutions

**S.K. Dash, Savita Rai, U.C. Mohanty, and S.K. Panda**

**Abstract** The purpose of this study is to examine the advantages of using higher resolution regional model in simulating the temperature and precipitation over India. The Regional Climate Model version 3 (RegCM3) has been integrated to simulate the Indian summer monsoon rainfall for a number of years at two horizontal resolutions 55 and 30 km. The characteristics of interannual variations in the contrasting monsoon years 2002 and 2003 have been examined in details at these resolutions. Comparison shows that the model simulated area weighted average magnitudes and spatial distribution of rainfall over India during June to September months reasonably compare with the respective gridded rainfall values of India Meteorological Department (IMD). Model simulated rainfall values with 30 km resolution are closer to the IMD values as compared to the simulated precipitation at 55 km model resolution. Also the spatial distribution of rainfall in RegCM3 with 30 km is more realistic than that of 55 km resolution. Comparison with NCEP/NCAR analysed fields shows that RegCM3 with 30 km resolution performs better than that with 55 km resolution in simulating the upper and lower level winds over India. It may be noted that both temperature and rainfall are important weather parameters for the farmers in terms of agricultural productions. Dynamical downscaling of the high resolution model simulated weather parameters will eventually help in agricultural risk management.

S.K. Dash (✉) • S. Rai • U.C. Mohanty • S.K. Panda
Centre for Atmospheric Sciences, IIT Delhi, Hauz Khas, New Delhi, India
e-mail: skdash@cas.iitd.ernet.in; savita1559@gmail.com; mohanty@cas.iitd.ernet.in; sampadpanda@gmail.com

S.D. Attri et al. (eds.), *Challenges and Opportunities in Agrometeorology*,
DOI 10.1007/978-3-642-19360-6_2, 

## 2.1 Introduction

The spatial variability of monsoon rainfall is observed to be large and there were several occasions when some parts of the country received heavy rainfall while at the same time some other parts had serious rainfall deficiency. In the recent past, the monsoons of 2002 and 2003 have exhibited very contrasting characteristics so far as rainfall over India is concerned. Large deficient rain in July 2002 over most of the country was reported in the year 2002. On the other hand, 2003 has been reported as a normal monsoon year. In 2002, the seasonal rainfall over the country as a whole was 81% of its long period average and hence it was declared as an All India drought monsoon year (Kalsi et al. 2004). The most important aspect of 2002 monsoon was that the rainfall in July was the lowest in the past 102 years. Month wise, the rainfall was normal in June, extremely subdued in July, normal in August and nearly normal in September. On the other hand in the year 2003, total seasonal monsoon rainfall over the country as a whole was 102% of its long term average. The rainfall activity in 2003 was very good during the months of June and July, though August and September were little subdued. Rajeevan et al. (2004) using 8-parameter and 10-parameter power regression models could not predict the large deficiency of rainfall of July 2002. Based on the model forecasts of European Centre for Medium range Weather Forecasts (ECMWF), Gadgil et al. (2002) summarised that June, July and August rainfall was deficient only over the southwestern peninsular and near normal over rest of the country.

It has been demonstrated that for examining the weather features in greater detail, regional models are more suitable than the global models. Today computationally it is affordable to increase the resolution of regional models so as to resolve regional climatic features reasonably well. There have been some attempts in the past to simulate monsoon features and extreme weather events over India by regional models. Bhaskaran et al. (1996) simulated the Indian summer monsoon using a regional climate model with a horizontal resolution of 50 km nested with global atmospheric GCM. Their study showed that regional model derived precipitation is larger by 20% than GCM. Ji and Vernekar (1997) simulated the summer monsoons of 1987 and 1988 by using the National Centers for Environmental Prediction (NCEP) Eta model nested in the Center for Ocean-Land-Atmosphere (COLA) GCM. Their comparative studies showed that for 1987, the Eta model simulates deficient summer monsoon rainfall over northern and peninsular India and the Indonesian region and excess rainfall over southeast China, Burma and the sub-Himalayan region compared to 1988. Azadi et al. (2001) used MM5 to simulate western disturbances during January 1997 over the Indian region and to predict precipitation associated with it. Bhaskar Rao et al. (2004) simulated many observed features of the Indian summer monsoon such as sea level pressure, 925 hPa temperature, low level wind and precipitation using MM5. The Regional Climate Model version 3 (RegCM3) has also been successfully integrated to simulate the salient features of Indian summer monsoon

circulation and rainfall (Dash et al. 2006; Shekhar and Dash 2005). They found that the RegCM3 successfully simulate the 850 hPa westerly flow and the 200 hPa easterly flow. Also the seasonal mean summer monsoon rainfall simulated by the model is close to the GPCC values. They have also found that RegCM3 successfully simulates the temperature pattern at 500 hPa over the Indian Peninsula and Tibet. In their study it was inferred that RegCM3 can be effectively used to study monsoon processes over the South Asia region. Shekhar and Dash (2005) have examined the effect of Tibetan snowfall in the month of April on the Indian summer monsoon circulation and associated rainfall using RegCM3 with 55 km resolution. Model simulations show that when 10 cm of snow-depth in April is prescribed over Tibet, summer monsoon rainfall in entire India reduces by about 30%. Singh et al. (2006) used RegCM3 over East Asia regions and showed promising performance of this regional model in simulating important characteristics of monsoon circulations.

The objective of the current paper is to examine the performance of RegCM3 at two different resolutions 55 and 30 km so as to compare the important features of simulated summer monsoon in the contrasting years 2002 and 2003. A brief description of RegCM3, experimental design and data used are given in Sect. 2.2. Sections 2.3–2.6 discuss the characteristics of upper level wind, lower level wind, temperature at 500 hPa and rainfall for both the resolutions of RegCM3 respectively and the conclusions are summarized in Sect. 2.7.

## 2.2 Model, Initial Data and Experimental Design

RegCM3, an upgraded version of the Abdus Salam International Centre for Theoretical Physics (ICTP) regional climate model RegCM2 originally developed by Giorgi et al. (1993a, b), is a compressible, grid point model with 14 vertical layers and hydrostatic balance. There are two categories of landuse such as MM4 vegetation and Global Land Cover Characterization (GLCC) which determine surface properties like albedo, roughness, moisture etc. at each grid point. MM4 vegetation has 13 different types and GLCC has similarly 20 types of lands. The model dynamical core is essentially the same as that of the hydrostatic version of MM5 (Grell et al. 1994). The model includes cumulus parameterization schemes, large scale precipitation scheme, planetary boundary layer (PBL) parameterization, state-of-the-art surface vegetation/soil hydrology package, the Biosphere-Atmosphere Transfer Scheme (BATS), Ocean flux parameterization, pressure gradient scheme, explicit moisture scheme, the radiative transfer scheme and the ocean-atmosphere flux scheme.

The complete RegCM3 modelling system consists of four modules: Terrain, ICBC, RegCM and Postprocessor. Terrain and ICBC are the two components of RegCM preprocessor. These program modules are run in sequence. Following Dash et al. (2006) in this study, Grell convective precipitation scheme with Arakawa-Schubert (AS) closure has been used. It has been widely used within both MM5 and

RegCM modeling frameworks. It is a mass flux scheme that includes the moistening and heating effects of penetrative updrafts and corresponding downdrafts.

For simulating the monsoon circulation features the central grid point for model domain is chosen at 80°E and 20°N. In the 55 km resolution domain chosen is 50°E to 109°E and 4°S to 41°N and there are 101 grid points along a latitude circle and 120 points along the longitudinal direction. In case of 30 km resolution there is one-way nesting with a larger domain at 90 km resolution as shown in Fig. 2.1. In the 90 km resolution the domain chosen is 51°E to 109°E and 4°S to 42°N and there are 64 grid points along a latitude circle and 72 points along the longitudinal direction. While in case of 30 km resolution the domain chosen is 66°E to 98°E and 6°N to 36°N and there are 120 grid points along both the latitude circle and the longitudinal direction.

The elevation data used are obtained from the United States Geological Survey (USGS). Terrain heights and land use data are used at 30 min resolution. In both the years 2002 and 2003, simulations at 55 and 30 km resolutions cover the months

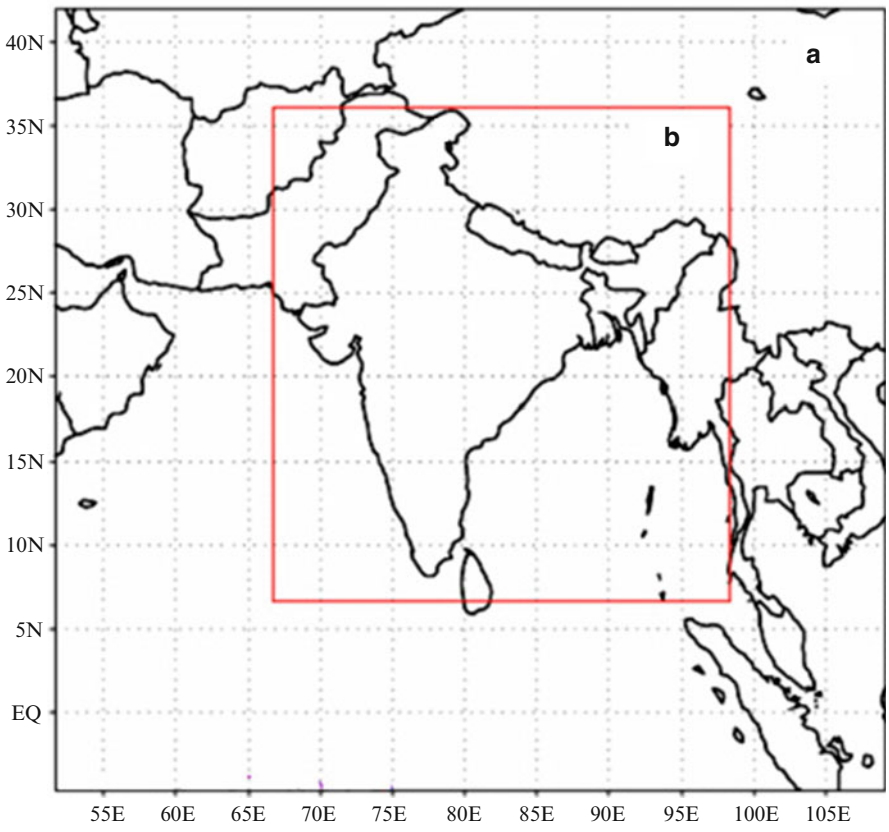


**Fig. 2.1** One way nesting of domains at (**a**) 90 km and (**b**) 30 km for the Indian region

from April to September in the ensemble mode with nine-members starting from 25th April to 3rd May. The data for initial and lateral boundary conditions have been obtained from the National Centers for Environmental Prediction (NCEP) Reanalysis (NNRP1) and Sea Surface Temperature (SST) that are collected from the National Oceanic and Atmospheric Administration (NOAA) 4-times daily and weekly datasets respectively.

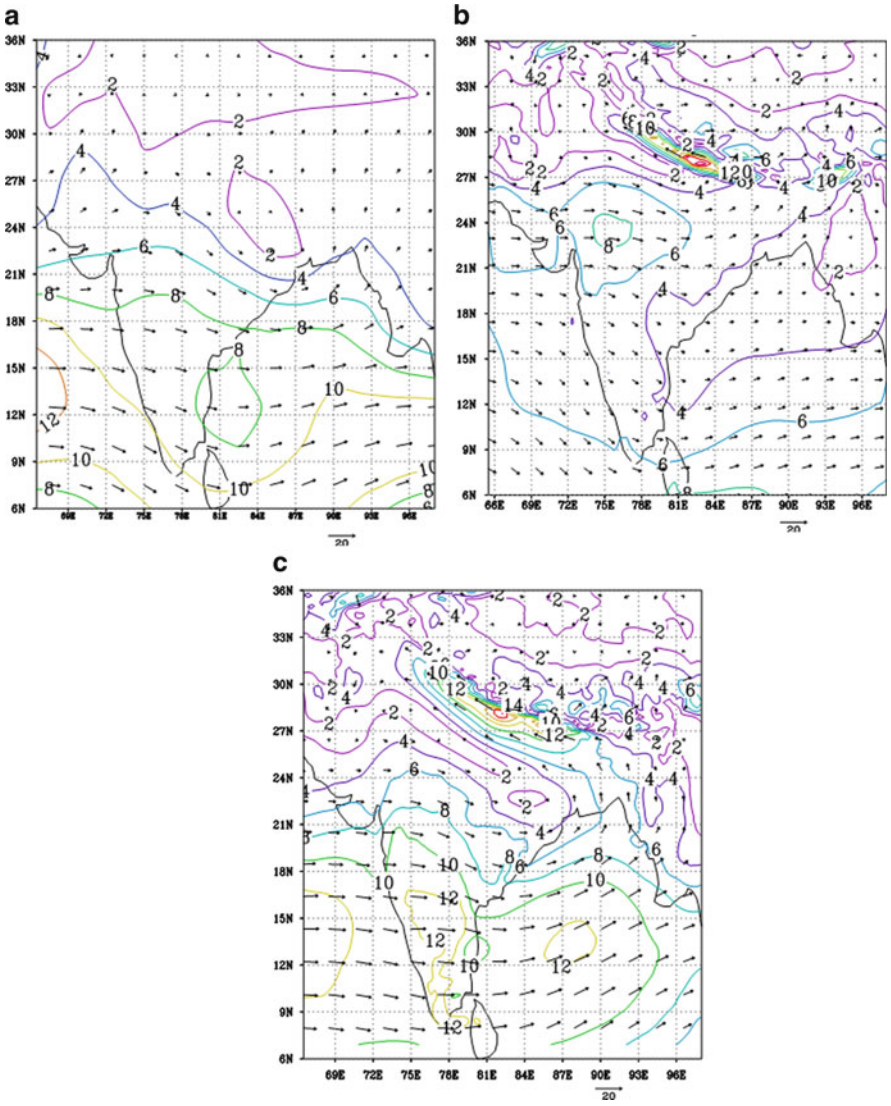


**Fig. 2.2** Mean winds (JJAS) at 850 hPa in 2002 (**a**) NCEP/NCAR reanalysis, (**b**) RegCM3 at 55 km and (**c**) RegCM3 at 30 km

## 2.3 Lower Level Wind

The averages of seasonal mean winds of the nine ensemble members simulated by RegCM3 in 2002 and 2003 with 55 and 30 km resolutions at 850 hPa levels are depicted in Figs. 2.2 and 2.3 respectively. In the year 2002, the maximum

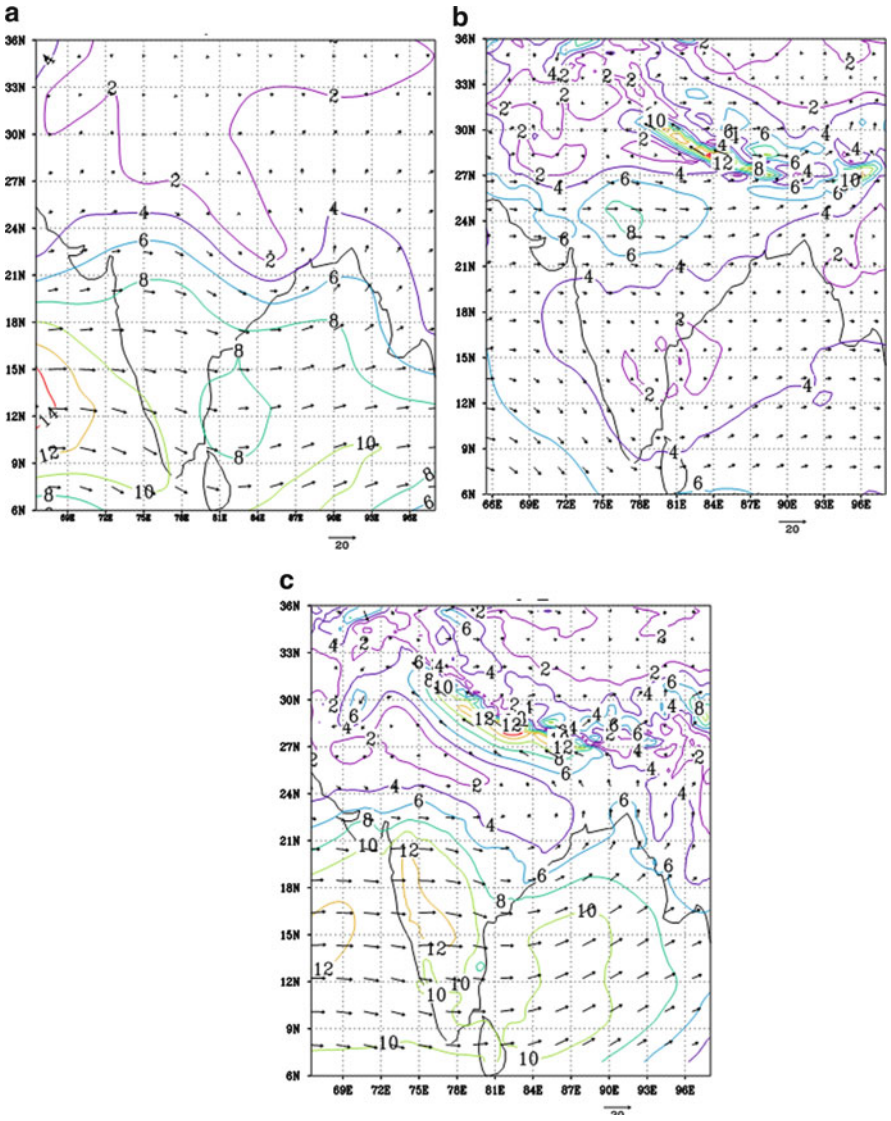


**Fig. 2.3** Mean winds (JJAS) at 850 hPa in 2003 (**a**) NCEP/NCAR reanalysis, (**b**) RegCM3 at 55 km and (**c**) RegCM3 at 30 km

strength of the Somali jet at 850 hPa is 12 m/s at 30 km resolution which is closer to NCEP/NCAR reanalysis while in case of 55 km the difference is more. Across the monsoon trough the maximum values are 8 m/s and 4 m/s in case of 30 and 55 km respectively. The westerly wind over the peninsula has the speeds of 10–12 m/s, 4–6 m/s and 8–10 m/s in case of 30 km model resolution, 55 km model resolution and NCEP-NCAR respectively. Similar pattern is seen for the year 2003. The maximum strength of the Somali Jet at 850 hPa level in case of 30 km resolution is 12 m/s which is very close to the NCEP/NCAR reanalysis value of 14 m/s. While in 55 km resolution the corresponding wind strength is 6 m/s, along the west coast the wind speeds are 12 m/s, 4 m/s and 10 m/s for resolutions 30, 55 km of RegCM3 and NCEP/NCAR respectively. The westerly wind simulated by RegCM3 over peninsula has the same speed of 10–12 m/s for both the years 2002 and 2003.

## 2.4 Upper Level Wind

The observed NCEP/NCAR reanalysed wind and the ensemble averages of the seasonal mean winds simulated by RegCM3 at 200 hPa level in the years 2002 and 2003 are shown in Figs. 2.4 and 2.5 respectively. In the year 2002 maximum strengths of the easterly jet across the peninsula are 22 m/s and 18 m/s at 30 and 55 km model resolutions respectively. Both the values are close to the NCEP/NCAR reanalysis value of 20 m/s. Upper level easterly wind strength over Tibet is 20 m/s at both 30 and 55 km model resolutions. In 2003, the wind speed ranges over the peninsula are 20–22 m/s, 18–20 m/s and 16–18 m/s in case of 30 km model resolution, NCEP/NCAR reanalysis and 55 km respectively. Upper level wind strength over Tibet is 24 m/s in the 30 km model resolution whereas both in NCEP/NCAR reanalysis and 55 km resolution the corresponding strength is 20 m/s. At 30°N and 85°E, the wind strength is 12 m/s at both 30 and 55 km model resolutions.

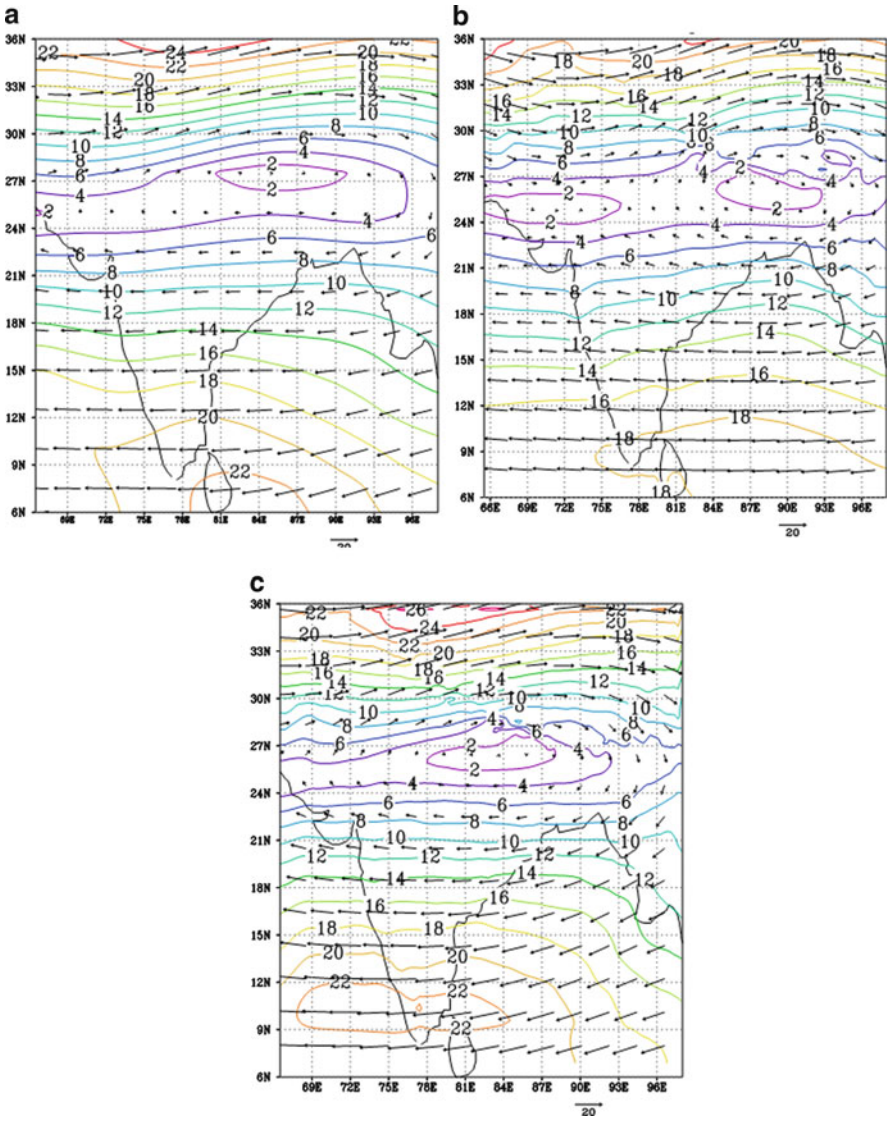


**Fig. 2.4** Mean winds (JJAS) at 200 hPa in 2002 (**a**) NCEP/NCAR reanalysis, (**b**) RegCM3 at 55 km and (**c**) RegCM3 at 30 km

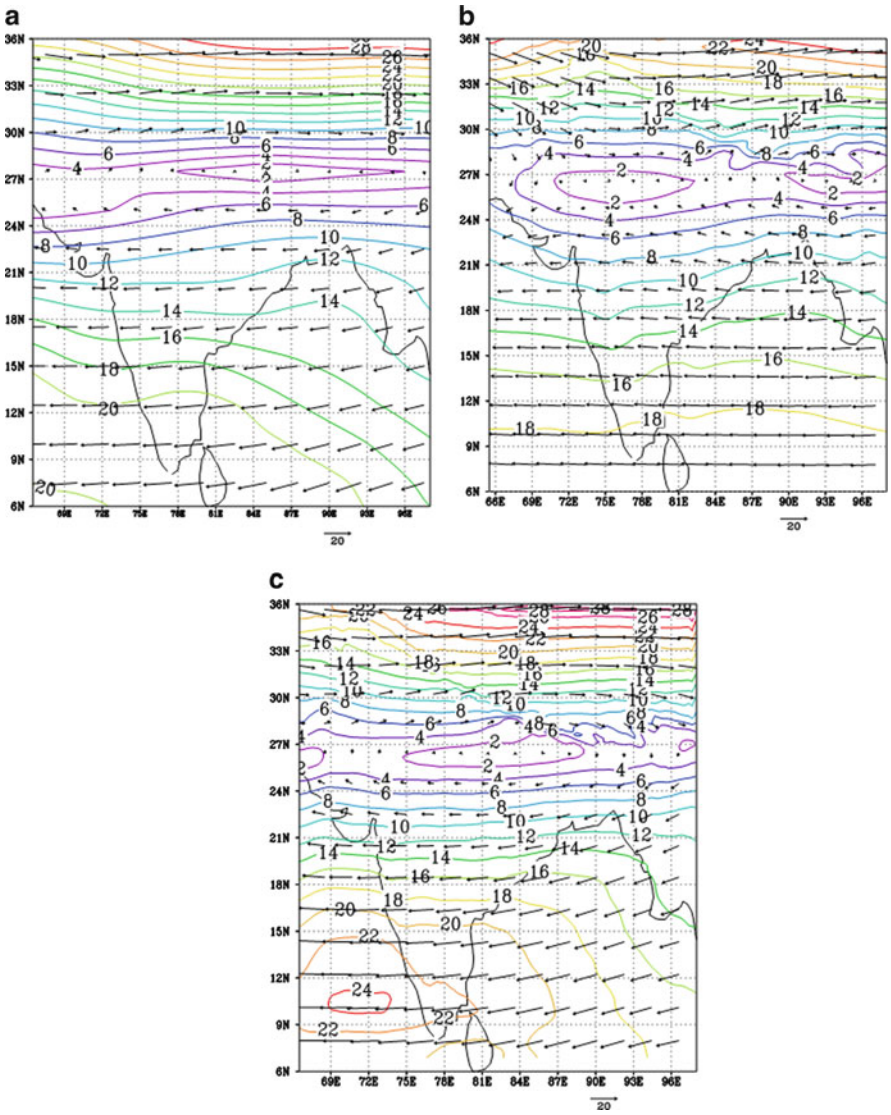


**Fig. 2.5** Mean winds (JJAS) at 200 hPa in 2003 (**a**) NCEP/NCAR reanalysis (**b**) RegCM3 at 55 km (**c**) RegCM3 at 30 km

## 2.5 Temperature at 500 hPa

Depict the NCEP/NCAR reanalysis and RegCM3 simulated JJAS mean temperatures at 500 hPa with 55 and 30 km resolutions respectively for the years 2002 and 2003. As shown in Fig. 2.6 the mean maximum temperature over Tibet is 272 K at both 30

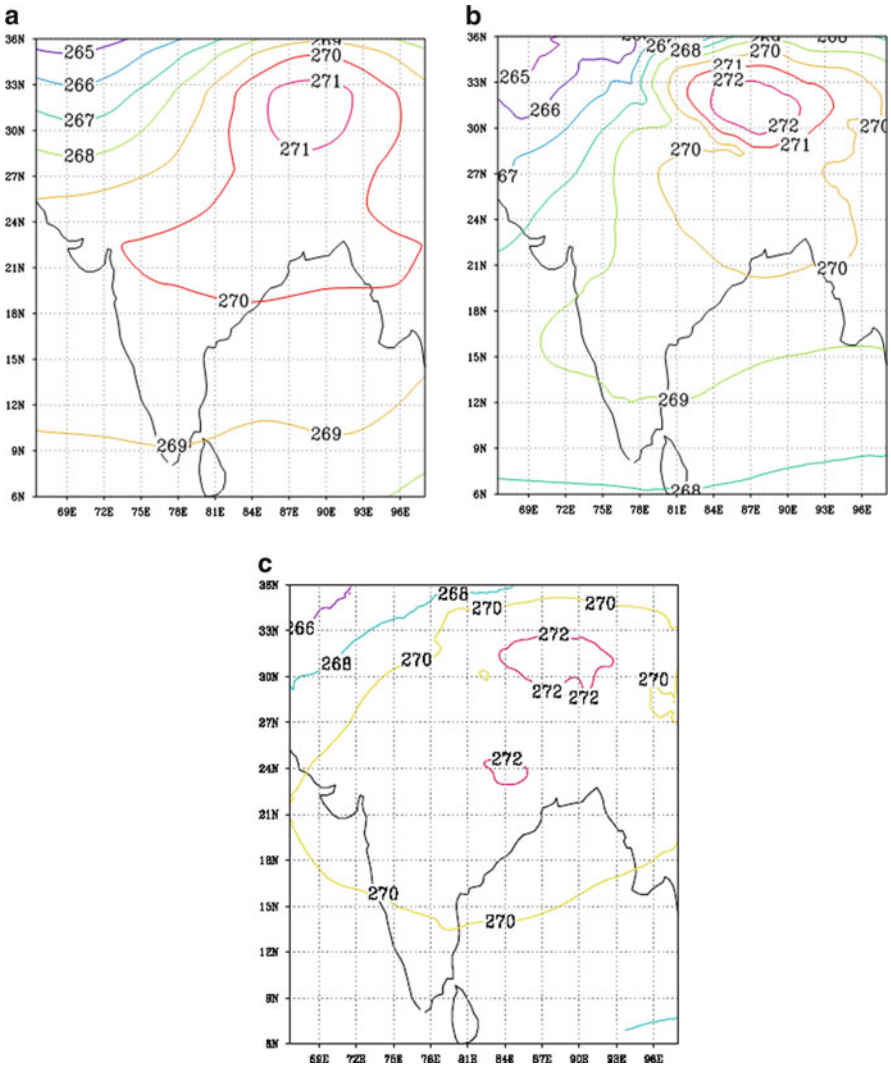


**Fig. 2.6** Mean temperatures (JJAS) at 500 hPa in 2002 (**a**) NCEP/NCAR reanalysis, (**b**) RegCM3 at 55 km and (**c**) RegCM3 at 30 km

and 55 km model resolutions in 2002. The corresponding mean temperature at 500 hPa in the NCEP/NCAR reanalysis is 271 K. Over the Indian Peninsula the mean simulated temperature in the 55 km resolution is similar to that of NCEP/NCAR but it is more in case of 30 km model resolution for both the years 2002 and 2003. The corresponding value in NCEP/NCAR reanalysis is 272K Figures 2.6 and 2.7.

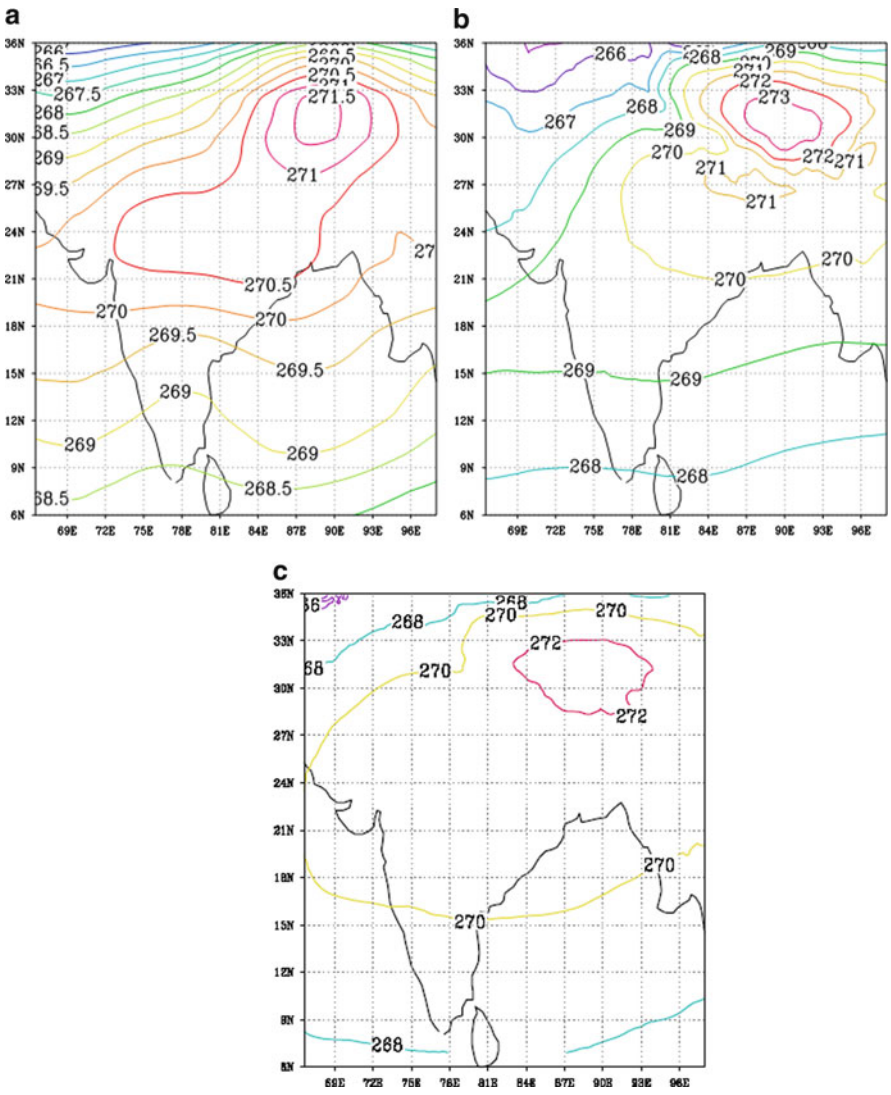


**Fig. 2.7** Mean temperatures (JJAS) at 500 hPa in 2003 (**a**) NCEP/NCAR reanalysis, (**b**) RegCM3 at 55 km and (**c**) RegCM3 at 30 km

## 2.6 Rainfall

The monthly and seasonal rainfall simulated in two consecutive years 2002 and 2003 with two different model resolutions of 55 and 30 km are discussed here. For better and close comparison of rainfall simulated by the model and the IMD observed rainfall, area weighted averaging has been done at the model grids. This

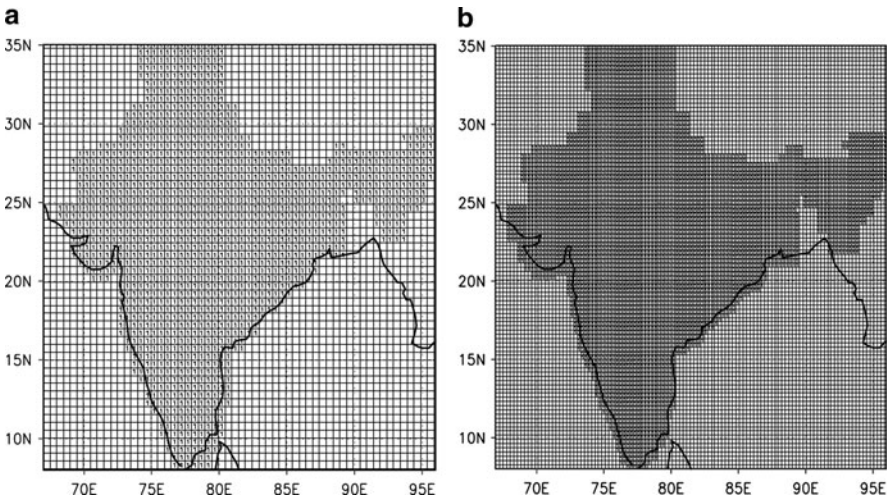


**Fig. 2.8** Grid boxes used for calculating rainfall over Indian landmass in RegCM3 simulations at (**a**) 55 km and (**b**) 30 km resolutions

method is similar to that used by IMD with the observed sub-divisional rainfall. It is known that IMD calculates ISMR based on the area weighted average sub divisional rainfall. As mentioned earlier RegCM3 at 55 km has 118 × 99 grids across the Indian landmass and at 30 km it has a total of 118 × 118 grids. The grid boxes marked '1' in Fig. 2.8a, b are those, which cover all the meteorological subdivisions of IMD as closely as possible. In this study, the model simulated monthly and seasonal rainfall are computed at the grids over Indian landmass. Figures 2.9 and 2.10 show the grid averaged rainfall of IMD and those simulated by RegCM3 with 55 and 30 km resolutions in July of both the years 2002 and 2003 respectively. Figures 2.11 and 2.12 show corresponding values for JJAS.

IMD has generated monthly mean rainfall at regular 10 × 10 grids over the India landmass (Rajeevan et al. 2005). For the analysis, daily rainfall data of 6,329 stations were considered during 1951–2003. There were only 1,803 stations with a minimum 90% data availability during that period. In their analysis, the interpolation method proposed by Shepard (1968) has been followed. This method is based on the weights calculated from the distance between the station and the grid point and also the directional effects. Standard quality controls were performed before carrying out the interpolation analysis. Quality of the present gridded rainfall analysis was also compared with similar global gridded rainfall data sets. Comparison revealed that the present gridded rainfall analysis is better in more realistic representation of spatial rainfall distribution. The IMD gridded rainfall dataset is being extensively used for many applications in validation of climate and numerical weather prediction models and also for studies on monsoon variability (Rajeevan et al. 2006; Dash et al. 2009).

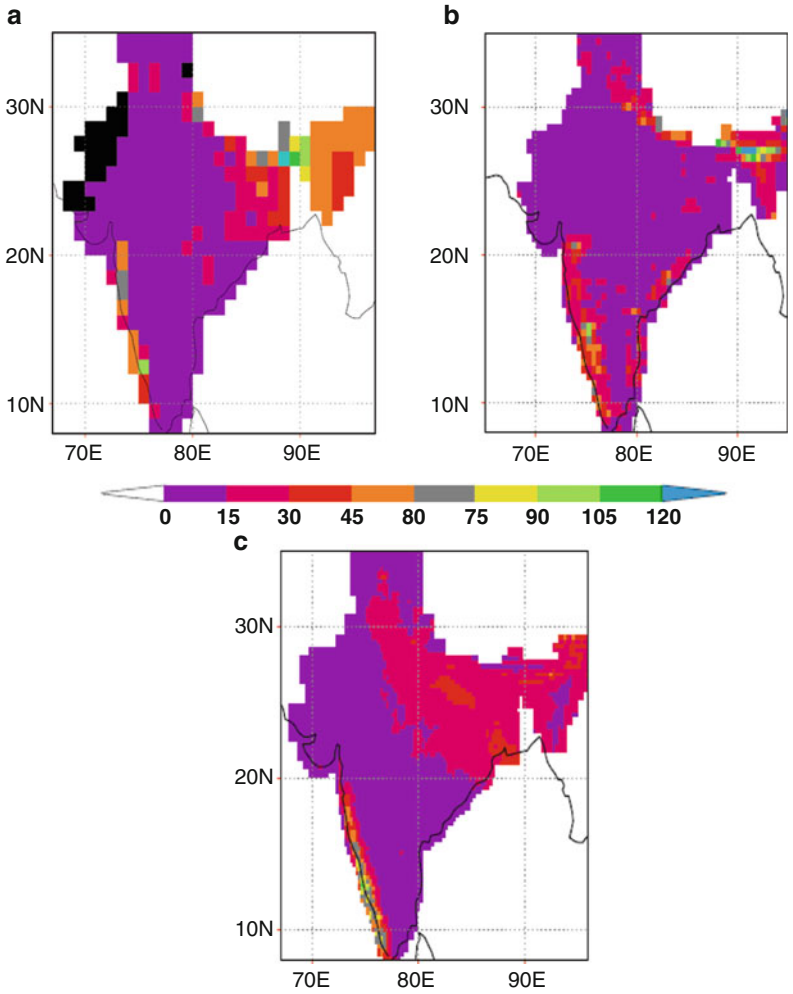


**Fig. 2.9** July 2002 mean rainfall (cm) at the grids over Indian landmass (**a**) IMD 1-degree, (**b**) RegCM3 55 km and (**c**) RegCM3 30 km

In July 2002 very little rain was observed except in the west coast and north-east of India (Fig. 2.9a) while in July 2003 good amount of rainfall was recorded throughout the country (Fig. 2.10a). This contrasting rainfall is clearly seen for higher resolution simulation of RegCM3 in comparison to resolution of 55 km. Figure 2.9a, c show that there is good amount of rainfall in west coast, some parts of coastal Andhra, coastal Orissa, along the foothills of Himalayas and north east India whereas there is very less rainfall in north-west and some parts of central India while Fig. 2.9b shows very less rainfall in coastal Orissa and north east India. On the other hand in 2003, most of the country received good amount of rainfall except north-west India as shown in Fig. 2.10.

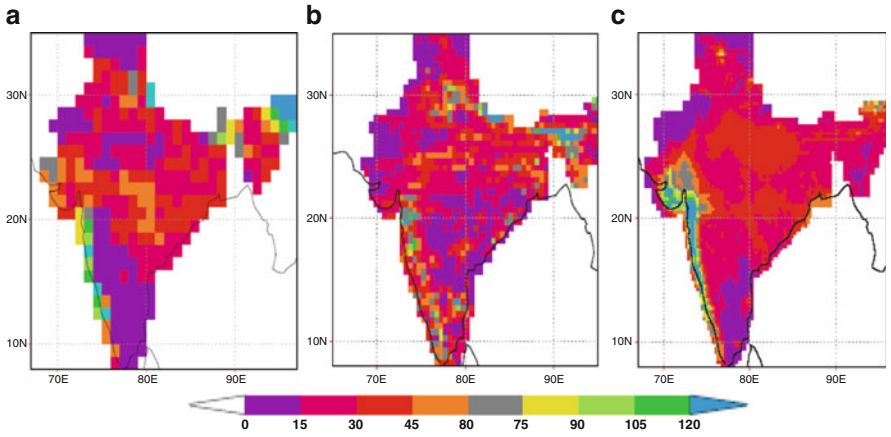


**Fig. 2.10** July 2003 mean rainfall (cm) at the grids over Indian landmass (**a**) IMD 1-degree, (**b**) RegCM3 55 km and (**c**) RegCM3 30 km

Figure 2.9c shows that in the simulations with 30 km grid size maximum rainfall is 75–90 cm. The model with 55 km simulates maximum rainfall of 90–105 cm (Fig. 2.9b) over west coast whereas the corresponding observed value is 50 cm (Fig. 2.9a). Simulated rainfall over Bihar, West Bengal and Orissa is 1–15 cm which is less than the corresponding observed value of 10–25 cm. However, precipitation simulated by RegCM3 at 30 km exactly matches with the observed values. Simulated rainfall over North-West India at both 55 km and 30 km lies between 1 and 15 cm. These are close to the observed rainfall value of 0–15 cm for the year 2002. The observed and simulated mean rainfall in the month of July at 55 and 30 km resolutions in the year 2003 are depicted in Figs. 2.10a–c respectively. Over west coast of India, the simulated rainfall is 80–120 cm for all the three cases. Comparing with observed rainfall over the central India, we found that higher resolution of 30 km predicted much accurate rainfall than 55 km resolution.

Figure 2.11a–c show the monthly mean rainfall of IMD and those simulated by RegCM3 with 55 and 30 km resolutions for the year 2002 respectively. The spatial distribution of rainfall shows differences in pattern for model simulated and IMD values, but some similarities exists in the zones of maximum and minimum. Simulated precipitation range rainfall for both of the resolutions over the west coast is 200–300 cm (Fig. 2.11b, c) which is similar to the corresponding observed value (Fig. 2.11a). Over Bihar and Gangetic west Bengal rainfall values lies between 100 and 200 cm for both the observed and RegCM3 simulated with 30 km resolution while with 55 km resolution these rainfall values lies between 50 and 100 cm. This shows that the RegCM3 simulated rainfall with 55 km is less than that observed over Gangetic plain. However, higher resolution of RegCM3 at 30 km depicts nearly same distribution of rainfall. Figure 2.12a–c show the monthly mean rainfall of IMD and RegCM3 simulated with 55 and 30 km respectively for

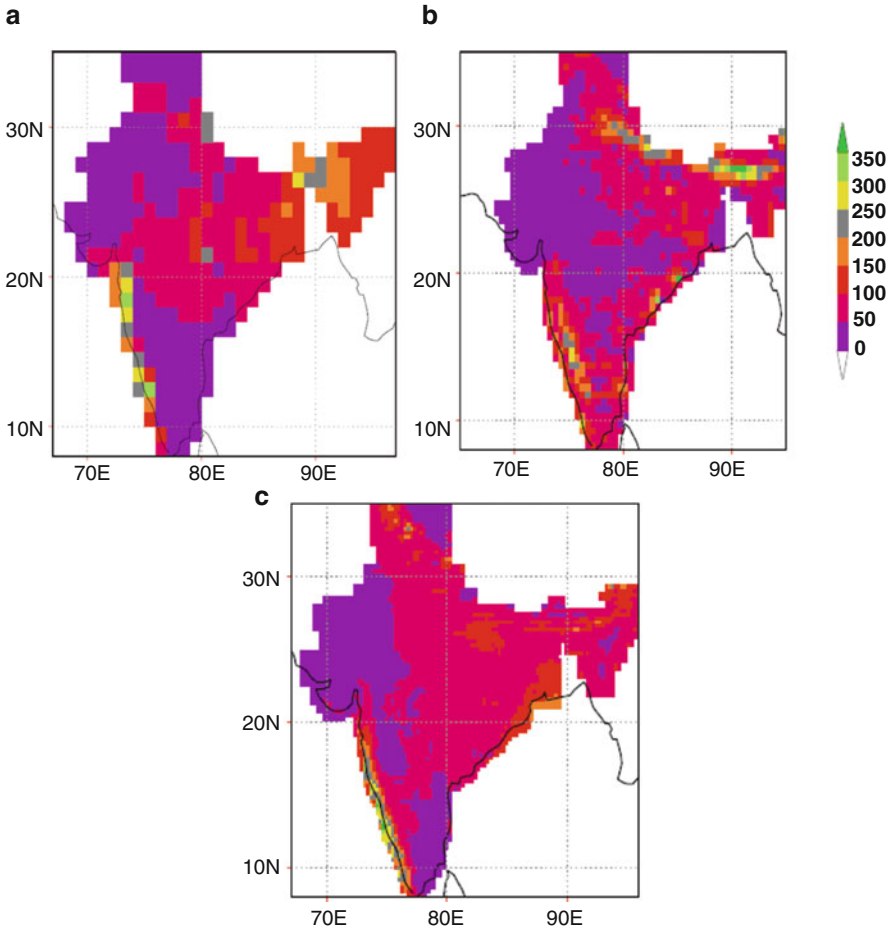


**Fig. 2.11** JJAS 2002 mean rainfall (cm) at the grids over Indian landmass (**a**) IMD 1°, (**b**) RegCM3 55 km and (**c**) RegCM3 30 km

the year 2003. Over west coast of India, the observed rain and that simulated by RegCM3 with 30 km resolution are more than 200 cm which is reasonably good in comparison to 55 km resolution value lying between 100 and 200 cm. Simulated rainfall values are up to 200 cm over Gangetic plain and up to 100 cm over the North-West India with both the resolutions of model.

Table 2.1 shows monthly mean rainfall values simulated by RegCM3 with 55 and 30 km resolutions using 9-ensemble members and IMD rainfall values for the years 2002 and 2003. In 2002, the area weighted average JJAS rain amount are 70.9 cm, 69.0 cm and 70.6 cm in case of 30 km, 55 km and IMD respectively. In 2003 these values are 90.7 cm and 88.3 cm with 30 and 55 km resolutions respectively while the corresponding observed value is 89.4 cm. Simulated rainfall by RegCM3 with 30 km resolution shows an overestimate of about 0.4% while with

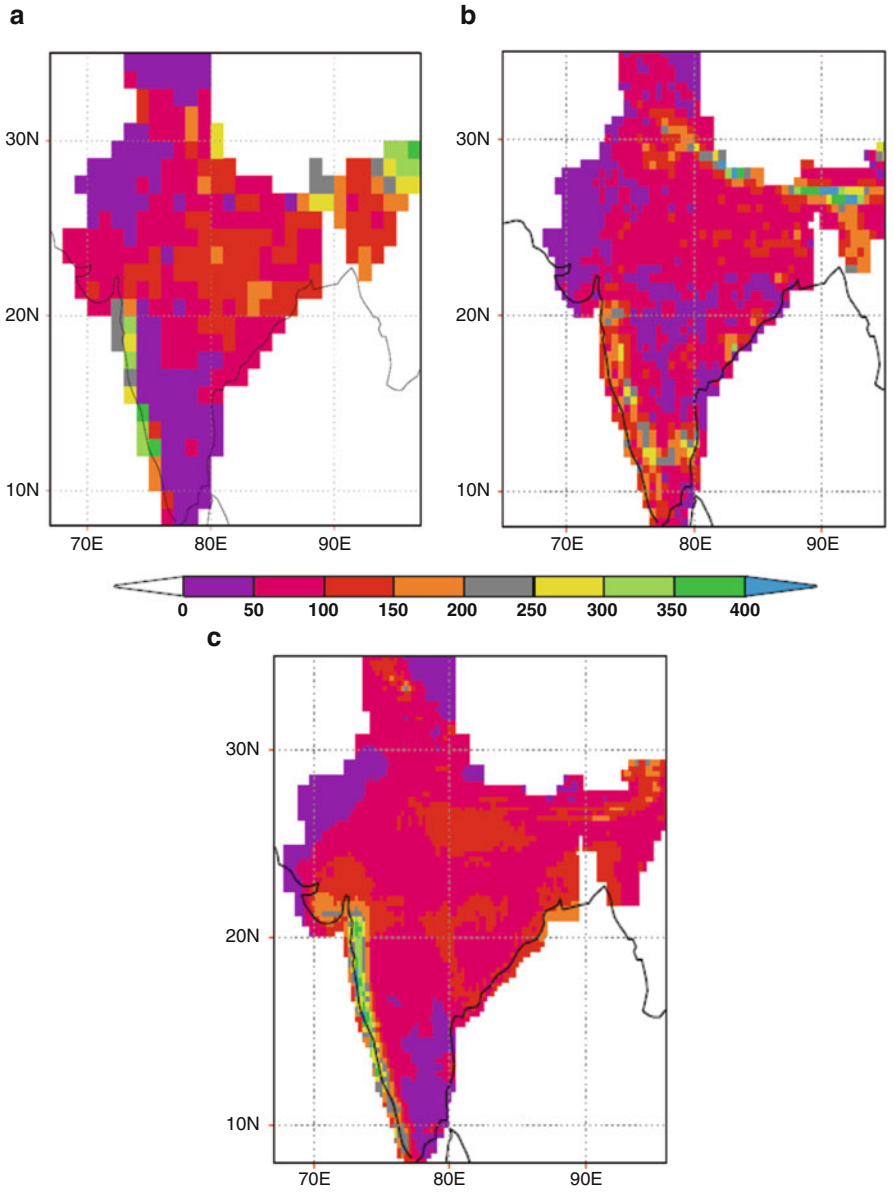


**Fig. 2.12** JJAS 2003 mean rainfall (cm) at the grids over Indian landmass (**a**) IMD 1°, (**b**) RegCM3 55 km and (**c**) RegCM3 30 km

55 km resolution rainfall value is underestimated by about 2.3% in 2002. While in 2003, simulated rain amount is overestimated by 1.4% and underestimated by 1.3% in 30 and 55 km model resolutions respectively. These results indicate that area

**Table 2.1** Comparison of RegCM3 simulated rainfall (cm) at resolutions 55 and 30 km with observed rainfall of IMD for the years 2002 and 2003

| | 2002 | | | | | | 2003 | | | | | |
|---|---|---|---|---|---|---|---|---|---|---|---|---|
| | IMD | | RegCM3-55 km | | RegCM3-30 km | | IMD | | RegCM3-55 km | | RegCM3-30 km | |
| Months | Magnitude (cm) | % departure from normal | Magnitude (cm) | % departure from normal | Magnitude (cm) | % departure from normal | Magnitude (cm) | % departure from normal | Magnitude (cm) | % departure from normal | Magnitude (cm) | % departure from normal |
| June | 16.2 | 104.2 | 15.9 | 102.2 | 16 | 102.6 | 16.9 | 108.7 | 19.1 | 122.7 | 18.3 | 117.4 |
| July | 14.2 | 48.3 | 13.9 | 47.3 | 14.9 | 50.5 | 31.4 | 106.7 | 30.2 | 102.5 | 30.9 | 105 |
| August | 24.8 | 95.7 | 23.1 | 89 | 24.3 | 93.7 | 24.6 | 94.9 | 23 | 88.7 | 24.6 | 95.1 |
| September | 15.4 | 89.6 | 16.1 | 93.4 | 16.9 | 98.2 | 16.5 | 96 | 16.1 | 93.4 | 16.9 | 98.2 |
| JJAS | 70.6 | 80.2 | 68.9 | 78.3 | 72 | 81.7 | 89.4 | 101.5 | 88.3 | 100.2 | 90.7 | 103 |

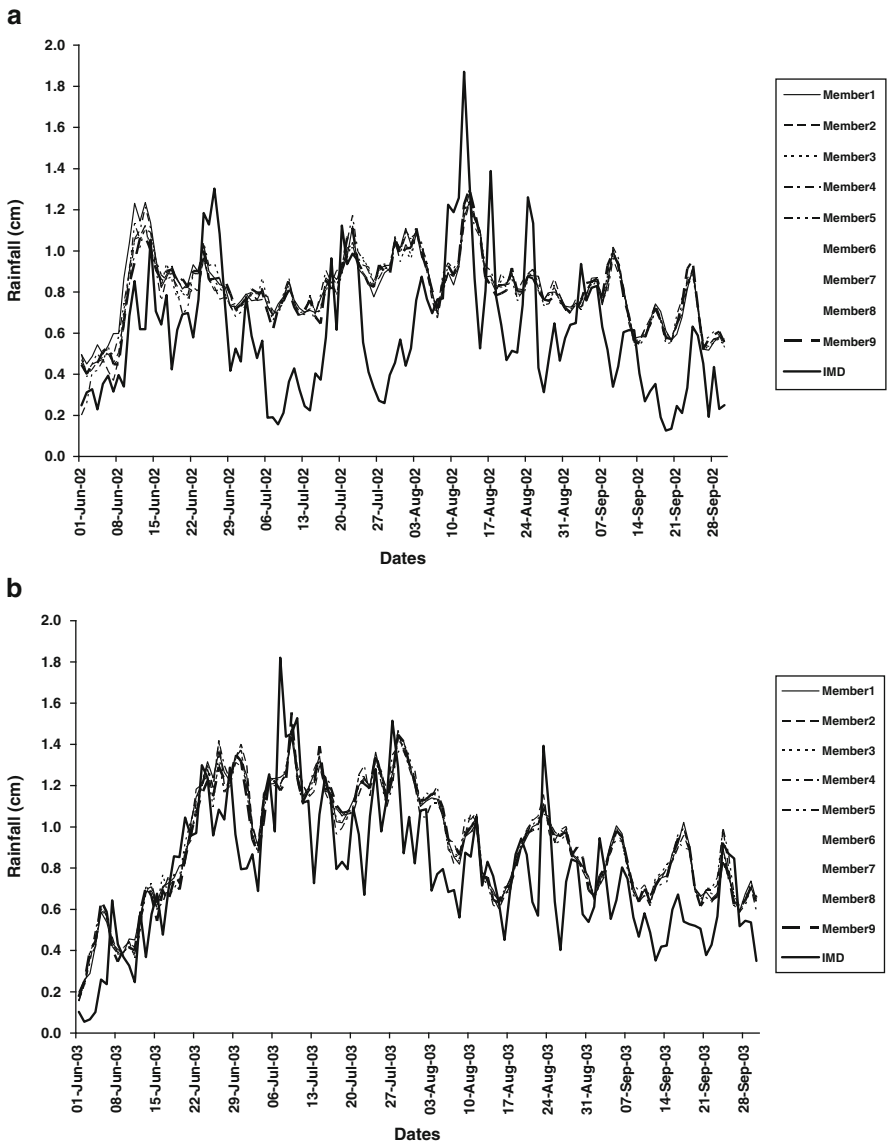


**Fig. 2.13** Daily standardised rainfall series simulated by individual ensembles at 30 km resolution compared with that of IMD (**a**) 2002 (**b**) 2003

weighted average rainfall over India is better simulated by the RegCM3 at higher resolution of 30 km and are more accuracy in comparison to 55 km resolution.

Figures 2.13 and 2.14 show the daily standardised rainfall simulated by nine ensembles individually with 30 and 55 km resolutions respectively in the years

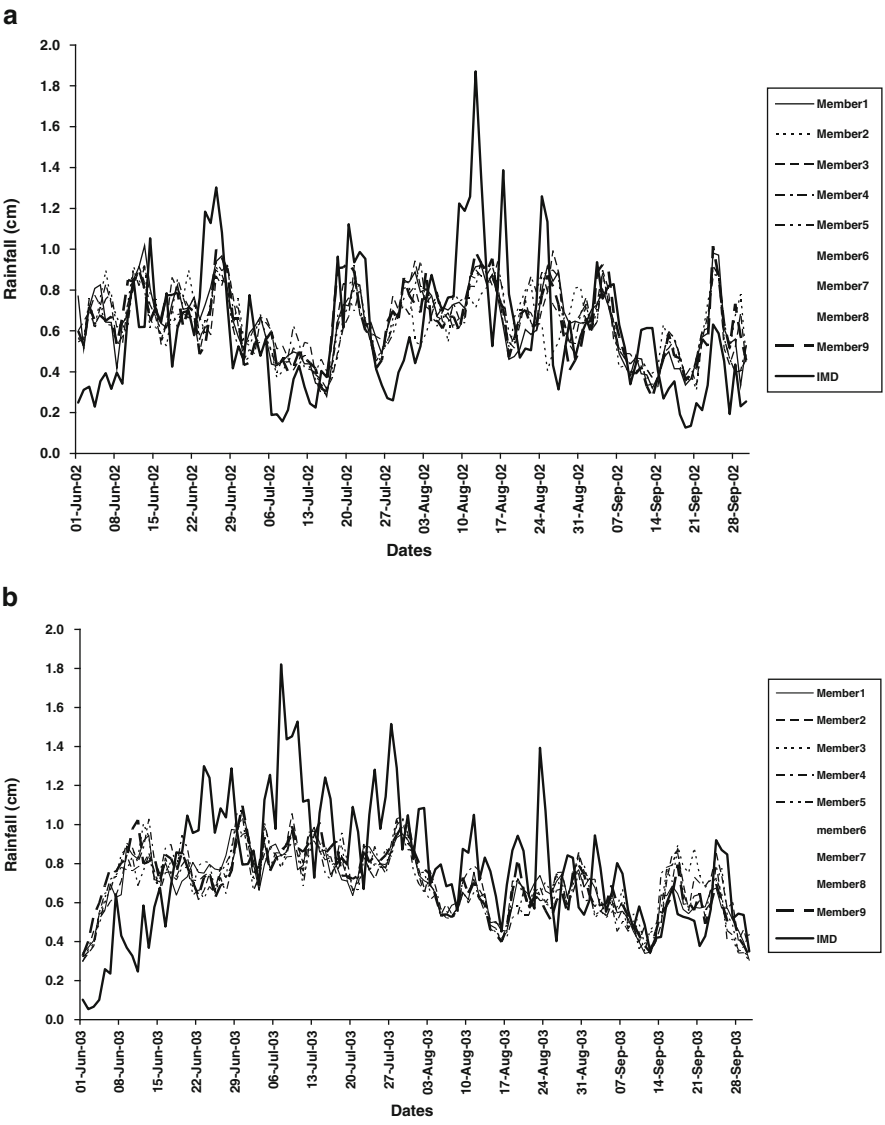


**Fig. 2.14** Daily standardised rainfall series simulated by individual ensembles at 55 km resolution compared with that of IMD (**a**) 2002 (**b**) 2003

2002 and 2003. Figure 2.15 shows the daily accumulated rainfall simulated by RegCM3 with 30 and 55 km along with IMD daily rainfall time series, starting from 1st June up to 30th September. These figures demonstrate the advantages of using higher resolution of 30 km compared to 55 km.

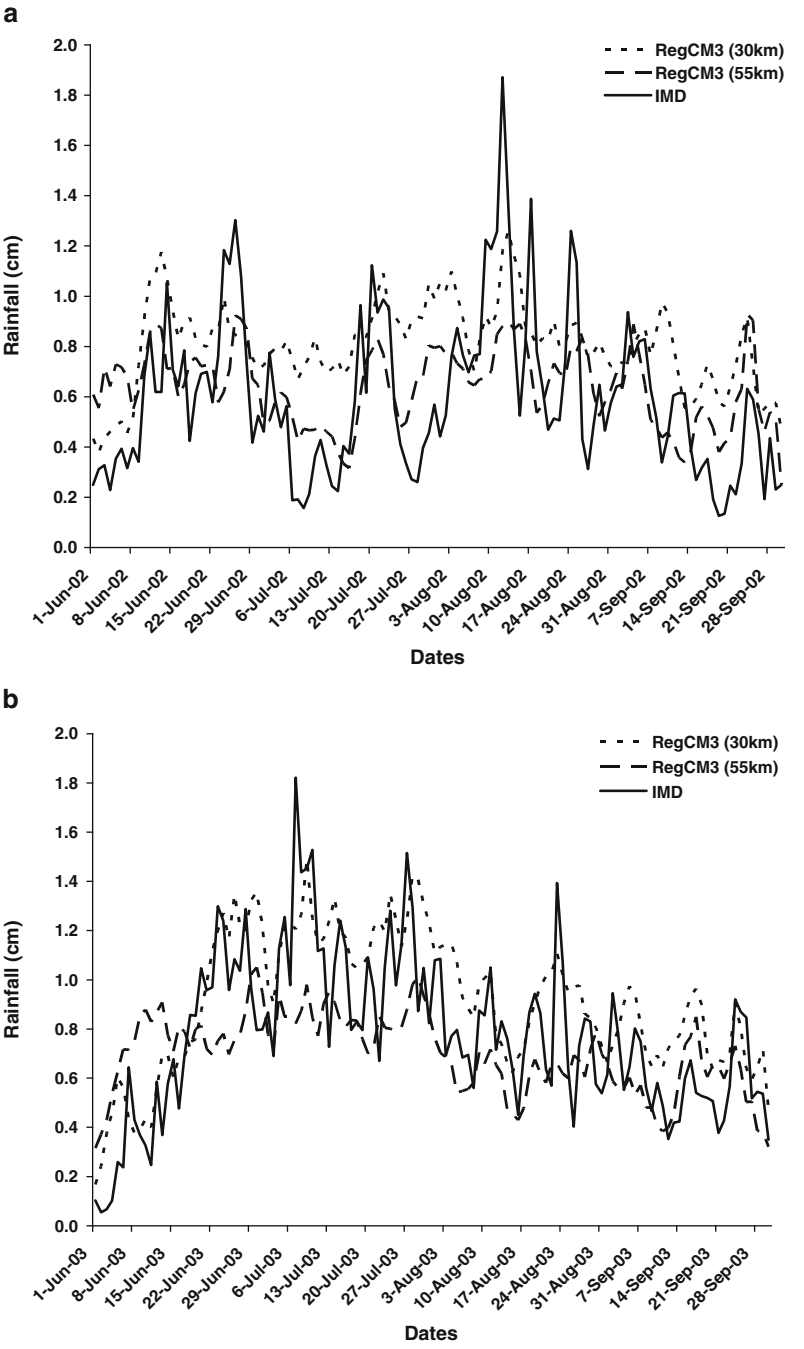


**Fig. 2.15** Daily ensemble mean rainfall simulated at 30 and 55 km of RegCM3 and IMD rainfall from 1st June to 30th September (**a**) 2002 and (**b**) 2003

## 2.7 Conclusions

In this study characteristics of summer monsoon circulation, rainfall and temperature simulated by RegCM3 at two different resolutions 55 and 30 km in the contrasting monsoon years 2002 and 2003 are compared in detail. The initial and boundary conditions for model integration are obtained from the analyses of NCEP/NCAR. Also the physical parameterization schemes of the two simulations are same. Results indicate that in both the years 2002 and 2003, higher resolution RegCM3 at 30 km predicts much closer wind to NCEP/NCAR reanalysis field at 850 hPa than that at 55 km model resolution. Also across the peninsula the strength of the easterly jet is well simulated by RegCM3 at 30 km resolution in both the years 2002 and 2003. In general, the maximum strengths of the Tibetan anticyclone and the easterly jet over peninsula are more in the year 2003 compared to those in 2002 in both the simulations of RegCM3 at 55 and 30 km. The temperatures at 500 hPa based on both the simulations of RegCM3 are close to NCEP/NCAR reanalysis in 2002 and 2003. Comparison of rainfall shows that higher resolution of RegCM3 at 30 km simulates much better rainfall magnitude and distribution close to that of IMD in both 2002 and 2003. The percentage rainfall departure from normal is minimum at 55 km model resolution in July of both the years 2002 and 2003. These percentage values are much closer to observed IMD at 30 km model resolution. Comparison of daily rainfall simulated by individual ensembles shows that at 30 km model resolution the time series are much closer to each other than in 55 km model resolution. In most of the months 55 km model simulation underestimates rainfall values in comparison to 30 km model simulation. In sum, results of this study demonstrate the advantages of using higher resolution RegCM3 in simulating the characteristics of summer monsoon over India. However, it is essential to conduct more detailed study by considering large number of contrasting years and also examining other important features of Indian summer monsoon including intra seasonal variabilities.

## References

Azadi M, Mohanty UC, Madan OP, Padmanabhamurti B (2001) Prediction of precipitation associated with a western disturbance using a high-resolution regional model – role of parameterization of physical processes. Meteorol Appl 7:317–326

Bhaskar Rao DV, Ashok K, Yamagata T (2004) A numerical simulation study of the Indian summer monsoon of 1994 using NCARMM5. J Meteorol Soc Jpn 82(6):1755–1775

Bhaskaran BR, Jones G, Murphy JM, Noguer M (1996) Simulations of the Indian summer monsoon using a nested regional climate model: domain size experiments. Clim Dyn 12:573–578

Dash SK, Shekhar MS, Singh GP (2006) Simulation of Indian summer monsoon circulation and rainfall using RegCM3. Theor Appl Climatol 86(1-4):161–172

Dash SK, Kulkarani MA, Mohanty UC, Prasad K (2009) Changes in the characteristics of rain events in India. J Geophys Res 114:12. doi:10.1029/2008JD 010572

Gadgil S, Srinivasan J, Nanjundiah RS, Kumar KK, Munot AA, Kumar KR (2002) On forecasting the Indian summer monsoon: the intriguing season of 2002. Curr Sci 4:394–403

Giorgi F, Marinucci MR, Bates GT (1993a) Development of a second generation regional climate model (RegCM2). Part I: boundary-layer and radiative transfer processes. Mon Wea Rev 121: 2794–2813

Giorgi F, Marinucci MR, Bates GT, De Canio G (1993b) Development of a second-generation regional climate model (RegCM2). Part II: convective processes and assimilation of lateral boundary conditions. Mon Wea Rev 121:2814–2832

Grell GA, Dudhia J, Stauffer D (1994) A description of the fifth-generation Penn-State/NCAR mesoscale model. NCAR technical report note TN-398, National Center for Atmospheric Research, Boulder, Colorado, USA

Ji Y, Vernekar AD (1997) Simulation of the Asian summer monsoons of 1987 and 1988 with a regional model nested in a global GCM. J Clim 10:1965–1979

Kalsi SR, Hatwar HR, Subramanian SK, Rajeevan M, Jayanthi N, Shyamala B, Jenamani RK (2004) IMD Monograph, Synop Meteorol No. 2/2004, pp 105

Rajeevan M, Pai DS, Dikshi SK, Kelkar RR (2004) IMD's new operational models for long-range forecast of southwest monsoon rainfall over India and their verification for 2003. Curr Sci 86(No.3):422–31

Rajeevan M, Bhate J, Kale JD, Lal B (2005) Development of a high resolution daily gridded rainfall data for the Indian region. IMD Met Monogr, Climatol No. 22/2005, pp 27

Rajeevan M, Jyoti B, Kale JD, Lal B (2006) Development of a high resolution daily gridded rainfall data for the Indian region: analysis of break and active monsoon spells. Curr Sci 91(3):296–306

Shekhar MS, Dash SK (2005) Effect of Tibetan spring snow on the Indian summer monsoon circulation and associated rainfall. Curr Sci 88(No. 11):1840–1844

Shepard D (1968) A two-dimensional interpolation function for irregularly spaced data, Proc. 23 ACM Nat'l Conf., Princeton, NJ, Brandon/Systems Press, 517–524

Singh GP, Jai-Ho Oh, Jin-Young K, Ok-Yeon K (2006) Sensitivity of summer monsoon precipitation over east Asia to convective parameterization schemes in RegCM3. SOLA 2:29–32

# Chapter 3
# Simulation of Heavy Rainfall in Association with Extreme Weather Events: Impact on Agriculture

**U.C. Mohanty, S. Pattanayak, A.J. Litta, A. Routray, and O. Krishna Kishore**

**Abstract** The extreme weather systems like thunderstorms, tropical cyclones, heavy rainfall and monsoon depression evolve through different scales of processes. The genesis and development of weather events involve complex interaction mechanism of mesoscale convective organization embedded in large-scale circulation. The skill of prediction of rainfall associated with extreme weather events as well as its impact on agriculture has been demonstrated through the climatological concept and the numerical simulations with the WRF modeling systems.

## 3.1 Introduction

The tropical weather and climate systems are more dominated by physical forcing (complex land-air-ocean interaction processes) than the dynamical forcing unlike in the mid-latitude, and hence weather prediction in tropics is more challenging task for the meteorological community. Although there have been significant improvements in numerical weather prediction (NWP) in last three decades, the prediction of extreme weather events is still a difficult and challenging task for the operational forecasters, particularly in the developing nations. Convective activity is one of the major processes in the atmosphere influencing the local and large-scale weather in the tropics. The Southeast Asia is mainly dominated by the summer monsoon and the tropical ocean regions act as main reservoirs of heat and moisture in supplying the necessary energy to the establishment and maintenance of the large scale circulation and associated monsoon activity over Indian subcontinent. A late

U.C. Mohanty (✉) • S. Pattanayak • A.J. Litta • A. Routray • O. Krishna Kishore
Centre for Atmospheric Sciences, Indian Institute of Technology, Delhi, Hauz Khas, New Delhi 110016, India
e-mail: mohanty@cas.iitd.ernet.in; sujata05@gmail.com; ajlitta@gmail.com; ashishroutray.iitd@gmail.com; osurikishore@gmail.com

S.D. Attri et al. (eds.), *Challenges and Opportunities in Agrometeorology*,
DOI 10.1007/978-3-642-19360-6_3, 

or early onset of the monsoon or an untimely break period in the monsoon may have devastating effects on agriculture even if the mean seasonal rainfall is normal. At the same time, meso-convective activity embedded with large-scale/synoptic circulations lead to extreme weather events like intense tropical cyclones (TCs), severe thunderstorms (STSs), and monsoon depressions (MDs) etc. have time and again contributed a large amount of precipitation in terms of rain, snow or hail which has a very hazardous impact on Indian agriculture.

Weather forecasting is important for each and every agricultural operation. The forecast of the sowing rains is one event for which the weather forecaster provides a critical input for the agriculture. At other stages of crop growth a combination of weather elements like rain, temperature, cloudiness, humidity, solar radiation, wind, evaporation and soil moisture become crucial for good crop production. Strong winds, heavy and torrential rains and the worst of all the storm surges are the most devastated elements of tropical cyclones, causing a lot of damage in the coastal region. Also, the agriculture of low laying delta regions are worst affected by costal inundation and intrusion of saline water due to storm surges. At the same time, farmers use various techniques for the mitigation of dry season e.g. changing sowing dates, using different types of seeds, storage of water, multiple cropping, relay cropping and intercropping etc. Hail is one of the most shocking natural perils for farmers. Hail occurs overnight whereas other perils like drought give farmer's time to agonize and cope. Although there are numerous hail factors influencing crop damage (kinetic energy, number of hailstones of relatively large diameter, momentum, mass, mean diameter), damage appears to best correlated with maximum hailstone size. Timely and reasonably accurate weather/climate forecast of these high impact weather events can significantly reduce the loss of lives, damage to properties and an awareness of the events to the general public as well as the planners for scheduling their action to a great extent. Hence, as far as the model forecast is concerned, high-resolution non-hydrostatic mesoscale models are expected to provide possibly the best forecast.

A brief description of the modeling system used in this study is given in Sect. 3.2. The simulation of severe thunderstorms is presented in Sect. 3.3. The simulations of intense tropical cyclones are provided in Sect. 3.4. Section 3.5 deals with the simulation of heavy rainfall and monsoon depression and the conclusions in Sect. 3.6.

## 3.2 Modeling System

The Weather Research and Forecasting (WRF) Model is a next-generation mesoscale forecast model that will be used to advance the understanding and the prediction of mesoscale convective systems. It features multiple dynamical cores, a 3-dimensional variational (3DVAR) data assimilation system, and a software architecture allowing for computational parallelism and system extensibility. The WRF model will be used for a wide range of applications, from idealized research

to operational forecasting, across scales ranging from meters to thousands of kilometers. WRF can resolve the small-scale weather features such as front, localized convection, hurricane core, and topographic effect much better than the global model.

The Weather Research and Forecasting (WRF) model contains two dynamic cores: the Non-hydrostatic Mesoscale Model (NMM – Janjic 2003) core, developed at the National Centers for Environmental Prediction (NCEP) and the Advanced Research WRF (ARW – Skamarock et al. 2005) core, developed at the National Center for

Atmospheric Research (NCAR). NMM runs are initialized through the same basic mechanism as the ARW runs: the WRF preprocessing system (WPS) reads GRIB data from an initializing model and interpolates it onto the target WRF domain grid. However, the functionality of the WPS had to be expanded to handle the horizontal staggering, map projection, and vertical coordinate used by the NMM, as each is distinct from its ARW counterpart. The NMM is a fully compressible, non-hydrostatic mesoscale model with a hydrostatic option. The model uses a terrain following hybrid sigma-pressure vertical coordinate. NMM model surfaces are terrain-following sigma surfaces near the ground, purely isobaric above a prescribed pressure value (typically about 420 hPa), and relax from terrain following to isobaric over the intervening depth. Further details of the vertical coordinate can be found in Janjic (2003). While ARW model's vertical coordinate is a terrain-following hydrostatic pressure coordinate.

NMM model uses a forward-backward scheme for horizontally propagating fast waves, implicit scheme for vertically propagating sound waves, Adams-Bashforth scheme for horizontal advection, and Crank-Nicholson scheme for vertical advection. The same time step is used for all terms. The dynamics conserve a number of first and second order quantities including energy and entropy (Janjic 1984), while ARW model uses higher order numerics. This includes the Runge-Kutta second and third order time integration schemes, and second to sixth order advection schemes in both horizontal and vertical directions. It uses a time-split small step for acoustic and gravity-wave modes. The dynamics conserves scalar variables. Both models support a variety of capabilities, which include real-data simulations, full physics options, non-hydrostatic and hydrostatic (runtime option), one-way static nesting and applications ranging from meters to thousands of kilometers. Table 3.1 gives a brief illustration of the two WRF dynamic systems.

Along with WRF, a three dimensional variational data assimilation system was developed based on fifth generation Mesoscale Model (MM5) 3DVAR system (Barker et al. 2004). The analysis system must be able to properly resolve all variables and scales of importance of the assimilation system. This formidable problem will be addressed incrementally by analyzing scales and variables, which we currently know how to do and developing techniques to perform the analysis at smaller scales and with additional analysis variables. 3DVAR analysis scheme is capable of analyzing most standard meteorological data, and more recently included a number of non-traditional data types (e.g. SSM/I radiances and radar radial velocity). The WRF assimilation research will strive to develop the "forward

**Table 3.1** A brief illustration of the two WRF dynamic systems

| ARW | NMM |
|---|---|
| Terrain following sigma vertical coordinate | Hybrid sigma to pressure vertical coordinate |
| Arakawa C-grid | Arakawa E-grid |
| Third order Runge-Kutta time-split differencing | Adams-Bashforth time differencing with time splitting |
| Conserves mass, entropy and scalars using up to sixth order spatial differencing equation for fluxes (fifth order upwind diff. is default) | Conserves kinetic energy, enstrophy and momentum using Second order differencing equation |
| NCAR physics package | Eta/NAM physics |
| Noah unified land-surface model | Noah unified land-surface model |

**Table 3.2** Model configuration of different convective activity

| | Thunderstorm | Tropical cyclone | Heavy rainfall/monsoon depression |
|---|---|---|---|
| Radiation parameterization | GFDL/GFDL | GFDL/GFDL | Rrtm/dudhia |
| Surface layer parameterization | Janjic similarity scheme | NCEP GFS scheme | Janjic similarity scheme |
| Land surface parameterization | NMM Land surface scheme | NMM Land surface scheme | Noah land surface scheme |
| Cumulus parameterization | Grell-Devenyi ensemble scheme | Simplified –Arakawa-Schubert | Grell-Devenyi ensemble scheme |
| PBL parameterization | Mellor-Yamada-Janjic | YSU | YSU |
| Microphysics | Ferrier scheme | Ferrier scheme | Ferrier scheme |

models" (and their adjoints) by which the WRF model fields can be transformed and interpolated to the observation locations and values for each of these data, and for these operators to be portable to alternative assimilation algorithms (e.g. alternative 3DVAR systems, 4DVAR, ensemble-based DA, etc.).

Initial and boundary conditions for all the following cases are derived from 6-hourly global final analysis (FNL) at 1.00 × 1.00 grids generated by National Center for Environmental Prediction (NCEP)'s global forecast system (GFS). Table 3.2 briefly describes the model configuration of different convective activities.

## 3.3 Simulation of Severe Thunderstorm

Thunderstorm is a mesoscale system of space scale a few kilometers to a couple of 100 km and time scale of less than an hour to several hours. Severe thunderstorms form and move from northwest to southeast over the Eastern and Northeastern

states of India (i.e., Gangetic West Bengal, Jharkhand, Orissa, Assam and parts of Bihar) during the pre-monsoon season (April–May). They are locally called "Kal-baishakhi" or "Nor'westers". Strong heating of landmass during mid-day initiates convection over Chhotanagpur Plateau, which moves southeast and gets intensified by mixing with warm moist air mass from head Bay of Bengal (BoB). It produces heavy rain showers, lightning, thunder, hail-storms, dust-storms, surface wind squalls, down-bursts and tornadoes. The northwest India gets convective dust-storms called locally Andhi in this season. These severe thunderstorms associated with thunder, squall lines, lightning, torrential rain and hail cause extensive loss in agriculture, damage to property and also loss of life.

The casualties reported due to lightning associated with thunderstorms in this region are the highest in the world. The strong wind produced by the thunderstorm is a real threat to aviation. The highest numbers of aviation hazards are reported during occurrence of these thunderstorms. In India, 72% of tornadoes are associated with Nor'westers. India is among the countries in the world having large frequency of hail. Reviewing the annual reports of India Meteorological Department from 1982 to 1989, Nizamuddin (1993) finds that there were 228 hail days (about 29 per year) of moderate to severe intensity. Hail size comparable to mangoes, lemons and tennis balls has been observed. Eliot (1899) found that out of 597 hailstorms in India 153 yielded hailstones of diameter 3 cm or greater. These events killed 250 persons and caused extensive damage to winter wheat crops. These severe thunderstorms have significant socio-economic impact in the eastern and northeastern parts of the country. An accurate location specific and timely prediction is required to avoid loss of lives and property due to strong winds and heavy precipitation associated with these sever weather system.

One of the main difficult tasks in weather prediction is the thunderstorm forecasting mainly because of its rather small temporal spatial extension and the inherent non-linearity of their dynamics and physics (Orlanski 1975). Accurate simulation requires knowledge about "where" and "when" storms will develop and how they will evolve. The high resolution non-hydrostatic mesoscale models with sophisticated parameterization schemes for the important physical processes would be very useful tool for reasonably accurate prediction of these severe thunderstorms (Weiss et al. 2007). Several studies related to the simulation of severe thunderstorm events using WRF-NMM model have been performed (Kain et al. 2006; Litta and Mohanty 2008; Litta et al. 2009). In the present study, an attempt is made to simulate a severe thunderstorm event that occurred over Kolkata (22.65° N, 88.45° E) on 21 May 2007, using WRF-NMM model and validated the model results with observational data.

The occurrence of pre and post monsoon thunderstorms over Indian continent is a special feature. Thunderstorms are associated with heavy rainfall during short duration of 2–3 h. It is useful for vegetations when it is in hot summer season. A severe thunderstorm occurred over Kolkata on 21 May 2007 at 1100 UTC is taken here for the present study. A squall line was reported over MO Kolkata at 1100 UTC from northwesterly direction with maximum wind speed of 19 $ms^{-1}$ and lasted for 1 min. This intense convective event produced 20 mm rainfall over

Kolkata. For this event, synoptic chart analysis shows low-level cyclonic circulation lies over Jharkhand/Gangetic West Bengal (GWB) and extended up to mid tropospheric levels. Coastal winds of Orissa/GWB are westerly to southeasterly. Good moisture incursion over East and North-East states was noticed (Mohanty et al. 2007). In the present simulation study, the model was integrated for a period of 24 h, starting from 21 May 2007 at 0000 UTC as initial values. A single domain with 3-km horizontal spatial resolution was configured.

Kolkata DWR composite radar reflectivity pictures on 21 May 2007 from 0800 to 1100 UTC is shown in Fig. 3.1. By analyzing DWR pictures, scattered echoes are developed near Dumka at 0800 UTC and moving south eastwards at 0900 UTC. This echo is intensified into a squall line (30 km north of Kolkata) at 1000 UTC. This squall line moved further in southeast direction. NMM model simulated composite radar reflectivity on 21 May 2007 from 0800 UTC to 1100 UTC is shown in Fig. 3.2. By analyzing NMM model simulated composite radar reflectivity pictures, scattered echoes developed north-west of Kolkata at 0800 UTC. This echo was moving south eastwards at 0900 UTC and intensified at 1000 UTC. This echo moved further in southeast direction. The model well simulated this squall line

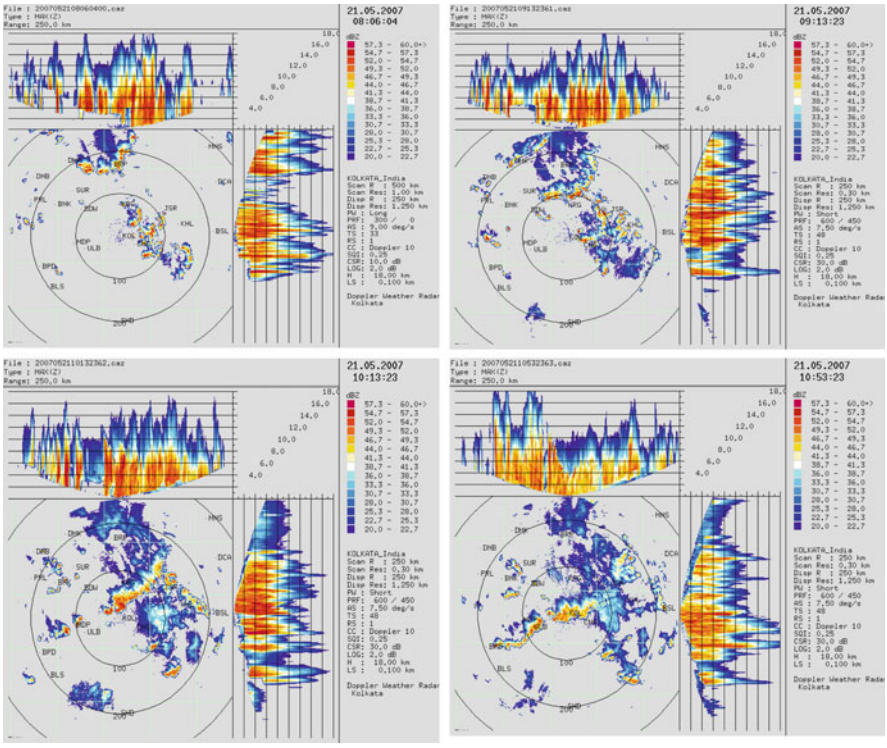


**Fig. 3.1** Kolkata DWR composite radar reflectivity pictures from 0800 to 1100 UTC on 21 May 2007

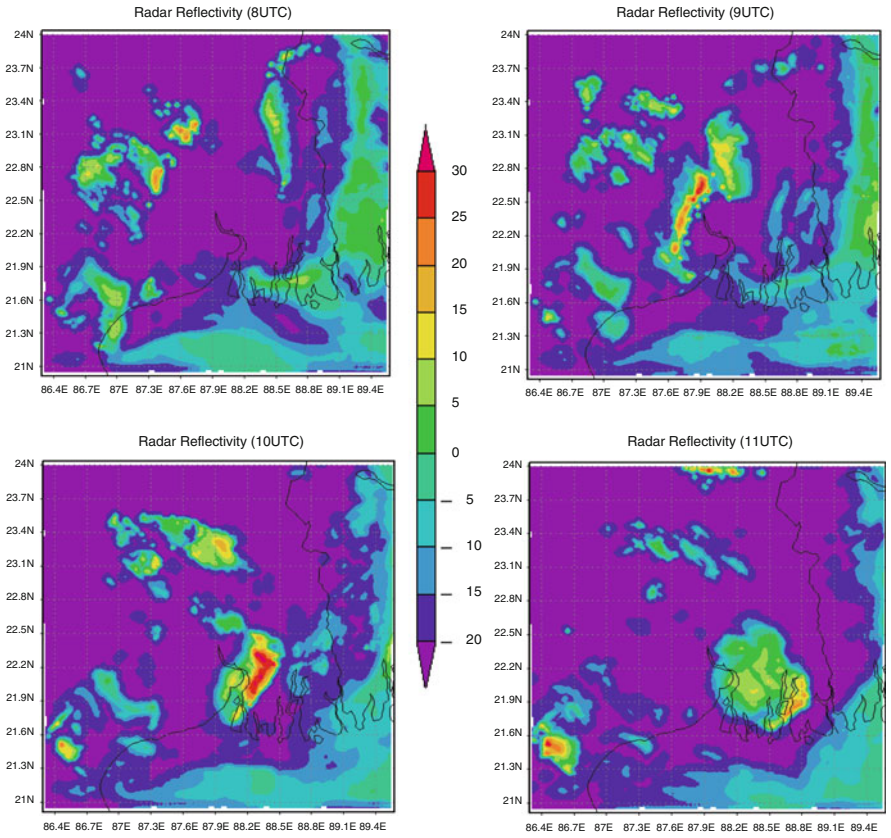


**Fig. 3.2** WRF-NMM simulated composite radar reflectivity pictures from 0800 to 1100 UTC on 21 May 2007

movement with simulated composite radar reflectivity fields. Variation of convection in the atmosphere depends upon dynamics as well as thermodynamic instability indices. A number of stability indices are devised in order to detect the likely occurrence of thunderstorms. The NMM model simulated skew-t plot and corresponding stability indices of Kolkata (22.65° N, 88.45° E) at 1100 UTC on 21 May 2007 is illustrated in Fig. 3.3. The skew-t plot shows that the atmosphere was convectively unstable at 1100 UTC. The NMM model simulated CAPE value (2314 $Jkg^{-1}$) is high and is a favorable condition for severe thunderstorms. The model simulated TT index at 1100 UTC is showing a very high value (46). Examination of all the model simulated stability indices clearly indicated that NMM model has well captured the instability of the atmosphere at 1100 UTC for the occurrence of a severe thunderstorm.

Figure 3.4a shows the inter-comparison of observed (AWS) and NMM model simulated diurnal variation of surface temperature (°C) over Kolkata valid for

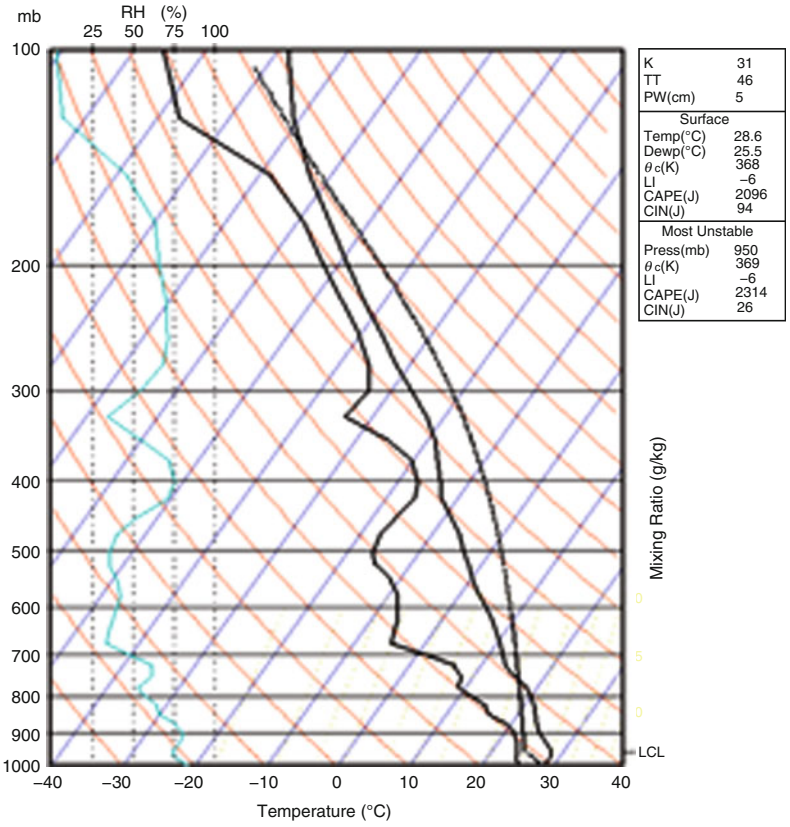


**Fig. 3.3** The NMM model simulated skew-t plot of Kolkata at 1100 UTC on 21 May 2007

21 May 2007 at 0000 UTC to 22 May 2007 at 0000 UTC. From the figure, we can clearly see that model captured the variation with drop in temperature at 1000 UTC, 1 h before the observed. Observed temperature showed a sudden drop from 30°C to 24°C at 1100 UTC whereas the model simulation shows a drop from 33°C to 27°C at 1000 UTC. Figure 3.4b shows the inter-comparison of observed and NMM model simulated accumulated progressive rainfall at Kolkata valid for 21 May 2007 at 0000 UTC to 22 May 2007 at 0000 UTC. Model has able to capture 18.5 mm of rainfall at 1000 UTC, which is close to the actual observation (20.0 mm). Model has predicted the rainfall at 1000 UTC, which is 1 h prior to the actual thunderstorm occurrence (1100 UTC). Relative humidity at surface level has also been taken into account, as it is an essential factor in intense convection. Model has captured (Fig. 3.4c) the rising of relative humidity values during the model simulated thunderstorm hour as in the observation. The observed relative humidity values peaked from 69% to 97% at 1100 UTC whereas model showed a sharp rise from around 56% to 86% at 1000 UTC, which is 1 h prior to the observed.

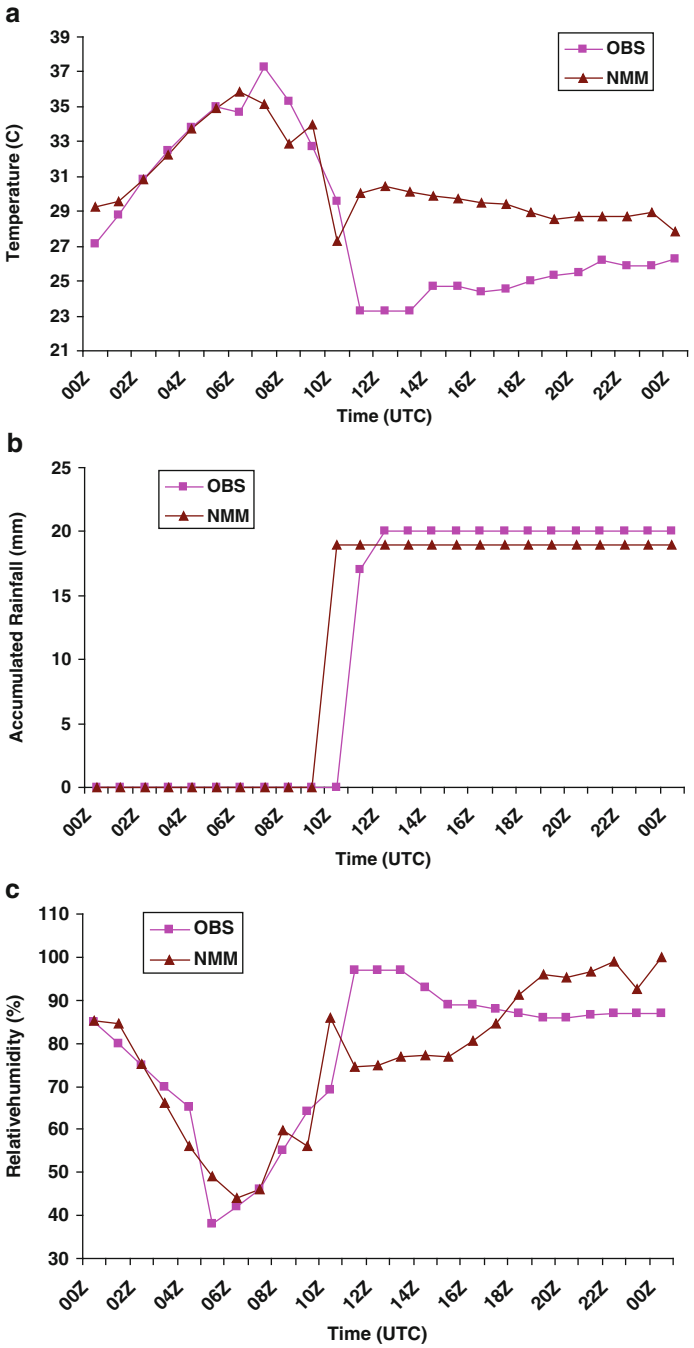


**Fig. 3.4** (**a–c**) The inter-comparison of observed and WRF-NMM model simulated diurnal variation of (**a**) temperature (°C) (**b**) accumulated rainfall (mm) (**c**) relative humidity (%) over Kolkata valid for 21 May 2007 at 0000 UTC to 22 May 2007 at 0000 UTC

## 3.4 Simulation of Tropical Cyclones

Tropical cyclones are among nature's most violent manifestations and potentially a deadly meteorological phenomenon. These are large low-pressure storms that form over the tropical oceans of the Earth's low latitudes, typically between 30°N and 30°S. The Bay of Bengal is a potentially energetic region for the development of cyclonic storms and about 7% of the global annual tropical storms forms over this region. Moreover, the Bay of Bengal storms are exceptionally devastating, especially when they cross the land (Pattanayak and Mohanty 2008). Thus the Bay of Bengal tropical cyclone is the deadliest natural hazard in the Indian sub-continent. It has significant socio-economic impact on countries bordering the Bay of Bengal, especially India, Bangladesh and Myanmar. At the same time, Arabian Sea contributes 2% of the global annual tropical storms. Therefore, reasonably accurate prediction of these storms is important to avoid the loss of lives. The trend of the tropical cyclones is increasing from 1905 to recent years and there has been a net 0.8°C increase in SST during this period. Also there is a drastic increase in the TC trend from 1995 onwards (Holland and Webster 2007). Bell and Chelliah (2006) provide a detailed summary of natural variability for long period tropical cyclones.

Tropical cyclones cause variety of damages. The major causes of damage are strong wind, storm surge and heavy precipitation. Strong wind can cause damage to tall structures, crops, power supply and communication systems. It also causes loss of life and generates devastating storm surges. Storm surge causes coastal flooding, damages to property, loss of life and intrusion of saline water in coastal areas. Intrusion of saline water in turn causes loss of soil fertility in coastal areas. While effects of strong wind and storm surge are concentrated within few tens of kilometers from the coastline, heavy rainfall often affects hundreds of kilometers from the coast. Flooding due to heavy rainfall may occur even after the storm has lost its hurricane intensity. In general, heavy precipitation follows the storm and the magnitude of precipitation varies with the intensity of the storm. Heavy rainfall causes loss of life, destruction of vegetation, crops and livestock and contamination of water supply. Hence, there is a direct impact on agriculture with the severe land falling tropical cyclones. The loss of life and property due to tropical cyclone disaster can be significantly reduced by reasonably accurate forecast of the storm and associated surge. In the present study, an attempt is made to simulate severe tropical cyclones that occurred over Bay of Bengal (Case I: Mala) and Arabian Sea (Case II: Gonu), using WRF-NMM model and validated the model results with observational data.

### *3.4.1 Case-I*

The cyclone Mala has developed over the warm tropical ocean, near 9.5° N, 90.5° E, around 0300 UTC 25 April 2006 with the central mean sea level pressure of 996 hPa and the maximum sustainable wind of 25 kts. The system remained at that stage for

further 6 h i.e. up to 0900 UTC 25 April 2006. By 0900 UTC 25 April 2006, it was turned into deep depression stage. Then the system became cyclonic storm after 1200 UTC 25 April 2006. At 0000 UTC 26 April 2006, the clear-cut cyclonic storm with the center of the storm at 10.5° N and 89.0° E with the central pressure of 994 hPa and maximum surface wind of 45 kts was observed. The system remained in cyclonic stage up to 0000 UTC 27 April 2006. Then around 0300 UTC 27 April 2006, it became severe cyclonic storm with central pressure of 990 hPa and the maximum sustainable wind of 55 kts. The system became very severe cyclonic storm (VSCS) by 1200 UTC 27 April 2006 with the central mean sea level pressure of 984 hPa and the maximum surface wind of 65 kts. The storm remained in VSCS for a period of 42 h i.e. up to 0600 UTC 29 April 2006. The maximum observed central pressure was 954 hPa with the pressure drop of 52 hPa. The observed maximum sustainable surface wind was 100 kts. The very severe cyclonic storm crossed the Arakan coast at about 100 km south to Sandoway around 0700 UTC 29 April 2006. The system remained on the land for further 12 h and caused a lot of devastation in the underlying coastal areas.

Figure 3.5a, b represents the day-3 forecast of mean sea level pressure and wind at 850 hPa valid at 0000 UTC 29 April 2006. At the Day-3 forecast, model simulation shows that, the storm moved northeastward from (13.7° N/91.2° E) to (17.7° N/93.2° E) in last 24 h with a MSLP of 960 hPa which is nearly matching with that of the observation. The maximum observed MSLP was 954 hPa with the pressure drop of 52 hPa. The WRF-NMM model simulated the maximum MSLP of 960 hPa with the pressure drop of 45 hPa. Figure 3.6a, b represents the 24 h accumulated precipitation valid at 0300 UTC 29 April 2006. Figure 3.6a represents 24 h accumulated precipitation as a merged analysis of Tropical Rainfall Measuring Mission (TRMM), TMI and rain gauges observations carried out by National Aeronautics and Space Administration (NASA) valid for 0300 UTC 29 April

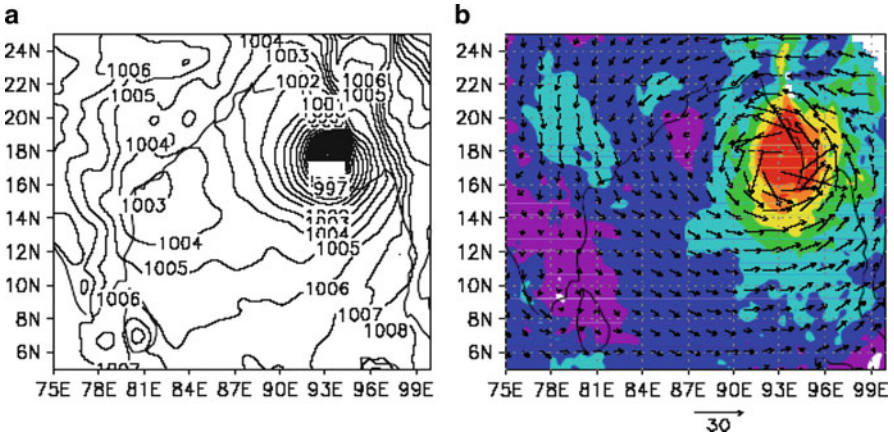


**Fig. 3.5** Simulation of mean sea level pressure & wind at 850 hPa for case-I (Mala) (**a**) MSLP for Day-3 and (**b**) wind for Day-3

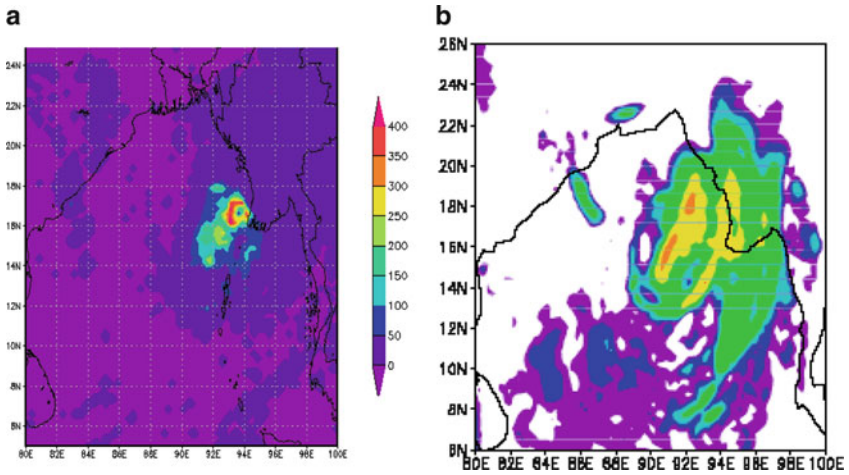


**Fig. 3.6** (**a** and **b**) 24 h accumulated precipitation valid at 0300 UTC 29 April 2006. (**a**) Observed from TRMM and (**b**) simulated with WRF-NMM (Day-3)

2006. Figure 3.6b represents the Day-3 forecast of accumulated precipitation valid at 0300 UTC 29 April 2006 from WRF-NMM. The observed precipitation is about 40 cm in Day-3 whereas the model could simulate the precipitation of 32 cm. The track of the cyclone as obtained with the model simulations from different initial conditions are evaluated and compared with the best-fit track obtained from India Meteorological Department (IMD). Figure 3.7 represents the track of the cyclone Mala as obtained with model simulations from different initial conditions. Results show that, in each case the cyclone moves to the Arakan coast, whatever the initial condition is being chosen. The vector displacement errors (VDEs) are also calculated at every 12 h interval and the detailed of the VDEs are provided in Table 3.3.

### *3.4.2 Case-II*

The tropical storm Gonu has developed as a depression over the east central Arabian Sea with center near lat 15.0° N, long 68.0° E at 1800 UTC 01 June 2007. It moved westwards and intensified into a cyclonic storm at 0900 UTC 02 June 2007 near lat 15.0° N, long 67.0° E. It remained in that stage for 15 h i.e. up to 0000 UTC 03 June 2007. By 0000 UTC 03 June 2007, it intensified into a severe cyclonic storm with the central pressure of 988 hPa and centered at lat 15.5° N, long 66.5° E and the storm remained in that stage for next 18 h i.e. up to 1500 UTC 03 June 2007. Continuing its northwestward movement, it further intensified into a very severe cyclonic storm by 1800 UTC 03 June 2007 and lay centered at lat 18.0° N, long 66.0° E with the central pressure of 980 hPa. It sustained in that stage for next 18 h i.e. up to 1500 UTC 04 June 2007. By 1500 UTC 04 June 2007, the system

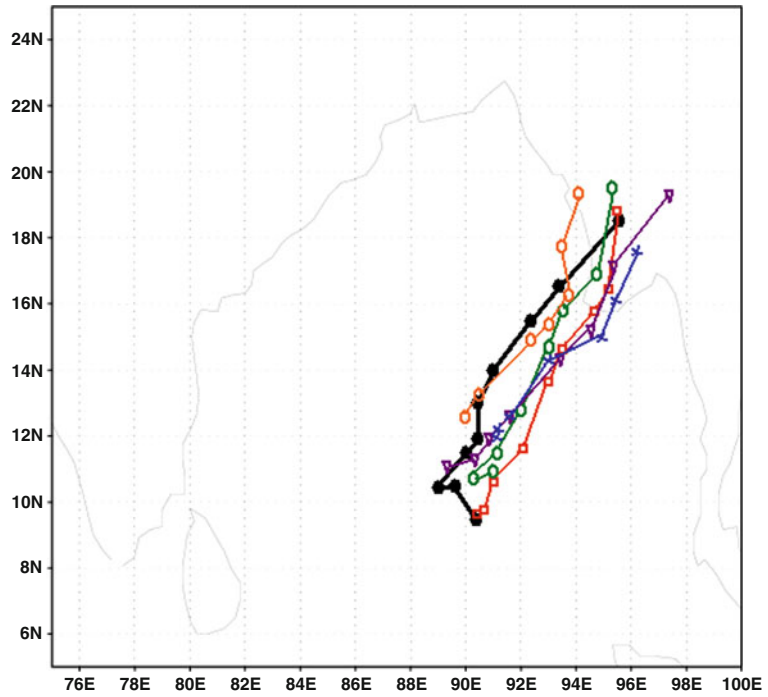


**Fig. 3.7** Track of the cyclone Mala

**Table 3.3** Vector displacement errors for case-I (Mala)

| Initial time of model integration | 00 h | 00 h | 12 h | 36 h | 48 h |
|---|---|---|---|---|---|
| Mala-1(2500) | 118.0 | 118.0 | 98.3 | 148.1 | 202.1 |
| Mala-2(2512) | 80.8 | 80.8 | 71.1 | 248.2 | 372.3 |
| Mala-3(2600) | 22.2 | 22.2 | 74.5 | 228.9 | 295.6 |
| Mala-4(2612) | 35.1 | 35.1 | 115.9 | 323.6 | 546.6 |
| Mala-5(2700) | 55.5 | 55.5 | 124.1 | 323.6 | 571.4 |
| Mean error | 62.3 | 62.3 | 96. 7 | 254.4 | 397.6 |

moved west-northwestwards and further intensified as a super cyclonic storm and lay centered at lat 20.0° N, long 64.0° E with the minimum central pressure of 920 hPa. It remained in the super cyclonic storm stage for the next 6 h i.e. up to 0000 UTC 05 June 2007. Then the storm further moved in northwestward direction and weakened into a very severe cyclonic storm by 2100 UTC 04 June 2007 and lay centered over northwest Arabian Sea at lat 20.5° N, long 63.5° E with the minimum central pressure of 935 hPa. The storm remained in that stage for the next 48 h i.e. up to 2100 UTC 06 June 2007. Then the storm gradually weakened, moved northwestward and crossed the Makran coast near lat 25.0° N, long 58.0° E between 0300 and 0400 UTC 07 June 2007 as a cyclonic storm.

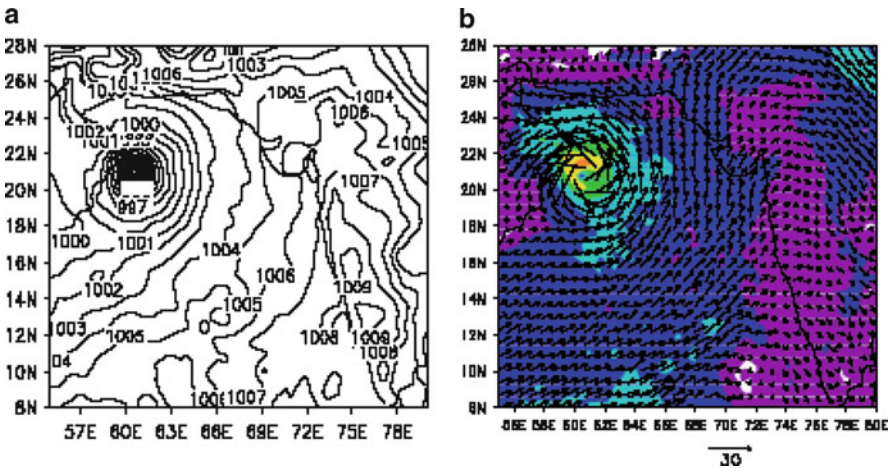


**Fig. 3.8** Simulation of mean sea level pressure & wind at 850 hPa for case-II (Gonu), (**a**) MSLP for Day-3 and (**b**) wind for Day-3

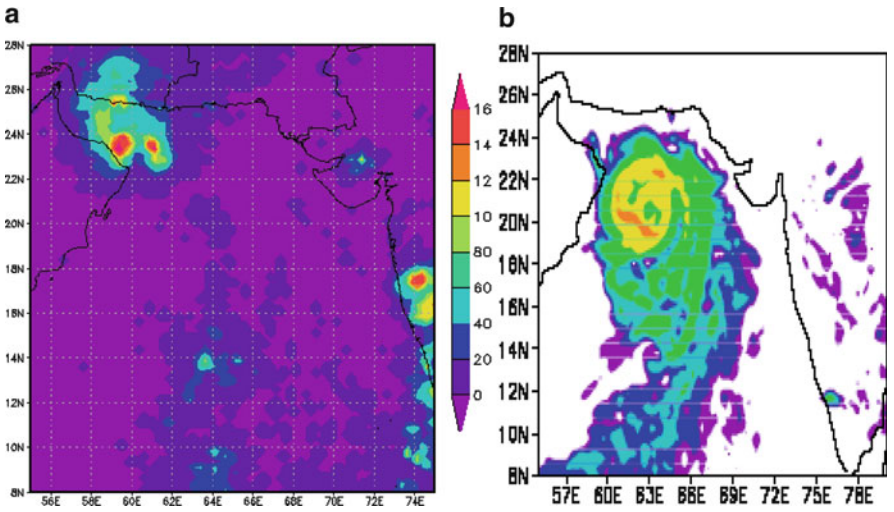


**Fig. 3.9** (**a** and **b**) 24 h accumulated precipitation valid at 0300 UTC 06 June 2007. (**a**) Observed from TRMM and (**b**) simulated with WRF-NMM (Day-3)

Figure 3.8a, b represents the day-3 forecast of mean sea level pressure and wind at 850 hPa valid at 0000 UTC 06 June 2007. The model simulation shows that the storm moved northwestward with the minimum central pressure of 981 hPa. The observed central pressure at that time was 970 hPa. The observed maximum sustained surface wind at that time was 77 kts, whereas the model could simulate the maximum wind of 66 kts. Figure 3.9 represents the 24 h accumulated

precipitation valid at 0300 UTC of 06 June 2007. Figure 3.9a represents 24 h TRMM accumulated precipitation valid at 0300 UTC of 06 June 2007. Figure 3.9b represents the Day-3 forecast of accumulated precipitation valid at 0300 UTC 06 June 2007 from WRF-NMM. The observed precipitation is about 16 cm in Day-3 whereas the model could simulate the precipitation of 14 cm. The track of the cyclone as obtained with both the model simulations from different initial conditions are evaluated and compared with the best-fit track obtained from IMD. Figure 3.10 represents the track of the cyclone Gonu as obtained with model simulations from different initial conditions. The vector displacement errors (VDEs) are also calculated at every 12 h interval and the detailed of the VDEs are provided in Table 3.4.

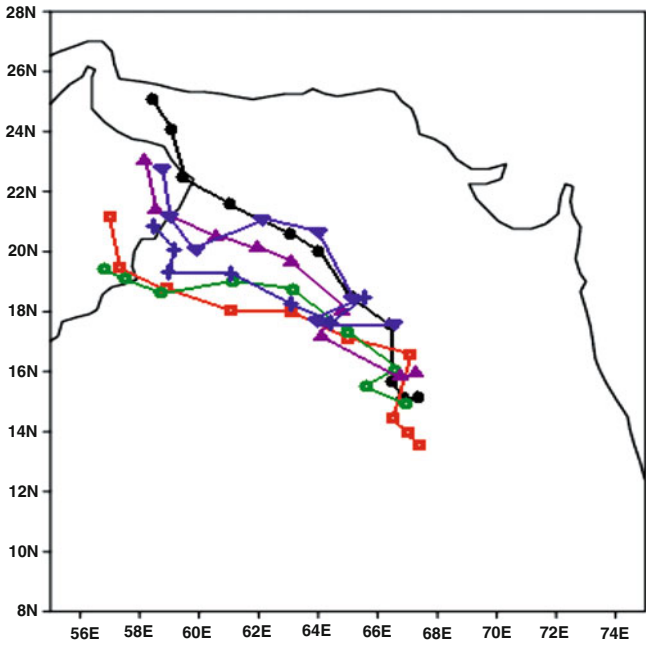


**Fig. 3.10** Track of the cyclone Gonu

**Table 3.4** Vector displacement errors for case-II (Gonu)

| Initial time of model integration | 00 h | 12 h | 24 h | 36 h | 48 h |
|---|---|---|---|---|---|
| Gonu-1(0200) | 100.0 | 95.0 | 88.5 | 128.1 | 142.0 |
| Gonu-2(0212) | 60.8 | 70.0 | 88.3 | 124.2 | 272.3 |
| Gonu-3(0300) | 32.0 | 65.4 | 140.7 | 188.0 | 225.0 |
| Gonu-4(0312) | 59.1 | 102.3 | 168.0 | 202.4 | 325.4 |
| Gonu-5(0400) | 50.1 | 84.1 | 125.1 | 223.6 | 371.0 |
| Mean error | 60.4 | 83.36 | 122.12 | 173.26 | 267.14 |

## 3.5 Simulation of Heavy Rainfall Events

South west (SW) monsoon is the main feature in the climate of India as well as the principal denominator of the prosperity of the country and the agro-economy. Most of the country as a whole receives 70% of the total annual rainfall except southern parts of peninsula, especially Tamil Nadu (Parthasarathy 1984) during this SW monsoon season. Hence, it is not only nourishes the kharif crops but enriches all sources of irrigation to enable cultivation of a wide variety of crops during rabi and pre-kharif season. As a result all sections of people starting from a farmer to the scientist and from a common man to the policy makers at the highest level are keen to know detail about the variation of weather of the season, its causes and effects especially on agriculture. Vulnerability and agricultural sustainability are primarily local issues, and depend critically on the amount and temporal distribution of rainfall received over a region.

Heavy rainfall pose a serious threat to many sectors particularly, agricultural sector. According Dash et al. (2009), the frequencies of moderate and low rain days considered over the entire country have significantly decreased in the last half century. On the basis of the duration of rain events it is inferred that long spells show a significant decreasing trend over India as a whole while short and dry spells indicate an increasing tendency with 5% significance. Field flooding during the plant growing season causes crop losses due to low oxygen levels in the soil, increased susceptibility to root diseases, and increased soil compaction due to the use of heavy farm equipment on wet soils. If the flood hit just as farmers start to harvest the crops, the losses to be very large. The flooding severely erodes upland soils where erosion puts some farmers out of business. The flooding also causes an increase in runoff and leaching of agricultural chemicals into surface water and groundwater. Another impact of heavy rainfall is that wet conditions at harvest time result in reduced quality of many crops. Vegetable and fruit crops are sensitive to even short-term, minor stresses, and as such are particularly vulnerable to weather extremes. Therefore, an accurate estimate of frequency, intensity and distribution of these events can significantly aid policy planning.

Over the Indian monsoon region in particular, the better simulation of weather events like heavy rainfall and monsoon depressions are important and routinely have resulted in flooding and significant loss to agriculture, life and property during the Indian monsoon. But the current mesoscale models have limited success in simulating these events over the region (Routray et al. 2005). The forecast performance of the mesoscale models critically depends on the quality of initial conditions (Pielke et al. 2006). Typically, large scale global analyses which provide the initial condition to the mesoscale models have limitations such as coarse resolution and inadequate representation of localized mesoscale features. Therefore, assimilation approaches like 3-dimensional variational data assimilation (3DVAR) that ingest local observations are important to develop improved analyses (Daley 1991) and hence the forecast. Vinod Kumar et al. (2007) adopted four dimensional data assimilation (FDDA) and surface data assimilation to study

tropical depressions over Bay of Bengal. The results suggested that improvement of monsoon depression simulations over Bay of Bengal were equivalent or better than that of increasing the model resolution from 30 to 10 km grid spacing. The main purpose of this study is to demonstrate the ability of the WRF-ARW mesoscale model in simulating the heavy rainfall events like Mumbai heavy rainfall (26–27 July 2005) and monsoon depressions (Case I: 2–4 August 2006 and Case II: 21–23 June 2007) with and without assimilation of Indian conventional and non-conventional observations using 3DVAR assimilation system.

### *3.5.1 Mumbai Heavy Rainfall*

This was a record-braking rain evnt, Santacruz received 94.4 cm within 24 h and the study by Jenamani et al. (2006) described details of the event. To simulate this localized and intense rainfall event, two numerical experiments with (3DV) and without (CNTL) data assimilation are carried out. For both the experiments, the model integrated 36 h from 0000 UTC of 26 July 2005 up to 1200 UTC of 27 July 2005. Figure 3.11 shows the temporal evolution of model and observed cumulative rainfall over Santacruz and Colaba IMD recording stations along 72.5° E. It is clearly observed that the record-breaking rainfall at Santacruz is significantly improved in the 3DV simulation (more than 78 cm) compared with the CNTL simulation (36 cm). In the same time, the 3DV experiment is also well simulated low rainfall amount over Colaba as compared to the CNTL simulation and trend is well match with the observations. Figure 3.12 shows the 24 h accumulated precipitation as obtained from CNTL and 3DV experiments and satellite estimates rainfall (TRMM) along with the IMD ground based rain gauge observations at and around Mumbai. The orientation and distribution of rainfall is well simulated in the 3DV

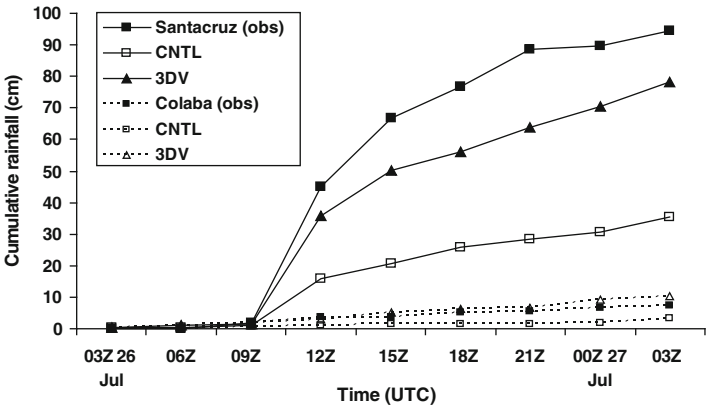


**Fig. 3.11** Observed and simulated 3-hourly interval cumulative rainfall (cm) over Santacruz and Colaba on 26–27 July 2005

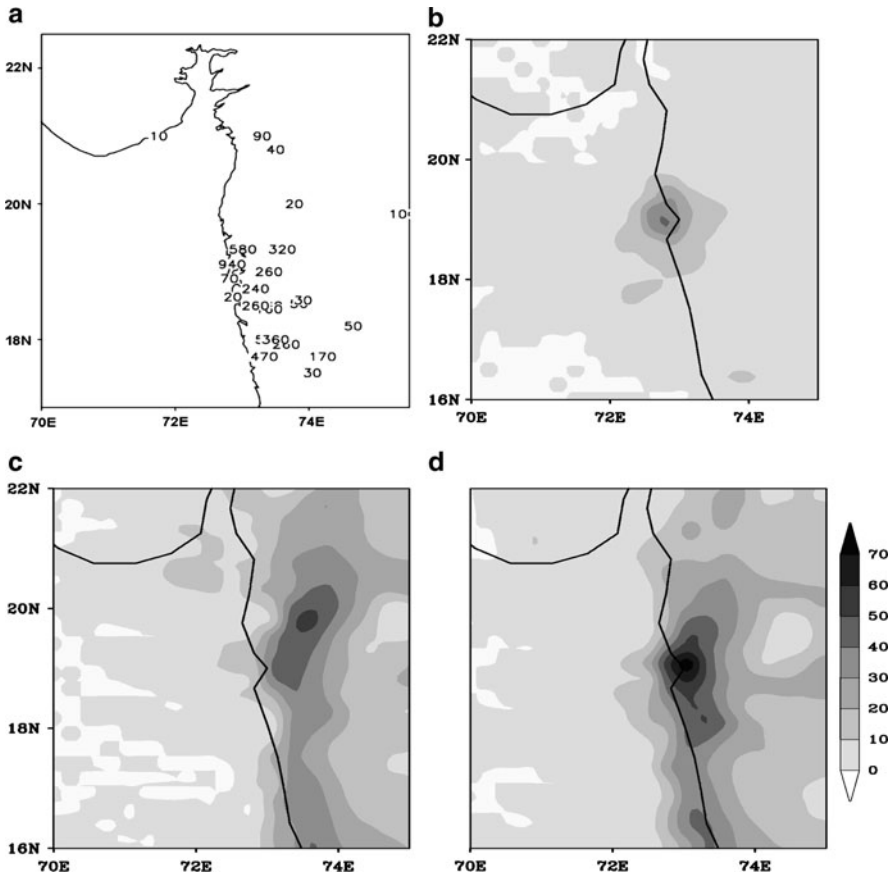


**Fig. 3.12** (**a**) IMD observed rainfall (mm) and 24 h accumulated rainfall (cm) for (**b**) TRMM (**c**) CNTL and (**d**) 3DV valid at 0300 UTC of 27 July 2005

experiment (Fig. 3.12d) and feature is very much match with the satellite estimated rainfall pattern (Fig. 3.12b). However, the CNTL experiment (Fig. 3.12c) shows the patch of maximum rain (50–60 cm) very much away from the observed location with a location error 120 km northeast of Santacruz, Mumbai. Further, we evaluate the model performance with 3DVAR based initial condition for the evolution of various meteorological parameters during this heavy rain event. Figure 3.13 shows the three hourly vertical cross sections (Time-pressure) of vorticity (Fig. 3.13a, b) and vertical velocity (Fig. 3.13c, d) obtained from CNTL and 3DV simulation starting from 0000 UTC 26 to 06 UTC 27 July 2005. Vertical cross section of vorticity obtained from 3DV simulation (Fig. 3.13b) exhibits structure of strong cyclonic vorticity (30–36 $\times$ $10^{-5}$ $s^{-1}$) at low and upper level. The feature is not noticed in the CNTL simulation (maximum vorticity is 21 $\times$ $10^{-5}$ $s^{-1}$ only at upper level). In the 3DV simulation, the positive vorticity increased gradually from developing stage to mature stage and then start decreasing after 1800 UTC.

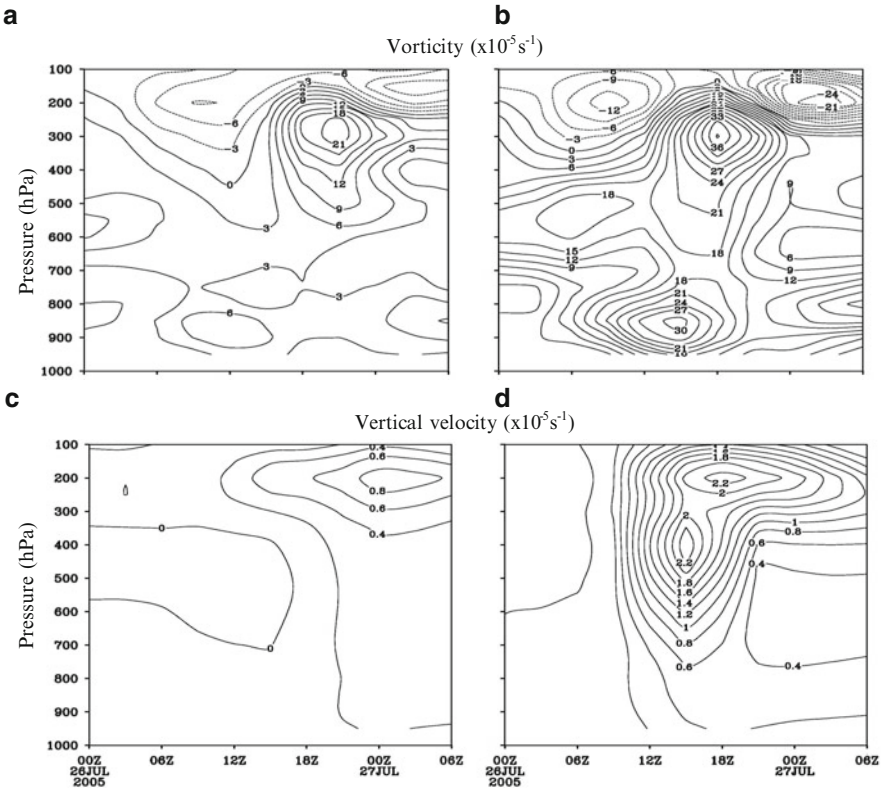


**Fig. 3.13** **(a–d)** Time-pressure cross section of vorticity ($10^{-5}$ $s^{-1}$) at Santacruz (19.11°N; 72.85°E) for (**a**) CNTL and (**b**) 3DV. Similarly, (**c** and **d**) are same as (**a** and **b**) but for vertical velocity (m/s)

The maximum cyclonic vorticity is found during the mature stage and extended up to upper atmosphere. This shows the gradual growth of the convective system which is well represented in the 3DV simulation. The strong negative vorticity (12–24 $\times$ $10^{-5}$ $s^{-1}$) at upper atmosphere around 200 hPa pressure level and above through out this period. The maximum upward velocity is 2.2 $ms^{-1}$ obtained from 3DV simulation (Fig. 3.13d) and found at mid-level (around 400 hPa) and upper atmosphere (around 200 hPa) during the mature stage (1200–1800 UTC). However, the maximum vertical velocity from CNTL simulation is 0.8 $ms^{-1}$ at upper atmosphere on 0000 UTC 27 July 2005. Similarly, the vertical cross section of divergence field (figures not provided) obtained from the 3DV simulation shows strong low-level convergence and upper-level divergence through out the period. The convergence is found from 0600 to 1800 UTC up to 600 hPa level with maximum value of 20 $\times$ $10^{-5}$ $s^{-1}$ at 1500 UTC. It can be inferred that the maximum convergence and vorticity precede and maximum vertical velocity follows the mature stage.

### 3.5.2 Monsoon Depressions

From the above case study, it is clear that the 3DVAR experiment improve the prediction of rainfall with the assimilation of conventional and non-conventional data. An attempt is also made here to study the impact of DWR data along with the GTS observation on the simulation of movement of monsoon depressions and associated heavy rainfall. In this purpose, three different numerical experiments are carried out such as CNTL (no assimilation), 3DV_GTS (only GTS observation) and 3DV_DWR (GTS and DWR). The model is integrated 54 h in all experiments from 0000 UTC of 2 August 2006 (case-1) and 21 June 2007 (case-2).

From Fig. 3.14, the 24 h accumulated rainfall for case-1 is well represented the intensity (150–250 mm) as well as spatial distribution i.e. maximum rainfall over the land and wide spread rainfall over oceanic region by the 3DV_DWR simulation (Fig. 3.14d). However, the TRMM (Fig. 3.14a) show maximum rainfall over oceanic regions. The Kalpana-1 satellite cloud image shows intense and wide spread convective clouds over the land as well as oceanic regions (figure not shown) which show good consensus with the rainfall simulated by the 3DV_DWR. Similarly, in case-2 (Fig. 3.14e–h), the spatial and temporal distribution of simulated rainfall from 3DV_DWR experiment (Fig. 3.14h) indicates that assimilation of DWR data resulted in a good simulation of rainfall during day-1. The CNTL experiment underestimates the rainfall (by 50–100 mm) over land. Another typical characteristic of the MD (Sikka and Gadgil 1980) is that heavier rainfalls are chiefly concentrated in the western and south western sectors of the depression and the 24 h rainfall generally ranges between 250 and 350 mm. These features are well resolved in the 3DV_DWR runs for both the cases. It is also noticed that the amount and spatial distribution of rainfall is improved in the 3DV_GTS simulations as compared to CNTL.

The spatial (Lat. 15°–25°N; Long. 75°–90°E) correlation co-efficient (CC) and RMSE of rainfall between TRMM and the model outputs are calculated over the land (mask out the ocean part) for day-1. The RMSE values are found less in 3DV_DWR simulation (30.35 in case-1 and 22.79 in case-2) as compared with the 3DV_GTS (34.85 in case-1 and 37.40 in case-2) and CNTL (40.46 in case-1 and 41.37 in case-2) simulations. Similarly, the CC is improved in the 3DV_DWR (0.74 in case-1 and 0.77 in case-2) as compared to 3DV_GTS (0.56 in case-1 and 0.51 in case-2) and CNTL (0.32 in case-1 and 0.20 in case-2) experiments. This study clearly depicts the capability of DWR radial velocity and reflectivity in the prediction of quantitative prediction of rainfall. Figure 3.15a, b represents the model simulated track of two MDs from all the experiments along with observed track. The mean vector displacement errors (VDEs) with 6-h interval are shown in Fig. 3.15c. It is observed that (Fig. 3.15c) the mean initial position error is least in the case of 3DV_DWR (60 km). It is well known that the reduction in initial position error causes better track prediction (Holland 1984). Therefore, the track of the systems is improved in 3DV_DWR experiment with least VDEs. However, the track of the MDs is also improved in the 3DV_GTS simulation as compared to CNTL simulated track. The 24-h (48 h) forecast errors (in kms) are 127 (93) in

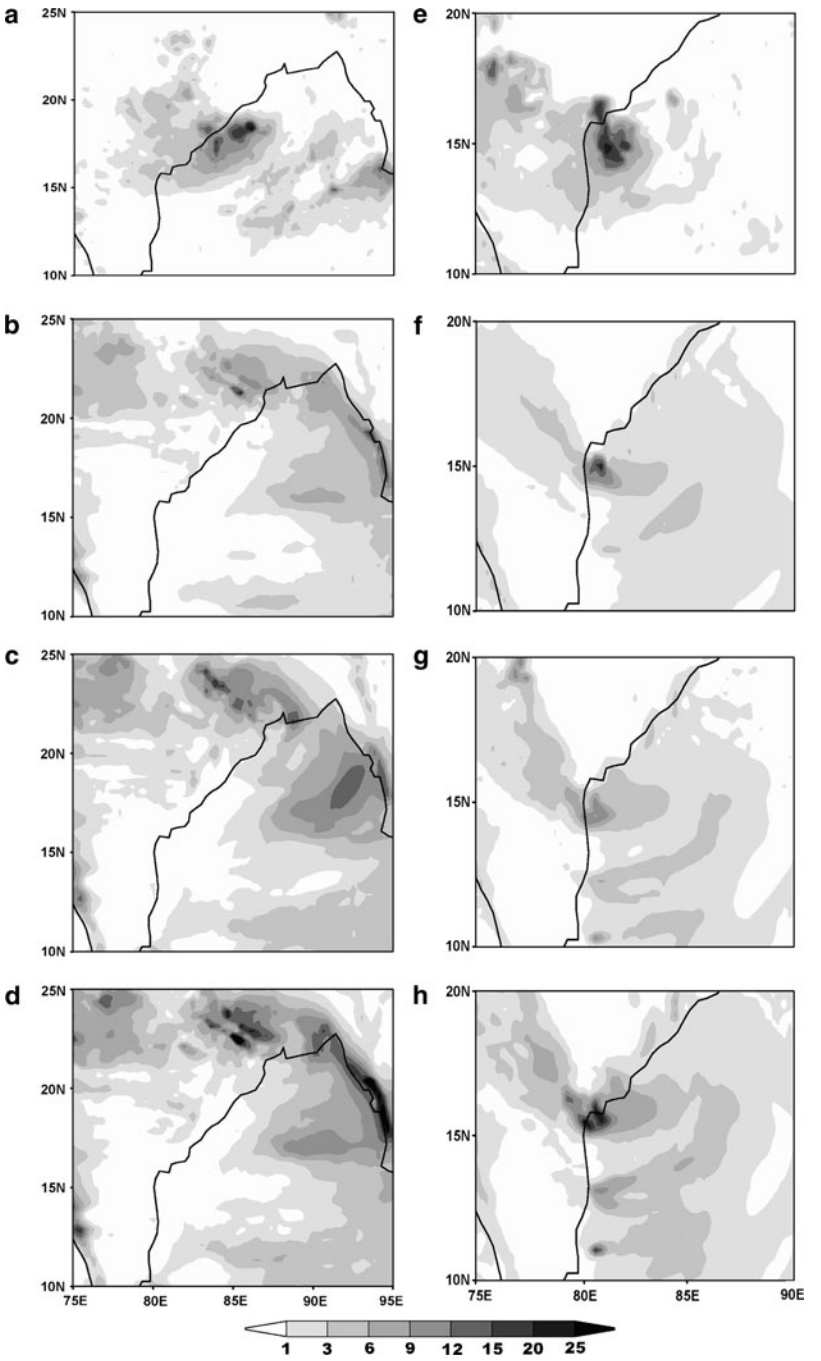


**Fig. 3.14 (a–h)** 24 h accumulated precipitation (cm) for day-1 (**a**) TRMM (**b**) CNTL (**c**) 3DV_GTS and (**d**) 3DV_DWR valid at 0300 UTC of 03 August 2006. Similarly, (**e–h**) are same as (**a–d**) respectively but for case-2 valid at 0300 UTC of 22 June 2007

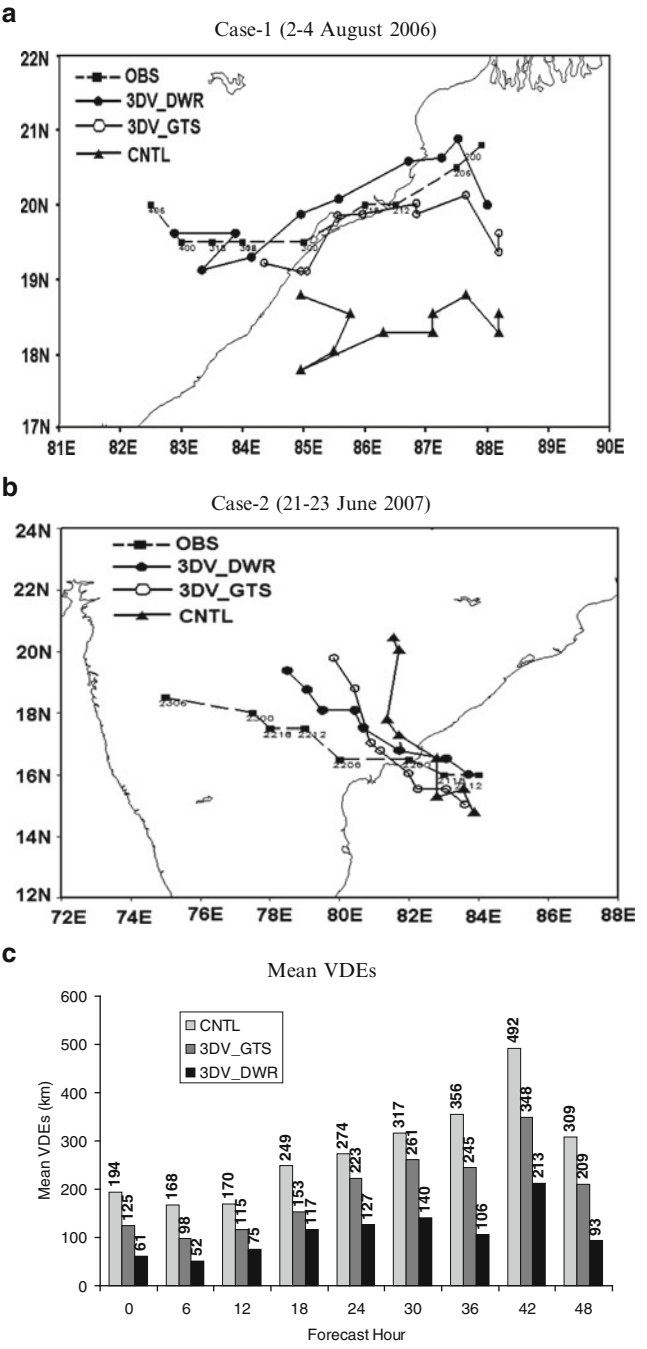


**Fig. 3.15** **(a–c)** Hourly track (observed and simulated) and VDEs from CNTL; 3DV_GTS and 3DV_DWR for (**a**) track for case-1 (**b**) same as (**a**) but for case-2 (**c**) mean VDEs for case-1 and case-2

3DV_DWR while for 3DV_GTS and CNTL the errors are 223 (209) and 274 (309) kms respectively. Overall results show that the forecast errors are reduced significantly in assimilation experiments particularly with DWR data as compared with the other experiments.

## 3.6 Conclusions

The model simulation studies of severe thunderstorm, tropical cyclone, heavy rainfall and monsoon depression lead to the following broad conclusions:

The WRF-NMM model simulated meteorological parameters such as relative humidity, rainfall and temperature are consistent with each other and all are in good agreement with the observation even though 1 h time lag exists. From the model simulated spatial plots of composite radar reflectivity, we can clearly see the squall line movement as in DWR images. The model simulated thermodynamic derivatives of stability indices are good enough with the values indicating a deeper layer around Kolkata favorable for intense convective activity. Thus the dynamic and thermo-dynamic properties of the atmosphere are well captured by WRF-NMM for the occurrence of a severe thunderstorm over Kolkata on 21 May 2007 at 1000 UTC, and agree reasonably well with the observations

The WRF-NMM model also could simulate most of the features of the cyclones Mala and Gonu with reasonable accuracy. The intensity of the tropical cyclones in terms of MSLP and maximum sustainable wind illustrates that the model underestimates the intensity of the storm. The pattern of distribution of precipitation is reasonably well predicted for both the cyclone cases. The track forecast with WRF-NMM is found to be reasonably accurate over this part of the world. The mean vector displacement error clearly demonstrates the forecast skill of the WRF-NMM in terms of track prediction. However, intensity of cyclone need further research for better performance.

The WRF-ARW model with improved initial condition is able to simulate with reasonably good accuracy the amount, intensity, timing and spatial distribution of this unusual rain event as compared to CNTL simulation. From the 3DV simulation, the analyses of the dynamical parameters at the location of heavy precipitation revealed that the maximum convergence and vorticity precede the mature stage, however the maximum vertical velocity follows it. The CNTL simulation failed to represent these types of features during the simulation period.

The northwestward movement and location of the depression are well represented in the assimilation experiments mainly in the 3DV_DWR and agree with the IMD observations. The model precipitation fields compared well with the TRMM rainfall estimates and the Kalpana-1 visible satellite convection imagery which also reflected in the statistical skill scores. The MDs track is also well simulated by the 3DV_DWR experiment, reasonably match with the IMD observed track. The VDEs are significantly improved in the assimilation experiments as compared to CNTL simulation, however, the values are found less in the DWR

assimilation experiment for both the cases. The intensity and structure of the MDs is thus better simulated with the DWR assimilation.

Overall, WRF modeling systems are able to broadly reproduce several features of these intense convective activities leading to extreme weather events and heavy rainfall in tropics. However, more realistic initial conditions with advanced data assimilation techniques of observational data from various platforms is required for the better prediction of these extreme weather events with state-of-the-art mesoscale models.

## References

Barker DM, Huang W, Guo YR, Xiao Q (2004) A three-dimensional variational (3DVAR) data assimilation system for use with MM5: implementation and initial results. Mon Weather Rev 132:897–914

Bell GD, Chelliah M (2006) Leading tropical modes associated with interannual and multidecadal fluctuations in north Atlantic hurricane activity. J Climate 19:590–612

Daley Roger (1991) Atmospheric data analysis, Cambridge atmospheric and space science series. Cambridge University Press, Cambridge, p 457

Dash SK, Kulkarni MA, Mohanty UC, Prasad K (2009) Changes in the characteristics of rain events in India. J Geophys Res 114:12

Eliot J (1899) Hailstorm in India during the period 1883–1897 with a discussion on their distribution. I Met Mem 6:4

Holland GJ (1984) Tropical cyclones in the Australian/Southwest Pacific region. II: Hurricane. Aust Meteor Mag 32:17–33

Holland GJ, Webster PJ (2007) Heightened tropical cyclone activity in the North Atlantic: natural variability or climate trend? Philos Trans R Soc A 365:2605–2716

Janjic ZI (1984) Non–linear advection schemes and energy cascade on semi–staggered grids. Mon Weather Rev 112:1234–1245

Janjic ZI (2003) A nonhydrostatic model based on a new approach. Meteorol Atmos Phys 82:271–285

Jenamani R, Bhan SC, Kalsi SR (2006) Observational/forecasting aspects of the meteorological event that caused a record highest rainfall in Mumbai. Curr Sci 90:1344–1362

Kain JS, Weiss SJ, Levit JJ, Baldwin ME, Bright DR (2006) Examination of convection-allowing configurations of the WRF model for the prediction of severe convective weather: the SPC/NSSL spring program 2004. Weather Forecast 21(2):167

Kumar V, Chandrasekar A, Alapaty K, Niyogi D (2007) The impact of assimilating soil moisture, surface temperature, and humidity and the traditional four dimensional data assimilation on the simulation of a monsoon depression over India using a mesoscale model. J Appl Meteorol Climatol 47:1393–1412

Litta AJ, Mohanty UC (2008) Simulation of a severe thunderstorm event during the field experiment of STORM programme 2006, using WRF-NMM model. Curr Sci 95(2):204–215

Litta AJ, Mohanty UC, Bhan SC (2009) Numerical simulation of a Tornado over Ludhiana (India) using WRF-NMM model. Meteorol Appl 17:64–75

Mohanty UC, Sikka DR, Madan OP, Pareek RS, Kiran Prasad S, Litta AJ et al (2007) Weather summary pilot experiment of Severe Thunderstorms-Observational and Regional Modeling (STORM) Programme – 2007, Kharagpur

Nizamuddin S (1993) Hail occurrences in India. Weather 48:90–92

Orlanski I (1975) A rational subdivision of scales for atmospheric processes. Bull Am Meteorol Soc 56:527–530

Parthasarathy B (1984) Interannual and long term variability of Indian summer monsoon rainfall. Proc Indian Acad Sci Earth Planet Sci 93:371–385

Pattanayak S, Mohanty UC (2008) A comparative study on performance of MM5 and WRF models in simulation of tropical cyclones over Indian seas. Curr Sci 95(7):923–936

Pielke RA Sr, Matsui T, Leoncini G, Nobis T, Nair U, Lu E, Eastman J, Kumar S, Peters-Lidard C, Tian Y, Walko R (2006) A new paradigm for parameterizations in numerical weather prediction and other atmospheric models. Natl Weather Dig 30:93–99

Routray A, Mohanty UC, Das AK, Sam NV (2005) Study of heavy rainfall event over the west-coast of India using analysis nudging in MM5 during ARMEX-I. Mausam 56:107–120

Sikka DR, Gadgil S (1980) On the maximum cloud zone and ITCZ over the Indian longitudes during the southwest monsoon. Mon Weather Rev 108:1122–1135

Skamarock WC, Klemp JB, Dudhia J, Gill DO, Barker DM, Wang W, Powers JG (2005) A description of the advanced research WRF version 2, NCAR tech note, NCAR/TN–468 + STR, 88 pp

Weiss SJ, Kain JS, Bright DR, Levit JJ, Carbin GW, Pyle ME, Janjic ZI, Ferrier BS, Du J, Weisman ML, Xue M (2007) The NOAAHazardous weather testbed: collaborative testing of ensemble and convection-allowing WRF modelsand subsequent transfer to operations at the Storm Prediction Center. 22nd Conference Weather Analysis Forecasting/18th Conference on Numerical Weather Prediction, Salt Lake City, Utah, American Meteorological Society, CDROM 6B.4

# Chapter 4
# Representation of Uncertainties in Seasonal Monsoon Predictions Using a Global Climate Model

**Sarat C. Kar**

**Abstract** A seasonal prediction system is being developed at NCMRWF under the Seasonal Prediction and Application to Society (SeaPrAS) programme. Ensemble integrations have been carried out using the Indian global Climate model (In-GLM1) for 23 monsoon seasons with observed, climatological and persisted sea surface temperature forcing. It is found that the model simulated climatology is reasonably good, however, inter-member ensemble spread of rainfall is quite large over the Indian monsoon region. Examination revealed that the inter-member variance is not purely due to internal dynamics. For making seasonal predictions, these uncertainties and systematic errors have to be represented. There are also large uncertainties in the SST predictions from various models and a method has been developed to incorporate these uncertainties while making seasonal predictions using prescribed SSTs. After establishing the usability of the model for seasonal predictions, the prediction system is being tested for real time for monsoon seasons since 2006.

## 4.1 Introduction

Rainfall during the Indian summer monsoon season (June, July August and September) show considerable interannual and intraseasonal variability. Prediction of the Indian summer monsoon both in interannual time scale and intraseasonal timescale are quite important for the economy of the subcontinent as the Indian economy is largely dependent on agriculture. Prediction of the seasonal mean monsoon at least one season in advance is one of the most important and challenging problems in tropical climate. The seasonal mean monsoon circulation in the

S.C. Kar (✉)
National Centre for Medium Range Weather Forecasting, Ministry of Earth Sciences, A-50, Sector-62, Noida, UP, India
e-mail: sckar@ncmrwf.gov.in

S.D. Attri et al. (eds.), *Challenges and Opportunities in Agrometeorology*,
DOI 10.1007/978-3-642-19360-6_4, 

tropics is potentially more predictable. This is because the low-frequency component of the tropical variability is primarily forced by slowly varying boundary forcing, which evolves on a slower time scale than that of the weather systems themselves. Influence of the El Nino Southern Oscillation (ENSO) on the Indian monsoon rainfall has been investigated (Sikka 1980; Shukla 1987). Goswami (1998) had examined interannual variation of Indian summer monsoon in a GCM and had evaluated the role of external conditions versus internal feedbacks. Kar et al. (2001) had examined long-term simulations of a global model with observed and climatological SST. Goswami and Xavier (2005) have examined the dynamics of internally generated interannual variability of Indian summer monsoon in a GCM. Kang et al. (2004) have estimated the potential predictability of summer monsoon rainfall in a dynamical seasonal prediction system with systematic error correction. NCMRWF, over the years, has successfully developed and made operational a deterministic medium-range weather forecasting system. There has been demand from several user agencies for extended range prediction (monthly and seasonal time-scales). Whereas efforts have been made to improve operational monsoon prediction at IMD using statistical methods, dynamical extended-range prediction efforts have continued at several organizations in India including that at NCMRWF.

In a stand-alone atmospheric model, various land surface processes are coupled with atmosphere through the land-surface process parameterization schemes, but the Sea Surface Temperatures (SSTs) are prescribed as external conditions. Large uncertainties exist in the forecasted SSTs from other SST prediction models. Therefore, it is essential to incorporate these uncertainties in the seasonal prediction models when real-time forecast runs are made in seasonal timescales. It is also important to understand the structure and behaviour of the internal variability, relate it to the systematic errors of the model, and represent these uncertainties in the final seasonal predictions. Main objective of this report is to document the strength and weaknesses of the two-tire system (a global model forced with prescribed SSTs) used in the seasonal prediction system. Section 4.2 of this report describes the seasonal prediction system, the model and data used. In Sect. 4.3, results are presented with discussion. Section 4.4 concludes the report.

## 4.2 The Seasonal Prediction System

Seasonal Prediction & Application to Society (SeaPrAS) programme at NCMRWF has been initiated for preparing seasonal predictions from users' point of view. The objective is to improve the capacity in India's resource management to cope with the impacts of climate variability. SeaPrAS shall be a platform for policymakers & resources managers to have access to, and make use of, information generated by climate prediction models. It is expected that the SeaPrAS programme shall provide the planners with more reliable seasonal climate prediction information and guidance on who could be the potential beneficiaries of the predictions. Associated

application systems shall also be developed for energy demand, water resource management, agriculture- drought prediction, crop yield. Work is in Progress towards this end.

The global model used for this study is the Indian global model (In-GLM1). This global climate model is the climate version of the NCMRWF's medium-range weather forecast model (older version). Several modifications were made to utilize the model for seasonal prediction and to study the seasonal to interannual variability of the climate system. More details of the model may be found at Kanamitsu et al. (1991), Kar (2002, 2007). The model was initialized with the NCEP-II reanalysis data (ftp.nomad3.ncep.noaa.gov) valid for April 15, 16, 17, 18, 19, 20, May 01, May 05, May 10 and May 15 of each year and seasonal simulations were carried out. All other surface characteristics at the initial stage of the model were set to climatology except for sea surface temperature (SST). The land surface properties such as wetness, temperature, snow, ice cover etc. evolve along with model simulations. For studying the monsoon variability, the model is forced with weekly optimum interpolation (OI) sea surface temperature (SST) data, Reynolds and Smith (1994). For prediction purpose, forecasted SSTs are downloaded from other Centres. These are described later in the report.

## 4.3 Results and Discussion

The model climatology for seasonal rainfall has been compared against the CMAP rainfall climatology for the corresponding period (1982–2004). The model's rainfall climate is reasonably good and all the essential features of rainfall pattern over the Indian region are simulated well by the model (figure not shown). The overestimation of rainfall by the model over the Arabian Sea and under-estimation of rainfall over the Bay of Bengal and the Gangetic plain is evident. Maximum underestimation in rainfall simulations is seen over the central Bay of Bengal as a zonal stretch around 10 N extending up to Western Pacific Ocean. Year to year variation of rainfall during the monsoon season over the Indian region (area averaged) from model simulations with observed SST and observation has been examined. An examination of the simulated and observed rainfall for these years over the Indian region suggests that there are some years, where simulations are not correct. However, some years such as 1988, 1987, 1994, 1997, 2002 the model hindcast simulations agree well with observation. Examination of temporal correlation coefficients of observed rainfall with the ensemble mean simulated rainfall with observed SST forcing shows that over India the correlation values are very low, only a small pocket has the value greater than 03 or 0.4. More about climatological patterns and interannual variability are provided in Kar (2007).

In order to examine the systematic error structure of the model simulated fields, the seasonal ensemble mean rainfall, zonal wind (U) and meridional wind (V) have been compared with CMAP rainfall and NCEP-II reanalysis datasets. The systematic error variance of these fields for the 23 monsoon seasons are shown in Fig. 4.1.

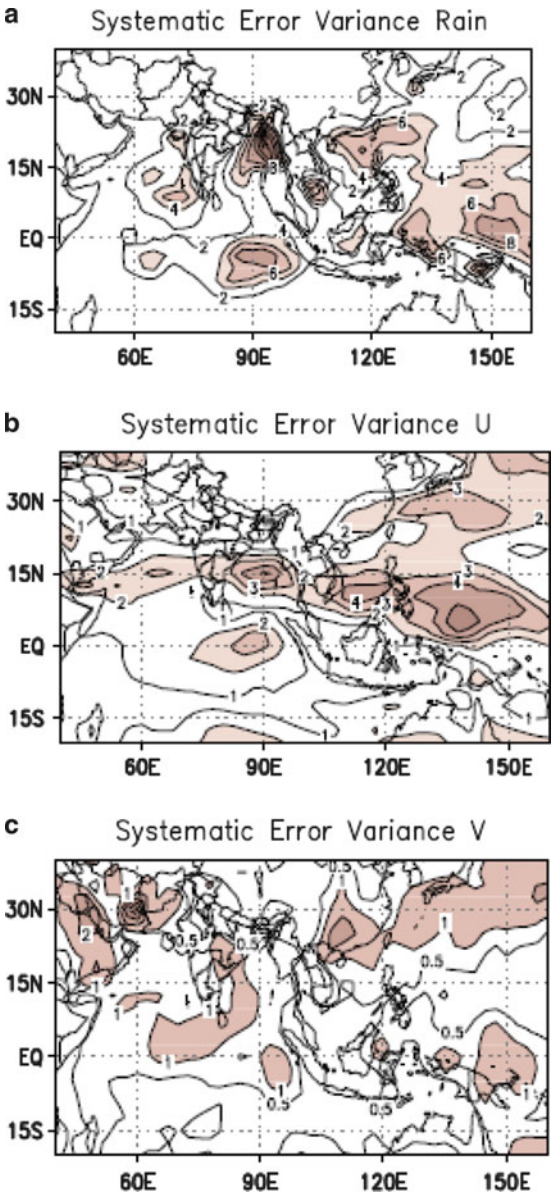


**Fig. 4.1** Systematic error variance from model simulations (**a**) rainfall, (**b**) zonal wind (u) and (**c**) meridional wind

In Fig. 4.1a, error variance of rainfall shows that model has large systematic error over the Indian Ocean to the west of Indonesia, centred around 10 S, 90E. Another zone of large error is off the south-west coast of India. The maximum error is along the Arakkan coast and north Bay of Bengal. There are also large errors in Western pacific. In the tropics, the latent heat release due to condensation shall drives the wind circulation. Therefore, in this region, the wind fields and rainfall are very

closely related. In the zonal wind systematic error variance plot [Fig. 4.1b], it is seen that there is a zonal band of zonal wind error along 12 N extending from the Arabian Sea to the Bay of Bengal and dipping southward extending to the West Pacific. In the equatorial Indian Ocean too, there is a large zonal wind error. The systematic error variance for the meridional winds are shown in Fig. 4.1c. A band of wind error extends from the equatorial Indian Ocean northward to the peninsular India.

Following Kang et al. (2004), the externally forced interannual variance for seasonal mean rainfall have been computed, as shown in Fig. 4.2a. It is seen that in the Indian region, a large part of the rainfall variability in interannual timescales forced by SST occur over the Indian seas. Two bands of maxima in the variability occur where there are rainfall maxima. Over the Pacific, especially central and eastern Pacific, the SST forced variability are also large (not shown in figure). Due

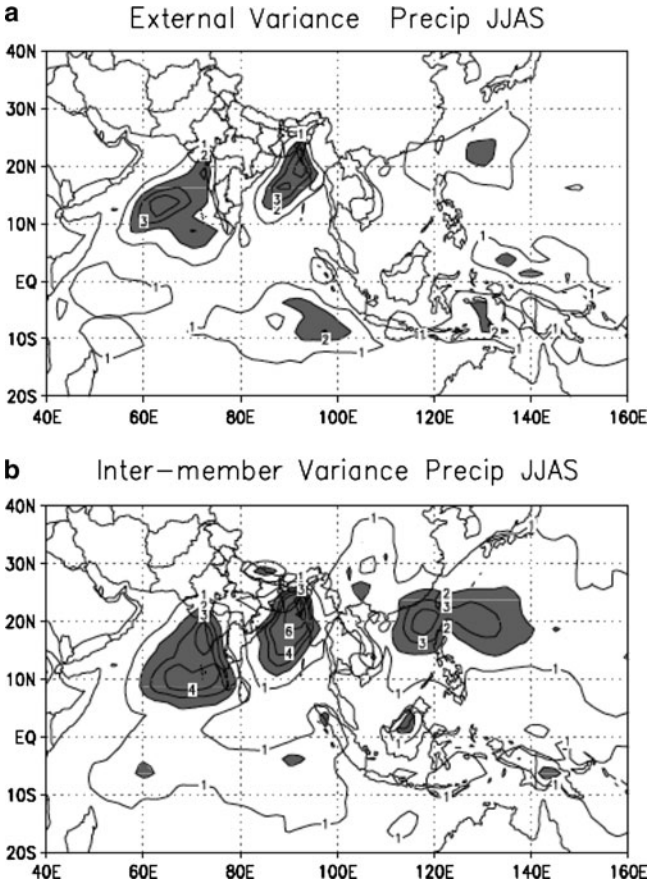


**Fig. 4.2** (**a**) Externally forced interannual variance for model simulated rainfall, and (**b**) inter-member rainfall variance

to local effect of interannually varying SST, there are some variability of rainfall in the Indian Ocean south of equator. As already mentioned, for this study, 10 member ensemble runs were made for each monsoon season. The inter-member variance is used by many authors (e.g. Kang et al. 2004) to describe the variability caused by internal dynamics. The inter-member variance in the present model simulations for rainfall are shown in Fig. 4.2b. It is seen that the variance is quite large in the Indian region, with magnitudes almost comparable to the SST forced variance. However, there are major differences in shape and orientation of the inter-member variance. The pattern of inter-member variance is almost similar to the systematic error variance. Therefore, it may be said that the model systematic errors define the inter-member spread.

In Fig. 4.3a, the ensemble spread over the Indian monsoon region is plotted against the model simulated ensemble mean rainfall climatology. Ideally, if the ensemble spread is caused by uncertainties in dealing with physical processes in the model, the spread should reflect this aspect. In the tropical region, convection is the most important physical process apart from radiation. Convective heating and moistening define the tropical circulation. There are several deficiencies in the manner in which the convection processes are included in a global model. In the figure it is seen that as the rainfall amount increases, the spread also increases. When the rainfall amount is low, the spread is also less. This shows that there shall be large uncertainty in predictions of flood monsoon years as compared to drought monsoon years. To examine if the inter-member spread is modulated by the SST, it has been correlated with the observed SST used in the model simulations. It is seen that indeed, the inter-member spread is correlated to large scale interannual variability of SSTs, and at many regions, the correlation coefficients are statistically significant. Therefore, it is concluded that the inter-member spread is not entirely due to internal dynamics, rather it gets modulated by interannually varying SST forcing. To estimate the internal variability generated by this model, the model was integrated for 23 monsoon seasons with climatological SST. The internal variance computed from runs with climatological SST runs is shown in Fig. 4.3b. It is seen that the internal variance is quite large in the Indian region and is similar to the systematic error variance for rainfall. Over large part of the country, rainfall variability in interannual timescale is due to internal dynamics in these model simulations.

At this point, it is worthwhile to examine how in the model ensemble spread increases as forecast length increases. For this purpose, ensemble forecasts up to 6-days have been carried out for each day of a monsoon season. Ensemble spread has been computed for each day of forecast as the root mean square of deviations of all the ensemble members from the ensemble mean of the forecasted day. Figure 4.4 shows the ensemble spread (mm/day) for Day-1, Day-2, Day-4 and Day-6 forecasts. It is interesting to note that the distribution and amount of spread is different for different length of forecasts. In Day-1 forecasts, the spread over most of the Indian region is between 2 and 4 mm/day. Over the west coast, and surrounding oceanic region, the spread is about 4 mm/day. Over parts of Gujarat and Rajasthan including parts of Uttar Pradesh, the spread is less than 2 mm/day.

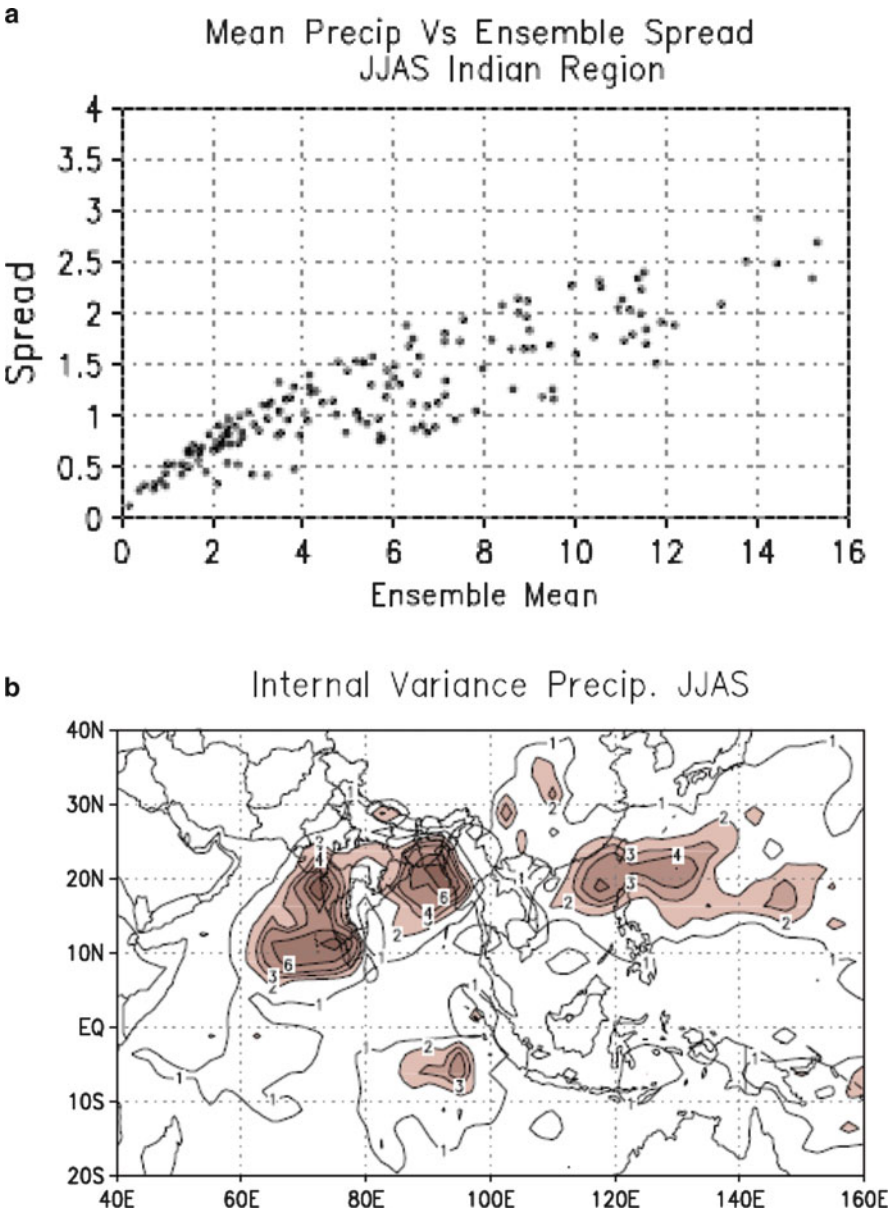


**Fig. 4.3** (**a** and **b**) Scatter diagram of ensemble mean climatology of rainfall and ensemble spread, (**b**) internal variance of simulated rainfall obtained from runs with climatological SST

Spread is quite large (8–12 mm/day) over Thailand and surrounding countries. In Day-2 and Day-4 forecasts, the spread over the Indian region has increased. The west coast, the eastern region and the Bay of Bengal have now a spread of

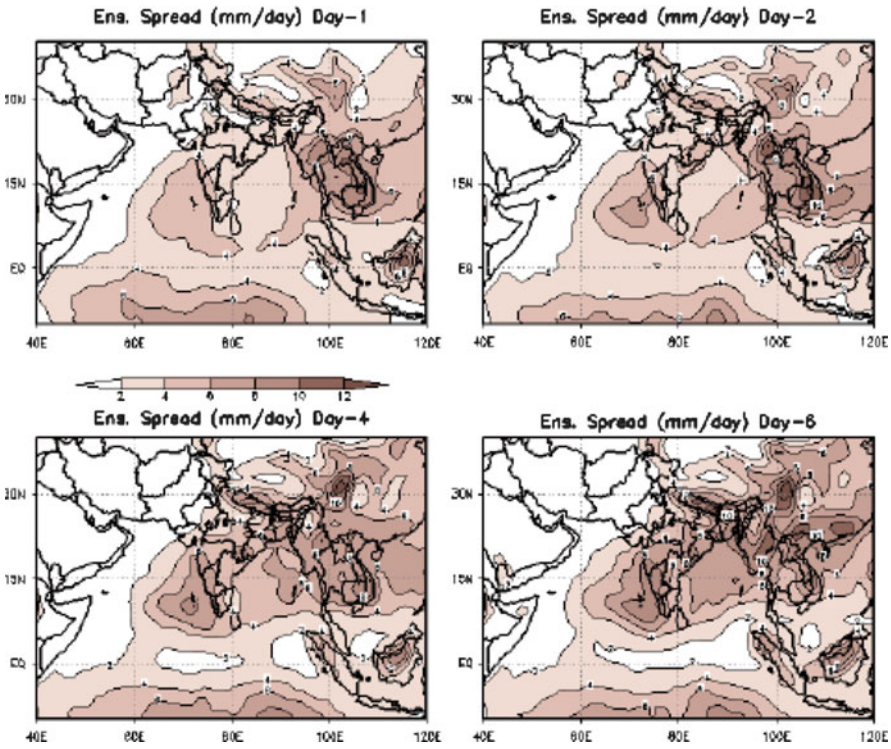


**Fig. 4.4** Ensemble spread (mm/day) for Day-1, Day-2, Day-4 and Day-6 forecasts. Contour levels are 2, 4, 6, 8, 10 mm/day. Regions with spread more than 2 mm/day are shaded

6 mm/day. Near the equatorial Indian Ocean region, the spread has reduced to less than 2 mm/day. By Day-6, the spread over most parts of the Indian region has further increased to 6 mm/day or more. There are pockets where spread is 8 mm/day and increasing to 10 mm/day. Over the equatorial Indian Ocean, the spread is further reduced. The model has a systematic bias and the ensemble spread is clearly demonstrating this bias. As the forecast length is further increased up to seasonal timescales, the ensemble spread start to display variations within a season. It is seen that the spread is more or less large over the Indian region, if the monsoon is active. The magnitude of spread is less if rainfall activity is subdued over the Indian region.

### *4.3.1 Real-Time Monsoon Prediction System*

The main problem for real time prediction with an atmospheric model is to have the prediction of boundary conditions like SST, which influences the monthly and seasonal mean anomalies. Since monsoon 2007, a set of forecasts of SST anomalies

obtained from IRI, USA are being used in the seasonal prediction system. In this report, we describe real-time predictions made for 2008 monsoon. During pre-monsoon months of 2008, moderate La Nina conditions were prevailing over the equatorial Pacific Ocean. Several ocean models and coupled ocean atmosphere models were indicating that during monsoon months, La Nina conditions shall weaken further and ENSO neutral conditions shall prevail. However, there was large variations in the predictions of SST by different models. It was considered appropriate to represent this uncertainty in the SST predictions into the global model used for seasonal predictions. Three scenarios of SST for summer months for 2008 were received from IRI. The seasonal (JJAS) mean anomalies of SST are shown in Fig. 4.5a. On to this anomaly, a perturbation was added and subtracted to generate other two SST scenarios. This perturbation represents the uncertainties in SST predictions (Fig. 4.5b).

Using these SST anomalies, the IN-GLM1 model was integrated for preparing monsoon rainfall forecasts for 2008. For each SST scenario, 6 member ensemble runs were made using observed initial conditions of April 6–11, 2008. Therefore, there were 18 members in total. The NCMRWF real-time global analysis data were used as initial conditions for the IN-GLM1 model. Rainfall anomalies (mm/day) from each member run are shown in Fig. 4.6. It I seen that the model responds to these three SST scenarios, and over the Indian monsoon region, the model provides different scenarios of rainfall activity. However, there are some robust signal which do not change much with different SST forcing nor with different initial conditions. Ensemble mean of these three sets of runs are shown in Fig. 4.7. Based on these results, a forecast was prepared for rainfall on April 13, 2008. Considering the bias

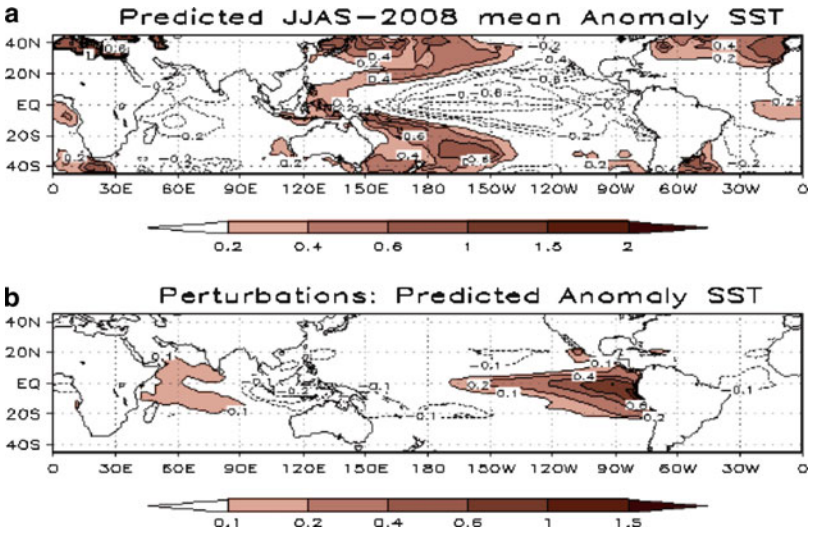


**Fig. 4.5** (**a** and **b**) Seasonal mean (JJAS) anomalies of predicted SST used in model simulations and (**b**) perturbation used to represent uncertainties in ST predictions

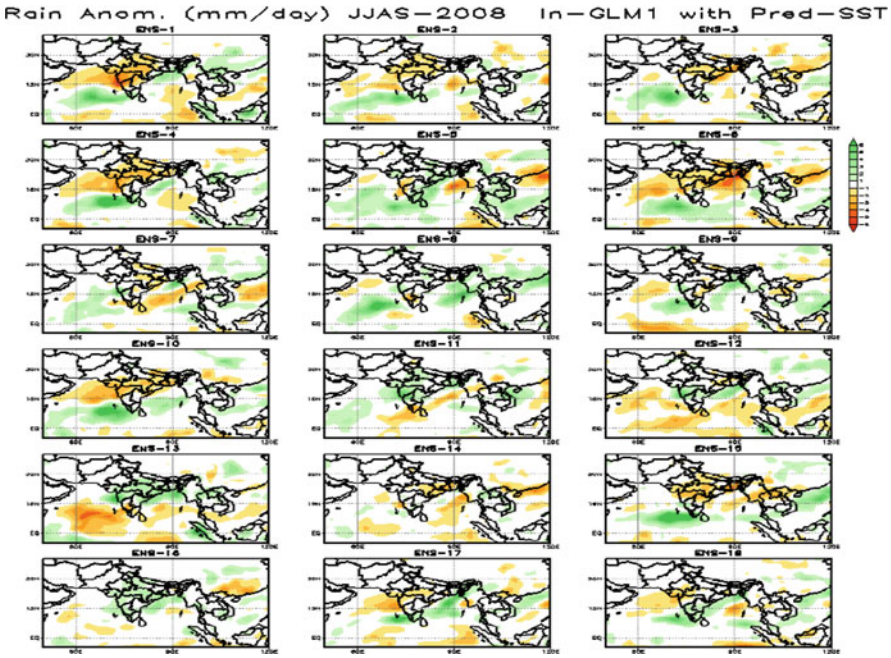


**Fig. 4.6** Predicted rainfall anomalies from each ensemble member with three scenarios of predicted SST for 2008 monsoon season

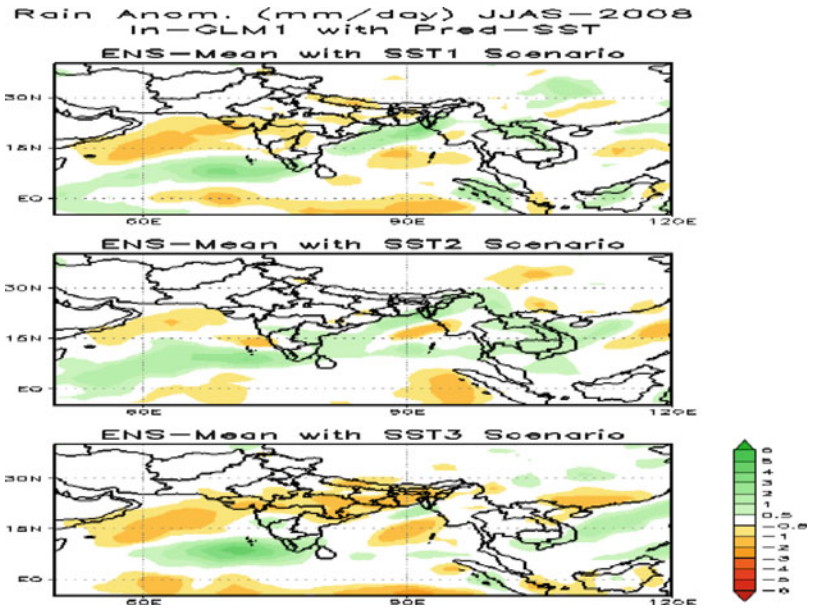


**Fig. 4.7** Ensemble mean of predicted rainfall anomalies from each of the three scenarios of predicted SST for 2007 monsoon season

in the model as well as other strength and weaknesses, the forecast given was that India shall experience below normal to normal monsoon rainfall during monsoon season of 2008. In order to update the forecast, similar exercise was made in May 2008 with model initial conditions of May and updated SST predictions. At the end of the season, IMD noted that for the country as a whole, the seasonal rainfall from 1st June to 30th September was 98% of its long period average (LPA). There were several deficiencies in the regional features of predicted seasonal anomalies of rainfall. It may however be noted that skill of dynamic models in predicting seasonal mean anomalies of monsoon rainfall is low. Therefore, a probabilistic seasonal prediction system has been developed. However, to ensure reliability of predictions, more test runs are being carried out. The probabilistic scheme is being calibrated.

## 4.4 Conclusions

Considering the limitations of statistical methodologies utilized by the IMD for seasonal monsoon prediction, a seasonal prediction system based on global dynamic model is being developed at NCMRWF. This development is being made under the Seasonal Prediction and Application to Society (SeaPrAS) programme. The Indian global Climate model (In-GLM1) has been integrated for 23 monsoon seasons with observed, climatological and persisted sea surface temperature forcing. For each season, simulations have been carried out using ten ensemble members. It is found that the model simulated climatology is reasonably good, however, inter-member ensemble spread of rainfall is quite large over the Indian monsoon region. Examination revealed that the interannually varying SST modulates the inter-member variance and therefore, this variance may not be purely due to internal dynamics. For making seasonal predictions, these uncertainties and systematic errors have to be represented. This observation provides a basis for a probabilistic prediction scheme based on a probability distribution function from the ensemble members. There are also large uncertainties in the SST predictions from various models and a method has been developed to incorporate these uncertainties while making seasonal predictions using prescribed SSTs. It was found that the model responds to local and remote SST variations reasonably well, after establishing the usability of the model for seasonal predictions, the prediction system is being tested for real time predictions for monsoon seasons since 2006. A probabilistic prediction system has also been developed and being calibrated. The prediction system has to be tested for large number of years in real-time to have enough confidence in predictions.

## References

Goswami BN (1998) Interannual variation of Indian summer monsoon in a GCM: external conditions versus internal feedbacks. J Climate 11:501–522

Goswami BN, Xavier PK (2005) Dynamics of 'Internal' interannual variability of Indian summer monsoon in a GCM. J Geophys Res 110:D24104. doi:10.1029/ 2005JD006042

Kanamitsu M, Alpert JC, Campana KA, Caplan PM, Deaven DG, Iredell M, Katz B, Pan HL, Sela J, White GH (1991) Recent changes implemented into the global forecast system at NMC. Weather Forecast 6:425–435

Kang IS, Lee J, Park CK (2004) Potential predictability of summer mean precipitation in a dynamical seasonal prediction system with systematic error correction. J Climate 17:834–844

Kar SC (2002) Description of a high-resolution global model (T170/L28) developed at NCMRWF. Research report 1/2002, NCMRWF, 28 pp

Kar SC (2007) Global model simulations of interannual variability of the Indian summer monsoon using observed SST variability, NCMRWF research report, NMRF/RR/3/2007, 40 pp

Kar SC, Masato Sugi, Nobuo Sato (2001) Interannual variability of the Indian summer monsoon and internal variability in the JMA global model simulations. J Meteorol Soc Jpn 79(2):607–623

Reynolds RW, Smith TM (1994) Improved global sea surface temperature analyses. J Climate 7:929–948

Shukla J (1987) Interannual variability of monsoon. In: Fein JS, Stephens PL (eds) Monsoons. Wiley, New York, pp 399–464

Sikka DR (1980) Some aspects of the large-scale fluctuations of summer monsoon rainfall over India in relation to fluctuations in the planetary and regional scale circulation parameters. Proc Indian Acad Sci Earth Planet Sci 89:179–195

# Chapter 5
# Intra Seasonal Variability of Rainfall in India on Regional Basis

**Manish K. Joshi, K.C. Tripathi, Avinash C. Pandey, and I.M.L. Das**

**Abstract** ISMR with its annual, seasonal and daily variability affects most of social, economic and human activities throughout the Indian subcontinent. In particular, the drought and floods not only affect all types of agricultural products but is also responsible for loss of human lives and property. Late or prolonged monsoon break can lead to catastrophic effects. The knowledge of the intra seasonal and inter annual variability of daily rainfall climatology can be used profitably for crop production. In the present study, the 60 years long NCEP reanalysis data of precipitation rate has been spectrally analyzed on decadal basis to find out the periodicity in All-India, Southwest (SW) and Southeast (SE) precipitation patterns. There is not much change observed in decadal spectra over the last six decades so long as the low frequency components are concerned but the higher frequency components have been found to be a gradually increasing factor in the temporal variation on decadal scale during the last three decades. The rain pattern in the SW region does not exhibit much variation on decadal scale during last six decades implying that the SW region is nearly non-evolving and follows the characteristic pattern of the region. In the SE region the strength of the signals corresponding to higher frequency cycles keep changing from decade to decade. It is concluded that SE region is more stable in temporal variability than the SW region.

M.K. Joshi (✉) • K.C. Tripathi
K. Banerjee Centre of Atmospheric & Ocean Studies, Institute of Interdisciplinary Studies, University of Allahabad, Allahabad 211 002, India
e-mail: manishkumarjoshi@gmail.com; kctripathi@gmail.com

A.C. Pandey
Department of Physics, University of Allahabad, Allahabad 211 002, India
e-mail: avinashcpandey@rediffmail.com

I.M.L. Das
M. N. Saha Centre of Space Studies, University of Allahabad, Allahabad 211 002, India
e-mail: profimldas@yahoo.com

S.D. Attri et al. (eds.), *Challenges and Opportunities in Agrometeorology*,
DOI 10.1007/978-3-642-19360-6_5, 

## 5.1 Introduction

Rainfall is the end product of a number of complex atmospheric processes which vary both in space and time (Luk et al. 2001). Knowledge of the space-time variability of rainfall is important for meteorology, hydrology, agriculture, telecommunications, and climate research. Rainfall has been long analyzed by means of standard statistics such as average value, variance, coefficient of variation and percentiles (Laughlin et al. 2003).

Krishnamurti and Bhalme (1976) reported the presence of the spectral peaks at 10–20 day in pressure and other data. While Krishnamurti and Ardanuy (1980) used longer surface pressure data and observed 10–20, 20–30 and 30–40 day variability. Murakami reported the existence of 5 day and 15 day peak while viewing the spectral analysis of Indian monsoon (Murakami 1977). The spectral analysis of a 70 year record of daily precipitation was performed to search for periodicities on subseasonal time scales during the summer monsoon and reported the presence of 40–50 day spectral peak corresponding to Madden Julian oscillation over most portion of India south (Hartmann and Michelsen 1989). The seasonal variability of spectral peaks in the 40–50 day range for winds and precipitation in the tropical Pacific and Indian Ocean region was studied (Hartmann and Gross 1988). Further, it was reported that the HIM time series is simple in structure with only the annual oscillation and its first two harmonics accounting for almost the entire variability (Rangarajan 1994). The Homogeneous Indian Monsoon (HIM) region rainfall was analysed for the epoch 1871–1990 using Singular Spectral Analysis (Rangarajan 1994).

Singular Spectrum Analysis (SSA) was applied to the Indian Summer Monsoon Rainfall (ISMR) series for extracting the statistically significant oscillations with periods 2.8 and 2.3 years from the white noise of the ISMR series (Vijayakumar and Kulkarni 1995).

In recent years, (Peters et al. 2002) has presented a power law behavior in the distribution of rainfall over at least four decades. Scargle periodogram and wavelet transform methods were used, to study the periodicity of Indian Summer Monsoon Rainfall (ISMR) changes between 1871 and 2004 and review the possible influence of solar activity on the rainfall (Lihua et al. 2007). The seasonal monsoon rainfall is found to consist of two dominant intraseasonal oscillations with periods of 45 and 20 days and three seasonally persisting components, by using Multichannel Singular Spectrum Analysis (MSSA) of daily rainfall anomaly (Krishnamurthy and Shukla 2007). The variability and long-term trends of extreme rainfall events over central India have been examined and it was reported that inter-annual, inter-decadal and long-term trends of extreme rainfall events are modulated by the SST variations over the tropical Indian Ocean (Rajeevan et al. 2008).

The purpose of this paper is to investigate the regular variations in rainfall over All-India and the two regions namely Southwest (SW) and Southeast (SE). A central part of the study is the spectral analysis of a 60 year record of daily rainfall data from. The goal of this analysis is to evaluate the changes that are taking place

in the pattern in All-India as well as the two regions defined above on the decadal basis and to observe the spectra of Daily Rainfall Climatology (DRC) of All-India and the two regions to investigate the broad features in the regions.

## 5.2 Data Used and Methodology

The 60 years (1948–2007) NCEP reanalysis data of precipitation rate has been spectrally analyzed on decadal scale to find out the periodicity in rainfall of All-India (66°E to 90°E and 5°N to 35°N), SW (73°E to 76°E and 11°N to 20°N) and SE (77°E to 80°E and 8°N to16°N) regions. The decadal spectra have been used to evaluate the changes that are taking place in the rain pattern and the daily rainfall climatology has been used to investigate the broad features of the rain pattern in these regions.

If R(m,n) be the precipitation for the nth day of the mth year of the 60 years NCEP data, then the DRC of the nth day, $R_c(n)$, is defined as:

$$R_c(n) = \frac{1}{60}\sum_{m=1}^{60} R(m,n)$$

Prior to perform spectral analysis, the high frequency fluctuations in the DRC have been removed by applying a 5-day running mean to obtain more accurate periodicities of rainfall.

## 5.3 Results and Discussion

Figure 5.1 shows the decadal spectra of precipitation over All-India for the period (a) 1948–1957, (b) 1958–1967, (c) 1968–1977, (d) 1978–1987, (e) 1988–1997 and (f) 1998–2007 respectively. There is not much change observed in decadal spectra of All-India over the last six decades so long as the low frequency components are concerned. In contrast, the higher frequency components, the 80th or other nearby harmonics corresponding to a cycles of 40–50 days (usually called the MJ oscillation), has been found to be a gradually increasing factor in the temporal variation on decadal scale during the last three decades. The gradually increasing energy of these signals can be seen from Fig. 5.1d–f.

Figure 5.2 shows the decadal spectra of precipitation over SE for the period (a) 1948–1957, (b) 1958–1967, (c) 1968–1977, (d) 1978–1987, (e) 1988–1997 and (f) 1998–2007 respectively. Apart from the annual and other components present in the All-India rainfall pattern, the harmonics from 150 to 270 are also found to be important in SE region. The dominant cycles between the harmonics 150–270 are variable on inter decadal basis. Some signals appear in some decades in an

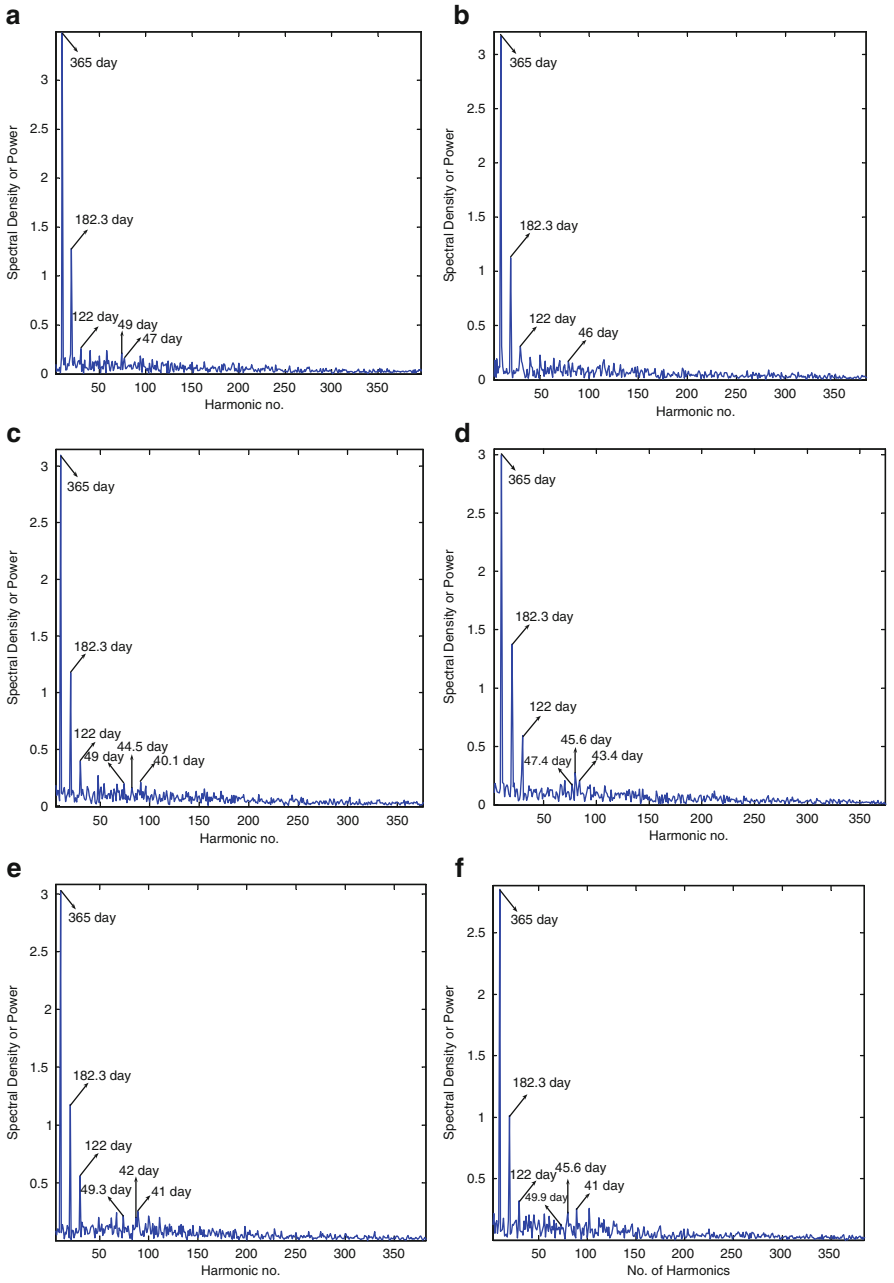


**Fig. 5.1** Discrete Fourier transform of precipitation for all-India region over the period (**a**) 1948–1957, (**b**) 1958–1967, (**c**) 1968–1977, (**d**) 1978–1987, (**e**) 1988–1997, (**f**) 1998–2007

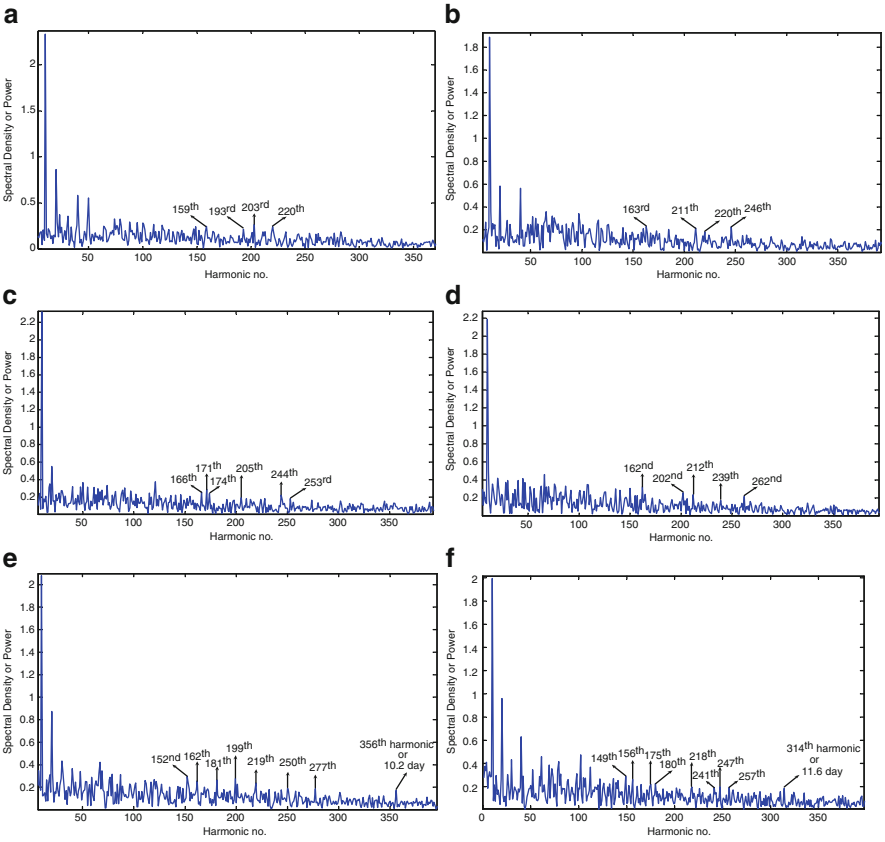


**Fig. 5.2** Discrete Fourier transform of precipitation for SE region over the period (**a**) 1948–1957, (**b**) 1958–1967, (**c**) 1968–1977, (**d**) 1978–1987, (**e**) 1988–1997, (**f**) 1998–2007

unpredictable way like the 277th harmonic in the 1988–1997 periods which is not present in any other decade. The second last and the last decade contains an important harmonic of 356 and 314 as shown in Fig. 5.2e, f respectively, indicating that the pattern of rainfall in the SE region is 'evolving' on a decadal basis.

Figure 5.3 shows the decadal spectra of precipitation over SW for the period (a) 1948–1957, (b) 1958–1967, (c) 1968–1977, (d) 1978–1987, (e) 1988–1997 and (f) 1998–2007 respectively. As far as low frequency components are considered, the rainfall pattern in the SW region does not exhibit much variation on decadal scale during last six decades. The spectrum of all decades for SW region contains the annual cycle of 365 day, semiannual cycle of 182.3 day, terannual cycle of 122 day and the quadannual cycle of 91 day. In addition to this, the other prominent cycles present in the first decade, are quite similar to those present in other decades. Thus it can be concluded that the SW region is nearly non-evolving and follows the characteristic pattern of the region.

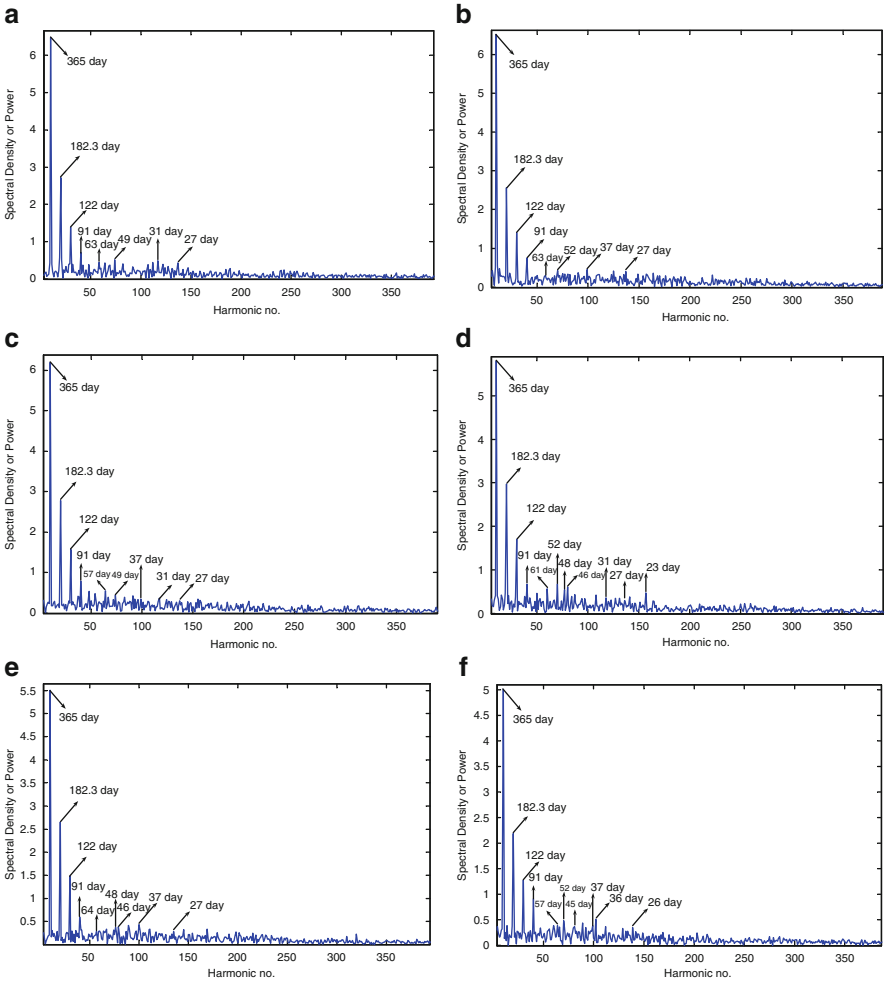


**Fig. 5.3** Discrete Fourier transform of precipitation for SW region over the period (**a**) 1948–1957, (**b**) 1958–1967, (**c**) 1968–1977, (**d**) 1978–1987, (**e**) 1988–1997, (**f**) 1998–2007

Figures 5.4–5.6 show the DFT of DRC for All-India, SE, and SW regions respectively, after excluding the more dominant cycles viz. annual, semiannual and terannual to observe the relative strength of other cycles. Besides, the annual, semiannual and terannual the other dominating cycles present in the spectrum of DRC for All-India rainfall are the cycles of 91 day, 45 day, 36 day, 18 day, 14 day and 10 day. The quadannual cycle and the 36 day cycle were also observed in the spectra of SE and SW regions. The cycle of 45 day that corresponds to Madden Julian Oscillations also referred as MJO and the 18 day cycle was observed in the spectra of SW and All-India region. The spectrum of DRC of SW region contains two important cycles of 60 day and 52 day which are clearly distinct as prominent

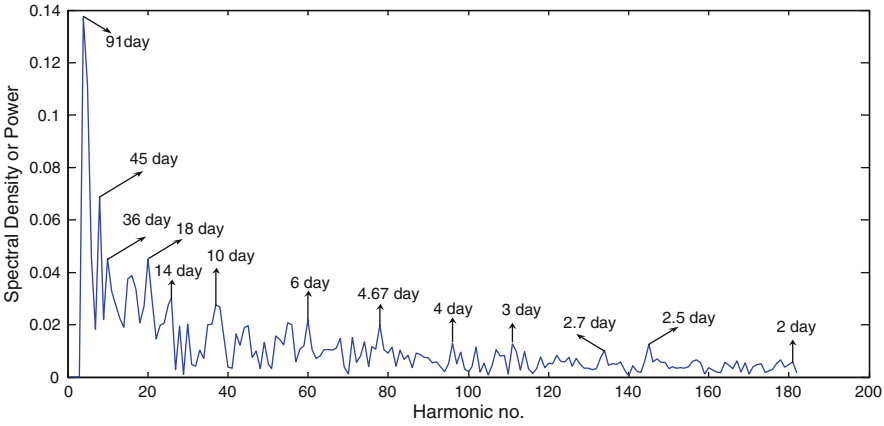


**Fig. 5.4** DFT of DRC excluding annual, semiannual and terannual cycles for All-India region

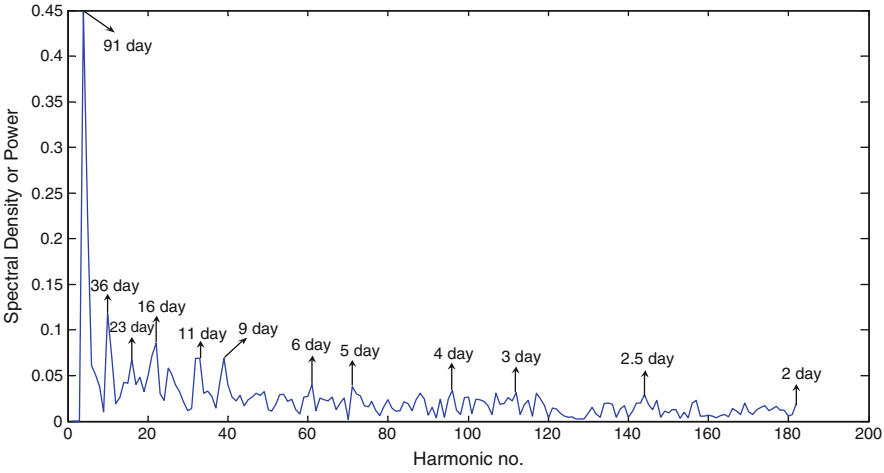


**Fig. 5.5** DFT of DRC excluding annual, semiannual and terannual cycles for SE region

peaks in the Fig. 5.6. These two prominent peaks were neither observed in the spectra of All-India nor in the SE region. The high frequency cycles i.e. the cycle of 6 day, 4 day, 3 day and 2.5 day were also observed in the spectra of all regions. In addition to this, the cycle of 5 day was observed in SE and SW region.

The basic difference in the spectra of SE region when compared with the spectra of All-India lies in the ratio of strengths of annual and other cycles representing intraseasonal and other smaller variations. While in the All-India pattern, the annual cycle singly dominates the rainfall; in the SE regions, other variations have significant strengths. This is obvious in the sense that All-India rainfall is nonetheless, an average over the smaller regions. However this fact leads to the conclusion that there are other regions which exhibit relatively less variations on small time scales.

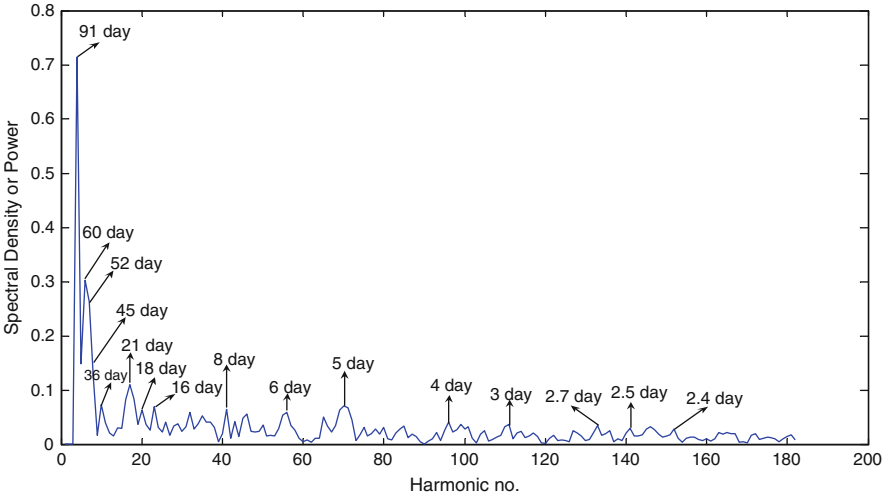


**Fig. 5.6** DFT of DRC excluding annual, semiannual and terannual cycles for SW region

Indeed SW region is one such region. It is observed that that the annual cycle is more dominant as is seen from the spectra. Thus, the SW region is much less responsible to local temporal rain as compared to the SE region. This conclusion cannot be reached on the basis of the analysis of simple variance as, in that case, overall variability will be reflected and no the relative strengths of local and global and temporal signals.

Analysis of spectra of climatology of rain over All-India, SE and SW regions confirms that this pattern is a characteristic pattern of the Indian rainfall. This can be seen in the relatively strong signals of 91 day cycle for the SW region as compared to SE and All-India regions.

## 5.4 Conclusion

Temporal pattern of the precipitation over India is analysed on regional basis. The spectra of the regions are investigated on decadal basis and the relative strengths of the low and high order harmonics are compared. It is observed that temporally local pattern of rain have more profound effect on the overall feature in the SE region than in the SW region. This feature is also reflected in the All-India rainfall pattern. Further, it is seen that the high frequency cycles, the harmonics around the MJ oscillations, have shown an increase in strength in the last three decades for the all India and SE rain patterns. However, the SW pattern remains comparatively more stable. It may be concluded that the pattern of the SE precipitation is evolving on decadal basis and an increase in the strength of MJ oscillation may be evident in the next couple of decades. Study of spectra on finer resolutions and their intercomparison may further inform the society of the local rain patterns.

## References

Hartmann DL, Gross JR (1988) Seasonal variability of the 40–50 day oscillation in wind and rainfall in the tropics. J Atmos Sci 45(19):2680–2702

Hartmann DL, Michelsen ML (1989) Intraseasonal periodicities in Indian rainfall. J Atmos Sci 46 (18):2838–2862

Krishnamurti TN, Ardanuy P (1980) The 10 to 20-day westward propagating mode and "breaks in the monsoons". Tellus 32:15–26

Krishnamurti TN, Bhalme HN (1976) Oscillations of a monsoon system. Part I. Observational aspects. J Atmos Sci 33:1937–1954

Krishnamurthy V, Shukla J (2007) Intraseasonal and seasonally persisting patterns of Indian monsoon rainfall. J Climate 20:3–20

Laughlin GP, Zuo H, Walcott J, Bugg AL (2003) The rainfall reliability wizard-a new tool to rapidly analyse spatial rainfall reliability with examples. Environ Model Softw 18:49–57

Lihua M, Yanben H, Zhiqiang Y (2007) The possible influence of solar activity on Indian summer monsoon rainfall. Appl Geophys 4(3):231–237

Luk KC, Ball JE, Sharma A (2001) An application of artificial neural networks for rainfall forecasting. Math Comput Modell 33:883–699

Murakami M (1977) Spectrum analysis relevant to Indian monsoon. Pure Appl Geophys 115(5–6): 1145–1166

Peters O, Hertlien C, Christensen K (2002) A complexity view of rainfall. Phys Rev Lett 88(1):1–4

Rajeevan M, Bhate J, Jaswal AK (2008) Analysis of variability and trends of extreme rainfall events over India using 104 years of gridded daily rainfall data. Geophys Res Lett. doi:10.1029/2008GL035143

Rangarajan GK (1994) Singular spectral analysis of homogeneous Indian monsoon (HIM) rainfall. J Earth Syst Sci 103(4):439–448

Vijayakumar R, Kulkarni JR (1995) The variability of the interannual oscillations of the Indian summer monsoon rainfall. Adv Atmos Sci 12(1):95–102

# Chapter 6
# Assimilation of Surface Observations in a High Resolution WRF Model

**Dipak K. Sahu and S.K. Dash**

**Abstract** In this study surface parameters such as dry-bulb temperature, dew-point temperature and wind speed at 8:30 IST (0300 UTC) from 32 Government Inter Colleges (GICs) in Uttarakhand are assimilated into a high-resolution Weather Research and Forecasting (WRF) version 2.2 model by using Three-Dimensional Variational (3DVAR) surface data assimilation technique. These surface weather observations are made in a programme entitled Participation of Youth in Real-time/field Observations to Benefit the Education (PROBE), which was initiated by the Department of Science and Technology (DST), India in the state of Uttarakhand in 2003. The WRF model has been integrated over the Uttarakhand domain at a horizontal resolution of 5 km. The assimilation of surface weather parameters have resulted in a noticeable impact on the horizontal and vertical distributions of temperature and wind fields. Also the comparison of simulated fields obtained with and without surface data assimilation in the model indicates comparatively less error after assimilation.

## 6.1 Introduction

Land surface is an important interface that exchanges energy between the earth and the atmosphere. Also surface parameters are crucial to the simulation of weather parameters by numerical methods. Because of lack of high quality spatial distributions of surface weather parameters those are not assimilated into mesoscale models and hence the difficulty in reasonable mesoscale predictions. To improve local weather simulations, it is necessary to collect and assimilate high resolution surface observations into a mesoscale model. In the past, several studies (Ruggiero et al. 1996;

D.K. Sahu (✉) • S.K. Dash
Centre for Atmospheric Sciences, Indian Institute of Technology Delhi, Hauz Khas, New Delhi 110 016, India
e-mail: dipakmath@gmail.com; skdash@cas.iitd.ac.in

S.D. Attri et al. (eds.), *Challenges and Opportunities in Agrometeorology*,
DOI 10.1007/978-3-642-19360-6_6, 

Alapaty et al. 2001; Alapaty et al. 2008; Stauffer et al. 1991; Vinodkumar et al. 2008a, b) have been conducted to improve simulations of weather parameters by using direct or model analyzed surface observations. The study conducted by Ruggiero et al. (1996) described a system for the frequent intermittent assimilation of surface observations into a mesoscale model. Results from a case study indicated that the frequent intermittent assimilation of surface data can provide a superior mesoscale forecast. Alapaty et al. (2008) and Vinodkumar et al. (2008a) have investigated the effect of indirect surface data assimilation using Flux-Adjusting Surface Data Assimilation System (FASDAS). Their results indicate that FASDAS consistently improved the accuracy of the model simulations. Further Vinodkumar et al. (2008b) investigated the impact of land surface processes and data assimilation on mesoscale convection and precipitation for a heavy rain event associated with offshore troughs over the Indian monsoon region. Their results showed that surface data assimilation simulated the strongest vertical wind velocity fields as well as the associated potential vorticity fields as compared with the model simulation from NCEP reanalysis initial and boundary conditions ($2.5^\circ \times 2.5^\circ$). In an earlier study Stauffer et al. (1991) presented a direct continuous assimilation of standard resolution rawinsonde and meso-alpha surface observations throughout the model integration rather than at the initial time. Within the planetary boundary layer they also investigated the effect of data assimilation by using four-dimensional data assimilation technique based on Newtonian nudging. The main objective of their study was to effectively utilize the combined strength of these two simple data systems while avoiding their individual weaknesses. Assimilation of surface wind and moisture data throughout the model planetary boundary layer generally showed a positive impact on the simulated precipitation. Xavier et al. (2008) assimilated the satellite and conventional meteorological data by using analysis nudging to study the effect of increased vertical and horizontal resolution as well as convective parameterization. The significant result from their study indicated that the improvements in the simulation using nudging run are better than the improvements in the simulation due to high-resolution and cumulus parameterization sensitivity.

Uttarakhand is located in the northern part of India and has a total geographic area of 51,125 $km^2$. Approximately 93% of Uttarakhand is covered by Himalayan Mountains and about 64% of the mountains are forest. This state has sparse weather data available for use in numerical weather prediction (NWP). Under a program entitled the Participation of Youth in Real-time/field Observations to Benefit the Education (PROBE) initiated by the Department of Science and Technology (DST), Met Labs are successfully installed in several Government Inter Colleges (GICs) in Uttarakhand. One of the objectives of this initiative is to use the surface weather observations in a high-resolution Weather Research and Forecasting (WRF) model to examine their impact on the local weather prediction. Initiated from Uttarakhand in 2003, this PROBE program has now spread over different states in India including NCR-Delhi, Orissa and Tamilnadu. Currently under this program, a good set of surface meteorological parameters has been collected from Uttarakhand in the last 3 years. In the present study these data are utilized in the data assimilation scheme of the WRF model.

In the present study surface observations such as dry-bulb temperature, wind speed and dew point temperature have been assimilated into Three-Dimensional Variational (3DVAR) data assimilation technique of the WRFV2.2 model in order to examine the impact of additional data in the local weather simulations. The surface observations are used at a minimum distance of about 5 km in the horizontal. Section 6.2 in this paper describes the WRF model in brief and the experimental design. Section 6.3 gives the details of observations used in the 3DVAR surface data assimilation (SDA) model simulations. Section 6.4 analyzes the statistical errors in terms of relative errors (REs) and root mean square differences (RMSDs). Sections 6.5 and 6.6 discuss the horizontal and vertical structures of the parameters before and after assimilation. Finally conclusions are given in Sect. 6.7.

## 6.2 Model Description and Experimental Design

The state-of-the-art WRF is the result of collaborative effort among the NCAR Mesoscale and Microscale Meteorology (MMM) Division, the National Oceanic and Atmospheric Administration's (NOAA), National Centers for Environmental Prediction (NCEP), Forecast System Laboratory (FSL), the Department of Defense's Air Force Weather Agency (AFWA), Naval Research Laboratory (NRL), the Centre for Analysis and Prediction of Storms (CAPS) at the University of Oklahoma, and the Federal Aviation Administration (FAA) and a number of other university scientists. WRF model is designed to replace existing U.S. research models (e.g., MM5) and operational models (e.g., Eta) under a common software architecture. The performance of WRF has been demonstrated to be comparable or even better than MM5 and other existing mesoscale models in weather forecasting (Gallus et al. 2005; Grams et al. 2006). A detail description of the model equations, physics and dynamics are available in Dudhia (2004). WRF is a limited area, non-hydrostatic, with terrain following eta-coordinate mesoscale modeling system designed to serve both operational forecasting and atmospheric research needs. There are a wide range of physical parameterization schemes available in WRF. After conducting a number of sensitivity studies we have selected the following physical parameterization schemes in this study. The schemes used include Ferrier (new Eta) microphysical parameterization, the ensemble Grell-Devenyi cumulus parameterization (Grell and Devenyi 2002), Dudhia shortwave radiation (Dudhia 1989) and Rapid Radiative Transfer Model (RRTM) longwave radiation (Mlawer et al. 1997), the Yonsei University (YSU) planetary boundary layer (PBL) scheme (Noh et al. 2003), the thermal diffusion land surface model and Monin-Obukhov surface layer scheme.

Advanced Research WRF (ARW) dynamic core version 2.2, is used in this study. Following two numerical experiments have been conducted in this study. In the single domain experiment the model is centered at 30.2°N and 79.4°E with $76 \times 78$ horizontal grid points in the longitudinal and latitudinal directions at

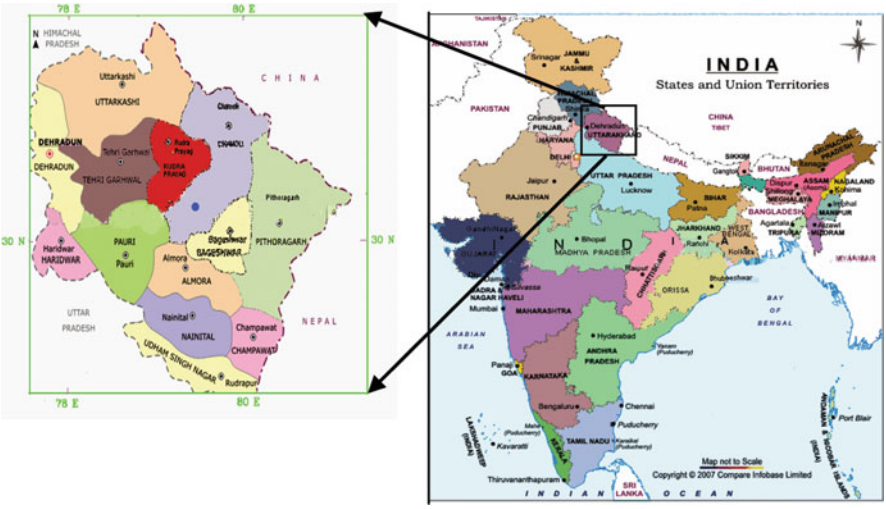


**Fig. 6.1** Domain used for WRF integration covering Uttarakhand state

horizontal resolution of 5 km as shown in Fig. 6.1. The Mercator map projection is used as the model horizontal coordinates. The model has been integrated vertically up to 100 hPa with 27 terrain-following sigma levels.

This single domain run referred to as control run (CTRL) in the text was conducted by using the NCEP-NCAR Final Analysis (FNL) at $1^\circ \times 1^\circ$ grid resolution to prepare initial and lateral boundary conditions. The second experiment, henceforth referred to as surface data assimilation run (SDA) was conducted with modified initial and lateral boundary conditions by assimilating additional surface observations at 32 stations with the help of 3DVAR data assimilation scheme available with WRFV2.2. Barker et al. (2004) and Lorenc et al. (2000) provide a detail description of the 3DVAR system used in this study. In SDA case three different experiments, the first from 0000 UTC 02 Dec to 0000 UTC 03 Dec 2006, the 2nd from 0000 UTC, 11 Dec to 0000 UTC, 12 Dec 2006 and the 3$^{rd}$ from 0000 UTC, 27 Dec to 0000 UTC, 28 Dec 2006 each for 24 h were conducted. These three experiments will be referred to as EXP1, EXP2 and EXP3 subsequently.

## 6.3 Observational Data Used

In this study we have used the surface measurements from U-PROBE (DST, 2007), since no other reliable data are available over the region of interest. U-PROBE programme initiated by DST aims at making climate and weather science education interesting and useful where school children and teachers participate actively. Under this programme about 97 Met Labs are functioning in Uttarakhand state till today. However, we have selected data from 32 stations shown in Fig. 6.2a in

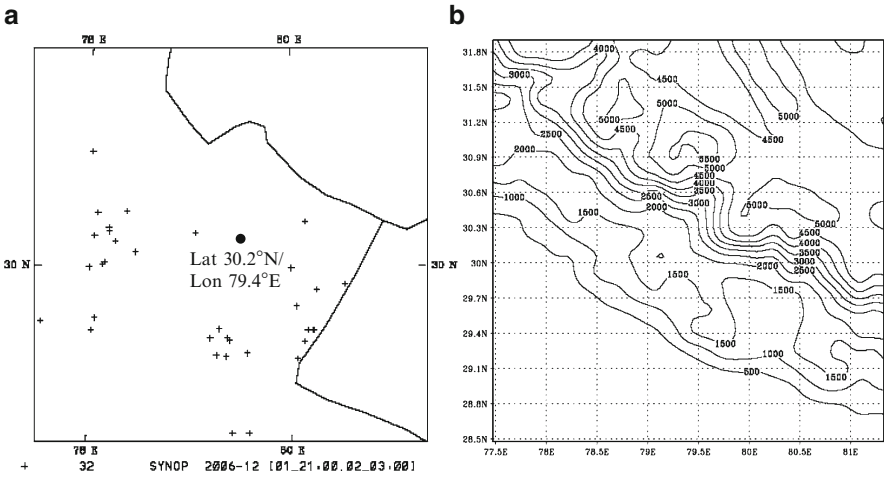


**Fig. 6.2** (**a**) Location of 32 Met Labs from which surface data are assimilated (**b**) Terrain heights used in WRF-ARW model

this study. Under U-PROBE all the surface measurements of dry-bulb temperature, wind speed and dew point temperature were made at 08.30 IST as required by the model configuration. The domain selected in this study has very complex terrain which includes some parts of the Himalaya. The terrain heights used in the model are shown in Fig. 6.2b, so that the relative heights of stations shown in Fig. 6.2a can be conveniently assessed. Thus we assimilated surface weather parameters in 5 km WRF-ARW model at 0300 UTC (08.30 IST) to prepare the updated initial and lateral boundary conditions for 24 h model integration.

## 6.4 Relative Errors and RMSDs

A comparative study has been conducted between the CTRL and SDA at three different stations Rishikesh, Newtehri and Thal in case of the three numerical experiments EXP1, EXP2 and EXP3. To estimate errors between the two model simulations and observed values, relative errors (REs) are calculated at each station for each parameter between CTRL and observations on one hand and SDA and observations on the other.

Relative error between CTRL simulations and observations, RE-ctrl $= \left|\frac{(C-O)}{O}\right|$

Relative error between SDA simulations and observations, RE-sda $= \left|\frac{(D-O)}{O}\right|$

Here C represents the CTRL model output at 0300 UTC, D represents the SDA model output and O represents the observational value at 0300 UTC (08.30 IST).

Also the respective difference between the CTRL and SDA simulations represented by the root-mean-square difference (RMSD) is given by

$$\mathrm{RMSD} = \sqrt{\frac{1}{N}\sum_{i=1}^{N}(C_i - D_i)^2}$$

Here $C_i$ and $D_i$ represent the CTRL and SDA predicted values respectively at a particular time of the 3 h output of 24 h model integration. N is the number of model output time in the 24 h model integration, in this case N = 9. It is well known that RMSD is a good estimate of the average difference and RE is a relative difference measure (Bonnardot and Cautenet 2009). Table 6.1 shows the RE-ctrl and RE-sda for dry-bulb temperature, dew point temperature and relative humidity at Thal, Rishikesh and Newtehri. The additional variable wind speed is available only at Newtehri and hence has been considered here. Wind speeds are not available at Thal and Rishikesh. Comparison shows that at all the three stations RE-sda is comparatively less than RE-ctrl, which implies the advantages of surface data assimilation in the SDA experiment. Generally a good agreement between observation and forecast leads to a smaller value of RMSE. But here smaller value of RMSD indicates the additional surface data has less impact on respective weather parameters and larger value indicates more impact. Table 6.2 represents the RMSD between the CTRL and SDA at all the three studied stations. It shows that in case of temperature the RMSD is less compare to other parameters and this result again leads to the inference that assimilation of surface observations from additional 32 Met Labs has improved the simulations. However, the impact is less in case of temperature compared to that of relative humidity, dew point temperature and wind speed.

## 6.5 Spatial Errors in Meteorological Parameters

### *6.5.1 Analysis at 850 hPa*

The spatial distribution of difference in wind speed and dew point temperature at 850 hPa are shown in Figs. 6.3 and 6.4 respectively. The difference is calculated by simply subtracting the SDA model simulations from CTRL model simulation at each 3 h model output. The spatial differences in dry-bulb temperature and relative humidity are also analyzed at 850 hPa but not shown in figures to save space. Level 850 hPa is chosen because in more than half of the domain the terrain heights are greater than 1 km [Fig. 6.2b]. It is found that the maximum difference in dry-bulb temperature is up to 1°C and the minimum difference is 0.5°C. In case of EXP1 the model simulates higher temperature in SDA in most part of the domain. However, EXP2 and EXP3 simulated higher temperature in case of CTRL. Figure 6.3 shows that maximum and minimum differences in wind speed between CTRL and SDA at 850 hPa are 2.4 m/s and 0.9 m/s respectively. It is seen from Fig. 6.3 that in most parts of the domain captured differences are up to 0.8–0.9 m/s and certain parts up

**Table 6.1** Relative Errors (REs) between the measured parameters at 03UTC and corresponding control (CTRL) and data assimilation (SDA) experiments

| | Thal (29.45°N, 80.16°E) | | | | | | Rishikesh (30.04°N, 78.15°E) | | | | | | Newtehri (30.22°N, 78.26°E) | | | | | | | |
|---|---|---|---|---|---|---|---|---|---|---|---|---|---|---|---|---|---|---|---|---|
| | Temperature | | Dew point temperature | | Relative humidity | | Temperature | | Dew point temperature | | Relative humidity | | Temperature | | Dew point temperature | | Relative humidity | | Wind speed | |
| Analysis time | CTRL | SDA | CTRL | SDA | CTRL | SDA | CTRL | SDA | CTRL | SDA | CTRL | SDA | CTRL | SDA | CTRL | SDA | CTRL | SDA | CTRL | SDA |
| 2-Dec-06 03UTC | 0.828 | 0.828 | 4.048 | 2.217 | 0.833 | 0.729 | 0.118 | 0.089 | 2.369 | 1.136 | 0.585 | 0.401 | 0.088 | 0.07 | 16.35 | 9.24 | 0.769 | 0.56 | 3.452 | 3.27 |
| 11-Dec-06 03UTC | 0.579 | 0.557 | 0.6 | 0.369 | 0.337 | 0.275 | 0.303 | 0.301 | 0.586 | 0.49 | 0.049 | 0.019 | 0.719 | 0.7 | 1.162 | 0.84 | 0.401 | 0.35 | 5.765 | 5.1 |
| 27-Dec-06 03UTC | 0.733 | 0.712 | 3.2 | 2.173 | 0.722 | 0.609 | 0.336 | 0.336 | 1.329 | 1.091 | 0.318 | 0.213 | 0.566 | 0.55 | 11.59 | 7.92 | 0.669 | 0.57 | 2.622 | 1.82 |

**Table 6.2** Root Mean Square Differences (RMSDs) of day-1 between control (CTRL) and data assimilation (SDA) experiments

| | Thal (29.45°N, 80.16°E) | | | | Rishikesh (30.04°N, 78.15°E) | | | | Newtehri (30.22°N, 78.26°E) | | | |
|---|---|---|---|---|---|---|---|---|---|---|---|---|
| Experiments | Temperature | Wind speed | Dew point temperature | Relative humidity | Temperature | Wind speed | Dew point temperature | Relative humidity | Temperature | Wind speed | Dew point temperature | Relative humidity |
| 2-Dec-06 | 0.143 | 0.204 | 4.361 | 7.346 | 0.109 | 0.325 | 3.595 | 5.511 | 0.0642 | 0.182 | 4.847 | 7.219 |
| 11-Dec-06 | 0.108 | 0.28 | 0.609 | 3.219 | 0.103 | 0.127 | 0.641 | 2.367 | 0.0455 | 0.255 | 0.61 | 2.799 |
| 27-Dec-06 | 0.152 | 0.293 | 2.998 | 7.634 | 0.066 | 0.452 | 1.924 | 4.011 | 0.0557 | 0.264 | 2.335 | 4.881 |

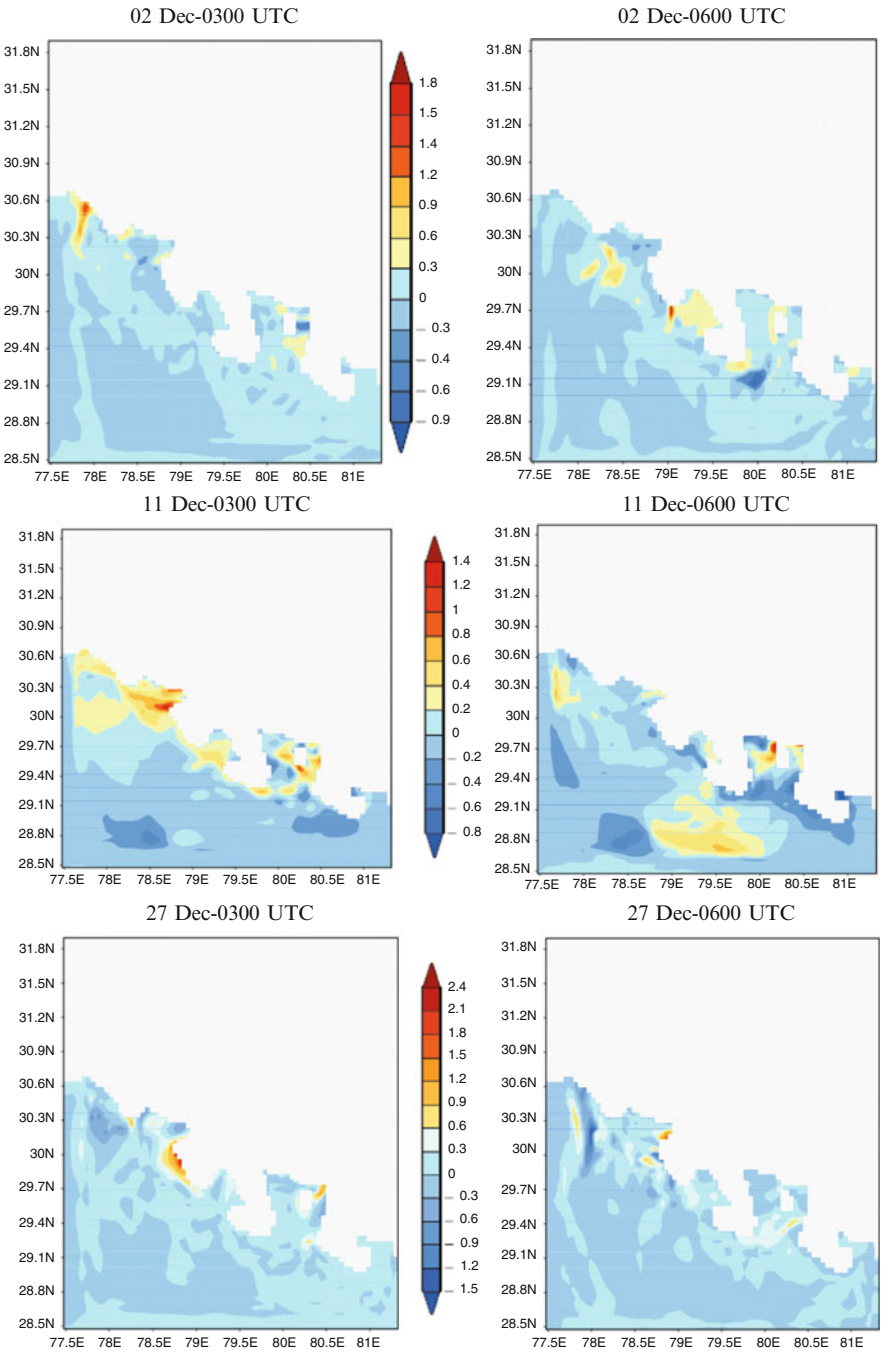


**Fig. 6.3** Horizontal distributions of wind speed differences at 850 hPa between CTRL and SDA simulations

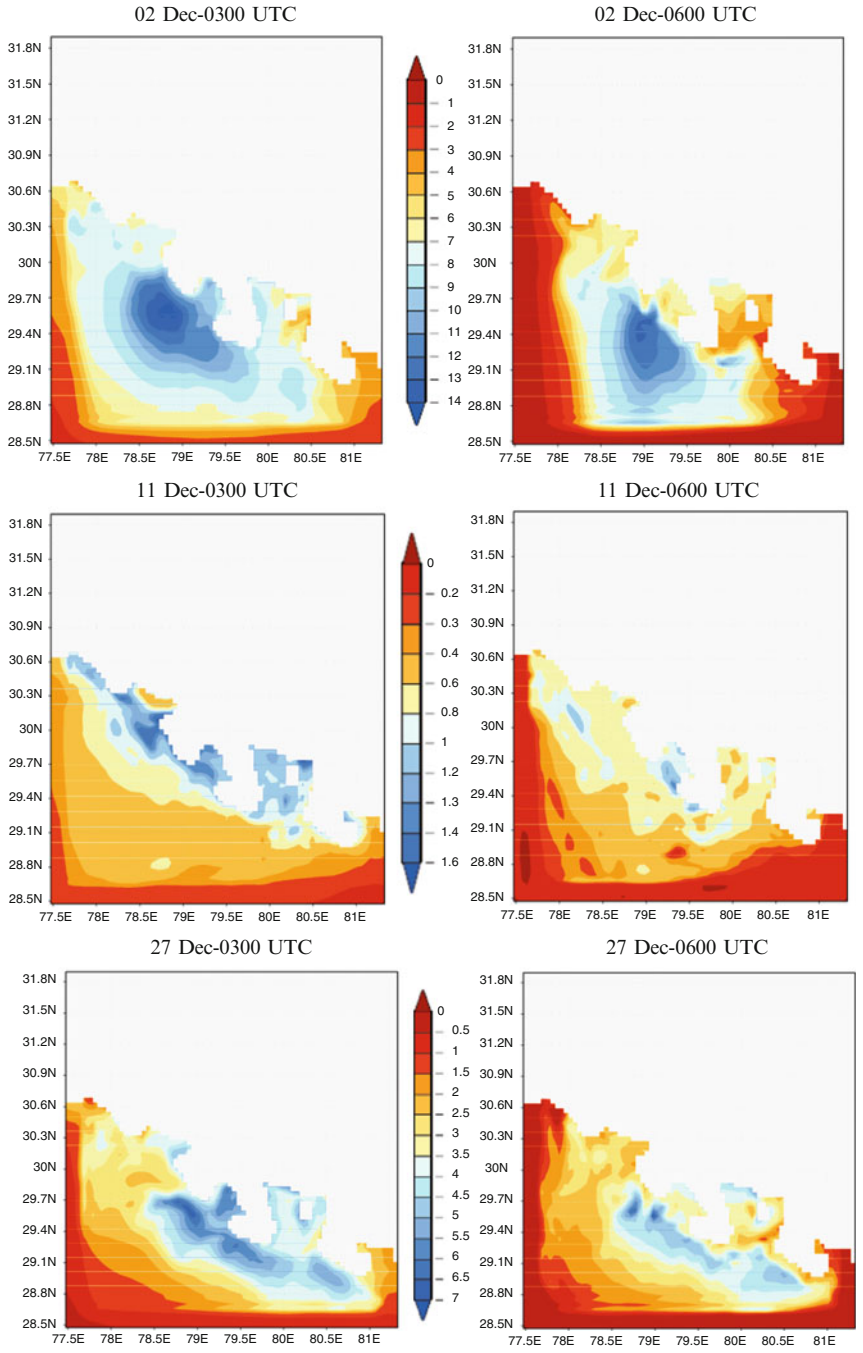


**Fig. 6.4** Horizontal distributions of dew-point temperature differences at 850 hPa between CTRL and SDA simulations

to 2–2.4 m/s between CTRL and SDA. Figure 6.4 shows that maximum and minimum spatial differences between CTRL and SDA at 850 hPa in dew point temperature are up to 14°C and 1.6°C for EXP1 and EXP2 respectively. It is seen from Fig. 6.4 that SDA model simulates maximum dew point temperature than CTRL in all three experiments. Spatial difference of relative humidity at 850 hPa is maximum up to 15% in EXP1. From all the three experiments it is seen that SDA simulates maximum values of relative humidity than CTRL simulations at both 0300 and 0600 UTC.

### *6.5.2 Analysis at 500 hPa*

Figures 6.5 and 6.6 depict the differences in wind speed and dew point temperature at 500 hPa in each experiment. Here also the difference is calculated by simply subtracting the model simulations of SDA from those of CTRL model simulation at each 3 h model output for each described parameters. The spatial differences in dry-bulb temperature and relative humidity are also analyzed at 500 hPa but the figures are not shown. It is seen that the maximum and minimum differences in the dry-bulb temperature at 500 hPa are up to 1.5°C and 0.5°C in EXP2 and EXP3 respectively. Similarly Fig. 6.5 shows that the differences in wind speed at 500 hPa are maximum up to 6 m/s in case of EXP1 and 2 and the minimum is 1.5 m/s in EXP3. It is seen from Fig. 6.5 that the differences in wind speed in each experiment are comparatively less at 0600 UTC than at 0300 UTC. The results are very good at 850 hPa level. Figure 6.6 depicts that the maximum differences in dew point temperature are up to 30°C in EXP2 and 3 and in EXP1 it is 16°C. Also in Fig. 6.6 the differences in dew point temperature is comparatively less at 0600 UTC than at 0300 UTC. It is also found that the differences in relative humidity at 500 hPa are maximum up to 40–50% in EXP1 and 2 and in EXP3 it is up to 30%.

## 6.6 Effect of Surface Data Assimilation on Vertical Structures of Meteorological Variables

In this section the impact of assimilating additional surface observations on the vertical profiles of dry-bulb temperature, wind speed and dew point temperature at three selected stations such as Thal (29.45°N/80.16°E), Rishikesh (30.04°N/78.15°E) and Newtehri (30.22°N/78.26°E) has been examined. Figure 6.7 depicts the variations in vertical profiles of wind speed between CTRL and SDA simulations in EXP1 and 2. It is seen that there is a maximum variation up to 2 m/s at lower level of the atmosphere and the variations are distinctly visible up to 700 hPa. From Fig. 6.7b, it is seen that at Newtehri the variations in vertical profiles of wind speeds are significant up to 600 hPa. In Fig. 6.8 there are noticeable

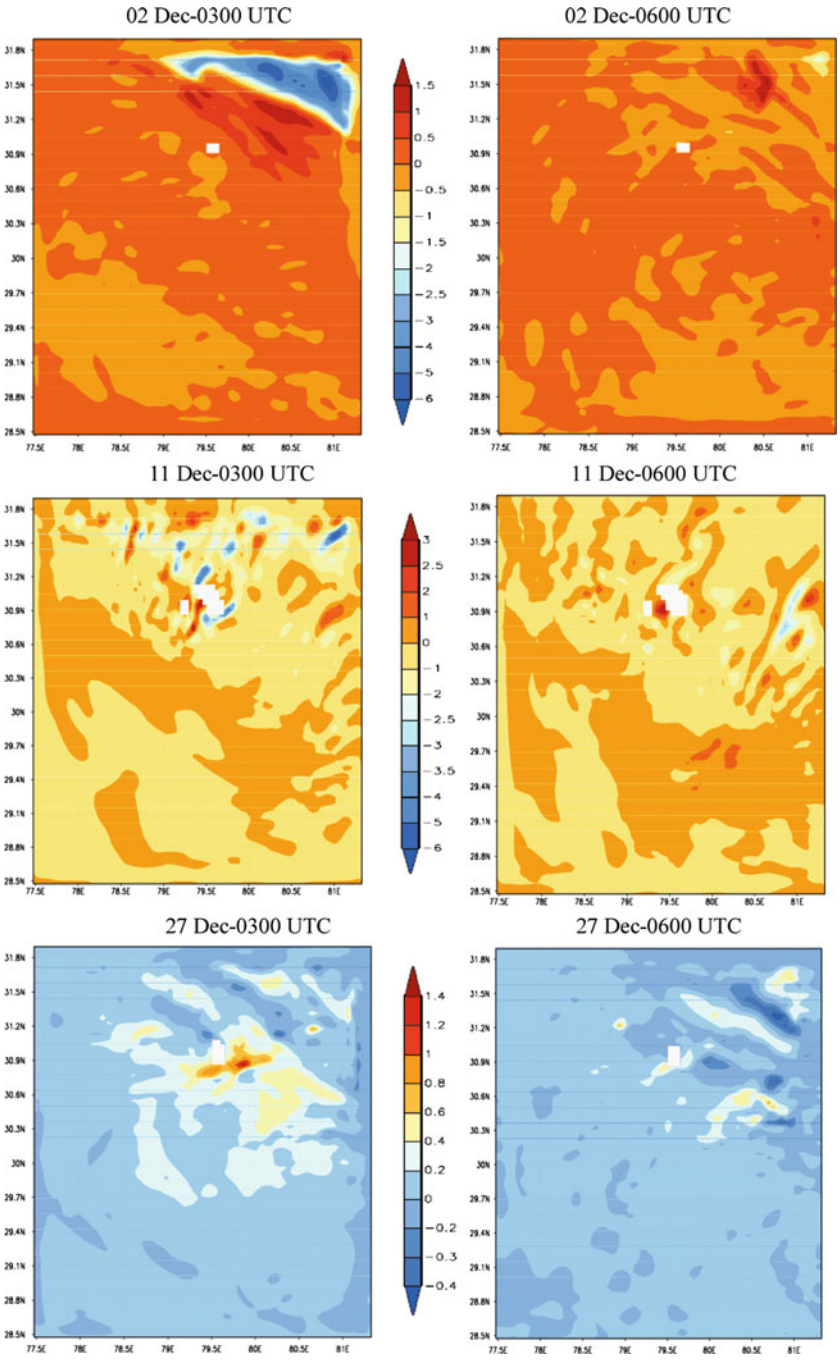


**Fig. 6.5** Horizontal distributions of wind speed differences at 500 hPa between CTRL and SDA simulations

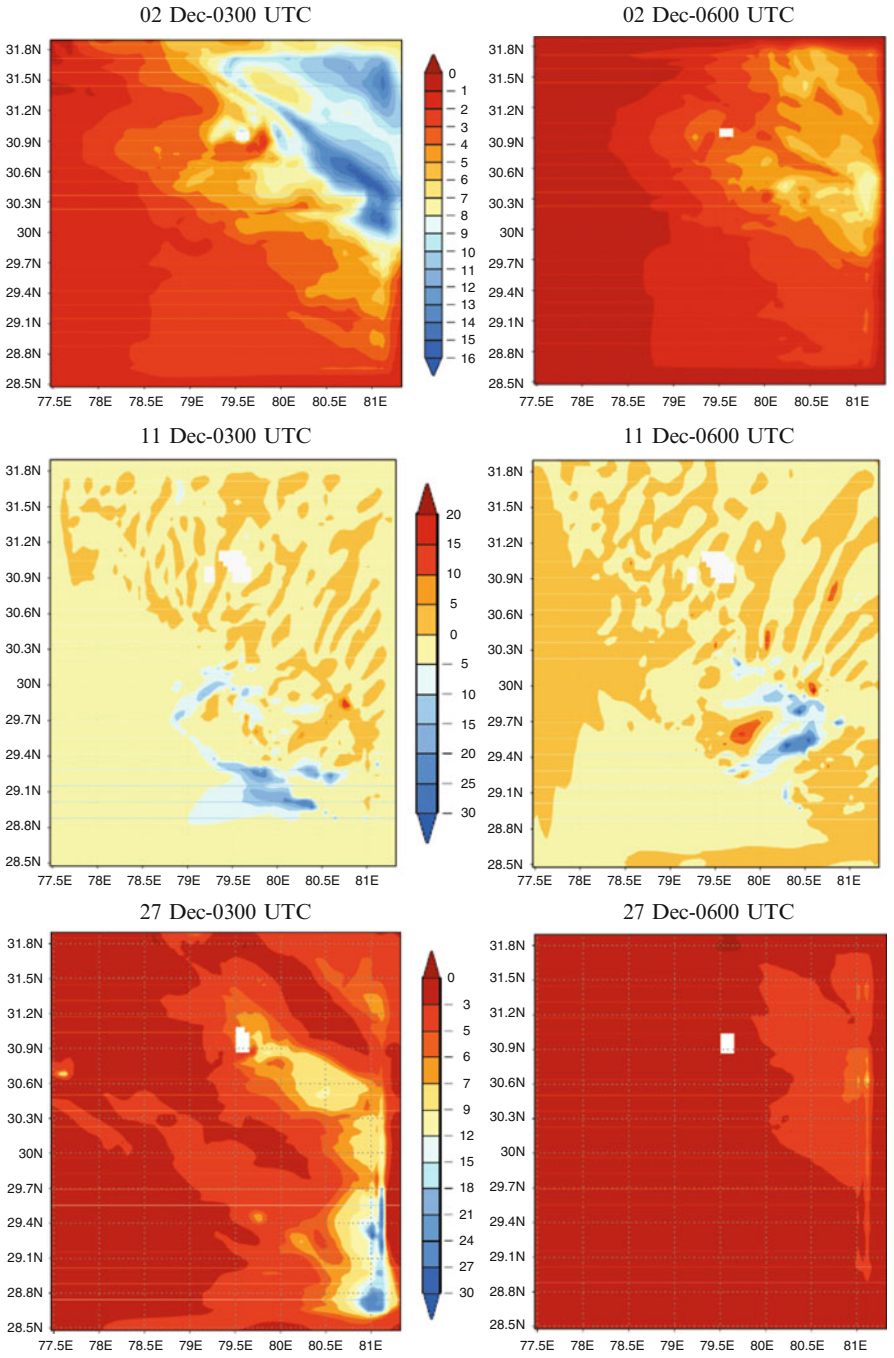


**Fig. 6.6** Horizontal distributions of dew-point temperature differences at 500 hPa between CTRL and SDA simulations

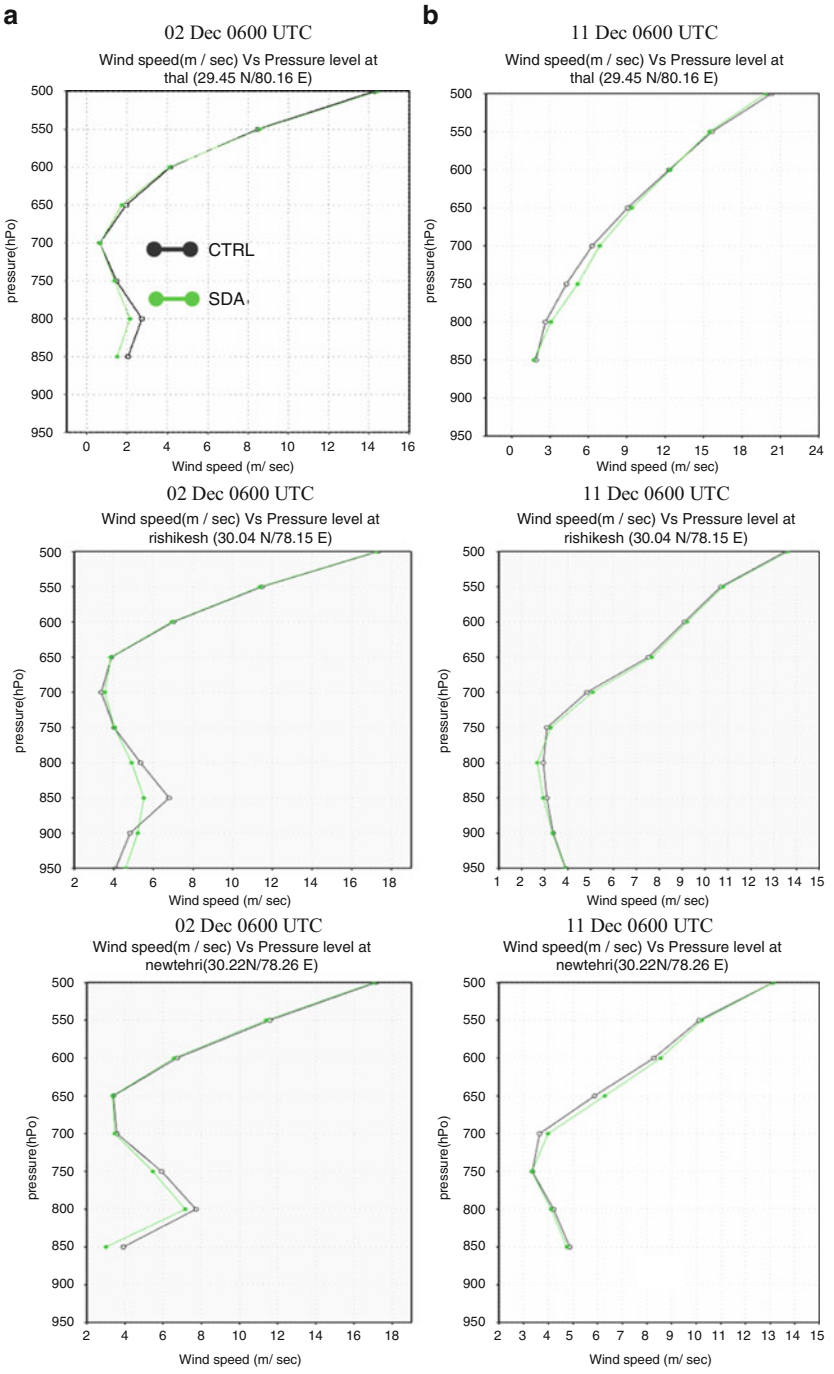


**Fig. 6.7** Comparison of vertical profiles of wind speeds in (**a**) EXP1 (02 Dec–03 Dec 2006) and (**b**) EXP2 (11 Dec–12 Dec 2006) between CTRL and SDA simulations

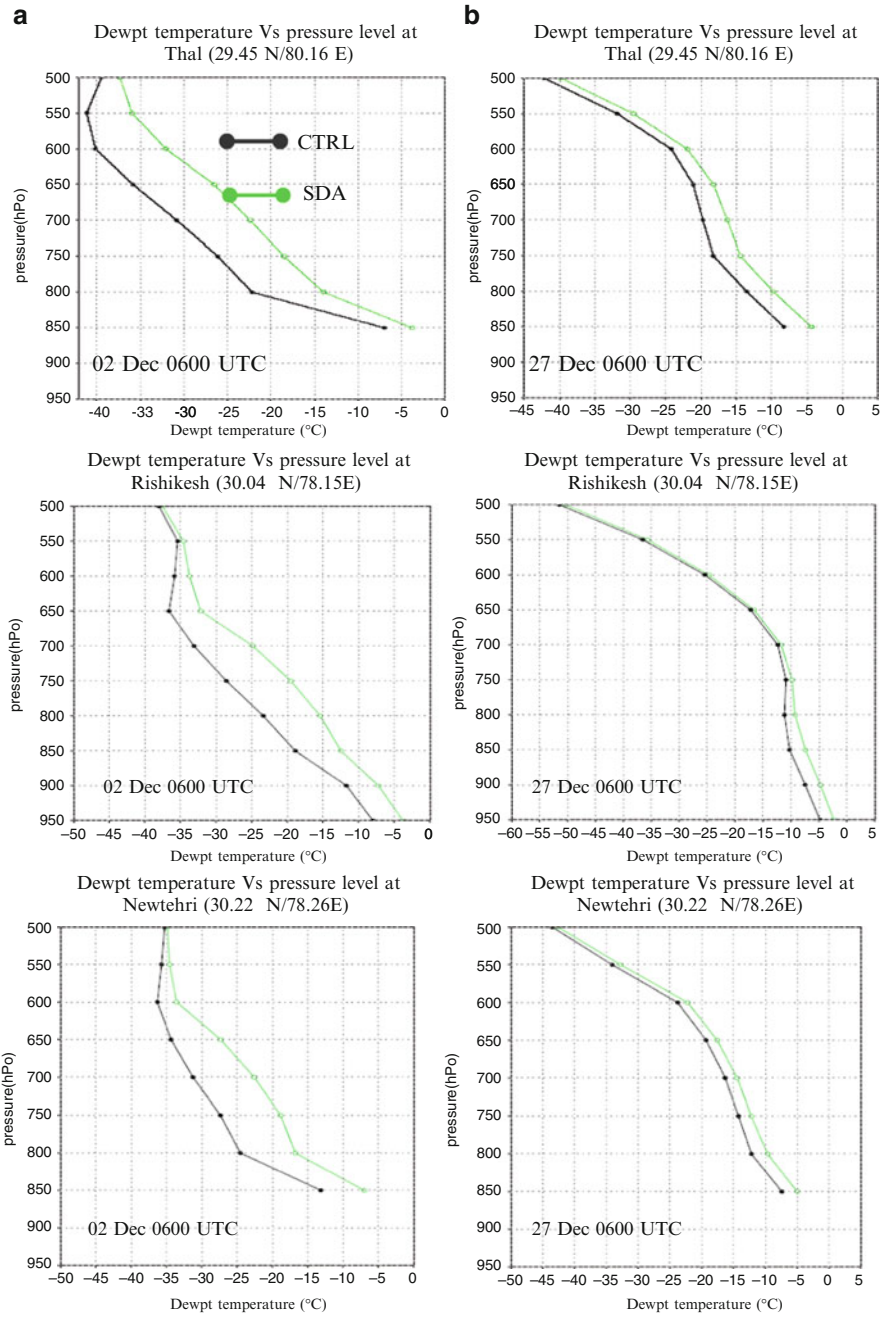


**Fig. 6.8** Comparison of vertical profiles of dew point temperatures in (**a**) EXP1 (02 Dec–03 Dec 2006) and (**b**) EXP3 (27 Dec–28 Dec 2006) between CTRL and SDA simulations

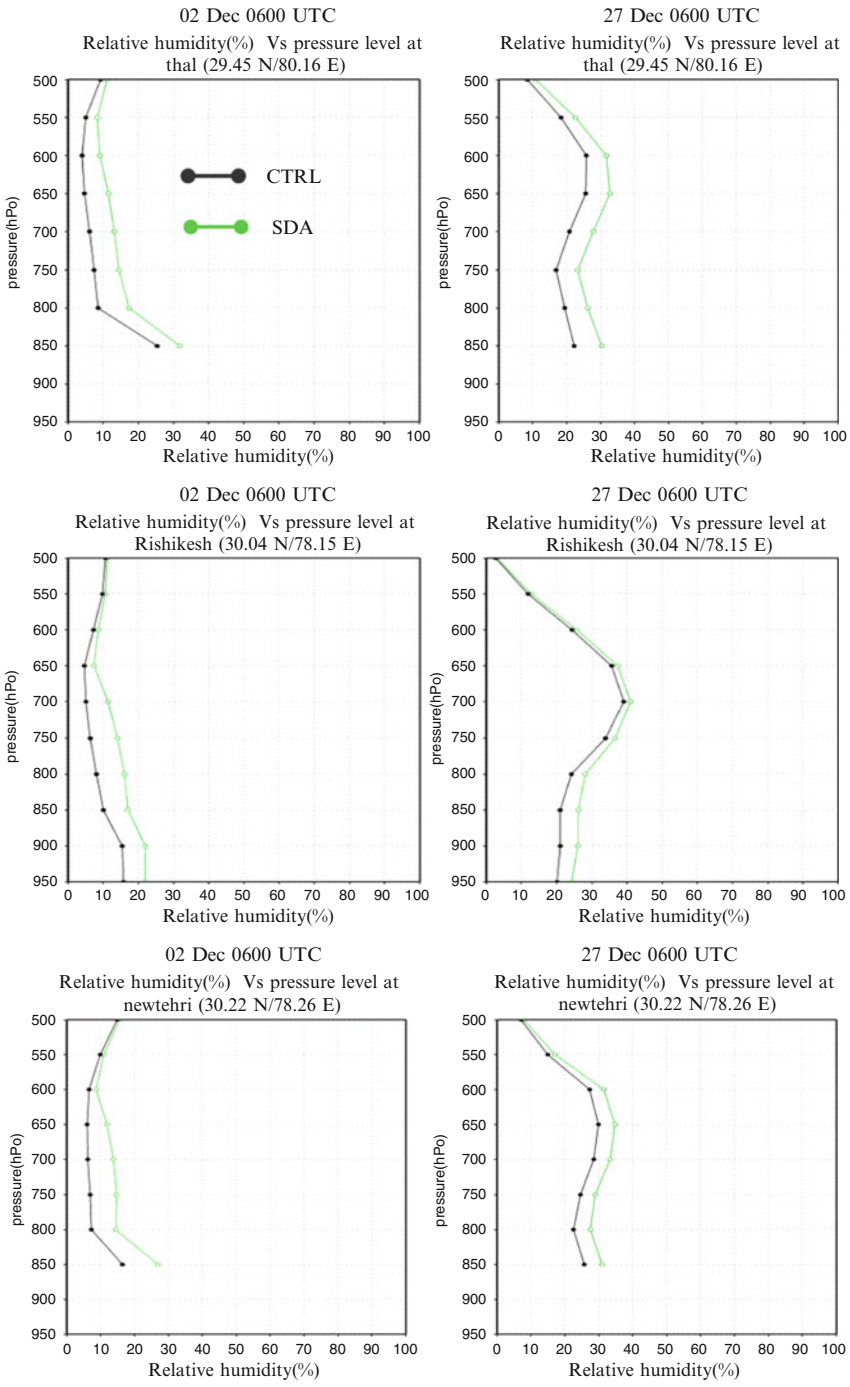


**Fig. 6.9** Comparison of vertical profiles of Relative humidities in (**a**) EXP1 (02 Dec–03 Dec 2006) and (**b**) EXP3 (27 Dec–28 Dec 2006) between CTRL and SDA simulations

variations in the vertical profile of dew point temperatures at all the selected stations of EXP1 and 3. It may be noted that results of all the three experiments are analyzed, but figures of EXP2 are not shown to save space. The variations of dew point temperature are about 5°C at the surface in EXP1 and it is comparatively less in EXP3. It is found that the variation in vertical profiles of dew point temperature in EXP2 is less compared to other two experiments. In Fig. 6.9 there are also noticeable variations in the vertical profiles of relative humidity and the maximum variation is up to 10% at the surface level at all three stations in EXP1 and 3 and gradually decreases towards the upper atmosphere. In case of relative humidity also the results of all the three experiments are examined, but figures of EXP2 are not shown. It is found from EXP2 that the difference in vertical profiles of relative humidity between CTRL and SDA is maximum up to 5% at the surface level which is comparatively less than the other two experiments and it also gradually decreases towards the upper level of the atmosphere. It may be noted that there is very less difference in dry-bulb temperature at the surface level between CTRL and SDA simulations. It is found that the maximum differences in dry-bulb temperature obtained in EXP1 are up to 0.6°C and 0.5°C at Rishikesh and Newtehri respectively.

## 6.7 Conclusions

This study has been conducted to examine the impact of assimilating additional surface observations over Uttarakhand state of India in a high resolution WRFV2.2 model by using 3DVAR data assimilation technique. The impacts on the horizontal and vertical distributions of dry-bulb temperature, wind speed, dew point temperature and relative humidity are examined in detail. Results indicate that there are some noticeable differences between the simulated fields obtained from CTRL and SDA runs. Analysis of the vertical profiles of the meteorological parameters at three different stations indicate significant differences in dew point temperature, relative humidity and wind speed after 3DVAR data assimilation. But in case of dry-bulb temperature profiles the difference is comparative less. There is a maximum improvement of 24.6% in temperature at Rishikesh and also a maximum of 30.6% in case of wind speed at Newtehri. Results also show that the improvements are quite large in dew point temperature and relative humidity with maximum of up to 52% and 62% respectively. Based on the above results it is inferred that additional surface data, when assimilated into a high resolution regional model are able to improve the simulations of meteorological parameters. The performance of 3DVAR assimilation may further improve by continuous assimilation of surface observations, not only at initial time but also at different time steps throughout the integration.

## References

Alapaty K, Seaman NL, Niyogi DS, Hanna AF (2001) Assimilating surface data to improve the accuracy of atmospheric boundary layer simulations. J Appl Meteorol 40:2068–2082

Alapaty K, Niyogi DS, Chen F, Pyle P, Chandrasekhar A, Seaman N (2008) Development of the flux-adjusting surface data assimilation system for mesoscale models. J Appl Meteorol Climatol 47:2331–2350

Barker DM, Huang W, Guo YR, Bourgeois A, Xiao XN (2004) A three-dimensional variational data assimilation system for MM5: implementation and initial results. Mon Weather Rev 132:897–914

Bonnardot V, Cautenet S (2009) Mesoscale atmospheric modeling using a high horizontal grid resolution over a complex coastal terrain and a wine region of South Africa. J Appl Meteorol Climatol 48:330–348

DST (2007) U-PROBE Annual Data Report, Department of Science and Technology, Govt. of India, pp 147

Dudhia J (1989) Numerical study of convection observed during the winter monsoon experiment using a meso-scale two-dimensional model. J Atmos Sci 46(20):3077–3107

Dudhia J (2004) The weather research and forecasting model (version 2.0). In: 2nd international workshop on next generation NWP model. Yonsei University, Seoul, pp 19–23

Gallus WA, Correia J, Jankov I (2005) The 4 June 1999 derecho event: a particularly difficult challenge for numerical weather prediction. Weather Forecast 20:705–728

Grams JS, Gallus WA, Koch SE, Wharton LS, Loughe A, Ebert EE (2006) The use of a modified Ebert-Mcbride technique to evaluate mesoscale model QPF as a function of convective system morphology during IHOP 2002. Weather Forecast 21:288–306

Grell GA, Devenyi D (2002) A generalized approach to parameterizing convection combining ensemble and data assimilation techniques. Geophys Res Lett 29(14), Article 1693, 4

Lorenc AC, Ballard SP, Bell RS, Ingleby NB, Andrews PLF, Barker DM, Bray JR, Clayton AM, Dalby T, Li D, Payne TJ, Saunders FW (2000) The Met. Office global three-dimensional variational data assimilation scheme. Q J R Meteorol Soc 126:2991–3012

Mlawer EJ, Taubman SJ, Brown PD, Iacono MJ, Clough SA (1997) Radiative transfer for inhomogeneous atmospheres: RRTM, a validated correlated-k model for the longwave. J Geophys Res 102(D14):16663–16682

Noh Y, Cheon WG, Hong SY, Raasch S (2003) Improvement of the K-profile model for the planetary boundary layer based on large eddy simulation data. Bound Layer Meteorol 107:401–427

Ruggiero FH, Sashegyi KD, Madala RV, Raman S (1996) The use of surface observations in four-dimensional data assimilation in a mesoscale model. Mon Weather Rev 124:1018–1033

Stauffer DR, Seaman NL, Binkowski FS (1991) Use of four dimensional data assimilation in a limited area mesoscale model Part-II: effects of data assimilation within the planetary boundary layer. Mon Weather Rev 119:734–754

Vinodkumar V, Chandrasekhar A, Alapaty K, Niyogi D (2008a) The impacts of indirect soil moisture assimilation and direct surface temperature and humidity assimilation on a mesoscale model simulation of an Indian monsoon depression. J Appl Meteorol Climatol 47:1393–1412

Vinodkumar V, Chandrasekhar A, Niyogi D, Alapaty K (2008b) Impact of land surface representation and surface data assimilation on the simulation of an off-shore trough over the Arabian sea. Glob Planet Change. doi:10.1016/gloplacha.2008.12.004

Xavier VF, Chandrasekar A, Rahman H, Niyogi D, Alapaty K (2008) The effect of assimilation of satellite and conventional meteorological data for the prediction of a monsoon depression over India using a mesoscale model. Meteorol Atmos Phys. DOI:10.1007/s00703-008-0314-7

# Chapter 7
# An Evaluation of the Simulation of Monthly to Seasonal Summer Monsoon Rainfall over India with a Coupled Ocean Atmosphere General Circulation Model (GloSea)

**D.R. Pattanaik, Ajit Tyagi, U.C. Mohanty, and Anca Brookshaw**

**Abstract** The performance of the UK Met Office's coupled ocean-atmosphere General Circulation Model (GCM) is evaluated in simulation of summer monsoon rainfall over Indian monsoon region. The UK Met Office's Global Seasonal (GloSea) forecasting model is initialized at 0000 UTC of 1st May and integrated for a period of 6 month with 15 ensemble members to generate the model forecast. These experiments have been conducted in similar approach from 1987 to 2002 (16 years) to have monthly as well as seasonal forecast of individual year. The model simulated rainfall is compared with the verification analysis (Xie-Arkin) during the monsoon season from June to September (JJAS).

The monthly forecast climatology from June to September separately and the seasonal forecast climatology (June to September; JJAS) of rainfall are well simulated by the model with two maxima viz., one over the west coast of India and other over the head Bay of Bengal region. However, the rainfall magnitude over the west-coast of India is less in the model simulation for monthly as well as in seasonal simulation. The model has shown good skill in simulation of seasonal (JJAS) mean rainfall over the Indian monsoon region. However, a little overestimation in rainfall is noted (approximately 4%) when considered the Indian monsoon region covering the land region and surrounding oceanic regions. The pattern correlation during JJAS shows highly significant correlation coefficients (CCs) over the global tropics (0.91) and Indian monsoon region (0.82). Similarly the Root

D.R. Pattanaik (✉) • A. Tyagi
India Meteorological Department (IMD), New Delhi, India
e-mail: drpattanaik@gmail.com; ajit.tyagi@gmail.com

U.C. Mohanty
Centre for Atmospheric Sciences, Indian Institute of Technology Delhi, Hauz Khas, New Delhi 110 016, India
e-mail: mohanty@cas.iitd.ernet.in

A. Brookshaw
Met Office, Exeter, United Kingdom

S.D. Attri et al. (eds.), *Challenges and Opportunities in Agrometeorology*,
DOI 10.1007/978-3-642-19360-6_7, 

Mean Square Error (RMSE) during JJAS is found to be less (1.01) over the global tropics than the Indian monsoon region (1.68). The interannual variability of forecast ensemble mean rainfall over the Indian monsoon region shows similar behaviour with that of verification rainfall variability with Correlation Coefficient of about 0.43 during the 16 years period from 1987 to 2002. The Anomaly Correlation Coefficients (ACCs) between verification and simulated rainfall during 1987–2002 over the Indian monsoon region is quite significant (more than 0.6 during some years). Overall, it can be stated that the performance of the UK Met Office's seasonal mean simulation is reasonably good.

## 7.1 Introduction

The extended range forecast from monthly to seasonal scale in tropics is one of the most challenging tasks in atmospheric sciences. The climate forecasting of precipitation in monthly to seasonal scale has significant implication in policy planning and national economy for the agro-economic country like India. The Indian summer monsoon rainfall forecasting in long-range has been initiated more than a century ago (Blanford 1884). The methods include; statistical, empirical and dynamical. In last few decades, many statistical (Shukla and Mooley 1987; Gowariker et al. 1991; Sahai et al. 2003) as well as dynamical (Palmer et al. 1992; Chen and Yen 1994; Sperber and Palmer 1996; Soman and Slingo 1997; Shukla et al. 2000; Saha et al. 2006; Pattanaik and Kumar 2010) models have been developed for the seasonal prediction of precipitation. The scientific basis of these dynamical seasonal forecasting is that, in tropics, the lower-boundary forcing (sea surface temperature (SST), sea-ice cover, land-surface temperature and albedo, vegetation cover and type, soil moisture and snow cover etc.), which evolve on a slower time-scale than that of the weather systems themselves, can give rise to significant predictability of statistical characteristics of large-scale atmospheric events (Charney and Shukla 1981). Several observational and modelling studies (Charney and Shukla 1981; Palmer and Anderson 1994) provide evidence that boundary forcing in the tropics contribute significantly to the internal variability of the tropical as well as monsoon circulations. Atmospheric General Circulation Models (AGCM) and Global Coupled GCMs (CGCMs) are the main tools for dynamical seasonal scale prediction. Though in dynamical model, significant improvement has been made through the improvement of the model physics and dynamics in last few years, but present day AGCM could not able to simulate mean and interannual variability of Indian summer monsoon very successfully (Kang et al. 2002). It is also found that the skill of the AGCM is poorer in simulating Indian monsoon; probably this is due to lack of proper representation of realistic sea surface temperature (SST). In recent years, it is found that the forecast errors in the seasonal prediction can be reduced through the combinations of the ensemble members forecast (Brankovic et al. 1990; Brankovic and Palmer 1997). Therefore, the focus is now mainly on multi-model ensemble/super ensemble forecast (Krishnamurti et al. 1999; Wu et al. 2002;

Wang et al. 2004 and Chakraborty and Krishnamurti 2006) for the seasonal and interannual prediction of monsoon. The methods like simple ensemble mean (Peng et al. 2002; Pavan and Doblas-Reyes 2000; Doblas-Reyes et al. 2000; Stephenson and Doblas-Reyes 2000; Palmer et al. 2004), regression improved ensemble mean (Peng et al. 2002; Kharin and Zwiers 2002), bias removed ensemble mean (Kharin and Zwiers 2002) and the multi model super ensemble (Krishnamurti et al. 1999) are included in the ensemble forecast. One approach is to generate the ensemble member forecast based on combination of forecasts obtained from model with perturbed initial conditions. Lorenz (1969) demonstrated that small perturbations in the initial conditions could produce a very different result in the final states.

Now a number of operational Numerical Weather Prediction (NWP) centres and a number of climate prediction centres around the world are making climate prediction at seasonal scale using AGCMs and global coupled GCMs. Seasonal forecasting group, Met Office, UK is one of them. It can be mentioned here that a project was initiated for the Development of a European multi-model ensemble system for seasonal to inter-annual prediction (DEMETER) by generating retrospective forecasts (or simulations) as part of the EU project DEMETER (Palmer et al. 2004). The main objective of the project was to develop a well-validated European coupled multi-model ensemble forecast system for reliable seasonal to interannual prediction. In this paper, comparative study of the seasonal mean and interannual variability of Indian summer monsoon rainfall obtained from UK Met Office's Global Seasonal (GloSea) forecasting model during the summer monsoon season from June to September (JJAS) has been carried out by taking 15 member ensemble forecast for 16 years (1987–2002). The rainfall for verification analysis is obtained from the global monthly precipitation using gauge observations, satellite estimates and numerical model outputs (Xie and Arkin 1996).

## 7.2 Details of Model and Model Products

The model hindcast is based on GloSea model, which is similar to the HadCM3 climate version of the Met Office Unified Model, with a number of improvements for seasonal forecasting purposes. Details of the model physics and discussion of the performance of HadCM3 can be found in Gordon et al. (2000). The atmospheric component is version HadAM3 (Pope et al. 2000), with a horizontal resolution of 3.75° east-west and 2.5° north-south and 19 vertical levels. The oceanic component has 40 vertical levels (compared to 20 in HadCM3) with zonal grid spacing at 1.25° and meridional grid spacing of 0.3° near the equator increasing to 1.25° pole ward of the mid-latitudes (compared to 1.25° resolution east-west and north-south in HadCM3). A coastal tilting scheme has been included, to enable specifications of the land-sea mask at the ocean resolution. Like HadCM3, the GloSea coupled GCM contains no flux corrections or relaxations to climatology. The model is initialized at 0000 UTC of 1st May and integrated for a period of 6 months in each year separately during the 16 years from 1987 to 2002. These experiments have been

carried out in similar approach from 1987 to 2002 (16 years) to obtain monthly as well as seasonal forecast of individual year. Each year simulation consists of 15-member ensemble. The GloSea model simulated precipitation is validated with the verification analysis rainfall obtained from the Xie-Arkin (1996) in the corresponding month/season of same years. The different verification methods used here are the correlation coefficient (CC), anomaly correlation co-efficient (ACC) and root mean square error (RMSE).

Initial ocean conditions for the GloSea simulations are obtained by forcing the ocean component with momentum, heat and fresh water fluxes from the ECMWF ERA40 reanalysis. The method described by Palmer et al. (2004) has been used to generate perturbed initial conditions for the ensemble members. Sets of wind stress and SST perturbations, designed to represent observed uncertainties in these parameters, are pre-defined using historical differences between quasi-independent analysis datasets. A series of wind stress perturbations, sampled from the pre-defined set, is applied with positive and negative signs to the ERA40 momentum fluxes and used in the ocean assimilation. In each simulation, instantaneous SST perturbations from the predefined set are added to each of the assimilation sequences to obtain a 15-member ensemble (Graham et al. 2005). The SST perturbations are added to the temperature field in the top 40 m of the ocean. Thus, perturbations are applied to the ocean initial state only, with unperturbed ERA40 analyses being used to initialize the model atmosphere and land components. The perturbations are devised such that all the resulting members (perturbed or not) are equally likely descriptions of the system.

## 7.3 Results and Discussion

The performance of numerical models can be evaluated by comparing model-simulated parameters with the observations. Therefore, it is very important and must to have observations for the verifications of the model performance. India Meteorological Department (IMD) has a good observational network of rainfall observations mainly spaced over land. On the other hand, numerical models simulate rainfall over land as well as over water body (over the whole domain of interest). Rajeevan et al. (2006) has recently generated a high resolution ($1^\circ \times 1^\circ$ lat./long.) gridded daily rainfall dataset for the Indian land region based on IMD observations. Xie and Arkin (1996) had made an attempt to merge and reproduce rainfall distributions over land and ocean with the use of surface observations, satellite data, buoys data and outputs from numerical models (GCM). Initially the observed gridded rainfall obtained from IMD is compared with the Xie-Arkin rainfall over Indian landmass to test the reliability of the Xie-Arkin rainfall to be used for evaluation of the performance of the GloSea model in simulation of rainfall during summer monsoon over India.

### 7.3.1 *Comparison of Xie-Arkin Rainfall with IMD (Observed) Rainfall*

Figures 7.1 and 7.2 show the monthly climatology (during 1987–2002) of rainfall for June, July, August and September obtained from IMD and Xie-Arkin respectively. The two maxima viz., one over west coast of India and other over the north east India as reported in observed rainfall in June (Fig. 7.1a) is matching well over the land region in Xie-Arkin rainfall (Fig. 7.2a). Similarly the active monsoon months of July and August with more rainfall (more than 7 mm/day) over the central India as reported in observed rainfall Fig. 7.1b, c is also well captured in Xie-Arkin rainfall (Fig. 7.2b, c). The retreat phase of monsoon in September with

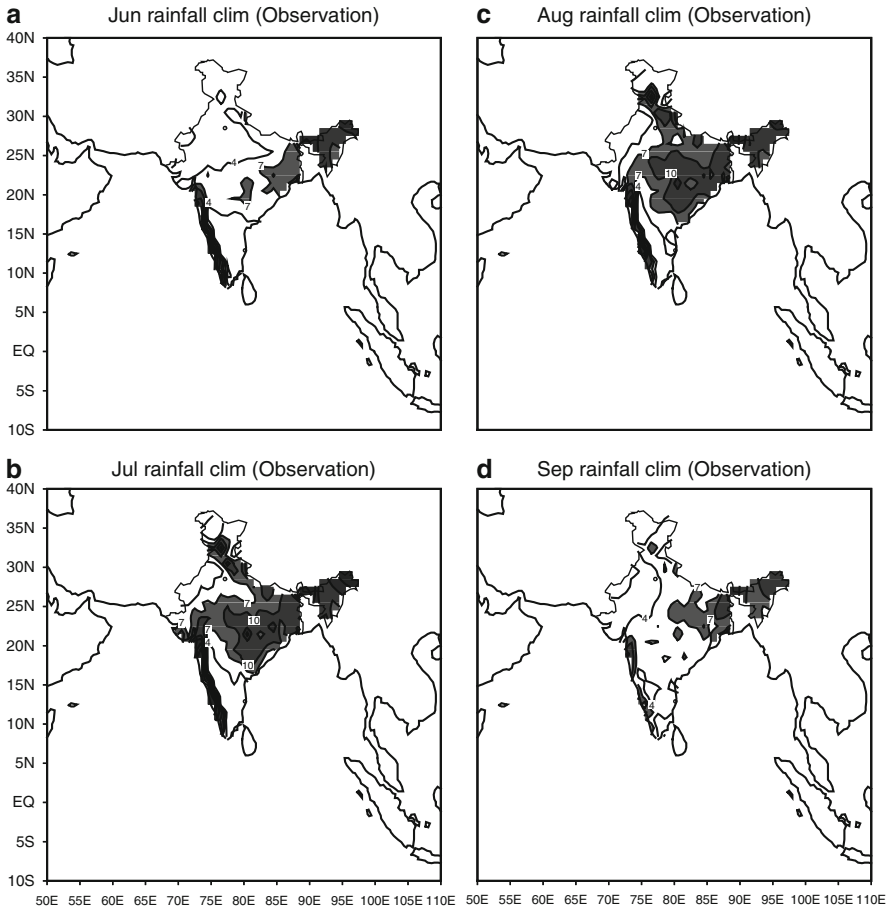


**Fig. 7.1** Spatial monthly climatological observed rainfall distribution (mm/day) obtained from IMD for the 16 years period from 1987 to 2002 valid for (**a**) June (**b**) July (**c**) August and (**d**) September. Rainfall with more than 7 mm/day is *shaded*

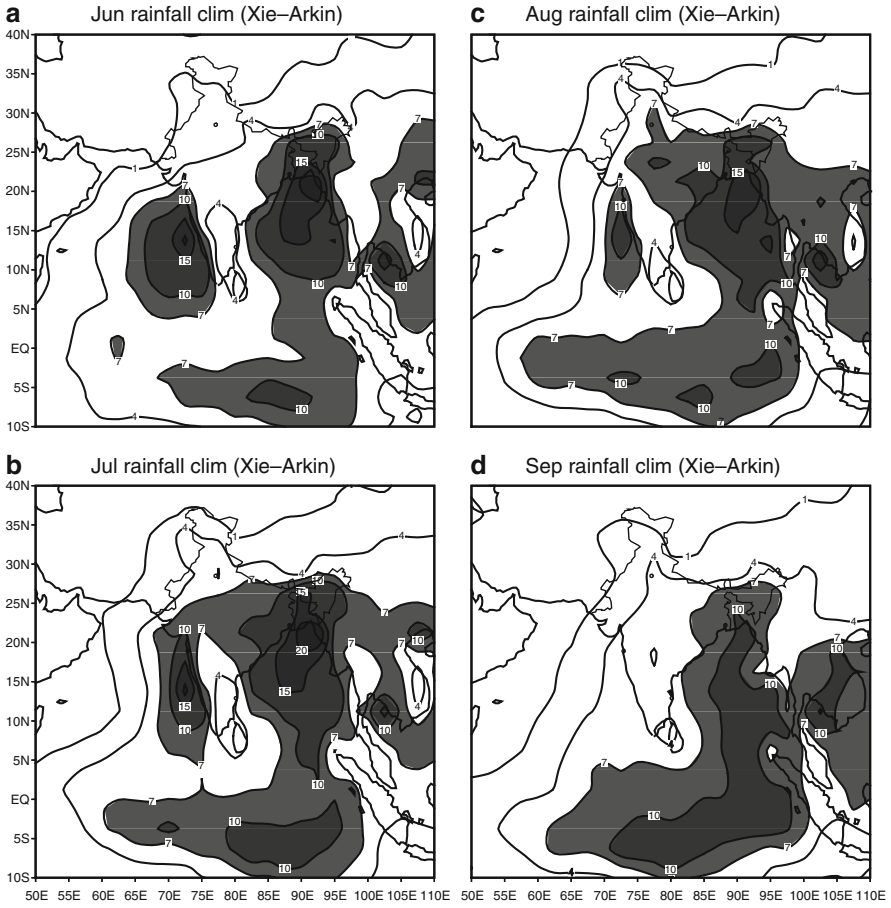


**Fig. 7.2** Spatial monthly climatological observed rainfall distribution (mm/day) obtained from the verification analysis (Xie-Arkin) for the 16 years period from 1987 to 2002 valid for (**a**) June (**b**) July (**c**) August and (**d**) September. Rainfall with more than 7 mm/day is *shaded*

less rainfall over the central part of India and more over northeast India as reported in the observation (Fig. 7.1d) is also almost identical in case of Xie-Arkin rainfall (Fig. 7.2d).

Like the monthly rainfall the seasonal observed rainfall during June to September (JJAS) as shown in Fig. 7.3a is also similar in distribution with that of mean JJAS Xie-Arkin rainfall (shown in Fig. 7.5a). Both the figures show identical maximum rainfall belt (more than 7 mm/day) over west coast of India and over the northeastern and adjoining Indo-Gangetic belt. Thus the representation of Xie-Arkin rainfall is almost identical with the observed rainfall over Indian region. Therefore, Xie-Arkin rainfall can be used for the verification purpose over the Indian monsoon region covering the Indian land mass and the surrounding areas. Hence in following sub-sections the model forecast is compared with the Xie-Arkin

rainfall analysis (Xie-Arkin) (hereafter referred as verification analysis). Over the Indian land region, the interannual variability of seasonal rainfall obtained from IMD observations showed many extreme years (Fig. 7.3b). The spatial rainfall

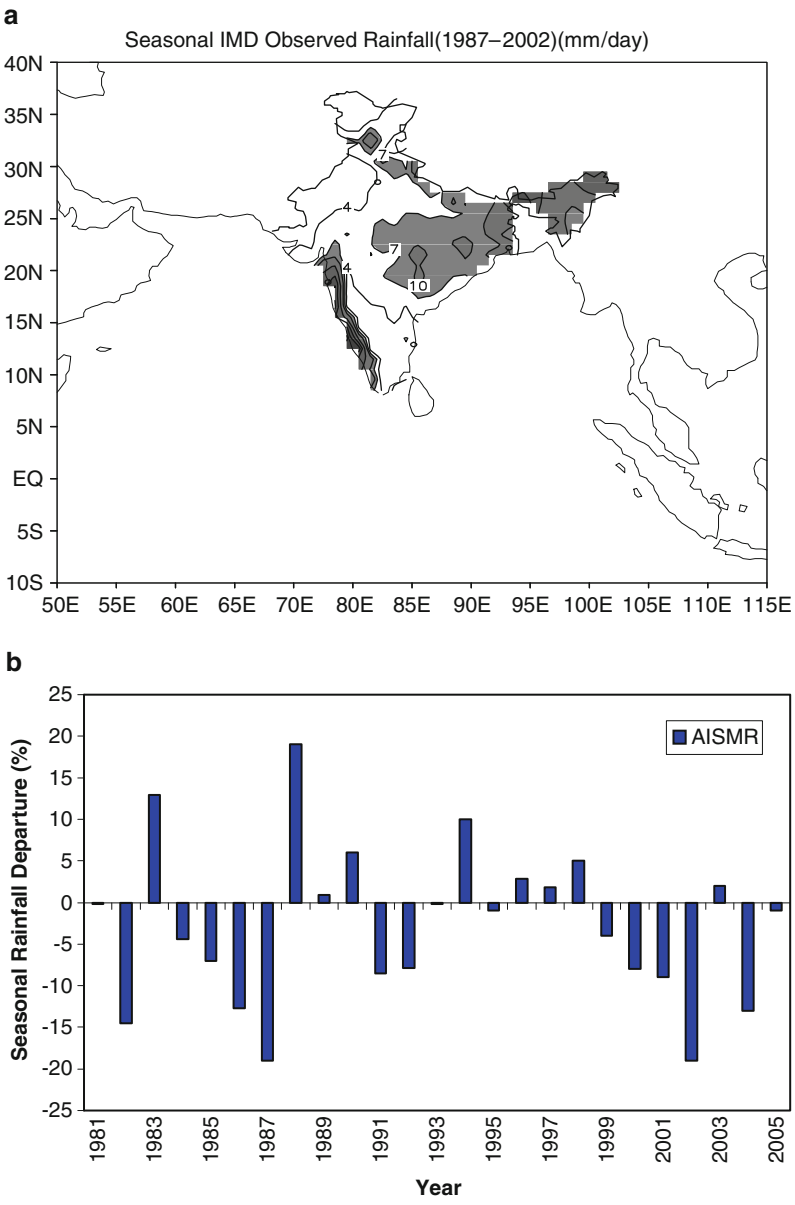


**Fig. 7.3** (**a**) Spatial monthly climatological observed rainfall distribution (mm/day) obtained from IMD for the 16 years period from 1987 to 2002 with rainfall $>$ 7 mm/day is *shaded*. (**b**) The standardised anomalies JJAS rainfall from IMD

anomaly during two contrasting year (1987 is deficit year and 1988 is excess year) and also the recent deficient year of 2002 as seen in the observed rainfall is very much identical with the Xie-Arkin rainfall (Fig. not shown).

### 7.3.2 Simulation of Mean Monsoon

The model climatology is represented here by retrospective forecasts (or "model simulations"), made with a 15-member ensemble, over the 16-year period from 1987 to 2002. Therefore, for each new forecast, there is a reference set of 240 ($15 \times 16$) simulations. As shown in Fig. 7.2 for the Xie-Arkin rainfall the corresponding spatial map of monthly means forecast rainfall from 240 members during June to September is shown in Fig. 7.4. The rainfall map plotted in Figs. 7.2 and 7.4 is in mm/day and a value more than 7 mm/day is shaded. It is seen from Figs. 7.2 and 7.4 that the forecast climatology during the month of June (Fig. 7.4a) is almost identical with verification (Fig. 7.2a) climatology with two maxima, one near the west coast of India and other over the head Bay of Bengal. However, the west coast maximum is slightly under estimated and it is confined only over smaller area at northern portion of the coast in forecast climatology (Fig. 7.4a). During the month of July the forecast climatology (Fig. 7.4b) shows similar patterns with corresponding verification climatology (Fig. 7.2b). The rainfall maxima over the head Bay of Bengal region and west coast of India and the rain shadow regions of Tamilnadu and north western part of India in the month of July are well captured in forecast climatology (Fig. 7.4b). However, the model simulation shows that the west coast maximum is under estimated and it is confined only to northern portion in forecast climatology (Fig. 7.4b) similar to the pattern of June forecast climatology (Fig. 7.4a). It is noticed that model simulated rainfall for the month of August (Fig. 7.4c) is in good agreement with the verification rainfall climatology (Fig. 7.2c) with two maxima, one over head Bay of Bengal and other over west coast of India. The two rain shadow regions such as Tamilnadu and north western India are also well simulated by the model in the month of August (Fig. 7.4c). The rainfall pattern during August is almost similar with that of July rainfall patterns, however, slight reduction in rainfall over the main land of India is noticed both in forecast (Fig. 7.4c) as well as verification climatology (Fig. 7.2c). From Fig. 7.2d it is noticed that the rainfall distribution indicate the withdrawal features of monsoon during September. During the withdrawal phase of monsoon in September the forecast climatology (Fig. 7.4d) is in close resemblance with the verification climatology (Fig. 7.2d). However, rainfall simulated with GloSea model is overestimated in the north central India over the Gangetic and Brahmaputra valley stretching from the Bay of Bengal region particularly during September and during the peak monsoon months of July, August (Fig. 7.4b–d). On the other hand, model simulated rainfall is underestimated over the west coast of India during July, August and September. Like the monthly pattern, the seasonal climatology (June to September; JJAS) from model forecast (Fig. 7.5b) shows almost similar rainfall

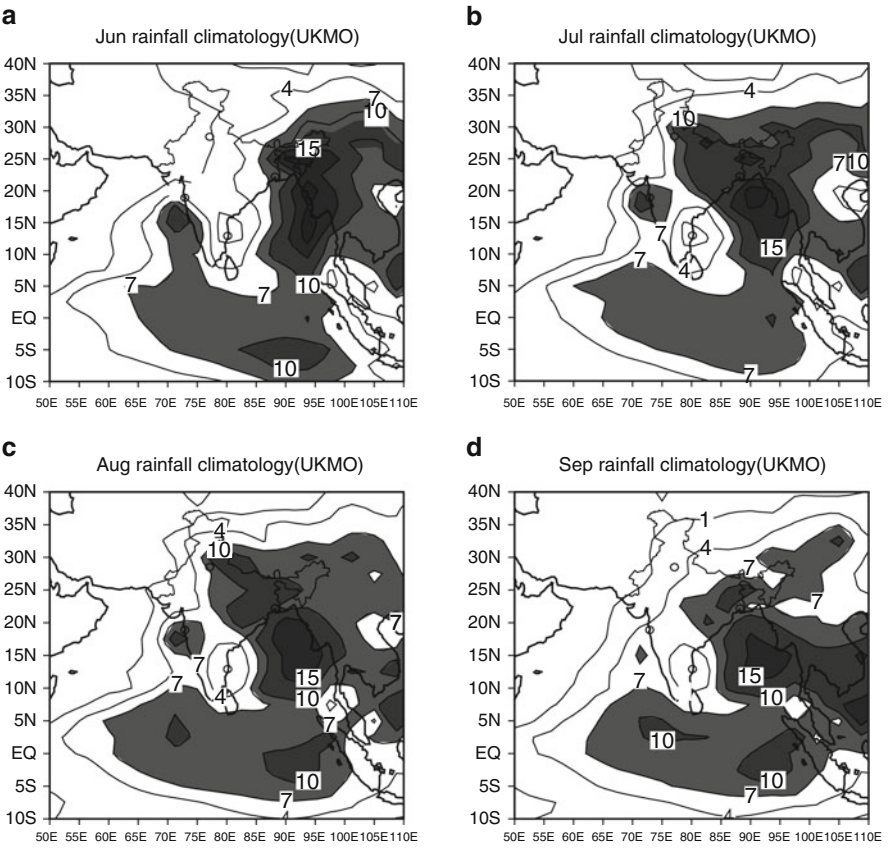


**Fig. 7.4** Spatial monthly climatological UK Met office's model forecast rainfall distribution (mm/day) for the 16 years period from 1987 to 2002 valid for (**a**) June (**b**) July (**c**) August and (**d**) September. Rainfall with more than 7 mm/day is *shaded*

distribution pattern with rainfall climatology obtained from the verification analysis (Fig. 7.5a) and is in close resemblance in terms of magnitude as well as spatial distribution. The coupled model could capture both the rainfall maxima over the west-coast of India and north Bay of Bengal region which is in good agreement with the verification analysis. Like in the monthly forecast rainfall during July to September as shown in Fig. 7.4b–d, the seasonal forecast rainfall also shows overestimation in the north central India over Gangetic and Brahmaputra valley stretching from the Bay of Bengal region. These features are shown in Fig. 7.5c by taking difference between verification and forecast rainfall over that region, which indicates negative difference over the north central India over Gangetic and Brahmaputra valley stretching from the Bay of Bengal region.

In order to study the pattern correlation of verification and model forecast output over the different regions, the seasonal (JJAS) climatology of verification analysis

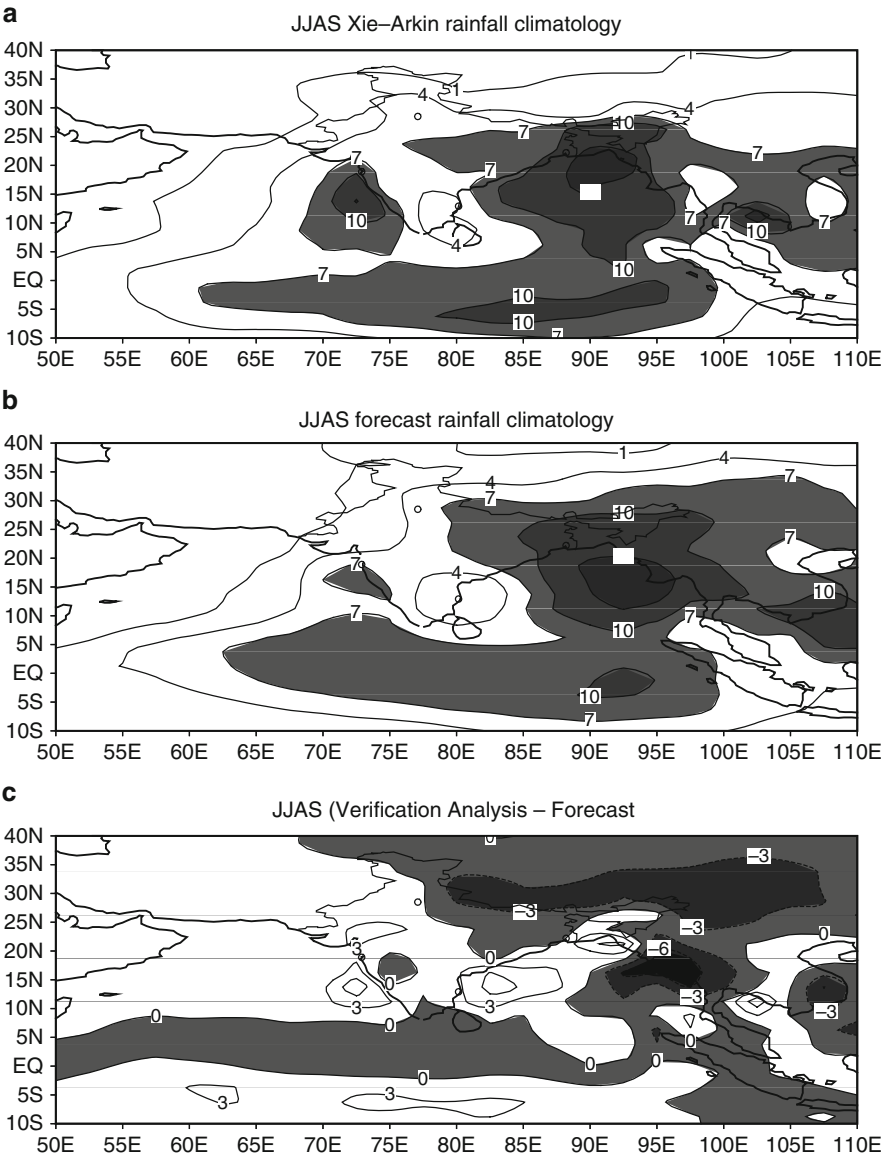


**Fig. 7.5** Spatial seasonal (June–September) climatological rainfall distribution (mm/day) for the 16 years period from 1987 to 2002 valid for (**a**) from (Xie-Arkin) (**b**) UK Met Office's model forecast and (**c**) the difference (**a**)–(**b**). Rainfall more than 7 mm/day is *shaded* in '(**a**)' and '(**b**)' and the negative values are *shaded* in '(**c**)'

is correlated with seasonal climatology of model forecast and the corresponding Correlation Coefficients (CCs) are given in Table 7.1. The CCs for 3 month forecast (June to August; JJA) is also included in Table 7.1. It is seen from Table 7.1 that the

**Table 7.1** The Correlation Coefficient (CC) and Root Mean Square Error (RMSE) between observed rainfall climatology and model hindcast climatology during the 16 years period from 1987 to 2002 for June to August (JJA) and June–September (JJAS)

| | Correlation coefficient | | RMSE (mm/day) | |
|---|---|---|---|---|
| Regions | JJA | JJAS | JJA | JJAS |
| Indian region (70°E–95°E, 5°N–35°N) | 0.72 | 0.76 | 2.56 | 2.17 |
| Indian monsoon region (50°E–110°E, 10°S–35°N) | 0.79 | 0.83 | 1.81 | 1.68 |
| Global tropics (0–360°E, 30°S–30°N) | 0.91 | 0.91 | 1.00 | 1.01 |

mean patterns show significant CC over the global tropics (0.91) followed by Indian monsoon region (0.79) and even also for the smaller Indian region (0.72). Though, the mean seasonal rainfall is slightly more in model forecast than verification, the seasonal climatology of model simulation is similar with that of verification climatology over the entire tropical belt including the Indian monsoon region.

### *7.3.3 Simulation of Interannual Variability*

The General Circulation Model (GCM) has an "average" behaviour or climatology similar to real atmosphere in large spatial and temporal scale. As model integration proceeds, there is a tendency for results to increasingly resemble the model climatology, introducing a systematic bias into the forecasts. To remove this bias, forecasts are expressed in terms of deviations from the GCM's own climatology - a process referred to as calibration. In any current prediction, the deviation of the model from its own climatology provides the forecast of how the real atmosphere is expected to deviate from real climatology.

The year-to-year variation of Indian rainfall from 1987 to 2002 indicates many extreme years and also the normal years. The standardised anomalies of Indian summer monsoon rainfall obtained from the India Meteorological Department (IMD) as shown in Fig. 7.3b indicates many extreme years during these 16 years mentioned above. Based on the criteria of $\pm 1$ Standard Deviation, 1987 and 2002 are considered to be deficit year and 1988 and 1994 are considered to be excess years during this period. In order to study the interannual variability of model simulation the year-to-year variation of JJAS total rainfall for 15-member ensemble over the entire Indian monsoon region bounded by 50°E–110°E and 10S°N–35°N from 1987 to 2002 for the verification analysis and the model forecast is illustrated in Fig. 7.6. The Indian monsoon region is considered as the study area, which is the same as chosen by Krishnamurti et al. (2004) for verification of DEMETER results. In case of model forecast the rainfall from 1987 to 2002 plotted in Fig. 7.6 is the simple ensemble mean of 15 members in each year. It is seen that the mean is more in case of model's forecast (711.7 mm) against the observation (683.4 mm). The correlation between observed and forecast rainfall plotted in Fig. 7.6 is found to be 0.43. However, over the land only region of India the seasonal mean forecast rainfall during JJAS is about 20% less compared to the observed mean JJAS rainfall

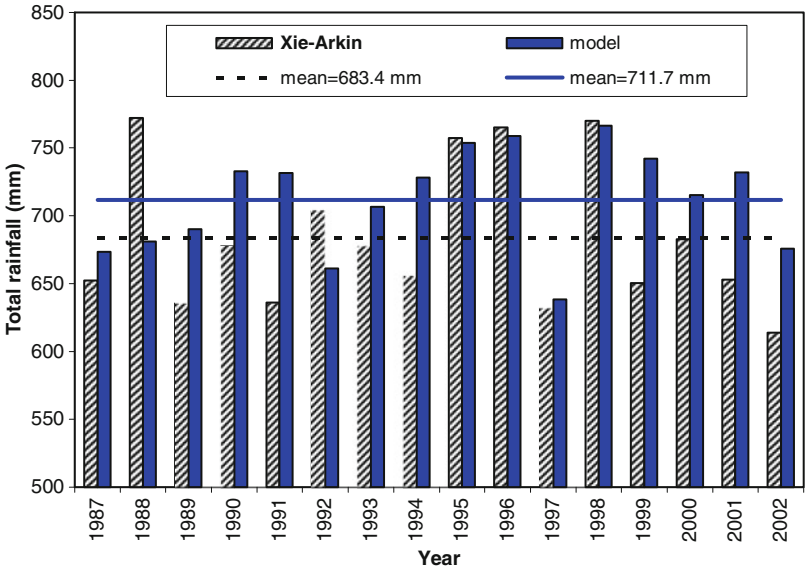


**Fig. 7.6** Year-to-year variation of mean rainfall (mm) from observation (Xie-Arkin) and Met Office's model simulations for the Indian monsoon region (50°E–110°E, 10°S–35°N) during the 16 years period from 1987 to 2002

of 889 mm obtained from IMD observation. Similarly the CC between IMD rainfall and the forecast rainfall over the land only region of India is also poor. It is also seen from Fig. 7.6 that the monsoon rainfall obtained from the model during few years such as during 1987, 1995, 1996, 1997, 1998 are very close to verification analysis. However, it is noticed from Fig. 7.6 that significant difference occurs between verification and forecast rainfall during some years (1988, 1991, 1999 and 2001). It may be mentioned here that although many earlier studies (Sperber et al. 2001; Ji and Vernekar 2000) have noted poor performance of forecasts in prediction of Asian monsoon a season in advance, the skill of the forecast shown here is hopeful since the seasonal as well as monthly forecast is well simulated in the model.

In order to study the skill of seasonal climate forecasts for individual seasons, the verification and forecast anomaly for a few recent years (1994, 1997, 1998 and 2002) have been plotted and are shown in Figs.7.7–7.10 respectively. Out of these 4 years, 1994 is an excess monsoon rainfall year with JJAS rainfall departure of +10%, 2002 is a deficient monsoon year with JJAS rainfall departure of −19% and 1997 & 1998 are normal years with JJAS rainfall departure of +2% and +5% respectively. While plotting these anomalies a local linear bias correction is applied (a posteriori) by expressing the forecasts relative to the model climatology, as defined from 225 realizations (15 × 15 members). In all cases, the cross-validation technique is used, in which the (15-year) reference climatology for each simulation is constructed without the year of the simulation itself. Cross-validation simulates typical real-time operational practice of using a fixed period for the reference model

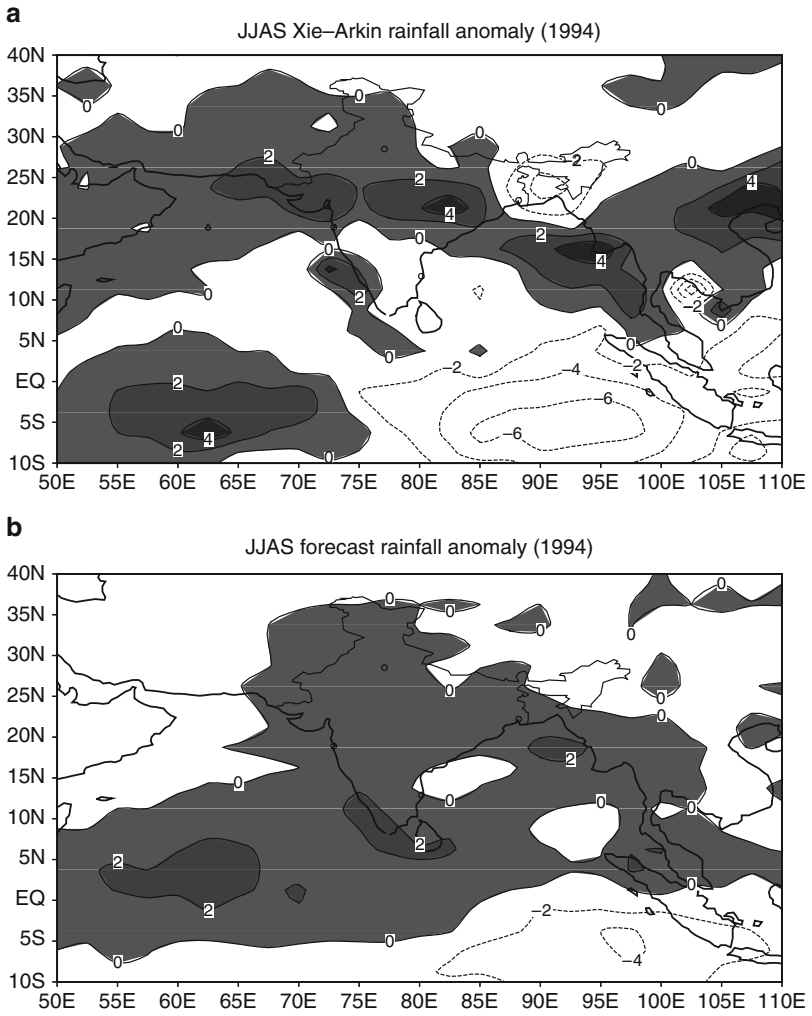


**Fig. 7.7** Seasonal (June–September; JJAS) rainfall anomalies (*positive anomalies are shaded*) for 1994 in mm/day valid for (**a**) observation (Xie-Arkin) (**b**) UK Met Office's model forecast

climatology, which does not extend to the current forecast year, and therefore provides a more faithful representation of real-time skill. The rainfall received over India during the monsoon season (JJAS) in 1994 is excess which is also indicated by the verification JJAS rainfall anomaly (Fig. 7.7a). The rainfall obtained from the model forecast also shows large positive anomalies over most parts of the country during monsoon season in 1994 (Fig. 7.7b). It is found that many El Nino years are associated with negative rainfall departure over India but one strong El Nino year of 1997 is associated with positive departure of rainfall (Fig. 7.3b). Slingo and Annamalai (2000) while examining the response of Indian summer

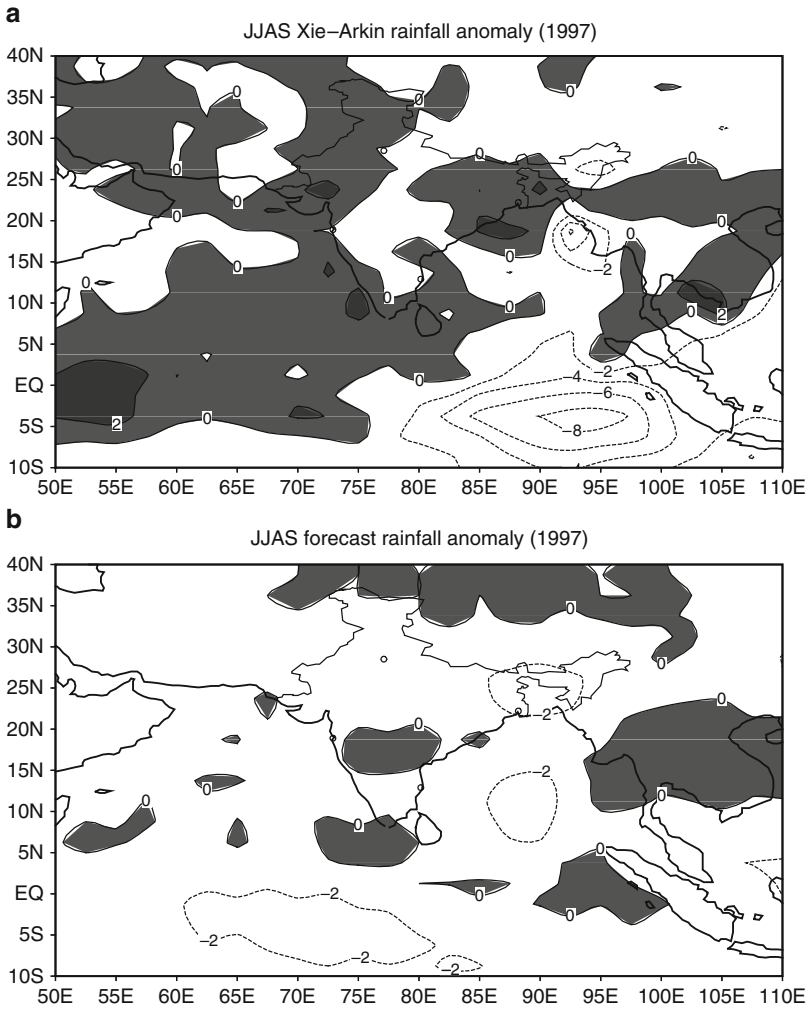


**Fig. 7.8** Seasonal (June–September; JJAS) rainfall anomalies (*positive anomalies are shaded*) for 1997 in mm/day valid for (**a**) observation (Xie-Arkin) (**b**) UK Met Office's model forecast

monsoon to the major El Nino, they found that sea surface temperature (SST) anomalies associated with strong El Nino do not always affect the Indian monsoon rainfall in the same manner like the year 1997 when the monsoon rainfall was above normal over many parts of India (Fig. 7.8a). However, the forecast anomaly for the year 1997 shows negative anomalies over most parts of the country (Fig. 7.8b). Followed by the El Nino year of 1997, the year 1998 was moderate La Nina year and the monsoon rainfall over India was with positive departure of rainfall (Fig. 7.3b). The verification rainfall during 1998 shows positive departure over northeast India, northern India, west coast of India and southern peninsular India

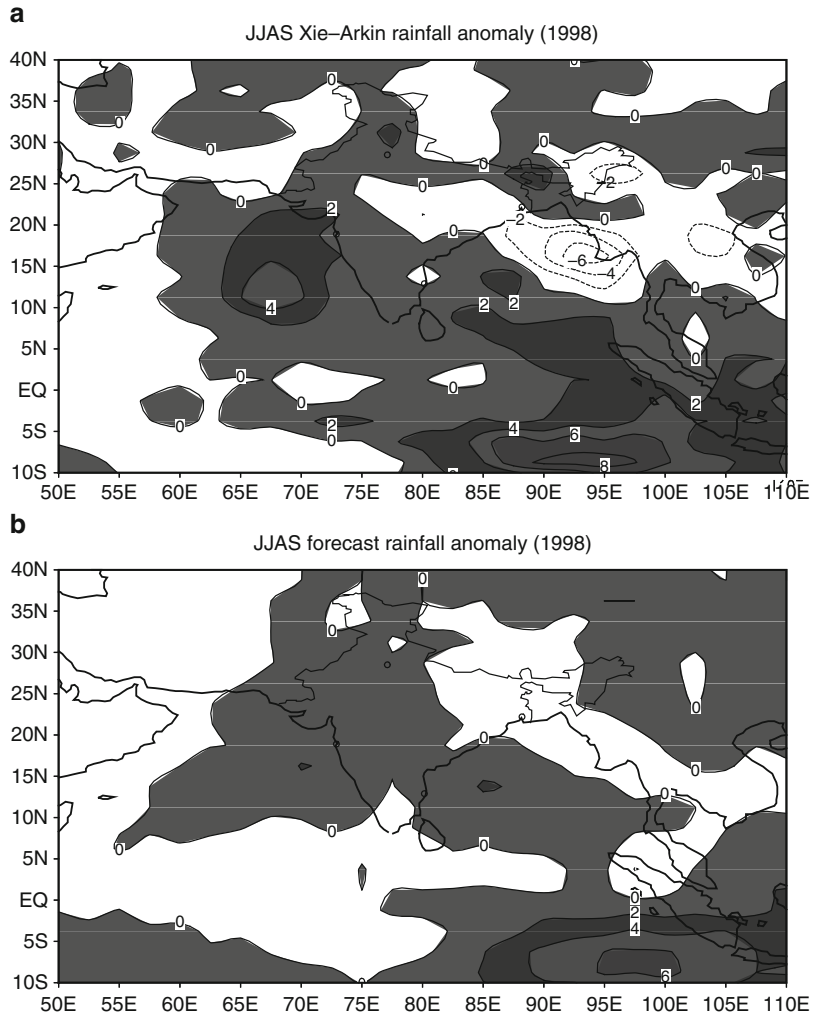


**Fig. 7.9** Seasonal (June–September; JJAS) rainfall anomalies (*positive anomalies are shaded*) for 1998 in mm/day valid for (**a**) observation (Xie-Arkin) (**b**) UK Met Office's model forecast

(Fig. 7.9a). In case of forecast departure (Fig. 7.9b) the patterns are in well agreement with that of observed anomaly (Fig. 7.9a) over most parts of India except some parts of northeast India. During the recent deficient year of 2002, the verification rainfall departure is negative over the entire country except some parts of north east India (Fig. 7.10a). It may be mentioned here that none of the global model could able to predict this large deficiency of rainfall over India during 2002. The model forecast here could able to show negative departure over most parts of the country (Fig. 7.10b). However, a belt of excessive rains in the interior of India over the Gangetic and Brahmaputra valley persists in forecast departure

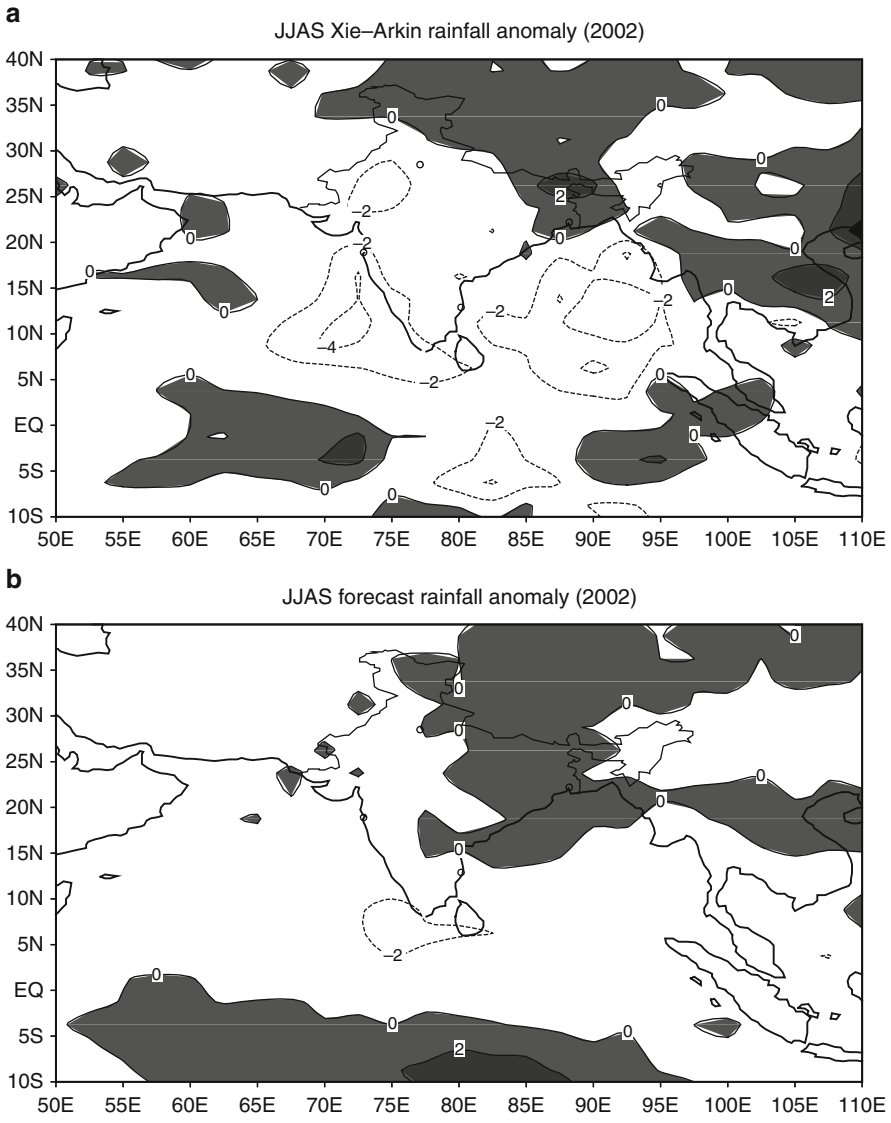


**Fig. 7.10** Seasonal (June–September; JJAS) rainfall anomalies (*positive anomalies are shaded*) for 2002 in mm/day valid for (**a**) observation (Xie-Arkin) (**b**) UK Met Office's model forecast

(Fig. 7.10b) though it is not seen in verification anomaly. As shown earlier similar patterns of excessive rainfall belts over the Gangetic and Brahmaputra valley also persists in the model forecast during July to September on monthly scale (Fig. 7.2) and during the season as a whole (Fig. 7.5b). In another contrasting El niño and La niña years of 1987 and 1988 (Fig. not shown), the rainfall anomalies obtained from the model forecast is in close resemblance with the verification anomalies over

India in El Nino year of 1987 whereas, the excess monsoon rainfall of 1988 is not captured well in the model.

### *7.3.4 Precipitation Forecast Skill*

The skill of seasonal anomaly forecast has been evaluated on year-to-year from 1987 to 2002 based on the Anomaly Correlation Coefficient (ACC) and Root Mean Square Error (RMSE) between verification and forecast rainfall over the Indian monsoon region and global tropics. The ACC and RMSE on year-to-year basis have been calculated and are shown in Figs. 7.11 and 7.12 respectively. In addition, ACC calculated for June to September (JJAS) and June to August (JJA) are also given in Figs. 7.11 and 7.12. For calculating ACCs between verification and forecast rainfall, the JJAS forecast rainfall is interpolated to 2.50 × 2.50 lat-long grids coincide with the verification rainfall grids obtained from Xie-Arkin during all 16 years. It is seen from Fig. 7.11 that the ACCs vary from year to year both over the Indian monsoon region (Fig. 7.11a) as well as the global tropics (Fig. 7.11b) bounded by 0–360°E, 30°S–30°N. It is found that over the global tropics ACCs values are comparatively higher than that of the corresponding ACCs over the Indian monsoon region during most of the years. Over the Indian monsoon region, though most of the years indicate positive ACCs (in some years ACCs $> 0.6$), slight negative ACCs are also noticed during few years as indicated in Fig. 7.11a. The negative ACCs could be due to mismatching of spatial distribution of model simulated anomaly and verification anomaly over the Indian monsoon region. The ACCs value during JJAS is the maximum with positive sign for the year 1998 followed by 1994, 1995, 1992, 1991 and 2002. Thus, the higher values of ACCs can provide some useful guidance on whether to expect above or below normal monsoon rainfall a season in advance. Though it is also seen from Fig. 7.11a, b that ACCs over global tropics are almost same during JJA and JJAS, but a little differences are present over the Indian monsoon region (Fig. 7.11a) particularly in 1987, 1990, 1991. It is observed that the ACCs is more over the Indian monsoon region during JJAS compared to JJA for the years 1987, 1989, 1991, 1994, 1997, 1998 and less in the rest of the years of the 16 years period. Similarly, as shown in Fig. 7.12, the RMSE value is also little higher over the Indian monsoon region (more than 3.0 mm/day) during some years compared to RMSE values over the tropics (less than 1.5 mm/day). Unlike ACCs, the RMSE value is higher over the Indian monsoon region in the season JJAS compared to that of JJA during all the years. Comparing the ACCs and RMSE values in each individual years, it is seen from Figs. 7.11 and 7.12 that in some individual years like 2002 & 2001, the RMSE is comparatively lower than other years with the magnitude of corresponding ACC is very small. Thus, for the superior skill of the seasonal forecast smaller RMSE is needed and a slight improvement for the ACC for seasonal forecasts of the monsoon is required and more efforts could be made to achieve the same.

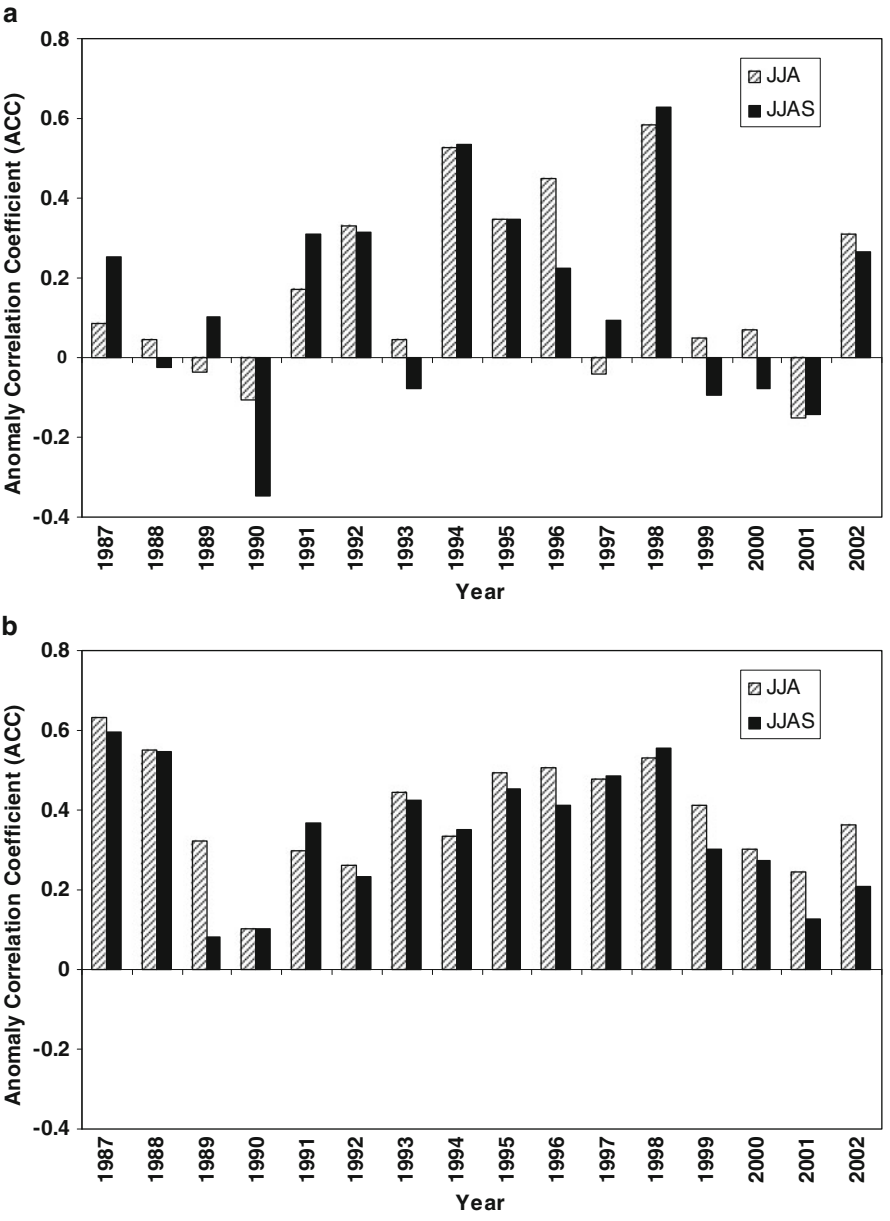


**Fig. 7.11** Seasonal (June–August; *JJA* and June to September; *JJAS*) Anomaly Correlation Coefficient (*ACC*) for the 16 years period from 1987 to 2002 valid for (**a**) the Indian monsoon region (50°E–110°E, 10°S–35°N) and (**b**) global tropics

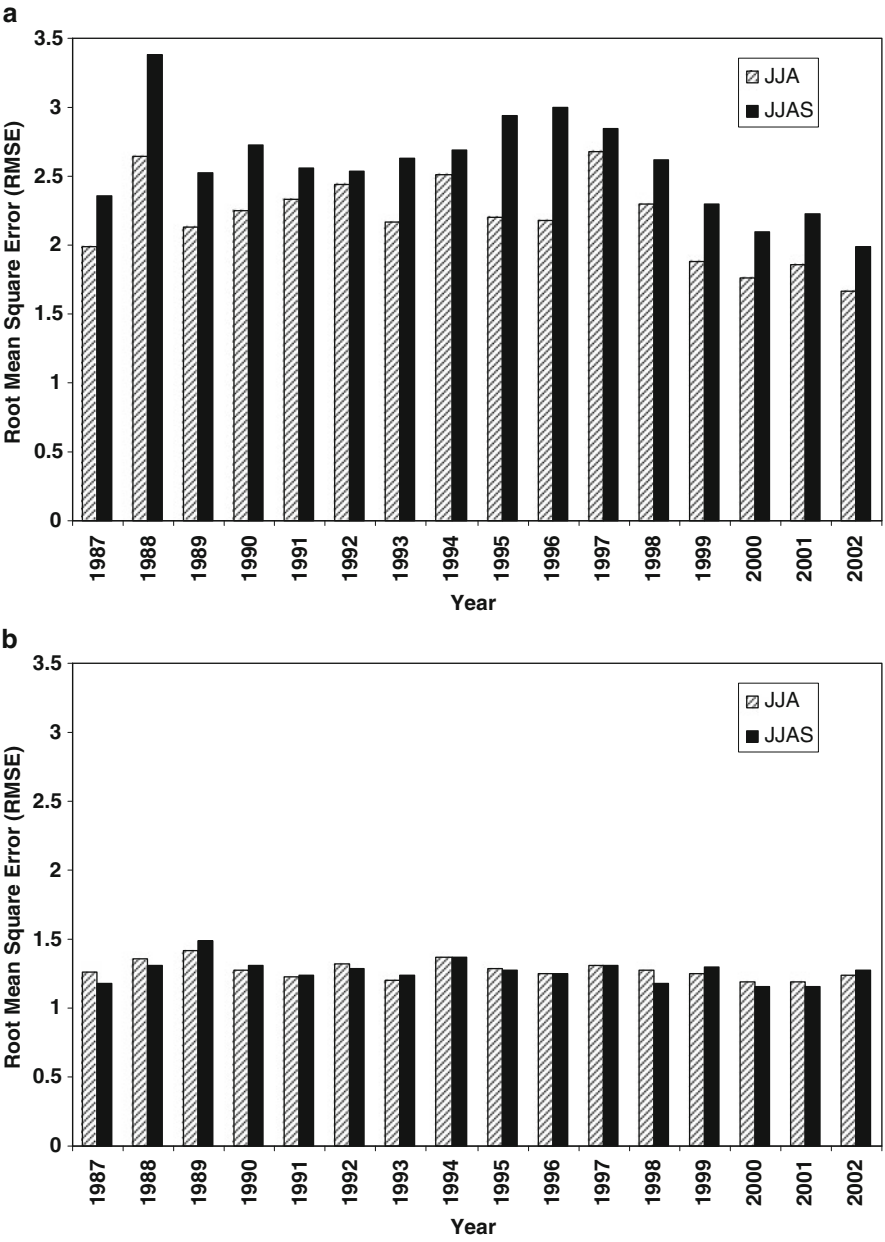


**Fig. 7.12** Seasonal (June–August; *JJA* and June–September; *JJAS*) Root Mean Square error (*RMSE*) for the 16 years period from 1987 to 2002 valid for (**a**) the Indian monsoon region (50°E–110°E, 10°S–35°N) and (**b**) global tropics

It can be stated here that the present analysis of UKMO model (GloSea3) simulation shows reasonable skill of rainfall (in global tropics as well as in Indian monsoon rainfall region), although the skill is poor over the land-only region of India continent. The real time forecast can be used in refined manner (probabilistic forecast) by using suitable statistical techniques over the Indian monsoon region. The recently upgraded UKMO seasonal forecast model (GloSea4), which has HadGEM3 as its atmospheric component with some additional improvement is expected to do better over the India monsoon region.

## 7.4 Summary and Discussion

The UK Met office monthly (from June to September) as well as seasonal (JJAS) forecasted rainfall from 240 members during 16 years period (1987–2002) is compared with the rainfall obtained from the Xie-Arkin (verification analysis) during the same period. From the above results, following broad conclusions can be drawn:

The UK Met office's model is well efficient in simulation of rainfall in the monthly forecast climatology from June to September as well as in the seasonal forecast climatology (JJAS) with two maxima one over the west coast of India region and other over the head Bay of Bengal. In model simulation, the west-coast rainfall maximum is slightly underestimated in Met Office's simulation and confined to only northern part of west-coast of India with smaller area. This may be due to model performance where model could not able to simulate locally organized convection properly over the Western Ghats mountain region during monsoon season. Though the model able to capture seasonal climatology very well, a belt of excessive rain in the interior of India over the Gangetic and Brahmaputra valley stretching from north Bay of Bengal persists in case of seasonal climatology. It is seen that the climatology mean rainfall is more in case of model's simulation (711.7 mm) against the verification analysis (683.4 mm) over the entire Indian monsoon region bounded by 50°E–110°E and 10°S–35°N. However, over the land only region of India the seasonal mean model forecast rainfall is about 20% less than the corresponding observed rainfall. The correlation coefficient between verification and forecast climatology during JJAS and JJA are in close resemblance over the Global tropics and Indian monsoon region with significant CCs. This result also supports earlier study that the predictability and the interannual variability of Asian summer monsoon rainfall in a model are dependent on the model simulation of the climatological mean monsoon (Sperber and Palmer 1996).

The year-to-year variations of forecast ensemble mean of JJAS total rainfall over the Indian monsoon region bounded by 50°E–110°E, 10°S–35°N show similar behaviour in some years with a CC of 0.43 during the 16 years period from 1987 to 2002. However, the correlation is poor when land only of India is considered. In this study, the Anomaly Correlation Coefficients (ACCs) between verification and forecast rainfall over Indian monsoon region during 1987–2002 indicate large

positive value (more than 0.6) during many years. Similarly, the Root Mean Square Error (RMSE) also varies from 1.5 to about 3.3 mm/day over the Indian monsoon region during the period from 1987 to 2002. For the superior skill of the seasonal forecast, further improvement is needed to have smaller RMSE and a slight improvement for the ACC for seasonal forecasts of the monsoon.

**Acknowledgements** The authors are thankful to the Director General of Meteorology for encouragement and for providing all facility to carry out this study. Thanks to UK Met office for providing the hindcast from GloSea model. Thanks are also due to NASA for making available the TRMM rainfall data used in the present study.

## References

Blanford HF (1884) On the connection of the Himalayan snowfall with dry winds and seasons of draughts in India. Proc R Soc Lond 37:3–22

Brankovic C, Palmer TN (1997) Atmospheric seasonal predictability and estimates of ensemble size. Mon Weather Rev 125:859–874

Brankovic C, Palmer TN, Molenti F, Tibaldi S, Cubasch U (1990) Extended range predictions with ECMWF models: time lagged ensemble forecasting. Q J R Meteorol Soc 116:867–912

Chakraborty A, Krishnamurti TN (2006) Improved seasonal climate forecasts of the South Asian summer monsoon using a suite of 13 coupled ocean-atmosphere models. Mon Weather Rev 134(6):1697–1721

Charney JG, Shukla J (1981) Predictability of monsoons. In: Lighthill J, Perce RP (eds) Monsoon dynamics. Cambridge University Press, Cambridge, pp 99–109

Chen TC, Yen MC (1994) Interannual variation of the Indian monsoon simulated by the NCAR Community Climate Model: effect of the tropical Pacific SST. J Clim 7:1403–1415

Doblas-Reyes FJ, Déqué M, Piedelievre JP (2000) Multimodel spread and probabilistic forecasts in PROVOST. Q J R Meteorol Soc 126:2069–2087

Gordon C, Cooper C, Senior CA, Banks H, Gregory JM, Johns TC, Mitchell JFB, Wood RA (2000) The simulation of SST, sea ice extents and ocean heat transports in a version of the Hadley Centre coupled model without flux adjustments. Clim Dyn 16:147–168

Gowariker V, Thapliyal V, Kulshrestha SM, Mandal GS, Sen Roy N, Sikka DR (1991) A power regression model for long-range forecast of southwest monsoon rainfall over India. Mausam 42:125–130

Graham RJ, Gordon M, Mclean PJ, Ineson S, Huddleston MR, Davey MK, Brookshaw A, Barnes R (2005) A performance comparison of coupled and uncoupled versions of the Met Office seasonal prediction General Circulation Model. Tellus 57A:320–339

Ji Y, Vernekar AD (2000) Simulations of the Asian summer monsoons of 1987 and 1988 with a regional model nested in a global GCM. J Clim 10(8):1965–1979

Kang IS, Jin K, Wang B, Lau KM, Shukla J, Krishnamurthy V, Schubert SD, Waliser DE, Stern WF, Kitoh A, Meehl GA, Kanamitsu M, Galin VY, Satyan V, Park CK, Liu Y (2002) Intercomparison of the climatological variations of Asian summer monsoon precipitation simulated by 10 GCMs. Clim Dyn 19(5–6):383–395

Kharin VV, Zwiers FW (2002) Climate predictions with multimodel ensembles. J Clim 15: 793–799

Krishnamurti TN, Kishtawal CM, LaRow TE, Bachiochi DR, Zhang Z, Williford CE, Gadgil S, Surendran S (1999) Improved weather and seasonal climate forecasts from multimodel superensemble. Science 285:1548–1550

Krishnamurti TN, Mitra AK, Yun WT, Vijaya Kumar TSV, Dewar WK (2004) Seasonal climate forecasting of the Asian monsoon using multiple coupled models. FSU Report No. 04–05, June 2004

Lorenz EN (1969) Atmospheric predictability as revealed by naturally occurring analogues. J Atmos Sci 26:636–646

Palmer TN, Anderson DLT (1994) The prospects for seasonal forecasting: a review paper. Q J R Meteorol Soc 126:2013–2033

Palmer TN, Brankowic C, Viterbo P, Miller MJ (1992) Modelling interannual variations of summer monsoons. J Clim 5:399–417

Palmer TN, Alessandri A, Andersen U, Cantelaube P, Davey M, Délécluse P, Déqué M, Díez E, Doblas-Reyes FJ, Feddersen H, Graham R, Gualdi S, Guérémy JF, Hagedorn R, Hoshen M, Keenlyside N, Latif M, Lazar A, Maisonnave E, Marletto V, Morse AP, Orfila B, Rogel P, Terres JM, Thomson MC (2004) Development of a European multi-model ensemble system for seasonal to inter-annual prediction (DEMETER). Bull Am Meteorol Soc 85:853–872

Pattanaik DR, Kumar A (2010) Prediction of summer monsoon rainfall over India using the NCEP climate forecast system. Clim Dyn 34:557–572

Pavan V, Doblas-Reyes J (2000) Multimodel seasonal hindcasts over the Euro-Atlantic: skill scores and dynamic features. Clim Dyn 16:611–625

Peng P, Kumar A, Van den Dool H, Barnston AG (2002) An analysis of multimodel ensemble predictions for seasonal climate anomalies. J Geophys Res 107(D23):4710. doi:10.1029/2002JD002712

Pope VD, Gallani ML, Rowntree PR, Stratton RA (2000) The impact of new physical parameterisations in the Hadley centre climate model: HadAM3. Clim Dyn 16:123–146

Rajeevan M, Bhate J, Kale JD, Lal B (2006) High resolution daily gridded rainfall data for the Indian region: analysis of break and active monsoon spells. Curr Sci 91:296–306

Saha S, Nadiga S, Thiaw C, Wang J, Wang W, Zhang Q, Van den Dool HM, Pan HL, Moorthi S, Behringer D, Stokes D, Pena M, Lord S, White G, Ebisuzki W, Peng P, Xie P (2006) The NCEP climate forecast system. J Clim 19:3483–3517

Sahai AK, Pattanaik DR, Satyan V, Grimm AM, Alice M (2003) Teleconnections in recent time and prediction of Indian summer monsoon rainfall. Meteorol Atmos Phys 83:217–227

Shukla J, Mooley DA (1987) Emperical prediction of the summer monsoon rainfall over India. Mon Weather Rev 115:695–703

Shukla J, Anderson J, Baumhefner D, Brankovic C, Chang Y, Kalnay E, Marx L, Palmer TN, Paolino DA, Ploshay J, Schubert S, Straus DM, Suarez M, Tribbia J (2000) Dynamical seasonal prediction. Bull Am Meteorol Soc 81:2593–2606

Slingo JM, Annamalai H (2000) The El Nino of the century and the response of the Indian summer monsoon. Mon Weather Rev 128:1778–1797

Soman MK, Slingo J (1997) Sensitivity of Asian summer monsoon to aspects of sea surface temperature anomalies in the tropical Pacific Ocean. Q J R Meteorol Soc 123:309–336

Sperber KR, Palmer T (1996) Interannual tropical rainfall variability in general circulation model simulations associated with the Atmospheric Model Intercomparison Project. J Clim 9:2727–2750

Sperber KR, Brankovic C, Deque M, Frederiksen CS, Graham R, Kitoh A, Kobayashi C, Palmer T, Puri K, Tennant W, Volodin E (2001) Dynamical seasonal predictability of the Asian summer monsoon. Mon Weather Rev 129(9):2226–2248

Stephenson DB, Doblas-Reyes FJ (2000) Statistical methods for interpreting Monte Carlo ensemble forecasts. Tellus 52A:300–322

Wang B, Kang IS, Lee JY (2004) Ensemble simulations of Asian-Australian monsoon variability by 11 AGCMS. J Clim 17(4):803–818

Wu MLC, Schubert S, Kang IS, Waliser D (2002) Forced and free intraseasonal variability over the south Asian monsoon region simulated by 10 AGCMs. J Clim 15(20):2862–2880

Xie-Arkin (1996) Analyses of global monthly precipitation using gauge observations, satellite estimates, and numerical model predictions. Journal of Climate 9:840–858

# Chapter 8
# Prediction of Monsoon Variability and Subsequent Agricultural Production During El Niño/La Niña Periods

**M.V. Subrahmanyam, T. Satyanarayana, and K.P.R. Vittal Murthy**

**Abstract** It is well know that the south west monsoon or popularly known summer monsoon dictates the economy of the sub-continent. A good monsoon year results in good rainfall increased production and a boom in the economy on the contrary a bad monsoon year with deficit rainfall results in decrease in the yield and a subsequent reduction in agricultural production and economy of the country. Indian Government and Indian scientists did a wonderful job in increasing the agricultural production to cater to the needs of increased population. However, in years of El Niño the monsoon activity and the monsoon rainfall is below normal and results in a decrease in production. In order to get a sustainable development, this is the area where serious scientific measures are to be implemented to get sustained development. It is possible to achieve this difficult task, because El Niño sends a forewarning signal in December with an increased abnormal SST of the coast of the Brazil in Pacific. The aim and objective of the present article is to focus about the phenomena of El Niño and La Niña, the mechanism the manifestation and the intensity. The reduction in monsoon circulation in fluxes and rainfall. This was amply described by estimating the oceanic fluxes, which will send clear signals as to the intensity of an El Niño and La Niña. In this article the yearly all India grain production from 1953 to 2007 was also examined. The increasing trend can be interpreted as the proper agro technical measures and use of complex fertilizers (intensive

M.V. Subrahmanyam (✉)
South China Sea Institute of Oceanology, Chinese Academy of Science, Beijing, China
e-mail: mvsm.au@gmail.com

T. Satyanarayana
Department of Environmental Sciences, Acharya Nagarjuna University, Guntur, AP, India
and
Central Research Institute for Dryland Agriculture, Hyderabad 500 059, India
e-mail: satya_1006@yahoo.co.in

K.P.R.V. Murthy
Department of Meteorology and Oceanography, Andhra University, Visakhapatnam, AP, India
e-mail: kprvm@yahoo.com

S.D. Attri et al. (eds.), *Challenges and Opportunities in Agrometeorology*,
DOI 10.1007/978-3-642-19360-6_8, 

cultivation) besides increase in the land under cultivation (bringing waste lands into irrigated fields – extensive cultivation. From the sequential March of grain production it is seen that the El Niño years resulted in deficit in production. It is suggested that proper agro management techniques can at least decrease the deficit in production. Various management programs in this direction were also suggested.

## 8.1 Introduction

### *8.1.1 Monsoon*

Monsoon winds blow from cold to warm regions because cold air takes up more space than warm air. Monsoons blow from the land toward the sea in winter and from the sea toward land in the summer. India's winters are hot and dry. The monsoon winds blow from the northeast and carry little moisture. The temperature is high because the Himalayas form a barrier that prevents cold air from passing onto the subcontinent. The summer monsoons enter to the subcontinent from the southwest. The winds carry moisture from the Indian Ocean and bring heavy rains from June to September. The summer monsoons are welcomed in India because farmers depend on the rains to irrigate their land.

The Asian monsoon is characterized by a seasonal reversal of surface winds and a distinct seasonality of precipitation. The fundamental driving mechanisms of the monsoon cycle are the cross-equatorial pressure gradients resulting from differential heating of land and ocean, modified by the rotation of the earth and the exchange of moisture between the ocean, atmosphere and land (Webster 1987). Strong seasonality of wind and rainfall patterns, the monsoon regions also experience a high degree of variability on intrapersonal, interannual, and interdecadal timescales (Clark et al. 2000). The variability of the Asian monsoon is linked with the El Niño–Southern Oscillation (ENSO). The occurrence of El Niño is generally associated with a weak monsoon, and La Niña is associated with a strong monsoon (Webster and Yang 1992). The connection between the Asian monsoon and ENSO appears to be statistically nonstationary (Troup 1965).

Several studies have been carried out on the role of air-sea interaction processes over the Indian Ocean (Cadet and Diehl 1984; Shukla and Mishra 1977; Weare 1979; Rao and Goswami 1988; Mohanty and Ramesh 1993). These studies are mainly concentrated on the relationship between sea surface temperature anomalies over Arabian Sea and summer monsoon rainfall over India. Shukla (1987) found that heavy (deficit) rainfall is followed by negative (positive) SST anomalies, but the magnitude of the SST anomalies for the premonsoon months is small and insignificant. Joseph and Pillai (1984) obtained the same results. On the contrary, the studies of Rao and Goswami (1988) suggest that SST in the southeast Arabian Sea during the premonsoon season is significantly correlated with ISM rainfall. The study of Ramesh Kumar et al. (1986) indicated that large negative anomalies off the Somali and Arabian coasts are associated with good monsoon rainfall over India.

The relationship between the SST in the Eastern Equatorial Indian Ocean (EEIO) and monsoon rainfall was studied by Sadhuram (1997). Their study indicated that SST anomaly during October and November in the EEIO is useful for monsoon rainfall prediction.

The origin and amount of moisture being transported to the Indian subcontinent during the southwest monsoon season was also studied by many investigators. Pisharoty (1965) utilizing the data collected during IIOE, examined the moisture budget and found that evaporation from Arabian Sea to be the main contributor for summer monsoon rainfall. Saha and Bavadekar (1973) using additional upper air data concluded that 70% of moisture flux from the south Indian ocean accounts for the bulk of moisture needed for summer monsoon rainfall. The intraseasonal variations of moisture budget have also been examined by several scientists (Ramamurthy et al. 1976; Ghosh et al. 1978; Howland and Sikdar 1983; Cadet and Reverdin 1981a, Sadhuram and Ramesh Kumar 1988). While the importance of evaporation over the Arabian Sea is suggested by Ghosh et al. (1978), Murakami et al. (1984), the role of cross equatorial (Cadet and Reverdin 1981a, b; Howland and Sikdar 1983; Sadhuram and Ramesh Kumar 1988; Ramesh Kumar and Sadhuram 1989; Ramesh Kumar et al. 1999). Most of these studies suggest that the cross equatorial moisture flux provides an important source of moisture for the ISM rainfall though the evaporation from the Arabian Sea is quite significant. Most of the above mentioned studies have used only limited data sets as no long term observation were available. Now with the availability of daily and twice daily reanalysis results from NCEP/NCAR project various aspects of monsoon can be studied in detail which can throw more light on the different phases of monsoon activity. In the present study, an attempt is made to understand the role of low level flow on the ISM rainfall. In the present study, the possible linkages between the Indian summer monsoon rainfall and surface meteorological fields (latent heat) were investigated during the El Niño years and La Niña years.

India is an agricultural country, 80% of the population depends on agricultural production. Indian Government has initiated number of steps to increase agriculture production, which is known as green revolution. On the agronomy side better varieties of agricultural seeds have been produced, which are high yielding, drought resistant and reduce the crop life period. More hydrological products are initiated, so that the river waters are utilized in a better fashion, by constructing dams across the rivers and providing water to more access of land, so that the agricultural land is increase, which is known as extensive cultivation. Research was also on for better utilization of water, so that water is utilized fully by the agricultural crop, but not wasted by percolation or de-percolation or by excessive runoff. Drip irrigation is an example in this direction. Better agro technical measures and proper utilization of specified fertilizers (natural and Bio fertilizer is better than chemical fertilizer) and proper and accurate utilization of insecticides and pesticides will also ensure increase yield per acre. So by the intensive and extensive cultivation of agricultural production can be increased.

In spite of the technological development mentioned above the agricultural production in the country very much depends on the timely rainfall received from

monsoons in normal quantities (extensive rainfall leads to floods deficit rainfall leads to drought). Both the disasters, there is substantial crop damage and loss of production. El Niño and La Niña are related to SST off the coast of Brazil in Pacific. El Niña in Spanish means child Christ because this phenomena manifests the greater half of December around Christmas La Niña (surprisingly means girl Christ) is opposite of El Niño. During El Niño, SSTs are more than normal during La Niña, they are less than normal respectively. Both the phenomena related to summer monsoon (ref). El Niño results in deficit rainfall and La Niña manifests excessive rainfall. As there is a gap of 6 months there is sufficient time to plan for the coming event of El Niño and La Niña. One can change the cropping pattern and apply proper agro technical measures aimed at achieving sustainable development with the production loses at a minimum level.

## 8.2 Data Methodology

In the present study, to find the possible linkages between the Indian summer monsoon rainfall and surface meteorological fields (latent heat) were investigated during the El Niño years and La Niña years. One of the reliable global data set is available from NCEP (National Centre for Environmental Prediction).NCEP Reanalysis data set has been used for the present study. The data is having resolution of $2.5^\circ \times 2.5^\circ$ grid. We have used the latent heat flux of every month average over Arabian Sea for the monthly analysis and mean of JJAS for seasonal analysis. El Niño and La Niña period chosen for this study is from the ENSO Years based on Oceanic Niño Index (ONI) http://ggweather.com/enso/oni.htm. We have used the monthly and seasonal for all India and sub divisional wise rainfall data, which are available at http://www.tropmet.res.in. All India food grain production from 1953–2006 was utilized to study effect Indian monsoon rainfall on food grain production. The detrend food grain production data the relationship with rainfall were analyzed.

## 8.3 Results and Discussion

### *8.3.1 Variation of Oceanic Latent Heat Flux*

The southwest monsoon rain fall is having the impact on the Indian agriculture. In this article we studied how the Latent Heat flux is influencing the rainfall in the India. The mean variation of LHF anomaly during the monsoon season (JJAS) over Arabian Sea has been given in the Fig. 8.1. Gradual decrease of red colour indicates the El Niño episodes and blue indicates the La Niña episodes. Gradual decrease of color changes from Strong to weak episodes and the green colour indicates the

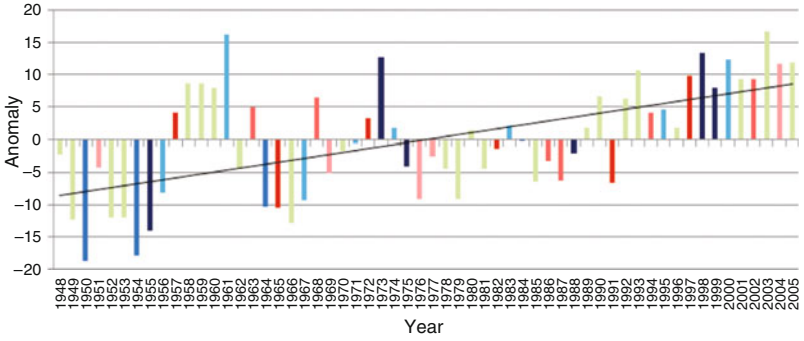


**Fig. 8.1** Mean variation of latent heat flux anomaly over the Arabian Sea during Southwest monsoon season (JJAS)

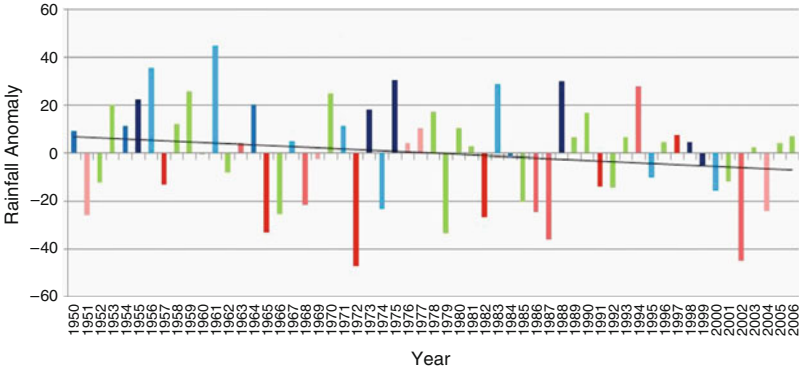


**Fig. 8.2** Variation of all India Rainfall anomalies during Southwest Monsoon season

normal monsoon. There is a much variations observed since 1950 to early 1990s. After that the variation of anomalies are shows the positive. It indicates the LHF is increasing by its values after early 1990s. The trend for the LHF anomalies is positive, it clearly indicates that the LHF is increasing may be due to global warming. The sea surface temperature (SST) in the Indian Ocean shows a warming trend in recent decades (Swadhin et al. 2007) can be related in increasing of LHF, which depends on, temperature, and wind. The North Indian Ocean shows SST warming of about 0.4°C during 1958–2000 (Bijoy Thompson et al. 2008).

## *8.3.2 Variation of All India Rainfall*

Figure 8.2 depicts the mean monsoon rainfall anomaly over the period 1950–2006 and is showing the decreasing trend. The red colour (Strong El Niño in the dark red

colour and weak El Niño in the light red colour) depicts the El Niño episode and light colour depicts the weak El Niño. The blue colour (strong La Niña in dark blue and weak La Niña in light blue colour) depicts the La Niña episodes. The maximum negative anomaly is observed on 1972, which is a strong El Niño episode, similarly in the moderate El Niño episode in the year 2002 showing the negative anomaly, during these episodes the rainfall is less than the normal monsoon episode. It is observed positive anomaly is also observed during the El Niño episodes during the moderate El Niño episode during 1994. The maximum positive anomaly is found in the weak La Niña episode during the year 1961. During the Strong La Niña episodes and moderate episodes showing only positive anomaly, where as moderate La Niña having negative anomaly also. Significant positive anomalies observed in the La Niña episodes and negative anomalies during the El Niño episodes.

### *8.3.3 Monthly and Season Wise Variation in Latent Heat Flux*

Figure 8.3 shows the variation of latent heat flux during the monsoon months and the seasonal mean over Arabian Sea. LHF decreases from June to September. The same feature can be observed in the all the episodes except during strong El Niño, strong La Niña and weak La Niña episodes. During Strong El Niño episode the LHF is higher and continued in the July where as in the strong La Niña LHF is higher in July than June and in the weak La Niña June and July are having the same LHF.

The departure of LHF in relation to normal monsoon over Arabian Sea is studied in particular to the monsoon months (JJAS) during El Niño and La Niña episodes are given in the Fig. 8.3. During the Strong El Niño event the LHF is higher than normal monsoon during all the June, July, August and September months.

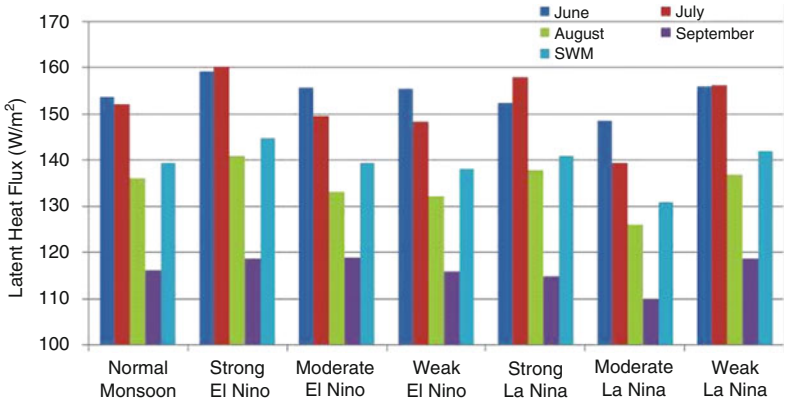


**Fig. 8.3** Variation of latent heat flux during the normal monsoon, El Niño and La Niña episodes in the months of June, July, August, September and southwest monsoon (SWM) season over Arabian Sea

In the moderate El Niño episodes it is observed that during June, and September are higher, where as in the months July and August it is lower than the normal monsoon. In the weak El Niño episodes June month shows the higher and the rest of the months it is lower. It was observed that during the El Niño episodes the LHF is higher during the June. In the moderate El Niño episode LHF is higher than normal during June and September, where as lower during July and August. During the weak El Niño June month LHF is higher where as in other months LHF is lower.

During strong and moderate La Niña episodes, LHF is lower in June and September and higher in July and August. In the contrary during the weak La Niña episodes the LHF is higher in all the months. From these observations, it can be concluded that higher LHF during July is an important for the strong El Niño episodes. The weak La Niña episodes LHF is higher during all the months.

### *8.3.4 Monthly and Season Wise Variation in all India Rainfall*

Figure 8.4 depict the mean variation of variation of all India rainfall during normal monsoon, El Niño and La Niña episodes. From the figure it is observed that during the El Niño episodes the rainfall is below normal monsoon, expect in the weak El Niño episode. During La Niña episodes the all India rainfall is more than the normal monsoon rainfall. The June month rainfall is necessary for the crops, during strong El Niño episode the rainfall is less when compared with all other episodes. During the strong El Niño episode the rain fall is far below the normal monsoon rainfall, it effects the crop growth which leads to lower production of crop. In the month of July the variation of rainfall is increasing from the strong to weak episode of El Niño. The same feature can be seen in the month of September. In August in the moderate El Niño episode the rainfall is higher than the strong and weak El Niño episodes. The rainfall is higher in the months of June, August and September during the strong La Niña episode, whereas during the month of July the rainfall is higher in the moderate

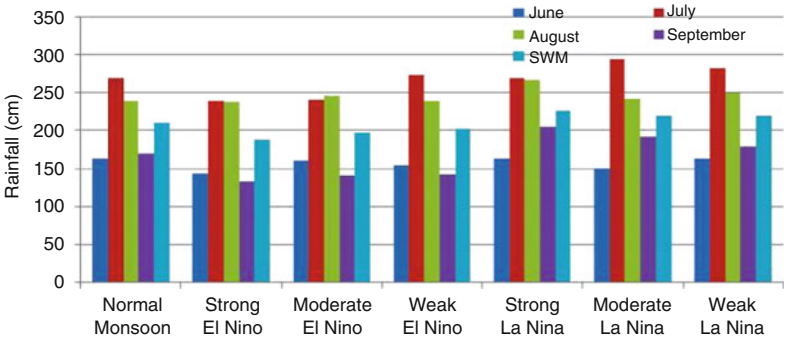


**Fig. 8.4** Mean variation of all India mean rainfall during El Niño, La Niña and normal monsoon episodes in June, July, August, September and Southwest monsoon season

La Niña episode. The clear picture of El Niño can be seen in the months of July and September as the rainfall increasing from Strong to weak episodes and the La Niña feature can be seen in the month of September decreasing rainfall from the strong to weak episodes. The mean picture of the monsoon month shows the clearly that during El Niño episodes the rainfall is decreasing from strong to weak episodes and increasing during the La Niña episodes from strong to weak episodes.

### *8.3.5 Variations in Rainfall Departures During El Niño and La Niña Period*

Figure 8.5 depict the mean variation of departures from El Niño and La Niña episodes with the normal monsoon. During the strong El Niño episode, the departures are negative it shows during the strong El Niño episode the rainfall is less when compared with the mean normal monsoon period and is positive during the La Niña episodes, there may be some exceptions like during moderate El Niño episode during in the month of August the rainfall is higher than the other El Niño episodes and higher rainfall can be seen in the month of July in the weak El Niño episode. During the moderate La Niña the rainfall is lower when compared with the other La Niña episodes.

### *8.3.6 Variation of Rainfall at Subdivision Level*

#### 8.3.6.1 Over Coastal Andhra Pradesh

Mean variation of rainfall in the coastal Andhra Pradesh is given in the Fig. 8.6a From the figure shows a slight decreasing trend in the rainfall over coastal

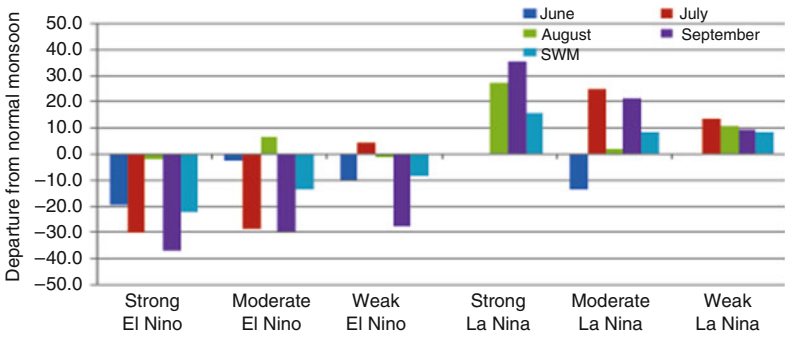


**Fig. 8.5** Mean variations of departures from El Niño and La Niña episodes with the normal monsoon

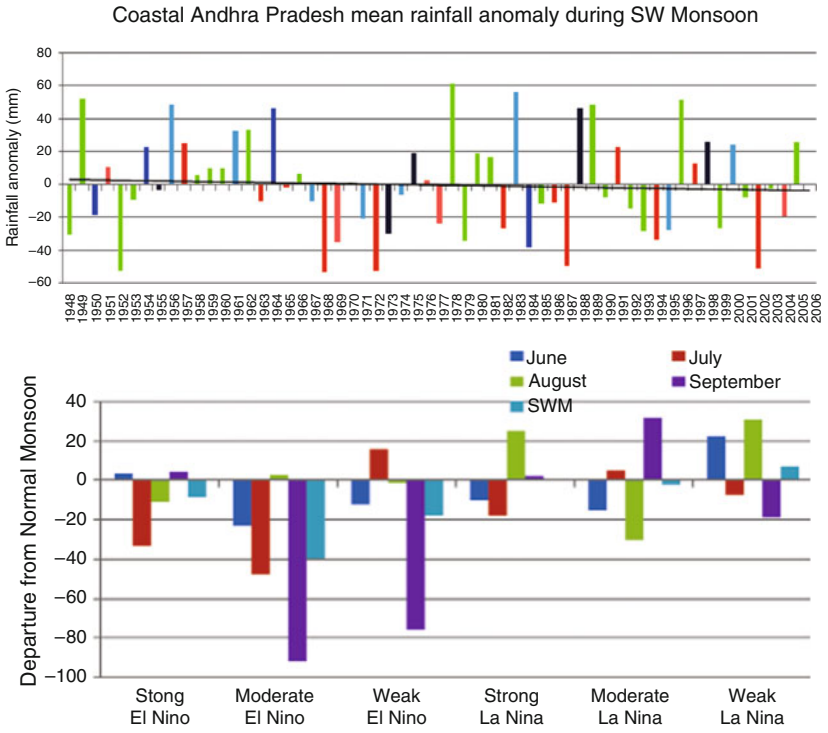


**Fig. 8.6** **(a)** Mean variation of rainfall in the coastal Andhra Pradesh region. **(b)** Departure of coastal Andhra Pradesh rainfall from the El Niño and La Niña episodes with the normal monsoon

Andhra Pradesh. The El Niño, La Niña and normal monsoon episodes can be seen in the different colours. El Niño episodes in the red and La Niña episodes in blue colour. The strong colour indicates the strong episode and light colour indicates the weak episodes for El Niño and La Niña. Significant higher positive anomalies can be observed during La Niña episodes and normal monsoon and lower anomalies in the El Niño episodes. Negative anomalies can be observed during the strong and moderate La Niña episodes also. The higher positive rainfall anomaly of around 60 observed during the normal monsoon and higher negative anomaly of 53 observed during moderate El Niño episode.

Figure 8.6b depicts departure of rainfall from the El Niño and La Niña episodes with the normal monsoon. The departure is negative in the El Niño episodes. The departure is higher in the months of September during moderate and weak El Niño episodes and reasonable negative departures in the month of July. Significant positive departures can be seen in August in Strong La Niña, in September during moderate La Niña and in June and September months in weak La Niña episodes. Negative departures can be seen in the months of June and July during strong La Niña episode. in June and August months during moderate La Niña and in July and September months of weak La Niña episodes.

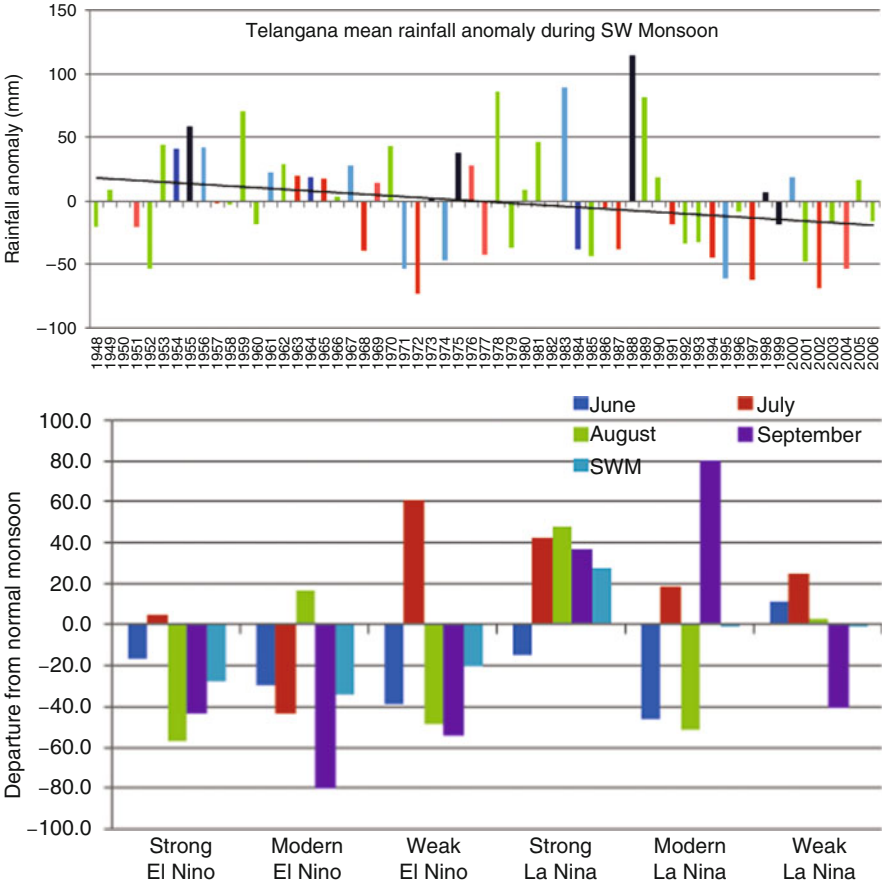


**Fig. 8.7** **(a)** Mean rainfall anomaly in the Telangana region. **(b)** Departure of Telangana region rainfall during El Niño and La Niña episodes with normal monsoon

### 8.3.6.2 Variation of Rainfall Over Telangana

Figure 8.7a shows the mean variation of rainfall anomaly in the Telangana region. In the telangana region the mean seasonal rainfall shows decreasing trend. The colour codes are same as earlier. During 1988 significant higher positive anomaly can be observed. Significant higher positive rainfall can be observed during La Niña episodes and normal monsoon. During the strong La Niña episode the higher positive anomaly was observed in the year 1988. And the higher negative anomaly observed during strong El Niño episodes in the year 1972.

Departure of Telangana rainfall from the normal monsoon during El Niño and La Niña episodes are given in the Fig. 8.7b. Negative departures can be seen during the El Niño episodes. Significant higher departure observed in the July month during weak El Niño episode. Positive departure can be seen in the La Niña

episodes. Significant negative departure can be seen in the June and August months of moderate La Niña episode and in the September month of weak La Niña episode.

### 8.3.6.3 Variation of Rainfall Over Rayalseema

Mean southwest monsoon rainfall variation in the Rayalseema region is shown in the Fig. 8.8a. The seasonal rainfall is near to normal rainfall. In all El Niño episodes the rainfall is lesser than the normal rainfall, there are some exceptions also. In the La Niña episodes the rainfall is higher than the normal. The higher positive rain fall anomaly of 85 in the year 1996 during normal monsoon and higher negative anomaly of 45 also observed during normal monsoon in the year 1952.

Departures of rainfall during El Niño and La Niña episodes with normal monsoon are given in the Fig. 8.8b. During the strong El Niño episode positive departure

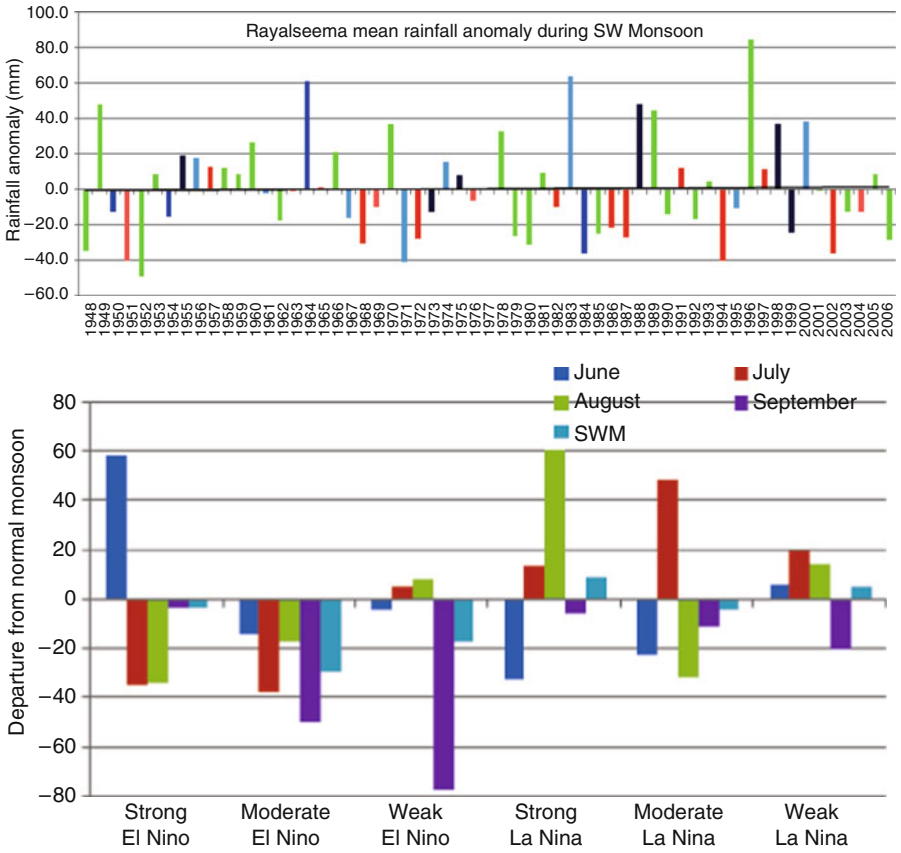


**Fig. 8.8** **(a)** Mean variation of rainfall in the Rayalseema region in the southwest monsoon season. **(b)** Departures of rainfall during El Niño and La Niña episodes with normal monsoon

can be seen in the month of June and during the strong La Niña episode negative departure can be seen. The maximum negative departure can be seen in the weak El Niño episode in the month of September. And maximum positive departure can be seen in the month of August during strong La Niña episode. During the moderate La Niña the maximum positive departure can be seen in the month July.

### *8.3.7 Spatial Distribution Ocean Latent Heat Fluxes Comparison During El Niño and La Niña Periods*

Large seasonal and inter annual variability in SST exists in the western and southeast tropical Indian Ocean. The processes, viz; latent heat flux, radiative flux, advection and entrainment play major roles in SST. Inter annual variability of heat flux is found to have greater influence on SST in most parts of the Indian Ocean (Behra et al. 2000). They have simulated the SST anomalies over different regions in Indian Ocean and found that latent heat dominates in all the regions. Advection and net heat flux are found to be dominant in the equatorial Indian Ocean. Warming observed in 1982–1983 (El-Niño) was due to the high latent heat flux. Interannual variability of heat fluxes could not be compared as there were no earlier studies for the same years. However, latent heat flux which is found to play a dominant role in SST variability, the distribution of latent heat flux under summer and winter monsoon seasons (Rao and Sriram 2005). The role of the latent heat flux plays vital role to explain the advent and performance of monsoon systems as revealed by some radiation and heat flux parameters (Subramaniyam 2006). Figure 8.9a, b shows the latent heat flux during El Niño and La Niña periods. It shows wide contrast between El Niño and La Niña. The figure shown to the left is LHF during El Niño. It is evident that LHF is intense and covering large area. Even though the areal extent is same, the intensity is less in La Niña. These fluxes are estimated in the month of June. It is observed that the contrast is more in June. We can use it is an indicator for performance of the monsoon rainfall.

### *8.3.8 Agriculture Production and Its Relationship with Rainfall*

The increasing trend of agriculture production can be interpreted as the proper agro technical measures and use of complex fertilizers (intensive cultivation) besides increase in the land under cultivation bringing waste lands into irrigated fields. The detrended yields find removing the increased trend pattern in agriculture production calculated deviation in all India annual rainfall. This is graph shows detrended yield which can be related to meteorological parameters like rainfall to find the relationship. Figure 8.10 depicts the it is showing that yield reduction coincide with rainfall

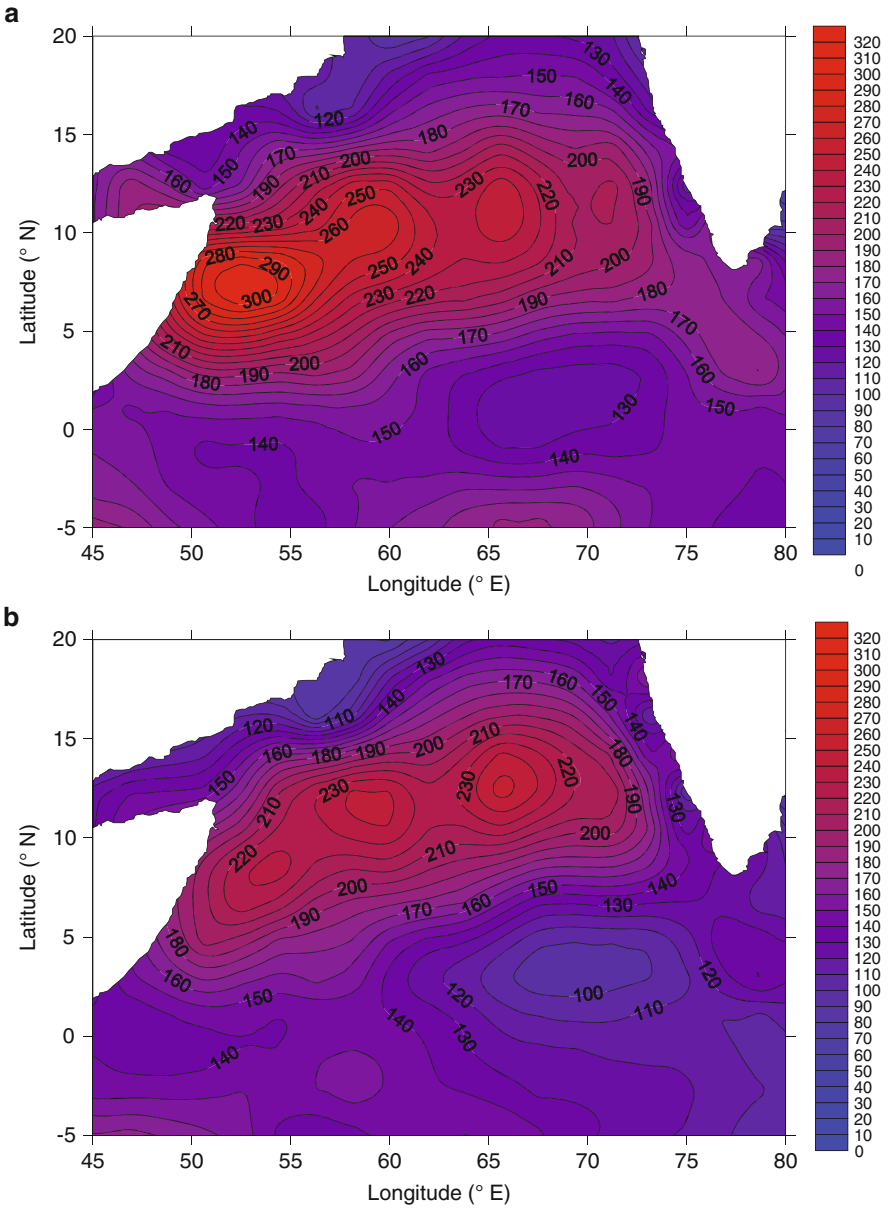


**Fig. 8.9** Mean special distribution of latent heat flux during (**a**) El Niño and (**b**) La Niña episodes in the month of June

negative deviations which is coincide the El Niño periods .High yield amount coincide with positive deviations which is coincide with La Niña periods. Some exemption also find during El Niño and La Niña periods.

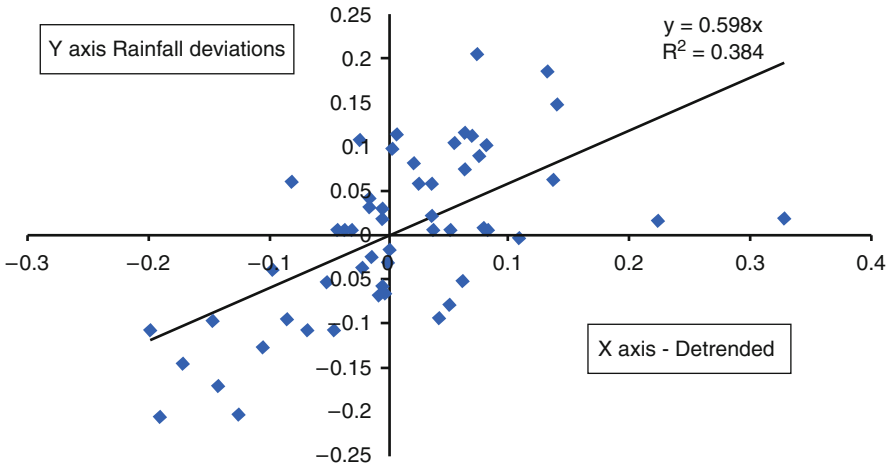


**Fig. 8.10** The graph between detrended yield and rainfall deviations

## 8.4 Conclusions

The teleconnections for Indian summer monsoon are impartment for prediction and planning. El Niño and La Niña in December gives sufficient time (6 months) for the prediction of Asian Summer monsoon. The intensity of El Niño and La Niña is very much related to the Oceanic fluxes in the Indian Ocean. The Ocean Fluxes especially Latent heat flux over Arabian Sea shows an Increasing trend. The mean monsoon LHF is showing the positive trend and all India rainfall showing the negative trend. The LHF and all India rainfall are showing the negative correlation . The important conclusion of this study is Latent Heat Flux differ very much during El Niño and La Niña episodes in June, which gives in an important clue to agricultural and ecological planning.. During the strong El Niño (La Niña) the LHF is higher (lower) and the rainfall is lower (higher). The departure of LHF and all India rainfall is also showing the same feature. Departure from the normal monsoon can reveal how the rainfall varying during the El Niño and La Niña episodes. The food production increased because of proper agro technical measures like better seed varieties, improved complex fertilizers and well tested insecticides and fungicides, but yet there is a decreasing trend during El Niño periods the sustainable development should be aimed at taking consideration of low rainfall in June and July months during El Niño. Alternate crops which require less water are to be planed, which will ensure sustainable development.

## References

Behra SK, Salvekar PS, Yamagata T (2000) Simulation of interannual SST variability in the tropical Indian ocean. J Climate 13:3487–3499

Cadet DL, Diehl BC (1984) Interannual variability of surface fields over the Indian Ocean during recent decades. Mon Wea Rev 112:1921–1935

Cadet D, Reverdin G (1981) Water vapour transport over the Indian ocean during summer 1975. Tellus 33:476–487

Cadet D, Reverdin G (1981b) Water Vapour Transport over the Indian Ocean during Summer 1975. Tellus 33:476–487

Clark CK, Cole JE, Webster PJ (2000) Indian ocean SST and Indian summer rainfall: predictive relationships and their decadal variability, J Climate 13:2503–2519

Gangadhava Rao LV, Shree Ram P (2005) Upper ocean physical processes in the tropical Indian ocean, A monograph prepared under CSIR Emeritus Scientist Scheme. National Institute of Oceanography, Goa

Ghosh SK, Pant MC, Dewan BN (1978) Influence of the Arabian Sea on the Indian summer monsoon. Tellus 30:117–125

Howland MR, Sikdar DN (1983) The moisture budget over the N.E. Arabian Sea during pre-monsoon and monsoon onset. Mon Wea Rev 111:2255–2268

Joseph PV, Pillai PV (1984) Air-sea interaction on a seasonal scale over north Indian Ocean. Part I: Interannual variations of sea surface temperature and Indian summer monsoon rainfall. Mausam 35:323–330

Mohanty UC, Ramesh KJ (1993) Characteristics of certain surface meteorological parameters in relation to the interannual variability of Indian summer monsoon. Proc Indian Acad Sci (Earth Planet Sci) 102(1):73–87

Murakami T, Nakazawa T et al (1984) On the 40–50 day oscillation during the 1979 northern hemisphere summer. Part. II, Heat and Moisture budget. J Meteor Soc Jpn 62:469–484

Pisharoty PR (1965) Evaporation from the Arabian Sea and the Indian southwest monsoon. In: Proceedings of the symposium on meteorological results of the IIOE. India Meteorological Department, Bombay, pp 43–54

Ramamurthy K, Jambhunathan R et al (1976) Moisture distribution water vapour flux over the Arabian Sea during active and weak spells of southwest monsoon. Ind J Met Hydrol Geophys 27(2):127–140

Ramesh Kumar MR, Sadhuram Y (1989) Evaporation over the Arabian Sea during two contrasting monsoons. Meteorol Atmos Phys 41:87–97

Ramesh Kumar MR, Sathyendranath S et al (1986) Sea surface temperature variability over North Indian Ocean – a study of two contrasting monsoon seasons. Proc Indian Acad Sci Earth Planet Sci 95(3):435–446

Ramesh Kumar MR, Shenoi SSC et al (1999) On the role of the cross equatorial flow on summer monsoon rainfall over India using NCEP/NCAR reanalysis data. Meteorol Atmos Phys 70:201–213

Rao KG, Goswami BN (1988) Interannual variations of sea surface temperature over the Arabian Sea and the role of low level flow on the summer monsoon rainfall over the Indian subcontinent during two contrasting monsoon years in an Monsoon: a new perspective. Mon Wea Rev 116:558–568

Sadhuram Y (1997) Predicting monsoon rainfall and pressure indices from sea surface temperature. Curr Sci 72(3):166–167

Sadhuram Y, Ramesh Kumar MR (1988) Does evaporation over the Arabian Sea play a crucial role in moisture transport across the west coast of India during an active monsoon period? Mon Wea Rev 116:307–312

Saha KR, Bavadekar SN (1973) Water vapour budget and precipitation over the Arabian Sea during the northern summer. Q J R Meteor Soc 99:273–278

Shukla J (1987) Monsoons. In: Fein JS, Stephens PI (eds) Interannual variability of Monsoons. Wiley, New York, pp 399–464
Shukla J, Misra BN (1977) Relationships between sea surface temperature and wind speed over the Central Arabia Sea and monsoon rainfall over India. Mon Wea Rev 105:998–1002
Subramaniyam (2006) Role of North Indian Ocean in the advent and performance of monsoon systems as revealed by some radiation and heat flux parameters. PhD, Andhra University, India
Swadhin KB et al (2007) What causes the Indian Ocean warming? Geophys Res Abstr 9:10950
Thompson B, Gnanaseelan C et al (2008) North Indian Ocean warming and sea level rise in an OGCM J. Earth Syst Sci 117:169–178
Troup AJ (1965) The southern oscillation. Quart J Roy Meteor Soc 91:490–506
Weare BC (1979) A statistical study of the relationship between ocean surface temperature and the Indian monsoon. J Atmos Sci 26:2279–2291
Webster PJ (1987) Monsoons. In: Fein JS, Stephens PI (eds) The elementary monsoon. Wiley, New York, pp 399–464
Webster PJ, Yang S (1992) Monsoon and ENSO: selectively interactive systems. Q J R Meteor Soc 118:877–926

# Chapter 9
# Improved Seasonal Predictability Skill of the DEMETER Models for Central Indian Summer Monsoon Rainfall

**Ravi P. Shukla, K.C. Tripathi, Sandipan Mukherjee, Avinash C. Pandey, and I. M. L. Das**

**Abstract** A method to improve the predictability of the seven models in the DEMETER project is proposed. This technique has been applied to investigate the effect on the predictability of seasonal precipitation (June–July–August) in the central Indian region. Three best models of DEMETER have been selected based on error and correlation analysis and standard deviation of the observed data. It is found that the ensemble mean prediction, when using these three models is better than the ensemble mean prediction when using all the seven models. It is also observed that the root mean square error is reduced when the ensemble mean of the models is taken. At the same time it is also observed that the ensemble mean does not, in every case, give better forecast skill scores in case of dichotomous forecasts which tell the skill of the models in forecasting rare events.

## 9.1 Introduction

Seasonal timescale climate predictions are important for the society for a variety of reasons (Thomson et al. 2000; Hartmann et al. 2002). Predictability is affected by perturbations in the initial conditions as well as the uncertainty in the representation of partial differential equations as a finite-dimensional set of ordinary differential

R.P. Shukla (✉) • K. Tripathi • S. Mukherjee
K. Banerjee Center of Atmospheric & Ocean Studies, University of Allahabad, Allahabad 211002, India
e-mail: ravishukla72@gmail.com; kctripathi@gmail.com; mukherjee.sandipan@rediffmail.com

A.C. Pandey
M. N. Saha Centre of Space Studies, University of Allahabad, Allahabad 211002, India
e-mail: avinashcpandey@rediffmail.com

I.M.L. Das
Department of Physics, University of Allahabad, Allahabad 211002, India
e-mail: profimldas@yahoo.com

S.D. Attri et al. (eds.), *Challenges and Opportunities in Agrometeorology*,
DOI 10.1007/978-3-642-19360-6_9, 

equations in a digital computer. At present it is not possible to theoretically estimate a probability distribution of such model uncertainty (Palmer 2001). An approach to overcome uncertainties arising out of such model uncertainty is to take an ensemble of semi-independent global climate models, called the Multi-Model Ensemble (MME) (Palmer et al. 2004). It has been established that multi-model ensemble makes more reliable forecasts than individual members, or an ensemble of many members of a single model, under the funded research projects such as Prediction Of climate Variations On Seasonal to Interannual Time-scales (PROVOST) (Palmer and Shukla 2000), Dynamical Seasonal Prediction (DSP) (Shukla et al. 2000; Palmer and Shukla 2000) and Development of European Multi-model Ensemble system for seasonal to inTER-Annual Prediction (DEMETER) (Palmer et al. 2004) established by the European Center for Medium-Range Weather Forecast (ECMWF). In such ensemble forecasts, the uncertainties in the initial state are addressed through an ensemble of different ocean initial conditions for each model.

The DEMETER project consists of seven global coupled ocean-atmosphere models viz. CERF (European Center for Research and Advanced Training in Scientific Computation, France), ECMWF, INGV (Instituto Nazionale de Geofisica e Vulcanologia, Italy), LODYC (Laboratoire d'Oceanographie Dynamique et de Climatologie, France), METF (Centre National de Recherches Meteorologiques, Meteo-France, France), UKMO (The Met Office, UK) and MAXP (Max Planck Institut fur Meteorologie, Germany). Each model consists of nine individual members.The Multi-model Ensemble technique has also been useful when predicting the winds at 850 hPa between the Madagaskar and Western Australia (Rai et al. 2008).

Most of the Indian subcontinent receives 70–90% of its annual rain fall during the summer monsoon. Prediction of All India seasonal mean Rainfall (ISMR) is useful for the country's policy makers as it is of great importance for agricultural planning as well as management of droughts and floods which directly affect country's agricultural production, economy and human loss (Gadgil and Rao 2000). Therefore, understanding and predictability of ISMR has been a subject of several scientific investigations since long (Blanford 1884, 1886). A recent advancement in the prediction of ISMR is that of real time forecasting technique (Xavier and Goswami 2007). Seasonal forecasting of the Indian summer monsoon rainfall has been widely studied (Kumar et al. 1995; Krishnamurthy and Shukla 2000). Predictability of the seasonal mean rainfall by the AGCM using different initial conditions, boundary condition and models has been recently studied (Kang and Shukla 2006; Kang et al. 2004; Shukla and Fennessy 1994).

Owing to the importance of the ISMR for the Indian subcontinent, a variant of multi-model ensembling technique is applied for the seasonal prediction of precipitation in the central Indian region (73–83°E, 18–27°N) for the period 1980–2001. The technique used in the present study consists of applying Multi-model ensembling to three better models of DEMETER selected on the basis of RMS error and correlation coefficient with the observed precipitation. This model is referred to as the Selected Multi-Model Ensembling (SMME). The predictive skills

of the DEMETER model, MME and SMME have been compared. The study may be further undertaken by comparing the variants proposed herein with the super-ensemble method of multi-model ensembling (Krishnamurthy et al. 1999).

This paper is divided into followings sections. Section 9.2 gives a brief description of the model and data. Section 9.3 describes the forecast skill score measure. Results of mean prediction predictive skill and categorical forecast measures with respect to observations have been discussed in Sect. 9.4 and concluding remarks are presented in Sect. 9.5.

## 9.2 Model and Data

The data used in the present study is 22 year hind cast of model generated data of the DEMETER project models. The data has been obtained from the International Center for theoretical Physics (ICTP), Trieste, Italy under joint collaboration between ICTP and Centre of Ocean–Land–Atmospheric (COLA) Studies, USA, through Targeted Training Activity (TTA) program. The DEMETER hindcasts were started from 1 February, 1 May, 1 August and 1 November to assess the seasonal dependence on prediction skill. Each hindcast comprises an ensemble of nine members.

The observed rainfall data used is the gridded rainfall data ($1^\circ \times 1^\circ$ resolution) from India Meteorological Department (IMD) for the period 1980–2001 based on 1,803 station (Rajeevan et al. 2006). The time series corresponding to 1980–2001 is used for our analysis.

## 9.3 Methodology

An ensemble of nine ocean initial conditions is taken to address the uncertainties in the initial state for each model. MME is done by taking the average of such ensemble forecasts. The outputs of the DEMETER models and the observed precipitation are averaged over the central Indian region and the mean is subtracted (anomaly retained) before doing the analysis.

### *9.3.1 Categorical Forecast Skill for Dichotomous Forecasts*

Categorical (dichotomous) forecast skills refer to the ability of the models to predict the rare events (Wilks 1995). For the dichotomous forecasts, the data is divided into two classes: rare events and normal events. Rare event is defined as one in which the data is outside the range of standard deviation. A normal event is one when the observed data is under the standard deviation of the observed data.

For evaluating the categorical forecast skills in the present study, the data is normalized by dividing with the respective standard deviations. Since the standard deviation of the normalized data is 1, a rare event happens when the modulus of the normalized observed precipitation exceeds 1. A normal event is one when the modulus of the normalized observed precipitation remains less than 1. A rare event is called "event" in this context.

The contingency table is a useful way to see what types of errors are being made. It shows the frequency of "yes" and "no" forecasts and occurrences. A "yes" in the contingency table denotes the occurrence of the "event". Following quantities are defined:

*Hit (H)* – event forecast to occur, and did occur
*Miss (M)* – event forecast not to occur, but did occur
*False alarm (F)* – event forecast to occur, but did not occur
*Correct negative (N)* – event forecast not to occur, and did not occur

Following skill measures are defined for the individual models, MME and SMME:

$$Accuracy = \frac{H+N}{Total} \quad \text{Total} = \text{H} + \text{M} + \text{N} + \text{F}$$

$$Bias = \frac{H+F}{H+M}$$

$$\text{False alarm ratio } (Far) = \frac{F}{H+F}$$

$$\text{Probability of false detection } (Pofd) = \frac{F}{N+F}$$

$$\text{Probability of detection } (Pod) = \frac{H}{(H+M)}$$

$$\text{Threat score } (Ts) = \frac{H}{(H+M+F)}$$

$$\text{Heidke skill score } (Hss) = \frac{[(H+N)-(correct_{random})]}{[Total-(correct_{random})]}$$

$$(correct_{random}) = \frac{[(H+M)(H+F)+(N+M)(N+F)]}{Total}$$

$$\text{Equitable threat score } (Ets) = \frac{(H-H_{random})}{(H+M+F-H_{random})}$$

$$H_{random} = \frac{[(H+M)(H+F)]}{Total}$$

## 9.4 Results and Discussion

The mean prediction of precipitation over the region (73–83°E, 18–27°N) has been studied for the period 1980–2001. In Table 9.1 RMS error and correlation coefficient of DEMETER model outputs with the observed precipitation have been shown. Standard deviation of the observed precipitation is 1.12.

**Table 9.1** Root Mean Square (RMS) error and Correlation Coefficient (r) computed for total rainfall obtained from DEMETER seasonal forecast system and observations. (Standard deviation of observed data = 1.12)

| Model | UKMO | ECMW | INGV | LODY | MAXP | METF | CERF |
|---|---|---|---|---|---|---|---|
| RMS error | 1.13 | 1.23 | 1.35 | 1.41 | 1.05 | 1.09 | 1.15 |
| r | 0.32 | −0.07 | 0.00 | −0.04 | 0.29 | 0.07 | 0.07 |

**Table 9.2** Root Mean Square (RMS) error and Correlation Coefficient (r) computed multi-model ensemble (MME) and SMME

| Model | MME | SMME |
|---|---|---|
| RMS error | 1.121 | 1.029 |
| r | 0.097 | 0.34 |

Tables 9.1 and 9.2 show the RMS errors and correlation coefficients of MME, SMME and DEMETER models with the observed precipitation. It can be seen from these tables that the predictability skills of MAXP, METF and UKMO models are comparable to that of MME. However, none of the models, including the MME, has better predictability skills than the SMME.

The issue of the possibility of a subset of the seven models being used for MME prediction has also been dealt with. Three best models, namely MAXP, METF and UKMO, have been selected on the basis of error analysis and correlation coefficient (Table 9.1) for the SWMME models. It can be seen that the SMME gives better results than the MME (Table 9.2).

The deviation (anomaly component) for the spatial ensemble mean of DEMETER model outputs and observed precipitation of the central Indian region for the 22 year period (1980–2001) for June-August (JJA) is shown in Fig. 9.1. The deviation (anomaly component) for the spatial average of MME and SMME models and the observed precipitation is shown in Fig. 9.2.

Categorical forecast verification has been performed for rainfall for the individual DEMETER models, MME and SMME. Contingency table, based on the definition of 'Yes' and 'No' forecasts, is shown in Table 9.3. The categorical forecast verification has been quantified by calculating dichotomous forecast skill measures and is given in Table 9.4.

Accuracy is greater than 0.50 for the individual models and MME. The accuracy is 0.727 and 0.68 for MAXP and SMME respectively. Since the bias is greater than 1, it can be argued that all the models are over predicting. Probability of detection (POD) for MAXP and UKMO is 0.50. Probability of detection (POD) for SMME is 0.25. False alarm ratio (FAR) is minimum for MAXP. FAR and POD are 1 and 0 respectively, both for METF and LODY, showing that these models fail to predict rare events. Probability of false detection (POFD) is small (0.22) for SMME, CERF and MAXP which indicates that the fraction of "events" which were "wrongly" forecast is small. Threat score (TS) measures accuracy when the correct negative has been removed from the forecast and it is found 0.25 and 0.20 for MAXP and UKMO respectively. Equitable Threat Score (ETS) and Hedkie Skill Score (HSS) are also larger for the MAXP, UKMO, ECMW, CERF and SMME.

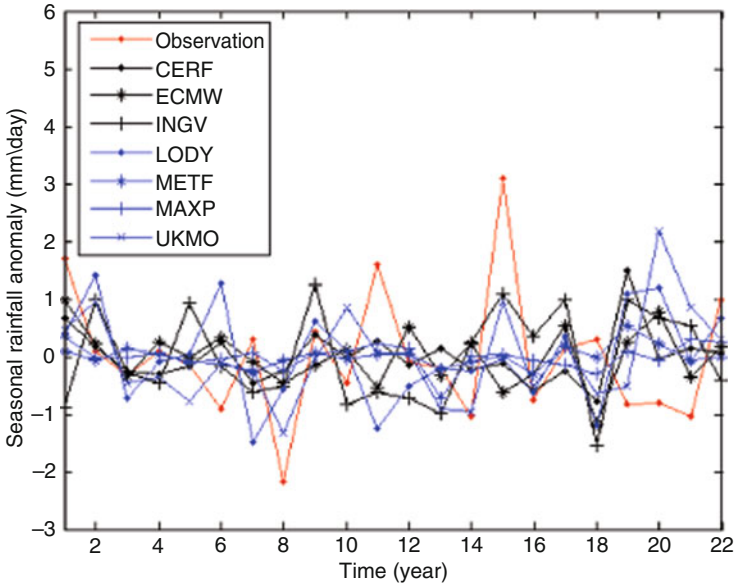


**Fig. 9.1** Time series of observation and individual model outputs of the DEMETER project for seasonal (JJA) precipitation anomaly averaged over central India for the period 1980–2001

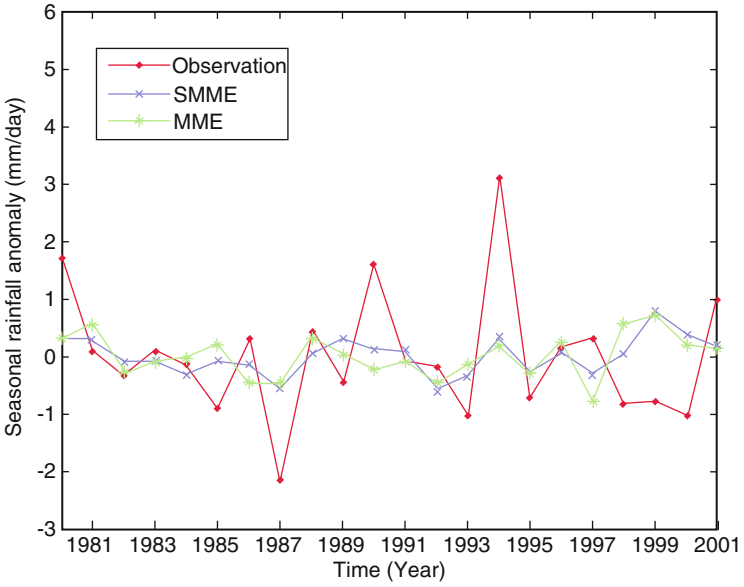


**Fig. 9.2** Time series of observation, multi-model ensemble (MME) and selected multi-model ensemble (SMME) of the individual model outputs of the DEMETER project for seasonal (JJA) precipitation anomaly averaged over central India for the period 1980–2001

**Table 9.3** Contingency table for the individual model, MME and SMME

| Model | | | Observed | |
|---|---|---|---|---|
| | | | Yes | No |
| UKMO | Forecast | Yes | 2 | 6 |
| | | No | 2 | 12 |
| ECMW | Forecast | Yes | 1 | 4 |
| | | No | 3 | 14 |
| INGV | Forecast | Yes | 1 | 8 |
| | | No | 3 | 10 |
| LODY | Forecast | Yes | 0 | 6 |
| | | No | 4 | 12 |
| METF | Forecast | Yes | 0 | 5 |
| | | No | 4 | 13 |
| MAXP | Forecast | Yes | 2 | 4 |
| | | No | 2 | 14 |
| CERF | Forecast | Yes | 1 | 4 |
| | | No | 3 | 14 |
| MME | Forecast | Yes | 1 | 6 |
| | | No | 3 | 12 |
| SMME | Forecast | Yes | 1 | 4 |
| | | No | 3 | 14 |

**Table 9.4** Categorical skill scores for individual models, MME and SMME

| Model | Accuracy | Bias | POD | FAR | POFD | TS | ETS | HSS |
|---|---|---|---|---|---|---|---|---|
| UKMO | 0.636 | 2.0 | 0.5 | 0.75 | 0.33 | 0.2 | 0.06 | 0.12 |
| ECMW | 0.68 | 1.25 | 0.25 | 0.8 | 0.22 | 0.125 | 0.012 | 0.025 |
| INGV | 0.5 | 2.25 | 0.25 | 0.88 | 0.44 | 0.083 | −0.061 | −0.13 |
| LODY | 0.54 | 1.5 | 0 | 1 | 0.33 | 0 | −0.12 | −0.28 |
| METF | 0.59 | 1.25 | 0 | 1 | 0.277 | 0 | −0.11 | −0.25 |
| MAXP | 0.727 | 1.5 | 0.5 | 0.66 | 0.22 | 0.25 | 0.13 | 0.22 |
| CERF | 0.68 | 1.250 | 0.250 | 0.800 | 0.222 | 0.125 | 0.013 | 0.025 |
| MME | 0.59 | 1.75 | 0.25 | 0.86 | 0.33 | 0.10 | −0.03 | −0.06 |
| SMME | 0.682 | 1.25 | 0.25 | 0.80 | 0.22 | 0.125 | 0.013 | 0.025 |

It has been pointed out that the SMME model has better predictability skills than all the other models including the MME when RMS error and correlation coefficients were compared. On the basis of categorical forecast skills, however, it can be seen that individual models (Table 9.4) may outperform MME and SMME both. Evaluation of categorical forecast skills is important for the actual comparison of models as it informs us of the model's ability to detect rare events. The purpose of calculating categorical forecast skill scores is, in the present case, to strengthen the argument that the ensemble mean forecast is not always better than the best individual model of DEMETER project.

It is also interesting to mention that CERF and ECMW models are showing same dichotomous skill scores (Table 9.4). However, from Table 9.1 it is clear that RMS error and correlation coefficients are different for the both models. Since the

dichotomous forecast skills refer to the capability of predicting the rare events only, we conclude that both are equivalent when predicting the rare events.

## 9.5 Conclusion

The models outputs of the DEMETER project have been analyzed for the prediction of seasonal (JJA) anomalies of the precipitation in the central Indian region for the period 1980–2001. Alternative technique for MME is proposed and its performance is evaluated. The technique, selected multi-model ensembling (SMME), consists of selecting three better individual models on the basis of error and correlation analysis and averaging the results over the models as is done in MME. It has been observed that the SMME model has better prediction skills than all the individual models and MME. The MME does not, in every case, has better prediction skills than the individual models when RMS error and correlation coefficients are considered. However, the SMME has shown better skills than all the individual models. Further, on the basis of categorical forecasts, it is seen that MME and SMME do not always give better prediction than individual models.

## References

Blanford HF (1884) On the connection of the Himalaya snowfall with dry winds and seasons of drought in India. Proc R Soc Lond 37:3–22

Blanford HF (1886) Rainfall of India. Mem India Meteorol Dept 2:217–448

Gadgil S, Rao PRS (2000) Famine strategies for variable climate – a challenge. Curr Sci 78:1203–1215

Hartmann HC, Pagano TC, Sorooshian S, Bales R (2002) Confidence builders: evaluating seasonal climate forecast for user prospective. Bull Am Meteor Soc 83:683–698

Kang IS, Shukla J (2006) Dynamical seasonal prediction and predictability. In: Wang B (ed) The Asian Monsoon. Springer, Heidelberg, pp 585–612

Kang IS, Lee JY, Park CK (2004) Potential predictability of summer mean precipitation in a dynamical seasonal prediction system with systematic error correction. J Clim 17:834–844

Krishnamurthy V, Shukla J (2000) Intraseasonal and interannual variability of rainfall over India. J Clim 13:4366–4377

Krishnamurthy TN, Kishtawal CM, LaRow TE, Bachiochi DR, Zhang Z, Williford CE, Gadgil S, Surendran S (1999) Improved weather and seasonal climate forecasts from multimodal super-ensemble. Science 285:1548–1550

Kumar KK, Soman MK, Kumar KR (1995) Seasonal forecasting of Indian summer monsoon rainfall: a review. Weather 50:449–467

Palmer TN (2001) A nonlinear dynamical prospective on model error: a proposal for non local stochastic dynamic parameterization in weather and climate prediction models. Quart J R Meteor Soc 127:279–304

Palmer TN, Shukla J (2000) Editorial to DSP/PROVOST. Q J R Meteorol Soc 126:1989–1990

Palmer TN, Alessandri A, Andersen U, Cantelaube P, Davey M, Délécluse P, Déqué M, Diez E, Doblas-Reyes FJ, Feddersen H, Graham R, Gualdi S, Guérémy JF, Hagedorn R, Hoshen M, Keenlyside N, Latif M, Lazar A, Maisonnave E, Marletto V, Morse AP, Orfila B, Rogel P,

Terres JM, Thomson MC (2004) Development of a European multimodel ensemble system for seasonal-to-interannual prediction (DEMETER). Bull Am Meteorol Soc 85:853–872

Rai S, Pandey AC, Tripathi KC, Dwivedi S (2008) Predictive skill of DEMETER models for wind prediction near Madagascar. Indian J Mar Sci 37:62–69

Rajeevan M, Bhatt J, Kale JD, Lal B (2006) High resolution daily gridded rainfall data for the Indian region: analysis of break and active monsoon spells. Curr Sci 91:296–306

Shukla J, Fennessy MJ (1994) Simulation and predictability of monsoons in Proceedings of the international conference on monsoon variability and prediction technology report WCRP-84, Geneva. World Climate Research Programme, pp 567–575

Shukla J, Anderson J, Baumhefner D, Brankovic C, Chang Y, Kalnay E, Marx L, Palmer T, Paolino D, Ploshay J, Schubert S, Straus D, Suarez M, Tribbia J (2000) Dynamical Seasonal Prediction. Bull Am Meteorol Soc 81:2653–2664

Thomson MC, Palmer TN, Morse AP, Cresswell M, Connor SJ (2000) Forecasting disease risk with seasonal climate predictions. Lancet 355:1559–1560

Wilks DS (1995) Statistical methods in atmospheric sciences. Academic, San Diego, pp 233–390

Xavier PK, Goswami BN (2007) Analog method for realtime forecasting of summer monsoon sub-seasonal variability. Mon Wea Rev 135:4149–4160

# Chapter 10
# Simulation of Indian Summer Monsoon Circulation with Regional Climate Model for ENSO and Drought Years over India

**Sandipan Mukherjee, Ravi P. Shukla, and Avinash C. Pandey**

**Abstract** Indian summer monsoon circulation including the monsoon rainfall has been simulated with the regional climate model (RegCM3) for two different years associating an ENSO and a drought year. The horizontal resolution of the model is 60 Km covering the entire Indian subcontinent. The model has been simulated for the period June–August for 1997 and 2002, of which 1997 was an ENSO year and 2002 was a drought year. The model sensitivity is examined by using two convective schemes (Kuo type and Grell) and by simulating the characteristics monsoon features of wind at 850 hPa and 200 hPa, temperature at 500 hPa, along with the mean seasonal rainfall over central India (70–90E and 15–25N). We find that the important monsoon circulation features are well simulated by the model including the low mean seasonal rainfall of 2002 over India. We have also find that between the two different parameterization schemes, the Grell runs are giving better results than the other for the rainfall fields. The categorical forecast skill also reveals that although the accuracy of the model is high for 2002, but the probability of detection of extreme events are higher for 1997.

S. Mukherjee (✉)
K. Banerjee Center of Atmospheric and Ocean Studies, University of Allahabad, Allahabad 211002, India
e-mail: mukherjee.sandipan@rediffmail.com

R.P. Shukla
Department of Physics, University of Allahabad, Allahabad 211002, India
e-mail: ravishukla72@gmail.com

A.C. Pandey
M. N. Saha Center of Space Studies, IIDS, University of Allahabad, Allahabad 211002, India
e-mail: avinashcpandey@rediffmail.com

S.D. Attri et al. (eds.), *Challenges and Opportunities in Agrometeorology*,
DOI 10.1007/978-3-642-19360-6_10, 

## 10.1 Introduction

For the prediction of natural systems a variety of models have been proposed. Models have been improved from simple conceptual Lorenz equations to complex global climate models. General circulation models (GCMs) are yet not capable of predicting the behaviour of local or regional climatic systems. To overcome the deficiency, regional climate models with a higher resolution are constructed for limited areas. Thus to capture the small-scale physical processes that drive important local surface variables and for improved predictions of those variables, regional climate modeling is necessary. Again from the computational point of view, it is possible to increase the resolution of regional models so as to resolve regional climatic features very well. Several regional models are in use today for a wide variety of weather and climatic research and applications including operational weather forecasting (Giorgi 1990; Dudhia 1993; Bhaskaran et al. 1996).

Rainfall over India varies both in space and time during summer monsoon seasons and the large scale rainfall plays an important role in the agriculture planning, disaster and water resource management of the Indian subcontinent (Gadgil and Rao 2000). The Indian summer monsoon circulation features with the associated rainfall and its variation is still an interesting problem. There have been some studies to simulate monsoon features and extreme weather events over India by regional models. Bhaskaran et al. (1996) simulated the summer monsoon circulation with a regional model nested in a GCM found that regional model derived precipitation is 20% larger than a GCM. Patra et al. (2000) made a comparative study on the performances of MM5 and regional atmospheric modeling system in simulating the Bay of Bengal cyclones. The effect of initial conditions on the simulation of the super cyclone of Orissa was explored by Trivedi et al. (2002) using MM5 model. Dash et al. (2006) have extensively used the regional climate model (RegCM3) to simulate the monsoon circulation over India and have tested the sensitivity of the model incorporating snow over the Tibetan region.

In our present study we have used the regional climate model to simulate the monsoon circulation features associated with rainfall over the Indian subcontinent for two different years, 1997 and 2002 and compared the circulation pattern with the observed data as the former year was an ENSO year and the later was a drought year. The sensitivity of the model is also explored with different physical parameterization schemes. In Sect. 10.2, a brief description of the model is given along with the initial and boundary condition data. In Sect. 10.3, characteristic monsoon circulation features of wind (850 and 200 hPa), temperature at 500 hPa, and rainfall is analyzed and compared for the two different events and a conclusion has been drawn in Sect. 10.4.

## 10.2 Model and Experimental Design

The regional climate model used in the present work is the version of RegCM3 developed by Giorgi et al. (1993a, b). The dynamical core of the regional climate model is equivalent to hydrostatic version of fifth generation NCAR, U.S., mesoscale model (MM5). The model is a compressible, grid point model with 18 vertical levels in sigma coordinate. The physics parameterization used in the simulation includes the radiative transfer package of NCAR CCM3. A planetary boundary layer schemes and the convective precipitation scheme of modified Kuo scheme and Grell scheme (Grell 1993) is used. These two different precipitation schemes are used to explore the sensitivity of the model. The model also includes an ocean flux parameterization and pressure gradient scheme. Different land surface processes are described by Biosphere–Atmosphere Transfer scheme or BATS (Dickinson et al. 1989). BATS consists of a vegetation layer, three soil layers for soil water content and a force restore method to calculate the temperature of surface soil layer and a subsurface soil layer. BATS is mainly a state-of-the-art land surface model that is used by researchers for long periods.

In the present study, the model is simulated over the domain and topography as shown in Fig. 10.1. The computational domain of the model includes the entire Indian subcontinent only excluding the extreme eastern Himalayan regions. A normal Mercator projection is used with the grid cells of 60 $\times$ 60 km size. For the model integrations, the central longitude and central latitude is chosen at 80° E and 20° N. Terrain heights and land use data are generated from the global data set of the United States Geographical Survey (USGS) at 10 min resolution. The initial conditions for the model used are from the NCEP reanalysis dataset-2 (2.5° $\times$ 2.5°, L17). The SST data used for the model initialization is the monthly mean and obtained from NOAA optimum interpolated (OI) SST v2, (OISST). The model has been simulated for two different years 1997 and 2002, from June 1 to August 30 and the mean monsoonal circulation feature is investigated and compared with the NCEP/NCAR reanalysis fields as well as the IMD gridded datasets.

## 10.3 Results

In this section, we have explored some of the important characteristics features of Indian summer monsoon circulation along with rainfall in detail for the two different years and are compared with corresponding fields from the NCEP/NCAR reanalysis. Some of the important monsoon circulation includes westerly jet at 850 hPa, the easterly jet at 200 hPa, the temperature at 500 hPa and the surface pressure pattern. We have mainly explored the variability of the wind fields and the temperature at 500 hPa along with the rainfall.

The observed wind flow of 850 hPa for 1997 and 2002 along with the model simulated wind is given in Figs. 10.2–10.4. The observed mean wind field for JJA of

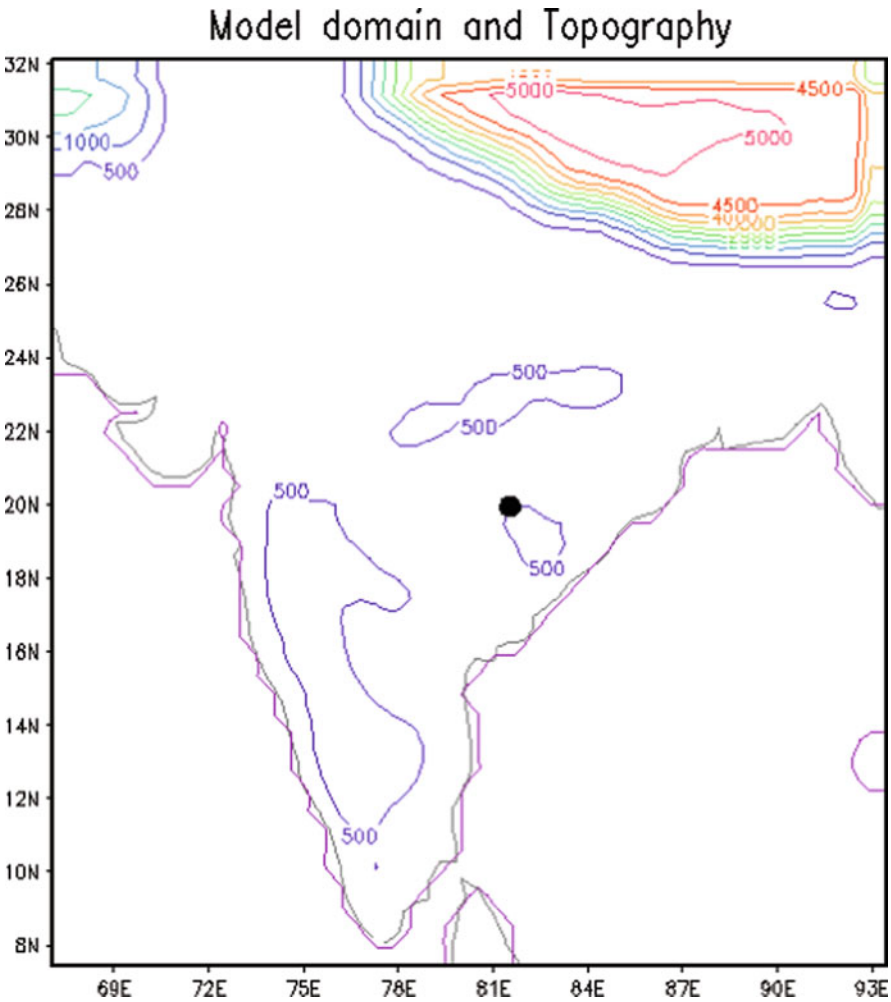


**Fig. 10.1** The model domain along with the surface elevation. The *dark spot* indicates the center of the model simulation at (80 E and 20 N)

1997 and 2002 is given in Fig. 10.2a, b. A strong westerly wind prevails for both the years over the peninsular region of India and the observed maximum strength of the JJA mean westerly wind at 850 hPa is found to be 7.4 m/s for 1997 and that of 6.9 m/s for 2002. Using the Grell scheme (Fig. 10.3a) we find that JJA mean westerly wind is 8 m/s and that of 7.0 m/s for the Kuo scheme (Fig. 10.3b) for 1997. When the 2002 wind field of 850 hPa is simulated using the same parameterization we find that the simulated mean wind is of 7.7 m/s for Grell scheme (Fig. 10.4a) but it is a fraction smaller for the Kuo scheme (Fig. 10.4b) and is 6.7 m/s. Although both the schemes have reasonably well simulated the mean wind

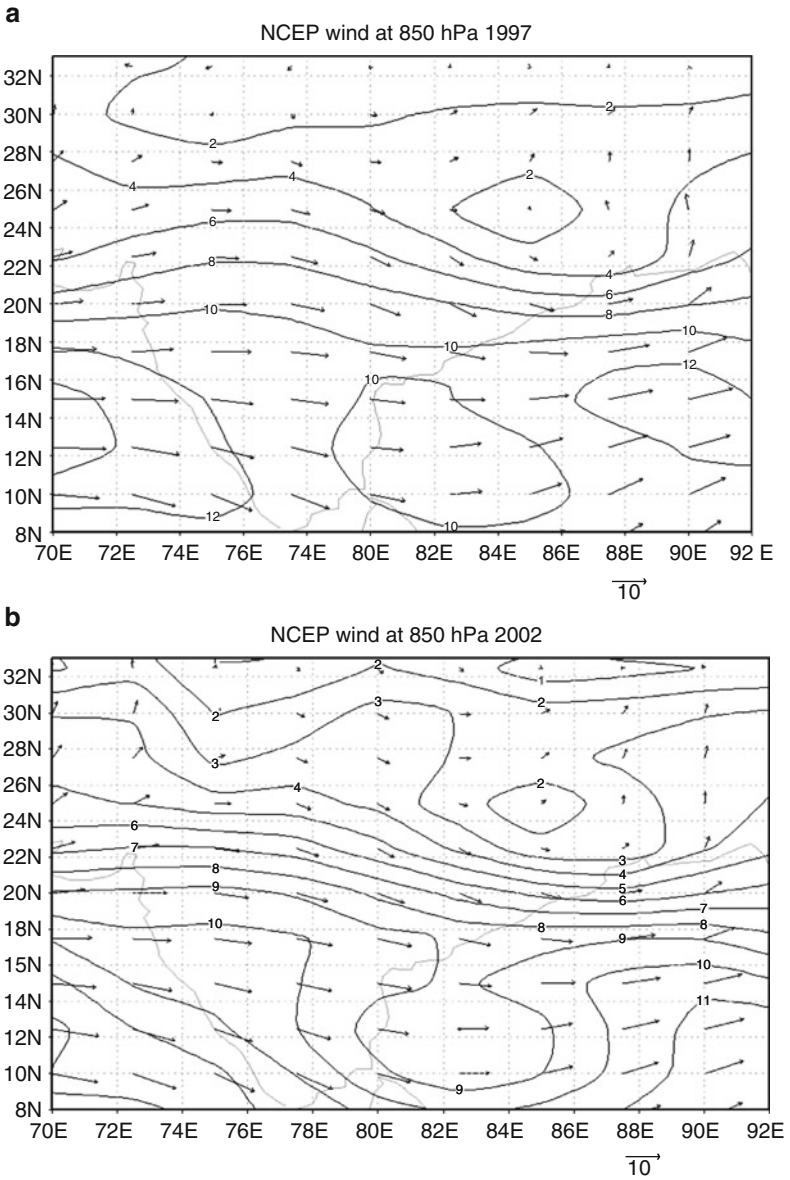


**Fig. 10.2** (**a** and **b**) Observed NCEP/NCAR reanalysis wind fields of 850 hPa for 1997 and 2002

fields of JJA of 1997 and 2002, the Grell scheme is found to simulate the mean wind 13% more than actual for 2002.

Similarly when the 200 hPa wind fields are simulated for 2002 using the same parameterization schemes, we found that both the Grell and Kuo schemes are

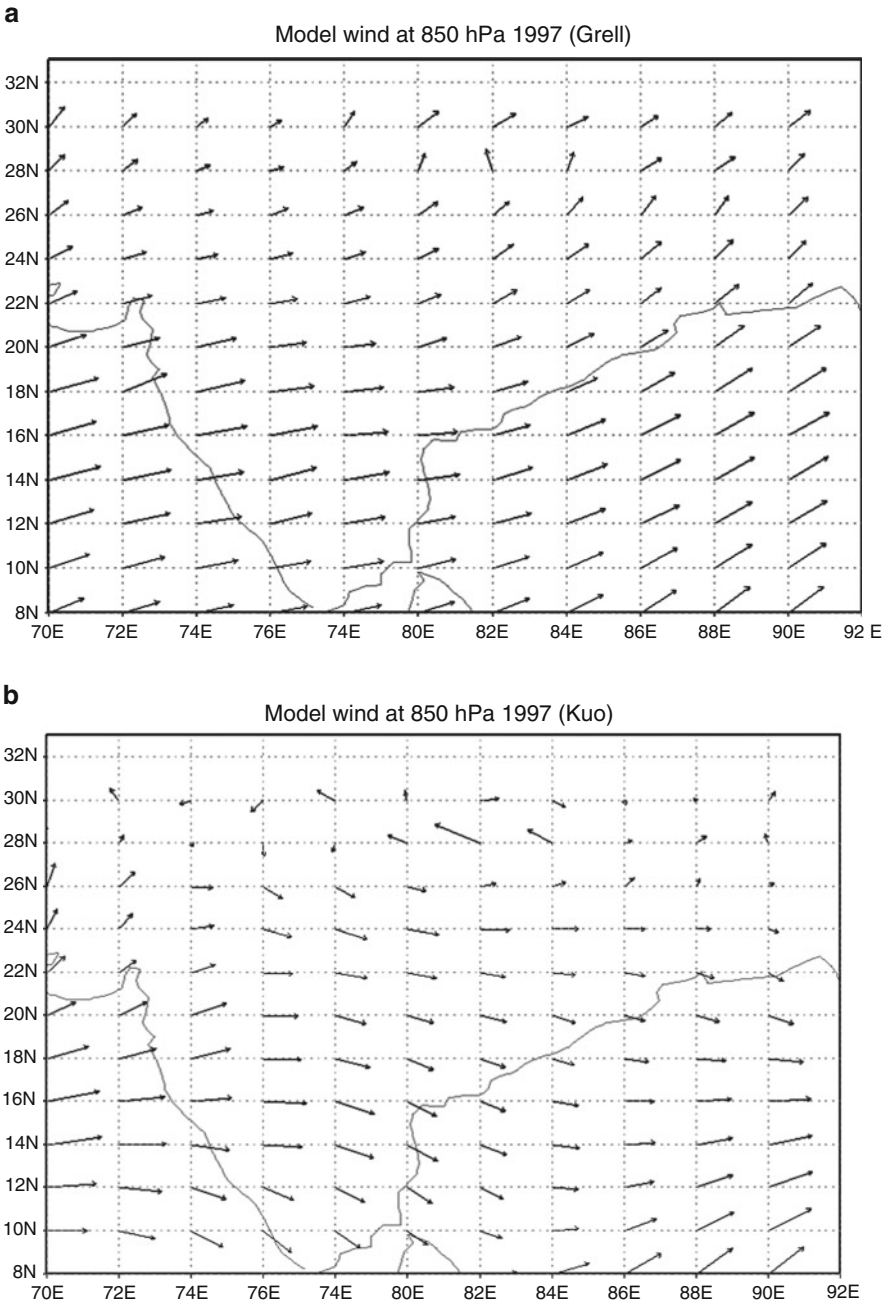


**Fig. 10.3** (**a** and **b**) Model simulated wind fields of 850 hPa for 1997 using Grell and Kuo schemes

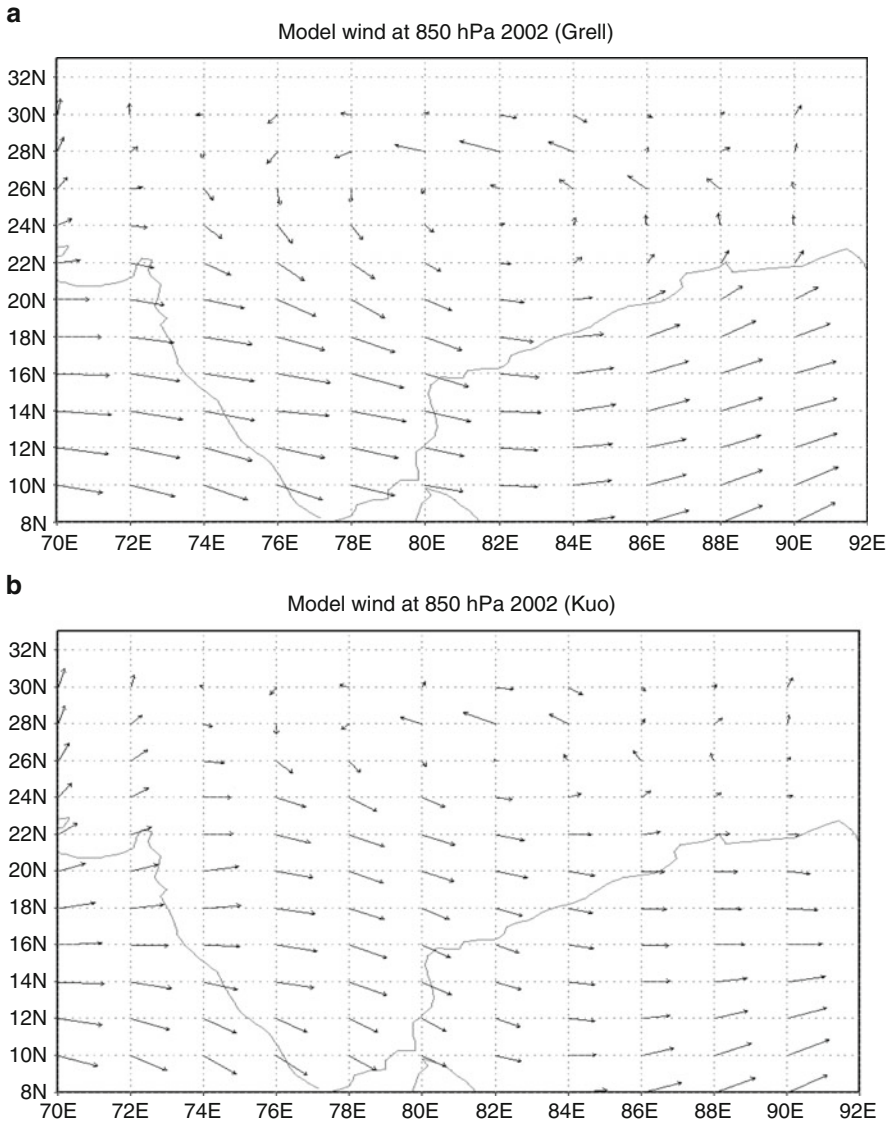


**Fig. 10.4** (**a** and **b**) Model simulated wind fields of 850 hPa for 2002 using Grell and Kuo schemes

simulating the mean wind well. The Grell scheme exactly matches the observed mean wind speed of 12.3 m/s and the Kuo scheme simulates a fraction larger with 12.5 m/s. In case of 1997, the observed mean wind over India for JJA is found to be 11 m/s. Simulating this wind field with two different parameterizations; we find that Grell scheme simulates the mean wind 20% less than the actual.

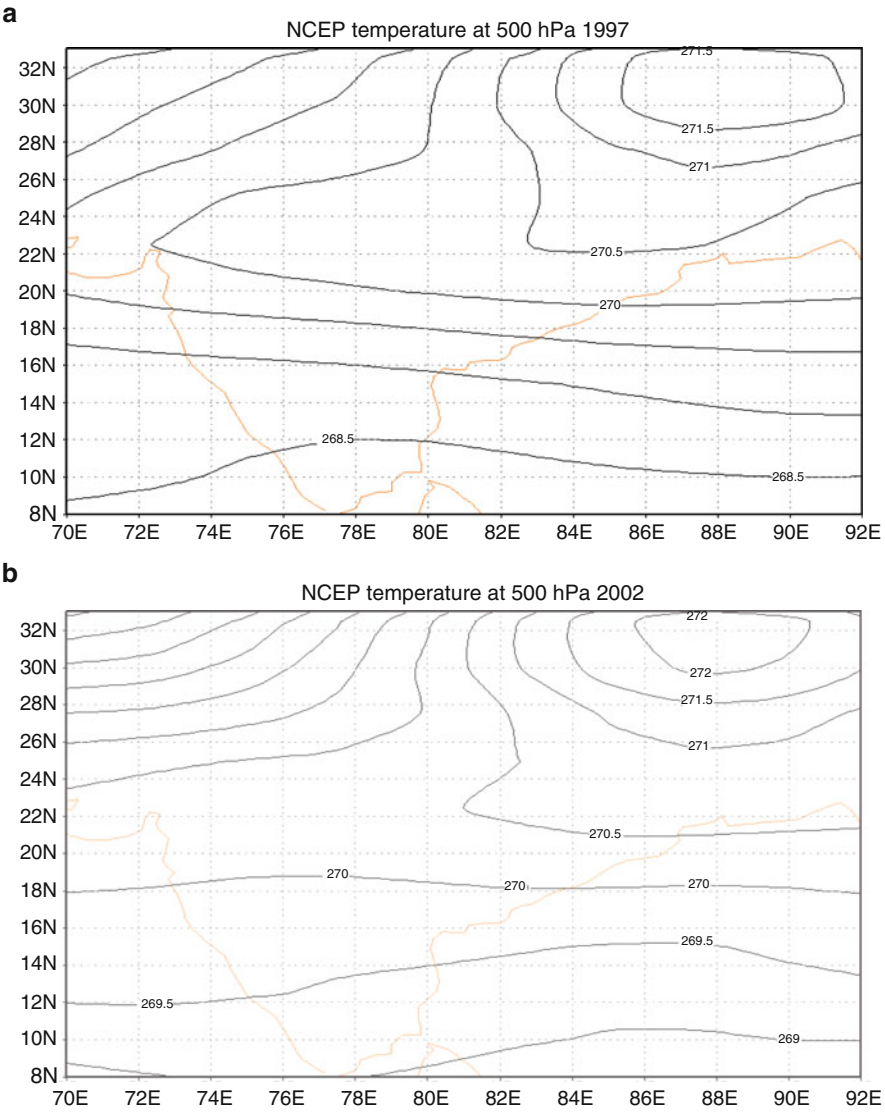


**Fig. 10.5** (**a** and **b**) Observed NCEP/NCAR reanalysis temperature fields of 500 hPa for 1997 and 2002

Figure 10.5a, b shows the observed mean temperature of JJA of 500 hPa for 1997 and 2002, respectively. The observed mean temperature for 1997 is found to be 269.5 K and that of 2002 is 269.9 K. The simulated temperature by Grell and Kuo schemes are shown in Fig. 10.6a, b for 1997 and in Fig. 10.7a, b for 2002. We find that the simulated mean temperature for 2002 on Grell run is 270.0 K to and that of the Kuo run is 269.5 K. The Grell scheme simulates reasonable results than the Kuo.

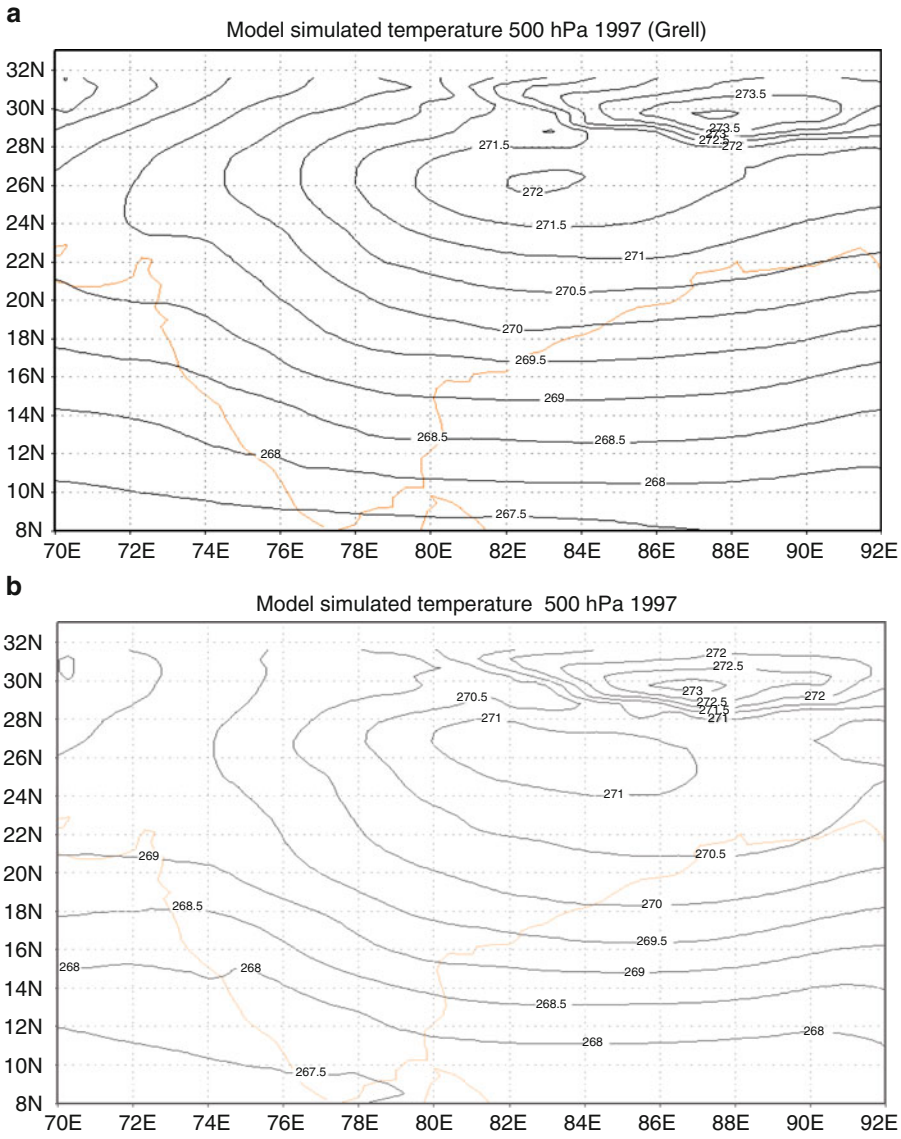


**Fig. 10.6** (**a** and **b**) Model simulated temperature fields of 500 hPa for 1997 using Grell and Kuo schemes

The standardized anomaly variation of rainfall of JJA over the central India (70–90E and 15–25N) for 1997 and 2002 is shown in Figs. 10.8 and 10.9 respectively. The rainfall variations are compared with the IMD station datasets which are linearly interpolated to a homogeneous grid over India. The standardized anomaly is calculated by removing the seasonal mean from the data. Although 1997 was an

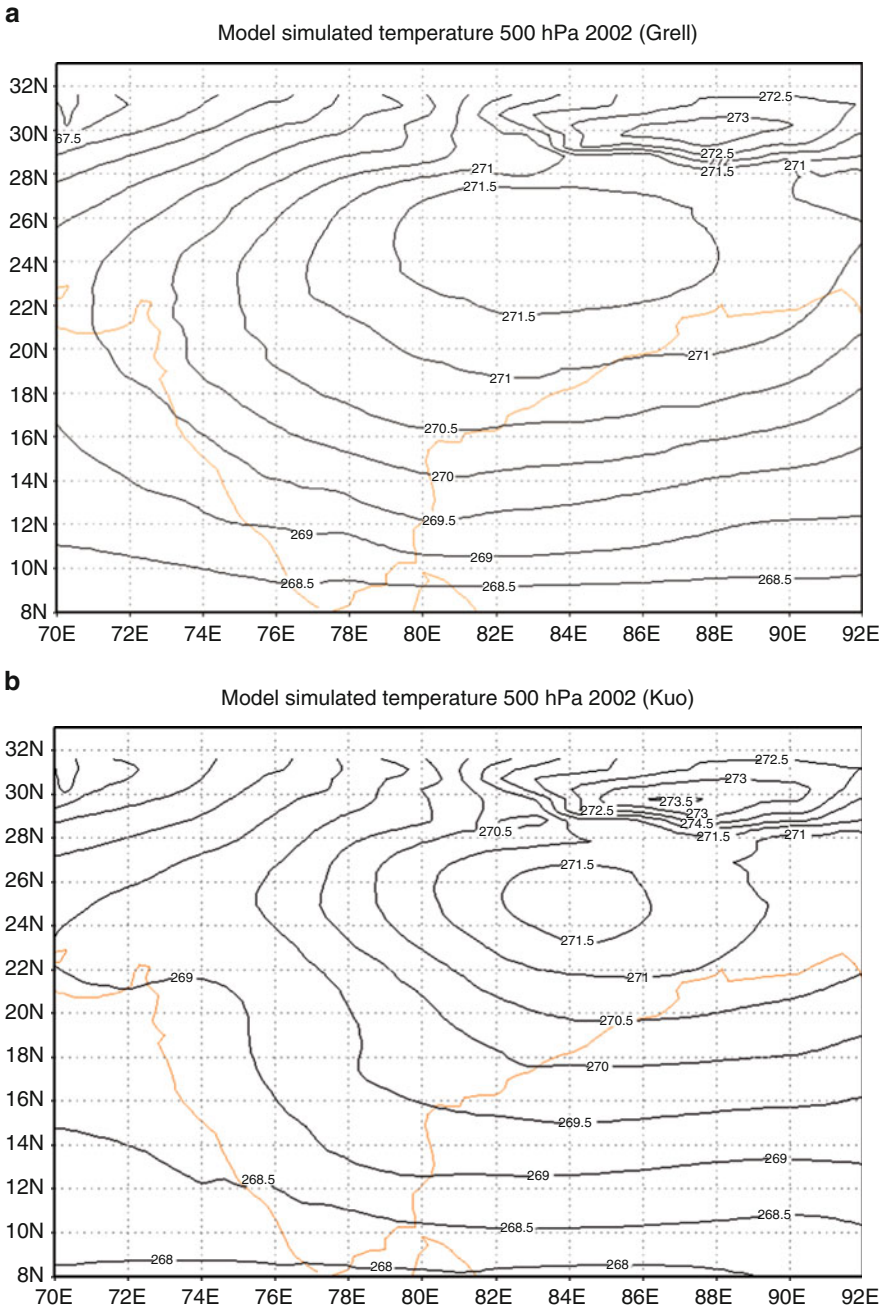


**Fig. 10.7** (**a** and **b**) Model simulated temperature fields of 500 hPa for 2002 using Grell and Kuo schemes

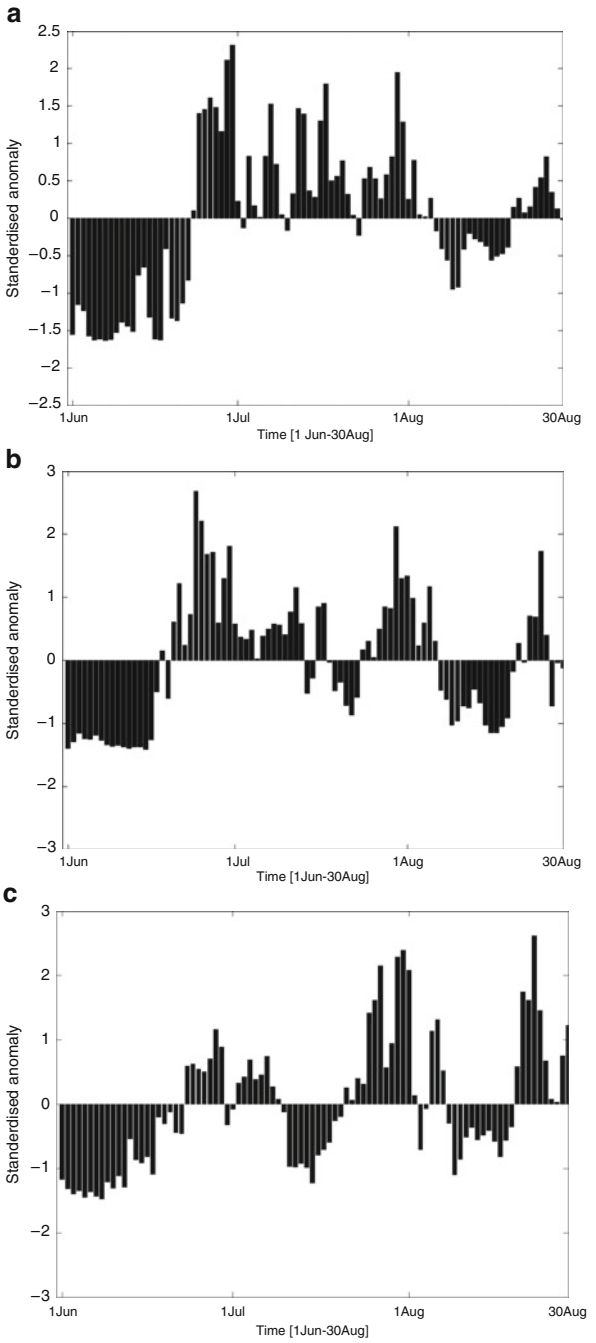


**Fig. 10.8** (**a–c**) Standardized anomaly of rainfall over central India (70–90E and 15–25 N) with (**a**) Grell scheme. (**b**) Kuo scheme. (**c**) IMD data for 1997

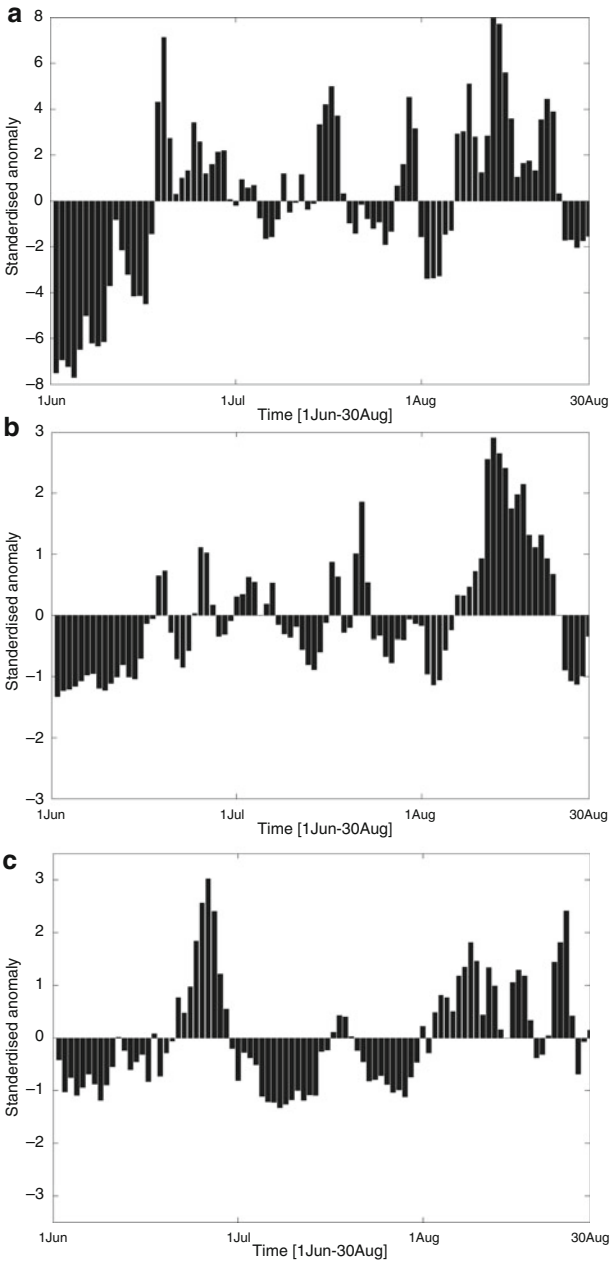


**Fig. 10.9** (**a**–**c**) Standardized anomaly of rainfall over central India (70–90 E and 15–25 N) with (**a**) Grell scheme. (**b**) Kuo scheme. (**c**) IMD data for 2002

**Table 10.1** Categorical forecast skill measures for the model simulated of seasonal rainfall over central for 1997 and 2002. Only the Grell scheme results are compared with IMD observed data

| Year | Schemes | Accuracy | POD | FAR | POFD | TS | ETS | HSS |
|---|---|---|---|---|---|---|---|---|
| 1997 | Grell | 0.67 | 0.21 | 0.85 | 0.24 | 0.09 | 0.00 | −0.01 |
| 2002 | Grell | 0.73 | 0.06 | 0.39 | 0.12 | 0.04 | −0.03 | −0.07 |

ENSO year, we find that the rainfall distribution during this year was nearly normal and an average seasonal rainfall of JJA over central India was 9 mm/day which is just little below the seasonal average of 10–15 mm/day for central region (Krishnamurthy and Shukla 2000), though we have excluded the rainfall pattern for September. The simulation of rainfall by Grell scheme for 1997 yields an average seasonal rainfall of 10.04 mm/day which is in good agreement with the observed value. The Kuo scheme simulates very low average seasonal rainfall of 3.0 mm/day virtually concluding the failure of the scheme. We find that the correlation between the IMD gridded data and Grell run data is 0.55 and that of IMD data and Kuo run data is 0.61 but the bias [mean(observed data) – mean (simulated data)] is found to be very high for Kuo run and is equal to 5.9 which is not the case for Grell run. Here the bias is respectively low and equal to −1.1.

For 2002, we find that the average seasonal rainfall over the central Indian region is 7.1 mm/day which is much lower than the normal seasonal rainfall of India. This leads to 2002 as a drought year. When the seasonal rainfall is simulated with Grell scheme we find it 8.3 mm/day with a correlation of 0.40 with the IMD data and a bias of −1.2. The Kuo run for 2002 fails drastically with a mean seasonal rainfall of 2.3 mm/day with correlation of 0.36 and bias 4.8. Categorical forecast skill measure for only the Grell scheme and for both the years is shown in Table 10.1. The accuracy is of the model is better for 2002, which is 0.71 but the probability of detection (POD) is higher for 1997 although the false alarm rate (FAR) and the probability of false detection (POFD) of 2002 is less than 1997.

## 10.4 Conclusion

The regional climate model (RegCM3) has previously been tested for the monsoon circulation by Dash et al. (2006) and the effect of snow cover is also tested by them. Dimri and Ganju (2007) have also explored the winter climatic behaviour of northern India with RegCM3. In the present study, we have explored the effect of change in the sea surface temperature during ENSO period on the monsoon circulation. We have also tested the sensitivity of the climate model for a drought year. The change in the monsoon circulation features are then compared for these two different weather events.

We find that between the two different cumulus parameterization schemes, Grell scheme is more superior to the Kuo scheme in simulating rainfall fields. In case of wind field though, the Grell scheme has simulated 13% more for 850 hPa and that of

20% less for 200 hPa for 2002. The temperature variation of 500 hPa is well simulated for both the years by Grell scheme with a very little deviation from the observed value. The mean seasonal rainfall is reasonably well predicted for the drought year of 2002 by the Grell scheme. The comparison of the forecast measure for 1997 and 2002 shows that the accuracy of the model is better for 2002, but the probability of detection of extreme events is higher for 1997.

## References

Bhaskaran BR, Jones G, Murphy JM, Noguer M (1996) Simulations of the Indian summer monsoon using a nested regional climate model: domain size experiments. Clim Dyn 12:573–578

Dash SK, Shekhar MS, Singh GP (2006) Simulation of Indian summer monsoon circulations and rainfall using RegCM3. Theor Appl Climatol 86:161–172

Dickinson RE, Erico RM, Giorgi F, Bates GT (1989) A regional climate model for the western United states. Clim Change 15:383–422

Dimri AP, Ganju A (2007) Wintertime seasonal scale simulation over western Himalaya Using RegCM3. Pure Appl Geophys 164:1733–1746

Dudhia J (1993) A nonhydrostatic version of the Penn State/NCAR mesoscale model: validation tests and simulation of an Atlantic cyclone and cold front. Mon Wea Rev 121:1493–1513

Gadgil S, Rao PRS (2000) Famine strategies for a variable climate – A challenge. Curr Sci 78:1203–1215

Giorgi F (1990) Simulation of regional climate using a limited area model nested in a general circulation model. J Climate 3:941–963

Giorgi F, Marinucci MR, Bates GT (1993a) Development of a second generation regional climate model (RegCM2). Part I: boundary-layer and radiative transfer processes. Mon Wea Rev 121:2794–2813

Giorgi F, Marinucci MR, Bates GT, De Canio G (1993b) Development of a second-generation regional climate model (RegCM2). Part II: convective processes and assimilation of lateral boundary conditions. Mon Wea Rev 121:2814–2832

Grell GA (1993) Prognostic evaluation of assumptions used by cumulus parameterizations. Mon Wea Rev 121:754–787

Krishnamurthy V, Shukla J (2000) Intraseasonal and interannual variability of rainfall over India. J Clim 13:4366–4377

Patra KP, Santhanam MS, Potty KVJ, Tewari M, Rao PLS (2000) Simulation of tropical cyclones using regional weather prediction models. Curr Sci 79(1):70–78

Trivedi DK, Sanjay J, Singh SS (2002) Numerical simulation of a super cyclonic storm, Orissa 1999: impact of initial conditions. Meteorol Appl 9:367–376

# Chapter 11
# Changes in surface temperature and snow over the Western Himalaya Under Doubling of Carbon Dioxide ($CO_2$)

**P. Parth Sarthi, S.K. Dash, and Ashu Mamgain**

**Abstract** Global warming has caused the world's surface temperature to rise at an unprecedented rate and these changes have caused the snow and ice to melt rapidly. The variability of temperature as consequence of global warming plays a crucial role on the snow over the western Himalaya which is a natural water reservoir by releasing large quantity of fresh water throughout the year in the important rivers of north India. The change in snow as an impact of global warming over this region may affect the water resources in north Indian rivers. The decline of water in snow fed rivers, with disappearance and melting of snow, glaciers and ice sheets may have a direct impact on the lives of millions of people who depend on these snow-fed rivers and hence there may be economic losses.

The impact of the Himalayan snow on Indian Summer Monsoon Rainfall (ISMR) and Land surface Hydrology in the northern Indian during Indian Summer Monsoon (ISM) region is vital and therefore it is necessary to examine their variability in past, present and future time slices. Since Western Himalaya (WH) snow does have a relation with ISMR and also important holy rivers like the Ganga originates, therefore the domain of WH is chosen for the current study. The Model for Interdisciplinary Research On Climate (MIROC3.2 hires) simulated snow depth and surface temperature in experiments twentieth century simulation (20c3m) and doubling of $CO_2$ simulation (1pctto2x) are utilized. To know the response of doubling of $CO_2$ in atmosphere on snow depth and surface temperature over WH, the model simulated snow depth and surface temperature is analyzed under the doubling of $CO_2$ (1pctto2x) and twentieth century (20c3m) simulation. snow depth is decreased more in 1pctto2x in compare to 20c3m simulation. It is found that the

P.P. Sarthi (✉)
Centre for Environmental Sciences, Central University of Bihar, Patna 800014, India
e-mail: drpss@hotmail.com

S.K. Dash • A. Mamgain
Center for Atmospheric Sciences, Indian Institute of Technology Delhi, Hauz Khas, New Delhi-110016, India
e-mail: skdash@cas.iitd.ac.in; ashumam@gmail.com

S.D. Attri et al. (eds.), *Challenges and Opportunities in Agrometeorology*,
DOI 10.1007/978-3-642-19360-6_11, 

increase of surface temperature and decrease of snow depth are more during May to December with positive and negative trends in surface temperature and snow depth respectively.

## 11.1 Introduction

snow is regarded as an important indicator of climate change because of its influence on energy and moisture budget on the earth surface. The increase or decrease in snow depth directly influences the prevailing surface temperature and leads to change in wind circulation pattern. Thus snow depth anomaly provides a sink or source of the surface temperature. When snow depth is more over an area, more radiation is required to melt the snow and small amount of radiation is left to warm the earth surface. The inverse is true in the case of less snow depth over the area. This is the classic temperature-snow feedback mechanism, which is key component in climate models. The snow/sec-ice feedback has a significant impact on the sensitivity of a climate model. If a marginally snow-covered area warms, snow tends to melt, lowering the albedo, and hence leading to more snowmelt (the ice-albedo feedback). This is the basis for predictions of enhanced warming in seasonally snow covered regions as a result of global warming.

The link between the Himalayan winter snow and ISMR has been recognized by Blanford (1884), Walker (1910), Dey and Kumar (1983), and Dickson (1984). The linear correlation coefficients between December-to-March snow extent in the Himalayas and June-to-September monsoon rainfall were found to be approximately −0.6 by Dey and Kumar (1983) and Dickson (1984). Kripalani et al. (2003) presented the monthly climatology and variability of the Indian National Satellite (INSAT) derived snow cover estimates over the western Himalayan region. They suggested that the changes in observed snow cover extent and snow Depth due to global warming may be a possible cause for the weakening winter snow-ISMR relationship. Using Regional Climate Model (RegCM3), a sensitivity experiment based on snow depth anomaly over Tibet has been conducted and associated changes in circulation pattern and rainfall over India were examined by Dash et al. (2007).

The snow in the Himalaya is a sensitive indicator of climate change. The Himalayan region as a whole has warmed by about 1.8°F since the 1970s (Shrestha et al. 1999; UNEP 2002). Earlier studies show decline in snow depth/cover over most parts of the world due to global warming (IPCC). The observational studies also indicated that the northern hemisphere annual snow cover extent has decreased by about 10% since 1966. The observational studies indicated a decrease in snow extent over the past decade (Robinson and Serreze 1995; Karl et al. 1993; Groisman et al. 1994). Reduction in snow cover during the mid to late 1980s was strongly related to temperature increase in snow covered area. There were highly significant interannual and multidecadal correlations between increase in the northern hemisphere spring land temperature and a reduction in the northern hemisphere spring snow cover (IPCC 2001).

The simulation of climate change projects a reduction in the extent and duration of snow cover in response to the warming condition (Kattenbergg et al. 1996). Hengchun and Mather (1997) used many general circulation models and suggested under double $CO_2$ scenarios, the increase of surface temperature all over the globe. They suggested possible changes in snow accumulation due to increasing $CO_2$. Wright et al. (2005) run the climate model based on IS92a emission scenario to represent future climate and shown an increase of surface temperature which leads to significant decrease in the net volume of ice.

The water derived from snow melting in the Himalaya region is used for drinking, agriculture, and power generation therefore a systemic and sustained study of hydro-meteorological processes of snow regime is necessary for evaluating changes in the hydrology of Mountain Rivers. The variation in snow depth over the Himalaya will affect the monsoon rainfall and surface runoff especially over northern India.

In this paper, it is aimed to study the response of the snow depth and surface temperature variability in twentieth century and doubling of $CO_2$ experiments. The introduction along with literature survey is kept in Sect. 11.1. The Sect. 11.2 describes the selection of the IPCC AR4 model and data for the current study. The results and discussions are briefly outlined in Sect. 11.3. Conclusions are placed in Sect. 11.4.

## 11.2 Sensitivity Experiments Using MIROC Model

Important rivers in northern India originate from the Himalayas. The snow/glacier over the Western Himalaya is the main contributor of water in those rivers. Therefore, it is necessary to understand the characteristics and behavior of snow depth and surface temperature over the WH. The characteristics of snow depth and surface temperature provide an insight to develop understanding on its impact on hydrological condition. For the current study, the selected domain for WH is 72°–80°E and 30°–39°N.

Program for Climate Model Diagnosis and Inter-comparison (PCMDI), at the Lawrence Livermore National University, USA, is volunteered to collect model simulated output, which are contributed by world leading modeling centers. Climate model simulated output of the past, present and future climate was collected by PCMDI mostly during the years 2005 and 2006, and this archived data is kept under phase 3 of the Coupled Model Inter-comparison Project (CMIP3). Based on climate models simulated result, various scientific research papers have given contribution in Fourth Assessment Report (AR4) of the International Panel on Climate Change (IPCC).

All coupled climate model, as used in CMIP3, do not simulate snow depth but they simulate snow cover mainly. Since the aim of the current study is to analyze the response of snow depth along with surface temperature, therefore only those models are selected which simulates snow Depth. The list of climate models, which

**Table 11.1** Climate models with their IPCC ID, affiliated country, their resolution, key references and convection schemes

| S. No. | IPCC ID | Country | surface resolution | Key reference | Convection scheme |
|---|---|---|---|---|---|
| 1 | MIROC 3.2 (Hires) | Japan | 1.1 × 1.1 | K-1 model developers (2004) | AS |
| 2 | CGCM3.1 | Canada | 3.7 × 3.7 | Flato et al. (2000) | MC |
| 3 | CNRM-CM3 | France | 2.8 × 2.8 | Salas-Meliá et al. (2005) | MF |
| 4 | BCC-CM1 | China | 1.9 × 1.9 | Not available | – |
| 5 | BCCR-BCM2.0 | Norway | 2.8 × 2.8 | Furevik et al. (2003) | MF |

*AS* Arakawa-Schubert, *MC* Moist Convection adjustment, *MF* Mass Flux based

simulated snow Depth, is given below in Table 11.1. The details of the above listed models are available at http://www.pcmdi.llnl.gov/ipcc/model_documentation/.

The surface resolution of the above listed models is varying from 1.1° × 1.1° to 3.7° × 3.7°. As WH is a small region, so higher surface resolution model will provide more number of data points in chosen domain. Therefore, MIROC 3.2 (Hires) model of Japan is found suitable for the current study. MIROC 3.2 (Hires) model simulated snow depth and surface temperature data for the period of 1900–2000 and 2001–2080 in the experiments of twentieth century "20c3m and "1pctto2x" respectively is considered for the analysis to understand the role of $CO_2$ on snow depth and surface temperature over WH. The details of the twentieth century and Doubling of $CO_2$ experiment are available IPCC official web site.

## 11.3 Changes in snow Depth and surface temperature

The annual variation in mean of November to April snow depth in 20c3m and 1pctto2x experiments is shown in Fig. 11.1a, b. The values are ranging from 0.7 to 1.1 m in Fig. 11.1a. The mean snow depth (Fig. 11.1a) does not show any significant change. In Fig. 11.1b, the mean of November to April snow depth is ranging from 0.4 to 1.1 m. and a gradual decreasing in mean snow depth is found when $CO_2$ is doubled. It is important to note that the mean of November to April snow depth is showing a sharp decrease from 2052 onwards.

In Fig. 11.2, variation during 20c3m and 1pctto2x simulation is depicted for 20c3m and 1pctto2x. The pattern in mean monthly variation of snow depth in both experiments is well agreed to each other. It is found that the mean monthly values of snow depth in each month during 20c3m are excess in comparison to 1pctto2x simulation. The minimum value of snow depth is noticed during August–September in 20c3m; from there it slowly increases in the respective months and finally attained the peak in the month of April and May. From the month of June, its starts decreasing and meet the minimum values in the month of August/September. Similarly, in 1pctto2x, the mean monthly values of snow depth are noticed in the month of September. From October onwards, it started to increase and attains

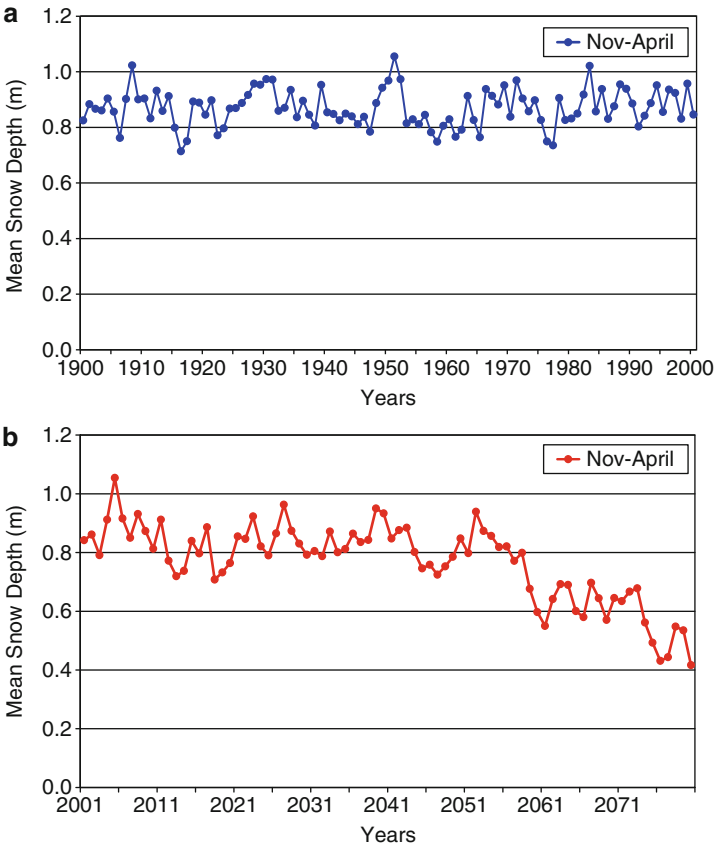


**Fig. 11.1** (**a** and **b**) Annual variation in mean of Nov-April snow depth (m) in (**a**) 20c3m and (**b**) 1pctto2x

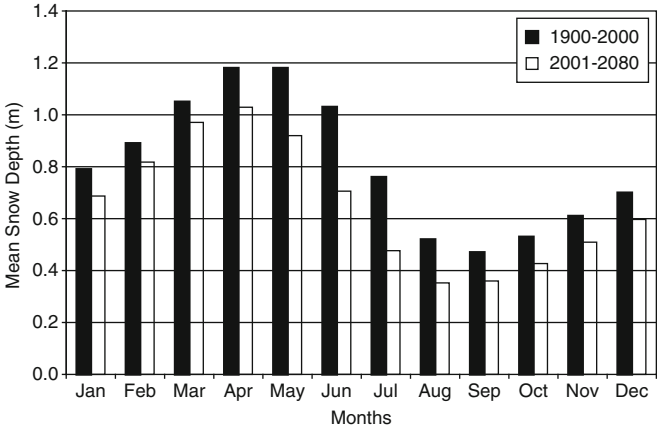


**Fig. 11.2** Variation of mean monthly snow depth (m) in 20c3m and 1pctto2x experiments

maximum values of snow depth in the month of April. From May onwards, the snow depth is decreasing and attained its lowest values in the month of August/September.

Figure 11.3a, b show monthly variation of surface temperature and snow depth in 20c3m and 1pctto2x experiments. In both figures, the increase in surface temperature is well agreed with decrease in snow depth especially during months of May to December. From the months of January to April, surface temperature and snow depth does not show significant relation. It seems that the surface temperature is influencing snow depth during May–December over WH.

Figure 11.4 shows the monthly variation in trend (negative) values of snow depth in 20c3m (in 101 years) and 1pctto2x (in 79 years). The pattern of trend values is well agreed to each other during April–December in both experiments. During January to March, the pattern is not same for experiments. In both

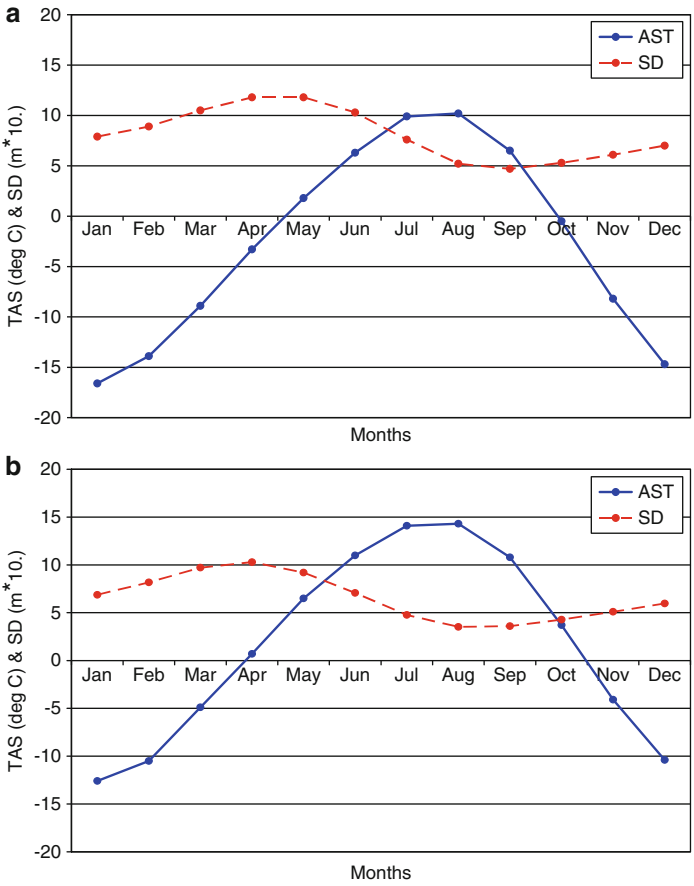


**Fig. 11.3** (**a** and **b**) Mean monthly variation of atmospheric surface temperature (AST) and snow depth (SD) in experiments (**a**) 20c3m and (**b**) 1pctto2x

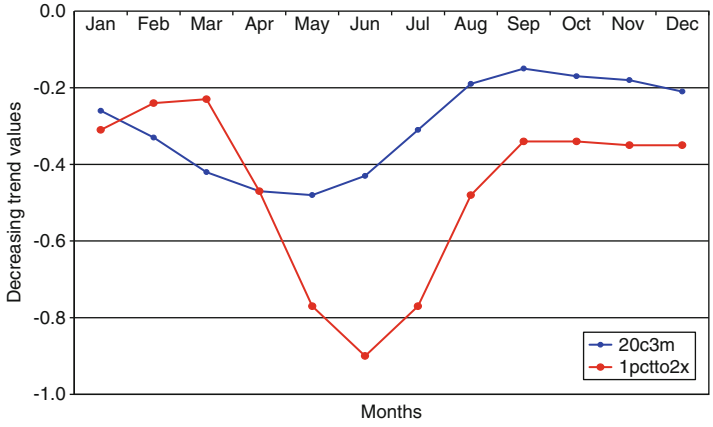


**Fig. 11.4** Decreasing trend in snow depth anomaly (m) in 20c3m (in 101 years) and 1pctto2x (in 79 years)

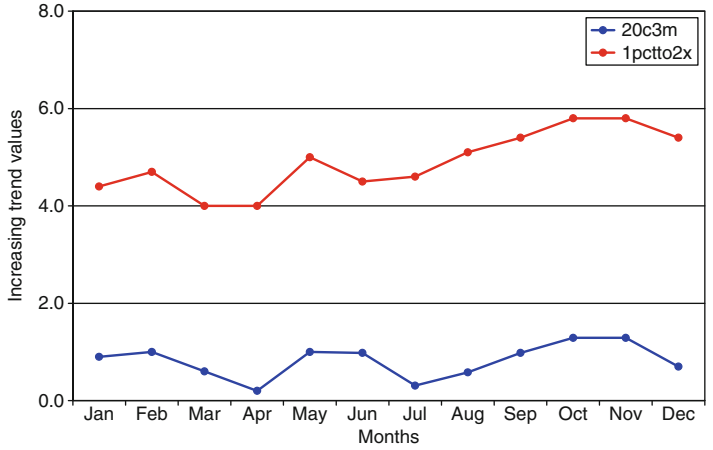


**Fig. 11.5** Increasing trend in surface temperature anomaly (m) in 20c3m (in 101 years) and 1pctto2x (in 79 years)

experiments, it is found that during May–December, trend (negative) values are more in 1pctto2x and less in 20c3m. The trend (negative) values are found maximum in June and minimum in September in both experiments.

The monthly variation of trend (positive) values in surface temperature anomaly in 20c3m and 1pctto2x are shown in Fig. 11.5. The values of trend (positive) are maximum in 1pctto2x and minimum in 20c3m experiment whereas pattern of both series shows a very good agreement in all months except month of April and June. A sharp increase in trend (positive) values are noticed from July to December.

The trend (positive) values are not very significant during January to June in both experiments.

## 11.4 Conclusions

The important results of this study indicate that model simulated annual variation of mean of November to April snow depths undergo a remarkable change in doubling of $CO_2$. The snow depth may slowly attain its low value from the year 2052 onwards. The mean monthly values during 1900–2000 (20c3m) are more compared to those in the period 2001–2080 (1pctto2x). In both the experiments, the inverse relation between snow depth and surface temperature exists during May–December with stronger magnitude in 1pctto2x compared to 20c3m simulation. The monthly variations of trend values of negative and positive snow depths and surface temperature anomalies are more in doubling of $CO_2$ (1pctto2x) case compared to those in the twentieth century simulation (20c3m). These results show the clear impact of $CO_2$ on the snow depth over the Western Himalaya.

## References

Blanford HF (1884) On the connection of the Himalayan snow with dry winds and seasons of drought in India. Proc R Soc Lond 37:3–22

Dash SK, Sarthi PP, Shekhar MS (2007) Influence of Eurasian and Tibetan snow on Indian Summer Monsoon. In: Vinayachandran PN (ed) Understanding and forecasting of monsoons. Centre for Science and Technology of the Non-Aligned and Other Developing Countries (NAM S & T Center), New Delhi, pp 108–118

Dey B, Kumar B (1983) Himalayan winter snow cover area and summer monsoon rainfall over India. J Geophys Res 88:5471–5474

Dickson RR (1984) Eurasian snow cover versus Indian monsoon rainfall – an extension of Hahn and Shukla results. J Clim Appl Meteorol 23:171–173

Flato GM, Lee WG, McFarlane NA, Ramsden D, Reader MC, Weaver AJ (2000) The Canadian Centre for Climate Modelling and Analysis Global Coupled Model and its climate. Climate Dyn 16:427–450

Furevik T, Bentsen M, Drange H, Kindem IKT, Kvamstø NG, Sorteberg A (2003) Description and evaluation of the Bergen climate model: ARPEGE coupled with MICOM. Climate Dyn 21:27–51

Groisman PYa, Karl TR, Knight RW (1994) Changes of snow cover, temperature, and radiative heat balanceover the Northern Hemisphere. J Clim 7:184–204

Hengchun Ye, Mather JR (1997) Polar snow cover changes and global warming. Int J Climatol 17 (2):155–162

IPCC (2001) In: Houghton JT et al (eds) Climate change 2001, the scientific basis. Cambridge University Press, Cambridge

Karl TR, Groisman PYa, Knight RW, Heim RR (1993) Recent variations of snow cover and snowfall in North America and their relation to precipitation and temperature variations. J Clim 6:1327–1344

Kattenberg A, Giorgi F, Grassl H, Meehl GA, Mitchell JFB, Stouffer RJ, Tokioka T, Weaver AJ, Wigley TML (1996) Climate change 1995: the science of climate change. In: Houghton JT, Meira Filho LG, Callander BA, Harris N, Kattenberg A, Maskell K (eds) Contribution of working group I to the second assessment report of the intergovernmental panel on climate change. Cambridge University Press, Cambridge, p 572

Kripalani RH, Kulkarni A, Sabade SS (2003) Western Himalayan snow cover and Indian monsoon rainfall: a re-examination with INSAT and NCEP/NCAR data. Theor Appl Climatol 74:1–18

K-1 Model Developers (2004) K-1 Coupled Model (MIROC) Description. K-1 Technical Report 1 (edited by Hasumi H, Emori S), Center for Climate System Research, University of Tokyo, Tokyo, Japan, p 34 [http://www.ccsr.utokyo.ac.jp/kyosei/hasumi/MIROC/tech-repo.pdf]

Robinson DA, Serreze MC (1995) Recent variations and regional relationships in Northern Hemisphere snow cover. Ann Glaciol 21:71–76

Salas-Meliá D, Chauvin F, Déqué M, Douville H, Gueremy J, Marquet P, Planton S, Royer J, Tyteca S (2005) Description and validation of the CNRM-CM3 global coupled model. CNRM Tech Rep 103, p 36

Shrestha AB, Wake CP, Mayewski PA, Dibb JE (1999) Maximum temperature trends in the Himalaya and its vicinity: an analysis based on temperature records from Nepal for the period 1971–94. J Clim 12:2775–2787

UNEP (2002) Impact of global warming on mountain areas confirmed by UNEP-backed mountaineers. GRID-Arendel News, United Nationas Environmental Program, June 5, 2002. http://www.grida.no/inf/news/news02/news41.htm

Walker GR (1910) Correlations in seasonal variations of weather. Mem India Meteorol Dept 21:22–45

Wright A, Wadham J, Siegert M, Luckman A, Kohler J (2005) Modelling the impact of superimposed ice on the mass balance of an arctic glacier under scenario of future climate change. Ann Glaciol 42(1):277–283

# Chapter 12
# Simulation of Tornadoes over India Using WRF-NMM Model

**A.J. Litta, U.C. Mohanty, S.C. Bhan, and M. Mohapatra**

**Abstract** A severe thunderstorm produced a tornado (F0 on the Fujita-Pearson scale), close to Ludhiana airport (Punjab), north-west region of India (30.8° N, 76.0° E) on 15 August 2007. Another severe thunderstorm produced a tornado (F3 on the Fujita-Pearson scale) which affected Rajkanika block of Kendrapara district of Orissa (20.7° N, 86.6° E) in the afternoon of 31 March 2009. An attempt is made to simulate this rare events using Non-hydrostatic Mesoscale Model (NMM) core of the Weather Research and Forecasting (WRF) system with a spatial resolution of 3 km for a period of 24 h. The results of the study can be utilized for now casting of severe thunderstorms.

## 12.1 Introduction

Tornadoes are a rare weather phenomenon involving a violently rotating column of air, which is in contact with both a cumulonimbus cloud and the surface of the earth. Spawned from powerful thunderstorms, tornadoes can cause fatalities and devastate a neighborhood in seconds. Tornadoes come in many sizes but are typically in the form of a visible condensation funnel, whose narrow end touches the earth and is often encircled by a cloud of debris. The tornadoes can pick up motor cars and even buses, twist steel bridges and destroy houses and factories along their path. Tornadoes have been observed to occur in every continent except Antarctica.

A.J. Litta (✉) • U.C. Mohanty
Centre for Atmospheric Sciences, Indian Institute of Technology, Delhi, Hauz Khas, New Delhi 110 016, India
e-mail: ajlitta@gmail.com; mohanty@cas.iitd.ernet.in

S.C. Bhan • M. Mohapatra
India Meteorological Department, Lodi Road, New Delhi 110 003, India
e-mail: scbhan@gmail.com; mohapatra_imd@yahoo.com

S.D. Attri et al. (eds.), *Challenges and Opportunities in Agrometeorology*,
DOI 10.1007/978-3-642-19360-6_12, 

This dangerous phenomenon occurs mostly in the United States, but occasionally occurs in other parts of the world. India is also not free from occurrences of such tornadoes.

A comprehensive pre-monsoon (March–May) tornado climatology was developed for the eastern parts of the Indian subcontinent particularly West Bengal and Orissa. The most comprehensive works were by Petersen and Mehta (1981), which documented 51 possible tornadoes across Bengal, 18 of which in each case killed 10 people or more. Twelve of these occurred from 1838 to 1963 and 24 occurred after 1968. However, there might exist a tendency to report only the relatively significant tornadoes that leave more damage and attract more attention. Between 1972 and 1978, 13 tornado events occurred in the area approximately coinciding with Bangladesh. Considering the entire area of the country, this gives a frequency rate of occurrence of about $1 \times 10^{-5}$ year$^{-1}$ km$^{-2}$ (Goliger and Milford 1998). Goldar et al. (2001) documented 36 possible spring tornadoes over West Bengal, 14 of which killed ten people or more during 1890–1900. Other studies such as Singh (1981) have listed a few tornadoes for India and the associated wind speeds have been estimated to be of the order of 200–400 km h$^{-1}$.

Northwest India does not frequently experiences this violent weather phenomenon; but there have been a few cases over the region. In northern Delhi, 28 people were killed and 700 were injured by a tornado that cut a path 5 km long and about 50 m wide on 17 March 1978. Another tornado is reported to have killed ten people near Ludhiana (Punjab) on 10 March 1975 (Kumar and Singh 1978; Kumar et al. 1979). Although only a few tornadoes occur over this part of the country, they have a great potential of causing damage to property and loss of life. It is, therefore, essential to investigate the occurrence of tornadoes with the capabilities of high resolution mesoscale models in simulating these highly localized events.

Extensive efforts have been made for several decades to reveal the generation mechanism and structure of tornadoes. Because of the short lifetime and the small horizontal scales of the vortices, however, comprehensive data that reveal their structure and generation process have not been obtained so far. However, the recent developments of computer technology and mesoscale numerical models have allowed a numerical simulation to be a promising tool to reveal the dynamics of tornadoes (Noda and Niino 2005). In the present study, an attempt is made to simulate two recent tornadoes that occurred over Ludhiana on 15 August 2007 and over Orissa on 31 March 2009 using a Non-hydrostatic Mesoscale Model (NMM) core of the Weather Research and Forecasting (WRF) system developed by the National Oceanic and Atmospheric Administration (NOAA)/ National Centers for Environment Prediction (NCEP). The outline of this paper is as follows: Sect. 12.2 gives a brief description of both tornado events; Sect. 12.3 presents the description of numerical model and configurations. The results and discussion are described in Sect. 12.4 and the conclusions in Sect. 12.5.

## 12.2 Case Description

### *12.2.1 Case 1-Tornado over Ludhiana*

A tornado was reported to affect the agricultural fields close to Ludhiana Airport in the afternoon of 15 August 2007. The phenomenon occurred at about 1100 UTC and covered a distance of about 1–1.5 km in agricultural fields of Ucchi Mangli and Sahanewal villages. The tornado moved south-southeastwards covering the distance of about 0.75–1 km. It then turned, west-southwards for about 100–200 m and then moved in a zigzag way. The phenomenon was so destructive that a few big trees were uprooted, heavy branches were snapped of the trees, tin roof of a tube well room was blown away and a bund maker weighing about 80 kg was reportedly lifted to a height of 60–70 ft and was seen rotating in the debris. The whole of the standing water in the paddy field was sucked in and the field was left dry. The plants of Sorghum crop were found flattened in west southwest and northeast direction indicating clockwise rotation in the tornado. The tornado began to weaken by 1115 UTC and disappear completely by 1120 UTC. Considering these damages, the intensity of this tornado can be estimated to be of F0 (18–32 $ms^{-1}$) according to Fujita-Pearson scale (Fujita 1981).

The records of the meteorological observatory situated at Ludhiana Airport, about 1–1.5 km from the site of the tornado, which records hourly observations from 0000 UTC to 1200 UTC during the day have been used to describe weather over the region. The observation report indicated that the sky was mainly sunny in the morning of 15 August 2007 with light southerly winds. A temperature of 29°C with 85% relative humidity was recorded at 0300 UTC. By 0600 UTC, the temperature rose to 32°C with 68% relative humidity and 4 okta low clouds were observed. Cumulus clouds developed in the afternoon and 6 okta cumulonimbus clouds were observed at the time of the event. Though, only 0.3 mm rain was recorded at the observatory. General weather phenomenon reported by the observatory during the day were mist and haze from 0345 to 0925 UTC, thunderstorm from 1113 to 1120 UTC and funnel cloud from 1105 to 1120 UTC. The weather radar situated at Patiala (about 80 km southeast of Ludhiana) reported scattered cumulonimbus clouds at a distance of about 200 km north-northeastwards of Patiala at 0600 UTC. No radar echoes were reported from 0700 to 1000 UTC. The radar reported a cumulonimbus cloud with its top at 6 km and located about 80 km northwest of Patiala (close to the area of occurrence of the tornado) at 1100 UTC.

### *12.2.2 Case 2-Tornado over Orissa*

A severe thunderstorm produced a tornado, which affected Rajkanika block of Kendrapara district of Orissa in the afternoon of 31 March 2009. This tornado was embedded in a severe squall line. The devastation caused by the tornado consumed

15 lives, left several injured with huge loss of property. The origin of the tornado was at Ostia village of Rajkanika and the tornado touched down in this village according to eye witnesses at 1110 UTC of 31 March 2009. It then passed over Barada, Badatala, Asasa, Baghabuda, Gobindpur, Kantapada, Gobindapur, Ganja, Achutapur, Mukundapur, Manaidiha, Dasabhagaria, Mangalpur and Dalikainda villages. The tornado moved from northeast to southwest from Ostia village to Ganja and then from north-northwest to south-southeast towards Dalikaenda village. The duration of the tornado was 10 min. The most affected area may be approximately of 0.6 km in width and 6 km in length covering the above villages. Hence, it moved with the speed of about 36 km $h^{-1}$. The Baghabuda village under Rajkanika Panchayat witnessed the maximum devastation. The phenomenon was so destructive that most of the trees either broke apart or fully uprooted, the bamboo bush of about 15 ft diameter was completely uprooted and all the electricity poles including power transmitter were laid down to ground. The fishes weighing about 1–2 kg were scattered here and there in the village which were thrown away by the tornado from a nearby pond. Some RCC roofs of non-structural concrete buildings were blown away by 30–40 ft. Considering these damages associated with the tornado over Rajkanika can be estimated to be a strong tornado with an intensity of F3 (70–92 $ms^{-1}$) according to Fujita-Pearson scale (Fujita 1981).

With the occurrence of tornado, heavy lightning, thunder and moderate to heavy hailstorm occurred which was accompanied by rain for about an hour and broken lightning persisted till evening (1230 UTC). The hailstone diameter was confined to less than 2 cm at most places and at some places their diameters ranged from 2 to 5 cm. In the approaching funnel cloud a very bright red color was observed up to a height of 50–100 m above ground, which looked peculiarly reddish at the touch down point. The analysis of current weather observations from Chandbali (nearest meteorological observatory), which lies at about 5 km to the north-northeast of Rajkanika, indicated that the cumulonimbus cloud developed to the south of Chandbali at about 1030 UTC. The first thunder was heard at 1035 UTC and continued till 1250 UTC. The rainfall started at Chandbali at 1100 UTC and continued till 1230 UTC. The hailstorm commenced over the station at 1110 UTC and continued till 1210 UTC. Chandbali reported 41.0 mm of rainfall and hail stones with diameter of about 3 cm. The environmental temperature over Chandbali gradually increased from 27.4°C at 0000 UTC and reached up to 30°C prior to the occurrence of tornado (1100 UTC). It suddenly fell thereafter to become 21.6°C at 1200 UTC. It increased again and became 25.0°C at 1500 UTC.

## 12.3 Modeling System

The Non-hydrostatic Mesoscale Model (NMM) core of the Weather Research and Forecasting (WRF) system is a next-generation mesoscale forecast model that is used to advance the understanding and the prediction of mesoscale intense convective systems. The WRF-NMM model is an efficient, state-of-art and flexible

mesoscale modeling system for use across a broad range of weather forecast and idealized research applications, with an emphasis on horizontal grid sizes in the range of 1–10 km. Several studies related to the simulation of severe thunderstorm events using NMM model have been performed (Kain et al. 2006; Litta and Mohanty 2008).

The NMM is a fully compressible, non-hydrostatic mesoscale model with a hydrostatic option (Janjic 2003). The model uses a terrain following hybrid sigma-pressure vertical coordinate. The grid staggering is the Arakawa E-grid. The model uses a forward-backward scheme for horizontally propagating fast waves, implicit scheme for vertically propagating sound waves, Adams-Bashforth scheme for horizontal advection, and Crank-Nicholson scheme for vertical advection. The same time step is used for all terms. The dynamics conserve a number of first and second order quantities including energy and entropy.

In the present simulation, the model was integrated for a period of 24 h, starting at 0000 UTC of 15 August 2007 for the first case and starting at 0000 UTC of 31 March 2009 for the second case as initial values. A single domain with 3 km horizontal spatial resolution was configured, which is reasonable in capturing the mesoscale cloud clusters. Initial conditions for the 3 km domain are derived from 6-hourly FNL Global Analyses at $1.0^\circ \times 1.0^\circ$ grids. Analysis fields, including temperature, moisture, geopotential height and wind, are interpolated to the mesoscale grids by the WRF preprocessing system (WPS). These derived fields are used as initial conditions for the present experiments. There are 38 unequally spaced sigma (non-dimensional pressure) levels in the vertical. The physical parameterizations used in this study are Geophysical Fluid Dynamics Laboratory (GFDL) for long wave and short wave radiation, NMM Land surface scheme for land surface, Mellor Yamada Janjic (MYJ) scheme for planetary boundary layer, Ferrier scheme for microphysics and Janjic similarity scheme for surface layer. The cumulus parameterization used for this study is Grell-Devenyi cloud ensemble scheme (Grell and Devenyi 2002). This is a multi-closure, multi-parameter, ensemble method with typically 144 sub-grid members. Table 12.1 gives a brief illustration on the model configuration of the present study.

**Table 12.1** NMM model configuration

| Dynamics | Non-hydrostatic |
|---|---|
| Horizontal spatial resolution | 3 km |
| Integration time step | 6 s |
| Map projection | Rotated latitude and longitude |
| Horizontal grid system | Arakawa E-grid |
| Vertical co-ordinate | Terrain-following hybrid (sigma-pressure) vertical coordinate (38 sigma levels) |
| Radiation parameterization | GFDL/GFDL |
| Surface layer parameterization | Janjic similarity scheme |
| Land surface parameterization | NMM land surface scheme |
| Cumulus parameterization | Grell-Devenyi ensemble scheme |
| PBL parameterization | Mellor-Yamada-Janjic |
| Microphysics | Ferrier (new eta) scheme |

## 12.4 Results and Discussion

Asnani (2005) have described some of the favorable meteorological conditions for severe convection in respect of tornado-genesis. They include plentiful supply of moisture in the lower levels, presence of convective instability in a sufficient measure in deep layer, the lifting mechanism to produce low-level convergence and upper level divergence to initiate and augment the release of convective instability and strong vertical wind shear of the horizontal winds. The following section describes the above mentioned features obtained from the WRF-NMM model.

### *12.4.1 Surface and Upper air Pattern*

The prediction of the dominant convective mode is based on the assessment of magnitude of vertical motion, which is needed to initiate convection (May and Rajopadhyaya 1999). Observations as well as theoretical calculations show that most tornadoes show a strong vertical upward motion at the centre, which is of the same order of magnitude as horizontal component of wind (Asnani 2005). Figure 12.1a shows the time-height cross section of model simulated pressure vertical velocity ($Pas^{-1}$) over Ludhiana valid from 0000 UTC of 15 August 2007 to 16 August 2007 and Fig. 12.1b over Rajkanika valid from 0000 UTC of 31 March 2009 to 0000 UTC of 1 April 2009. The figure shows a high upward velocity with a magnitude of $-12$ Pa $s^{-1}$ over Ludhiana at 1100 UTC on 15 August 2007, which is consistent with the tornado occurrence. The Fig. 12.1b clearly shows a strong upward velocity with a magnitude of $-40$ Pa $s^{-1}$ over Rajkanika at 0900 UTC on 31 March 2009, which is the model predicted tornado hour. The model well simulated high magnitude pressure vertical velocity at the tornado site for both the cases, which is an important factor related to tornado genesis.

Figure 12.2a illustrates the model simulated moisture convergence at 850 hPa at 1100 UTC of 15 August 2007. The maximum convergence (convergence is positive and divergence is negative) over Ludhiana happens at 1100 UTC which is consistent with the weather report. Figure 12.2b illustrates the model simulated moisture convergence at 850 hPa at 0900 UTC of 31 March 2009. This figure shows maximum convergence over Rajkanika at 0900 UTC which is again consistent with the tornado occurrence. In both the tornado cases, the model well simulated strong convergence over the tornado site during the model predicted tornado hour. Most of the severe thunderstorms produce heavy rainfall during their lifecycle of 1–3 h (Vaidya 2007). The time-series plots of 3-hourly NMM model simulated and TRMM accumulated rainfall over Ludhiana valid for 15 August 2007 at 0000 UTC to 16 August 2007 at 0000 UTC is given in the Fig. 12.3a. The model simulated accumulated rainfall at Ludhiana is 15.96 mm which is close to the TRMM accumulated rainfall (26.0 mm). The model results in terms of intensity,

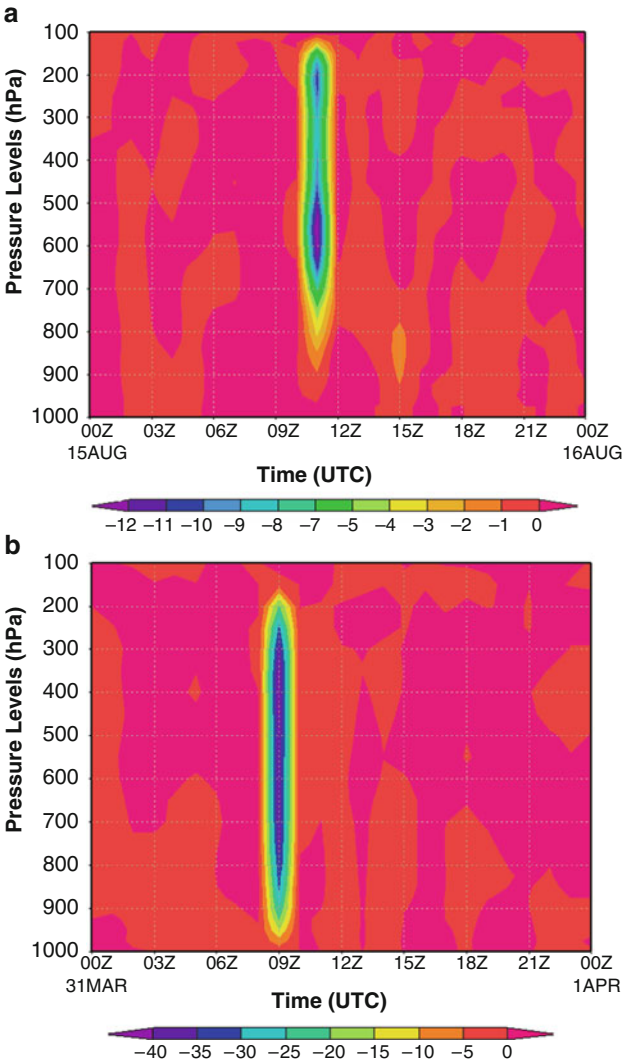


**Fig. 12.1** (**a** and **b**) Time-Height cross section of simulated pressure vertical velocity ($Pas^{-1}$) (**a**) over Ludhiana valid from 0000 UTC of 15 August 2007 to 0000 UTC of 16 August 2007 and (**b**) over Rajakanika valid from 0000 UTC of 31 March 2009 to 0000 UTC of 1 April 2009

time and location are very close to the observation. The inter-comparison of 3-hourly model simulated rainfall and observed rainfall at Chandbali meteorological station valid from 0000 UTC of 31 March 2009 to 0000 UTC of 1 April 2009 is illustrated in Fig. 12.3b. The figure clearly shows a high rainfall (35.44 mm) over Chandbali between 0900 UTC to 1100 UTC during the model simulated tornado hour, which is very close to the actual observation (41.0 mm).

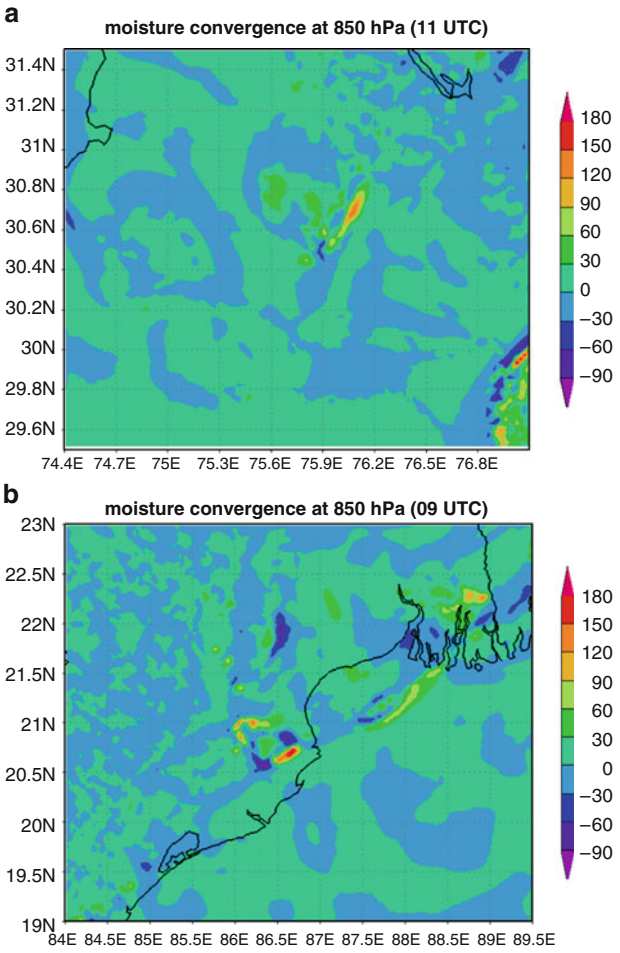


**Fig. 12.2** (**a** and **b**) The model simulated moisture convergence at 850 hPa valid at (**a**) 1100 UTC of 15 August 2007 and (**b**) 0900 UTC of 31 March 2009

Studies have indicated that a meso-cyclonic flow results in the formation of a severe vortex like a tornado (Asnani 2005). The plants of Sorghum crop were found flattened in west southwest and northeast direction indicating clockwise rotation in the tornado of Ludhiana. To the western side of the track the uprooted trees were aligned from north to south and to the eastern side of the track the uprooted trees were aligned from south to north in the case of tornado over Orissa. It indicated that the ground circulation associated with the tornado was cyclonic and hence this particular tornado was associated with a cyclonic vortex. However, the observations are not sufficient to draw a conclusion that there was a development of vortex or suction vortex in the vicinity of these latest tornadoes. The model simulated surface wind at 1100 UTC of 15 August 2007 is given in Fig. 12.4a.

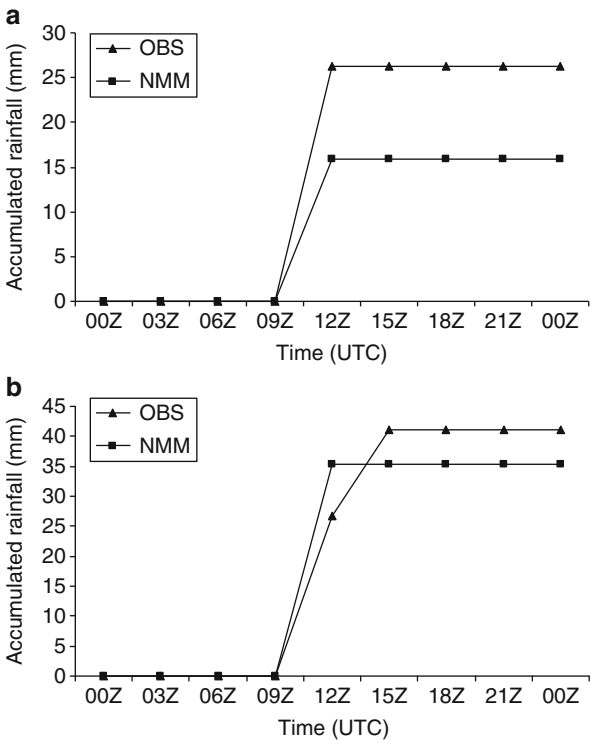


**Fig. 12.3** (**a** and **b**) The inter-comparison of (**a**) 3-hourly NMM model simulated and TRMM accumulated rainfall (mm) over Ludhiana valid for 15 August 2007 at 0000 UTC to 16 August 2007 at 0000 UTC (**b**) 3-hourly NMM model simulated and observed accumulated rainfall (mm) over Chandbali station valid from 0000 UTC of 31 March 2009 to 0000 UTC of 1 April 2009

The cyclonic rotation is visible in the figure during the tornado hour with a maximum wind speed of 12 $ms^{-1}$. The model simulated surface wind at 0900 UTC of 31 March 2009 is presented in Fig. 12.4b. The tornado vortex is clearly visible at the model predicted s between 20.5–21°N and 86–87°E with a maximum speed of 20 $ms^{-1}$. The model failed to capture the intensity of wind speed in both the cases. However, the core of the strongest winds is shown very close to the site of actual occurrence of the event.

### *12.4.2 Instability Indices from the Model*

An attempt is made to examine different stability indices, which acts as indicators of severe convective activity. The NMM model simulated skew-t plot of Ludhiana at 1100 UTC on 15 August 2007 is illustrated in Fig. 12.5a and over Rajkanika at 0900 UTC on 31 March 2009 in Fig. 12.5b. The skew-t plots show that in both the cases the atmosphere was convectively unstable for an occurrence of severe thunderstorms over Ludhiana and Rajkanika. Convective Available Potential Energy (CAPE) represents the amount of buoyant energy available to accelerate a parcel vertically and a CAPE value greater than 1500 J $kg^{-1}$ is suggested by

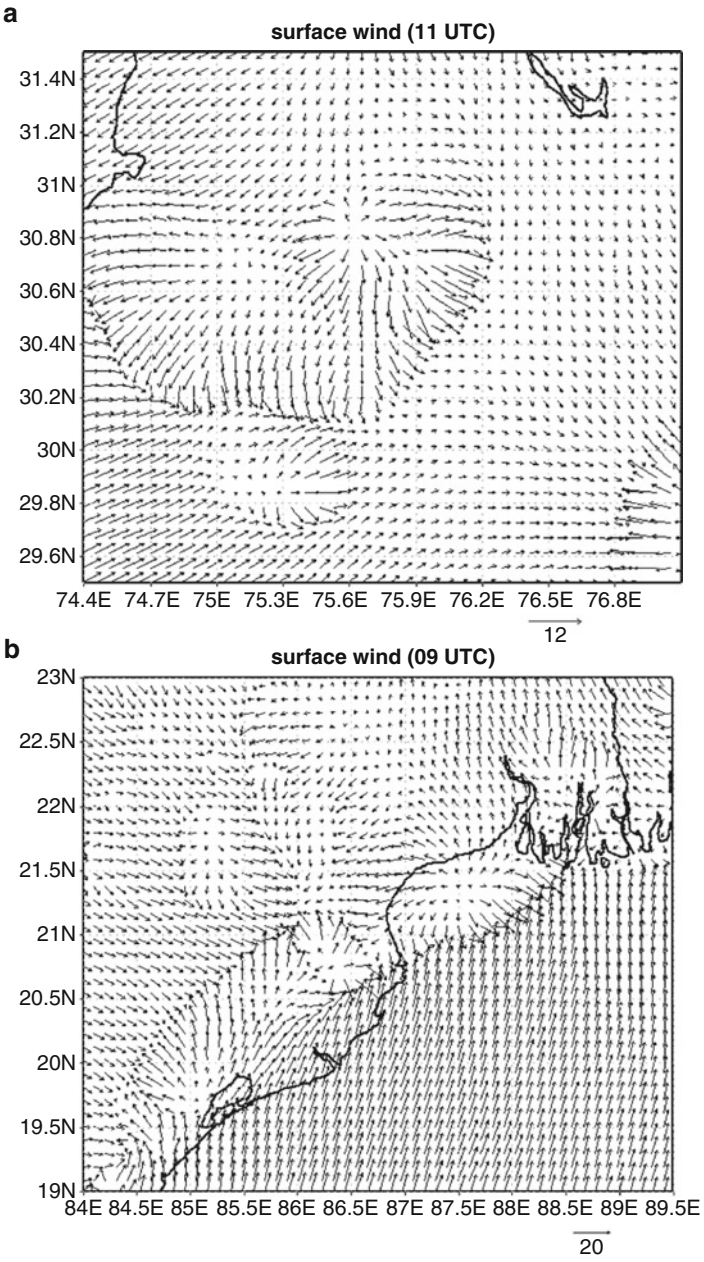


**Fig. 12.4** (**a** and **b**) The model simulated surface wind valid at (**a**) 1100 UTC of 15 August 2007 (**b**) 0900 UTC of 31 March 2009

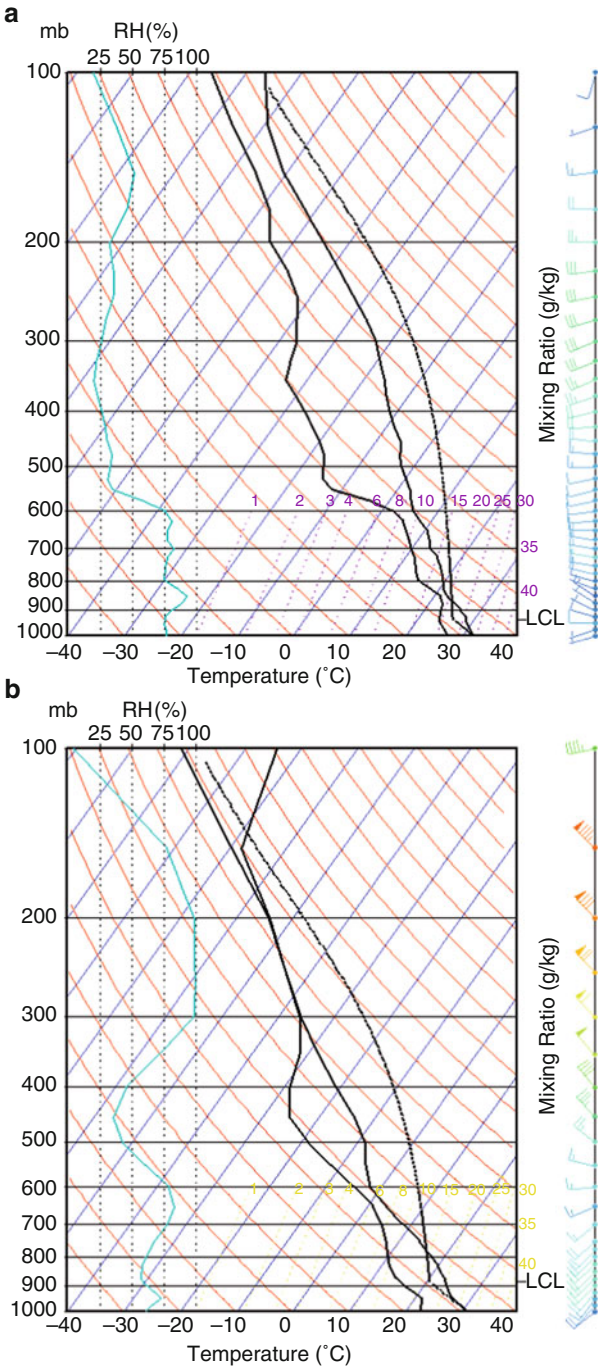


**Fig. 12.5** (**a** and **b**) The model simulated skew-t plot (**a**) over Ludhiana at 1100 UTC on 15 August 2007 (**b**) over Rajkanika at 0900 UTC on 31 March 2009

**Table 12.2** NMM model simulated stability indices at Tornado hour for both cases

| Stability index | Description | Critical level | Case 1 1100 UTC | Case 2 0900 UTC |
|---|---|---|---|---|
| Lifted index | $T_{500} - T_{parcel}$ | $< -6$ | $-8$ | $-8$ |
| Total totals | $(T_{850} - TD_{850}) - 2(T_{500})$ | $> 48$ | 47 | 51 |
| CAPE | $\int_{z=LFC}^{z=LNB} g \frac{[\theta_{vp}(z) - \theta_v(z)]}{\theta_v(z)} dz$ | $> 1{,}500$ | 3,437 | 3,584 |

Rasmussen and Wilhelmson (1983) as being necessary for supercells to form. Johns et al. (1993) and Korotky et al. (1993) extended the use of CAPE for tornadic environments to include high CAPE-low shear as well as low CAPE-high shear situations. Table 12.2 shows the model simulated stability indices at both cases with critical levels for severe thunderstorms. The NMM model simulated a high CAPE value which is 3,437 J $kg^{-1}$ during the tornado hour for the first case and 3,584 J $kg^{-1}$ for the second tornado case (Table 12.2).

The Lifted Index (LI) measures the difference between a parcel's temperature compared with the environmental temperature at 500 hPa, after the parcel has been lifted from the Lifting Condensation Level (Air Weather Service Technical Report 1990). LI has proved useful for indicating the likelihood of severe thunderstorms. The chances of a severe thunderstorm are best when the LI is less than or equal to $-6$. This is because air rising in these situations is much warmer than its surroundings and can accelerate rapidly and create tall and violent thunderstorms. Values less than $-9$ reflect intense instability. The NMM model is able to capture a low value which is $-8$ at tornado hour of both cases (Table 12.2).

Miller (1972) introduced the Total Totals Index (TTI) for identifying areas of potential thunderstorm development. It accounts for both static stability and the presence of 850 hPa moisture. A TTI of greater than 48 indicates favorable conditions for development of severe thunderstorms; a value of 50 indicates favorable conditions for tornadoes (Air Weather Service Technical Report 1990). The NMM model simulated TTI value is 47 for the first case and 51 for the second case (Table 12.2). The CAPE and TTI show a high value and LI presented a low value during tornado hour, which is a favorable condition for severe thunderstorm occurrence.

## 12.5 Conclusions

The model simulation studies of the tornado of 15 August 2007 over Ludhiana (Punjab) and the tornado of 31 March 2009 over Rajkanika (Orissa) lead to the following broad conclusions:

The model simulated meteorological parameters such as wind speed, pressure vertical velocity and moisture convergence at 850 hPa are consistent with each

other and all are in good agreement with the observation in terms of the region of occurrence of the intense convective activity for both the tornado cases. The model simulated tornado hour over Ludhiana is exactly matching with the actual occurrence. However, model simulated tornado occurred 2 h prior to the actual occurrence of tornado over Rajkanika.

The WRF-NMM model has well captured the vertical motion. It is found that the pressure vertical velocity is produced at proper location and time in the case of tornado over Ludhiana with a magnitude of $-12$ Pa $s^{-1}$. The model simulated well the updraft with a magnitude of $-40$ Pa $s^{-1}$ in the case of tornado over Rajkanika during the model simulated tornado hour. The wind speed is not in good agreement with the observation for both the tornado cases; however, the core of the strongest winds is shown to be very close to the site of actual occurrence of the event. The intensity of 3-hourly rainfall rates are in good agreement with the observation for both the tornado cases. In the first case model is able to simulate 15.96 mm against 26.0 mm over Ludhiana and for the second case 35.44 mm against 41.0 mm over Chandbali.

The model simulated thermodynamic derivatives of stability indices such as CAPE, LI, and TTI indicate a deep instable layer around Ludhiana and Rajkanika favorable for intense convective activity like tornado during model simulated tornado hour.

Thus the dynamic and thermo-dynamic properties of the atmosphere are well simulated by WRF-NMM for the occurrence of tornado over Ludhiana and also over Rajkanika, and agree reasonably well with the observations. The results of these analyses demonstrated the capability of high resolution WRF-NMM model in simulation of severe thunderstorm produced tornadoes.

## References

Air weather service technical report 79/006 (1990) The use of the skew T, Log P diagram in analysis and forecasting. Air weather service, Scott AFB, Illinois

Asnani GC (2005) Tropical meteorology (Revised Edition), vol II. Indian Institute of Tropical Meteorology, Pune

Fujita T (1981) Tornadoes and downbursts in the context of generalized planetary scale. J Atmos Sci 38:1511–1534

Goldar RN, Banerjee SK, Debnath GC (2001) Tornado in India and neighborhood and its predictability. Regional Met. Centre, Alipore, Kolkata. Issued by Office of the Additional Director General of Meteorology (Research), Meteorological Office of India Meteorological Deptartment, Pune, India

Goliger AM, Milford RV (1998) A review of worldwide occurrence of tornadoes. J Wind Eng Ind Aerodyn 74:111–121

Grell GA, Devenyi D (2002) A generalized approach to parameterizing convection combining ensemble and data assimilation techniques. Geophys Res Lett 29(14):1693

Janjic ZI (2003) A nonhydrostatic model based on a new approach. Meteorol Atmos Phys 82:271–285

Johns RH, Davies JM, Leftwich PW (1993) Some wind and instability parameters associated with strong and violent tornadoes, 2. Variations in the combinations of wind and instability

parameters. The Tornado: its structure, dynamics, prediction and hazards. Geophys Monogr Am Geophys Union 79:583–590
Kain JS, Weiss SJ, Levit JJ, Baldwin ME, Bright DR (2006) Examination of convection-allowing configurations of the WRF model for the prediction of severe convective weather: The SPC/NSSL spring program 2004. Weather Forecast 21(2):167
Korotky W, Przybylinski RW, Hart JA (1993) The Plainfield, Illinois, tornado of August 28, 1990: The evolution of synoptic and mesoscale environments. The Tornado: its structure, dynamics, prediction and hazards. Geophys Monogr Am Geophys Union 79:611–624
Kumar S, Singh MS (1978) Satellite study of development of severe thunder/hailstorms over south Punjab on 10 March 1975. Indian J Met Hydrol Geophys 29(4):754–756
Kumar S, Singh J, Raj H (1979) Severe weather outbreak associated with intersection of sub-tropical jet stream with squall line. Vayu Mandal 9(1&2):46–47
Litta AJ, Mohanty UC (2008) Simulation of a severe thunderstorm event during the field experiment of STORM programme 2006, using WRF-NMM model. Curr Sci 95(2):204–215
May PT, Rajopadhyaya DK (1999) Vertical velocity characteristics of deep convection over Darwin. Aust Mon Weather Rev 127:1056–1071
Miller RC (1972) Notes on analysis and severe storm forecasting procedures of the air force global weather central AWS TR 200 (revised) air weather service scott air force base, Illinois
Noda AT, Niino H (2005) Genesis and structure of a major Tornado in a numerically-simulated supercell storm: importance of vertical vorticity in a gust front. SOLA 1:005–008
Peterson RE, Mehta KC (1981) Climatology of tornadoes of India and Bangladesh. Arch Meteorol Geophys Bioklimat 29B:345–356
Rasmussen RM, Wilhelmson RB (1983) Relationships between storm characteristics and 1200GMT hodographs, low-level shear and stability. In: Preprints of 13th conference on severe local storms. American Meteorological Society, Tulsa, pp 55–58
Singh R (1981) On the occurrence of tornadoes in India. Mausam 32(3):307–314
Vaidya SS (2007) Simulation of weather systems over Indian region using mesoscale models. Meteorol Atmos Phys 95:15–26

# Chapter 13
# A Pilot Study on the Energetics Aspects of Stagnation in the Advance of Southwest Monsoon

**Somenath Dutta and Lt. Vishwarajashree**

**Abstract** An attempt has been made to understand dynamically the stagnation in the advancement of southwest monsoon from an energetics point of view. Recent four cases of stagnation of duration more than 10 days during 2002–2006 have been selected. For each case, different energy terms, their generation and conversion among different terms have been computed during the stagnation period and also during the pre-stagnation pentad over a limited region between 65°E and 90°E, 5°N and 30°N. These computations are based on NCEP 2.5° × 2.5° re-analysed daily composite data during different stagnation period and during corresponding pre-stagnation pentad.

From this study it is found that:

- In most of the cases there is a reduction in zonal kinetic energy ($K_z$) and in eddy kinetic energy (KE) during stagnation period compared to pre-stagnation pentad.
- In all cases, during stagnation as well as in the pre stagnation pentad, barotropic eddy energy transfer dominates over baroclinic eddy energy transfer.
- In most of the cases there is a reduction in the generation of zonal available potential energy [G ($A_z$)] during stagnation period compared to pre-stagnation pentad.
- In most of the cases there is a reduction in the conversion from zonal available potential energy to zonal kinetic energy [C ($A_z$, $K_z$)] during stagnation period compared to pre-stagnation pentad.

S. Dutta (✉)
Meteorological Office, Pune, India
e-mail: dutta.drsomenath@gmail.com

Lt. Vishwarajashree
INS Garuda, Cochin, India

S.D. Attri et al. (eds.), *Challenges and Opportunities in Agrometeorology*,
DOI 10.1007/978-3-642-19360-6_13, © Springer-Verlag Berlin Heidelberg 2011

## 13.1 Introduction

The normal onset date of southwest monsoon over Kerala is 1st June and the date of covering the entire country is 15th July. But there are wide variations to this travel time of monsoon in different years. Whereas the onset of Indian Summer monsoon over Kerala is of importance, the advance of monsoon over other parts of the country is also equally important. The advance of monsoon is not a continuous process rather it is pulsatory in nature. There are several years when stagnation occurs and the northward or westward propagation of monsoon is arrested. Most of the years there are only short lulls of 7–10 days, but there are years when this stalling of the stagnation of monsoon continues for over 2 weeks period. Such stagnation causes concerns to the farmers and other weather dependent activities.

Keshavamurty and Awade (1970) found that maintenance of mean monsoon trough against frictional dissipation is mainly due to work done by horizontal pressure gradient. Their study also indicates a loss in standing eddy kinetic energy by rising of relatively colder air and sinking motion of relatively warmer air.

Rao and Rajamani (1972) studied the heat source and sinks and generation of available potential energy of the atmosphere over the Indian region during southwest monsoon season. Their computation showed a net generation of APE over the region of study.

Krishnamurty and Ramanathan (1982) have shown that a sharp rise in the rotational kinetic energy is an interesting aspect of onset of Indian Summer Monsoon (ISM). Awade and Bawiskar (1982) have shown that bad monsoon activity is associated with large divergence of heat at sub-tropics and large convergence of heat at extra tropics. According to Pasch (1983) the onset of planetary scale monsoon is preceded by an organization of cumulus convection on the planetary scale. Awade et al. (1985) have shown that in good monsoon years there is large divergence of momentum in subtropics, while there is large convergence of momentum in mid latitude. They argued that this situation leads to a stronger westerly in mid-latitude and stronger easterly at tropics. Krishnamurty (1985) has shown that divergent kinetic energy, must be transferred to rotational kinetic energy, available potential energy must be transferred to divergent kinetic energy via rising motion over warm region/sinking motion over cold region. He has also shown that available potential energy is maintained via heating of warmer air and cooling of colder air. Rajamani (1985a) computed the diabatic heating and generation of APE over south Asia for typical monsoon month July 1963. The study has inferred positive generation of both zonal and standing eddy APE. Rajamani (1985b) made a study on available potential energy (APE) and its transformation into kinetic energy. This study shows that differential heating between Asian landmass and Indian ocean causes the generation of zonal APE ($A_z$), a part of which is converted into zonal kinetic energy ($K_z$). The study also indicates that diabatic heating generates standing eddy APE (AE), which is again converted into standing eddy kinetic energy. Ramasastry et al. (1986) brought out some features of the process of stagnation. Krishnamurti and Surgi (1987) have shown that around

the period of the onset of monsoon rains over India, there is a sharp rise in the conversion of zonal available potential energy ($A_z$) to zonal Kinetic energy ($K_z$).

Yanai et al. (1992) have shown that reversal of north-south temperature gradient in the layer between 700 and 200 hPa triggers the onset of South Asian monsoon. George and Mishra (1993) had examined the temporal variations of the zonal and eddy kinetic and available potential energy in association with the formation, growth and maintenance of vortex during southwest monsoon. Their study indicated that barotropic eddy energy transfer dominates over baroclinic eddy energy transfer. They have also showed that C ($K_z$, $K_E$) > C ($A_E$, $K_E$). Biswas et al. (1998) have studied the role of the mechanical barrier of the Himalayan massif – Tibetan plateau and the mid tropospheric sub-tropical ridge in the stagnation in the advance of southwest monsoon.

Krishnamurti et al. (1998) studied the energetics of south Asian monsoon. Using FSU Gobal spectral model at T 170 resolution, they examined the maintenance of the monsoon. This study indicates that differential heating leads to the growth of APE, which is next passed on to the divergent motions and then finally divergent K.E. is converted to rotational K.E, which of course critically depends on the orientation of the isopleths of $\psi$ and $\chi$. Results of the study by Wu and Zhang (1998) are in conformity with that of Yanai et al. (1992). These studies indicate that during the onset of South Asian monsoon there is a sudden increase in the zonal available potential energy.

Raju et al. (2005) studied the onset characteristics of the southwest monsoon over India. Their study reveals that the low level kinetic energy, vertically integrated generation of kinetic energy and net tropospheric moisture can be used as potential predictors to predict the onset of Southwest monsoon. Rao and Mohanty (2007) have shown that the onset of the Indian southwest monsoon over the Bay of Bengal is discernible by a gradual increase in the adiabatic generation of kinetic energy, while over the Arabian Sea it is first noticeable by a steep and abrupt increase of generation.

From the foregoing discussion it appears that hardly there is any study on the energetic aspects of stagnation, although there are ample studies on energetics during onset and energetics on monsoon disturbances.

The present study aims at analyzing the energetic aspects of stagnation of southwest monsoon.

## 13.2 Data

The different cases of stagnation period in the advance of SW monsoon have been obtained from the isochrones of monsoon advance prepared by the India Meteorological Department. For the present study we have used data for $u$, $v$, $\omega$, $T$, $rh$ obtained from NCEP/NCAR. We have used daily composite data of the above fields for the stagnation period and for pre-stagnation pentad of individual cases over the limited region between 5°N and 30°N, 65°E and 90°E.

## 13.3 Methodology

First, from the temperature data, at each grid point, heating rate $\frac{\dot{Q}}{C_p}$ has been computed using first law of thermodynamics $\frac{\dot{Q}}{C_p} = \frac{dT}{dt} - \frac{\alpha}{C_p}\omega$. In the computation of $\frac{dT}{dt}$, tendency has not been taken care of. Then, following Krishnamurty and Bounoua (2000), zonal average, area average, deviation from the area average, deviation from zonal average and finally the departure of the zonal average from area average of different field have been computed. These have again been used to compute zonal available potential energy ($A_z$), zonal kinetic energy ($K_z$), eddy available potential energy ($A_E$), eddy kinetic energy ($K_E$), generation of zonal available potential energy [$G(A_z)$], generation of eddy available potential energy [$G(A_E)$], conversion of $A_z$ to $A_E$ [$C(A_z, A_E)$], conversion of $A_z$ to $K_z$ [$C(A_z, K_z)$], conversion of $A_E$ to $K_E$ [$C(A_E, K_E)$] and conversion of $K_z$ to $K_E$ [$C(K_z, K_E)$] following Krishnamurty and Bounoua (2000). These computations have been made for the stagnation period and also for corresponding pre-stagnation pentad for different stagnation cases being studied.

## 13.4 Case Studies

The following cases were identified for which the further advance of SW monsoon had been stalled by more than 12 days.

Here we shall discuss the energetics during stagnation period and during corresponding pre-stagnation period for different stagnation cases. Energy flow diagram depicting different energy terms, generation terms and conversion terms for all the four cases under study have been shown in Figs. 13.1–13.4.

**Case – I:** *Stagnation during 5th July–18th July and pre-stagnation pentad during 30th June–4th July 2002*

The year 2002, demarcated to be an all India drought year, had been anomalous in a multitude of features during the SW monsoon season. The unusual delay occurred in covering the entire country is one among these. It was some parts of NW India, which were left out, during the period of the stagnation (5–18 July 2002) considered in the present study. An anticyclone sitting over the central parts of the country prevented the formation of any intense low-pressure systems and consequently further advance in SW monsoon. For this case the energy flow diagrams corresponding to pre-stagnation pentad and stagnation period are given in Fig. 13.1a, b respectively.

These figures indicate that there is a reduction in $G(A_z)$, $G(A_E)$, $K_z$, $C(A_z, K_z)$ and $C(A_E, K_E)$, during stagnation period as compared to during corresponding pre-stagnation pentad.

**Case – II**: *Stagnation during 20th July–14th August and pre-stagnation pentad during 15th–19th July 2002*

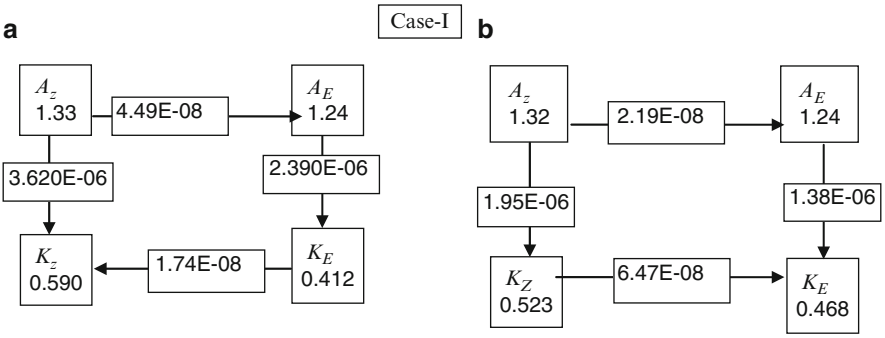


**Fig. 13.1** (**a**) Pre-Hiatus pentad 30 June–04 July 2002. (**b**) Hiatus period 5 July–18 July 2002

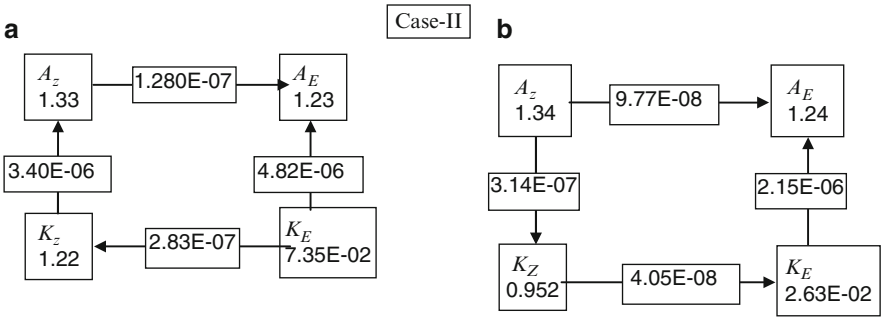


**Fig. 13.2** (**a**) Pre-Hiatus pentad 15–19 July 2002. (**b**) Hiatus period 20 July–14 August 2002

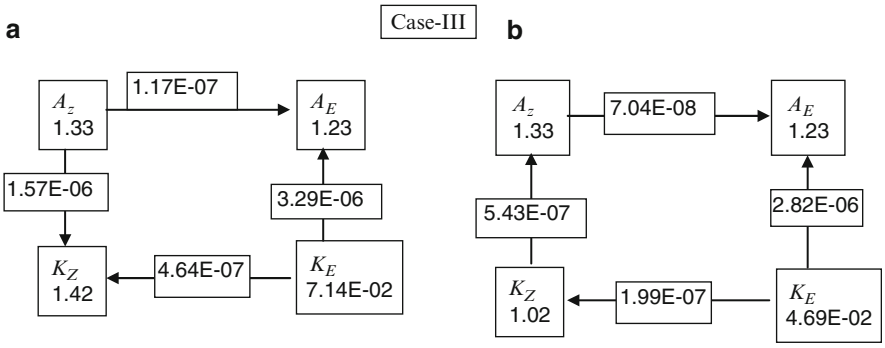


**Fig. 13.3** (**a**) Pre-Hiatus pentad 14–18 June 2004. (**b**) Hiatus period 19 June–03 July 2004

An anticyclone sitting over the central parts of the country prevented the formation of any intense low-pressure systems and consequently further advance in SW monsoon.

The energy flow diagrams for this case corresponding to pre-stagnation pentad and stagnation period are given in Fig. 13.2a, b respectively. It can be seen from figures that except $K_z$, $K_E$ and $C(A_z, K_E)$ for all the energy, energy generation

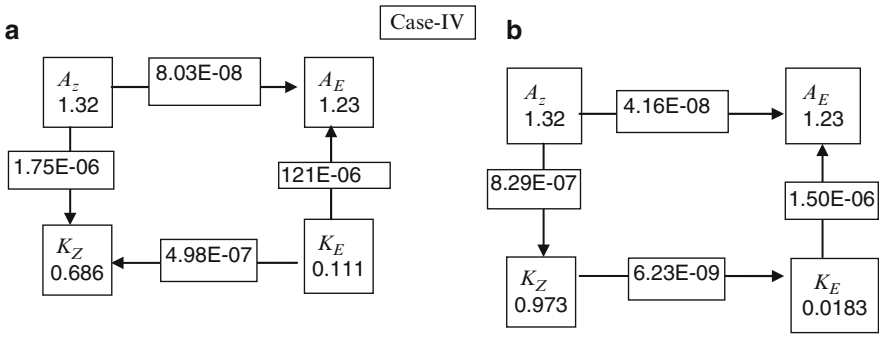


**Fig. 13.4** (**a**) Pre-Hiatus pentad 02–06 June'06. (**b**) Hiatus period 07 June–22 June'06

and conversion terms there is either enhancement or practically no change during stagnation period as compared to during corresponding pre-stagnation pentad. It can be seen that the magnitude of barotropic energy conversion, i.e., magnitude of $C(K_z, K_E)$ has reduced during stagnation. It can also be seen that in contrary with the energetics of a typical baroclinic wave, where $A_E$ is converted to $K_E$, here $A_E$ is being converted from $K_E$.

**Case – III**: *Stagnation during 19th June – 03rd July 2004 and pre-stagnation pentad from 14th to 18th June 2004*

Prior to the occurrence of the stagnation in advance, the SW monsoon had covered nearly 2/3rd area of the country. It was rather a rapid advance during the pre-stagnation period, under the influence of two intense vortices in the form of deep depressions, one over the Arabian Sea during 10–13 June and the other over the Bay of Bengal during 11–14 June.

The energy flow diagrams for this case corresponding to pre-stagnation pentad and stagnation period are given in Fig. 13.3a, b respectively. They show that for this case, there is a considerable reduction in $G(A_z)$, $C(A_z, K_z)$, $K_z$ and $K_E$ during stagnation period as compared to during corresponding pre-stagnation pentad.

From these figures it can be seen that similar to the previous case, in this case also there is a reduction in the magnitude of barotropic energy conversion. Similar to previous case here also $A_E$ is being converted from $K_E$ both during hiatus and pre-hiatus pentad.

**Case – IV**: *Stagnation during 7th–22nd June 2006 and pre-stagnation pentad from 2nd to 6th June 2006*

The stagnation in advance occurred along the latitude 22°N in the western and roughly along longitude 85°E in the eastern parts of the country. A low pressure area formed over the North Bay during the pre-stagnation period moved rapidly inland and dissipated. Also there occurred mid latitude westerly intrusion in the mid and upper tropospheric levels, as revealed by the passage of a series of high amplitude troughs in the upper air charts.

Energy flow diagram for the stagnation and pre-stagnation period for this case are shown in Fig. 13.4a, b. From these figures it can be seen that for this case, there is a reduction in $G(A_Z)$, $G(A_E)$, $C(A_Z, K_Z)$, $C(A_E, K_E)$ and $K_E$ during stagnation

period as compared to those during pre-stagnation pentad. From these figures it can be seen that similar to the last three cases, in this case also there is a reduction in the magnitude of barotropic energy conversion during hiatus and also $A_E$ is being converted from $K_E$ both during hiatus and pre-hiatus pentad.

## 13.5 Discussion

Total four cases have been studied. In most cases it has been found that during stagnation the magnitude of $C(K_Z, K_E)$ has been reduced as compared during pre-stagnation pentad.

It has also been seen that out of four cases, in three cases there are fall in $C(A_Z, K_Z)$. From the expression of $C(A_Z, K_Z)$, it appears that it is positive if there is rising motion of relatively warmer air and sinking motion of relatively colder air. During the advance of Southwest monsoon (SWM), northern latitude is having warm anomaly and southern latitude is having cold anomaly. This sets up a solenoidal circulation with a rising limb over warmer north and sinking limb over colder south. This causes surface southerly and the advance in SWM, this also cause $C(A_Z, K_Z)$ positive. Now, when north is relatively colder and south is relatively warmer, then this solenoidal circulation is either reversed or weakened, resulting in arrest of monsoon advance. Hence in the above-mentioned seven cases, due to reversal or weakening of $C(A_Z, K_Z)$, monsoon advance is stalled. It may be due to weakening or reversal of the north-south temperature gradient pattern.

The above result is in conformity with the findings of Biswas et al. (1998), where it was argued that massif Himalaya acts as an barrier to the passage of westerly trough, causing northerly cold advection to the west of it, which may lead to a weakening of above mentioned north-south temperature gradient.

In these cases, $G(A_Z)$ have also been observed to be reduced during stagnation, which is due to reduction in the net heating. Reduction in the net heating appears to be mainly due to rising motion of unstable relatively warmer air over southern latitude and sinking motion of unstable relatively colder air over northern latitude during stagnation. As in the zonal kinetic energy budget $C(A_Z, K_Z)$ is a source term, hence reversal or weakening of $C(A_Z, K_Z)$ also results in a reduction in $K_Z$ also, which further results into deceleration in monsoon advance. Another interesting point to note that in most cases, in contrary with the energetics of a typical baroclinic wave, where $A_E$ is converted to $K_E$, $A_E$ is being converted from $K_E$.

## 13.6 Conclusion

In most of the cases under study, a fall in $G(A_Z)$ during stagnation period has been observed.

A fall in $C(A_Z, K_Z)$ during stagnation period as compared to during pre-stagnation pentad has been observed in most of the cases.

There are observed reduction in $K_Z$ and in the magnitude of $C(K_Z, K_E)$ during stagnation as compared to during pre-stagnation pentad.

In most cases eddy baroclinic energy conversion during pre-stagnation pentad as well as during stagnation, takes place in the direction opposite to eddy baroclinic energy conversion in case of a typical baroclinic wave.

## References

Awade ST, Bawiskar SM (1982) Meridional transport of sensible heat in contrasting monsoon activity: spherical harmonic analysis. PAGEOPH 120:229–248

Awade ST, Totagi MY, Bawiskar SM (1985) Interaction of monsoon with northern hemisphere mid-latitude circulation. Proc Indian Acad Sci (Earth Planet Sci) 94:147–157

Biswas NC, De US, Sikka DR (1998) The role of Himalayan massif Tibetan plateau and mid-tropospheric sub-tropical ridge over north India during the advance phase of the south west monsoon. Mausam 49:285–300

George L, Mishra SK (1993) An observational study on the energetics of the onset monsoon vortex, 1979. Q J R Meteorol Soc 119:755–778

Keshavamurty RN, Awade ST (1970) On the maintenance of the mean monsoon trough over north India. Mon Weather Rev 98:315–320

Krishnamurti TN (1985) Summer monsoon experiment – a review. Mon Weather Rev 113:1590–1626

Krishnamurti TN, Bounoua L (2000) An introduction to numerical weather prediction techniques. CRC Press Inc, Boca Raton, pp 1–286

Krishnamurti TN, Ramanathan Y (1982) Sensitivity of monsoon onset of differential heating. J Atmos Sci 39:1290–1306

Krishnamurti TN, Surgi N (1987) Observational aspects of summer monsoon. In: Chang CP, Krishnamurti TN (eds) Monsoon meteorology. Oxford University Press, New York, pp 3–25

Krishnamurti TN, Sinha MC, Jha B, Mohanty UC (1998) A study of south asian monsoon energetics. J Atmos Sci 55(15):2530–2548

Pasch RJ (1983) On the onset of the planetary scale monsoon. Report No. 83–9, Department of Meteorology, Florida state university, Tallahassee, pp 1–220

Rajamani S (1985a) Energetics of the monsoon circulation over south Asia: I – Diabatic heating and generation of available potential energy. Mausam 36:7–12

Rajamani S (1985b) Energetics of the monsoon circulation over south Asia: Part-II – Energy terms and energy transformation terms. Mausam 36:405–412

Raju PVS, Mohanty UC, Bhatia R (2005) Onset characteristics of the southwest monsoon over India. Int J Clim 25(2):167–182

Ramasastry AA, De US, Vaidya DV, Sundari S (1986) Forty day mode and medium range forecasting. Mausam 37:305–312

Rao PLS, Mohanty UC (2007) Temporal characteristics of the Indian southwest monsoon. Nat Hazards 42(2):335–344

Rao KV, Rajamani S (1972) Study of heat sources and sinks and the generation of available potential energy in the Indian region during southwest monsoon. Mon Weather Rev 100:383–388

Wu G, Zhang Y (1998) Tibetan plateau forcing and the monsoon onset over south Asia and southern China sea. Mon Weather Rev 126:913–927

Yanai M, Li CF, Song ZS (1992) Seasonal heating of the Tibetan plateau and its effects on the evolution of the Asian summer monsoon. J Meteorol Soc Jpn 70:319–351

# Chapter 14
# Integrated Agrometeorological Advisory Services in India

**L.S. Rathore, S.K. Roy Bhowmik, and N. Chattopadhyay**

**Abstract** There is a considerable scope for decreasing the vulnerability of agriculture to increasing weather and climatic variability through weather forecast based agro-advisories. India Meteorological Department (IMD), Ministry of Earth Sciences (MoES), is operating an integrated Agro-Meteorological Advisory Service (AAS) at district level, in India, which represents a small step towards agriculture management in rhythm with weather and climate variability leading to weather proofing for farm production. Under AAS, needs of farming community was defined through ascertaining information requirement of diverse groups of end-users. It emerged, that prime need of the farmer is location specific weather forecast in quantitative terms. Hence, the same was developed and made operational in June, 2008. Thereafter, mechanism was developed to integrated weather forecast and climatic information along with agro-meteorological information to prepare district level agro-advisories outlining the farm management actions to harness favorable weather and mitigate impacts of adverse weather. A system has also been developed to communicate and disseminate the agro-meteorological advisories to strengthen the information out reach. The institutional dissemination channels such as farmer association, non-governmental organizations (NGOs), input suppliers, progressive farmers are also employed.

## 14.1 Weather Forecasting System for Agromet Advisory Service

IMD has started issuing quantitative district level (612 districts) weather forecast up to 5 days since 1st June, 2008. The products comprise of quantitative forecasts for seven weather parameters viz., rainfall, maximum temperature, minimum

L.S. Rathore • S.K.R. Bhowmik • N. Chattopadhyay (✉)
Agricultural Meteorology Division, India Meteorological Department, Pune, India
e-mail: lsrathore@ncmrwf.gov.in; skrb.imd@gmail.com; n.chattopadhyay@imd.gov.in

S.D. Attri et al. (eds.), *Challenges and Opportunities in Agrometeorology*,
DOI 10.1007/978-3-642-19360-6_14, 

temperatures, wind speed, wind direction, relative humidity and cloudiness. In addition, weekly cumulative rainfall forecast is also provided. IMD, New Delhi generates these products using Multi Model Ensemble (MME) technique based on forecast products available from number models of India and other countries. These include: T-254 model of NCMRWF, T-799 model of European Centre for Medium Range Weather Forecasting (ECMWF); United Kingdom Met Office (UKMO), National Centre for Environmental Prediction (NCEP), USA and Japan Meteorological Agency (JMA). The products are disseminated to Regional Meteorological Centres and Meteorological Centres of IMD located in different states. These offices undertake value addition to these products using synoptic interpretation of model output and communicate to 130 AgroMet Field Units (AMFUs), located with State Agriculture Universities (SAUs), institutes of Indian Council of Agriculture Research (ICAR) etc. on every Tuesday and Thursday.

Results show that MME forecasts have the better capability (compared to member models) to capture large scale rainfall features of summer monsoon, such as heavy rainfall belt along the west coast, over the domain of monsoon trough and along the foot hills of the Himalayas. The inter-comparison reveals that the ensemble forecast is able to provide more realistic spatial distribution of rainfall by taking the strength of each constituent model. The mean error as well as RMSE is found to be lowest in the ensemble forecasts both in magnitude and in the spatial area coverage. Results of errors statistics have clearly demonstrated the superiority of the MME over the member models. Among the member models ECMWF is found to be the best followed by JMA and NCEP GFS. The forecasts for other parameters namely maximum and minimum temperature, morning and evening relative humidity have also shown reasonably good skill. The results of the district level performance of the ensemble rainfall forecast show that the technique, in general, is capable of providing reasonably good forecast skill over most states of the country, particularly over the districts of the Central Zone where the monsoon systems are dominant. Though the procedure shows appreciable skill to predict occurrence or non-occurrence of light to moderate rainfall at the district level, but it has certain limitations to capture heavy rainfall events.

Inter-comparison of country mean spatial correlation coefficient (CC) of rainfall forecasts by MME and member models is presented in Fig. 14.1. The results show that MME is superior to each member model at all the forecasts (day 1 to day 5). Inter-comparison of threat score of rainfall forecasts by MME and member models at different rain thresholds is presented in Fig. 14.2. At all the rain thresholds, MME is better than each individual model.

State-wise performance of district level forecasts for day-5 is summarized in Table 14.1. Performance index is defined as the % of total districts with threat score more than 0.5 for rainfall thresholds of 2.5, 5, 10 and 15 mm. Threat score is defined as number of correct forecasts divided by total forecasts. The threat score ranges between 0 and 1, with 1 as the perfect score. The district level forecast skill is found to be reasonably good over most parts of the country.

An inter-comparison of distribution of rainfall over the coastal districts of Orissa, based on the MME forecasts against the observation of 16 June 2008 in

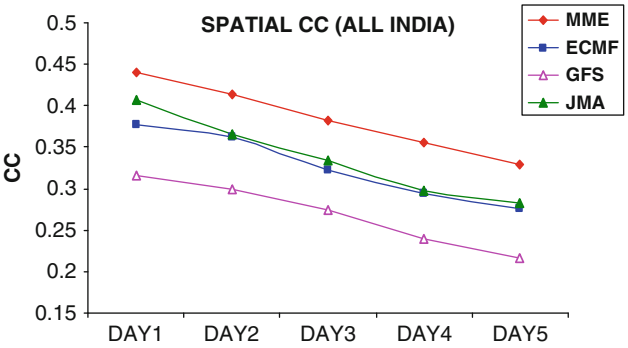


**Fig. 14.1** Inter-comparison of country mean spatial CC of day 1–day 5 rainfall forecasts by MME and member models for the period from 1 June to 30 September 2008

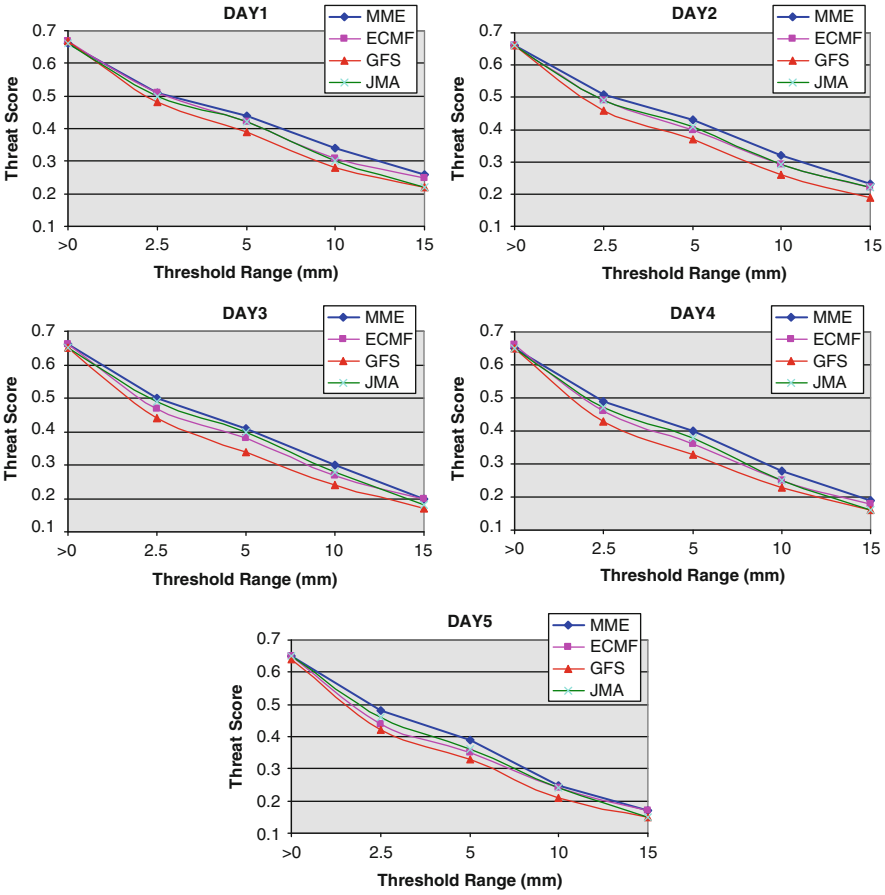


**Fig. 14.2** Inter-comparison of threat score of day 1–day 5 rainfall forecasts by MME and member models at different thresholds for the period from 1 June to 30 September 2008

**Table 14.1** State-wise district level performance skill of rainfall day 5 forecast (% of districts with threat score 0.5 and above for various rain thresholds)

| State | Total Dist. | 2.5 mm | 5 mm | 10 mm | 15 mm |
|---|---|---|---|---|---|
| Andaman & Nicobar | 2 | 100 | 100 | 100 | 50 |
| Arunachal Pradesh | 13 | 100 | 92 | 92 | 85 |
| Assam | 24 | 100 | 100 | 96 | 58 |
| Meghalaya | 7 | 100 | 100 | 100 | 86 |
| Nagaland | 8 | 100 | 100 | 100 | 13 |
| Manipur | 9 | 100 | 100 | 100 | 10 |
| Mizoram | 8 | 100 | 100 | 75 | 13 |
| Tripura | 4 | 100 | 100 | 100 | 10 |
| Sikkim | 4 | 100 | 100 | 75 | 25 |
| West Bengal | 19 | 100 | 95 | 84 | 32 |
| Orissa | 29 | 100 | 100 | 97 | 31 |
| Jharkhand | 18 | 100 | 100 | 100 | 39 |
| Bihar | 37 | 100 | 97 | 95 | 38 |
| Uttar Pradesh | 70 | 100 | 100 | 92 | 14 |
| Uttaranchal | 13 | 100 | 100 | 92 | 15 |
| Haryana | 19 | 100 | 84 | 26 | 5 |
| Chandigarh | 1 | 100 | 100 | 100 | 2 |
| Delhi | 1 | 100 | 100 | 7 | 5 |
| Punjab | 17 | 100 | 71 | 18 | 5 |
| Himachal Pradesh | 12 | 100 | 100 | 100 | 25 |
| Jammu & Kashmir | 17 | 100 | 65 | 24 | 5 |
| Rajasthan | 32 | 97 | 72 | 38 | 3 |
| Madhya Pradesh | 45 | 100 | 100 | 78 | 7 |
| Gujarat | 25 | 92 | 36 | 4 | 3 |
| Goa | 2 | 100 | 100 | 100 | 100 |
| Maharashtra | 33 | 100 | 88 | 55 | 21 |
| Chhattisgarh | 15 | 100 | 100 | 100 | 20 |
| Andhra Pradesh | 23 | 100 | 83 | 48 | 0 |
| Tamilnadu | 29 | 76 | 24 | 10 | 3 |
| Karnataka | 27 | 100 | 89 | 52 | 33 |
| Kerala | 14 | 100 | 100 | 100 | 79 |
| Lakshadweep | 1 | 100 | 100 | 100 | 100 |

presence of a monsoon depression is illustrated in Fig. 14.3. The results show that though the model (MME) underestimated rainfall amounts, it could capture heavy rainfall events for some districts as well.

The technique is constantly renewed and at present work is under way to compute weight for each of ECMWF, JMA, NCEP, NCMRWF and UKMO based on 2008 monsoon data for the five members MME to be used for weather prediction. Development work is also under way to design a MME method for probabilistic forecast to issue 3 days forecast based on very high resolution non-hydrostatic meso-scale models as the ensemble members to estimate risk for districts, making use of the new observations and infrastructure that would be available from the ongoing modernization programme of IMD. The documentation

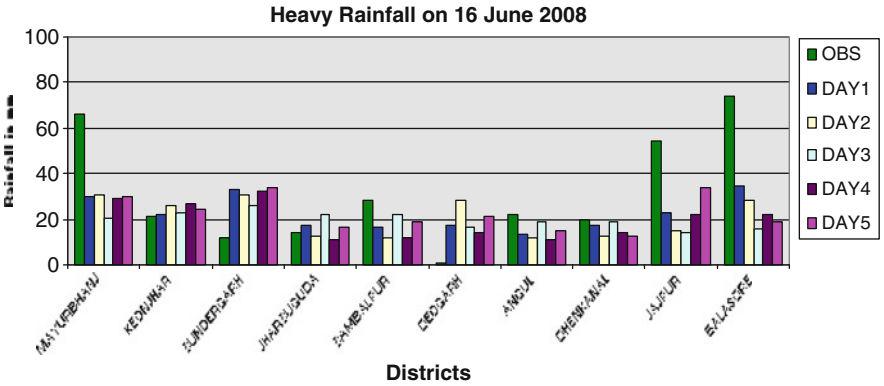


**Fig. 14.3** MME day 1–day 5 rainfall forecasts valid for 16 June 2008 for coastal districts of Orissa in association with a monsoon depression

of important weather system where forecast fails and preparation of concept paper for value addition procedure is also being taken up along with preparation of district level climatology of extreme weather events.

## 14.2 Agro-Meteorological Field Units (AMFUs)

The AAS is multidisciplinary and multi-institutional project. It involves all stakeholders such as State agricultural Universities (SAUs), Indian Council for Agriculture

Research (ICAR), Krishi Vigyan Kendras (KVK), Department of Agriculture & Cooperation, State Departments of Agriculture/Horticulture/Animal Husbandry/ Forestry (Up to District level offices), NGOs, Media Agencies, etc. Roles of various agencies and their inter-linkages are depicted in Fig. 14.4. This project is being implemented through five tier structure to set up different components of the service spectrum. It includes meteorological (weather observing and forecasting), agricultural (identifying weather sensitive stress and preparing suitable advisory using weather forecast), extension (two way communication with user) and information dissemination (Media, Information Technology, Telecom) agencies (Fig. 14.5).

The Ministry of Earth Sciences (MoES), Government of India, has set up a network of 130 AMFUs covering all agro-climatic zones of the country. These are opened and operated at State Agriculture Universities (SAUs), Indian Council of Agricultural Research institutions (ICAR), Indian Institute of Technology (IIT) by providing grant-in-aid from IMD. These units are responsible for recording agro meteorological observations, preparing medium range weather forecast based Agromet advisories for the districts falling under precinct of concerned agroclimatic zone and dissemination of the same. Concerned university/institute has appointed Nodal Officer and Technical Officers, who prepare the advisory

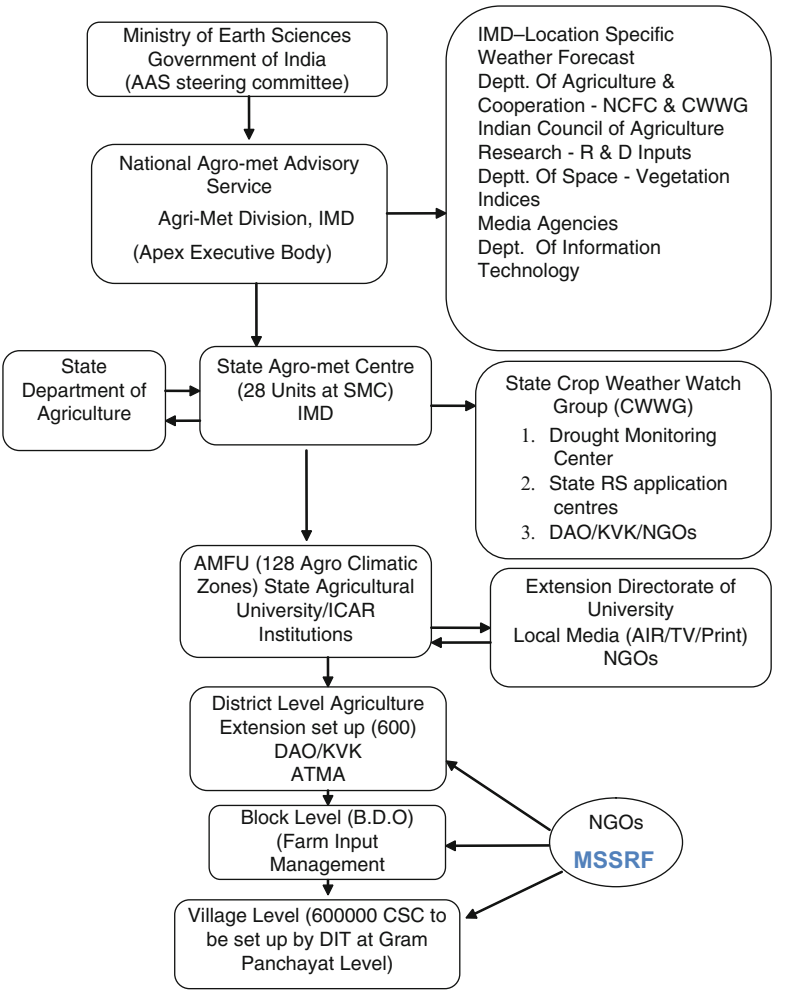


**Fig. 14.4** Collaborating organization and their linkages under integrated agromet services

bulletins in consultation with the panel of scientists drawn from various disciplines at these units.

## 14.3 Translating Forecast into Crop Advisories

Application of weather forecast to generate crop advisories is linked to accuracy, spatial domain of validity and temporal range. In view of these requirements of farming community, district level forecasts are issued for above listed parameters

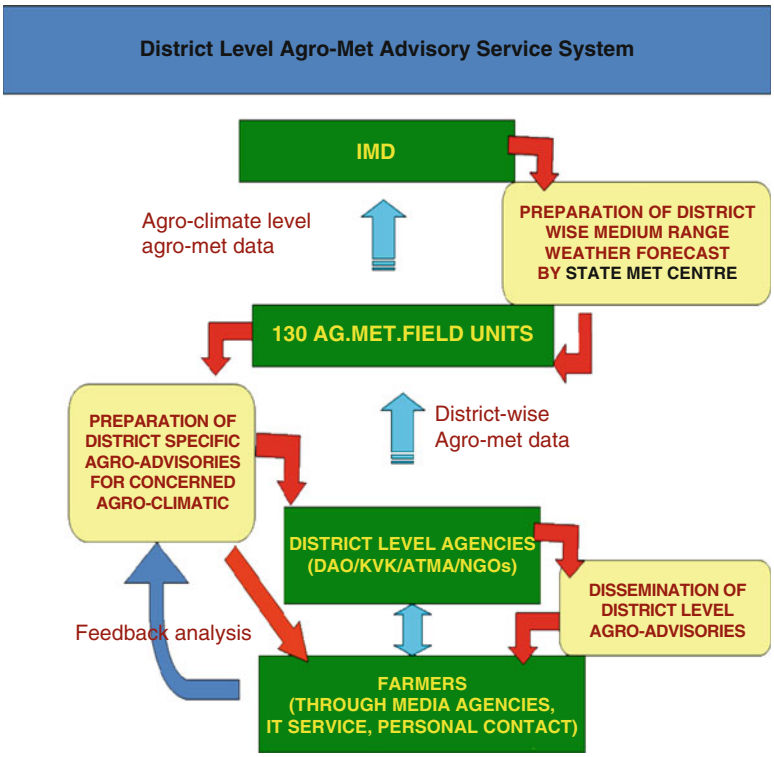


**Fig. 14.5** Integrated agrometeorological advisory service system

for next 5 days and same are translated into crop specific advisories keeping in view their phenological stages for farmer's guidance on cultural practices.

District-specific medium-term forecast information and advisories help maximize output and avert crop damage or loss. It also helps growers anticipate and plan for chemical applications, irrigation scheduling, disease and pest outbreaks and many more weather related agriculture-specific operations. Such operation include cultivar selection, their dates of sowing/planting/transplanting, dates of intercultural operations, dates of harvesting and also performing post harvest operations. Agromet advisories help increase profits by consistently delivering actionable weather information, analysis and decision support for farming situations such as: to manage pests through forecast of relative humidity, temperature and wind; manage irrigation through rainfall and temperature forecasts; protect crop from thermal stress through forecasting of extreme temperature conditions etc.

Under the AAS system, more focus has been started to be given to use the crop/soil simulation models to decide crop management strategies, for the given weather condition. Agricultural scientists at Agrometeorological Field Units have started using crop simulation models as a decision support tool for helping with weather forecast based farm management decision making as they are more objective.

For example, the Agro-meteorological Field unit can objectively assess the impact of skipping irrigation at a particular phenophase of a crop on its dry matter yield though with some uncertainties. Agrometeorologists can consider many of the factors involved, and answer the question with a reasonable estimate. The crop models are also be used as technique for prediction of different phenophases and final yield.

## 14.4 Agro-Meteorological Support for Farm Management

Weather based farm advisories as support system has been organized after characterization of agro-climate, including length of crop growing period, moisture availability period, distribution of rainfall and evaporative demand of the regions, weather requirements of cultivars and weather sensitivity of farm input applications. All this is used as background information. Following are the ingredients of a typical Agromet Advisory Bulletin to reap benefits of benevolent weather and minimize or mitigate the impacts of adverse weather;

1. District specific weather forecast, in quantitative terms, for next 5 days for rainfall, cloud, max/min temperature, wind speed/direction and relative humidity, including forewarning of hazardous weather event likely to cause stress on standing crop and suggestions to protect the crop from them.
2. Weather forecast based information on soil moisture status and guidance for application of irrigation, fertilizer and herbicides etc.
3. The advisories on dates of sowing/planting and suitability of carrying out intercultural operations covering the entire crop spectrum from pre-sowing to post harvest to guide farmer in his day–today cultural operations.
4. Weather forecast based forewarning system for major pests and diseases of principal crops and advises on plant protection measures.
5. Propagation of techniques for manipulation of crop's microclimate e.g. shading, mulching, other surface modification, shelter belt, frost protection etc. to protect crops under stressed conditions.
6. Reducing contribution of agricultural production system to global warming and environment degradation through judicious management of land, water and farm inputs, particularly pesticides, herbicides and fertilizers.
7. Advisory for livestock on health, shelter and nutrition.

The support on above is rendered through preparing district specific agrometeorological advisory bulletins which are tailored to meet the farmers' need and are made relevant to his decision making processes. The suggested advisories generally alter actions in a way that improves outcomes. It contains advice on farm management actions aiming to take advantage of good weather and mitigate the stress on crop/livestock. Hence, while formulating the bulletin one ought to know the crop condition. Ideally, farmer should place request to the AMFU/IMD either directly or via the extension officer. But more often than not, such information has to be

assessed through field observation, media reports, farmers' feedback, and remote sensing (NDVI etc.) observations. The desired information is also obtained by exploratory surveys or participatory methods of personal interactions with farmers. The critical issues in this regard as summarized by Hansen (2002) are followed and include: (a) site specificity – that farmers are aware of spatial variability and can recognize scale mismatches between the forecasts and their on farm decisions; (b) temporal specificity – including timing relative to decisions and impacts, highlighting factors such as onset of rainfall, dry spell distribution, and weather conditions during harvest; and, (c) skill of the forecast – often in different terms from the forecasters but relative to the other risks within their farming operations.

The bulletins are encoded in a format and language which is easy to comprehend by the farmer. The agrometeorologists first interpret the immediate past weather and the forecast for next 5 days and translate it into layman's terms so that the farmers can understand it. Thus, the agrometeorologists play a vital role in the encoding and decoding of the messages from the meteorologists to the agricultural sector. Also, interaction between the AMFUs and farmers to identify the weather sensitive decisions is promoted under the service. This step enables a relationship between the IMD, AMFUs, and the farmers so that they can identify or diagnose the gaps in weather information available from the IMD. As the interaction between the weather and agriculture is complex, it is not just a case of applying a simple solution and expecting implementation by the farmers. So, an awareness process to understand the influence of weather and climate on sustainable agricultural production as outlined by Sivakumar et al. (2000) is followed.

The Agro-met Advisory Bulletins are issued at district, state and national levels to cater the needs of local level to national level. The district level bulletins are issued by AMFUs and include crop specific advisories including field crops, horticultural crops and livestock. The State Level bulletin is a composite of district bulletins helping to identify the distressed district of the state as well as plan the supply of appropriate farm inputs such as seeds, irrigation water, fertilizer, pesticides etc. These bulletins are jointly prepared by State Meteorological Centre of IMD and AMFUs and mainly used by State Government functionaries. This is also useful to Fertilizer industry, Pesticide industry, Irrigation Department, Seed Corporation, Transport and other organizations which provide inputs in agriculture. This bulletin is a significant input to the State level Crop Weather Watch Group (CWWG) meeting. National Agromet Advisory Bulletins are prepared by National Agromet Advisory Service Centre, Division of Agriculture Meteorology, IMD, Pune, using inputs from various states. This bulletin helps identify stress on various crops for different regions of the country and suitably incorporate advisories. Ministry of Agriculture is prime user of these bulletins, which help take important decisions in Crop Weather Watch Group (CWWG) meetings at national level. The bulletins are also used by a large number of other agencies including fertilizer, pesticide industries.

## 14.5 Dissemination of Agrometeorological Bulletins

The task of AAS is to provide information to help farmers make the best possible use of weather and climate resources. While disseminating the information, it is presumed that the farmers possess relevant knowledge and skills. Although concerted efforts are being made to set up two way communications, but as of now the information flow is largely one-way. AS agro-meteorologists at Agrometeorological Field Units (AMFUs) have less frequent interaction with the farmers, good communication and working relationships have been set up with the agricultural extension, Krishi Vigyan Kendra (Agriculture Science Centres), Kisan (Farmer) Call Centre etc. to promote participatory methods for interactions with farmers. Due care is being taken regarding content of the message which must be relevant to the weather based decision making by the farmer. This involves the identification of weather & climate sensitive decisions and interactions between the weather forecasters from meteorological Centres of IMD and the agriculture scientists from Agriculture Universities and/or Institutes of Indian Council of Agriculture Research to develop weather based advisories and technological. Information is disseminated through multi-modes of delivery including mass and electronic media. It include, All India Radio, Television, Print Media (local news paper in different vernacular languages), internet (Web Pages) as well as group and individual relationships through email, telephone etc. The use of electronic media such as e-mail or the Internet is picking up as the access of these methods to the farming community is on significant rise. The agrometeorological bulletins always contain dynamic information hence, repetitive dissemination is being made. This reiterative process also helps to address large temporal and spatial variability having significant influence of weather and climate on agriculture. Critical factors for successful dissemination include relevance of information to weather and climate sensitive decision making in agriculture, followed by good outreach.

## 14.6 Evaluating the Impact of Agrometeorological Advisory Systems

Impact assessment of weather forecast based agro-advisory service was undertaken at 15 representative AAS units representing different agro-climatic zones. The report assesses the impact of weather based agro-advisories on cereals, millets, pulses, oilseeds, fruits, vegetables and cash crops selected for the study. The study period was spread over 3 years comprising of 3 Kharif and 3 Rabi seasons. National Centre for Agriculture Economics and Policy Research (NCAP), who was engaged as consultant for the project, helped to formulate the study plan, including devising sampling method, preparation of questionnaire, monitoring its implementation and data analysis. It has been found that in most of the cases, use of AAS advisories resulted in decline in the cost of cultivation up to 25% for the study crops. In some

cases, cost of cultivation did increase up to 10% as a result of follow up action on AAS advisories, but this was more than offset by the consequent increase in net returns up to 83%, with a modal value of 20%. The major crops which benefited most from the use of AAS service are paddy, wheat, pearl millet and fruits and vegetables. This proves the usefulness of AAS advisories. This also endorses the need for dissemination of AAS information to farmers on a wider scale and convincing them about its positive impacts on a sustainable basis. Equally important but the most challenging task would be to enhance the accuracy of weather forecast and to make the AAS more useful and demand-driven for the farm households (Rathore and Maini, 2008).

## References

Hansen JW (2002) Realizing the potential benefits of climate prediction to agriculture: issues, approaches, challenges. Agric Syst 74:309–330

Rathore LS, Maini, Parvinder (2008) "Economic impact assessment of agro-meteorological advisory service of NCMRWF". Report no. NMRF/PR/01/2008. Published by NCMRWF, Ministry of Earth Sciences, Government of India, A-50, Institutional Area, Sector – 62, Noida 201 307, pp 104

Sivakumar MVK, Gommes R, Baier W (2000) Agrometeorology and sustainable agriculture. Agric For Meteorol 103:11–26

# Chapter 15
# South-West Monsoon Variability and Its Impact on Dryland Productivity in Drought Affected Districts of Amravati Division in Maharashtra State

**G.U. Satpute and S.S. Vanjari**

**Abstract** Rain water is the most vital and a critical input for agricultural production in rainfed farming areas in Maharashtra state. Recent droughts in Vidarbha region had adversely affected the crop production and economic condition of dryland farmers. The present study was undertaken in Amravati division of Vidarbha for assessing drought potential and its impact on agricultural production.

The decadal variation of seasonal, monthly and weekly rainfall (1976–2005) on district and taluka level clearly indicated a remarkable change in rainfall pattern during the current decade (1996–2005) over earlier two decades (1976–1985 and 1986–1995). Drought study indicated a tendency of occurrence of drought successively for 3 years at all the district places of Amravati division during 30 years study period (1976–2005). Considerable reduction (12–54%) in rainfed crop yield of cotton, sorghum, soybean, pigeon pea and gram was observed in Amravati division during wide spread drought years over normal years. Such studies can be helpful in assessing climatic potential of the region in terms of moisture availability/ water deficit pattern during different crop growth periods which will be useful for better agricultural planning and developing water resources for providing protective irrigation.

G.U. Satpute (✉)
SWCE, Department of Soil and Water Conservation Engineering, Dr. Panjabrao Deshmukh Krishi Vidyapeeth, PO Krishi Nagar, Akola (MS) 444 104, India
e-mail: gusatpute@rediffmail.com

S.S. Vanjari
Department of Agronomy, Dr. Panjabrao Deshmukh Krishi Vidyapeeth, PO Krishi Nagar, Akola (MS) 444 104, India
e-mail: wanjari.sanjay@rediffmail.com

S.D. Attri et al. (eds.), *Challenges and Opportunities in Agrometeorology*,
DOI 10.1007/978-3-642-19360-6_15, 

## 15.1 Introduction

Rainfall is the most important natural hydrologic event and a unique phenomenon varying both in space and time. For the optimum development of water resources and for selection of crops and cropping sequences, and for planning of agriculture operations in a given region, basic knowledge of rainfall distribution during weeks, months, seasons and year is of vital importance. Rainfall or lack of it plays an important role in many of the agricultural and non-agricultural operations. According to Vairavan et al. (2002) to minimize risk, the climatological data of a location becomes very important to provide necessary information. Amongst different climatological parameters, rainfall data is only monitored regularly at a taluka level and can be used to study spatial and erratic nature of monsoon rainfall of the region.

Hence, the determination of rainfall amounts and patterns is of great importance and should continue to receive priority attention especially in the drought prone districts of Vidarbha region for securing optimum production and productivity levels in agriculture. Balogun (1972) discussed three widely used methods of expressing rainfall variability and showed that use of coefficient of variability is the most advisable when explaining the spatial variability of rainfall.

In this paper, south-west monsoon variability at 29 station in five drought affected districts of western Vidarbha have been reported considering decadal variation in rainfall amount on seasonal, monthly and weekly basis and corresponding coefficient of variability.

## 15.2 Materials and Methods

Weekly rainfall data for different taluka places in different drought affected districts of Vidarbha (Buldhana, Akola, Amravati, Washim and Yeotmal) for which a long length of record (30 years period) was available were selected. Weekly rainfall for 29 taluka places in five drought affected districts was collected from Indian Meteorology Department, Pune and Agro-meteorology Observatory, Dr. PDKV, Akola for 30 years (1976–2005). The location map of the study area is shown in Fig. 15.1. The data were aggregated to monthly, seasonal (June–September) and annual totals. The mean rainfall, standard deviation and coefficient of variation for seasonal, monthly and weekly periods were worked out as per Deka and Nath (2000).

The rainfall pattern of all the five drought affected districts in Amravati division have been studied considering decadal variation of rainfall amount on seasonal, monthly and weekly basis and corresponding coefficient of variation. The coefficient of variation is used to explain the spatial variability of rainfall and is estimated as

$$CV = \frac{\sigma}{\bar{x}} 100$$

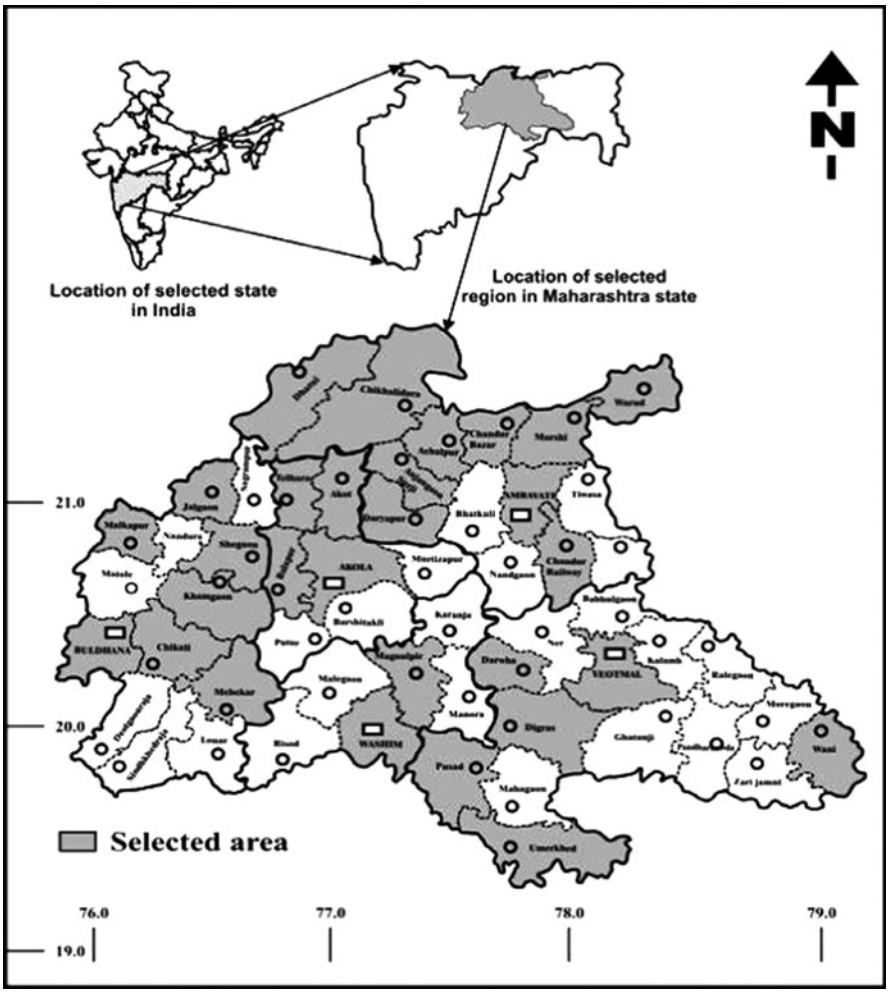


**Fig. 15.1** Location map of study area in western Vidarbha

Where,

CV – Coefficient of variation
$\sigma$ – Standard deviation
$\overline{x}$ – Mean

In this study, monsoon season rainfall was considered from 23rd to 39th meteorological weeks, while for monsoon monthly rainfall analysis of June, July, August and September months, the meteorological weeks considered were 23rd–26th, 27th–31st, 32nd–35th and 36th–39th week respectively. Decadal variation of seasonal and monthly rainfall at different taluka places and district wise averages of

corresponding parameters for different talukas is determined to analyze rainfall pattern in the region.

The agricultural droughts due to monsoon variability at different districts were determined by Satpute and Singh (2006) using climatological water balance approach according to Thornthwaite and Mather (1955). The reference evapotranspiration was computed using Penman Monteith equation as per the procedure given by Allen et al. (1998). Drought intensity was determined at all the district places considering aridity index (Ia) deviation estimated on annual basis and categorizing the intensity of drought years using different ranges of standard deviation suggested by Subramanyam and Sastri (1969). The taluka wise yields of different crops as reported by State Agriculture Department were used for verifying the results obtained from the study.

## 15.3 Results and Discussion

### *15.3.1 Annual and Seasonal Rainfall Analysis*

Annual and seasonal rainfall for 30 years period (1976–2005) at the selected taluka places in different drought affected districts of Vidarbha was averaged on district basis and corresponding station's annual and kharif seasonal average (June–September) is given in 15.1. From Table 15.1, it is revealed that on district level basis, average annual rainfall at Buldhana, Akola, Amravati, Washim, and Yeotmal districts was 724.8, 725.9, 869.0, 879.9 and 906.3 mm respectively. On district level basis, average annual rainfall shows less regional variation among Buldhana – Akola, Amravati – Washim and Yeotmal compared to a large variation at taluka level in respective districts. The 30 year seasonal mean rainfall shows less variation among Amravati, Washim and Yeotmal districts while that of Buldhana and Akola districts seasonal mean is near about same.

At district level, coefficient of variation of average annual rainfall (Table 15.1) was lowest at Washim district (26.9) and highest at Amravati district (39.0). Seasonal rainfall variation was less in Akola (31.8%) and Washim (31.6%) districts

**Table 15.1** Average annual and seasonal rainfall during 1976–2005 at different drought affected districts of Amravati division

| District | Average annual rainfall (mm) | Average seasonal rainfall (mm) | C.V. of rainfall, % | | Percentage of seasonal to annual rainfall, % |
|---|---|---|---|---|---|
| | | | Annual | Seasonal | |
| Buldhana | 724.8 | 634.9 | 30.3 | 35.5 | 87.6 |
| Akola | 725.9 | 627.6 | 30.4 | 31.8 | 86.5 |
| Amravati | 869.0 | 767.7 | 39.0 | 42.2 | 88.0 |
| Washim | 879.9 | 764.4 | 26.9 | 31.6 | 87.2 |
| Yeotmal | 906.3 | 790.4 | 31.3 | 33.5 | 87.2 |

and high in Amravati district (42.2%). The coefficient of variation of average seasonal rainfall at taluka level varies from 26% to 36% with the exceptions of Jalgaon-Jamod and Mehakar in Buldhana and Umarkhed in Yeotmal districts. In general, different stations in different drought affected districts received about 86–87% of annual rainfall in monsoon season (Table 15.1). The contribution of seasonal rainfall to annual rainfall varies from 84.1% to 93.0% at different taluka places in different drought affected districts of Vidarbha.

### *15.3.2 Monthly Rainfall Analysis*

Average monthly rainfall contribution to seasonal rainfall during 1976–2005 at different drought affected districts and district wise monthly coefficient of variation is presented in Table 15.2. From Table 15.2 it reveals that different stations in all the districts receive maximum rainfall in the month of July, followed by August, June and September. Contribution of average monthly to average seasonal rainfall on district level basis for the months of June, July, August and September was found to vary from 21.4% to 24.3%, 34.4% to 36.8%, 25.6% to 29.0% and 12.6% to 15.2% respectively in different districts. The monthly rainfall coefficient of variation for July was least, followed by August, June and September at different drought affected districts. Though, Table 15.2 shows more or less even rainfall distribution in each month at all district places, but at taluka level, there was wide variation in rainfall of monsoon months.

### *15.3.3 Decadal Behavior of Seasonal Rainfall*

The decadal behavior of average seasonal rainfall distribution in different districts during monsoon season as presented in Table 15.3 reveals that in Buldhana and Akola districts seasonal rainfall increased while the same is reduced in Washim and Amravati districts and was nearly constant in Yeotmal district in second decade

**Table 15.2** Average monthly rainfall in different drought affected districts of Amravati division (1976–2005)

| | | Percent contribution of monthly rainfall to seasonal rainfall, % | | | | Monthly rainfall, c. v., % | | | |
|---|---|---|---|---|---|---|---|---|---|
| District | Mean seasonal rainfall, mm | Jun | Jul | Aug | Sep | Jun | Jul | Aug | Sep |
| Buldhana | 634.9 | 24.3 | 34.4 | 26.5 | 14.9 | 59.3 | 44.1 | 60.8 | 91.7 |
| Akola | 627.6 | 21.5 | 36.4 | 26.9 | 15.2 | 71.3 | 46.0 | 57.9 | 92.2 |
| Amravati | 767.7 | 19.7 | 36.8 | 27.9 | 15.2 | 61.6 | 56.4 | 68.7 | 97.8 |
| Washim | 764.4 | 24.3 | 36.2 | 25.6 | 14.2 | 61.1 | 43.6 | 59.0 | 90.0 |
| Yeotmal | 790.4 | 23.0 | 36.6 | 27.9 | 12.6 | 57.6 | 47.4 | 58.5 | 106.5 |

**Table 15.3** Decadal behavior of average monsoon seasonal rainfall on district level basis in drought affected districts of Amravati division (1976–2005)

| District | 30 year seasonal mean, mm | Decadal mean seasonal rainfall, mm | | | Decadal mean seasonal rainfall as % of 30 year mean | | |
|---|---|---|---|---|---|---|---|
| | | 1976–1985 | 1986–1995 | 1996–2005 | 1976–1985 | 1986–1995 | 1996–2005 |
| Buldhana | 634.9 (35.5)[a] | 620.6 (31.0)[b] | 653.5 (42.5)[b] | 630.5 (31.3)[b] | 97.8 | 102.9 | 99.3 |
| Akola | 627.6 (31.8) | 621.8 (29.4) | 682.8 (36.9) | 578.4 (23.6) | 99.1 | 108.8 | 92.2 |
| Amravati | 764.4 (42.2) | 823.2 (38.6) | 773.2 (48.9) | 696.8 (37.1) | 107.7 | 101.2 | 91.2 |
| Washim | 767.7 (31.6) | 787.3 (23.4) | 747.5 (32.5) | 768.1 (38.7) | 102.5 | 97.4 | 100.1 |
| Yeotmal | 790.4 (33.5) | 804.0 (34.0) | 812.7 (35.7) | 754.4 (30.4) | 101.7 | 102.8 | 95.4 |

[a]Figure in parenthesis is coefficient of variation of 30 year seasonal rainfall.[b]Figure in parenthesis is coefficient of variation of decadal seasonal (June–Sept.) rainfall

(1986–1995) than that of first decade (1976–1985). The seasonal rainfall in third decade (1996–2005) is reduced in Buldhana, Akola, Amravati and Yeotmal districts while it was increased marginally in Washim district over that of second decade (1985–1996). Seasonal rainfall decreased in the current decade (1996–2005) at almost all the stations in different districts except for Buldhana, Jalgaon-Jamod, Malkapur, Washim, Morshi, Daryapur, Anjangaon and Darwha stations, where seasonal rainfall increased over 30 year mean. The coefficient of variation of decadal seasonal rainfall (Table 15.3) indicates in general lowest values in all districts except Washim in the current decade (1996–2005) over other two decades.

The percentages of decadal mean seasonal rainfall over that of 30 year mean seasonal rainfall (Table 15.3) indicates that in current decade all district except Washim shows considerable reduction (91–95%) in rainfall over the remaining two decades. During 1996–2005 (current) decade near about 21 taluka places shows 15–20% reduction in mean seasonal rainfall on district basis while individual year wise variation is quite high (40–60%).

The decadal changes in coefficient of variation of seasonal rainfall during 1976–2005 at different taluka stations in different drought affected districts of Amravati division as shown in Table 15.4 clearly indicates that 21 talukas during 1986–95 shows highest decadal c.v. followed by 1976–1985 (5) and least during current decade 1996–2005 (3). Tables 15.3 and 15.4 shows that with lower seasonal rainfall at maximum talukas during the current decade (1995–2005) having lowest c.v. clearly indicates uniformity in least rainfall received in the drought affected districts of the region.

### *15.3.4 Decadal Behavior of Monthly Rainfall*

The decadal behavior of average monthly rainfall distribution in different districts during monsoon season as presented in Table 15.5 reveals that for the month of June, rainfall percentage increased in second decade at all the drought affected districts of Vidarbha and a marginal increase was observed in third decade with respect to first decade except for Washim district. For the month of July, when

**Table 15.4** Coefficient of variation of seasonal rainfall and decadal changes in coefficient of variation of seasonal rainfall during 1976–2005 at different taluka stations in drought affected districts of Amravati division

| District | Taluka | C.V. of seasonal rainfall, % 1976–2005 | Decadal C.V. of seasonal rainfall, % | | |
|---|---|---|---|---|---|
| | | | 1976–1985 | 1986–1995 | 1996–2005 |
| Buldhana | Buldhana | 29.0 | 31.9 | 27.5 | 28.9 |
| | Chikhali | 30.4 | 33.8 | 38.4 | 17.2 |
| | Jalgaon | 38.2 | 34.0 | 38.2 | 42.6 |
| | Khamgaon | 33.6 | 29.1 | 45.6 | 23.0 |
| | Malkapur | 34.9 | 33.6 | 25.2 | 39.2 |
| | Mehekar | 40.1 | 22.7 | 53.4 | 27.8 |
| | Shegaon | 33.5 | 33.4 | 36.2 | 32.2 |
| Akola | Akola | 26.0 | 21.8 | 28.2 | 22.7 |
| | Akot | 34.4 | 31.4 | 45.9 | 22.9 |
| | Balapur | 32.1 | 28.2 | 38.2 | 27.4 |
| | Telhara | 33.4 | 32.1 | 37.8 | 25.2 |
| Amravati | Amravati | 27.4 | 14.1 | 28.8 | 40.6 |
| | Achalpur | 30.0 | 30.0 | 37.6 | 35.0 |
| | Anjangaon | 29.4 | 26.6 | 33.5 | 22.6 |
| | Chandur Baz. | 27.9 | 18.0 | 34.2 | 20.7 |
| | Chandur Rly. | 29.6 | 32.6 | 32.0 | 25.1 |
| | Chikhaldara | 30.7 | 25.1 | 38.6 | 18.3 |
| | Daryapur | 29.6 | 18.9 | 41.2 | 24.8 |
| | Dharni | 30.8 | 16.8 | 43.7 | 26.4 |
| | Morshi | 25.9 | 21.4 | 37.2 | 27.3 |
| | Warud | 36.3 | 25.9 | 35.2 | 25.0 |
| Washim | Washim | 29.1 | 23.9 | 33.6 | 19.7 |
| | Mangrulpir | 33.2 | 24.0 | 44.9 | 23.7 |
| Yeotmal | Yeotmal | 26.4 | 28.2 | 29.8 | 23.8 |
| | Darwha | 31.2 | 29.8 | 32.6 | 32.4 |
| | Digras | 32.1 | 37.6 | 36.5 | 20.8 |
| | Pusad | 35.3 | 36.9 | 36.6 | 34.9 |
| | Umarkhed | 38.3 | 38.2 | 36.9 | 30.6 |
| | Wani | 32.5 | 28.6 | 37.5 | 29.5 |

compared to first decade, rainfall percentage decreased in second decade at all the district places and continues to decrease in third decade except for Buldhana, Amravati and Washim districts while an increased trend was observed in the third decade in comparison with second decade except for Akola district.

Rainfall percentage for August in second and third decade compared with first decade shows an increasing trend at all district places in second decade but a decreasing trend was observed in third decade at most of the district places except for Washim. Also comparison of rainfall percentage in second and third decade shows decreasing trend in third decade at all district places. Rainfall percentage for September in second and third decade when compared with first decade shows decrease in rainfall in second decade which later increases in third decade at all the

**Table 15.5** Decadal behavior of average monthly rainfall on district level basis in drought affected districts of Vidarbha, during monsoon months (1976–2005)

| District | Contribution of monthly rainfall to seasonal rainfall, per cent | | | | | | | | | | | |
|---|---|---|---|---|---|---|---|---|---|---|---|---|
| | June | | | July | | | August | | | September | | |
| | 1976–1985 | 1986–1995 | 1996–2005 | 1976–1985 | 1986–1995 | 1996–2005 | 1976–1985 | 1986–1995 | 1996–2005 | 1976–1985 | 1986–1995 | 1996–2005 |
| Buldhana | 23.3 | 26.6 | 23.5 | 38.4 | 33.0 | 35.3 | 24.9 | 28.6 | 24.0 | 13.3 | 11.8 | 17.2 |
| Akola | 21.8 | 21.9 | 21.9 | 38.7 | 36.5 | 35.2 | 25.5 | 30.5 | 23.2 | 14.0 | 11.2 | 19.8 |
| Amravati | 19.7 | 21.9 | 19.5 | 38.5 | 35.2 | 37.2 | 28.4 | 30.2 | 24.1 | 13.4 | 12.7 | 19.2 |
| Washim | 24.0 | 27.5 | 22.7 | 36.2 | 33.7 | 39.7 | 22.9 | 26.9 | 25.4 | 16.8 | 11.9 | 12.3 |
| Yeotmal | 23.2 | 24.5 | 23.6 | 38.7 | 33.6 | 38.8 | 24.5 | 32.8 | 24.7 | 13.6 | 9.1 | 13.0 |

places except for Washim district. But rainfall percentage for September increased in the third decade with respect to second decade at all the districts.

From above discussion of Table 15.5, it can be concluded that the monsoon rainfall of the region showed shift of considerable amount of monsoon rainfall from the month of August to the month of September in the current decade of 1996–2005 over earlier two decades (1976–1995).

### *15.3.5 Decadal Behavior of Weekly Rainfall*

Weekly rainfall during June to September months (23rd–39th met. weeks) in different talukas of the drought affected districts shows a wide variation with coefficient of variation of 30 year seasonal weekly rainfall in the range of 113.1–149.0%. Amongst different talukas, Jalgaon-Jamod and Malkapur in Buldhana district, Balapur and Telhara in Akola district, Chandur-Railway and Warud in Amravati district and Umarkhed in Yeotmal district showed quite high coefficient of variation. However, decadal coefficient of variation of weekly rainfall in different talukas for 1976–1985, 1986–1995 and 1996–2005 decades as shown in Table 15.6 indicates that, in the former decade only two talukas are having high coefficient of variation values, followed by 11 talukas in the second decade and maximum 16 talukas in the latter decade (1996–2005).

These results indicates that in the current decade (1996–2005) maximum area (nearly 70% talukas) of the drought affected districts had received weekly rainfall with highest coefficient of variation, indicating most erratic distribution of monsoon rainfall in the current decade compared to other decades. These results of high decadal coefficient of variation of weekly rainfall during current decade (1996–2005) which were reverse of that of corresponding seasonal decadal rainfall with least C.V. was mostly responsible for maximum drought years during the study period in the region.

This type of micro level (Taluka wise) rainfall characterization study on regional basis is of great use for planning of different dryland agricultural crops in general and development of agriculture sector in particular through water resource development in the region.

### *15.3.6 Agricultural Drought Years and Dryland Crop Productivity*

Different types of agricultural droughts estimated by Satpute and Singh (2006), are arranged in Fig. 15.2 according to different drought intensity classes viz. disastrous, severe, large and moderate along with corresponding years annual rainfall, which reveals that at different stations total drought years varies from 13 to18 in number with corresponding percentage varying from 43.33% to 60.00%. Study of drought years in drought affected districts indicated a tendency of occurrence of drought

**Table 15.6** Coefficient of variation of decadal weekly rainfall during monsoon season at different taluka stations in drought affected districts of Amravati division

| District | Taluka | 30 year. seasonal weekly rainfall c. v. (%) | Decadal weekly c. v. (%) | | |
|---|---|---|---|---|---|
| | | | 1976–1985 | 1986–1995 | 1996–2005 |
| Buldhana | Buldhana | 116.0 | 110.6 | 117.9 | 117.6 |
| | Chikhali | 120.0 | 114.0 | 122.3 | 123.6 |
| | Jalgaon Ja. | 134.3 | 119.0 | 136.7 | 142.0 |
| | Khamgaon | 120.1 | 113.2 | 128.4 | 116.7 |
| | Malkapur | 129.6 | 126.2 | 118.6 | 136.9 |
| | Mehekar | 121.2 | 115.2 | 121.5 | 126.4 |
| | Shegaon | 126.0 | 120.8 | 134.0 | 122.7 |
| Akola | Akola | 117.0 | 114.4 | 117.0 | 117.8 |
| | Akot | 121.5 | 116.0 | 124.5 | 124.4 |
| | Balapur | 132.0 | 130.3 | 130.5 | 132.9 |
| | Telhara | 139.0 | 157.0 | 130.5 | 124.3 |
| Amravati | Amravati | 124.6 | 121.7 | 130.8 | 121.0 |
| | Achalpur | 124.0 | 124.6 | 113.4 | 130.8 |
| | Anjangaon | 126.1 | 117.2 | 130.8 | 129.8 |
| | Chandur Baz. | 120.4 | 118.1 | 115.8 | 128.2 |
| | Chandur Rly. | 149.0 | 120.0 | 193.3 | 120.8 |
| | Chikhaldara | 114.2 | 105.0 | 123.2 | 114.0 |
| | Daryapur | 123.1 | 110.8 | 109.5 | 138.6 |
| | Dharni | 118.1 | 115.8 | 114.8 | 123.3 |
| | Morshi | 114.6 | 109.5 | 118.1 | 116.9 |
| | Warud | 137.7 | 116.2 | 160.0 | 119.8 |
| Washim | Washim | 118.6 | 112.1 | 118.5 | 125.1 |
| | Mangrulpir | 124.4 | 123.9 | 123.5 | 126.7 |
| Yeotmal | Yeotmal | 114.7 | 111.9 | 109.8 | 122.8 |
| | Darwha | 115.8 | 107.4 | 123.2 | 117.1 |
| | Digras | 119.2 | 116.6 | 116.2 | 124.9 |
| | Pusad | 117.6 | 116.2 | 112.0 | 124.4 |
| | Umarkhed | 127.2 | 132.9 | 121.0 | 119.9 |
| | Wani | 117.7 | 119.3 | 124.1 | 103.8 |

successively for two or more years in all the districts and such sequences occurred during 1979–1981, 1983–1986, 1991–1992, 1994–1996 and 2002–2004 in some of the districts. The Fig. 15.2 indicates the tendency of occurrence of high intensity drought years successively for two or more years at all the district places which is a very serious climatic feature of the region. The same figure indicates that agricultural droughts also occur in high rainfall years indicating erratic distribution of rainfall during those years.

The different intensity droughts at different district stations as schematically presented in Fig. 15.2, indicates that varying intensity agricultural droughts occurred in the same year at all the stations during 1980, 1985, 1991, 1992, 1996 and 2002. However severe to large intensity agricultural droughts occurred at maximum stations during 1980, 1984, 1986, 1991, 1996, 2002 and 2004.

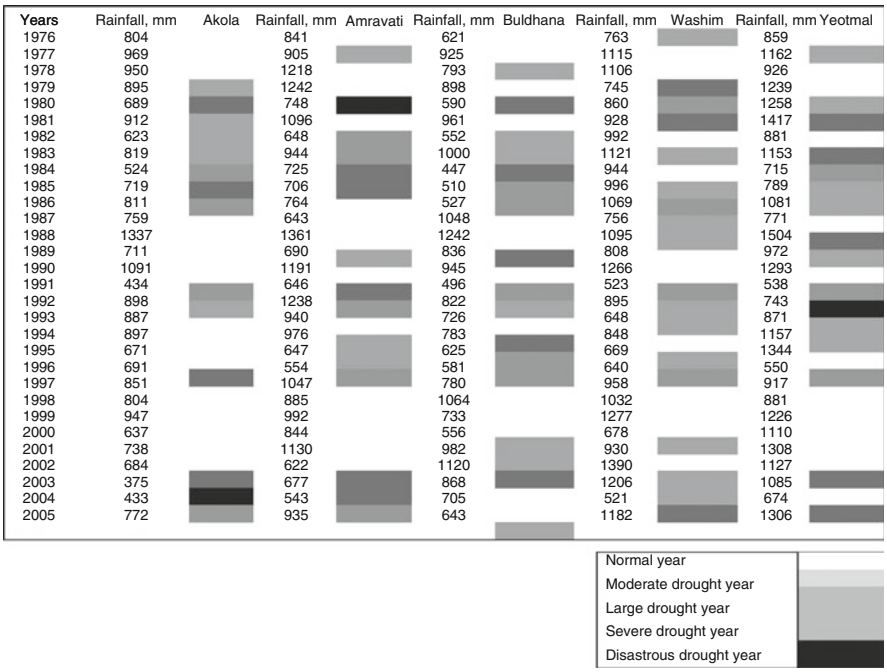


**Fig. 15.2** Schematic presentation of different intensity drought years at different districts in western Vidarbha

**Table 15.7** Percent reduction in dryland crop yields during wide spread droughts years over normal years in drought affected districts of Amravati division

| Districts | Green gram | Soybean | Sorghum | Cotton | Pigeon pea | Gram |
|---|---|---|---|---|---|---|
| Buldhana | 72.1 | 27.9 | 56.1 | 20.3 | −3.2 | 32.9 |
| Akola | 83.3 | 18.1 | 37.1 | 20.2 | 42.7 | 41.4 |
| Amravati | 87.7 | 49.6 | 60.9 | −1.4 | 6.4 | 3.2 |
| Washim | 22.9 | 16.8 | 52.3 | 24.0 | 15.2 | 7.9 |
| Yeotmal | 29.4 | 82.3 | 23.1 | −1.6 | 10.3 | −0.8 |
| Average | 53.6 | 37.3 | 45.2 | 11.9 | 13.8 | 15.9 |

Among above stated drought years at the selected stations in western Vidarbha, it is observed that intensity of drought during 1980, 1986, 1991, 1996 and 2004 was of higher severity for maximum stations.

The taluka wise yields of different crops for various talukas as reported by State Agriculture Department were used for verifying the results obtained from the study. A considerable reduction in the average yield of different dryland crops was observed during the widespread drought year's viz., 1984, 1986, 1991, 2002 and 2004 over normal years viz., 1987, 1990, 1997, 1998 and 1999 in the selected talukas of different drought affected districts. Percent reduction in the yield of green gram (mung), soybean, sorghum (kharif jowar), cotton, pigeon pea and gram in different talukas of various drought affected districts is presented in Table 15.7.

The data reveal that there is considerable reduction in the yield of green gram (53.6%). sorghum (45.2%) and soybean (37.3%) followed by gram (15.9%), pigeon pea (13.8%) and cotton (11.9%).

## 15.4 Conclusions

Decadal variation study showed reduction in seasonal rainfall in general in the current decade (1996–2005) in all the districts. Similarly decadal behavior of monthly rainfall for July showed reduction in the current decade in most of the districts except for Washim and Yeotmal districts. August showed reduction in rainfall in the current decade in all the districts. September showed an increase in rainfall in the current decade over earlier in all the districts. Weekly rainfall pattern in different talukas of different drought affected districts clearly shows highly erratic distribution in the current decade over remaining two decades.

The decadal variation of seasonal, monthly and weekly rainfall on district and taluka level clearly indicates a remarkable change in rainfall pattern of drought affected region during the current decade (1996–2005) over earlier two decades resulting to reduction in agricultural productivity and uncertainty in dryland agricultural production. This change in rainfall pattern of the studied area during current decade may indicate the effect of climate change.

Agricultural drought characterization study of 30 years period (1976–2005) in five drought affected districts indicated a very high tendency of occurrence of drought successively for two or more years in all the districts inspite of quite high rainfall received in the region Considerable reduction in the productivity of different dryland kharif crops during widespread drought years (1984, 1986, 1991, 2002 and 2004) over normal years (1987, 1990, 1997, 1998 and 1999) was observed in the selected talukas (29) of different drought affected districts of Amravati division. Hence for sustainable agricultural production under the impact of climate change in drought affected districts of Vidarbha, adoption of effective rainwater conservation and management systems suitable to geomorphology of the region is necessary.

## References

Allen RG, Pireira JS, Dacs D, Smith M (1998) Crop evapotranspiration, guideline for computing crop water requirements. FAO Irrigation and Drainage, pp 56

Balogun C (1972) The variability of rainfall in Nigeria. Niger J Sci 6:89

Deka RL, Nath KK (2000) Rainfall analysis for rainfall crop planning in the upper Brahmaputra valley zone of Assam. J Agrometeorol 2(1):47–53

Satpute GU, Singh RV (2006) Evaluation of agricultural drought in western Vidarbha. Proceedings of 40th annual convention and symposium of indian society of agricultural engineers, held at TNAU, Coimbatore, 19–24 Jan 2006, pp 4–6

Subramanyam VP, Sastri CRS (1969) Water balance study at Vishakapatnam. Annu Arid Zone Res 18(1 & 2):89–97

Thornthwaite WC, Mather JR (1955) The water balance budget and its use in irrigation. In: Stefferud A (ed) Water-yearbook of agriculture. Department of Agriculture, Washington, DC, pp 346–358

Vairavan K, Singh RD, Kananm K, Goheche C (2002) Sustainable agricultural planning with agro-meteorology observation. Madras Agric J 89(1–3):151–154

# Chapter 16
# Simulation of Growth and Yield Attributes of Wheat Genotypes Under Changing Climate in Recent Years in India

**S.D. Attri, K.K. Singh, and R.K. Mall**

**Abstract** Climate change is one of the most important global environmental challenges, with implications for food production and sustainability at global and national level. Therefore, question arises, how can productivity be increased while ensuring the sustainability of agriculture and the environment for future generations? Decision makers need information supplied by research to make informed choices about new agricultural technologies and to devise and implement policies to enhance food production and sustainability. Simulation experiments were conducted to evaluate growth and yield attributes of wheat genotypes under timely and late sown conditions in diverse environments in wheat growing regions of India using Dynamic Crop Growth Model i.e. DSSAT v4.5 Results indicate that the anthesis and maturity period generally varied by 2–14% and 2–10% in different genotypes under study in recent years. Grain number and yield of different cultivars generally varied between 4–27% and 6–26%, respectively.

## 16.1 Introduction

The challenges facing agriculture and assuring global food security and the sustainable management of natural resources are manifold and immensely complex. Agriculture is intimately tied to nature and hence subject to its vagaries. The variations in agricultural production put added stress on developing countries

S.D. Attri (✉) • K.K. Singh
India Meteorological Department, New Delhi 110 003, India
e-mail: sdattri@gmail.com; kksingh2022@gmail.com

R.K. Mall
India Meteorological Department, New Delhi 110 003, India
and
National Institute of Disaster Management, New Delhi, India
e-mail: mall_raj@rediffmail.com

S.D. Attri et al. (eds.), *Challenges and Opportunities in Agrometeorology*,
DOI 10.1007/978-3-642-19360-6_16, 

having their agrobased economy. India in recent years has made considerable progress in the field of agriculture; however, in order to keep pace with the increasing population, the growth in agricultural production should be sustainable in the long run. Uncertainties of weather and climate pose a major threat to food security of the country, which have increased under rapidly changing climate scenarios.

It is important to note that almost every aspect of agriculture from long term planning to tactical decisions in day-to-day agricultural operations is dependent on climate and weather. Thus, there is need for increasing agricultural production in a sustainable manner using state-of-art technology and resources efficiently. Efficient agrometeorological service is the need of the hour to advise the farming community well in advance to take full advantage of benevolent weather and precautions against malevolent weather to minimize losses. India in recent years has made considerable progress in the field of agriculture. However, in order to keep pace with the increasing population, the growth in agricultural production should be sustainable.

India is one of the greatest success stories of Green Revolution, and Wheat (*Triticum aestivum*) is the most important winter cereal of India and is grown during "rabi season" November to mid-April. India is now second largest producer of wheat in the world with production hovering around 70–78 million tons in the past few years and produced a record 78.40 million tons during crop year 2007–2008 (Nagarajan 2005; DES 2008). It accounts for approximately 12% of world's wheat production and is the second largest wheat consumer after China. Wheat production of 6.5 million tons in 1950–1951, was dwarfed by the 78.4 million tons produced in 2007–2008, a more than tenfold increase. This national production increase is reflected in increased yields per hectare that went from around 660 kg/ha in 1950–1951 to 2,785 kg/ha in 2007–2008. Alongside increased yields came an increase in area planted from nearly 9.8 million hectares in 1950 to 24 million hectares in 1990, to about 28 million hectares in 2007–2008 (DES 2008).

Wheat is one of the important staple foods in India and is grown under diverse sets of agro-climatic conditions. In India, it is grown in the region within latitudes 15°–32° N and longitudes 72°–92°E under irrigated conditions. Punjab, Haryana, Uttar Pradesh, Madhya Pradesh, Rajasthan and Bihar are the leading states of India contributing more than 90% of the Wheat for the country. India is now the 2nd largest wheat producer in the world after China. Wheat is sown during November to December and harvested during March to April. The wheat-marketing season in India is assumed to begin from April every year.

Weather variables are one of the key components which influence the wheat production and over which man has very little control. Weather abnormalities like, hailstorm, frost, high wind and extreme temperatures during wheat growing season leads to natural disasters affecting agricultural productivity. It has been observed that per hectare yield of wheat in India has fallen due to the temperature rising steadily in January and February, a time most crucial for the wheat crop during current decade.

During January and February of 2006, temperatures kept rising steadily due to prolonged absence of rain. The average day and night temperatures have been 4–6°C higher than the normal, most striking during February, in wheat sowing region of the country. With the rising temperatures, crop matures early. The response to temperatures varies with the stage of development, mainly booting (late ear development), anthesis (pollination and fertilization) and grain growth (a week after anthesis to maturity). Wheat is a crop, which needs low temperature for the kernel to form during booting stage. Crop encountered increased temperature during booting and anthesis stages, coinciding the end of January and with month of February of current year leading to reduction in grain number due to high temperature during booting. Besides rabi season of 2005–2006, yield estimates is also made for another wheat season, representing near normal weather condition to enable a comparison with the selected season yield and yield attributes.

Mechanistic crop growth models are now routinely used for assessing the impacts of climate change. There are several crop simulation models now available for the same crop that can be employed for impact assessment of climate change (Mall and Aggarwal 2002; Saxana et al. 2006; Mall et al. 2006). Crop weather models, in general, integrate current knowledge from various disciplines including agrometeorology, soil physics, soil chemistry, crop physiology, plant breeding, and agronomy, into a set of mathematical equations to predict growth, development and yield of a crop (Aggarwal and Kalra 1994; Hoogenboom 2000; Pathak et al. 2003; Sivakumar and Motha 2007; Aggarwal and Singh 2010). In India, substantial work has been done in last decade aimed at understanding the nature and magnitude of change in yield of wheat crop due to possible climate change using CERES-wheat and other crop simulation models (Aggarwal and Kalra 1994; Lal et al. 1998; Attri and Rathore 2003; Nain et al. 2004; Timsina and Humphreys 2006a, b; Mall et al. 2006; Pathak and Wassmann 2009).

Attri and Rathore (2003) used CERES-wheat dynamic simulation model and climate change scenarios projected by the middle of the current century, based on the latest studies, and analyses the impacts of concurrent changes of temperature and $CO_2$ on the growth, development and yields of wheat in northwest India. Table 16.4 shows the change in yield of different genotype of wheat under modified climate in rainfed and irrigated conditions. They found increase in wheat yield between 29–37% and 16–28% under rainfed and irrigated conditions especially in different genotypes were observed under a modified climate as shown in table. A 3°C increases in temperature or more shall cancel out the positive effects of $CO_2$.

Several studies have indicated decrease in yield of crops as temperature increases in different parts of India. The studies carried out by Sinha and Swaminathan (1991) and Aggarwal and Kalra (1994), show that on a 2°C increase in mean air temperature, rice yields could decrease by about 0.75 t/ha in the high yield areas and by about 0.06 t/ha in the low yield coastal. A temperature rise by 0.5°C in winter temperature is projected to reduce rain fed wheat yield by 0.45 t/ha in India (Lal et al. 1998). Attri et al. (2001) and Lal et al. (1998) and have reported that dynamic models have capability for reasonably simulating attributes of wheat cultivars.

The evaluation of genotypes is needed for deciding their suitability in particular region under climate change which has become more complex particularly in recent years. In view of above, simulation experiments have been carried out using crop growth simulation model to quantify growth, development, yield and yield attributes in the current decade (2000–2006) for popular wheat cultivars in India using dynamic simulation model viz. DSSAT 4.5. The model was also utilized to quantify the impact during 2005–2006 in relation to normal weather.

## 16.2 Data and Methodology

Agricultural system simulation models are predictive tools for assessing climate change impacts on crop production. Validated crop growth simulation model CERES-Wheat v 3.5 (DST 2006, Attri 2000, Mall and Singh 2000; Aggarwal et al. 2000) has been used to simulate attributes of popular wheat genotypes at wheat growing locations in India during 2000–2006. The details of commonly grown cultivars at different locations used in the study and normal weather year

**Table 16.1** Details of wheat genotypes grown in various parts of India

| Cultivar | Region | Locations | Sowing time | Duration |
|---|---|---|---|---|
| PBW-343 | North India | Jammu, Palampur, Ludhiana Hissar, Delhi, Pantnagar Roorkee | Normal | Medium |
| RAJ-3765 | Rajasthan | Sriganganagar, Jaipur | Normal | Medium |
| HD-2285 | Uttar Pradesh | Kanpur, Faizabad, Allahabad, Pusa, Sabour | Normal | Medium |
| C-306 | East India | Ranchi and Raipur | Normal | Medium |

**Table 16.2** Predominant soil types and near normal weather year considered for different locations

| Zones | Locations | Soil | Soil depth (cm) | Year |
|---|---|---|---|---|
| North India | Jammu | Sandy loam | 70 | 1999–2000 |
| | Palampur | Sandy clay loam | 90 | 1999–2000 |
| | Ludhiana | Sandy loam | 150 | 2001–2002 |
| | Hisar | Sandy loam | 150 | 2000–2002 |
| | Delhi | Sandy loam | 150 | 2001–2002 |
| | Pantnagar | Sandy loam | 105 | 1999–2000 |
| | Roorkee | Sandy loam | 150 | 2002–2003 |
| Rajasthan | Sriganganagar | Sandy loam | 90 | 2002–2003 |
| | Jaipur | Sandy loam | 150 | 2002–2003 |
| Uttar Pradesh | Kanpur | Sandy loam | 150 | 2001–2002 |
| | Faizabad | Sandy loam | 150 | 2000–2001 |
| | Allahabad | Sandy loam | 150 | 2003–2004 |
| East India | Pusa | Sandy loam | 150 | 2002–2003 |
| | Ranchi | Sandy clay loam | 80 | 2002–2003 |
| | Raipur | Vertisol | 120 | 2003–2004 |

selected for different station sand cultivars are presented in Tables 16.1 and 16.2 respectively.

Daily weather data on maximum and minimum temperatures, rainfall and radiation were used for 16 locations for first decade of this century. 15 November and 1 December were considered as sowing dates for the study. The management practices considered for this study are:

- Plant population: 90-plants/$m^2$,
- Row spacing: 20 cm
- Planting depth: 5 cm.
- Wheat cultivation is mostly irrigated in Indo-Gangetic plains.
- Fertilizer is applied as per package and practices of the crop.

Therefore, productivity of a given cultivar is primarily governed by the weather, particularly temperature and radiation.

Water use efficiency and nitrogen use efficiency are the indices generally used to estimate how efficiently the crop has utilized water and nitrogen resources which have been estimated as under:

$$\text{Water use efficiency (WUE, kg cm}^{-1}) = \text{Gy/ET}$$

$$\text{Nitrogen use efficiency (NUE, kg kg}^{-1}) = \text{Gy/N supply}$$

### *16.2.1 Simulation of Growth of Different Genotypes*

Growth, Yield attributes, Evapo-transpiration and N-uptake of different genotypes in major wheat growing i.e. North India, Rajasthan, Uttar Pradesh and East India during 2000–2006 (as per data availability) are depicted in Tables 16.3 and 16.4. The variations in anthesis and maturity period of all genotypes under study were of the order of 2–14% and 2–10% respectively. Grain number and yield of different cultivars generally varied between 4–27% and 6–26% respectively in different years in most of the cases. However, variations were higher in some years which may be due to unfavorable weather. The variations in ET and N - uptake were generally in the range of 4–10% and 2–14% respectively at different location and years.

The variations can mainly be attributed to unfavourable weather (temperature) in addition to water and nutrient stresses at critical stages. The variations in maximum and minimum temperatures computed at fortnight interval at different locations were of the order of −1.4 to +6.6°C and −5.2 to +8.0°C, respectively (Table 16.5). Abnormal temperatures mainly during booting to grain filling stage were associated with lower yield in different cultivars. However, in some cases, impact of other stresses was also observed.

**Table 16.3** Growth and yield attributes of different genotypes in North India

| Delhi | Anthesis date | Maturity date | Grain number | Yield | ET | N-uptake |
|---|---|---|---|---|---|---|
| **Delhi** | | | | | | |
| 2000–2001 | 112 | 155 | 12,563 | 5,671 | 376 | 167 |
| 2001–2002 | 110 | 154 | 12,684 | 2,478 | 366 | 176 |
| 2002–2003 | 114 | 157 | 10,867 | 4,849 | 321 | 158 |
| 2003–2004 | 112 | 155 | 13,186 | 4,701 | 358 | 166 |
| 2004–2005 | 110 | 152 | 12,166 | 5,460 | 332 | 166 |
| 2005–2006 | 111 | 154 | 10,481 | 4,725 | 379 | **173** |
| **Ludhiana** | | | | | | |
| 2000–2001 | 117 | 160 | 14,865 | 5,985 | 434 | 164 |
| 2001–2002 | 114 | 157 | 13,874 | 5,971 | 409 | 172 |
| 2002–2003 | 120 | 163 | 14,126 | 5,808 | 417 | 164 |
| 2003–2004 | 117 | 160 | 14,141 | 4,672 | 405 | 162 |
| 2004–2005 | 116 | 160 | 12,468 | 5,404 | 391 | 168 |
| 2005–2006 | 114 | 157 | 12,788 | 5,672 | 417 | 168 |
| **Palampur** | | | | | | |
| 2000–2001 | 136 | 179 | 13,503 | 5,028 | 372 | 148 |
| 2001–2002 | 124 | 167 | 14,308 | 3,714 | 324 | 153 |
| 2002–2003 | 140 | 183 | 13,707 | 3,456 | 305 | 143 |
| 2003–2004 | 124 | 167 | 9,947 | 1,989 | 324 | 140 |
| 2004–2005 | 121 | 166 | 12,146 | 5,880 | 339 | 145 |
| 2005–2006 | 134 | 177 | 13,946 | 5,382 | 373 | 141 |
| **Jammu** | | | | | | |
| 2000–2001 | 117 | 159 | 11,307 | 2,329 | 361 | 138 |
| 2001–2002 | 114 | 157 | 7,826 | 3,274 | 273 | 128 |
| 2003–2004 | 120 | 163 | 11,640 | 2,351 | 305 | 109 |
| 2004–2005 | 121 | 165 | 9,462 | 4,241 | 335 | 107 |
| 2005–2006 | 116 | 160 | 10,557 | 4,330 | 314 | 116 |
| **Pantnagar** | | | | | | |
| 2002–2003 | 116 | 159 | 14,643 | 5,691 | 351 | 139 |
| 2003–2004 | 113 | 156 | 14,619 | 4,330 | 330 | 150 |
| 2004–2005 | 109 | 153 | 12,478 | 5,580 | 353 | 153 |
| 2005–2006 | 110 | 153 | 12,204 | 5,105 | 359 | 156 |
| **Roorkee** | | | | | | |
| 2002–2003 | 114 | 156 | 13,987 | 6,243 | 385 | 157 |
| 2003–2004 | 110 | 152 | 14,392 | 4,699 | 411 | 147 |
| 2004–2005 | 108 | 151 | 14,698 | 6,802 | 449 | 151 |
| 2005–2006 | 110 | 153 | 13,657 | 4,197 | 357 | 145 |
| **Hisar** | | | | | | |
| 2000–2001 | 121 | 165 | 15,545 | 5,143 | 369 | 156 |
| 2001–2002 | 117 | 160 | 14,867 | 5,407 | 399 | 170 |
| 2002–2003 | 121 | 164 | 14,276 | 5,018 | 393 | 166 |
| 2003–2004 | 120 | 163 | 14,204 | 3,585 | 360 | 163 |
| 2004–2005 | 116 | 159 | 13,549 | 5,572 | 395 | 167 |
| 2005–2006 | 115 | 159 | 12,907 | 5,452 | 406 | 169 |

**Table 16.4** Growth and yield attributes of different genotypes in (a) Rajasthan (b) Uttar Pradesh and (c) East India

| Delhi | Anthesis date | Maturity date | Grain number | Yield | ET | N-uptake |
|---|---|---|---|---|---|---|
| **(a) Rajasthan** | | | | | | |
| Jaipur | | | | | | |
| 2002–2003 | 93 | 137 | 13,233 | 6,503 | 345 | 148 |
| 2003–2004 | 94 | 138 | 14,307 | 4,346 | 314 | 145 |
| 2004–2005 | 92 | 137 | 13,314 | 5,737 | 307 | 147 |
| 2005–2006 | 93 | 136 | 10,978 | 4,237 | 296 | 148 |
| **(b) Uttar Pradesh** | | | | | | |
| Kanpur | | | | | | |
| 2000–2001 | 97 | 141 | 22,973 | 6,546 | 367 | 182 |
| 2001–2002 | 102 | 147 | 18,890 | 6,133 | 349 | 184 |
| 2002–2003 | 102 | 147 | 17,488 | 6,395 | 345 | 173 |
| 2003–2004 | 97 | 140 | 24,109 | 6,902 | 374 | 177 |
| 2004–2005 | 90 | 134 | 15,974 | 6,822 | 317 | 159 |
| 2005–2006 | 93 | 137 | 17,022 | 6,679 | 351 | 184 |
| Allahabad | | | | | | |
| 2002–2003 | 94 | 138 | 14,367 | 5,925 | 297 | 191 |
| 2003–2004 | 93 | 137 | 7,487 | 5,763 | 306 | 165 |
| 2004–2005 | 90 | 134 | 12,707 | 5,172 | 281 | 145 |
| 2005–2006 | 91 | 134 | 16,867 | 5,810 | 358 | 182 |
| Faizabad | | | | | | |
| 2001–2002 | 93 | 137 | 17,304 | 6,682 | 326 | 154 |
| 2002–2003 | 91 | 136 | 15,489 | 6,744 | 308 | 148 |
| 2003–2004 | 96 | 141 | 19,073 | 6,135 | 324 | 148 |
| 2004–2005 | 93 | 137 | 16,368 | 6,408 | 221 | 154 |
| **(c) East India** | | | | | | |
| Raipur | | | | | | |
| 2000–2001 | 98 | 140 | 12,828 | 3,930 | 349 | 153 |
| 2001–2002 | 98 | 140 | 15,877 | 3,945 | 340 | 156 |
| 2002–2003 | 96 | 138 | 14,786 | 5,007 | 356 | 156 |
| 2003–2004 | 98 | 140 | 19,029 | 5,247 | 397 | 154 |
| 2004–2005 | 97 | 139 | 16,619 | 5,546 | 387 | 157 |
| 2005–2006 | 98 | 140 | 11,639 | 4,675 | 357 | 157 |
| Pusa | | | | | | |
| 2002–2003 | 93 | 137 | 15,506 | 6,749 | 313 | 161 |
| 2003–2004 | 91 | 135 | 16,646 | 6,216 | 309 | 164 |
| 2004–2005 | 88 | 132 | 14,947 | 6,547 | 320 | 156 |
| 2005–2006 | 91 | 135 | 16,006 | 5,442 | 311 | 168 |
| Ranchi | | | | | | |
| 2001–2002 | 108 | 151 | 20,660 | 4,870 | 354 | 148 |
| 2002–2003 | 109 | 152 | 20,427 | 5,945 | 394 | 147 |
| 2003–2004 | 110 | 152 | 12,790 | 2,558 | 310 | 146 |
| 2004–2005 | 106 | 148 | 18,308 | 4,972 | 345 | 150 |
| 2005–2006 | 108 | 150 | 13,165 | 3,426 | 338 | 138 |

**Table 16.5** Variation of (a) maximum and (b) minimum temperatures during crop growing period in various parts of India

| | 1–15 Jan | 16–31 Jan | 1–15 Feb | 16–28 Feb |
|---|---|---|---|---|
| (a) Maximum temperatures | | | | |
| Hisar | −0.9 | 1.1 | 5.0 | 3.9 |
| Sriganganagar | 0.1 | 1.1 | 6.0 | 6.4 |
| Delhi | −0.4 | 2.2 | 5.7 | 5.5 |
| Faizabad | −0.3 | 2.3 | 1.1 | 4.2 |
| Kanpur | 0.3 | 1.8 | 3.1 | 4.1 |
| Pantanagar | −1.4 | 0.5 | 2.5 | 3.5 |
| Pusa | 0.9 | 1.8 | 5.0 | 6.6 |
| Sabour | −1.2 | −0.8 | 2.6 | 2.8 |
| Ranchi | 1.5 | 1.7 | 3.2 | 4.5 |
| (b) Minimum temperatures | | | | |
| Hisar | −3.2 | −0.2 | 0.6 | 3.0 |
| Sriganganagar | 2.6 | 4.6 | 7.4 | 7.8 |
| Delhi | −1.5 | 1.4 | 2.5 | 4.5 |
| Faizabad | −5.2 | −3.0 | −1.5 | 0.6 |
| Kanpur | 0.0 | 1.8 | 1.9 | 5.2 |
| Pantanagar | 1.2 | 0.8 | 3.3 | 4.9 |
| Pusa | 3.2 | 2.7 | 4.0 | 8.0 |
| Sabour | −0.5 | 1.4 | 2.2 | 5.6 |
| Ranchi | −2.9 | −0.2 | −1.5 | 0.9 |

### *16.2.2 Growth and Yield Attributes of Timely Sown Crop*

The simulated grain yield, grain number and maturity period for the different locations sown on 15 November and 1 December in 2005–2006 and normal weather year are given in Figs. 16.1–16.4.

Wheat crop matures slightly earlier in 2005–2006 season compared to the normal weather year, due to above normal day and night temperature during January and February 2006 (Figs. 16.1a and 16.2a). The magnitude of reduction in maturity period is 3 days in north, 10 days in Rajasthan, 3 days in U.P and 2 days in east India. Figures 16.1c and 16.2c show significant reduction in grain number at all the locations ranging from 9% to 20%, as this growth parameter is sensitive to temperature stress during February month, coinciding with late ear development stage. As a combined effect, depicts decrease in grain yield by 16% in north India, 14% in Rajasthan, 7% in Uttar Pradesh and 8% in east India respectively (Figs. 16.1b and 16.2b).

### *16.2.3 Growth and Yield Attributes of Late Sown Crop*

The reduction in maturity period was observed of the order of 2 days in north, 4 days in Rajasthan, 2 days in U.P and 3 days in east India (Figs. 16.3a and 16.4a).

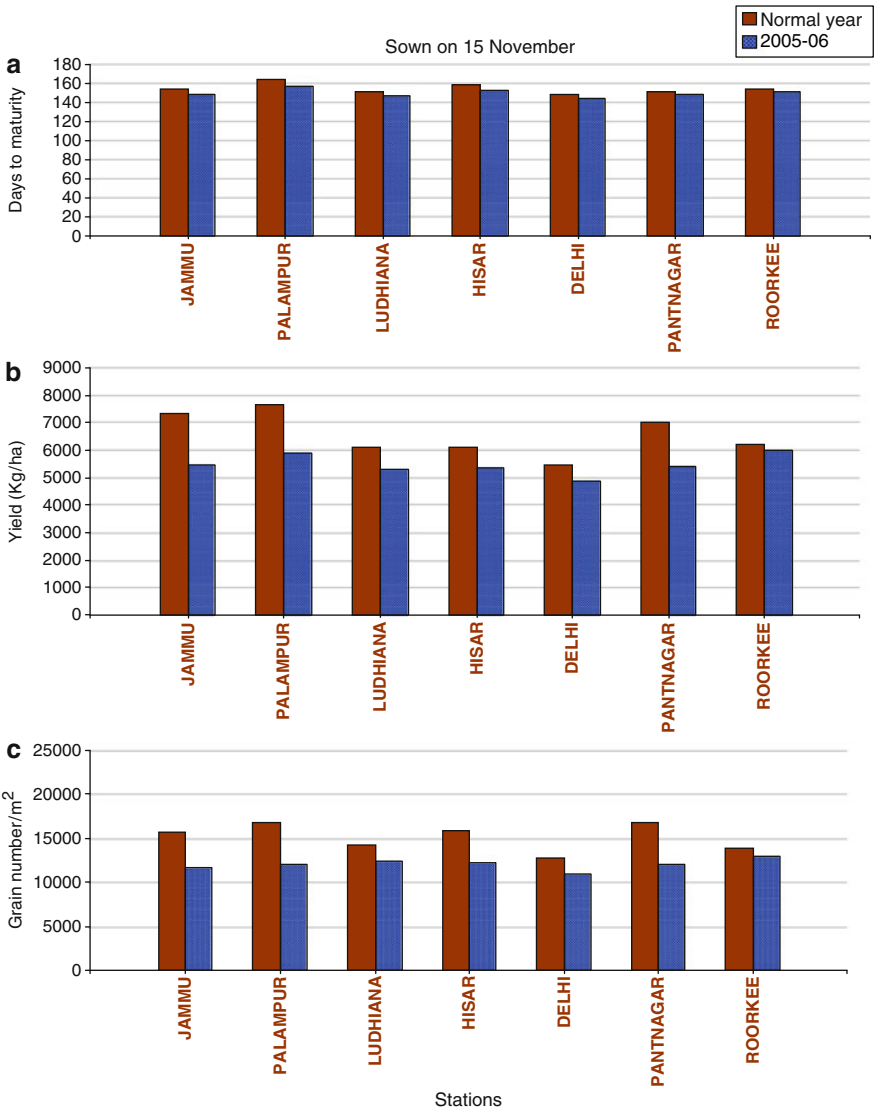


**Fig. 16.1** Variation of growth and grain attributes for 2005–2006 and normal year for timely sown crop in North India

However, reduction in grain number was significant ranging from 12% to 22% at all the locations (Figs. 16.3c and 16.4c). Grain yield simulated for 2005–2006 season compared with that of normal year, as shown in figs. 16.3b and 16.4b, clearly indicates the decrease by 9% in north India, 7% in Rajasthan, 10% in Uttar Pradesh and 5% in East India, respectively.

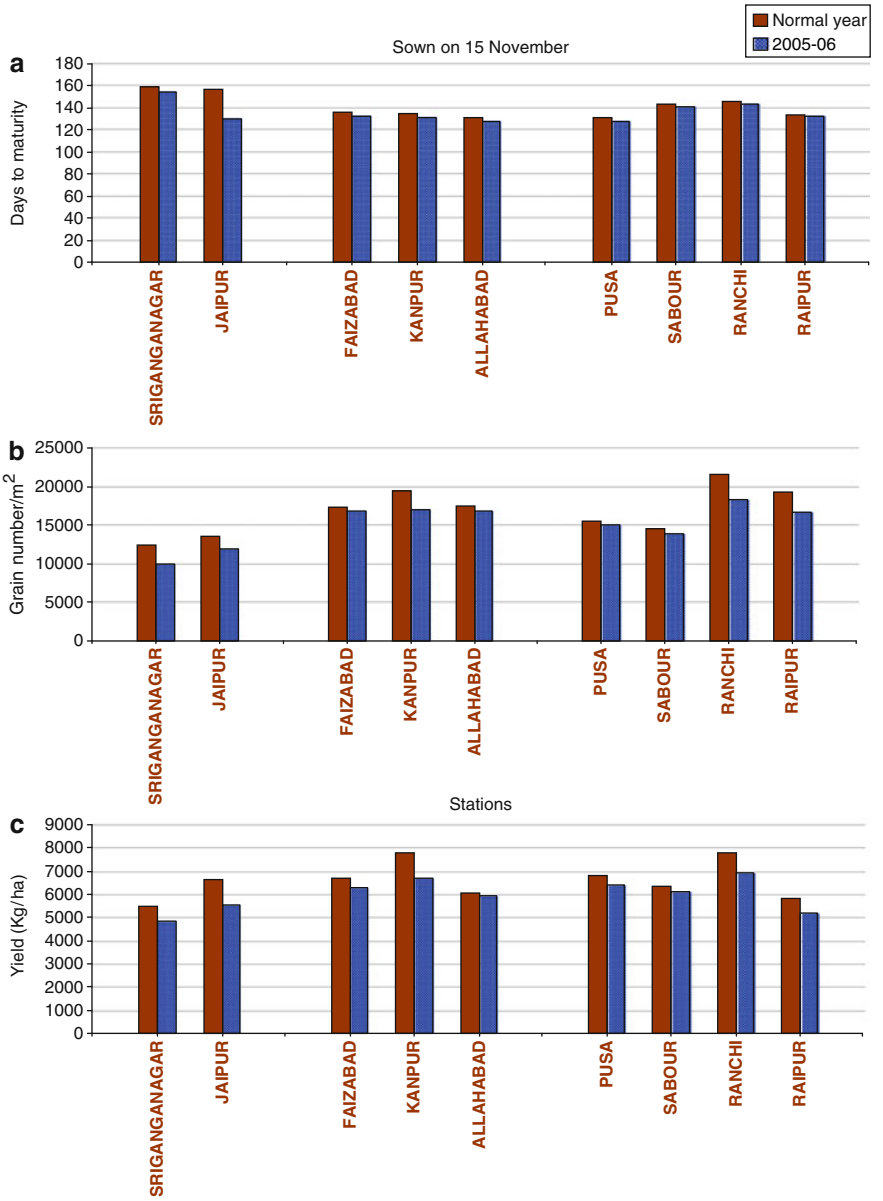


**Fig. 16.2** Variation of growth and grain attributes for 2005–2006 and normal year for normal sown crop in Rajasthan, Uttar Pradesh and East India

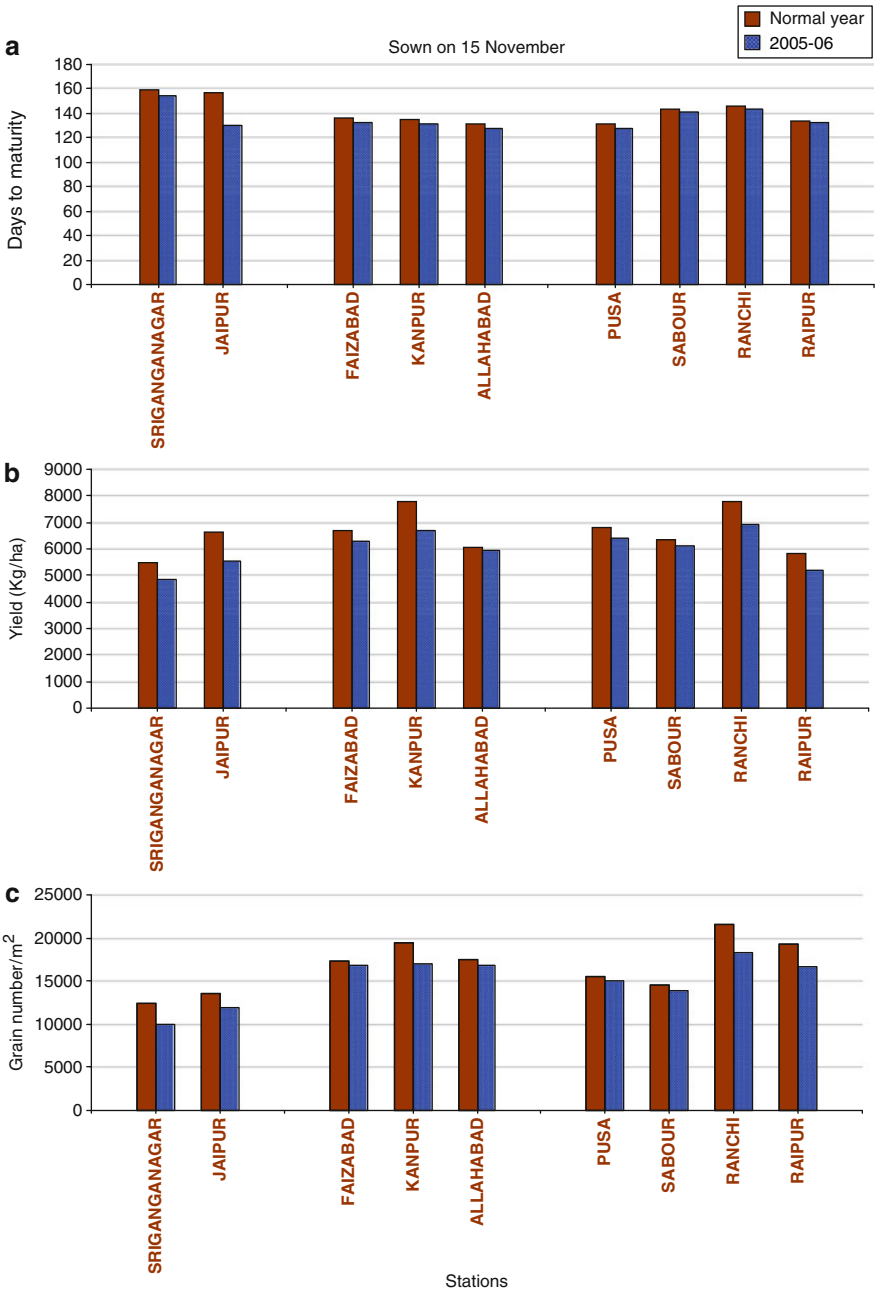


**Fig. 16.3** Variation of growth and grain attributes for 2005–2006 and normal year for late sown crop in North India

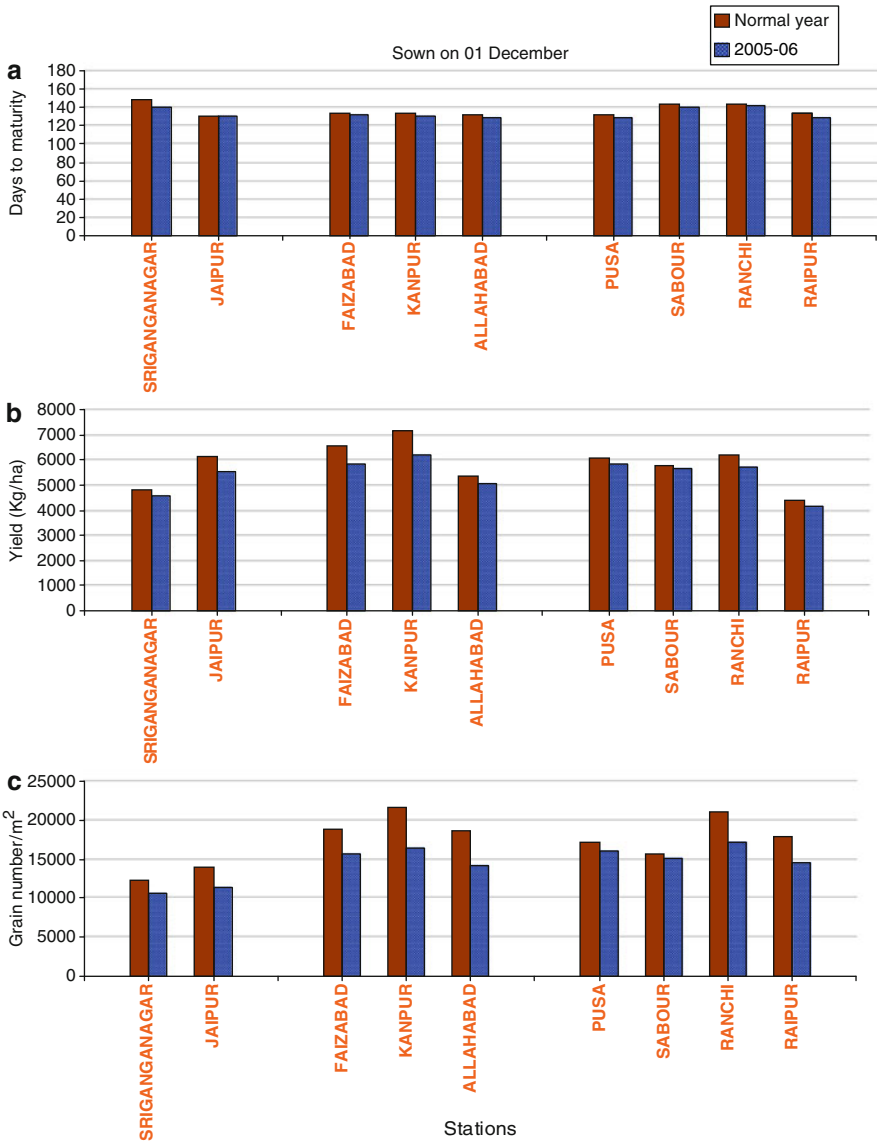


**Fig. 16.4** Variation of growth and grain attributes for 2005–2006 and normal year for late sown crop in Rajasthan, Uttar Pradesh and East India

## *16.2.4 Water and Nitrogen Use Indices*

Increasing production of wheat can result from efficient irrigation and nutrient management. Simulated water use efficiency (kg $cm^{-1}$) of different cultivars varied from 6 to 19 with average of about 14 in different years. However it was higher on

a few occasions. Mahmood and Ahmad (2005) have estimated WUE of the order of 8–17 at different level of soil moisture in wheat. Similar results have also been reported by Mandal et al. (2005).

NUE (kg $kg^{-1}$) generally varied from 14 to 42 with average of 32 in different years in genotypes under study. NUE of the order of 33 has been observed by Raun and Johnson (1999). Similar results have also been reported by Rahimizadeh et al. (2010) and Khichar et al. (2008).

## 16.3 Conclusion

1. Model simulation indicates that crop matures earlier by 2–4 days in different zone for both the sowing dates except crop sown on 15 November in Rajasthan where maturity occurs 10 days earlier.
2. Number of grains/$m^2$ are reduced in all 4 zones ranging from 9% to 22% due to above normal temperature during end of January and February month of current season.
3. Grain yield per hectare simulated for the crop sown on 15 November shows significant reduction by 22% in North India and Rajasthan while by 8% in U.P . and east India.
4. In case of crop sown on 1 December, model predicts reduction in grain yield per hectare by 7–10% in northwest India while it is only 5% in east India.
5. Anthesis and maturity period generally varied between 2–14% and 2–10% in different genotypes under study in recent years. However, grain number and yield of different cultivars generally varied between 4–27% and 6–26%, respectively.

## References

Aggarwal PK, Kalra N (1994) Simulating the effects of climatic factors, genotype and management on production of wheat in India. IARI, New Delhi

Aggarwal PK, Singh AK (2010) Implications of global climate change on water and food security. In: Ringler C et al (eds) Global change: impacts on water and food security. Springer, Heidelberg, pp 49–63. doi:DOI: 10.1007/978-3-642-04615-5_3

Aggarwal PK, Talukdar KK, Mall RK (2000) Potential yields of rice–wheat system in the Indo-gangetic plains of India. In: Rice wheat consortium paper series 10. RWCIGP, CIMMYT, New Delhi, p 16

Attri SD (2000) Weather based crop management using dynamic simulation model, Ph. D Thesis, GJ University of Science and Technology, Hisar (Haryana), India

Attri SD, Rathore LS (2003) Simulation of impact of projected climate change on wheat in India. Int J Clim 23:693–705

Attri SD, Singh KK, Kaushik A, Rathore LS, Mendiratta N, Lal B (2001) Evaluation of dynamic simulation model for wheat genotypes under diverse environments in India. Mausam 52 (3):561–66

DES (2008) Agricultural statistics at a glance. Directorate of Economics and Statistics, Ministry of Agriculture, Government of India, New Delhi

DST (2006) Report on wheat yield prediction using CERES-Wheat model for the season 2005–06 (K K Singh, A K Baxla, L S Rathore, Sunil and P K Singh)

Hoogenboom G (2000) Contribution of agrometeorology to the simulation of crop production and its applications. Agric Forest Meteorol 103:137–157

Khichar ML, Behal RK (2008) Impact of agrometeorological variables on nitrogen uptake and crude protein content of wheat under different planting and sowing environments. TROPICS 17(2):185–191

Lal M, Singh KK, Rathore LS, Srinivasan G, Suseendran SA (1998) Vulnerability of rice and wheat yields in NW India to future changes in climate. Agric Forest Meteorol 89:101–114

Mahmood N, Ahmad RN (2005) Determination of water requirements and response of wheat to irrigation at different soil moisture depletion levels. Int J Agric Biol. doi:1560–8530/2005/07–5–812–815

Mall RK, Aggarwal PK (2002) Climate change and rice yields in diverse agro-environments of India. I. Evaluation of impact assessment models. Clim Change 52(3):315–331

Mall RK, Singh KK (2000) Climate variability and wheat yield progress in Punjab using the CERES-wheat and WTGROWS models. Yayu Mandal 30(3–4):35–41

Mall RK, Singh R, Gupta A, Srinivasan G, Rathore LS (2006) Impact of climate change on Indian agriculture: a review. Clim Change 78:445–478

Mandal KG, Hati KM, Misra AK, Bandyopadhyay KK, Mohanty M (2005) Irrigation and nutrient effects on growth and water–yield relationship of wheat (Triticum aestivum L.) in central India. J Agron Crop Sci 191((6):416–425

Nagarajan S (2005) Can India produce enough wheat even by 2010? Curr Sci 89(9):1467–1471

Nain AS, Dadhwal VK, Singh TP (2004) Use of CERES-Wheat model for wheat yield forecast in central Indo-Gangetic plains of India. J Agric Sci (camb) 142:59–70

Pathak H, Wassmann R (2009) Quantitative evaluation of climatic variability and risks for wheat yield in India. Clim Change 93:157–175

Pathak H, Ladha JK, Aggarwal PK, Peng S, Das S, Singh Y, Singh B, Kamra SK, Mishra B, Sastri ASRAS, Aggarwal HP, Das K, Gupta RK (2003) Climatic potential and on-farm yield, trends of rice and wheat in the Indo-Gangetic plains. Field Crops Res 80(3):223–234

Rahimizadeh M, Kashani A, Zare-Feizabadi A, Koocheki A, Nassiri-Mahallati M (2010) Nitrogen use efficiency of wheat as affected by preceding crop, application rate of nitrogen and crop residues. AJCS 4(5):363–368

Raun WR, Johnson GV (1999) Improving nitrogen use efficiency for cereal production. Agron J 91:357–363

Saxana R, Bharadwaj V, Kalra N (2006) Simulation of wheat yield using WTGROWS in northern India. J Agrometeorol 8(1):87–90

Sinha SK, Swaminathan MS (1991) Deforestation, climate change and sustainable nutrition security: a case study of India. Clim Change 19:201–209

Sivakumar MVK, Motha RP (2007) Managing weather and climate risks in agriculture: summary and recommendations. In: Sivakumar MVK, Motha RP (eds) Managing weather and climate risks in agriculture. Springer, Berlin, pp 477–491

Timsina J, Humphreys E (2006a) Performance of CERES-rice and CERES-wheat models in rice-wheat systems: a review. Agric Syst 90:5–31

Timsina J, Humphreys E (2006b) Application of CERES-rice and CERES-wheat models in research, policy and climate change studies in Asia: a review. Int J Agric Res 1(3):202–225

# Chapter 17
# Strategies for Minimizing Crop Loss due to Pest and Disease Incidences by Adoption of Weather-Based Plant Protection Techniques

**N. Chattopadhyay, R.P. Samui, and L.S. Rathore**

**Abstract** Every year crops are being damaged by pests and diseases. Due to lack of proper operational forecasting system for the incidences of pests and diseases, it becomes difficult to adopt plant protection measures at right time. It has been established with fair degree of accuracy that climate/weather play major role in the incidences of pests and diseases. Thus there is great scope of utilizing meteorological parameters for the advance information of the occurrences of pests and diseases and ultimately scheduling of prophylactic measures can be taken scientifically and judiciously. Quite a number of studies on the relation between meteorological parameters and pest and disease incidences have already been made in India. In the present paper a comprehensive discussion has been made on the strategies, starting from development of weather based pests and diseases models to dissemination of the advance information to the farmers through different state of art information technology, are being taken to control and minimize of the loss of crops due to pests and diseases incidences.

## 17.1 Introduction

Though a substantial achievement in increasing the area of production and productivity of major crops have already been made in India, the periodical unabated explosions of pests and diseases in different regions of the country have made agriculture less remunerative and highly risk prone in the past one and half decades. An erratic monsoon and unfavourable weather conditions are attributed to unusually

N. Chattopadhyay (✉) • R.P. Samui
Agricultural Meteorology Division, India Meteorological Department, Pune, India
e-mail: n.chattopadhyay@imd.gov.in; rsamui@yahoo.com

L.S. Rathore
India Meteorological Department, Ministry of Earth Sciences, New Delhi 110 003, India
e-mail: lrathore@gmail.com

S.D. Attri et al. (eds.), *Challenges and Opportunities in Agrometeorology*,
DOI 10.1007/978-3-642-19360-6_17, 

high rate of pestilence on crops. Expert assessment reveals that around 22% of yield losses in major crops in the country can be attributed to insect pests. The current annual loss due to insects, pests and diseases in the agricultural sector in India is around Rs 15,000 crores. India consumes nearly Rs. 3,150 crore worth of pesticides annually in agriculture. Due to lack of knowledge of exact time of occurrence of these living entities, usually noxious chemicals are applied indiscriminately to control them. With increase in pest problems and resultant indiscriminate use of pesticides not only causes economic restrain on the farmers but also produce harmful side effect in the ground water and natural enemies present in the soil and environment and ecological imbalance. Among the various methods used to prevent the losses of crop due to pest and diseases, the weather based forewarning for operational crop protection is gaining importance.

There has been a long history of attempts to forecast the incidence of the disease and many forecasting schemes have been developed. Prediction of disease appearance does not always help in control but does enable farmers to reduce their losses in other way. For instance, there is no practicable short time control measure available for wheat leaf rust, but forecast issued early in the season allows farmers to plough up there wheat and plans some other crop or pasture their fields if serious out-break is indicated. Thus they can recover at least part of their season investment. Forecasting plant diseases occurrence on the basis of known weather requirements is well established in USA. In this country apple scab spray-warning services have been routine for almost 30 years. Some other diseases for which forecasting is regularly a part of the control programmed in one region or another include bacterial wilt of sweet corn, wheat leaf rust, late blight, tobacco blue mould.

Since last four decades, India Meteorological Department, Indian Council of Agricultural Research (ICAR), State Agricultural Universities and others are endeavoring to find out the interrelationship between meteorological parameters and the incidences of major pest and diseases of crop in the country. The ultimate aim of the study is to forewarn the outbreak of pest and diseases based on the prevailing weather conditions. In the present paper elaborate discussion was made on the on-going and future strategies of controlling pest and disease incidences on crops utilising weather information as well as dissemination of advance information of pest and disease incidences to the farmers using state of information technology.

## 17.2 Data, Methodology and Different Models for Operational Plant Protection

Both historical as well as current data of pest/disease, crop and weather data in the experimental firms are used. Besides model parameters from laboratory experiments are also used. Pest observation by using sex pheromone traps and lures are also used. Central Integrated Pest Management Centres, Directorate of Plant Protection, Quarantine and Storage (PPQ& S), Government of India,

Faridabad in collaboration with State Department of Agriculture and Indian Council of Agriculture monitors pest and disease situations on major crops every month by deputing their staff in the predetermined routes in the country (Figs. 17.1 and 17.2). Based on the survey report received from different parts of the country,

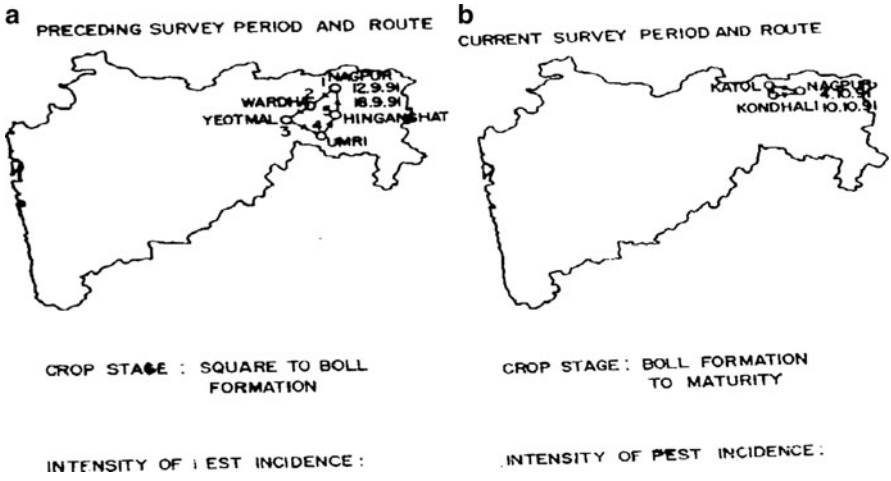


**Fig. 17.1** Pest surveillance data recorded by PPQ&S

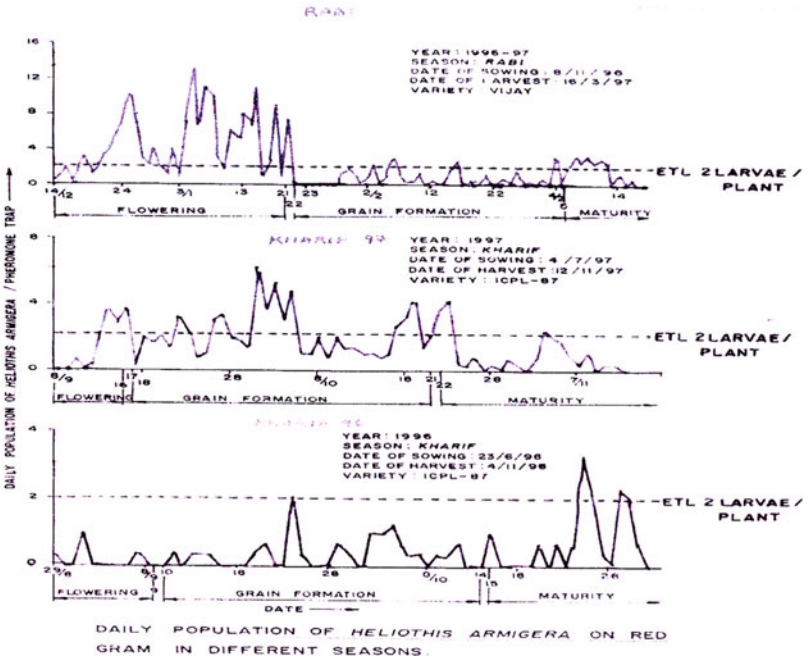


**Fig. 17.2** Daily pest observation at experimental field by pheromone trap

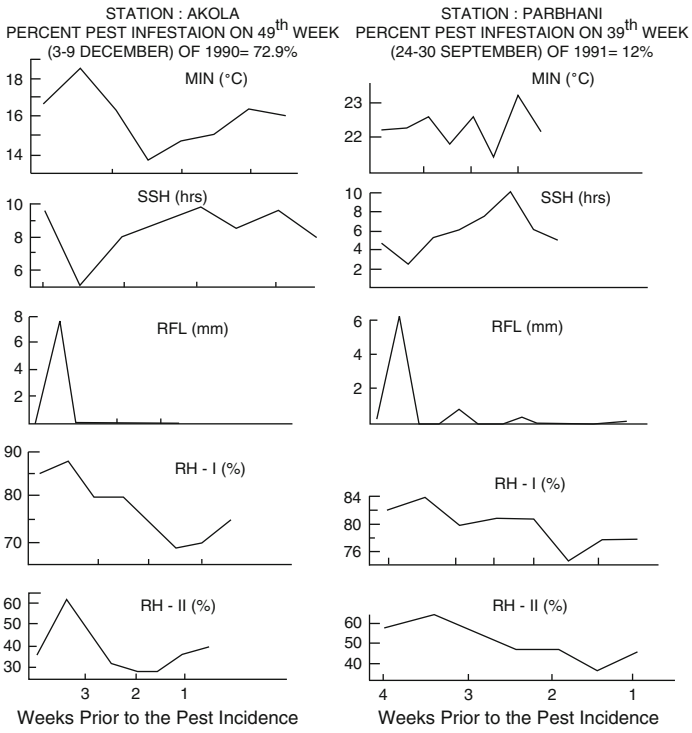


**Fig. 17.3** Variation of different meteorological parameters in the weeks preceding to the incidence of Heliothis

PPQ&S prepares Rapid Roving Survey Reports every month. The qualitative data from this surveillance are also used to develop the relation between weather parameters and pest/disease incidences.

Information on the synoptic situation from weekly weather reports and synoptic charts from different offices of India Meteorological Departments are also used. Usually graphical superimposition techniques as well as statistical analysis are made to understand the relation between the weather parameters and pest/disease incidences (Fig. 17.3). Critical values of the corresponding meteorological parameters favourable for the pest incidences are also worked out. In addition to that, Differential equations, multivariate analysis, population dynamics modeling, simulation modeling, stochastic, simple probabilistic models are also used. In India studies are made on simple prediction rules, crop-pest-weather relationships (correlation and regression), weather based advisories, effect of weather variables on insect development, Life tables, degree-day approach data mining and neural network techniques are being used for to develop pest, disease and weather models and its use in operational plant protection.

## 17.3 Sensitivities of Pest and Disease Incidences to Weather Parameters

Studies on the pests and disease of major corps in India like wheat, rice, sugarcane, jowar, cotton etc. in relation to weather factors have been done using the pest data obtained from 10 to 15 Agricultural Field stations in the country. Useful studies on some of the important pests and diseases like stem borer of rice, spotted bollworm of cotton, rusts of wheat, pyrilla of sugarcane, tikka leaf spot of groundnut, late blight of potato, green ear/ergot of bajra, green jassids and gall midge in rice, aphids, jassids, thrips and boll worms in cotton, gram pod borer, shoot fly, stem borer and mite in sorghum, soybean leaf miner, leaf spot and rust of groundnut, fig rust, fruit canker, Japanese beetle, Colorado potato beetle, stem and stalk borer of sugarcane were also made. From the study of Chattopadhyay and Samui 2003, it is observed that drop in mean temperature ($<28^{\circ}C$) in association of continuous rainfall was congenial weather condition for outbreak of stem borer on rice in Andhra Pradesh, Orissa, Karnataka and Punjab. Dubey and Yadav (1980) studied the effect of weather on the incidences of shootfly on jowar grown at New Delhi, Udaipur, Anantapur and Indore and found that higher maximum temperature (30–34°C) and lower relative humidity (40–75%) are conducive to egg laying and larval activities of the insect causing severe attack. Ravindra et al. (1999) found that minimum temperature about 20°C, morning relative humidity above 60%, clouding during most part of the day and rainfall above 0.5 mm aggravates the multiplication of pink bollworm at Akola in October. Similar studies were made by number of workers (Samui 1993; Suleman and Agashe 1965) in the country The method employed in the study is the statistical technique of finding correlation between the various meteorological factors and the pest or disease infestation and working out multiple linear regression equations expressing the relationship between the dependent variable (pest or disease incidence) and the independent variables (weather factors like rainfall, number of rainy days, humidity, sunshine etc.). Figure 17.4 (Graphical superimposition) and (Synoptic condition) shows that prolong dry condition, decrease in relative humidity (morning $< 80\%$ and evening $< 60\%$) and fall in minimum temperature 23°C below were found congenial for the outbreak of heliothis on cotton. Absence of rain due to withdrawal of southwest monsoon or break monsoon situation along with a fall in minimum temperature due to passage of western disturbances as an upper air system in North India is favourable synoptic situation for the outbreak of heliothis.

## 17.4 Pest Weather Calendar

Pest weather calendar is prepared based on results emerged from the different studies for operational crop protection measure during the peak infestation period. From this calendar, it is possible to assess the infestation of pest based on real time

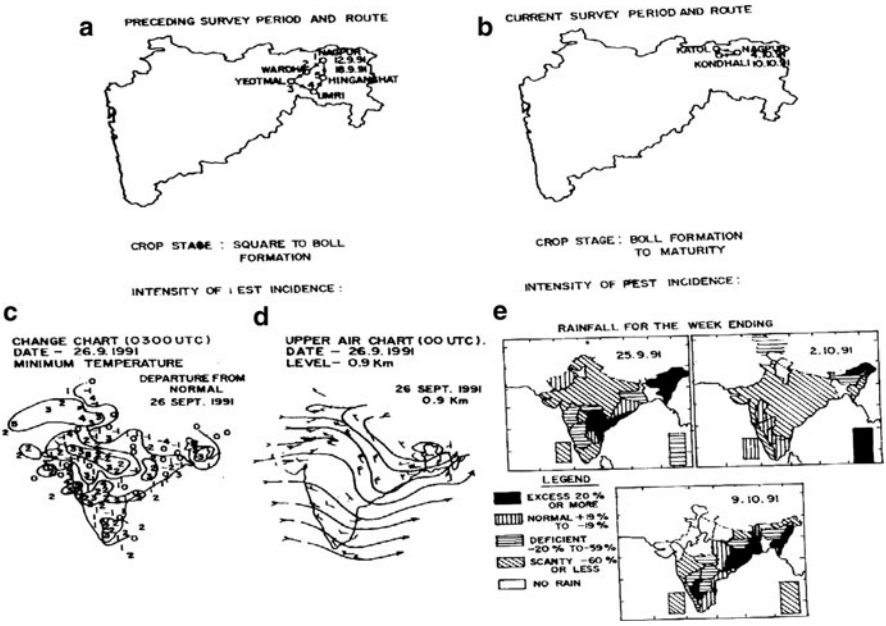


**Fig. 17.4** Weather and Heliothis information prior to the pest incidence

data of meteorological parameters. It is concentric circle where the important epochs of crop growth, corresponding standard weeks, dates and critical values of the meteorological parameters causing the pest infestation are included. This calendar along with the real time information on population density of pest and current weather would help agrometeorologists/agricultural scientists to forewarn the farmers about the possible attack of the pest on the crop.

## 17.5 Operational Plant Protection Through Integrated Agromet Advisory Service in India

India Meteorological Department (IMD), Ministry of Earth Sciences (MoES), is operating an integrated Agro-Meteorological Advisory Service (AAS) at district level, in India, which represents a small step towards agriculture management in rhythm with weather and climate variability leading to weather proofing for farm production. Under AAS, needs of farming community was defined through ascertaining information requirement of diverse groups of end-users. It emerged, that prime need of the farmer is location specific weather forecast in quantitative terms. Thereafter, mechanism was developed to integrated weather forecast and climatic information along with agro-meteorological information to prepare district level agro-advisories outlining the farm management actions to harness favorable

weather and mitigate impacts of adverse weather. IMD has started issuing quantitative district level (612 districts) weather forecast up to 5 days since 1st June, 2008. The products comprise of quantitative forecasts for seven weather parameters viz., rainfall, maximum temperature, minimum temperatures, wind speed, wind direction, relative humidity and cloudiness. In addition, weekly cumulative rainfall forecast is also provided. IMD, New Delhi generates these products using Multi Model Ensemble technique based on forecast products available from number models of India and other countries.

Under the Integrated Agromet Advisory Services launched in IMD a comprehensive strategies has been taken to minimized the crop loss by the pest and diseases by utilising, validating the information already available in IMD, State Agriculture University, ICAR and Regional Agriculture Research Stations etc. The forewarning package will be established by blending statistical, graphical and synoptic approaches. Meteorological parameters recorded at different Observational network like AWS, Agro AWS, different types of Agromet Observatories and Medium range weather forecasting used extensively to forewarn the incidence of pest and diseases at least 4–5 days in advanced. Besides it is planned that Agromet Products in relation to the pesticides application will be developed using GIS technology with the interface of high speed computing system on real time basis for the preparation of crop and location specific advisories for the farmers. Forewarning of pests and diseases by integrating all the above mentioned techniques through Agromet Advisory Services will solve the long standing problem of minimizing the loss of crop through Agromet Advisory Services of IMD.

## 17.6 Dissemination

In addition to different multi-channel dissemination system, agromet advisories under the project Integrated Agromet Advisory Service (IAAS) are being disseminated to the farming community in India through SMS and IVR (Interactive Voice Response Technology). Under the SMS system an information platform has been created which allows the existing Agromet Field Units (AMFUs) located at State Agriculture Universities (SAUs), institutes of Indian Council of Agriculture Research (ICAR), Indian Institute of Technology (IITs) etc. to provide the information in a convenient and timely manner. The advisories are crop and location specific and delivered within actionable time to the farmers. Under IVR system the information from AMFUs for each state are collected and then stored, and converted into voice where the farmer would be calling and receiving the desired information.

A number of private firms namely Reuter Market Light, Pune and Handygo, Delhi and Vritti Solution, Pune IFFCO Kisan Sanchar Limited (IKSL) are disseminating the agromet advisories generated under IAAS through SMS and Interactive Voice. At present 16 states namely Delhi, Uttar Pradesh, Punjab, Haryana, Rajasthan, Madhya Pradesh, Orissa, West Bengal, Gujarat, Karnataka,

Kerala, Tamilnadu, Andhra Pradesh, Bihar, Maharashtra and Himachal Pradesh have been covered under this service. Advisory are also disseminated through SMS to the farming community of Maharashtra in collaboration with the State Department of Agriculture, Government of Maharashtra Besides, there is a plan to disseminate this service through Narrowcasting Centre of Prasar Bharati, FM channel of AIR, Community Radio, Common Service Centre (CSC) of Departmental International Technology (DIT), NABARD, Tata Consultancy Services (TCS), NOKIA etc. The experience gained in the targeted states would be leveraged upon to create a scalable model which can expand across India and utilize the information developed for all the 615 districts of the country targeted to be in place by end of the year 2010. Besides this, there is a plan to disseminate this service through Narrowcasting Centre of Prasar Bharati, FM channel of AIR, Community Radio, and Common Service Centre (CSC) of Departmental International Technology (DIT). The ultimate aim of this initiative is to disseminate advisories in short range, medium range and extended range period for the 600 million farmers of the country on real time basis.

## 17.7 Economic Impact of Operational Plant Protection Through IAAS

In order to judge worthiness and role of the service in farm management its economic impact was assessed through conducting extensive feed back surveys under Agromet Advisory Services. The care was taken to isolate the economic impact of weather based advisories on different crops cultivated by weather-sensitive users. Under the AAS farmers utilized the advisories on stem borer on paddy get benefit of Rs. 10,000/ha. Similarly farmers utilized the advisories for leaf spot on turmeric get benefit of Rs. 25,000/ha.

## 17.8 Conclusion

Control of pests and diseases incidences on crops has become a great challenge to the agricultural community. In spite of modern pest management technique adopted for effective plant protection measures, there are incidences of heavy attack of pest and diseases leading to total crop failure at a particular region of the country. Among the different control measures, pesticides are widely applied to eradicate the pests and diseases of crops. Excessive and indiscriminate use of these noxious chemicals causes economic restrain on the farmers and ultimately imbalances the sustainable agriculture.

Efforts are being made to evolve guidelines for application of pesticides at the right time to minimise the pollution caused by the slow bio-degradation of these

noxious chemicals. Though considerable progress in this regards has already been achieved, more research work is needed to solve the vexed problem. In order to solve the problem, weather based plant protection measure is gaining importance in these days.

Climate and weather have great role to play for timely operational plant protection of pests and diseases. Relationships between weather conditions and pests and diseases incidences for number of crops have already been established accurately by different workers in India and abroad. Research work done by many investigators also suggests the view.

## References

Chattopadhyay N, Samui RP (2003) Weather based forewarning of stem borer (Scirpophaga incertulas) on rice. Mausam 54(3):695–704

Dubey RC, Yadav TS (1980) Shorgum shootfly (Arherigona soccata rondand) relation to temperature and humidity. Indian J Ent 42(2):273–274

Ravindra PS, Samui RP, Chattopadhyay N (1999) Forewarning of pink bollworm outbreak and pest weather calendar for operational crop protection in Vidarbha and Marathwada region of Maharashtra. Tropmet 99:485–490

Samui RP (1993) Forewarning of stemborer attack on sugarcane and pest weather calendar for operational crop protection at Gorakhpur, East Uttar Pradesh. Indian Sugar 43(8):627–639

Suleman M, Agashe NG (1965) In: Reddy PS (ed) Influence of climate on the incidence on tikka disease in groundnut. Publication and Information Division, ICAR, New Delhi

# Chapter 18
# Climate-Based Decision Support Tools for Agriculture

**Mark S. Brooks, Aaron P. Sims, Ashley N. Frazier, Ryan P. Boyles, Ameenulla Syed, and Sethu Raman**

**Abstract** Farmers consider many variables in making agricultural decisions. The farmer must often choose his inputs for the production function before variables such as weather are known. The uncertainties associated with weather can however be mitigated with the use of decision support tools. As the specific relationships of weather, disease development and crop maturity are determined through research, the value of weather-based decision support tools becomes more evident. The State Climate Office of North Carolina (SCO) at North Carolina State University, USA has successfully developed several agricultural decision support systems. These include climate-based decision support tools for peanuts, strawberries, cucurbits, turfgrass and tobacco. All are built in collaboration with agricultural scientists who have expertise in each respective crop. Real-time and historical data from the North Carolina Environment and Climate Observing Network (ECONet) in conjunction with high-resolution numerical models support the availability of the tools.

## 18.1 Introduction

Farmers consider many variables in making crop management decisions. Some are known and others are unknown. Farmers must often plan ahead without the benefit of knowing these variables, including weather. The uncertainties with weather can however be mitigated with the use of decision support tools. The essence of a decision support tool is to convey all available information in such a way that promotes efficiency in the decision making process. Climate-based decision support tools for agriculture help farmers make timely decisions about when to plant,

M.S. Brooks (✉) • A.P. Sims • A.N. Frazier • R.P. Boyles • A. Syed • S. Raman
State Climate Office of North Carolina, NC State University, Box 7236, Raleigh, NC 27695–7236, USA
e-mail: mark_brooks@ncsu.edu; aaron_sims@ncsu.edu; anfrazier@gmail.com; ryan_boyles@ncsu.edu; asyed@ncsu.edu; sethu_raman@ncsu.edu

S.D. Attri et al. (eds.), *Challenges and Opportunities in Agrometeorology*,
DOI 10.1007/978-3-642-19360-6_18, 

protect, and harvest their crop. Such tools combine high resolution climate data with agricultural information. Demonstrable value provides an incentive for growers to consider climate information in management decisions thereby reducing costs, increasing yields, and promoting more efficient use of resources.

The State Climate Office of North Carolina (SCO) at North Carolina State University, USA has been successful in developing decision support tools for crop management. The SCO is a public service center housed at North Carolina State University. It was acknowledged by the American Association of State Climatologists as one of the first officially recognized State Climate Offices. The mission of the SCO is to provide climate related services to state, local and federal agencies, businesses and the citizens of North Carolina. The products and services provided and technologies developed are adaptable to other geographies and climates.

## 18.2 CRONOS/NC ECONet

In cooperation with state agencies, the SCO maintains and operates the NC Environment and Climate Observing Network (ECONet), a network of high-quality environmental monitoring stations. ECONet stations record standard meteorological parameters plus other critical parameters such as solar radiation, soil temperature, soil moisture, and evaporation. To date, there are 36 ECONet stations in North Carolina. Weather data are archived in the Climate Retrieval and Observations Network of the Southeast (CRONOS) database. CRONOS archives data from the ECONet and several other monitoring networks as shown in Fig. 18.1. Data are publicly available through the climate office website. Data from the ECONet and CRONOS support a wide range of value-added applications and decision support tools (Fig. 18.2), including all of the products mentioned herein. The SCO has supported a variety of University and government agency projects with its expertise in environmental data acquisition, visualization, and dissemination.

## 18.3 Environment Modeling

For a grower, it is helpful to anticipate risk over the proceeding days. The anticipation of these risks is prognosticated through several high resolution numerical weather prediction models operated by the SCO, including MM5 and WRF (Grell et al. 1995; Skamarock et al. 2008). Models are centered over the southeast US and are run 4 times a day out 72 h and have varying grid resolutions of 12, 15, and 5 km for MM5 and WRF (Fig. 18.3). To improve forecasts, surface data from CRONOS are assimilated into MM5 at initialization and is part of a developing 3D variational data assimilation scheme for WRF. High resolution sea surface temperature (1.44 km) from AVHRR satellites are also assimilated at run time to help improve

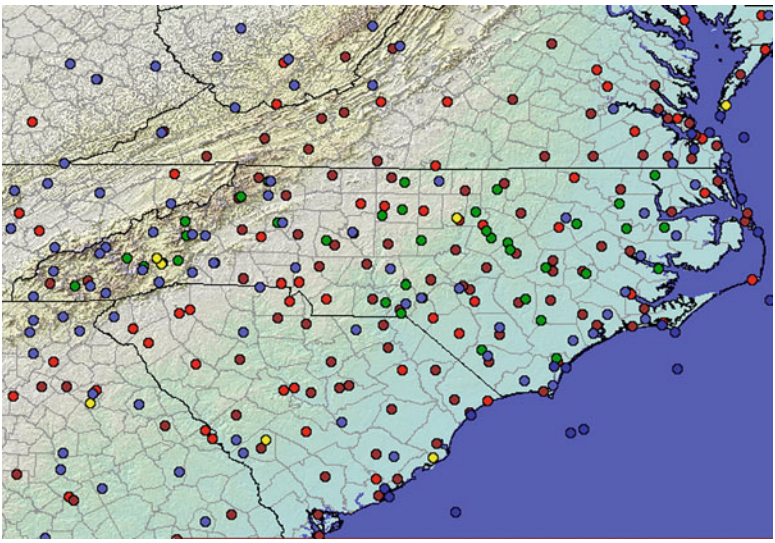

**Fig. 18.1** The locations of hourly weather stations in the NC CRONOS database. Each colored dot represents the location of a weather station that records hourly data. The color of the dot represents the type of network that the station is part of. Stations represented by green dots are NC ECONet stations, operated and maintained by the State Climate Office of North Carolina. Data are available online at http://wwww.nc-climate.ncsu.edu/cronos/

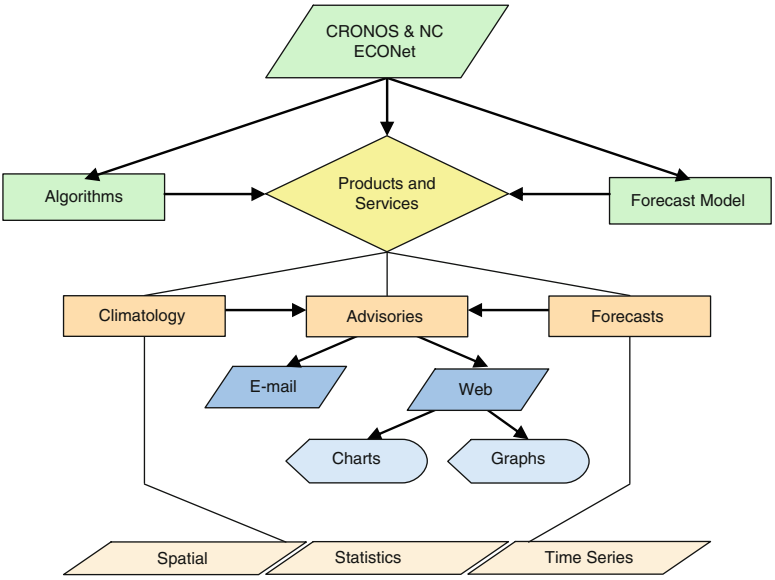


**Fig. 18.2** The State Climate Office of North Carolina's products and services are driven by the needs of clients with sensitivities to weather and climate. Climatology data feed real-time products, such as crop advisories for agriculture

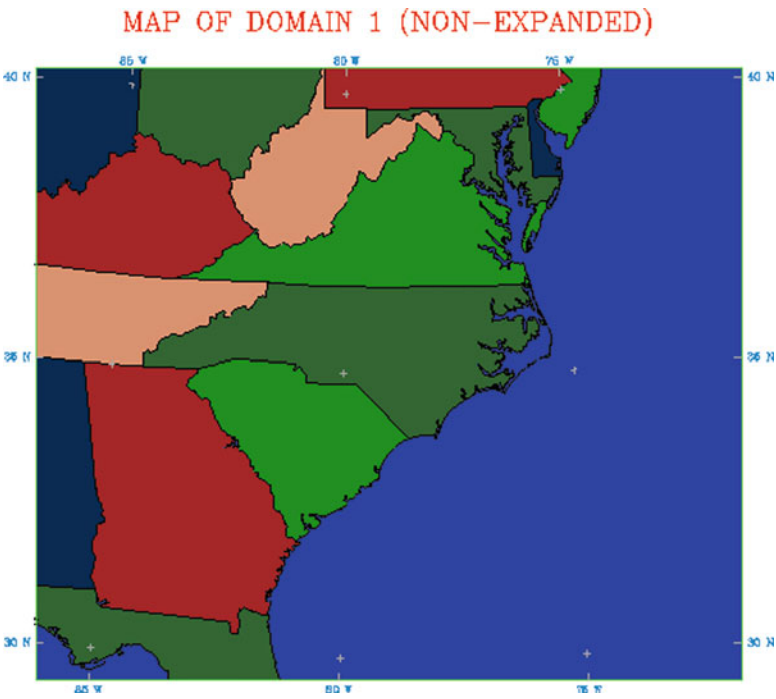


**Fig. 18.3** Extent of MM5 12 km domain centered over North Carolina, USA

initial conditions (Fig. 18.4). These models are used to forecast temperature, humidity, wind speeds and directions, rainfall, and some soil conditions.

Some risks include diseases that are airborne pathogens and are easily transported via wind. In addition to weather forecast models, the SCO is developing dispersion modeling capabilities to support the tracking and transport of pathogens using Flexpart-WRF (Fast and Easter 2006; Doran et al. 2008). This will enable the development of additional decision support tools for crops that are sensitive to airborne pathogens.

## 18.4 Peanut Crop

Leaf spot and Sclerotinia blight are the two most damaging peanut diseases in America. If uncontrolled, peanut leaf spot can cause yield losses of 50% or more in one season. Sclerotinia blight can spread rapidly under a peanut canopy and result in yield losses of up to 80%. The traditional approach is to repeatedly apply fungicides throughout the growing season. This is expensive and may create non-target problems, such as spider mites. Furthermore, water quality can be sustained due to less chemical runoff.

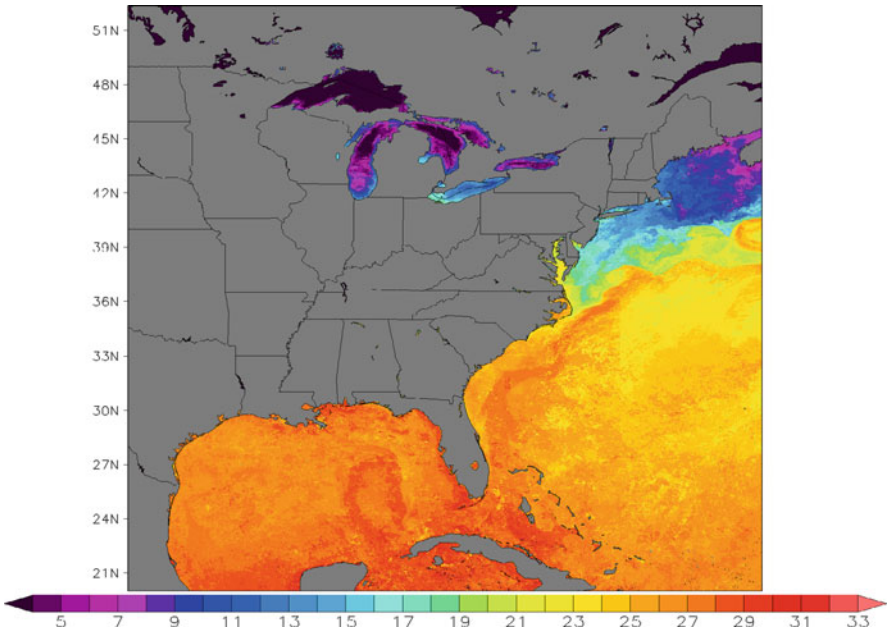


**Fig. 18.4** High resolution Coastwatch AVHRR sea-surface temperature data off the east and southern coast of the US for Jun 3, 2009

Fortunately, the relationship between disease development and weather is well established in literature (Cu and Phipps 1993; Langston, et al. 2002). In 2004, the SCO began working with agricultural scientists to develop a decision support tool for peanut farmers. The SCO developed techniques to automatically calculate the number of favorable disease hours for peanut leaf spot and Sclerotinia blight. The method is based on the concept of a disease triangle (Fig. 18.5). Daily e-mails are distributed during the growing season with estimations for locations throughout North Carolina. The algorithms consider specific environmental conditions such as air temperature, soil temperature, daily precipitation and relative humidity. Based on predetermined thresholds of these parameters, the daily count of favorable disease hours is incremented. Once a sufficient number of favorable hours have accumulated, conditions for disease development exist and an affirmative spray advisory is generated. If conditions do not yet exist for disease development, the advisory contains pertinent details for the grower including growing degree days and other statistics. The SCO also developed a graphical depiction of disease hours as shown in Fig. 18.6.

By helping growers identify the favorable times for disease development and fungicide application, time and money can be saved and crop yields can be increased. In the 2005 growing season, it is estimated that two sprays were saved across the state, which equates to USD $2.2 million in potential savings.

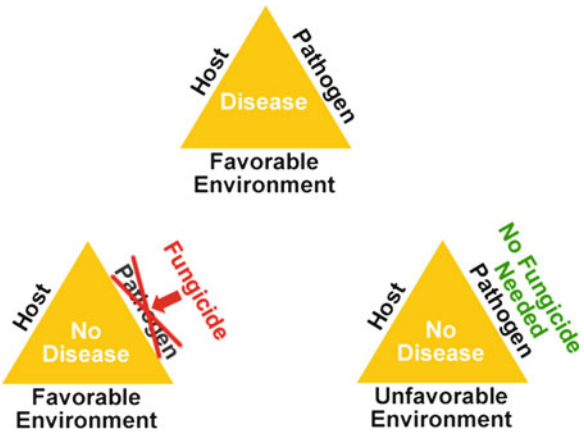


**Fig. 18.5** Disease advisories are based on the disease triangle. Disease will develop only if a pathogen encounters a susceptible host in a favorable environment. Applying a fungicide controls disease by removing the pathogen, but no fungicide is needed if conditions are not favorable for disease development

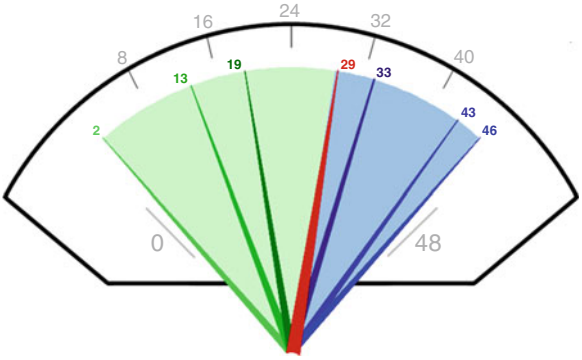


**Fig. 18.6** This graphic is designed to help a peanut grower visualize their risk for peanut disease. It is based on the number of favorable hours for disease development. The green arrows show the past 3 days of favorable disease hours. The red arrow shows where we are today. And the blue arrows show the proceeding 3 days of expected disease hours. This graphic is what decision support is all about – disseminating the latest, high quality information to a grower so that they can make the best production decisions

## 18.5 Strawberry

In the Southeast U.S., strawberries are another high value commodity crop worth about $96 million. Unfortunately, strawberry crop yields are easily diminished due to unfavorable or abrupt changes in the weather. For example, ice crystals forming in the plant tissue can destroy or significantly lower yield. However, action can be taken to mitigate crop losses. Row covers and/or irrigation can be used to insulate and protect strawberry crops against cold weather and freezing. Timing this has to be just right to achieve optimal effectiveness. Laying down covers too late may not provide enough insulation; irrigating too soon before a cold event may lead to

additional heat loss by evaporation. Due to the variable nature of weather and climate and local agricultural practices across our state, a crop advisory for one farm may not be appropriate for another. A more sophisticated, location-dependent advisory is needed.

Working with researchers and collaborators at NC State University, the SCO is developing a website that will ask strawberry growers several basic questions about the current status of their crop. The inputs needed to make a location-specific strawberry advisory are: (1) farm location, (2) type of groundcover between rows, (3) strawberry varieties being grown, (4) current crop stage, (5) recent irrigation or rainfall amounts, and (6) available row covers and irrigation equipment. Considering the current and forecasted crop risk, the grower's available row covers and irrigation capacity, an actionable advisory will be generated. The output generated is simple and intuitive in both maps and charts. If action is needed to protect the crop at the specified location, the specific action and timing will be recommended. This product is expected to be open to the public by the 2010 growing season.

## 18.6 Cucurbit

Another high value crop in the Southeast U.S. is cucurbits. Cucurbits are members of the gourd family and include cantaloupe, cucumber, pumpkin, squash and watermelon. As a group, these crops are valued at nearly $1.5 billion in the U.S. Cucurbit downy mildew (CDM) is one of the most important diseases in cucurbits. The disease is most common in humid climates with frequent rainfall, such as the eastern U.S. CDM is caused by the fungus Pseudoperonospora cubensis, which is an obligate biotroph, unable to survive without a living host. In the Northern Hemisphere, it moves from south to north as susceptible hosts become available, conditions are favorable, and inoculum is moved via air currents from infected plants to uninfected plants. CDM can kill plants by infecting its leaves, which impair necessary food production in the plant. It spreads rapidly and can destroy crops in 3–4 days (Thomas 1996; Holmes et al. 1998; Nusbaum 1944, 1948).

Fungicide treatments can be effective against CDM if properly timed. However, it is expensive and time consuming to routinely treat with fungicide. A more efficient approach is to only apply fungicide if the disease is likely to develop or spores are likely to land nearby. In collaboration with researchers at NC State University, the SCO began developing an automated CDM forecast system in 2008. A website is established that solicits reports from cucurbit growers and county extension agents. If cucurbit downy mildew is observed, it can be reported online. These reports are archived and will be used to alert other growers who may be in the path of the spores. Additionally, the reports are used to numerically model where spores are likely to travel during the proceeding 72 h. The model is based on the strength of the inoculum, local weather conditions, host, and stage of disease development.

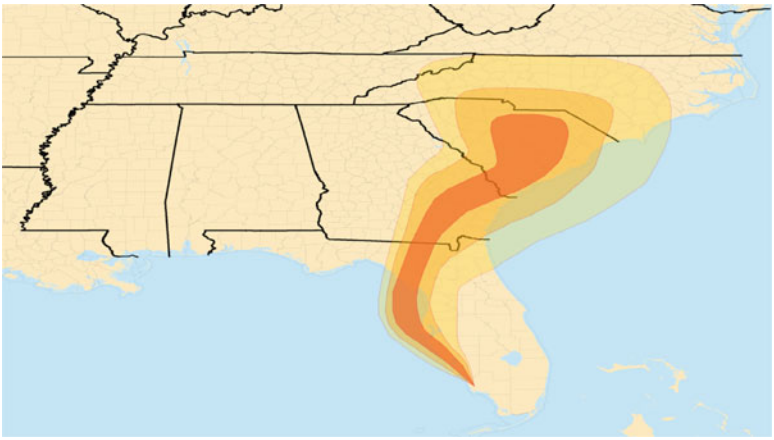

**Fig. 18.7** This sample graphic depicts varying levels of risk for cucurbit downy mildew. Cucurbit growers and county extension agents will be able to use these maps and accompanying information to prepare for the disease and protect their crop

Maps are then produced that depict levels of risk for CDM as shown in Fig. 18.7. Cucurbit growers will have access to these maps and accompanying information to prepare for the disease and protect their crop. The system will be fully operational by 2011.

## 18.7 Turfgrass

Golf is a popular leisure sport in the Southeast United States. Many golf courses, and homeowners alike, put enormous efforts into caring for their lawn– or turfgrass. This requires an enormous volume of irrigation. People tend to irrigate more than their turf actually needs to remain healthy and green. Due to severe droughts and water restrictions plus a need to improve water conservation, the SCO co-developed a turfgrass irrigation management system.

The Turf Irrigation Management System (TIMS) was launched in June 2007 by the Department of Crop Science and the State Climate Office at NC State University. TIMS is an irrigation decision-support tool, accessible to anyone in North Carolina via the Internet. It provides people with guidance for irrigation management of turf areas as shown in Fig. 18.8. Information on turf water use and turf species crop coefficients has been collated from a number of scientific studies and assimilated into a model on irrigation management. The development of the model has looked at a comparison of ET reference models and how they needed to be integrated with turf water use and irrigation system management information coupled with generalized soils information. Users provide their location, turfgrass species, soil type, and recent irrigation amounts. Based on recent daily temperatures, precipitation, and estimated evapotranspiration rates, a recommended irrigation amount is provided.

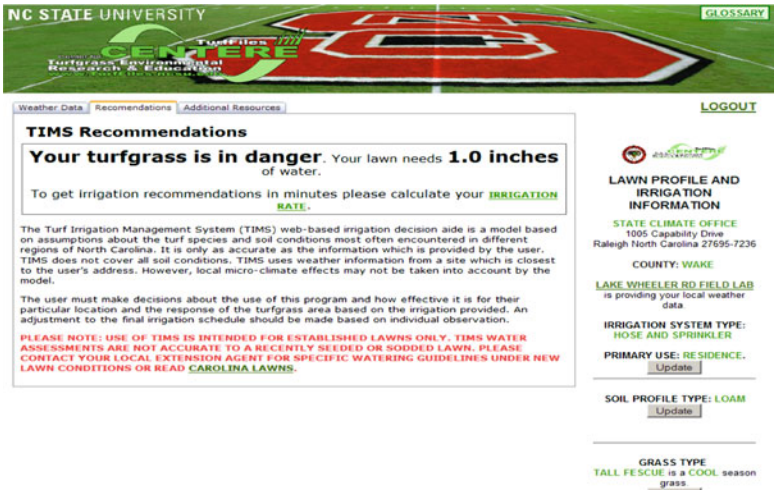


**Fig. 18.8** TIMS is an irrigation decision-support tool, accessible to anyone in North Carolina via the Internet. It provides people with guidance for irrigation management of turf area. The user inputs their location, turf type, soil type, and other environmental conditions. Calculations are made to estimate the amount of water actually needed to keep the turf healthy and green. Output is shown as inches of water needed or number of minutes needed to run their irrigation system

## 18.8 Tobacco

Tobacco is another valuable crop in the Southeast U.S. The crop is susceptible to the Tomato Spotted Wilt Virus (TSWV). Losses in the tobacco crop due to TSWV vary greatly depending on year and location. In addition to killing young plants, TSWV reduces the uniformity and leaf quality of infected plants that are not killed. The tobacco thrips (Frankliniella fusca) is the primary vector of TSWV in North Carolina tobacco. Winter and spring temperatures and rainfall are the primary factors that affect tobacco thrips population growth and dispersal. Based on this information, models have been developed that predict tobacco thrips flights in North Carolina. These models use area-specific, winter and spring temperature and rainfall data plus 15-day weather forecasts to predict the expected magnitude and timing of tobacco thrips flights and TSWV spread for an area of interest.

Working with researchers at NC State University, the SCO is developing software to help tobacco growers and extension agents gage the risk of thrips infestations and spread of TSWV. A webpage is being developed that will interview growers and use their input to generate a custom, location-specific advisory. Inputs include field location, disease history at the field, planting date, type of tobacco, and treatments available. Based on the input, calculations will be automatically run to find the historical temperature and precipitation data from the nearest weather station, degree day accumulations, and an overall risk assessment for thrips.

Output will be generated that will help tobacco growers and extension agents supplement their decision making. This output will include charts of the calculations and relevant graphs to illustrate the risk of thrips. The website will be ready in 2010.

## 18.9 Summary

Since the beginning of productive agricultural practices, growers have attempted to reduce their risk to weather. With advances in science and technology, tools are becoming available to help growers. The State Climate Office of North Carolina is leading the efforts to bridge the gap between agriculture and climate science in the Southeast U.S. Where there is actionable knowledge of the weather sensitivities to specific crops, the SCO can develop a decision support tool.

Many challenges still lie ahead. The most important need of all is more high quality environmental observations. If no data exist on the ground, the numerical weather models can do poorly and any climate-based decision support tool may also perform poorly. More data on the ground equals better forecasts, better products, and better services. Furthermore, research should continue and be supported with more funding in order to better establish the specific relationships between weather and climate and crop diseases. Only a few crops have had extensive research. Finally, atmospheric models, like WRF and MM5, produce reasonably good forecasts for up to 72 h. However, the resolution of these forecasts is still not ideal for farm-level use. More computing power is needed to resolve complex atmospheric simulations at extremely high resolution.

**Acknowledgements** The work mentioned herein is supported, in part, by the North Carolina Agricultural Research Service; Office of Extension, Engagement and Economic Development at NC State University; and the Center for Turfgrass Environmental Research and Education at NC State University. The authors would also like to acknowledge our collaborators: Dr. Barbara Shew, Department of Plant Pathology, NC State University; Dr. Gina Fernandez and Dr. Barclay Poling, Department of Horticulture, NC State University; Dr. George Kennedy and Dr. Hannah J. Burrack, Department of Entomology, NC State University; and Dr. Charles Peacock, Department of Crop Science, NC State University.

## References

Cu RM, Phipps PM (1993) Development of a pathogen growth response model for the Virginia peanut leaf spot advisory program. Phytopathology 83:195–201

Doran JC, Fast JD, Barnard JC, Laskin A, Desyaterik Y, Gilles MK, Hopkins RJ (2008) Applications of lagrangian dispersion modeling to the analysis of changes in the specific absorption of elemental carbon. Atmos Chem Phys 8:1377–1389

Fast JD, Easter RC (2006) A lagrangian particle dispersion model compatible with WRF. 7th WRF Users Workshop, NCAR, Boulder, 19–22 June, p 6.2

Grell GA, Dudhia J, Stauffer DR (1995) A description of the fifth generation penn state/NCAR Mesoscale Model (MM5). NCAR Tech. Note NCAR/TN-398+STR, 122 pp

Holmes GJ, Main CE, Keever TZ (1998) Forecasting long-distance movement of cucurbit downy mildew. In: Proceedings cucurbitaceae 1998, Pacific Grove, pp 186–188

Langston DB, Phipps PM, Stipes RJ (2002) An algorithm for predicting outbreaks of sclerotinia blight of peanut and improving the timing of fungicide Sprays. Plant Dis 86:118–126

Nusbaum CJ (1944) The seasonal spread and development of cucurbit downy mildew in the Atlantic coastal states. Plant Dis 28:82–85

Nusbaum CJ (1948) A summary of cucurbit downy mildew reports from Atlantic coastal states in 1947. Plant Dis 32:44–48

Skamarock WC, Klemp JB, Dudhia J, Gill DO, Barker DM, Duda MG, Huang XY, Wang W, Powers JG (2008) A description of the advanced research WRF version 3. NCAR Tech. Note NCAR/TN-475+STR, 113 pp

Thomas CE (1996) Downy mildew. In: Zitter TA, Hopkins DL, Thomas CE (eds) Compendium of cucurbit diseases. APS Press, St. Paul, pp 25–27

# Chapter 19
# Challenges in District Level Weather Forecasting for Tribal Region of Chhattisgarh State

**J.L. Chaudhary**

**Abstract** Agricultural production in many parts of India continues to be largely dependant on weather and climatic fluctuations despite several impressive advances made in the field of agricultural technology over the last few decades. Bastar Plateau ACZ (agro-climatic zone) is covering four districts i.e. Kanker, Dantewada, Bijapur and Bastar districts with a geographical area of around 39,000 sq. kms. Approximately 6.5 lakh hectares area is under rice crop in this tribal zone and total cultivated area happens to 1.0 million hectares covering other crops like pulses, oilseeds, minor millets, maize and other variable crops in post-kharif and rabi seasons etc. However, cropping intensity in this zone is 105% because of the fact that irrigation percentage is hardly 3–4%.

Under changing scenarios and availability of improved techniques of weather information, it is desirable to utilize the weather parameters as agricultural resource for the farmers in this tribal belt. In Bastar Plateau ACZ since year 1999, DST sponsored agroadvisory services project is functional at center S.G. CARS, Jagdalpur (earlier ZARS, Jagdalpur) in co-ordination with National Centre for Medium Range Weather Forecasting. Major objective of the project is to prepare agrometeorological advisory services bulletins (AABs) on the basis of medium range weather forecasting received from NCMRWF, preceding week weather data and current crop situation in consultancy with different disciplines. Main utility of the project has been found to be helping farmers regarding adjustment in routine production and post-harvest operations for achieving maximum productivity and economy, efficient use of weather sensitive inputs and fertilizers, pesticides and irrigation water. On the basis of feedback received from farmers, it has been found that farmers are making use of AABs in epidemic management and adjusting farming operations according to medium range weather forecasting. It has been

J.L. Chaudhary (✉)
S.G. College of Agriculture and Research Station, Kumhrawand, Jagdalpur 494 005, Chhattisgarh, India
e-mail: zars_igau@rediffmail.com

S.D. Attri et al. (eds.), *Challenges and Opportunities in Agrometeorology*,
DOI 10.1007/978-3-642-19360-6_19, 

found that if a forecast of sufficient skill can be generated, returns to the framers can increase substantially as losses many times are high.

From the monsoonal season of year 2008, the district level weather forecasting has been started and at AMFU Jagdalpur, the district level weather forecast is available through internet from Regional Meteorological Centre, Raipur. Earlier the AABs were prepared for the Bastar Plateau ACZ. Under changed system of Ministry of Earth Sciences Integrated agro advisory services project, in spite of availability of district level weather forecasting, AABs are not prepared district wise. This is because of the fact that specific features district wise are not available with the advisory panel responsible for preparation of AABs. At present, four districts are covered under Bastar Plateau ACZ viz. Bastar, Narayanpur, Bijapur and Dantewada. It is desired that district wise AABs are prepared for four districts for which specific features are required by the advisory panel. A preliminary effort has been made in this direction and some of the features are compiled. In addition to it, a kind of questionnaire has been prepared and sent to Deputy Directors of Agriculture of four districts.

## 19.1 Introduction

India's economy has been agricultural in nature. Excess climate anomalies, deficient and flooded rainfall years have a dramatic impact on the economy as well as on the living conditions of the inhabitants of the affected regions. Rice (*Oryza sativa* L.) crop is widely grown during the summer/ kharif season in Chhattisgarh region of Central India which is a pre-dominantly sub-humid agroclimatic region.

Rice is grown in about 3.8 million hectare area in Chhattisgarh state of which more than 80% is rainfed out of which Bastar region rice coverage area is approximately 6.5 lakh hectare area where irrigation facilities are mere 3–4%. The average productivity of rice in this tribal Bastar region is about 1.2 t/ha which is very low. There are three agro-climatic regions/zones viz. Chhattisgarh Plains, Northern Hill Region and Bastar Plateau zones in this Chhattisgarh region. The various districts and tehsils covered under each agro-climatic region are as follows:

| Agro-climatic region | Districts/tehsils covered |
|---|---|
| Chhattisgarh plains region | Raipur, Mahasamund, Dhamtari, Durg, Rajnandgaon, Kawardha, Bilaspur, Korba, Janjgir-champa, Raigarh and Kanker districts. |
| Bastar plateau zone | Bastar, Dantewada, Bijapur and Narayanpur districts. |
| Northern hill region | Surguja district, Jashpur district and Korea district. |

Under changing agricultural scenario and availability of improved weather information, it is desirable to utilize weather parameters as agricultural resource for input saving, pests-diseases management and yield improvement. It has been argued that mere presence of physical impacts is not sufficient to conclude that improved climate information would have economic benefits. For benefits to occur, economic systems need to possess the flexibility to utilize improved information and farmers need to be innovators in utilizing these advance information. In Bastar

Plateau Agroclimatic zone (ACZ) since year 1999, DST sponsored agro-advisory services project is functional at centre S.G. CARS, Jagdalpur (earlier ZARS, Jagdalpur) in co-ordination with National Centre for Medium Range Weather Forecasting, New Delhi and advanced information technology has helped a lot in faster dissemination of the information to ultimate users. Further, it has been found that characteristics of climate forecasts such as lead time and accuracy affect the value of forecast system.

Bastar Plateau ACZ is covering four districts i.e., Kanker, Bastar, Dantewada, Narayanpur and Bijapur with a geographical area of around 39,000 sq. kms. It is possible to have impact of AABs on approximately 1.0.million hectares area grown under various crops in this tribal zone through use of MRWF and through information technology available in present era. Crops grown are like pulses, oilseeds, minor millets, maize, other variable crops in post-kharif and rabi season etc. However cropping intensity in this zone is 105% because of the fact that irrigation percentage is hardly 3–4%. During 9 years of dissemination of AAB's, main utility of this project has been found to be helping farmers regarding adjustment in routine production and post-harvest operations for achieving maximum productivity and economy of different cropping systems, efficient use of weather sensitive inputs like fertilizers, pesticides and irrigation water in this ACZ and also in disease management in vegetables and rice crop. It has been found that if a forecast of sufficient skill can be generated, returns to the farmers can increase substantially as losses many times are high.

In the recent years, a greater emphasis has been given on studies of climate related studies like climatic change/ fluctuations. Some studies in this regard have been made (Chaudhary and Sastri 1999) in Chhattisgarh region of central India. In fact, agriculture and forestry are well adjusted to the mean climatic conditions and show little sensitivity to moderate variations around these means. The experience of the world is sufficient to convince people that even a temporary change of climate can have profound impact on agricultural production and on the use of energy and water resources (Gates 1988). With rice as a main crop under rainfed conditions, any slight small deviation of rainfall from mean is detrimental for its production and these cyclic variations of rainfall have profound impact on the productivity for which studies have already been conducted by Chaudhary et al. (1996) for undivided Bastar district. In some pockets like Bhanupratap-pur and Kanker, there is observed a sharp decreasing trend in annual rainfall.

Scarcity of water is a critical limitation to adoption of modern technology for increasing productivity of traditional rainfed rice growing areas in Chhattisgarh state including Bastar zone. Erratic distribution of rainfall and increased field water losses account for unreliability and shortage of water for crop production. Most of precipitation occurs between June to September and during this period about 50% of rainfall occurs in about 20–30 h (Pishroty 1987). This duration hardly accounts for 1% of total rainy season during which rainfed rice is grown. A large amount of water from these storms is lost by runoff, seepage and percolation. Shortage of water in this region results from uneven distribution of rains, significant gaps

between rain events and field water losses rather than from low seasonal or annual rainfall totals.

In the rice based farming system, it is must to have in depth knowledge about relevant features. Farmers traditionally impound water in the bunded rice fields up to 40–50 cms depth, compelling them to take local tall varieties like Safri which are of longer duration and having less yield potential. Hence, productivity of rice crop is low. These crop varieties flower in mid-October and mature by mid November while the monsoon withdraws by mid September. The method of rice cultivation is broadcast biasi system in which rice seeds are broadcast in the field with first showers of monsoon and fields are ploughed in the standing crop after 30–40 days when sufficient water is accumulated in the fields. This operation is called biasi. As the rice fields are not puddled, the percolation losses are very high and drought is a recurring feature in this area limiting the rice productivity to 1.2 ton per ha. Traditionally, rice is grown under continuous flooded condition and requires 1,500–2,000 mm water (Kandaih 1985). A feasible strategy is to alleviate this limitation is to harvest excess rainwater in a farm pond or OFR (On Farm Reservoir) during wet season and use conserved water for crop production in both wet (as insurance against drought) and dry seasons by adopting suitable crop and cropping systems (Rathore et al. 1996).

At present 5-day forecast for 7 weather parameters is available based on satellite cloud picture, numerical weather prediction model and other improved forecasting techniques. Major objective of the project is to prepare agrometeorological advisory bulletins (AABs) on the basis of medium range weather forecast received from RMC, IMD, Raipur preceding week weather data and current crop situation in consultancy with different disciplines.

## 19.2 Discussions

It has been suggested that mere presence of physical impacts was not sufficient to conclude that improved climate information would have economic benefits (Sonka 1986). For benefits to occur, economic systems need to possess the flexibility to utilize improved information. As the agroadvisory bulletins are sent to private traders, several newspapers, state administrators, agricultural department officials, university officials, dissemination officers including PRO, station director of AIR, station director of Doordarshan. In addition to it, about 15 progressive farmers have been selected in this area and agro-advisory bulletins are being personally handed over to them on every Tuesday/Wednesday. The district wise features compiled are shown in the tabulated form.

| District | Specific features |
|---|---|
| | *This district is in sub-humid tropics. Water harvesting potential is going less due to several factors of rainfall variability. There are hillocks, contour cultivation in practice and field leveling efforts have been started recently. |
| | *Finger millet, kodo, kutki are sown by end July. We can expect a field condition yield of about 10 q/acre for ragi, 8 q/acre for kodo, 5 q/acre for kutki. |
| | *Some perennial sources of irrigation are available in Bakawand. In kondagaon tehsil, there is good coverage of maize. |
| | *There is good coverage of pulses and oilseeds. |
| | *There is coverage of tuber crops like Colocasia, sweet potato, Amorphophallus and tapioca/cassava. |
| | *In rice crop, there is more infestation of gall midge, leaf folder and stem borer. |
| 1. Bastar | *Blast disease of rice is a significant feature for rice crop. |
| | *In this district, more rainfall pattern, higher temperature pattern and less of evaporation is observed. High water table happens to be a significant feature. |
| | *There is coverage of tuber crops like Discorea and colocasia. |
| | *There is fair coverage of vegetables. |
| | *In rice crop, there is infestation of hoppers, gundhi bug, leaf folders and stem |
| 2. Narayanpur | borer. |
| | *In this district, sandy soils are observed. Perennial streams, hot and dry weather condition is observed and low water table also happens to be a significant feature. Topography is undulating. *There is more coverage of niger, arhar and minor millets. |
| | *There is coverage of tuber crops like Discorea. |
| | *In minor millets, farmers' preference is rice and after major operations of rice are finished, they go for minor millets. Sometimes due to this, there is heavy infestation of insect-pests and diseases. |
| | *In rice crop, there is infestation of stem borer, cutworm and hoppers. |
| 3. Dantewada | *BLB of rice is a significant feature for rice crop. |
| 4. Bijapur | There is less coverage of vegetables. |

## 19.3 Summary and Conclusions

Implication is that our future agricultural planning must take account of these specific features. Short duration but high yielding varieties of different crops need to be developed in this region and brought under cultivation for successful agriculture including weather package as an input. Looking into the above specific instances, it can be seen that Medium Range Weather Forecast (MRWF) has great and significant value for farmers of Bastar Plateau Zone and dissemination process has improved to a significant extent. Reaching weather forecast and agricultural guidelines based upon MRWF will help the farmers in taking advantage of these information. Utilizing and incorporating these information's in day to day agricultural operations management and modifications is need of the hour to save precious weather sensitive inputs.

Further, flexible management styles are more costly than routine- oriented systems because they require additional management time and effort for increasing farming operations efficiency. Input cost levels also affect the value of forecasts as higher input costs reduce the value of climate forecast information. The decline in relative effect is particularly sharp when higher input prices are coupled with lower output prices. Lower relative values when input costs are high suggest that producers would be motivated to adopt cost reducing strategies in such an economic environment regardless of expected climate information. Underlying facts of economic impact is that management practices that take into account the rainfall variability over the region of interest (Bastar Plateau ACZ) are likely to generate a substantial increase in the sustained productivity. In addition, if it becomes possible to forecast critical events (such as dry or wet spells) and take preventive measures, we expect a further increase in yields. If a forecast of sufficient skill can be generated, returns to the farmer can increase substantially as losses many times are high. Earlier results indicated that modest improvements in forecast accuracy would have potentially significant value (Brown et al. 1986). A detailed analysis of every cropping system is required for identification of the value of those weather/climate events that have a large impact on productivity. Ultimately it can be said that availability of improved climate information and district wise features and preparation of ready hand AABs would lessen the negative aspects and exploit positive features of weather variability.

## References

Brown BG, Katz RW, Murphy AH (1986) On the economic value of seasonal precipitation forecasts: the fallowing/planting problem. Bull Am Meteorol Soc 67:833–841

Chaudhary JL, Sastri ASRAS (1999) Regional climate change and climatic swings with reference to production of rice and water resource potential in Chhattisgarh region of Central India. Trop Ecol 40(1):137–144

Chaudhary JL, Srivastava AK, Naidu D (1996) Climatic variations and their impact on agricultural productivity in Bastar district. Geog Rev India 58(1):82–89

Gates GM (1988) Climate and the climate system. In Schlesinger ME(ed) Physically based and simulation of climate and climate change, Part I, Kluwer, Dordrecht, pp 3–21

Kandaih A (1985) Modern concepts of water management in rice production. Proceedings of the 16th season of the international rice commission, Rice progress assessment and orientation in the 1980s, vol 34(2). International Rice Commission Newsletter, Los Banos, Laguna, Philippines, pp 153–162, 10–14 June 1985

Pishroty PR (1987) Water management and watershed management. Wasteland News 3(1):3–11

Rathore AL, Pal AR, Sahu RK, Chaudhary JL (1996) On-farm rainwater and crop management for improving productivity of rainfed areas. Agric Water Manage 31:253–267

Sonka ST (1986) Information management in farm production. Comput Elect Agric 1:75–85

# Chapter 20
# Agromet Information System for Farm Management

**M.C. Varshneya, N. Kale, V.B. Vaidya, Vyas Pandey, and B.I. Karande**

**Abstract** The global food security and sustainable agriculture are the key challenges before the scientific community in the present era of enhanced climate variability, rapidly rising population and dwindling resources. The agrometeorological information viz. weather forecast, soil status information along with agro-advisory is real input for efficient farm management. India had glorious scientific and technological tradition in the past. Our ancient astronomers and astrologers made a systematic study of meteorology. Kautilya's Arthashastra contains records of scientific measurement of rainfall and its application to the country's revenue and relief work. Kautilya emphasized observing and understanding the weather for better management of agricultural crops, way back in Third century B.C. This paper describes the application of ancient knowledge in forecasting the rainfall and generating information for farm management. Rainfall calendars are prepared for all the districts of Gujarat based on astrometeorological prediction. Paper further discusses the agrometeorological services being provided by India Meteorological Department. In addition to this, the unique attempt done by Government of Gujarat under Soil Health Card Program to provide the web based information to all the farmers of Gujarat, is also described in this paper.

## 20.1 Introduction

The global food security and sustainable agriculture are the key challenges before the scientific community in the present era of enhanced climate variability, rapidly rising population and dwindling resources. No part of the world is immune from meteorological extremes of one sort or another posing threat to the food security.

M.C. Varshneya (✉) • N. Kale • V.B. Vaidya • V. Pandey • B.I. Karande
Anand Agricultural University, Anand 388110, Gujarat, India
e-mail: mcvarshneya@gmail.com; yogirajvedashram@gmail.com; vaidya.vidyadhar@gmail.com; pandey04@yahoo.com; babankarande@yahoo.co.in

S.D. Attri et al. (eds.), *Challenges and Opportunities in Agrometeorology*,
DOI 10.1007/978-3-642-19360-6_20, 

Agrometeorology has to make most efficient use of the opportunities to develop efficient agrometeorological services which may cope up with risks. The agrometeorological information viz., weather forecast, soil status information along with agro-advisory is real input for efficient farm management. The ancient techniques of rainfall prediction were used by the farming community since last thousands of years. The rainfall prediction used to be given in traditional almanac.

Weather forecasting is probably the oldest of all "Sciences" and has played a major part in human history. Evidence indicates that Meteorology, as a science, is comparatively young, while as a branch of knowledge, it dates back to the origins of human civilization. Modern scientific knowledge on methods of weather forecasting has originated recently. But ancient indigenous knowledge is unique to our country. India had glorious scientific and technological tradition in the past. Our ancient astronomers and astrologers made a systematic study of meteorology. Even today, it is common that village astrologers (*pandits*) are right in surprisingly high percentage of their weather predications (Varshneya 2008).

Varahamihir's classical work, the Brihatsamhita, written around 500A.D., provides clear evidence that a deep knowledge of atmospheric processes existed even in those times. It was understood that rains come from the sun (Adidyat Jayate Vrishti) and that good rainfall in the rainy season was the key to bountiful agriculture and food for the people (Tamboli and Nene 2002). Kautilya's Arthashastra contains records of scientific measurement of rainfall and its application to the country's revenue and relief work. Kautilya emphasized observing and understanding the weather for better management of agricultural crops, way back in Third century B.C.

Rain is a basic need for farming similarly water is a must for every living beings. This basic need was well thought, considered and emphasized by our seers, astrologers and intellectuals. This natural phenomena of rainfall was given simile of phenomenon in human race; and hence Varahamihira wrote that cloud delivers rain. Varahmihir postulated different principles for the prediction of rainfall and weather (Tamboli and Nene 2002).

According to the ruling planet of a year, overall rainfall of that particular year should be anticipated as follows:

| | | |
|---|---|---|
| 1. | Sun | Moderate |
| 2. | Moon | Very heavy |
| 3. | Mars | Scanty |
| 4. | Mercury | Good |
| 5. | Jupiter | Very good |
| 6. | Venus | Good |
| 7. | Saturn | Very low (Stormy wind) |

Our Earth, the third planet from the Sun, orbits our local star along with eight other neighboring planets and is an integral part of the whole solar system. And being an integral part of the whole system, is affected by the whole system, comprised of the Sun, Moon and planets. They are among the chief causes of our weather, and natural disasters. Sun is the main, which affect weather and climate.

Mars and Pluto are responsible for increase in temperature. Different aspects between Moon, Venus and Neptune are responsible for rain. Saturn and Uranus are responsible for decrease in temperature. Mercury acts on wind and is responsible for movement of clouds. More number of planets in any one nadi gives effect of that nadi.

## 20.2 Modern Methods of Agromet Information

India Meteorological Department (IMD) started weather services for farmers in the year 1945. It was broadcast by All India Radio in the form of Farmer's Weather Bulletin (FWB). Subsequently, in the year 1976, IMD started Agro-Meteorological Advisory Service (AAS) from its State Meteorological Centers, in collaboration with Agriculture Departments of the respective State Governments. Though these services are being regularly provided by IMD for the past many years, the demand of the farming community could not be fully met due to certain drawbacks in the system. Prior to 2007, National Centre for Medium range Weather Forecasting (NCMRWF), Govt. of India, NOIDA (UP) was giving location specific rainfall and other five parameters for 5 days twice a week. NCMRWF is giving prediction based on Numerical Weather Prediction (NWP) technique with the help of super computer to 107 Agromet Advisory Field Units (AMFU) throughout the country. In view of that IMD launched Integrated Agromet Service in the country for 2007 in collaboration with different organizations/institutes. At present bulletins are being issued from three levels viz., National Agromet Advisory Bulletin, State Agromet Advisory Bulletin and District Agromet Advisory Bulletin.

Weather forecasting system already started issuing quantitative district level weather forecast up to 5 days from 1 June, 2008. The products comprise of quantitative forecasts for seven weather parameters viz., rainfall, maximum and minimum temperatures, wind speed and direction, relative humidity and cloudiness. IMD is generating these products based on a Multi Model Ensemble technique using forecast products available from a number of models of India and other countries like the UK, US and Japan.

1. Advisory service network: Based on the above forecast products and the crop information available from districts, the Agromet field units (AMFU) will prepare district-wise agro-advisories.
2. Advisory dissemination mechanism: These weather based advisories would be disseminated to the farmers through mass media dissemination, Internet etc. as well as through district level intermediaries. The advisories would be communicated through multi-channel dissemination system including All India Radio (AIR), Doordarshan, private television channels, FM radios, print media (newspapers), Internet (web pages of IMD, universities, etc.) and community Service Centres of Ministry of Information Technology, cell phone-SMS, district agricultural offices (DAO), kisan call centres.

## 20.3 Soil Health Card Program of Gujarat

The Government of Gujarat (GoG) after making a thorough assessment of the fact that available technologies have not either reached to all farmers in the state or not being adopted by them for some reasons or the other. GoG has decided to embark on a massive programme that will address few crucial areas in agriculture that require immediate attention and take up an awareness–cum-implementation plan across the state aiming at every individual farmer. Soil Health Card acts like a ration card, providing permanent identification and status of the land. For instance, recently ten samples of land from each of the 18,818 villages were taken and analyzed with the help of Gujarat Narmada Valley Fertilizer Corporation (GNFC), Gujarat State Fertilizer Corporation (GSFC), Indian Farmers Fertilizers Co-operative (IFFCO) and Indian Potash Ltd (IPL) and a comprehensive report was prepared about the status of land held by the individual farmers (Varshneya et al. 2008a).

Twelve lakh soil test data from farmer's field of all villages of Gujarat, as analyzed and reported from Soil Testing Labs, have gone into database. All the recommendations made by agricultural universities of Gujarat for farmers have been incorporated into database and crop specific information are generated. The guidelines are given for the interpretation of soil test data to adjust the fertilizer requirement of the crop as per updated recommendations made by the agricultural universities. The Soil Health Card provided to farmers contains information such as farmers name, account number, survey number, soil fertility (N, P, K, pH, EC values) their status, general fertilizer dose and manures recommended and soil-test based fertilizer to be given for each crop grown by the farmers.

Under SHC programme, along with soil test data, taluka wise long term daily rainfall and potential evapotranspiration have been used for water balance computation for different soil types of all 225 talukas of Gujarat state. Under different scenarios of soil, rainfall and PET the start, end and duration of crop growing seasons have been worked out. The long term daily rainfall (30–100 years for each taluka, climate of the district/taluka have been kept on web site for user community. The detail information on water balance computations, actual evapotranspiration, water surplus, water deficit, soil moisture storage and length of crop growing period under different soil types has been provided through website. The data required for working out the water balance computation are rainfall, potential evapotranspiration (PET), soil depth, bulk density, field capacity (FC) and Permanent Wilting Point (PWP) of the soil type. Based on average of 30 years of weekly normal potential evapotranspiration, the water balance is computed for different soil types within taluka. The main features of this water balance technique are calculation of soil moisture storage, actual evapotranspiration and water surplus. The ratio of AET (actual evapotranspiration) to PET (potential evapotranspiration) referred to as moisture availability index (MAI) is a good indicator of moisture availability crops. MAI $> 0.75$ is excellent for crop growth, MAI between 0.75 and 0.50 is good for crops, MAI between 0.50 and 0.25 indicates crop under moderate stress

and MAI $< 0.25$ means crop under severe stress. The start and end of crop growing period (CGP) and thereby length of crop growing period (LGP) is determined taking MAI $> 0.75$ for starting of season and MAI $< 0.5$ for end of season (Varshneya et al. 2008a). Based on length of growing period and risk involved each farmer is suggested for alternate crop planning and thereby increase in its income. All such information has been provided through Internet under soil health card program (http://shc.gujarat.gov.in) of Govt. of Gujarat that can be accessed by the farmers at anywhere anytime. The GoG has already provided internet connectivity through Website also provides FAQs, which are very useful to the farmers. Moreover, if farmer has any additional query, he can submit his request through email/phone/fax/mobile etc. and get the advisory from the respective scientists/officials.

## 20.4 Ancient methods

Astrologers used to play an important role in prediction of rainfall and subsequent crop yield. Observations on direction of wind, color and size of clouds, moon's conjunction with behavior of birds and animals were the principal elements considered for prediction of rainfall. The rules are simple and costly apparatus are not required. Observation coupled with experience over centuries enhanced to develop meteorology. The ancient/indigenous method of weather forecast may be broadly classified into two categories (Varshneya 2008).

1. Observational method
   - Atmospheric changes
   - Bio-indicators
   - Chemical changes
   - Physical changes
   - Cloud forms and other sky features
2. Theoretical methods (or) Astrological factors (or) planetary factors
   - Computation of planetary positions and conjunctions of planets and stars
   - Study of solar ingress and particular date of months
   - Study of Nakshatra Chakras
   - Study of Nadi Chakras
   - Dashatapa Siddhanta

### *20.4.1 Rainfall Calendar*

Varshneya et al. (2002) designed an almanac for farmers to predict rainfall distribution in next rainy season. The techniques gave prediction of onset and withdrawal

of monsoon and distribution of rainfall about 6 months in advance. Pictorial assistance is given to assist farmer in noting indication of commencement and withdrawal of monsoon. So that it is possible for the farmers to change the crops to decide area under kharif and rabi season. Vaidya (2004) briefly gave the relative advantage of "Nakshtra varsha" calendar for Maharashtra.

Based on astrology Anand Agricultural University, Anand has prepared Nakshtra-Charan wise forecast for eight agro climatic zones of Gujarat for 2005 monsoon (Varshneya et al. 2009). The almanac for 2006 was prepared by Anand Agricultural University, Anand, to predict rainfall distribution in next monsoon season on temporal (day to day) and spatial (different zones) basis, for farmers of Gujarat state (Varshneya et al. 2006). Gujarat was divided into eight agro-climatic zones. This almanac gave forecast for rainfall of each zone. The daily rainfall was characterized as no rainfall (0 mm), low rainfall (<2.5 mm), medium rainfall (5–10 mm), heavy rainfall (>10 mm). Simultaneously, agricultural operations to be carried out during that month and contingent crop planning according to the rainfall forecast was also suggested.

#### 20.4.1.1 Validation of Rainfall Prediction for Gujarat

The validation of this forecast on Yes/No basis indicated that accuracy ranged between 42% and 73% for various zones for the year 2005.Validation of rainfall forecast, for the year 2006, was done on Yes/No skill score (%) basis, for different zones of Gujarat. The average accuracy of rainfall forecast for state as a whole for June 40.4%, for July 62.5%, for August 52.5% and for September it was 50.9%. The validation of rainfall forecast for the year 2007, on Yes/No skill score basis for June, July, August, September and October month indicate that average accuracy was 67.9%, 73.1%, 63.3% and 58.8% for four regions viz., Middle Gujarat, South Gujarat, North Gujarat and Saurashtra respectively. On an average Monsoon Research Almanac published by AAU, Anand has shown 65.8% accuracy for Gujarat state (Varshneya et al. 2009). In year 2008, the daily rainfall predictions were made for 25 districts of Gujarat state. The validation of rainfall forecast on Yes/No basis was done by comparing it with actual average rainfall for a district as a whole for every month indicated that accuracy varied between 28.3% and 48.8% for different districts. Comparatively, the accuracy of forecast was good in the month of July. On an average Monsoon Research Almanac published by AAU, Anand has shown 36.8% accuracy for Gujarat state. Along with AAU's Monsoon Research Almanac-2008, rainfall predictions made by other astro-meteorologists for Gujarat were also validated. The average Y/N skill score was 38.6%, 42%, 45.1%, 46.8%, 51.6% and 59.9% for Patel Jasratbhai Surani, Dhansukh Shah, Girdharbhai Devjibhai, Pravinbhai Vora, Ratanbhai Mathuria, and Dheeraj Thumar respectively for June to September, 2008.

The validation was done with actual rainfall for each district and zone wise results are given in Table 20.1. The rainfall projection for the state as a whole was quite good with +6.3% departure from actual rainfall which was less than 10%.

**Table 20.1** Validation of rainfall projection for four regions of Gujarat

| S. No. | Name of region | Rainfall projection (Jun-Sep) (mm) | Actual rainfall (mm) | Normal rainfall (mm) | Rainfall projection (% departure from actual) | Actual rainfall (% departure from normal) |
|---|---|---|---|---|---|---|
| 1 | Middle Gujarat | 739.2 | 619.7 | 779.8 | 16.2 | −20.5 |
| 2 | North Gujarat | 605.3 | 565.3 | 575.4 | 6.6 | −1.8 |
| 3 | South Gujarat | 1,895.7 | 1,686.6 | 1,388.3 | 11.0 | +21.6 |
| 4 | Saurashtra | 641.1 | 765.4 | 494.8 | −19.4 | +54.7 |
| | State | 970.3 | 909.3 | 809.6 | +6.3 | +12.3 |

For North Gujarat also departure was +6.6% from actual rainfall. The state's rainfall was 12.3% higher than normal whereas our projections were also showing above normal rainfall for all zones except Saurashtra. The trend of rainfall projections for all zones was similar for district average. Our projection for the state as a whole was 19.8% higher than the normal rainfall, which gave correct trend of above normal prediction in Monsoon 2008.

### *20.4.2 Rainfall Prediction Based on Rainfall Conception Theory of Varah Mihir*

Amongst various astro-meteorological methods for rainfall forecasting, the Antariksha method, which is based on the sky observation, is most popular. The observations of rainfall conception based on 16 symptoms taken for the period (approx. 6 months i.e., 180 days) between Ashwin Krishna paksha (dark half of Ashwin month i.e., Oct-Nov., 2003 to Vaishakh Pournima (April-May month of 2004) was used for daily prediction of rainfall during ensuing monsoon season of 2004 for Barshi, Dist. Solapur (Varshneya et al. 2008b). Similarly, the predictions for the monsoon season of 2005, 2006, 2007 and 2008 were made from rainfall conception observations.

Following are the symptoms of Rain conception. Numbers for symptoms were given according to their priority in rain conception process (Table 20.2).

The analysis was done to find out the most important rainfall conception symptoms responsible for rainfall delivery. The analysis revealed that on an average for 5 years symptom number 1 i.e., observation of rainy clouds has the highest frequency of 79.6%, while the symptom number 4 i.e. Squalls has the lowest frequency (22.5%). It was also observed that the rainfall conception days were maximum (65 days) during 2005, while it was minimum (35 days) during 2007 indicating lower number of rain events during monsoon season of 2007.

The yes/no skill score for each month viz. June to October for the 5 years viz., 2004–2008 is given in Table 20.3. The average skill score for June, July, August, September and October months were 73.3%, 79.2%, 75.5%, 79.3% and 86.4%

**Table 20.2** Symptoms of rainfall conception

| | | | |
|---|---|---|---|
| 1. | Rainy clouds | 2. | Blood red color 15–20 min before sunrise |
| 3. | Blood red color 15–20 min after Sunset | 4. | Squalls |
| 5. | Wind direction | 6. | Cloud roaring |
| 7. | Lightening | 8. | Gusty weather |
| 9. | Rain – Tr. Amt | 10. | Rainbow |
| 11. | Ants (black or red) carrying eggs | 12. | Patangs flying (Flying insects) |
| 13. | Halo around moon | 14. | Halo around Sun |
| 15. | Hot and humid weather | 16. | Haze and 17) Dew |

**Table 20.3** Skill score (%) for rainfall prediction made for Barshi, Dist. Solapur (MS)

| S. No. | Month | 2004 | 2005 | 2006 | 2007 | 2008 | Average |
|---|---|---|---|---|---|---|---|
| 1 | June | 63.3 | 73.3 | 80.6 | 70.0 | 79.3 | 73.3 |
| 2 | July | 64.5 | 80.6 | 96.8 | 80.6 | 74.2 | 79.2 |
| 3 | August | 67.7 | 67.7 | 90.3 | 74.2 | 77.4 | 75.5 |
| 4 | September | 93.3 | 86.7 | 76.7 | 76.7 | 63.3 | 79.3 |
| 5 | October | 87.1 | 80.6 | 93.5 | 71.0 | 100.0 | 86.4 |
| | Average | 75.2 | 77.8 | 87.6 | 74.4 | 78.8 | 78.8 |

**Table 20.4** Skill score (%) of rainfall prediction considering border cases (192 + 1 calendar days) for Barshi (MS)

| S. No. | Month | 2004 | 2005 | 2006 | 2007 | 2008 | Average |
|---|---|---|---|---|---|---|---|
| 1. | June | 63.3 | 83.3 | 96.7 | 80.0 | 79.3 | 80.5 |
| 2. | July | 64.5 | 83.9 | 96.8 | 80.6 | 74.2 | 80.0 |
| 3. | August | 71.0 | 80.6 | 90.3 | 74.2 | 80.6 | 79.3 |
| 4. | September | 93.3 | 93.3 | 80.6 | 90.0 | 63.3 | 84.1 |
| 5. | October | 87.1 | 80.6 | 93.5 | 71.0 | 100.0 | 86.4 |
| | Average | 75.8 | 84.3 | 91.6 | 79.2 | 79.5 | 82.1 |

respectively. The yearly average skill score was 75.2%, 77.8%, 87.6%, 74.4% and 78.8% for the years 2004, 2005, 2006, 2007 and 2008 respectively. The overall average skill score for rainfall prediction was 78.8%. In general the skill score was good and it can be concluded that the rainfall prediction can be made successfully based on the rainfall conception observation with a better accuracy. If we consider border cases of rainfall prediction i.e., 192 $\pm$ 1 calendar days, then average accuracy for these 5 years is 82.1% (Table 20.4). Thus, it can be concluded that rainfall conception observations can be used successfully for rainfall prediction for that locality.

Hansen – Kuipers (HK) coefficient score for the season i.e. from June to October was calculated and it was ranged between 0.45 (2007) and 0.71 (2006). The average H.K. score was 0.56, indicating better skill of prediction. H.K. score ranged between 0 and 1, indicating no skill and perfect prediction respectively. Thus, our prediction for Barshi indicate average HK score of 0.56 means better skill of rainfall prediction.

The rainfall can be predicted well in advance and it was published in the daily newspapers viz., Daily Lokmat, Daily Sakal and Daily Saamana. The predictions

given in the news papers were used by the farming community in Barshi taluka of Solapur district for crop planning and farm operations. The dry spell in the month of July, 2004 and 2005 was very well predicted by Shri. Yogiraj Ved Vijnana Ashram, Barshi, which helped the farmers to take correct decision regarding crop planning and management.

## References

Tamboli PM, Nene YL (2002) Science in India with special reference to agriculture. Asian Agri-History Foundation, Secunderabad. email: ynene@satyam.net.in

Vaidya VB (2004) The long range forecast of Monsoon with Astronomy and local observations for Maharashtra. Asian Agri-Hist 8(4):323–324

Varshneya MC (2008) Blend of Ancient Wisdom and modern science of meteorology for improving agriculture. In: Souvenir of "International Symposium on Agrometeorology and Food Security (INSAFS)" held at CRIDA, Hyderabad during 18–21 Feb 2008, pp 1–5

Varshneya MC, Bhat VV, Joshi RM et al (2002) Nakshatra-varsha almanac-prepared for Maharashtra. Vijay Bhat, Pune, pp 1–22

Varshneya MC, Shekh AM, Pandey V, Patel HR et al (2006) Monsoon research Almanac prepared for Gujarat. Anand Agricultural University, Anand, pp 1–25

Varshneya MC, Kalyanasundaram NK, Patel RH, Sarvaiya JG, Pande V, Patel HK et al (2008a) Taking agricultural technologies to farmers-a massive ongoing effort in Gujarat. Indian J Fert 4 (10):19–22 and 25–28

Varshneya MC, Kale N, Vaidya VB, Pandey V et al (2008b) Forecasting and validation of rainfall for Barshi (M.S.) based on astro-meteorological principle of rainfall conception. In: Abstracts and Souvenir of Third National Seminar on "Agrometeorological Services for Farmers" held at AAU, Anand during 10–13 Nov, Oral-17, pp 1–15

Varshneya MC, Vaidya VB, Pandey V, Chimote LD, Damle KS, Shekh AM, Karande BI et al (2009) Forecasting of rainfall for Gujarat based on astrometeorology. Asian Agri-Hist 13(1):25–37

# Chapter 21
# Advanced INSAT Data Utilization for Meteorological Forecasting and Agrometeorological Applications

**P.C. Joshi, B. Simon, and B.K. Bhattacharya**

**Abstract** INSAT data along with in-situ and other satellite data play a key role in meteorological forecasting over Indian region, especially for agrometeorological applications. Presently, INSAT-3A and Kalpana1 are in orbit providing parameters such as OLR, precipitation, atmospheric motion vectors, upper tropospheric humidity etc. State of the art algorithms are developed and geophysical parameters are routinely getting retrieved. The products are being utilized for monitoring the weather as well as input to meso-scale models for forecasting. Forthcoming satellite INSAT-3D will have 'Imager' and a infrared 'sounder', providing humidity and temperature profile with a spatial resolution of 10 km. The availability of meteorological parameters from these satellites and their utilization is briefly discussed. Retrieval protocols for various land surface radiation and bio-physical parameters have been tested to estimate evapotranspiration for agro-meteorological applications.

## 21.1 Introduction

INSAT series of geostationary satellite was conceived in the early 1980s to meet the operational needs of meteorology and weather services in the country. The INSAT-1 series had four satellites carrying a Very High Resolution Radiometer (VHRR) onboard with two spectral bands for observation: visible (0.55–0.75 μm) and thermal infrared (10.5–12.5 μm). VHRR had spatial resolutions of 2.75 km in visible and 11 km in thermal infrared, with capability of providing half hourly images in normal scan mode. Last satellite in this series, INSAT-1D, provided observations much beyond its expected lifetime.

INSAT-2 series was designed and built indigenously based on the user feedbacks, and launched five satellites to ensure continuity of services. INSAT-2A and 2B were

P.C. Joshi (✉) • B. Simon • B.K. Bhattacharya
Space Applications Centre (ISRO), Ahmedabad 380 015, India
e-mail: pcjoshi35@hotmail.com; babysimon@gmail.com; bkbhattacharya@sac.isro.gov.in

S.D. Attri et al. (eds.), *Challenges and Opportunities in Agrometeorology*,
DOI 10.1007/978-3-642-19360-6_21, 

launched in 1992 and 1993 respectively, and carried VHRR with improved resolution of 2 km in visible and 8 km in thermal infrared bands. The enhanced imaging capability included three modes, viz., full frame, normal frame and sector mode of 5 min for rapid coverage of severe weather systems. INSAT-2C and INSAT-2D did not carry VHRR payload. INSAT-2E was launched in 1999, which carried an advanced VHRR payload operating in three channels – visible (2 km), thermal infrared and water vapour absorption band (8 km). Observations in the water vapour channel, operating in 5.7–7.1 μm band, enabled us to study the water vapour distribution and flow patterns in the lower troposphere (Bhatia and Gupta 1999a). INSAT-2E also carried a CCD camera with three channels – visible, near infrared and short wave infrared with 1 km resolution to map the vegetation and snow cover (Bhatia et al. 1999b). CCD also has the capability to estimate atmospheric aerosols over marine environments (Kaila et al. 2002). Presently, Kalpana1 (launched in September 2002) and INSAT-3A (launched in April 2003) satellites are available in this series. Kalpana1 is launched exclusively for meteorological observations, having only one payload onboard, i.e., VHRR, whereas INSAT-3A has VHRR and CCD similar to INSAT-2E (Joshi et al. 2003).

India is now planning to launch INSAT 3D by the end of 2009 and will carry infrared sounder for temperature and water vapour profiles and Imager with split thermal channels for accurate sea surface temperature retrieval. INSAT-3D is expected to boost the mesoscale studies and prediction of weather by providing three-dimensional information of atmospheric temperature and humidity with very high temporal repetivity (few hours).

The present paper describes the availability of the parameters from INSAT series of satellites and their applications in meteorological forecasting and agro-meteorology.

## 21.2 Meteorological Products from INSAT Series of Satellites

Various algorithm developments are taking place for deriving the meteorological parameters. As a demonstration few are listed below:

(a) Atmospheric Motion Vectors (AMV):
Atmospheric motion vectors (AMV) can be estimated (Kishtawal et al. 2009; Deb et al. 2008) from half-hourly INSAT triplet images (Fig. 21.1a). Infrared images are used for detection and movement of clouds for estimation of winds at cloud levels, while water vapor images are used to track the patterns of moisture for the same. Detection of AMV is based on the assumption that clouds and water vapour at different levels follow the atmospheric motion as rigid bodies. This assumption can be applied over a short interval of time, say, 30 min. Three consecutive INSAT-IR images at 30-min interval are needed to determine the AMVs. The displacement of cloud features in two successive images is the motion vector.

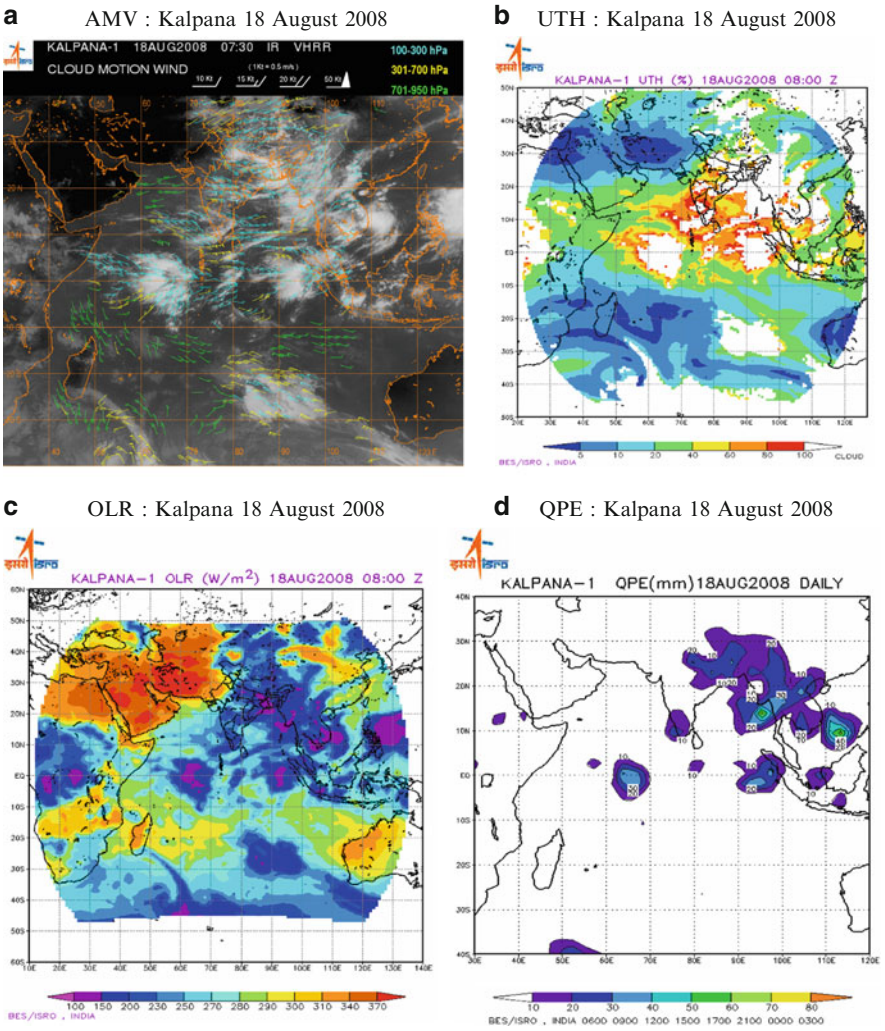


**Fig. 21.1** Kalpana derived Meteorological products (**a**) Atmospheric Motion Vector (**b**) Upper Tropospheric Humidity (**c**) Outgoing Longwave Radiation (**d**) Quantitative Precipitation Estimate for 18 August 2008

(b) Upper Tropospheric Humidity (UTH):
Upper tropospheric humidity can be estimated (Thapliyal et al. 2006) using brightness temperature observations in water vapour channel of VHRR. Figure 21.1b shows an example of UTH using Kalpana1 WV channel observations. UTH derived from INSAT-3A and Kalpana1 observations have been compared with the UTH computed from collocated radiosonde measurements and also with the Meteosat-5 derived UTH.

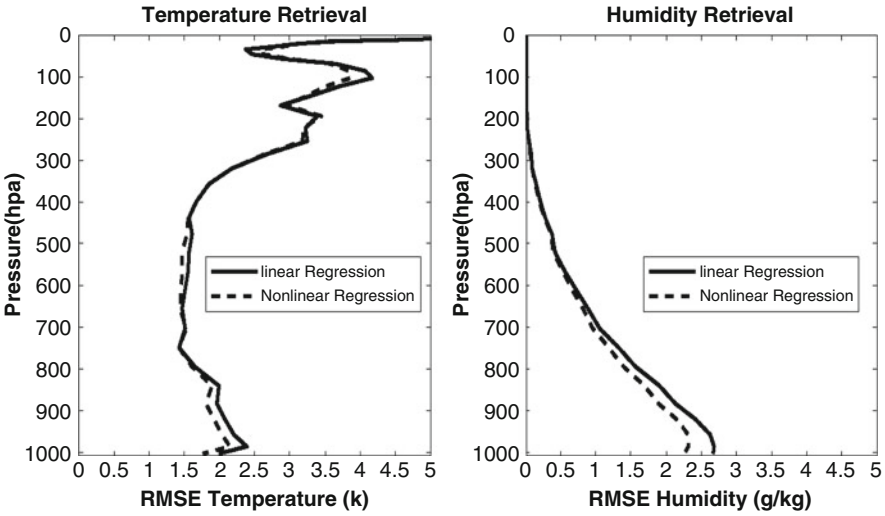


**Fig. 21.2** RMS accuracy of temperature and humidity profiles retrieval using simulated dataset for INSAT-3D Sounder channels

(c) Outgoing Longwave Radiation (OLR):
Outgoing longwave radiation (OLR) can be estimated (Singh et al. 2007) from IR channel observations of INSAT-VHRR by converting the narrowband infrared observations into broadband infrared flux using an empirical relationship (Fig. 21.1c).
OLR estimates are useful for earth radiation budget estimation and also for model diagnostics.

(d) Quantitative Precipitation Estimation (QPE):
QPE is derived (Gairola et al. 2008) based on the Arkin's method using 3 hourly cloud top temperature information inferred from thermal IR channel of VHRR accumulated over 2.5 × 2.5 latitude/longitude grids and correlated to rainfall (Fig. 21.1d). The QPE over the oceans fill up an important gap in rainfall measurements and is a key input to numerical weather models.

(e) Temperature and humidity profile from sounder
INSAT-3D Sounder observations will provide vertical profiles of temperature and humidity in clear-sky conditions besides total column ozone and various other derived products. Figure 21.2 shows simulated retrieval accuracies (Thapliyal et al. 2009) for temperature and humidity profiles retrieved from INSAT-3D Sounder.

## 21.3 Application of INSAT Data in Meteorological Forecasting

For agrometeorological purposes the important application of INSAT data is in the short and the medium range weather forecasting. The AMV's are important inputs for numerical models and are being routinely used for the operational and the R & D

activities. The rainfall prediction during the summer monsoon season is an agro-meteorological need. In this respect the onset of monsoon prediction and the prediction of the active break cycle of the monsoon are few much sought after applications. In the following few such applications are discussed.

The southwest monsoon season (June–September), accounts for more than 80% of the annual rainfall over India. The spatial and temporal distribution of summer monsoon rainfall over the country and its variability affects agricultural output significantly. A delay in the onset of the monsoon by a few weeks would affect agricultural activity while an early onset might not be utilized to its full advantage without an advanced forecast. Thus, the monitoring and forecasting of the summer monsoon onset over the Indian subcontinent is very important for the economy of the country. The onset, or the beginning of rainy season over South Kerala (southern tip of India) is normally declared based on rainfall, wind, temperature, moisture, cloud pattern, cloud type, and state of the sea, etc. It is very difficult to define the date of onset because all these parameters are highly variable in space and time. Rainfall criteria is operationally used for defining the onset of monsoon. The date of monsoon onset varied from 11 May in 1918–18 June in 1972. The normal onset date of the monsoon over Kerala is 1 June, with a standard deviation of about 8 days,

A diagnostic index of monsoon onset and withdrawal based on the monsoon hydrological cycle provides insight into the seasonal transition of the Indian monsoon. By studying the changes in mid-tropospheric water vapor from NOAA/TOVS (layer humidity) for several years over various regions of the Indian ocean, Bay of Bengal (BoB) and Arabian Sea (AS), Simon and Joshi (1994) found that mid-tropospheric water vapor content (700–500 hPa) over the western Arabian Sea (WAS) increased by 25% about 8–10 days before the monsoon onset. Simon et al. (2006), also have found that prior to the monsoon, total integrated water vapour build up takes place over the western Arabian Sea, in the region west of Somalia [50–65 E and 0–10 N]. This is also the region where the cross equatorial wind picks up the moisture before its movement to the Indian peninsula. This study has indicated that the build up of total integrated water vapour over this regions gives us a lead time of two and half weeks for the onset of monsoon over Kerala. Figure 21.3 shows the build up of total precipitable water vapour over Western Arabian Sea (peaking on 10th May) and the subsequent onset (on 28th may) after about two and half weeks during the year 2008.

In future INSAT-3D sounder will have the capability to estimate both the mid-tropospheric as well as total precipitable water. Thus the data will be useful for the prediction of onset of monsoon.

INSAT VHRR imagery on the day of the onset of monsoon in 2008 is shown in Fig. 21.4. The INSAT imagery is also useful in monitoring the progress of the monsoon as well as in delineating the heavy rainfall events based on cloud top temperature.

The Madden Julian Oscillation (MJO) is the dominant form of intra-seasonal variability in the Tropics and studying this helps in predicting the onset of monsoon and the active - break cycle of the monsoon. INSAT derived OLR can be used for

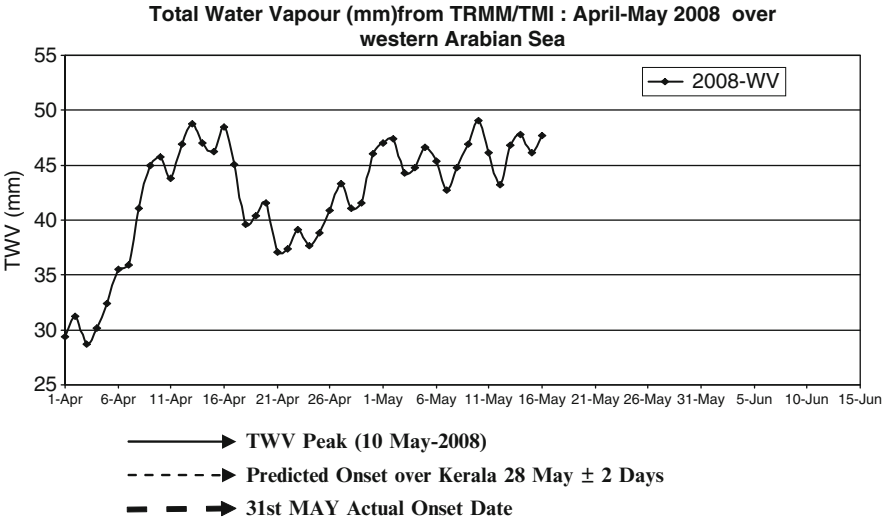


**Fig. 21.3** Variation of total water vapour peaking (mm) over the Western Arabian Sea during the onset of monsoon over Kerala using TRMM/TMI data

examining this behaviour of MJO. Figure 21.5 shows the Hovemoller diagram of Kalpana1 derived average OLR over the region around equator (5 N–5 S) in the year 2008. The low OLR values [<200 W/sq m] can be seen clearly moving west to east.

This is followed by a second MJO which started on 26th May and moved towards east. This is normally associated with the onset over Kerala. The axis of the east propagating MJO is shown in the diagram. The second phase of the MJO came over the same longitude by 29th May, and finally the onset took place on 31st May. This shows the periodicity of the MJO in the year 2008 was about 40 days. This oscillation also helps in predicting the active-break phase of the monsoon.

## 21.4 Land Parameters from INSAT Series of Satellites and Agrometeorological Applications

Data in red and near-infrared bands from CCD onboard INSAT-3A are used to retrieve NDVI (Bhattacharya et al. 2008). The VHRR onboard Kalpana1 and INSAT-3A satellites can give the estimates of the radiation parameters such as albedo (Bhattacharya 2009a), land surface temperature (Bhattacharya et al. 2009a), and surface insolation (Bhattacharya et al. 2009b). A brief discussion of these is given below. These parameters can be used for estimating regional evapotranspiration over different agro-ecosystems using surface energy balance approach.

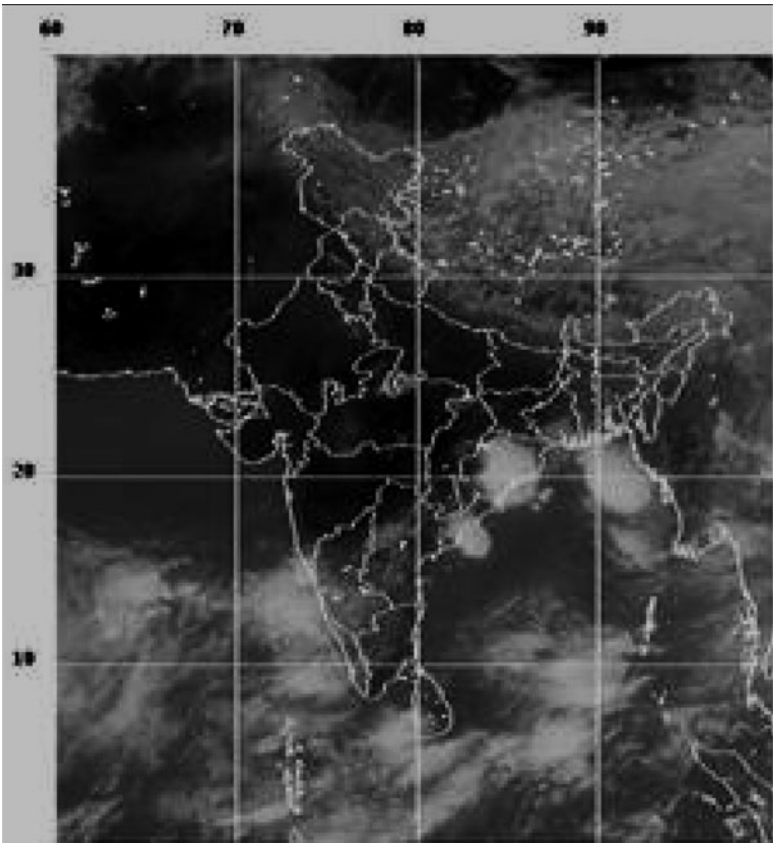

**Fig. 21.4** Monsoon onset over Kerala on 31st May 2008 captured using Kalpana1-IR image

### *21.4.1 Radiation Parameters*

The K1VHRR albedo was compared with aggregated MODIS AQUA noontime albedo over different land targets (agriculture, forest, desert, scrub and snow) that showed minimum differences over agriculture and forest. The comparison of spatial albedo over different landscapes (Fig. 21.6) yielded a root mean square deviation (RMSD) of 0.021 in VHRR albedo (9% of MODIS albedo). The root mean square error (RMSE) of MODIS AQUA albedo was found to be 0.024 as compared to in situ measurements. Typical resemblance of spatial outputs of MODIS AQUA albedo at its native (0.01°) and target grid (0.08°) and VHRR albedo (0.08°) over a patch in Northwestern India (24°–32° N, 74°–76° E) are shown in Fig. 21.6. A great heterogeneity of surface albedo values was observed over the landscape (Fig. 21.6). An output of monthly minimum surface albedo composite over Indian sub-continent is shown in Fig. 21.6. This clearly differentiates the higher to lower albedo zones among snow, desert and other land cover types over Indian landmass.

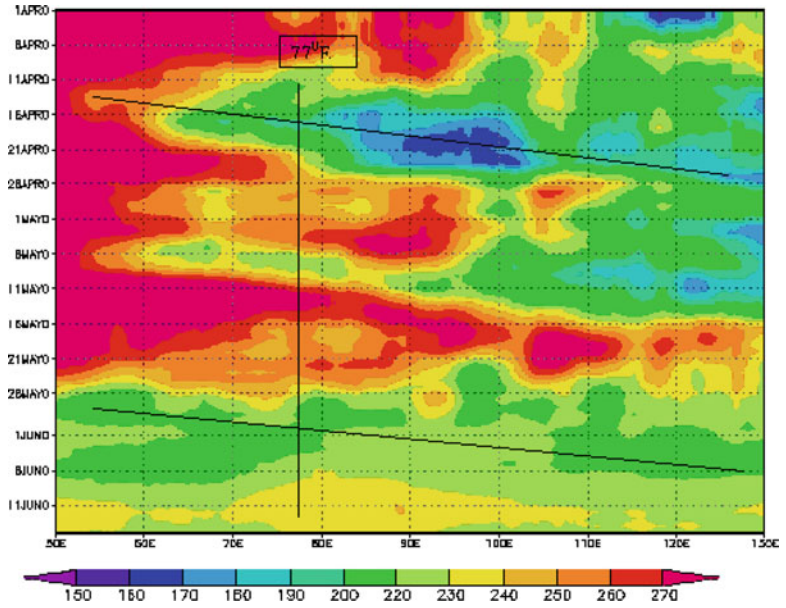


**Fig. 21.5** Propagation of Madden Julian Oscillation (MJO) derived using Kalpana OLR averaged over equator [5 N–5 S] during the pre monsoon rainfall and during onset phase

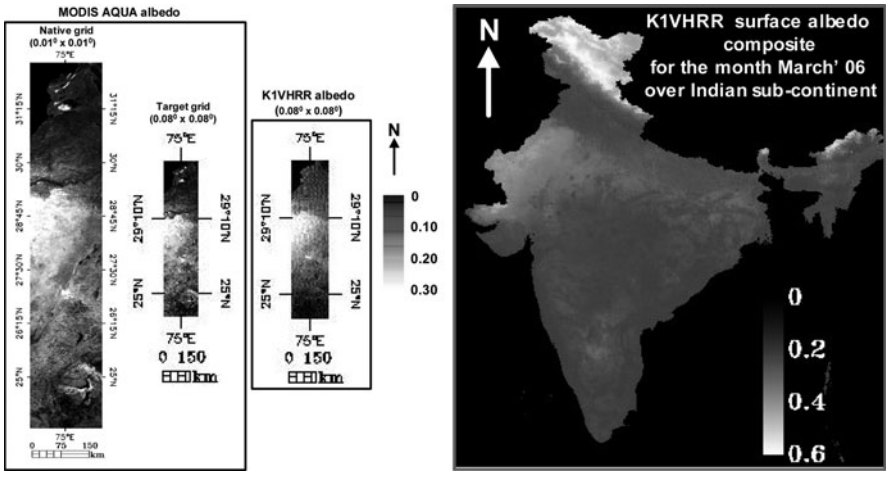


**Fig. 21.6** Comparison of K1VHRR and MODIS AQUA noontime albedo

The accuracy of VHRR LST was also verified over different land targets through intercomparison with aggregated MODIS AQUA LST (Bhattacharya et al. 2009a). The maximum RMSD was obtained over agriculture. Spatial comparison of VHRR and AQUA LST over homogeneous and heterogeneous landscape cutouts revealed

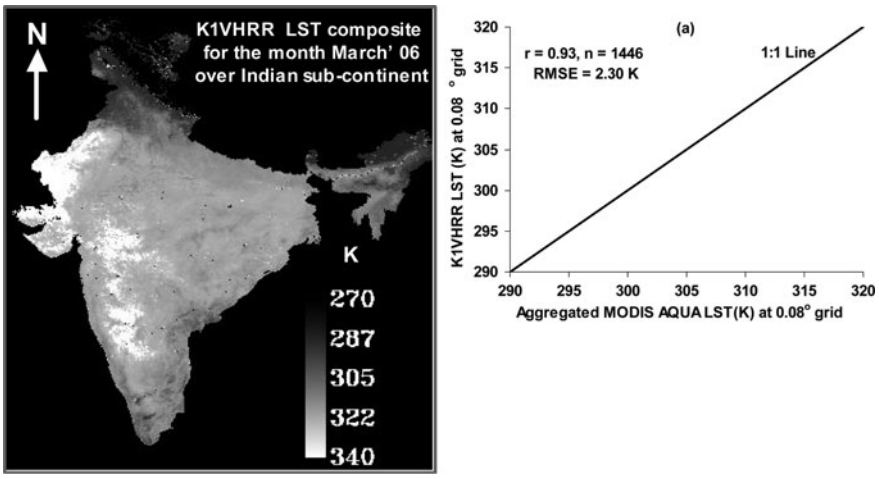


**Fig. 21.7** Comparison of noontime K1VHRR and MODIS AQUA LST

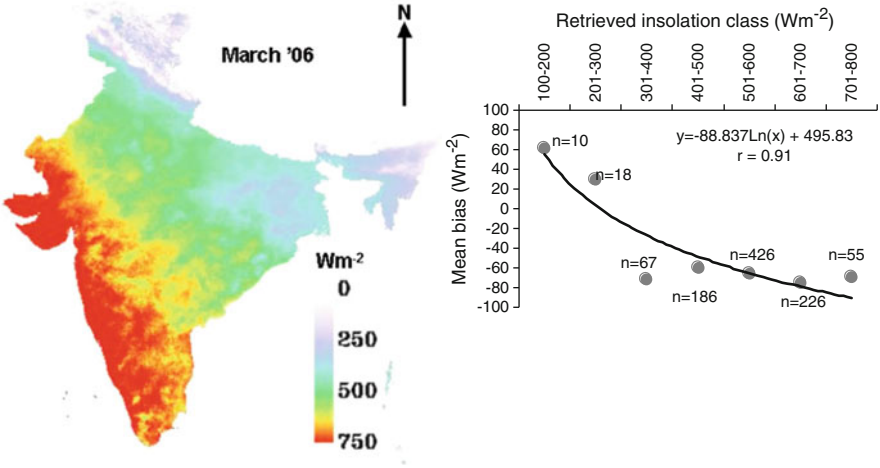


**Fig. 21.8** K1VHRR noontime insolation and assessment of bias of estimates

an overall RMSD of 2.3 K (Fig. 21.7). The inherent error of MODIS LST was found to be 1.7 K when compared to measurements over Indian agroecosystems.

The retrieved noontime surface insolation was found to produce high correlation ($r = 0.88$, $n = 988$) with in situ pyranometer measurements over continental, coastal and desert stations (Bhattacharya et al. 2009b). The root mean square error (RMSE) of retrieved noontime insolation was 13% of observed mean (Fig. 21.8). It was relatively higher in coastal stations as compared to the rest of the stations due to the complex interaction of water vapour and aerosols (dust, smoke and smog) in the atmosphere that is difficult to model analytically.

### 21.4.2 Biophysical Parameters

There was 10%–20% improvement in NDVI after atmospheric correction. NDVI profiles extracted from CCD output (Bhattacharya et al. 2008) showed logical temporal variation on different land targets such as agriculture, forest and desert. The INSAT 3A CCD 15-day NDVI composites at 10:30 LMT were compared with aggregated MODIS TERRA (11:00 LMT) 15-day NDVI over known targets. There were underestimates from CCD NDVI as compared to TERRA NDVI with systematic bias. The overall CCD RMSD was found to be 0.12 (Bhattacharya et al. 2008) with respect to TERRA with higher deviations at low vegetation conditions. A clear temporal dynamics of crop growth cycle has been captured (Fig. 21.9) during a rabi growing season in India over Indo-Gangetic plain when NDVI took its peak during 1st week of March and thereafter declines.

### 21.4.3 Regional Evapotranspiration (ET) over Agroecosystems

A two-step validation scheme (in situ vs. lumped estimates from K1VHRR and distributed estimates from MODIS AQUA vs. lumped) was followed to validate regional clear sky latent heat flux or ET estimates. When compared to in situ

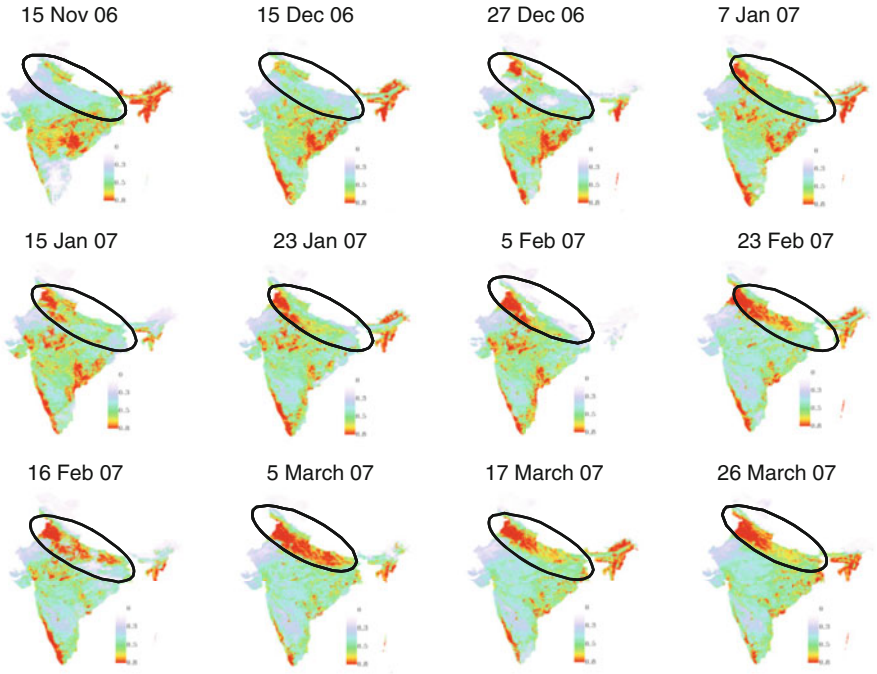


**Fig. 21.9** INSAT 3A CCD NDVI dynamics

measurements, the RMSE of daytime distributed latent heat flux estimates at landscape scale (Mallick et al. 2009) from MODIS AQUA was 24 $Wm^{-2}$ (R2 = 0.92, n = 135). The RMSD of regional or lumped estimates from K1VHRR as compared

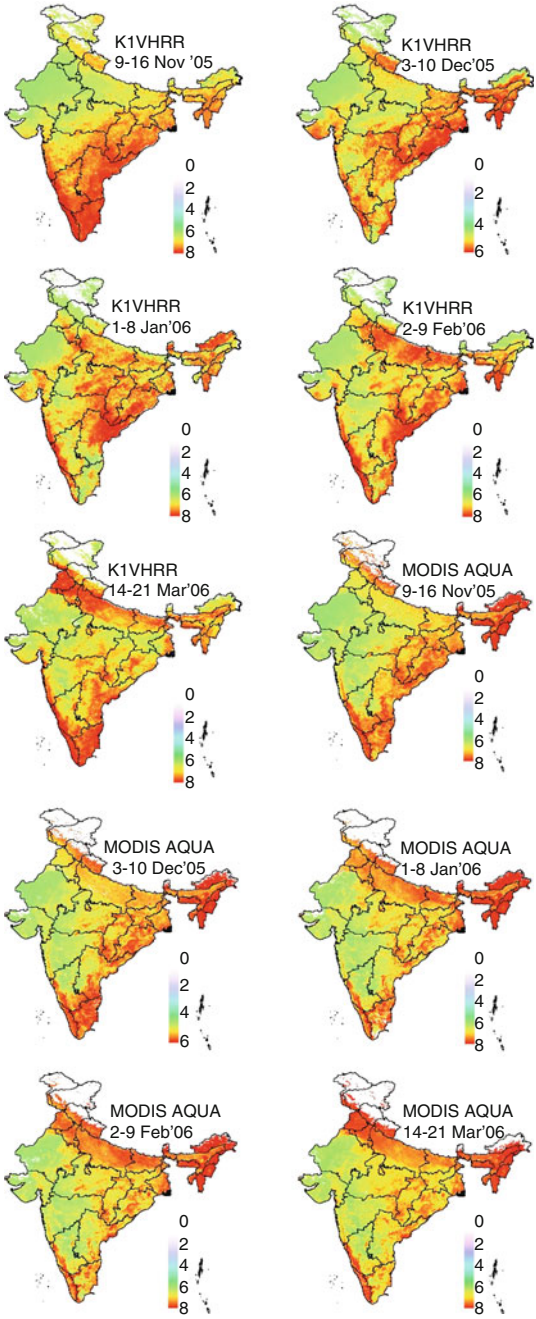


**Fig. 21.10** Comparison of K1VHRR and MODIS AQUA 8-day cumulative evapotranspiration (mm)

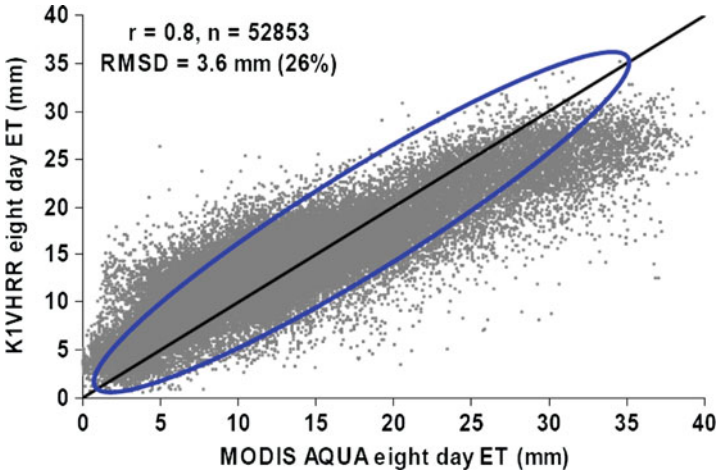


**Fig. 21.11** Wall-to-wall comparison of MODIS AQUA and K1VHRR 8-day cumulative clear sky evapotranspiration

to aggregated landscape scale estimates was found to be 39 $Wm^{-2}$ ($R2 = 0.52$, $n = 35$), which is about 25%. Typical examples of regional ET outputs from MODIS AQUA and K1VHRR are shown in Fig. 21.10.

The wall-to-wall comparison of K1VHRR and MODIS AQUA 8-day clear sky cumulative ET produced a correlation of the order of 80% (Fig. 21.11) over Indian agro-ecosystems during rabi (November - March) growing season. It was noticed that the deviations increased with higher order of sub-grid heterogeneity. The major issue in the ET estimation from optical and thermal remote sensing is the temporal data gaps due to cloud cover. Recently, have developed a technique for estimating ET fluxes both in clear and cloudy days using two-source model (e.g. ALEXI) applied to GOES data. The scheduled launch of INSAT 3D with six channel 'Imager' and 19 channel 'Sounder' would help improve the retrieval accuracy of core radiation variables. The improved spatial resolution would also reduce loss of sub-grid heterogeneity in the lumped ET computation. Daily integral from half-hourly ET fluxes, instead of only using noon-midnight data, would be attempted in future to capture the full potential of diurnal variability from geostationary sensor data. The development of an INSAT-based agro-meteorological monitoring system is indeed the need of the hour to strengthen national agro-advisory service.

## References

Bhatia RC, Gupta HV (1999a) Use of charged coupled device payload on INSAT-2E for meteorological and agricultural applications. Curr Sci 76:1444–1447

Bhatia RC, Bhushan B, Rajeswara Rao V (1999b) Applications of water vapour imagery received from INSAT-2E satellite. Curr Sci 76:1448–1450

Bhattacharya BK, Nigam R, Dorjee N, Panigrahy S (2008) Normalized difference vegetation index – towards development of operational products using INSAT 3A CCD data. In: Proceedings of ISRS symposium held at Ahmedabad

Bhattacharya BK, Mallick K, Padmanabhan N, Patel NK, Parihar JS (2009a) Retrieval of land surface albedo and temperature using data from Indian geostationary satellite – a case study for winter months. Int J Remote Sens 30(12):3239–3257

Bhattacharya BK, Mallick K, Padmanabhan N, Patel NK, Parihar JS (2009b) Retrieving noontime surface insolation for winter months using data from Indian geostationary meteorological satellite (KALPANA1). Curr Sci (under revision)

Deb SK, Kishtawal CM, Pal PK, Joshi PC (2008) A modified tracer selection and tracking procedure to derive winds using water vapour imager. J Appl Meteorol Climatol 47:3252–3263

Gairola RM, Mishra A, Varma AK (2008) Rainfall estimation using satellite microwave and INSAT/KALPANA1-IR Measurements over Indian land and Oceanic regions. In: National symposium on advances in remote sensing technology and applications with special emphasis on microwave remote sensing, Nirma University, Ahmedabad, 18–20 Dec 2008

Joshi PC, Narayanan MS, Bhatia RC, Manikiam B, Kiran Kumar AS, Jayaraman V (2003) Evolution of Indian Satellite meteorological programme. Mausam 54:1–12

Kaila VK, Kirankumar AS, Sundaramurthy TK, Ramakrishan S, Prasad MYS, Desai PS, Jayaraman V, Manikam B (2002) METSAT – a unique mission for weather and climate. Curr Sci 83:1081–1088

Kishtawal CM, Deb SK, Pal PK, Joshi PC (2009) Estimation of atmospheric motion vectors from Kalpana1 imagers. J Appl Meteorol Climatol 48:2410–2421

Mallick K, Bhattacharya BK, Rao VUM, Reddy Raji, Banerjee D, Hoshali S, Pandey V, Kar G, Mukherjee J, Vyas SP, Gadgil AS, Patel NK (2009) Latent heat flux estimation in clear sky days over Indian agroecosystems using noontime satellite remote sensing data. Agricultural and Forest Meteorology 149(10):1646–1665

Simon B, Joshi PC (1994) Determination of moisture changes prior to the onset of monsoon over Kerala using NOAA/TOVS satellite data. Meteorol Atmos Phys 53:223–231

Simon B, Rahman SH, Joshi PC (2006) Condition leading to onset of monsoon: a satellite perspective. Meteorol Atmos Phys 93(3–4):201–210

Singh R, Thapliyal PK, Kishtawal CM, Pal PK, Joshi PC (2007) A new technique for estimating outgoing longwave radiation using infr-red window and water vapour radiances from Kalpana1 VHRR. Geophys Res Lett 34:l23815. doi:10.1029/2007GL031715

Thapliyal PK, Shukla MV, Ajil KS, Shah S, Pal PK, Joshi PC (2006) Estimation of upper Tropospheric Humidity from water vapour channel of Very High Resolution Radiometer onboard INSAT-3A and Kalpana1 Satellites, Proc. SPIE, 6408, 40807, p 7. available at http://spiedl.org

Thapliyal PK, Ajil KS, Shukla MV, Pal PK, Joshi PC (2009) Improvement in humidity profile retrieval from sounder observations by linearizing the predictands in a hybrid regression retrieval. Journal of Applied Meteorology (Under revision)

# Chapter 22
# Data Mining: A Tool in Support of Analysis of Rainfall on Spatial and Temporal Scale Associated with Low Pressure System Movement over Indian Region

**Kavita Pabreja**

**Abstract** Weather is not just an environmental issue; it is a major economic factor. The rainfall over Indian region is of utmost importance to agriculture, aviation and transportation segments. We propose to enhance our understanding of formation and movement of clusters of Low Pressure System (LPS) over Indian region during the months of June to September using data mining and associating these clusters with rainfall. Data mining is a technique for finding and describing patterns in data, for helping to explain that data and make predictions from it and it is an evolving approach that has gained a lot of importance for extracting knowledge from meteorological datasets. The weather system can be thought of as a complex system whose various components interact in various spatial and temporal scales and these states exhibit a great deal of correlations at various spatial and temporal scales. Since the weather data are generally voluminous, they can be mined for occurrence of particular patterns that distinguish specific weather phenomena. The study is based on the datasets of 18 years (1984–2003) for LPS and rainfall. Year 1986 and 1987 are not included as these were very poor rainfall years. Clustering technique offered by Waikato Environment for Knowledge Analysis (WEKA) Weka (Weka 3-Data mining with open source machine learning software Available from:- http://www.cs.waikato.ac.nz/ml/weka/ Accessed 3 Aug 2008) tool for data mining has been used to identify the favored zones of formation, movement and dissipation of LPS over Indian region. The clusters hence generated have been correlated with actual rainfall datasets provided by Indian Meteorological Department (IMD). A hypothesis is drawn that as the cluster moves from South-East to North-West during the months of August-September, it causes rainfall from North-West to South-East quadrants.

K. Pabreja (✉)
Research Scholar-BITS, Pilani, C-3A/39C, DDA Flats, Janak Puri, New Delhi 110058, India
e-mail: kavita_pabreja@rediffmail.com

S.D. Attri et al. (eds.), *Challenges and Opportunities in Agrometeorology*,
DOI 10.1007/978-3-642-19360-6_22, 

## 22.1 Introduction

Recently there has been increased interest in the use of data mining techniques for weather interpretations and forecasts (Pabreja 2005). Statistical approaches to weather predictions have a long and distinguished history that predates modeling based on physics and dynamics. This trend continues today with new approaches based on machine learning algorithms. Based on the k-means approach, a quantitative snowfall forecast model has been developed for a station in Jammu and Kashmir, using surface meteorological data for 12 winters (Singh et al. 2005). Several data mining algorithms for classification using WEKA tool has been used to predict Forest Fires in Slovenia (Stojanova et al. 2006). Spatial clustering has also been used for the purpose of mining of Geographical data (Koperski et al. 1998; Han et al. 2001). Clustering Large Applications based upon RANdomized Search (CLARANS) was proposed in (Han et al. 2001) so as to improve the quality and scalability of Clustering LARge Applications (CLARA) that is a k-medoids method of spatial clustering. Two spatial data mining algorithms were developed in an approach similar to CLARANS (Ng and Han 1994).

In this work, we apply clustering technique for mining of Low Pressure System data for the duration of 18 years (1984–2003). Low Pressure System is an area with lower atmospheric pressure than its surrounding areas; this makes air from surrounding areas to flow into the low, the end result of which is probably cloudiness and precipitation.

We have used Grid Analysis and Display System (GrADS) to generate contours of rainfall on annual basis (http://www.iges.org/grads/). The rainfall dataset clusters are also been generated for identification of more precise association with LPS formation using WEKA. Finally LPS and rainfall datasets are also been analyzed using .xls files of records of eighteen years.

## 22.2 Description of the Dataset Used

We examined two different datasets: year 1984, 1985, 1988, 1989, 1990, 1991, 1992, 1993, 1994 and year 1995–2003 corresponding to LPS and Rainfall.

### *22.2.1 LPS Dataset*

The LPS data (Mooley and Shukla 1987; Sikka 2006) contains the serial number of the system in the year, the date of formation of the system (the date is also given on 1–122 scale : 1 for 1st June and 122 for 30th September), the intensity stage, and the location of the system for each day of existence (latitude °N and longitude °E correct to the first decimal). The intensity stage is given by 1 for Low, 2 for Depression, 3 for Deep Depression, 4 for Cyclonic Storm and 5 for Severe Storm.

**Table 22.1** A sample of LPS data for the year 1984

| S. No. | Date | Days | Long. | Lat. | Time int |
|---|---|---|---|---|---|
| | 2-Jun 1984 | 2 | 89 | 21 | 1 |
| | 3-Jun 1984 | 3 | 90 | 20 | 2 |
| | 4-Jun 1984 | 4 | 87.5 | 22 | 3 |
| | 5-Jun 1984 | 5 | 86.5 | 23 | 4 |
| 1 | 6-Jun 1984 | 6 | 86.5 | 23.5 | 5 |
| | 5-Jun 1984 | 5 | 67.5 | 18.5 | 1 |
| | 6-Jun 1984 | 6 | 67 | 20 | 2 |
| | 7-Jun 1984 | 7 | 67 | 19.5 | 3 |
| 2 | 8-Jun 1984 | 8 | 66.5 | 19.5 | 4 |
| | 11-Jun 1984 | 11 | 84.5 | 17.5 | 1 |
| | 12-Jun 1984 | 12 | 86 | 19 | 2 |
| | 13-Jun 1984 | 13 | 87 | 21.5 | 3 |
| | 14-Jun 1984 | 14 | 88 | 21.5 | 4 |
| | 15-Jun 1984 | 15 | 88.5 | 23.5 | 5 |
| | 20-Jun 1984 | 20 | 90 | 24.5 | 2 |
| | 22-Jun 1984 | 22 | 90 | 21.5 | 2 |
| | 23-Jun 1984 | 23 | 89 | 23 | 3 |
| | 24-Jun 1984 | 24 | 88 | 23 | 4 |
| 4 | 25-Jun 1984 | 25 | 88 | 23.5 | 5 |
| | 16-Jul 1984 | 46 | 89 | 19.5 | 1 |
| | 17-Jul 1984 | 47 | 88 | 20 | 2 |
| | 18-Jul 1984 | 48 | 83 | 20.5 | 3 |
| | 19-Jul 1984 | 49 | 76 | 22 | 4 |
| 8 | 20-Jul 1984 | 50 | 72.5 | 23.5 | 5 |
| | 30-Jul 1984 | 60 | 89 | 19.6 | 1 |
| | 31-Jul 1984 | 61 | 88.5 | 19.5 | 2 |
| | 1-Aug 1984 | 62 | 82.5 | 22 | 3 |
| | 2-Aug 1984 | 63 | 79 | 24 | 4 |
| 9 | 3-Aug 1984 | 64 | 76 | 25 | 5 |
| | 7-Aug 1984 | 68 | 89 | 20 | 1 |
| | 8-Aug 1984 | 69 | 88 | 22 | 2 |
| | 9-Aug 1984 | 70 | 84.5 | 22.5 | 3 |
| | 10-Aug 1984 | 71 | 83 | 23 | 4 |
| 10 | 11-Aug 1984 | 72 | 78 | 23 | 5 |

The datasets are set in the .csv format as required by the WEKA tool for data mining (Witten and Frank 2005). A small sample of the LPS data for the year 1984 is given in Table 22.1.

### *22.2.2 Rainfall Dataset*

The rainfall dataset given by IMD contains daily rainfall (in mm) for the years mentioned above. The data is correct up to 0.5° grid point (latitude and longitude).

The data is for the longitude 66.5°E–100.5°E and latitude 6.5°N–38.5°N for every day of the year. The dataset is in .grd format and has been converted to .txt file using a FORTRAN programme given below and finally into .xls format for analysis purpose.

```
      PROGRAM READ
      PARAMETER(ISIZ = 35,JSIZ = 32)
      DIMENSION RF(ISIZ,JSIZ)
      OPEN(7,FILE = 'input.grd',
+   FORM = 'UNFORMATTED',
      ACCESS = 'DIRECT',RECL = ISIZ*JSIZ*4,
+   STATUS = 'OLD')
      OPEN(10,FILE = 'output.DAT',+FORM = 'FORMATTED',
      STATUS = 'UNKNOWN')
55    FORMAT(20F8.1)
C     TAKE NDAY = 366 FOR LEAP YEARS NDAY = 365
      DO 101 IDAY = 1,NDAY
      READ(7,REC = IDAY)((RF(I,J),I = 1,ISIZ),J = 1,JSIZ)
      WRITE(10,55)((RF(I,J),I = 1,ISIZ),J = 1,JSIZ)
101 CONTINUE
      STOP
```

The daily rainfall dataset taken into consideration for the study is from longitude 66.5°E–90.0°E and latitude 15.0°N–25.0°N for the time period June to September. A very small sample of this data with rainfall values in mm is shown in Table 22.2.

**Table 22.2** A sample of rainfall dataset for the year 1984

| Dayn | | 73°E | 73.5°E | 74°E | 74.5°E | 75°E | 75.5°E |
|---|---|---|---|---|---|---|---|
| 106 | 25°N | 21 | 14.3 | 0.8 | 0.3 | 0 | 1.2 |
| 106 | 24.5°N | 80.9 | 3.7 | 0 | 0.3 | 0.1 | 1.3 |
| 106 | 24°N | 52.6 | 3.5 | 0.2 | 0 | 46.8 | 1.9 |
| 106 | 23.5°N | 36.9 | 39.7 | 1.5 | 4 | 0 | 3 |
| 106 | 23°N | 35.7 | 6 | 0.8 | 1.6 | 2.9 | 1.3 |
| 106 | 22.5°N | 8.4 | 35.5 | 1.9 | 1.5 | 0 | 0.6 |
| 106 | 22°N | 11.2 | 1.6 | 1.8 | 1.7 | 0.7 | 0 |
| 106 | 21.5°N | 9.7 | 10 | 8.1 | 2.3 | 15.4 | 0 |
| 106 | 21°N | 4.5 | 13.4 | 1.7 | 5 | 2.4 | 1 |
| 106 | 20.5°N | 4.3 | 6.1 | 6.6 | 19.1 | 5.8 | 1.4 |
| 106 | 20°N | 1.5 | 9.5 | 1 | 1.7 | 0.1 | 0 |
| 106 | 19.5°N | 0.3 | 0.9 | 0 | 0.7 | 0.4 | 0 |
| 106 | 19°N | 0 | 0 | 0 | 0 | 0 | 0 |
| 106 | 18.5°N | 0 | 0 | 0 | 0 | 0 | 0 |
| 106 | 18°N | 0 | 0 | 0 | 0 | 0 | 0 |
| 106 | 17.5°N | 1.7 | 0 | 0 | 0 | 0 | 0 |
| 106 | 17°N | 2.9 | 3.3 | 0 | 0.2 | 0 | 0 |
| 106 | 16.5°N | 1.9 | 1.9 | 4.3 | 6.7 | 1.2 | 21 |
| 106 | 16°N | 0 | 0 | 0.4 | 0.6 | 2.6 | 3.6 |

## 22.3 Technique Used

Low Pressure Area data as mentioned above has been analyzed using WEKA tool for data mining. WEKA is a collection of machine learning algorithms for data mining. It is an open Source Machine Learning Software in Java. It offers many techniques for mining of datasets. We have used Clustering technique of WEKA to group a set of objects into clusters so that the objects within a cluster have a high similarity in comparison to one another, but are dissimilar to objects in other clusters. The k-means method of clustering is used to generate clusters corresponding to the day of formation of the system to the day it dies. The tool provides various options to select/ reject the attributes on the basis of which the clustering should be done. The number of clusters required can also be selected. The groups that are identified are exclusive so that an instance belongs to only one group.

The k-means method first chooses k points at random as cluster centers. All instances are assigned to their closest cluster centre according to the ordinary Euclidean distance metric. Next the centroid/mean of the instances in each cluster is calculated. These centroids are taken to be new center values for their respective clusters. Finally, the whole process is repeated with the new cluster centers. Iteration continues until the same points are assigned to each cluster in consecutive rounds, at which stage the cluster centers have stabilized and will remain same forever.

GrADS is an interactive desktop tool that is used for easy access, manipulation, and visualization of earth science data. GrADS uses a 4-Dimensional data environment: longitude, latitude, vertical level, and time. Data sets are placed within the 4-D space by use of a data descriptor file. The format of the data may be either binary, GRD, GRIB, NetCDF, or HDF-SDS (Scientific Data Sets). Data may be displayed using a variety of graphical techniques: line and bar graphs, scatter plots, smoothed contours, shaded contours, streamlines, wind vectors, grid boxes, shaded grid boxes, and station model plots.

We have used the annual rainfall datasets in GRD format as provided by IMD and has been displayed in the form of contours.

## 22.4 Results

Using data mining technique has resulted in locating a cluster of formation of Low Pressure System on 1st day and a cluster of disappearance on 4th or 5th day of formation, on a spatio-temporal scale for the months of June-July and August-September separately, for a period of 9 years (year 1984, 1985, 1988, 1989, 1990, 1991, 1992, 1993, 1994) as shown in Figs. 22.1 and 22.3 respectively.

Similarly, a cluster of formation of Low Pressure System on 1st day and a cluster of disappearance on 4th or 5th day of formation, on a spatio-temporal scale for the

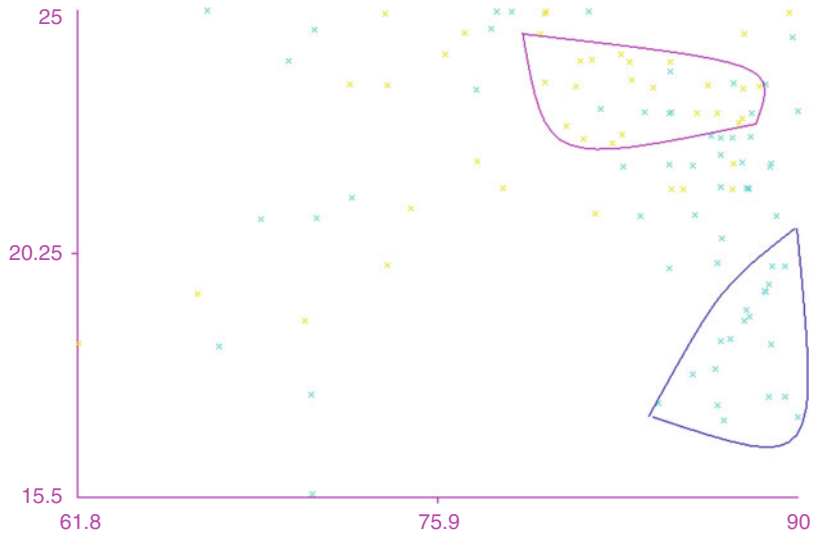


**Fig. 22.1** Clusters of formation and disappearance of LPS during June-July 1984, 1985, 1988–1994 *Blue* – data points of formation of LPS. *Yellow* – data points of disappearance of LPS

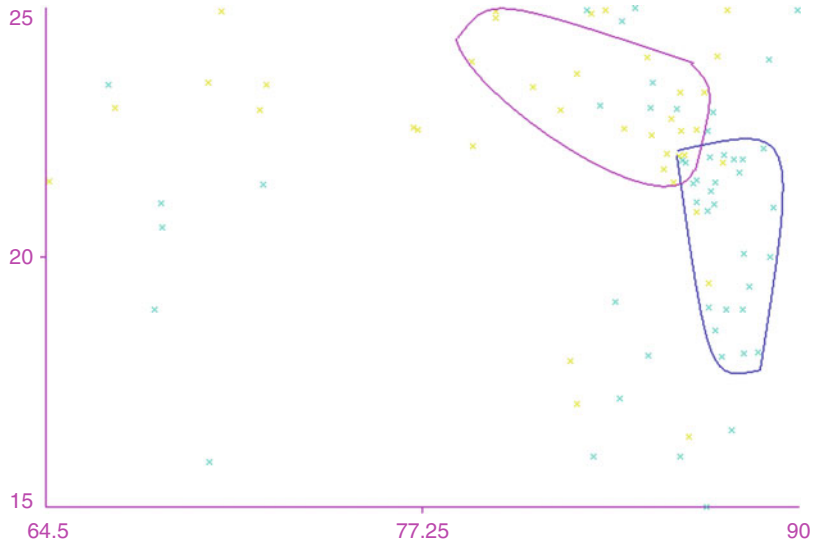


**Fig. 22.2** Clusters of formation and disappearance of LPS during June-July 1995–2004. *Blue* – data points of formation of LPS. *Yellow* – data points of disappearance of LPS

months of June-July and August-September separately, for a period of 9 years (year 1995–2003) are located as shown in Figs. 22.2 and 22.4 respectively. There is a strong resemblance between the location of clusters of formation and disappearance

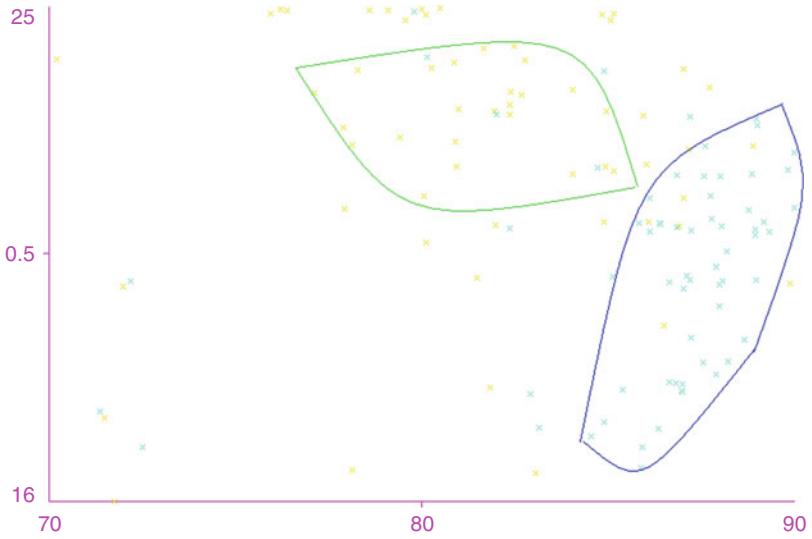


**Fig. 22.3** Clusters of formation and disappearance of LPS during Aug-Sept 1984, 1985, 1988–1994. *Blue* – data points of formation of LPS. *Yellow* – data points of disappearance of LPS

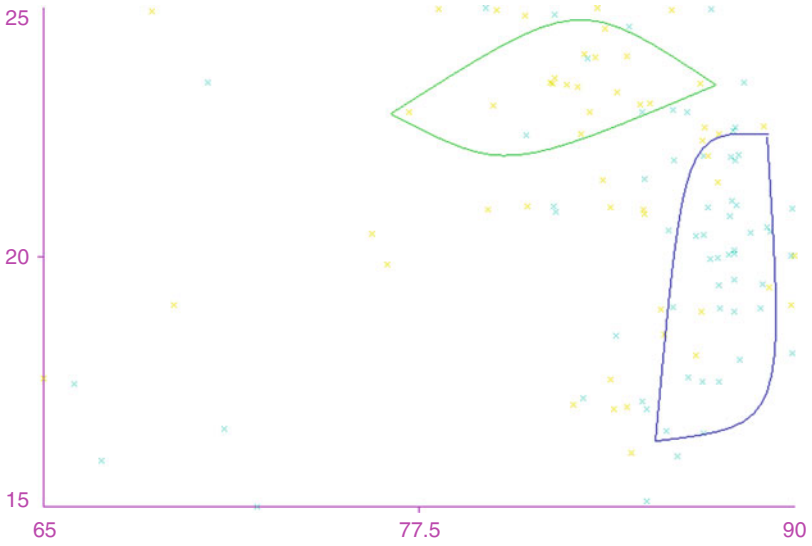


**Fig. 22.4** Clusters of formation and disappearance of LPS during Aug-Sept 1995–2004. *Blue* – data points of formation of LPS. *Yellow* – data points of disappearance of LPS

in Figs. 22.1 and 22.2, which is for Jun-July months. There is also a strong resemblance between the location of clusters of formation and disappearance in Figs. 22.3 and 22.4, which is for August-September months.

Hence the favored zones of formation and disappearance of LPS on a spatio-temporal scale, over Indian region during June to September have been identified.

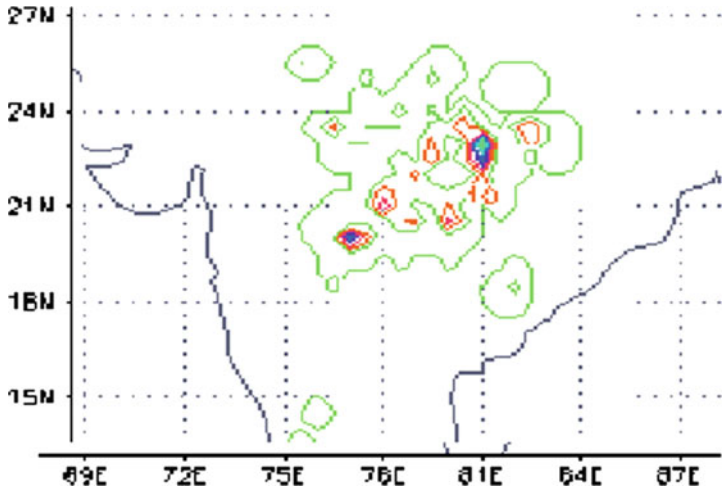


**Fig. 22.5** PCGrADs output contours for 1984 rainfall

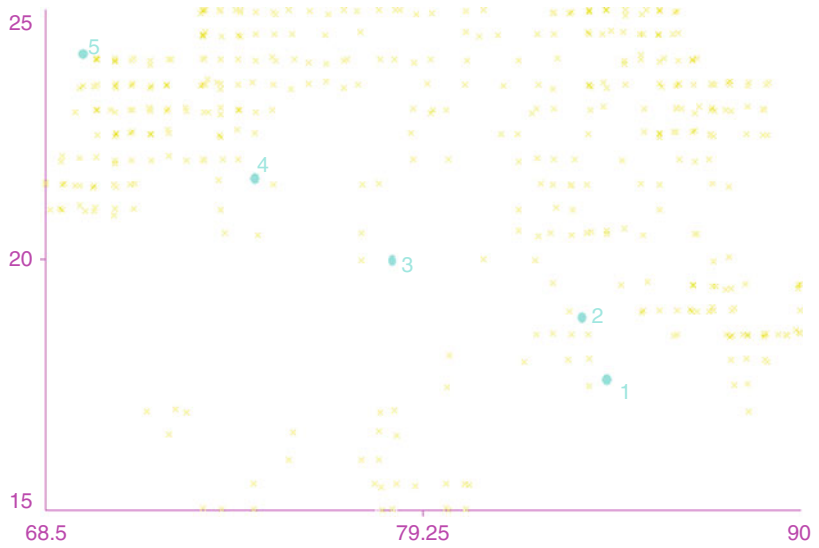


**Fig. 22.6** WEKA output Figures for rainfall on 10th Sept to 14th Sept, 1984 (Blue color circle shows LPS movement day-wise)

The contours displaying annual rainfall during the years 1984–2003 are generated using PCGrADS for the purpose of finding their association with the corresponding year's LPS formation. One such contour for the year 1984 is displayed in Fig. 22.5.

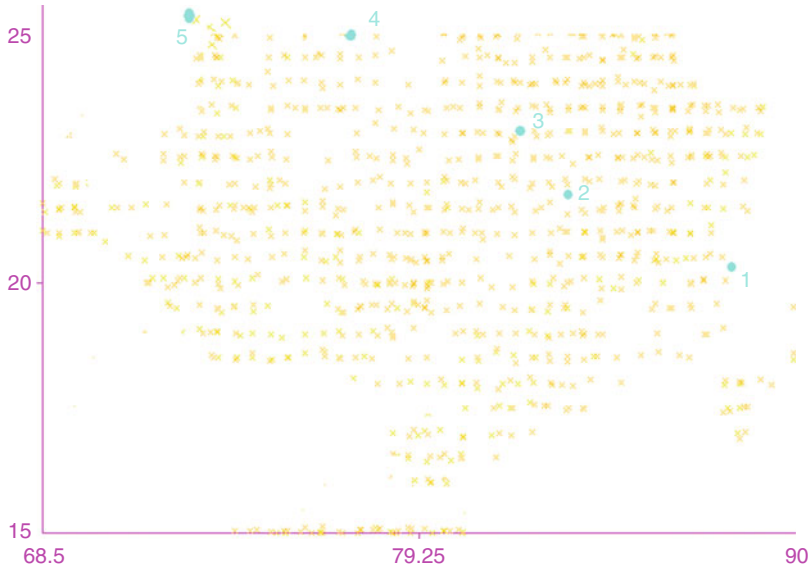


**Fig. 22.7** WEKA output Figures for rainfall on 1st Aug to 5th Aug, 1985 (Blue color circle shows LPS movement day-wise)

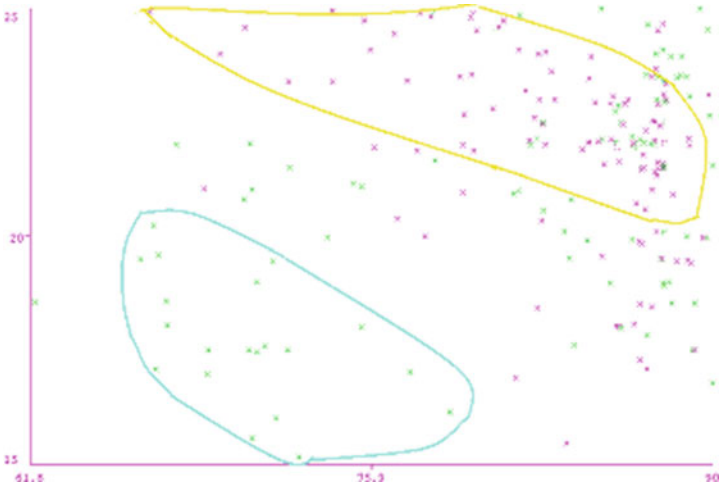

**Fig. 22.8** Clusters of LPS for 1984, 1985, 1988, 1989, 1990, 1991, 1992, 1993, 1994. Green represents LPS during June and Pink represents LPS during July

We have also generated clusters of rainfall on day-wise basis during the months of June to September for the years 1984–2004. One such cluster is shown in Fig. 22.4. These clusters and their corresponding values from excel sheet have helped devise a hypothesis that as the cluster moves from South-East to North-West during the months of August-September, it causes rainfall from North-West to South-East quadrants (as displayed in Figs. 22.6 and 22.7).

There is also an important finding that clusters of LPS move geographically from south to North corresponding to June to July. One such Figure is shown in Fig. 22.8.

## 22.5 Conclusions

There is a strong resemblance between the location of clusters of formation and disappearance in Figs. 22.1 and 22.2 which is for Jun-July months. There is also a strong resemblance between the location of clusters of formation and disappearance in Figs. 22.3 and 22.4 which is for August-September months. Hence the favored zones of formation on 1st day and disappearance of LPS on 3rd–5th day, on a spatio-temporal scale, over Indian region during June to September have been identified.

There is also an important finding that clusters of LPS move geographically from south to North corresponding to June to July. One such Figure is shown in Fig. 22.8.

The clusters of rainfall as shown in Figs. 22.6 and 22.7 and their corresponding values from excel sheet have helped devise a hypothesis that as the cluster moves from South-East to North-West during the months of August-September, it causes rainfall from North-West to South-East quadrant.

## 22.6 Future Scopes

Testing of hypothesis as drawn above is to be implemented within an appropriate data mining tool namely WEKA. This knowledge can also be verified and implemented using other data mining tools namely Tanagra and Rapidminer. The datasets being multidimensional can be manipulated to retrieve various reports by implementing OLAP cubes in Oracle 10 g or SQL Server 2005. The output provided by querying of the cubes may be input to data mining tools for association mining and hence new rules may be drawn.

**Acknowledgments** This study is based on the datasets made available by courtesy of Indian Meteorological Department, India. The author is thankful for the support and guidance provided by Dr. Rattan K. Datta, Former President - Indian Meteorological Society and Computer Society of India.

## References

Han J, Kamber M, Anthony K (2001) Spatial clustering methods in data mining: a survey. In: Geographic data mining. Taylor & Francis, London

Koperski K, Han J, Adhikary J (1998) Mining knowledge in geographical data. Commun ACM 26 (1):65–74

Mooley DA, Shukla J (1987) Characteristics of the westward – moving summer monsoon low pressure systems over the Indian region and their relationship with the monsoon rainfall. Center for Ocean-Land-Atmosphere Interactions, University of Maryland, College Park, MD

Ng R, Han J (1994) Efficient and effective clustering method for spatial data mining. In: Proceedings of international conference on very large databases, Santiago de Chile, Chile

Pabreja K (2005) Data mining techniques for spatio-temporal datasets with special reference to interpretation of weather patterns. In: International Brainstorming meeting on modeling and prediction over the Indian monsoon region-vision 2015

PCGrads software, tutorials. Available from:-http://www.iges.org/grads/

Sikka DR (2006) A study on the monsoon low pressure systems over the Indian region and their relationship with drought and excess monsoon seasonal rainfall, Center for Ocean-Land-Atmosphere Studies, Center for the Application of Research on the Environment, CTR - 217, May 2006, pp.60. Acc. No. COLA-21

Singh D, Ganju A, Singh A (2005) Weather prediction using nearest-neighbour model. Curr Sci 88 (8):1283–1289

Stojanova D, Panov P, Koblar A (2006) Learning to predict forest fires with different data mining techniques. Conference on data mining and data warehousing (SiKDD 2006), Ljubljana

Weka 3-Data mining with open source machine learning software Available from:- http://www.cs.waikato.ac.nz/ml/weka/.Accessed 3 Aug 2008

Witten IH, Frank E (2005) Data mining practical machine learning tools and techniques, 2nd edn. Morgan Kaufmann Publishers, San Francisco

# Chapter 23
# Information Systems as a Tool in Operational Agrometeorology: Applications to Irrigation Water Management in Emilia Romagna-Italy

**Federica Rossi**

**Abstract** Information systems are now widely used to support irrigation management in many Countries Interactive information systems facilitate the operation and management of irrigation systems and offer personalized forecasting to farmers, who are advised about the amount and timing of water supply to the different crops grown in their farms.

This paper reports about the current adaptation and mitigation tools in agricultural use of water adopted in Emilia Romagna, focusing on the use of information systems and the research applications in improving irrigation advices. Irrinet irrigation advisories is under revision, since research is involved to improve the degree of accuracy in estimation of actual evapotranspiration (ETc). Eddy covariance technique is used to measure Etc over a high water-demanding crop (kiwifruit orchard), allowing to calculated proper Kc values, to be used to improve irrigation advice to farmers.

## 23.1 Introduction

The development and the operational application of best practices for daily agriculture management are becoming more and more strategic to cope with climate changes and variability issues, and the concurrent needs for better use of strategic resources. Agrometeorology, as the synergic result of the integration of many sciences, has the intrinsic ability to provide substantial and relevant information for decision-makers to help preserve agricultural sustainability and environmental conservation.

F. Rossi (✉)
Consiglio Nazionale delle Ricerche, Institute of Biometeorology, Via P. Gobetti 101, 40129 Bologna, Italy
e-mail: f.rossi@ibimet.cnr.it

S.D. Attri et al. (eds.), *Challenges and Opportunities in Agrometeorology*,
DOI 10.1007/978-3-642-19360-6_23, 

Information systems are now widely used to support irrigation management in many Countries Efficient use of irrigation water is crucial in many countries due to a number of reasons, including weather conditions, crop stress, and cost of irrigation. Proper use of irrigation systems improve crop productivity and quality; improves control and efficiency of water use, especially when supplies are limited; reduces soil erosion on irrigation fields; and, increases income and/lowers production costs for farmers. Interactive information systems facilitate the operation and management of irrigation systems and offer personalized forecasting to farmers, who are advised about the amount and timing of water supply to the different crops grown in their farms.

The Mediterranean region has, in general, hot and dry summers that, mainly in the South and East areas impose significant irrigation requirements for many crops, winter crops and orchard included. Emilia Romagna, located in the Italian Po plane, is one of the European leading areas for fruit tree production. In this region, sector analyses indicate that for agriculture annual water consumption of 1.400 millions cubic meters over the 2.100 of available water, necessitating irrigation to meet the water requirements of the crops.

Surface water withdrawal is about 68% of the total, while 32% of the withdrawal (680 $Mm^3$/year) is from ground water. Ground water recharge may be even more seriously lowered by the predicted climate change. Serious subsidence problems and intrusion of sea water are occurring in many parts of the region, leading to major problems of soil salinity. Some areas have been classified as undergoing a trend toward desertification hazard.

Coping strategies include initiatives for demand management, many of them having the objective to reduce water supply to agriculture through more rational use recommendations. Local Authorities and Research Institutions are cooperating in developing information and educational programmes to encourage water saving, and in defining technical and agronomical approaches to address irrigation and to avoid water losses and overestimation of crop water consumption.

This paper reports about the current adaptation and mitigation tools in agricultural use of water adopted in Emilia Romagna, focusing on the use of information systems and the research applications in improving irrigation advices.

## 23.2 Best Management Practices for Water

A best practice may be defined as a practical, affordable approach to conserving water without sacrificing productivity, maximizing its use efficiency. Improvement of application efficiency (the ratio of water being withdrawn from a particular resource to the water available for target plant production) as well as resource conservation (efforts in reducing losses by a particular management or a system change) and saving (the ways to reduce use, improve application efficiency, re-utilize) are all part of the integrated management that is looked for in the region. The common

objective is the preservation of the target yield, namely quantity-quality, and the maintenance of traditional, high values agricultural vocational traits and landscape.

Technical and agronomic actions and suggestions are addressed both at basin and farm levels, and an increase of the efficiency of each of the virtual water chain processes is looked for. This increases the focus on the different steps of water transportation from the source to the field, including the efficiency of delivery to the farm, the efficiency within the farm including the efficiency of distribution systems till to physiological efficiency of the crops.

Dry farming techniques aim to conserve limited moisture during dry weather by reducing or even eliminating runoff and evaporation, thereby increasing soil absorption and retention of moisture. Deep ploughing, minimum tillage, weed control and mulching, adoption of windbreaks may all help in limiting evapotranspiration. Species selection (as early ripening varieties, drought resistant selections and rootstocks) may opportunely integrate management techniques as adoption of permanent water stress, controlled water stress, timing of irrigation during the more sensitive phases, applied when pertinent to the kind of crop and to local environmental and weather conditions.

## 23.3 The Information System IRRINET

The technical approach adopted to rationalize the use of water in Emilia Romagna is the irrigation advisory service provided to farmers via a system called Irrinet. Irrinet is a free-of-charge system managed by Consorzio di Bonifica per il Canale Emiliano Romagnolo (CER), aimed to support crop management with specific custom-built suggestions. CER is a consortium founded by the local authorities and from the different regional reclamation consortiums, that acts both as a water distributor and the most important water infrastructure, making water available through a channel from the Po River over a 3,000 $km^2$ area with a supply of 68 $m^3/s$ .

The first version of Irrinet was established in 1984 by using public founding to test telematics in agriculture (Videotex), and evolved in a Web interface in 1999. GIS extensions and advanced WEB interfaces were provided in 2002, and in 2003 Web plus SMS (IrriSMS) service started. So far, the advisories provided by Irrinet involve more than 9,000 farms, covering almost 25% of the irrigated area in the region, and the amount of farmers utilizing the service is constantly increasing.

The software details the irrigation advisories for the main crops grown in the region on the basis of water balance, calculated utilizing meteorological data (rain and evapotranspiration) provided by the Regional Meteorological Service, soil data by Regional Geological Service and crop parameters collected by the CER technical service during over 30 years of local experimentation. The suggestion about water amount needed and proper timing of irrigation is supported by graphs showing the trend of soil humidity from the beginning of the irrigation season.

The plant and soil model algorithm are shown in Figs. 23.1 and 23.2, and allow several calculations. For example, the amount of the actual infiltration of rain water

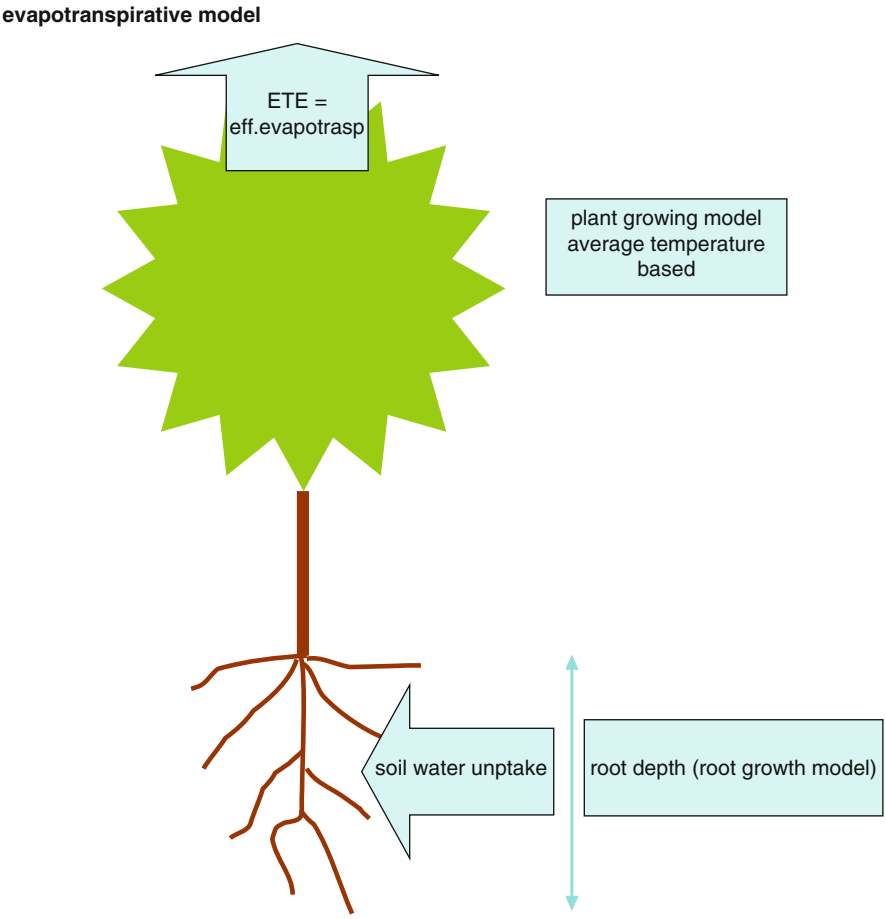


**Fig. 23.1** The plant evapotranspirative model, including algorithms on plant and root growth

in the soil, the simulation of root growth and the phenological development of crops, the estimation of stress status, the estimation of water table uptake, the calculation of water flow through soil layers, the real time simulation of the amount of water needed at root level may be provided.

Farmers may register to become full time users and archive their own farm data, that are definitely stored into the system, or may have access as anonymous users. Farmers regulated by Reg. CE 1257 on sustainable agriculture that follow Irrinet guidelines are recognized to obey to the rules of water management and are automatically certified. Some limitation to the diffusion of Irrinet to a larger amount of farmers still comes from the need to have a PC connected to internet. To expand the IrriWeb users and to better manage less interactive users, the SMS service is also active. This service has shown to bring several advantages also to regular users, too, since they do not need to access to the net for getting the irrigation scheduling,

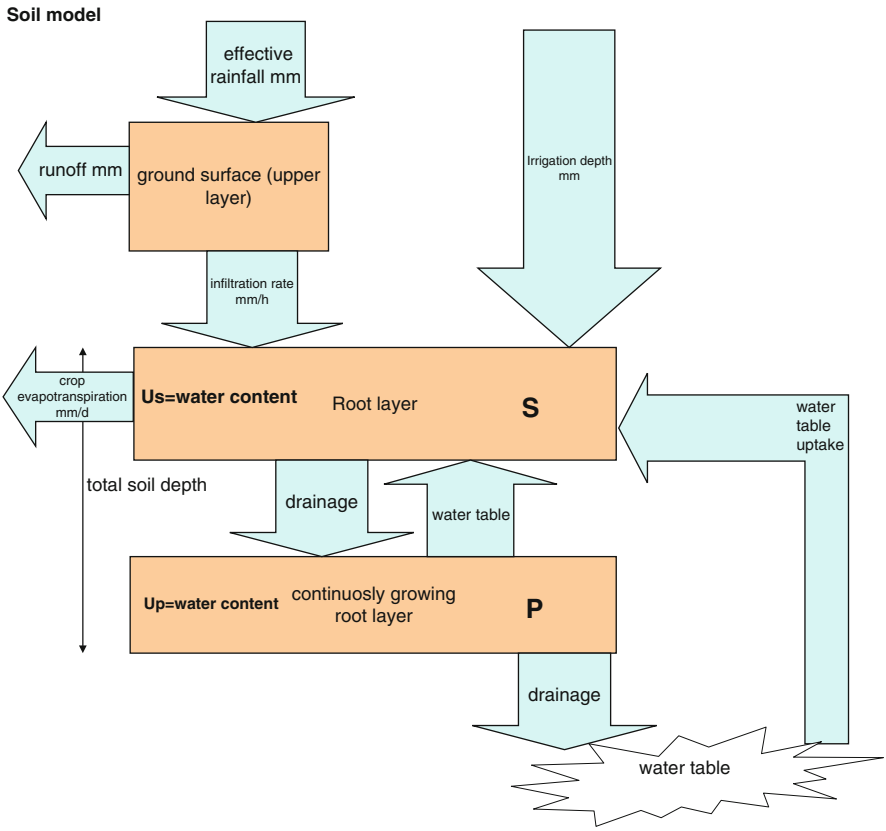


**Fig. 23.2** The scheme of the soil model module of IRRINET

and it has demonstrated to be flexible also in providing additional information like meteorological warning/disease alarms or advertising/technological updates.

In 2008, Anonymous unique users were 354, with 1.135 provided real-time irrigation scheduling; Registered users 1,056, with 25.582 real-time irrigation scheduling provided, the number of IrriSMS users was 140, with 10.994 SMS sent. In addition, almost 5,000 farmers are connected to a single Land Reclamation Bureau that directly provides the service to its associated. This is the Bureau Parmigiana Moglie, that covers a surface (partly plain, partly hilly) of about 215.000 ha, and includes 46 Municipalities belonging to provinces of Reggio Emilia, Modena and Mantova. Much of the area consists of farms growing natural meadows and mixed permanent meadows for fresh forage for dairy cows with milk destined to the production of Parmigiano-Reggiano (Parmesan) cheese. The regulation for feed rationing is strictly regulated since in the feeding of dairy cows a minimum of at least 35% of dry matter must be supplied by forage produced on the farm; and at least 75% by forage coming from the Region of Origin. Farms are considered suitable if having an area/cattle ratio of at least 0.33 ha per lactation cow in the plains and 0.50 ha in the

mountains. Should the farm area be less, the farmer must provide the necessary documentation proving the origin of the forage purchased.

Parmigiano Reggiano is recognized as one of the main Italian products and it is strictly bound to its place of origin (PDO), ideal environmental unit for its agricultural and cattle breeding traditions, from which the special qualities of the milk (needing a high content of casein) are derived. Meadow irrigation is an indispensable tool to ensure and maintain the stability of production of this high-values cheese. Irrinet produces advisories directly to the bureau, through which a Call Center operates to book and to distribute water (also directly opening the bulkheads of channels), indicating to each farm how much water is needed. The service is consulted 5,000 times a year.

In 2007, in total for the whole region, the application of Irrinet allowed an estimated water saving of more than 50 millions $m^3$.

## 23.4 Research Development for Irrinet Improvements

Further improvement of Irrinet irrigation advisories is necessary to enhance water savings techniques for local and general needs. Research is involved to improve the degree of accuracy in estimation of actual evapotranspiration (ETc) of many crops. As suggested in Allen et al. (1998), the calculation procedure of Etc in Irrinet consists of: identifying the crop growth stages, determining their lengths, and selecting the corresponding Kc coefficients; adjusting the selected Kc for frequency of wetting or climatic conditions during the stage; constructing the crop coefficient curve (Kc values determination for any period during the growing period); and calculating ETc as the product of ETo and Kc. ETo is calculated according to Penman-Montheith (P-M) model P-M is largely accepted for operational applications for its simplicity (Rana and Katerji 2000), but it has been criticized mainly for the contestable meaning of canopy resistance (Brutsaert 1982) and for not taking in account canopy architecture (Perrier 1975). Proper evapotranspiration fluxes measurements are under realization for some of the main crops with the finale purpose to adopt more properly, locally- derived, Kc.

Orchards are particularly interesting due to the prominent regional vocation on fruit tree production and the high amount of agricultural surfaces utilized for these crops. Irrigation optimization is very important under both environmental respect and farming purposes point of view, and a great concern is going to definitely maintain different crops in the pronest areas in order to limit production costs and impacts and facilitate crop management.

To make an example, Italy is the world's leading country in kiwifruit production. The presence of Actinidia deliciosa (kiwifruit) has been progressively increasing in Emilia Romagna, as this species is very suitable to local pedology and climate conditions. Actinidia, is, however, a very high water demanding crop (6,800 $m^3$/ha on average), so a proper estimation of water actually consumed in different areas is very urgent.

### 23.4.1 An Example: Eddy Covariance Applied to Kiwifruit Evapotranspiration Measurements

In 2008, the first-year micrometeorological measurements have been carried out over a representative kiwifruit-grown surface (cv. Hayward) trained at a T-shape, 3 × 5 spacing, drip irrigated with 4 emitters/plant (4 l/h each, total 16 l/h/plant) to assess orchard heat and evapotranspiration fluxes through the eddy covariance technique.

Between the two main growing areas of Actinidia, the hilly zone was selected for this first approach, due to increasing drought and desertification hazards assessed in one of the main growing areas of this crop (Valle Lamone Marzeno), in which impacts due to extensive agricultural water use are currently considered and mitigation measures under discussion.

Due to inhomogeneous landscape features, eddy covariance data quality check and control was particularly careful (three axis rotations of the anemometer was performed, and footprint analysis ensured the representativeness of fluxes) to best provide correctness of the measurements. Wind velocity and temperature fluctuations were measured by a three dimensional sonic anemometer (CSAT3-3D, Campbell Sci., USA). Water vapour concentration was measured by an open-path, infrared absorption gas analyser (IRGA) LI7500 (LiCor Inc, Lincoln, NE, USA). These instruments were installed at 5 m height from the ground (at about twice average tree height) on a mast located in a nearly central position of the orchard. On the top of the same mast, a net radiometer (NR Lite, Campbell Sci., USA) was placed to measure the net available energy at the surface. Heat flux in the soil was measured through three soil heat flux plates (HFP01, Campbell Sci., USA) placed at a depth of 5 cm in three different points at the same distance from the girth of the mast. Wind, water vapor and temperature were sampled at 10 Hz and stored on a data logger (CR1000, Campbell Sci.).

Eddy covariance post-processing was done to obtain 30-minute averages of fluxes.

Energy balance equation:

$$Rn = \lambda E + H + G$$

(where Rn is net radiation, λE is the latent heat flux of evapotranspiration, H the sensible heat flux and G the ground heat flux) was solved and the closure of the balance is shown for all the months in Fig. 23.3 to demonstrate the quality of the data collected.

Effective ETc of kiwifruit (mm/d) was calculated by dividing λE by the latent heat of water vaporization λ (2.45 MJ $kg^{-1}$). Then, a comparison between measured effective Etc and the potential ETs calculated following P-M- (where meteo data were from the e.c station), and following Hargreaves and Samani (1985) (where meteo data were from meteorological service data base) was done (Fig. 23.4), and Kc calculated accordingly. Temporal trends of both these coefficients together with

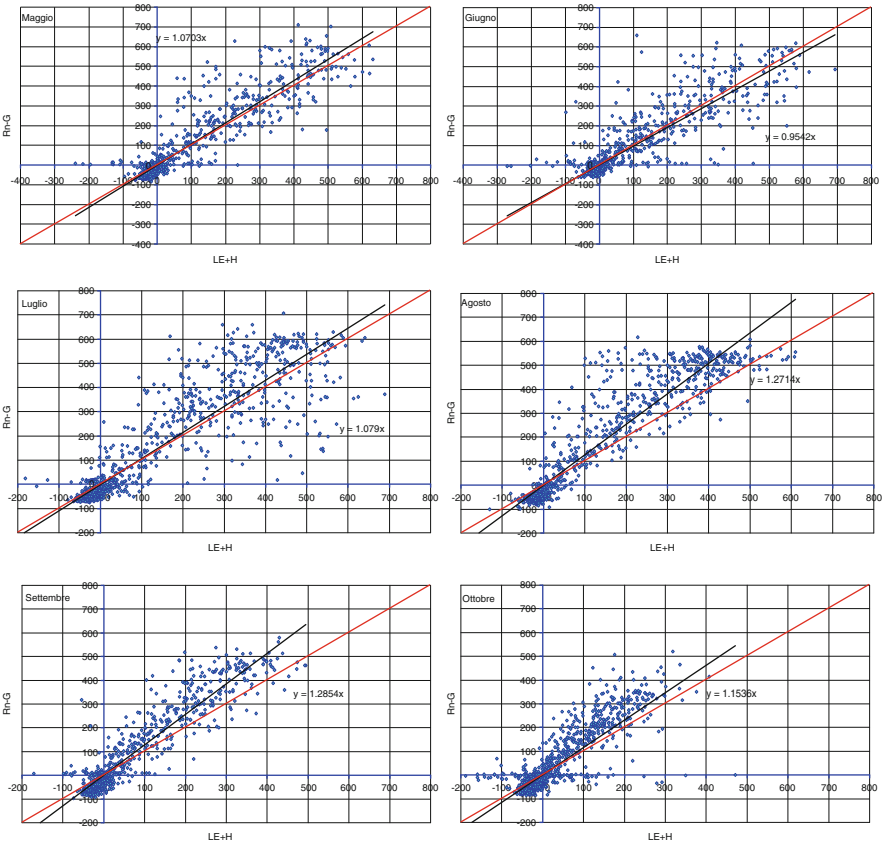


**Fig. 23.3** Energy balance closure in the different months of measurements

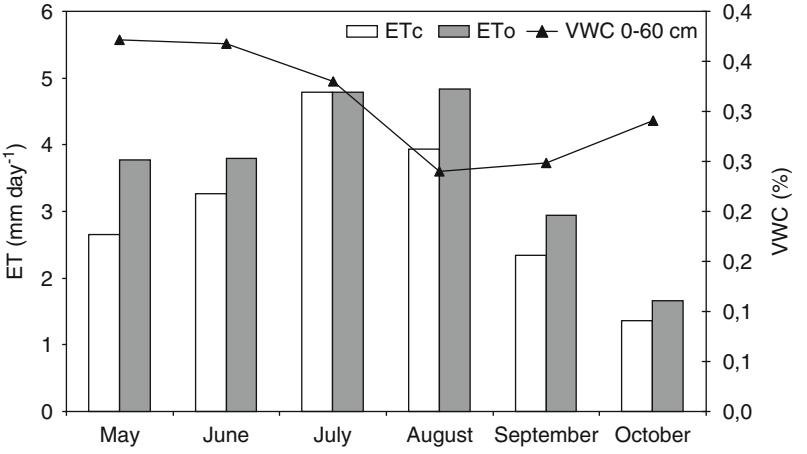


**Fig. 23.4** Measured crop evapotranspiration and reference evapotranspiration calculated in the different months, shown together with soil water content monitored by FDR sensors

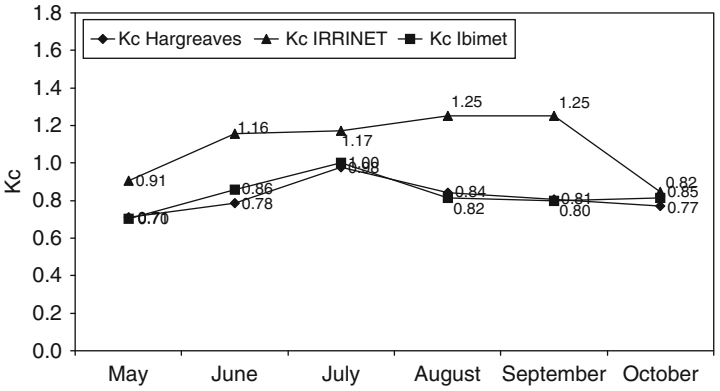


**Fig. 23.5** Trends of calculated Kc: Kc Ibimet is obtained by dividing Etc measured by eddy covariance crop evapotranspiration by ET0 calculated by P-M, Kc Hargreaves by ET0 calculated following Hargreaves, Kc Irrinet is the value embedded into the Irrinet advice programme

the values actually present in Irrinet are reported in Fig. 23.5. From the results obtained during this first year of observations, Kc values included in Irrinet appear higher throughout the whole season with respect to those obtained by our measurement. These last appear more congruent to suggest a correct water supply through irrigation in kiwifruit, at least in a representative hilly area avoiding dissipation due to an overestimation of crop evapotranspiration. Also, the use of Hargreaves formulation (1985) to derive ETo, in the tested condition, showed to suit well the results obtained by applying the more complex P-M.

## 23.5 Conclusions

Irrinet has been demonstrating, in its temporal evolution, to be a credible informative system to disseminate irrigation advisories, both under its technical content and diffusion aspects. Its operational applications have increased with time, and the system is reaching more and more farmers due to the progressive increase of diffusion of the net in the countryside and to the integration of mobile telephony facilities. Also, the way to present irrigation advisories (personalized and simple) appears to be sufficiently user-friendly to appeal to farmers (Rossi et al. 2004). Scientific support to check and possibly improve all aspects of the system is being reviewed. Actual ETc is under direct evaluation in the most water demanding agricultural systems. In 2009, for example, measurements will be repeated for one more growing season over kiwifruit grown in the hill, and similar measurements will start over the same species grown in the plane, to complete the local overview of water consumption. Spatial and temporal variability might be then considered in driving irrigation needs for such high demanding species. Furthermore, direct evaluation of evapotranspiration may offer useful information for environmental networks.

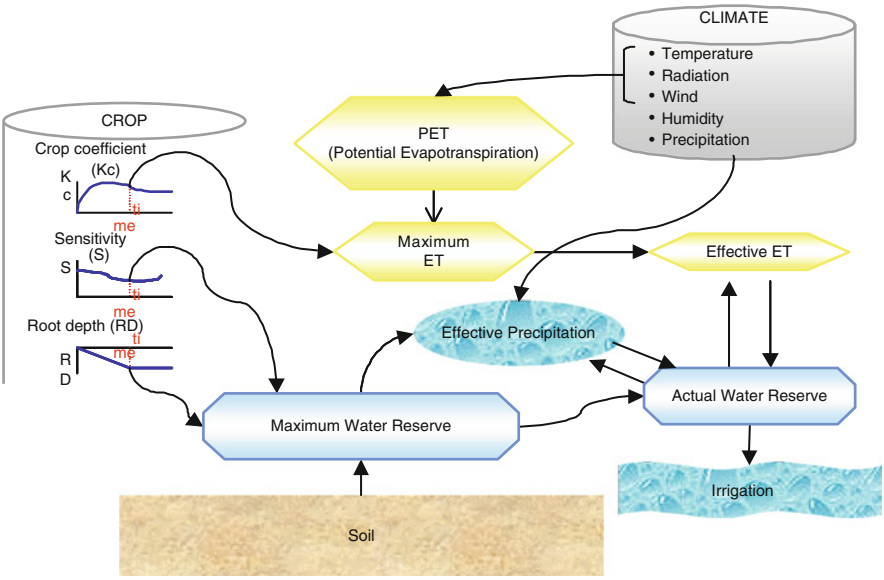


**Fig. 23.6** The scheme of the water balance model criteria

Locally determined Kc values may also, in fact, implement Criteria. Criteria is the soil water balance model developed for

Emilia Romagna (Marletto et al. 2001) (Fig. 23.6), that addresses local plans for water preservation and saving at basin level.

The example from Irrinet has been followed by many other Italian regions, that have developed their own interactive systems to provide farmers with irrigation advisories. Sicilia, for example, suffers from severe summer droughts which make irrigation indispensable for the majority of crops. The Kc coefficients embedded into Irrisias system, developed by Siciliana region, are also under revision, and direct monitoring of actual evapotranspiration through micrometeorological methods (eddy covariance, surface renewal, scintillometry) are carried out in the main high value orchard crops i.e. olive in Trapani area and orange in Catania plane. Further scaling up of the information to regional scale (Glenn et al. 2007) is also provided in several contexts of the Country. Local calibration of Kc will allow better quantification of crop needs at catchment scale in different regions of the Country, offering a concrete service to farmers and stakeholders.

**Acknowledgement** Drs. Paolo Mannini, Stefano Anconelli, Roberto Genovesi from CER Emilia Romagna are the persons who created and are supporting future development of Irrinet system. Thanks are due to Drs. Osvaldo Facini, Marianna Nardino, Teodoro Georgiadis of CNR- IBIMET for the collaboration in eddy covariance measurements, and to Dr. Raymond Motha, USDA, for the friendship and the suggestions.

## References

Allen GA, Pereira LS, Raes D, Smith (1998) Crop evapotranspiration – guidelines for computing crop water requirements – FAO Irrigation and drainage paper 56, FAO, Rome

Brutsaert WH (1982) Evaporation in the atmosphere: theory, history and applications. D. Reidel Publ, Dordrecht

Glenn EP, Huete AR, Nagler P, Hirschboeck KK, Brown P (2007) Integrating remote sensing and ground methods to estimate evapotranspiration. Crit Rev Plant Sci 26(3):139–168

Hargreaves GH, Samani ZA (1985) Reference crop evapotranspiration from temperature. Appl Eng Agric 1:96–99

Marletto V, Zinoni F, Criscuolo L, Fontana G, Marchesi S, Morgillo A, van Soethendal M, Ceotto E, Andersen U (2001) Evaluation of downscaled DEMETER multi-model ensemble seasonal hindcasts in a northern Italy location by means of a model of wheat growth and soil water balance. Tellus 57A:488–497

Perrier A (1975) Etude physique de l'évapotranspiration dans les conditions naturelles. Parts I, II, III Ann Agron 26: 1–16, 105–123, 229–243

Rana G, Katerji N (2000) Measurements and estimation of actual evapotraspiration in the field under mediterranean climate: a review. Eur J Agron 13:125–153

Rossi F, Nardino M, Genovesi R, Mannini P (2004) Irrinet emilia romagna: on-line decision support on irrigation. In: Online agrometeorological applications with decision support on the farm level. Dina Research Report No. 109, Tjiele

# Chapter 24
# Impact of Climate Change on Crop Water Requirements and Adaptation Strategies

**V.U.M. Rao, A.V.M. S. Rao, G.G.S.N. Rao, T. Satyanarayana, N. Manikandan, and B. Venkateshwarlu**

**Abstract** Water is an important for all forms of life and it is becoming scarce natural resource in the future owing to climate variability / change which aggravates the situation. Water resources are inextricably linked with climate. Climate change and variability would be the principal source of fluctuation in global food production, particularly in the semi-arid tropical countries of the developing world. In conjunction with other physical, social and political-economic factors, climate variability contributes to vulnerability to economic loss, hunger, famine and dislocation in the developing countries. Climate change impact studies reveal that annual average river runoff and water availability are projected to increase by 10–40% at high latitudes and in some wet tropical areas, and decrease by 10–30% over some dry regions at mid-latitudes and in the dry tropics. Crop water availability shortage and excess affects the growth and development of the plants, yields and quality of produces. Climate change, which affect the water availability resources, which in turn affect agriculture in many ways. For instance in soil plant processes with an increase in soil water deficit by changes in soil water balance. Long term climate change and its effect on crop water requirements of major cereal crops like wheat, maize, sorghum and millet in 1990, 2020 and 2050 were estimated by FAO CROPWAT program and the adaptation strategies to be taken to combat climate change effect were also discussed in this paper.

## 24.1 Introduction

Water is an important for all forms of life and is becoming scarce natural resource in the future owing to climate variability / change. It is crucial for crop production and best use of available water must be made for efficient crop production and high

V.U.M. Rao (✉) • A.V.M.S. Rao • G.G.S.N. Rao • T. Satyanarayana • N. Manikandan • B. Venkateshwarlu
Central Research Institute for Dryland Agriculture, Hyderabad, AP 500 059, USA
e-mail: vumrao54@yahoo.com

S.D. Attri et al. (eds.), *Challenges and Opportunities in Agrometeorology*,
DOI 10.1007/978-3-642-19360-6_24, 

yields. The relationships between crop, climate, water and soil are complex and many biological, physiological, physical and chemical processes are involved. Knowledge on reliable estimates of water required by different crops in a given set of climatological conditions of a region is great help in rational utilization of irrigation water for irrigation scheduling, planning of irrigation schemes and effective design of water saving and management systems. The average global surface temperature is projected to increase by 1.4–3°C from 1990 to 2100 for low-emission scenarios and 2.5–5.8°C for higher emission scenarios of greenhouse gases in the atmosphere (Mall et al. 2006). Warming of climate is observed over the past several decades and is consistently associated with changes in a number of components of the hydrological cycle and hydrological systems such as: changing precipitation patterns, intensity and extremes; increasing atmospheric water vapour; increasing evaporation; and changes in soil moisture and runoff. There is still substantial uncertainty in trends of hydrological variables because of large regional differences, and because of limitations in the spatial and temporal coverage of monitoring networks (Huntington 2006). The investigation by McCabe and Wolock (1992), based on an irrigation model, concluded that the increase in mean annual water use is strongly associated with the increase in temperature. On the other hand, the natural resource base of agriculture, is shrinking and degrading, and also adversely affecting production capacity of the ecosystem. However, demand for agriculture is rising rapidly with rise in population and per capita income and growing demand from industry sector.

India shares about 16% of the global population and 2.3% of global land but it has only 4.2% of the total fresh water resources from rainfall, ground water and rivers and per capita availability of water resources is about 4–6 times less as compared to world average. As per the government of India statistics of 2005–06, the net area sown is 142 Mha; whereas net irrigated area is only 60 Mha. Major part of the Indian food grain production comes from irrigated areas. Apart from that, the rainfed farming practiced in over 87 million ha area of the country contributes 40% of food supports of human and 60% of livestock population. But at the same time, it will not be possible to provide irrigation for more than half the cultivated area in the foreseeable future (Katyal 1998).

Monsoon is the most important climatic phenomenon occurring in the Indian subcontinent and the adjoining regions. It forms the backbone of Indian economy; a high degree of correlation exists between monsoon rainfall and agricultural Production. Almost 65–70% of annual rainfall in India is mainly received from southwest monsoon (June-September). Deficit or failure of southwest monsoon put tremendous pressure on the water resources and food basket of the Country. The impact of variability of the monsoon rainfall on the food grain production has remained large throughout the last century, despite the Green Revolution over the Indian region, (Abrol 1996; Gadgil et al. 1999). Thus, it is imperative that to study the potential impact of climate change on water requirements of crops and to evolve suitable policies for development of water resources and irrigation systems in the context of climate change scenarios. In India per capita surface water availability in

the years 1991 and 2001 were 2,309 and 1,902 $m^3$ and these are projected to reduce to 1,401 and 1,191 $m^3$ by the years 2025 and 2050 respectively (Kumar et al. 2005). Therefore, there is a need for proper planning, development of water resources for sustaining food grain production and livelihood of peasants living across India. The present study aimed to estimate the crop water requirements during 1990, 2020 and 2050 for the important cereal crops like wheat, maize, sorghum and millet and adaptation strategies also discussed.

## 24.2 Material and Methods

The crop water requirements (CWR) of crops under study were calculated using CROPWAT 4 Windows v 4.3 (Smith 1992, 1993). This program uses the FAO Penman-Monteith method (Allen et al. 1998) for calculating reference evapotranspiration (ETo). The crop coefficient (Kc) values were taken from the CROPWAT software. These coefficients present the relationship between references (ETo) and crop evapotranspiration (ETcrop) or ET crop = Kc * ETo. Value of Kc varies with the crop, stage of growth, growing season and the prevailing weather conditions.

The required weather input files (Normal monthly weather data files for the period 1961–90 for maximum and minimum temperature, relative humidity, wind speed, sunshine hours and rainfall) for CROPWAT programme have been collected from FAO database software New_LocClimV1.1 (FAO 2005) for the stations under study.

To generate weather data files for 2020 and 2050, HadCM3 GCM (Global Circulation Model) output was used and by using this weather data files, crop water requirements for 2020 and 2050 was estimated. The data on district-wise area (from 1999 to 2006) for all crops taken for study has been collected from website of Directorate of Economics and Statistics, New Delhi.

## 24.3 Results and Discussions

The results of crop water requirements analysis revealed that sizeable increase in water requirement is seen for wheat, maize, sorghum and millet crops during 2020 and 2050 when compared to 1990. However, there is significant differences have been noticed in the percent increase in crop water requirement and reference evapotranspiration (ETo) among the stations selected for this study and values are furnished in the tables. It is significant to note at this point is projections of water demands of India for the year 2025 and 2050 which is worked out by IWMI said that even with lower estimates projected by IWMI, there shall be substantial future increase in irrigation water requirements (Sharma 2006).

In general, the crop water requirement and reference evapotranspiration is high in early sown crop and less in late of sown crop i.e., 1 week before and after from the normal date of sowing except for wheat. It can be attributed that in general late sown crop in rabi season will have shorter crop duration than early sown crop. In addition to this, reduction in temperature and high relative humidity also reduces the reference evapotranspiration and crop water requirements. In the case of wheat (being a winter/rabi season) the crop water requirements are low for early sowing crop than the late sowing crop, as the reproductive stage of late sowing crop would coincide the summer period. Besides this, it can be noted here that the NATCOM reported that warming is relatively more during post monsoon and winter season, which is coinciding with the crop-growing season of wheat.

### *24.3.1 Crop Water Requirement and Reference Evapotranspiration for Wheat*

Crop water requirement and reference crop evapotranspiration of wheat for the base year 1990 is more at Hardoi (447–503 mm and 534–599 mm) followed by Vidisha and Sangrur (Table 24.1). It was less at Ganganagar (262–303 mm and

**Table 24.1** Crop water requirement and reference crop evapotranspiration for wheat during 1990, 2020 and 2050

| | 1990 | | 2020 | | 2050 | |
|---|---|---|---|---|---|---|
| Date of sowing | CWR | ETo | CWR | ETo | CWR | ETo |
| **Hardoi (Uttar Pradesh)** | | | | | | |
| 15-Nov | 447.2 | 538.8 | 459.6 (2.8) | 552.9 (2.6) | 473.4 (5.9) | 571.6 (6.1) |
| 22-Nov | 475.0 | 568.2 | 488.2 (2.8) | 583.3 (2.7) | 502.2 (5.7) | 602.1 (6.0) |
| 29-Nov | 503.1 | 599.1 | 516.9 (2.7) | 615.2 (2.7) | 531.3 (5.6) | 634.1 (5.8) |
| **Vidisha (Madhya Pradesh)** | | | | | | |
| 20-Oct | 415.8 | 526.7 | 425.0 (2.2) | 537.3 (2.0) | 438.6 (5.5) | 556.4 (5.6) |
| 27-Oct | 437.1 | 547.3 | 446.9 (2.3) | 558.8 (2.1) | 460.4 (5.3) | 577.6 (5.5) |
| 04-Nov | 462.5 | 573.0 | 473.2 (2.3) | 585.4 (2.2) | 486.5 (5.2) | 604.0 (5.4) |
| **Sangrur (Punjab)** | | | | | | |
| 20-Oct | 368.1 | 476.9 | 381.3 (3.6) | 491.3 (3.0) | 392.0 (6.5) | 506.0 (6.1) |
| 27-Oct | 391.1 | 496.2 | 405.4 (3.7) | 512.0 (3.2) | 416.3 (6.4) | 526.8 (6.2) |
| 04-Nov | 420.4 | 522.5 | 435.9 (3.7) | 539.9 (3.3) | 447.1 (6.3) | 554.9 (6.2) |
| **Sirsa (Haryana)** | | | | | | |
| 20-Oct | 264.6 | 357.9 | 275.2 (4.0) | 370.0 (3.4) | 283.3 (7.1) | 381.4 (6.6) |
| 27-Oct | 281.8 | 369.1 | 293.1 (4.0) | 382.1 (3.5) | 301.4 (7.0) | 393.5 (6.6) |
| 04-Nov | 305.8 | 387.8 | 317.8 (4.0) | 401.9 (3.6) | 326.4 (6.8) | 413.4 (6.6) |
| **Ganganagar (Rajasthan)** | | | | | | |
| 20-Oct | 261.6 | 353.7 | 272.3 (4.1) | 366.0 (3.5) | 280.0 (7.0) | 376.9 (6.5) |
| 27-Oct | 278.9 | 365.0 | 290.3 (4.1) | 378.3 (3.6) | 298.2 (6.9) | 389.1 (6.6) |
| 04-Nov | 303.0 | 383.9 | 315.2 (4.0) | 398.1 (3.7) | 323.4 (6.7) | 409.1 (6.6) |

Figures in parenthesis are percentage increase in crop water requirement and reference evapotranspiration over 1990 values

354–384 mm) and at Sirsa (265–306 mm and 358–388 mm). The percentage increase in crop water requirement and reference evapotranspiration is high at Sirsa and Ganganagar in 2020 (4–4.1% and 3.4–3.7%) and in 2050 (6.7–7.1% and 6.5–6.6%) when compared to base line year 1990 data. The increase is minimum at Vidisha (2.2–2.3% and 2.0–2.2%) in 2020 and in 2050 (5.2–5.5% and 5.4–5.6%). Though the absolute amount of crop water requirement and reference evapotranspiration is low at Ganganagar and Sirsa in 1990, the percentage increase is more in 2020 and 2050 at these places.

### *24.3.2 Crop Water Requirement and Reference Evapotranspiration for Sorghum*

The highest crop water requirement and reference crop evapotranspiration for sorghum in 1990 is noticed at Mahabubnagar (369–399 mm and 532–573 mm) followed by Khargaon and Solapur (Table 24.2). The lowest values are seen at Surat (305–313 mm and 427–439 mm) and in Banda.

**Table 24.2** Crop water requirement and reference crop evapotranspiration for sorghum during 1990, 2020 and 2050

| | 1990 | | 2020 | | 2050 | |
|---|---|---|---|---|---|---|
| Date of sowing | CWR | ETo | CWR | ETo | CWR | ETo |
| **Solapur (Maharashtra)** | | | | | | |
| 25-Jun | 349.3 | 482.3 | 379.5 (8.7) | 535.4 (11.0) | 407.1 (16.6) | 574.4 (19.1) |
| 02-Jul | 348.8 | 481.2 | 373.2 (7.0) | 526.0 (9.3) | 399.9 (14.7) | 563.7 (17.1) |
| 09-Jul | 348.4 | 480.5 | 367.7 (5.5) | 517.4 (7.7) | 393.3 (12.9) | 553.9 (15.3) |
| **Khargaon (Madhya Pradesh)** | | | | | | |
| 25-Jun | 366.6 | 531.7 | 371.5 (1.3) | 538.6 (1.3) | 380.6 (3.8) | 551.5 (3.7) |
| 02-Jul | 350.3 | 509.3 | 355.1 (1.4) | 516.0 (1.3) | 364.1 (3.9) | 528.7 (3.8) |
| 09-Jul | 334.7 | 487.6 | 339.6 (1.4) | 494.3 (1.4) | 348.3 (4.1) | 506.8 (3.9) |
| **Mahabubnagar (Andhra Pradesh)** | | | | | | |
| 25-Jun | 398.8 | 573.2 | 409.6 (2.7) | 588.8 (2.7) | 424.6 (6.5) | 609.0 (6.2) |
| 02-Jul | 383.4 | 552.4 | 393.7 (2.7) | 567.3 (2.7) | 409.1 (6.7) | 587.9 (6.4) |
| 09-Jul | 368.6 | 532.0 | 378.4 (2.7) | 546.3 (2.7) | 394.0 (6.9) | 564.2 (6.0) |
| **Banda (Uttar Pradesh)** | | | | | | |
| 25-Jun | 343.9 | 497.4 | 345.8 (0.5) | 505.7 (1.7) | 364.5 (6.0) | 526.2 (5.8) |
| 02-Jul | 326.7 | 474.9 | 332.5 (1.8) | 483.1 (1.7) | 347.0 (6.2) | 503.3 (6.0) |
| 09-Jul | 309.5 | 452.2 | 315.3 (1.9) | 460.3 (1.8) | 329.6 (6.5) | 480.2 (6.2) |
| **Surat (Gujarat)** | | | | | | |
| 25-Jun | 313.1 | 439.3 | 318.6 (1.8) | 447.0 (1.7) | 326.0 (4.1) | 457.4 (4.1) |
| 02-Jul | 308.9 | 432.9 | 314.3 (1.8) | 440.5 (1.8) | 321.7 (4.1) | 450.8 (4.1) |
| 09-Jul | 305.1 | 427.1 | 310.5 (1.8) | 434.6 (1.8) | 317.8 (4.2) | 444.7 (4.1) |

Figures in parenthesis are percentage increase in crop water requirement and reference evapotranspiration over 1990 values

The percentage increase in crop water requirement and reference evapotranspiration is found maximum at Solapur during 2020 (5.5–8.7% and 7.7–11.0%) and 2050 (12.9–16.6% and 15.3–19.1%) when compared to base line year 1990 data. The increase is minimum at Banda (0.5–1.9% and 1.7–1.8%) during 2020 and at Khargaon (3.8–4.1% and 3.7–3.9%) during 2050.

### *24.3.3 Crop Water Requirement and Reference Evapotranspiration for Maize*

Crop water requirement and reference crop evapotranspiration of maize is high at Jhabua (404–447 mm and 517–539 mm) followed by Udaipur and Karimnagar for the year 1990. It is less at Begusarai (353–388 mm and 449–489 mm) followed by Bahraich (Table 24.3). The percentage increase in crop water requirement and reference evapotranspiration is found maximum at Karimnagar in 2020 (2.0–2.1% and 2.0%) and at Begusarai (5.1–5.5% and 5.1–5.4%) in 2050 when compared to base line year 1990 data. The increase is minimum at Udaipur (0.9–1% and 0.9–1%) in 2020 and 2050 (3.1–3.2% and 3.1–3.2%).

**Table 24.3** Crop water requirement and reference crop evapotranspiration for maize during 1990, 2020 and 2050

| | 1990 | | 2020 | | 2050 | |
|---|---|---|---|---|---|---|
| Date of sowing | CWR | ETo | CWR | ETo | CWR | ETo |
| **Udaipur (Rajasthan)** | | | | | | |
| 25-Jun | 407.7 | 512.0 | 411.4 (0.9) | 516.7 (0.9) | 420.3 (3.1) | 527.7 (3.1) |
| 02-Jul | 388.8 | 490.6 | 392.4 (0.9) | 495.2 (0.9) | 400.9 (3.1) | 505.8 (3.1) |
| 09-Jul | 369.8 | 468.8 | 373.4 (1.0) | 473.3 (1.0) | 381.7 (3.2) | 483.7 (3.2) |
| **Jhabua (Madhya Pradesh)** | | | | | | |
| 20-Jun | 446.7 | 569.1 | 452.8 (1.4) | 577.1 (1.4) | 464.6 (4.0) | 591.8 (4.0) |
| 27-Jun | 424.5 | 542.6 | 430.6 (1.4) | 550.2 (1.4) | 441.9 (4.1) | 564.4 (4.0) |
| 04-Jul | 403.6 | 517.0 | 409.5 (1.5) | 524.4 (1.4) | 420.4 (4.2) | 538.1 (4.1) |
| **Bahraich (Uttar Pradesh)** | | | | | | |
| 25-Jun | 427.3 | 534.4 | 432.4 (1.2) | 541.0 (1.2) | 447.1 (4.6) | 558.5 (4.5) |
| 02-Jul | 407.4 | 512.4 | 412.1 (1.1) | 518.6 (1.2) | 426.5 (4.7) | 536.2 (4.6) |
| 09-Jul | 387.1 | 489.6 | 391.4 (1.1) | 495.5 (1.2) | 405.5 (4.8) | 512.2 (4.6) |
| **Karimnagar (Andhra Pradesh)** | | | | | | |
| 15-Jun | 444.1 | 560.4 | 453.3 (2.1) | 571.7 (2.0) | 459.7 (3.5) | 579.7 (3.5) |
| 22-Jun | 424.7 | 537.4 | 433.4 (2.0) | 548.3 (2.0) | 440.0 (3.6) | 556.4 (3.5) |
| 29-Jun | 406.0 | 515.0 | 414.4 (2.1) | 525.6 (2.0) | 421.2 (3.7) | 533.7 (3.6) |
| **Begusarai (Bihar)** | | | | | | |
| 17-Jun | 387.5 | 489.2 | 393.2 (1.5) | 496.2 (1.4) | 407.9 (5.3) | 514.4 (5.1) |
| 24-Jun | 370.0 | 467.8 | 374.7 (1.3) | 474.7 (1.5) | 388.9 (5.1) | 492.4 (5.3) |
| 30-Jun | 353.4 | 449.4 | 359.2 (1.6) | 456.4 (1.6) | 373.0 (5.5) | 473.6 (5.4) |

Figures in parenthesis are percentage increase in crop water requirement and reference evapotranspiration over 1990 values

### 24.3.4 Crop Water Requirement and Reference Evapotranspiration for Pearl Millet

The highest crop water requirement and reference crop evapotranspiration of pearl millet is observed at Barmer (324–352 mm and 486–525 mm) followed by Gulbarga and Ongole (Table 24.4). The lowest is noticed at Bhiwani (283–311 mm).

The percentage increase in crop water requirement and reference evapotranspiration is more at Ongole in 2020 (2.7–2.8% and 2.7–2.8%) and in 2050 at Gulbarga (5.6–6.0% and 5.4–5.8%) when compared to base line year 1990 data. The increase is less at Barmer (0.1–0.4% and 0–0.3%) in 2020 and in 2050 (2.6–3% and 2.5–2.9%). It can be noticed that the increment is more at two south Indian stations viz., Ongole and Gulburga and low at northwest Indian station Barmer.

## 24.4 Adaptation Strategies

The results of the study clearly indicate that, the impact of climate change could increase crop water requirement and influence negatively on yield levels unless their need is fulfilled. It is big challenge in the coming decades about increasing

**Table 24.4** Crop water requirement and reference crop evapotranspiration for pearl millet during 1990, 2020 and 2050

| | 1990 | | 2020 | | 2050 | |
|---|---|---|---|---|---|---|
| Date of sowing | CWR | ETo | CWR | ETo | CWR | ETo |
| **Barmer (Rajasthan)** | | | | | | |
| 05-Jul | 351.8 | 524.7 | 352.2 (0.1) | 524.9 (0.0) | 361.1 (2.6) | 537.9 (2.5) |
| 12-Jul | 337.8 | 505.3 | 338.6 (0.2) | 506.1(0.2) | 347.4 (2.8) | 518.9 (2.7) |
| 19-Jul | 323.7 | 485.5 | 325.0 (0.4) | 487.0 (0.3) | 333.5 (3.0) | 499.5 (2.9) |
| **Nasik (Maharashtra)** | | | | | | |
| 15-Jun | 294.3 | 438.3 | 299.9 (1.9) | 446.5 (1.9) | 306.8 (4.3) | 456.4 (4.1) |
| 22-Jun | 284.2 | 424.1 | 289.9 (2.0) | 432.2 (1.9) | 296.9 (4.5) | 442.3 (4.3) |
| 29-Jun | 274.2 | 409.7 | 279.9 (2.1) | 418.0 (2.0) | 287.0 (4.7) | 428.3 (4.5) |
| **Agra (Uttar Pradesh)** | | | | | | |
| 20-Jun | 288.1 | 427.2 | 290.5 (0.8) | 431.0 (0.9) | 300.4 (4.3) | 445.2 (4.2) |
| 27-Jun | 277.5 | 412.9 | 279.7 (0.8) | 416.4 (0.8) | 289.7 (4.4) | 430.7 (4.3) |
| 04-Jul | 266.4 | 397.8 | 268.4 (0.8) | 401.0 (0.8) | 278.4 (4.5) | 415.3 (4.4) |
| **Gulbarga (Karnataka)** | | | | | | |
| 15-Jun | 334.4 | 496.6 | 343.0 (2.6) | 509.2 (2.5) | 353.1 (5.6) | 523.6 (5.4) |
| 22-Jun | 325.2 | 483.4 | 333.5 (2.6) | 495.6 (2.5) | 344.0 (5.8) | 510.5 (5.6) |
| 29-Jun | 316.3 | 470.4 | 324.4 (2.6) | 482.4 (2.5) | 335.2 (6.0) | 497.7 (5.8) |
| **Ongole (Andhra Pradesh)** | | | | | | |
| 15-Jun | 330.5 | 488.6 | 339.6 (2.8) | 502.3 (2.8) | 348.2 (5.4) | 514.7 (5.3) |
| 22-Jun | 320.2 | 474.7 | 328.9 (2.7) | 487.9 (2.8) | 337.6 (5.4) | 500.4 (5.4) |
| 29-Jun | 309.4 | 460.1 | 317.8 (2.7) | 472.6 (2.7) | 326.5 (5.5) | 485.3 (5.5) |

Figures in parenthesis are percentage increase in crop water requirement and reference evapotranspiration over 1990 values

food production with less water particularly when the major river basins will have limited water resources and reduction in ground water availability. Improved water management practices that increase the productivity of irrigation water use may provide significant adaptation potential for all land production systems under future climate change. A number of adaptation policies are suggested in literatures. The policies suggest specific measures for water resources and agriculture that could reduce the potential adverse effects of climate change on crop evapotranspiration and yield. Micro-irrigation and resource conservation technologies (RCTs), economizing on water is to be promoted in a big way. The conjunctive use of water and diversification of rice-wheat is required for solving the emerging problem associated with climate change. At the same time, improvements in irrigation efficiency are critical to ensure the availability of water both for food production and for competing human and environmental needs. High volume of wastewater (18.4 million $m^3$/day) needs to be utilized for irrigation after their proper treatment. Options for autonomous adaptation are already available to farmers and communities to cope with the future water shortage related risk management and production enhancement activities. These include (i) Adoption of varieties with increased resistance to high temperature and drought. (ii) Modification of irrigation techniques, including amount, timing or technology. (iii) Improved water management to prevent water logging, erosion and leaching. (iv) Adoption of efficient technologies to 'harvest' water. (v) Conserve soil moisture (e.g. crop residue retention), and reduce siltation and saltwater intrusion. (vi) Modification of crop calendars, i.e., timing or location of cropping activities (Bates et al. 2008).

In general, projections suggest that the greatest relative benefit from adaptation is to be gained under conditions of low to moderate warming, and that adaptation practices that involve increased irrigation water use may in fact place additional stress on water and environmental resources as warming and evaporative demand increase.

## 24.5 Conclusions

The present study indicates the crop water requirement and reference crop evapotranspiration is high for maize followed by sorghum and wheat and the low for pearl millet in 1990. However, the lowest crop water requirement (260–300 mm) is noticed for wheat at northwest Indian stations like Sirsa and Ganganagar, which could be due to regional weather influence during crop growing season. In the case of percentage increase in crop water requirement and reference crop evapotranspiration, highest is noticed at Solapur for sorghum, Sirsa and Ganganagar for wheat, Karimnagar and Begusarai for maize in 2020 and 2050 respectively, and at Ongole and Gulburga for pearl millet. It is important to notice that though the actual values of crop water requirement and reference evapotranspiration is low at Ganganagar and Sirsa in 1990, the percentage increase is more in 2020 and 2050 at these places when compared to other wheat growing stations. These stations come under water

scarcity zone and adequate measures to augment irrigation water availability in order to sustain wheat production. However, given the potential adverse impacts on water resources that could be brought about by climate change, it is worthwhile to conduct more in-depth studies and analyses to gauge the extent of problems that the country may face. Climate change is posing a challenge in front of the scientists concerned with water resources, policy makers and most importantly farmers.

## References

Abrol IP (1996) India's agriculture scenario. In: Abrol YP, Gadgil S, Pant GB (eds) Climate variability and agriculture. Narosa Publishing House, London, pp 19–25

Allen RG, Pereira LS, Rase D, Smith XM (1998) Crop evapotranspiration. Guidelines for computing crop water requirements. Irrig. & Drain. Paper 56 Food and Agricultural Organisation, Rome

Bates BC, Kundzewicz ZW, Wu S, Palutikof JP (eds) (2008) Climate change and water. technical paper of the intergovernmental panel on climate change. IPCC Secretariat, Geneva

FAO (2005) New_LocClim. climatological database of the agromet group of FAO. Food and Agricultural Organisation, Rome

Gadgil S, Abrol YP, Seshagiri Rao PR (1999) On growth and fluctuation of Indian foodgrain production. Curr Sci 76(4):548–556

Huntington TG (2006) Evidence for intensification of the global water cycle: review and synthesis. J Hydrol 319:83–95

Katyal JC (1998) Soil, water and environmental Sciences In: Porceedings of brainstorming session on 'Scientists perception for agriculture-2020 NBPGR New Delhi, India, 4–5 June 1998

Kumar R, Singh RD, Sharma KD (2005) Water resources of India. Curr Sci 89(5):794–811

Mall RK, Gupta A, Singh R, Singh RS, Rathore LS (2006) Water resources and climate change: an Indian perspective. Curr Sci 90(12):1610–1626

McCabe GJ Jr, Wolock DM (1992) Sensitivity of irrigation demand in a humid-temperature region to hypothetical climate change. Water Resour Bull 28(3):533–543

Sharma BR (2006) Crop water requirements and water productivity: concepts and practices. Groundwater governance in Asia. http://www.waterandfood.org/gga/ Lecture%20Material/B.R. Sharma_CWR&WP.pdf

Smith M (1992) CROPWAT. A computer program for irrigation planning and management. Irrig. & Drain. Paper 46 FAO, Rome

Smith M (1993) CLIMWAT for CROPWAT. A climatic database for irrigation planning and management. Irrig, & Drain, paper, 49, Food and Agricultural Organisation, Rome

# Chapter 25
# Climate Change and Its Impact on Wheat and Maize Yield in Gujarat

**Vyas Pandey and H.R. Patel**

**Abstract** Modeled studies of the sensitivity of world agriculture to potential climate change have suggested that the overall effect of moderate climate change on world food production may be small, as reduced production in some areas is balanced by gains in others. The vulnerability to climate change is systematically greater in developing countries like India-which are mostly located in lower, warmer latitudes. In these regions, cereal grain yields are projected to decline. In view of the various uncertainties, climatic data of different stations of Gujarat have been analyzed to ascertain the climatic change/variability in the state and its likely impact on crop production using crop models.

The long period rainfall analysis showed slight increase in annual rainfall by 2.86 mm/year. The months of July and August are although the months of receiving higher rainfall, the analysis at Anand showed that June and September have received higher rainfall than that of July and August at several occasion. The rainfall intensity in terms of daily maximum rainfall also showed increasing trend. The maximum temperature was found to increase in different seasons. The rate of increase was between 0.2 and 0.5°C per decade, maximum being in summer season. Similarly, the minimum temperature was found to increase but with slightly lower rate of 0.2–0.3°C per decade in different seasons.

The impact analysis of climate change on wheat and maize yield was assessed using CERES-wheat and CERES-maize models. The calibrated models were subjected to simulate the wheat and maize yield under hypothetical weather condition that may be arising due to climate change. The climate scenario simulated for temperatures (±1 to ±3°C), radiation (±1 to ±3 MJ $m^{-2}$ $day^{-1}$) and $CO_2$ (440, 550 and 660 ppm against present concentration of 330 ppm) were well within the range of projected climate scenario by IPCC. Results revealed that increase in

V. Pandey (✉) • H.R. Patel
Department of Agricultural Meteorology, Anand Agricultural University, Anand 388 110, Gujarat, India
e-mail: pandey04@yahoo.com; hrpatel410@yahoo.com

S.D. Attri et al. (eds.), *Challenges and Opportunities in Agrometeorology*,
DOI 10.1007/978-3-642-19360-6_25, © Springer-Verlag Berlin Heidelberg 2011

temperature significantly reduced the wheat yield (−8 to −31%) while decrease in temperature increased the yield (10–26%). The effect of maximum temperature on maize yield had similar effect but the magnitude is marginal (− 4 to 6%) over whole range of temperature (±3°C) change. The minimum temperature had similar effect on wheat yield with less magnitude of variation (−14 to +19%), however on maize yield increasing trend was observed with increase in minimum temperature. Higher receipt of solar radiation had favourable effect on wheat and maize yield and lower receipt of radiation may cause decrease in yields of both the crops. The effect was higher in wheat crop (−50 to 40%) than maize (−18 to 8%). Under limited irrigation condition the higher solar radiation receipt may have adverse effect through heating and thereby reduction in yield. Increase in $CO_2$ had beneficial effect on both the crops. The over all response of climate change on maize crop is less than wheat crop.

## 25.1 Introduction

The Intergovernmental Panel on Climate Change (IPCC 2007) Fourth Assessment Report released in February 2007 has confirmed that warming of climate system is unequivocal, as is evident from observations of increases in global average air and ocean temperatures, widespread melting of snow and ice, and rising global mean sea level. At continental, regional, and ocean basin scales, numerous long-term changes in climate have been observed. These include changes in Arctic temperatures and ice, widespread changes in precipitation amounts, ocean salinity, wind patterns and aspects of extreme weather including droughts, heavy precipitation, heat waves and the intensity of tropical cyclones. The report has pointed out with high level of confidence that the warming is due to human activities. Global atmospheric concentrations of carbon dioxide, methane and nitrous oxide have increased markedly as a result of human activities since 1,750 and now far exceed pre-industrial values determined from ice cores spanning many thousands of years. The global increases in carbon dioxide concentration are due primarily to fossil fuel use and land-use change, while those of methane and nitrous oxide are primarily due to agriculture.

Modeled studies of the sensitivity of world agriculture to potential climate change have suggested that the overall effect of moderate climate change on world food production may be small, as reduced production in some areas is balanced by gains in others. The same studies find, however, that vulnerability to climate change is systematically greater in developing countries like India-which are mostly located in lower, warmer latitudes. In these regions, cereal grain yields are projected to decline under climate change scenarios, across the full range of expected warming.

In view of the various uncertainties, climatic data of different stations of Gujarat have been analysed to ascertain the climatic change/variability in the state and its likely impact on agriculture using crop models.

### 25.1.1 Biophysical Resources

Gujarat is the western-most state of India. It has a long (1,600 km) sea coast on the Arabian Sea. The Gulf of Cambay separates the Western peninsula (Saurashtra) from the arid district of Kutch. The hill ranges of Aravalli in the northeast, Saputara in east and Sahyadri in the southeast run along the eastern boundary of the state from the northern district of Banaskantha to its southern end. Topographically, Gujarat state is characterized by a large central alluvial plain and a peninsula, separated by the Gulf of Cambay. Kutch, the largest district, lies north of the peninsula, and on its northern border is the large rann (desert) of Kutch. Of the numerous rivers that flow westward across the plain, the most prominent, the Tapi, Narmada and Mahi, have perennial flow. With the exception of the northern-most part, the plain has assured rainfall. The state's area of 19.60 million ha accounts for about 6.0% of the total area of India. Its net sown area is 9.58 million ha, which is 6.75% of that of the country. Barren and uncultivated land (2.61 million ha) represents about 13.31% of the landmass of the state.

Gujarat is divided into eight agroclimatic zone (Fig. 25.1) based on rainfall, soils and cropping pattern. The distribution of cropping systems is determined largely by the climatic gradient and distribution of soils. Three types of tropical climate prevail across the state. An arid climate is seen in the extreme north and northwest,

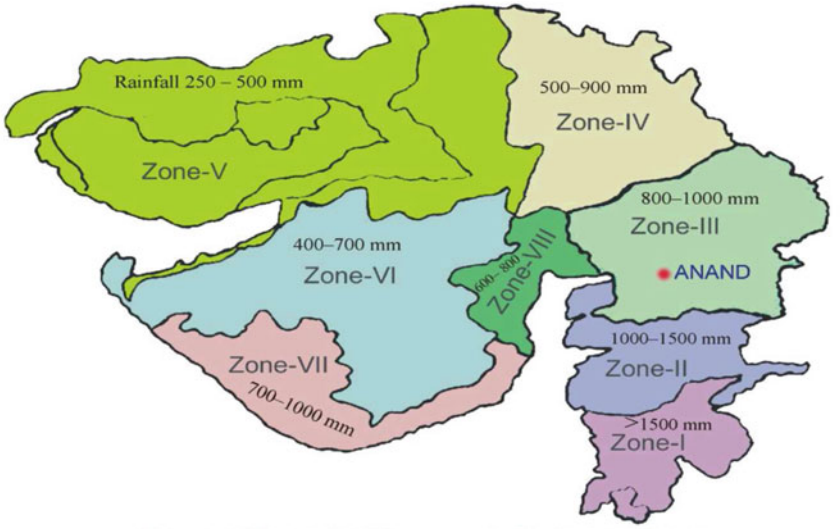


**Fig. 25.1** Agroclimatic zones of Gujarat

comprising Kutch, and western portions of Banaskantha, Patan and Jamnagar. The Surat, Narmada, Navsari, Valsad and Dangs districts in the extreme south have a sub-humid climate with good vegetative cover. The remaining parts of the state have a semi arid climate, relatively sparse vegetative cover, frequent droughts and susceptibility to soil erosion.

The monsoon normally sets in mid-June and withdraws by mid-September. The annual average rainfall of the state is 821 mm which is not reliable neither representative. Average annual rainfall ranges from as high as 1,900 mm in the sub-humid southeast to as low as 320 mm in the arid north. The distribution of rainfall, particularly wet and dry spell characteristics, has largely determined the traditional evolution of cropping patterns and agricultural practices. Much of the southern portion of the state experiences excess rainfall frequently. The northern and north-western parts of Gujarat receive less precipitation and experience frequent failures of monsoon.

## 25.2 Material and Methods

Fifty years (1958–2007) of rainfall and temperature data of Anand, Gujarat, India were used to analyse the variability at different time scales while district wise rainfall data were use to study the spatial variability of rainfall in the state. The impact analysis of climate change on wheat and maize yield was assessed using CERES-wheat and CERES-maize models, which were calibrated and validated using experimental data conducted at Anand (Anon 2007; Patel 2004; Patel et al. 2007). CERES models were subjected to simulate the wheat yield under hypothetical weather condition that may be arising due to climate change (Pandey et al. 2007). The climate scenario simulated for temperatures ($\pm 1$ to $\pm 3$°C), radiation ($\pm 1$ to $\pm 3$ MJ $m^{-2}$ $day^{-1}$) and $CO_2$ (440, 550 and 660 ppm against present concentration of 330 ppm) were well within the range of projected climate scenario by IPCC (2007). In the case of wheat crop two management conditions (Full irrigation and limited irrigation) were considered while for maize crop two cultivars (Ganga Safed-2 and GM-3) were selected. Looking to the interaction effect of climatic parameters the yield was simulated due to change in individual parameters as well as in combination with other one or two.

## 25.3 Results and Discussions

### *25.3.1 Climate Change/Variability*

#### 25.3.1.1 Rainfall Variability

Gujarat state receives about 95% of its annual rainfall through the influence of SW monsoon during June to September period. The subdivision wise rainfall analysis

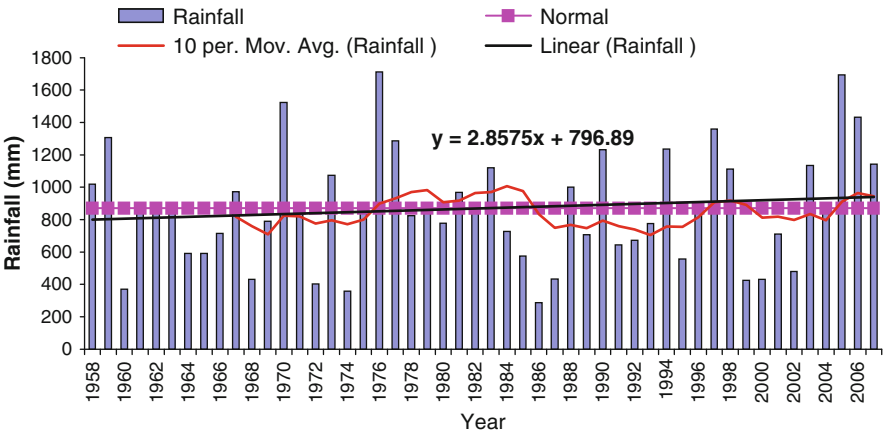


**Fig. 25.2** Annual rainfall variability and trend at Anand

revealed that Saurashtra & Kutch subdivision have mean annual rainfall of 428 mm with coefficient of variation of 44% and decreasing trend of −5% per 100 years while Gujarat sub division has mean annual rainfall of 863 mm with coefficient of variation of 32% and decreasing trend of −5% per 100 years.

Temporal and spatial variability of rainfall analysis suggested occurrence of floods and drought side by side (Pandey et al. 1999). Kutch having less rainfall (<350 mm) had highest annual rainfall variability (57%) while the Dangs having highest rainfall (1,792 mm) had lowest rainfall variability (29%). On monthly basis, the coefficient of variability is still higher, being >100% in Kutch even in monsoon months. Among four months of monsoon months, July contributes 35–45% of annual rainfall. Kutch is having 80% chances of getting low rainfall (<500 mm), the Dang and Valsad have 70% chances of getting higher rainfall (>1,500 mm). Kutch district and parts of Banaskantha, Patan, Surendranagar, Rajkot and Jamnagar districts were found prone to experience moderate to severe droughts in more than 30% of the years (Pandey et al. 1999).

The annual rainfall analysis at revealed that Anand showed slight increase in annual rainfall by 2.86 mm (Fig. 25.2). Although, the months of July and August are the months of receiving higher rainfall, the analysis at Anand showed that many a times June and September received higher rainfall than that of July and August. The rainfall intensity in terms of daily maximum rainfall also showed increasing trend at Anand.

### 25.3.1.2 Temperature

The maximum temperature at Anand was found to increase in all the three seasons (summer, monsoon and winter). The rate of increase was between 0.2 and 0.5°C per

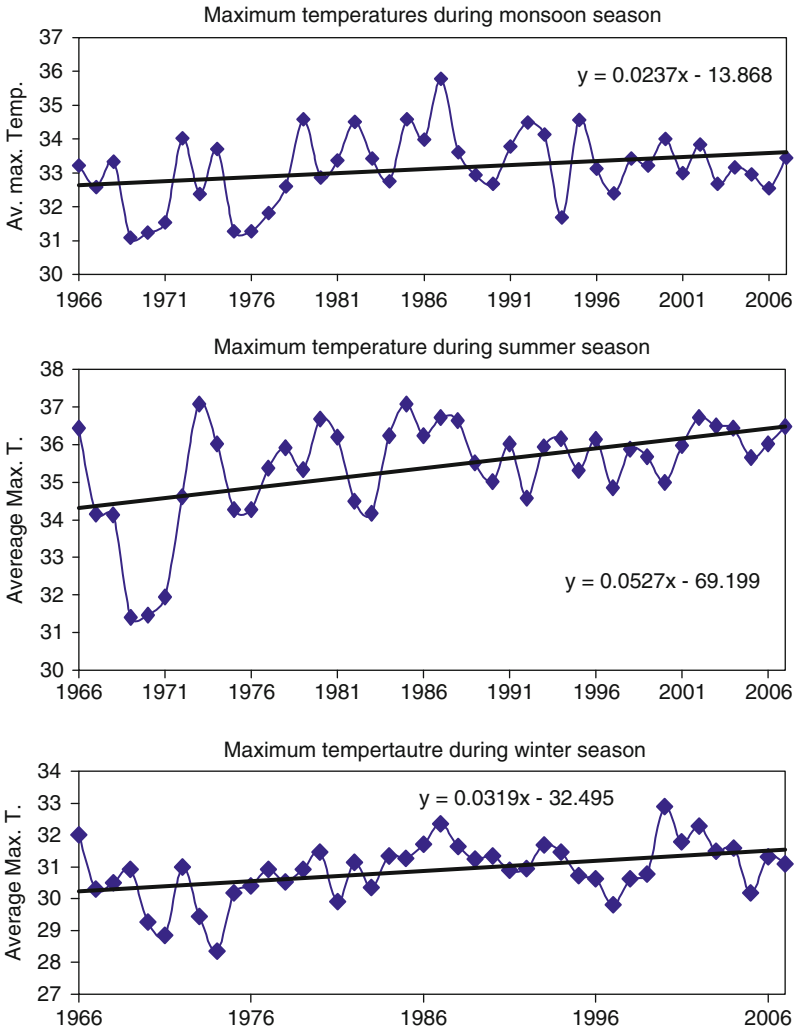


**Fig. 25.3** Trends of maximum temperature during different seasons at Anand

decade, maximum being in summer season (Fig. 25.3). Similarly, the minimum temperature was found to increase but with slightly lower rate of 0.2–0.3°C per decade in different seasons (Fig. 25.4). The rate of increase of maximum as well as minimum temperature was lowest during monsoon season and highest during summer season. Thus the higher temperature during summer season may further aggravate the summer season.

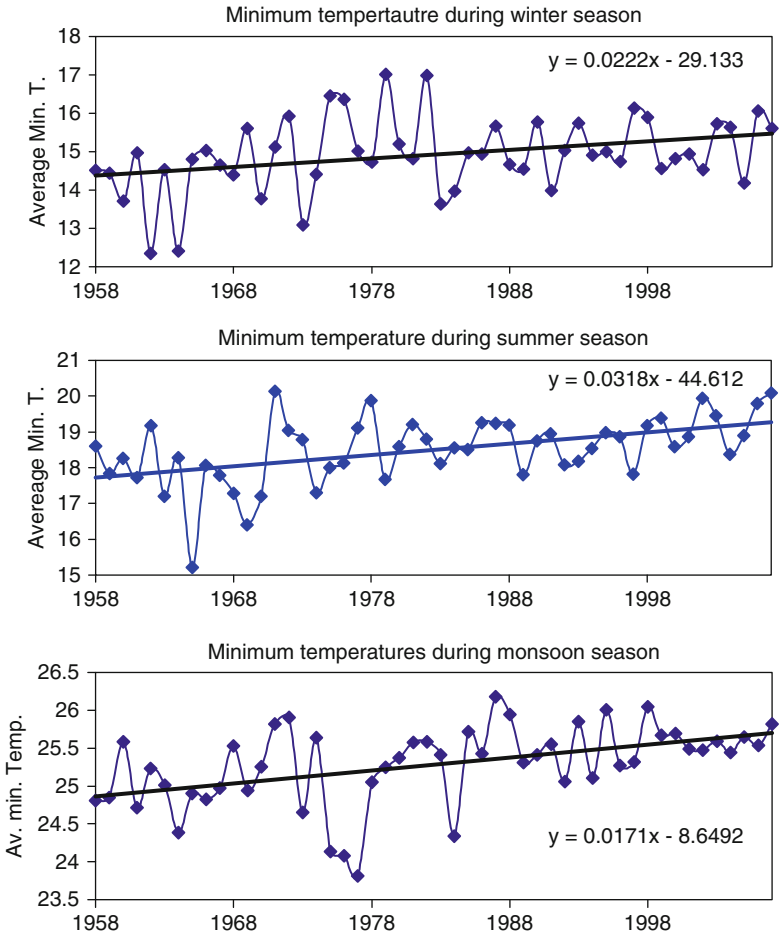


**Fig. 25.4** Trends of minimum temperature during different seasons at Anand

## *25.3.2 Impact Analysis*

### 25.3.2.1 Impact on Wheat Yield

Individual Effects of Temperature, Solar Radiation and $CO_2$ Concentration

The simulated grain yield of wheat by CERES-wheat model under incremental units of maximum temperature (1–3°C) showed gradual decrease in yield ranging from 3,546 to 2,646 kg $ha^{-1}$ (8–31%) under irrigated condition (Table 25.1). Under limited irrigation condition, yield reduction was recorded to the extent of 2,841–2,398 kg$ha^{-1}$ (9–23%). In general, increase in maximum temperature from

**Table 25.1** Simulated wheat yield due to varying temperature, solar radiation and $CO_2$ concentration under irrigated and limited irrigation conditions

| Parameters | Simulated grain yield (kg $ha^{-1}$) | | % Change in yield | |
|---|---|---|---|---|
| | Full irrigation | Limited irrigation | Full irrigation | Limited irrigation |
| MaxT (°C) | | | | |
| 3 | 2,646 | 2,398 | −31 | −23 |
| 2 | 3,091 | 2,668 | −19 | −14 |
| 1 | 3,546 | 2,841 | −8 | −9 |
| −1 | 4,206 | 3,190 | 10 | 3 |
| −2 | 4,485 | 3,358 | 17 | 8 |
| −3 | 4,817 | 3,641 | 26 | 17 |
| MinT (°C) | | | | |
| 3 | 3,288 | 2,874 | −14 | −8 |
| 2 | 3,460 | 2,948 | −10 | −5 |
| 1 | 3,692 | 3,039 | −4 | −2 |
| −1 | 4,118 | 3,140 | 7 | 1 |
| −2 | 4,226 | 3,195 | 10 | 3 |
| −3 | 4,581 | 3,234 | 19 | 4 |
| Solar radiation (MJ $m^{-2}$ $day^{-1}$) | | | | |
| 3 | 5,387 | 2,454 | 40 | −21 |
| 2 | 5,111 | 2,709 | 33 | −13 |
| 1 | 4,523 | 3,085 | 18 | −1 |
| −1 | 3,156 | 2,985 | −18 | −4 |
| −2 | 2,503 | 2,503 | −35 | −20 |
| −3 | 1,903 | 1,903 | −50 | −39 |
| $CO_2$ concentration (base value 330 ppm) | | | | |
| 440 | 4,630 | 3,695 | 21 | 19 |
| 550 | 5,687 | 4,327 | 48 | 39 |
| 660 | 6,465 | 4,876 | 68 | 57 |

1 to 3°C significantly reduced the wheat yield. The reduction in yield was mainly due to reduction in duration of anthesis and grain filling with rise in ambient temperature and vice versa. Similarly in case of gradual down scale of maximum temperature in the range of −1 to −3°C, totally reverse trend was observed. Similar trend was also noticed in case of increase and decrease in minimum temperature. The magnitude of effect of minimum temperature was quite less (−14 to +19%) than those due to maximum temperature (−31 to +26%). This showed that wheat yield was found to be highly sensitive to change in temperature under irrigated as well as under limited irrigation conditions.

The increase in solar radiation from 1 to 3 MJ $m^{-2}$ $day^{-1}$ resulted in increase in yield of wheat from 18 to 40% while reduction in solar radiation by −1 to −3 MJ $m^{-2}$ $day^{-1}$ caused decrease in wheat yield to the tune of −18 to −50%. However, under limited irrigation conditions the yield was found to decrease both under elevated as well as reduced solar radiation. This showed that under limited irrigation condition the higher solar radiation receipt may have adverse effect through heating and thereby reduction in yield. It may be noted that under lower solar

radiation regime, the yields under both conditions are same. The overall response of varying radiation to grain yield of wheat showed that the model was more sensitive to radiation than it was to temperature.

The effects of elevated carbon dioxide on simulated grain yield of wheat showed that due to gradual increase in $CO_2$ concentration from 440 to 660 ppm, the yield levels increased to the tune of 21–68% under irrigated condition. Under limited irrigated condition similar response were observed with slightly lower magnitude (19–57%). This showed that under climate change scenario, $CO_2$ enhancement proved beneficial for higher productivity. The increase in yield under increase in concentration in $CO_2$, may be due to most plants growing in experimental environments with increased levels of atmospheric $CO_2$, exhibit increased rates of net photosynthesis and reduced stomatal opening. Partial stomatal closure leads to reduced transpiration per unit leaf area and, combined with enhanced photosynthesis, often improves water-use efficiency.

## Combined Effect of Temperature and Solar Radiation

Under optimal condition, the effect of increase in temperatures was found to be nullified by similar increase in solar radiation (MJ $m^{-2}$ $day^{-1}$), as it is evident from the effect on yield (+2 to −4%), while decreasing temperature and radiation had negative effect (−3 to −25%) on grain yield (Table 25.2). This showed that the favourable effect of lower temperature was suppressed by negative effect of lower solar radiation regimes. Under limited irrigated condition, the decrease in yield up to 33% was observed due to increase in both temperature and radiation by 3 units, while lowering of temperature and radiation had marginal effect (+6 to −7%) on wheat yield. It can further be revealed that due to lowering of temperature and radiation by 3 units the wheat yields under fully irrigated condition was same as that of under limited irrigated condition.

**Table 25.2** Simulated wheat yield due to combined effect of temperature and solar radiation under irrigated and limited irrigation conditions

| | Simulated grain yield (kg $ha^{-1}$) | | % Change in yield | |
|---|---|---|---|---|
| Temperatures (°C) and SAR (MJ $m^{-2}day^{-1}$) | Full irrigation | Limited irrigation | Full irrigation | Limited irrigation |
| 3 | 3,670 | 2,083 | −4 | −33 |
| 2 | 3,790 | 2,486 | −1 | −20 |
| 1 | 3,917 | 2,799 | 2 | −10 |
| −1 | 3,738 | 3,292 | −3 | 6 |
| −2 | 3,453 | 3,273 | −10 | 5 |
| −3 | 2,892 | 2,892 | −25 | −7 |

### Combined Effect of Temperature, Solar Radiation and $CO_2$ Concentration

Model simulation was also carried out for combined effect of temperature, solar radiation and different levels of $CO_2$ concentration (440, 550 and 660 ppm) under fully irrigated and under limited irrigated conditions (Table 25.3). The results revealed that at $CO_2$ concentration of 440 ppm, the wheat yield was found to generally increase (−2 to 23%) with either increase or decrease of temperature and radiation up to 3 units under optimal condition. Under limited irrigated condition, however, the favourable effects were observed only under down scaling of the temperature and radiation regimes, the total effect being −23 to 26%. At higher $CO_2$ concentration of 550 ppm, the net effect on yield was favourable (23–51%) irrespective of whether temperature and radiation increased or decreased under full irrigation condition, while under limited irrigation condition, the negative effect (−12%) was observed at higher temperature and radiation (+3 units) regimes. Under doubling of $CO_2$ concentration (660 ppm) scenario, increase in yield levels are quite high (42–70% under full irrigation condition and −3 to +75% under limited irrigation condition) due to changes in both temperature and radiation by +3 units.

**Table 25.3** Simulated wheat yield due to interaction effect of temperature, solar radiation and $CO_2$ concentration under irrigated and limited irrigation conditions

| | Simulated grain yield (kg $ha^{-1}$) | | % Change in yield | |
|---|---|---|---|---|
| Temperatures (°C) and SAR (MJ $m^{-2}day^{-1}$) and $CO_2$ | Full irrigation | Limited irrigation | Full irrigation | Limited irrigation |
| 440 ppm | | | | |
| 3 | 4,369 | 2,410 | 14 | −23 |
| 2 | 4,699 | 2,896 | 22 | −7 |
| 1 | 4,726 | 3,287 | 23 | 6 |
| −1 | 4,550 | 3,920 | 19 | 26 |
| −2 | 4,255 | 3,929 | 11 | 26 |
| −3 | 3,776 | 3,776 | −2 | 21 |
| 550 ppm | | | | |
| 3 | 5,125 | 2,730 | 34 | −12 |
| 2 | 5,593 | 3,307 | 46 | 6 |
| 1 | 5,778 | 3,784 | 51 | 22 |
| −1 | 5,452 | 4,602 | 42 | 48 |
| −2 | 5,161 | 4,642 | 35 | 49 |
| −3 | 4,707 | 4,695 | 23 | 51 |
| 660 ppm | | | | |
| 3 | 5,781 | 3,015 | 51 | −3 |
| 2 | 6,332 | 3,476 | 65 | 12 |
| 1 | 6,541 | 4,226 | 70 | 36 |
| −1 | 6,229 | 5,201 | 62 | 67 |
| −2 | 5,950 | 5,262 | 55 | 69 |
| −3 | 5,537 | 5,439 | 44 | 75 |

The interaction effect of temperature, radiation and $CO_2$ concentration revealed that the response under irrigated condition was quite different than that under limited irrigated condition. Under fully irrigated condition the highest benefits are obtained at higher level of $CO_2$ concentration combined with one unit increase in temperature and radiation. The percentage change in yield decreased both ways i.e. either increasing or decreasing the parameters from the mean values. The percentage change in yield under limited irrigation condition was found to have increasing trend with decreasing (+3 to −3 units) temperature and radiation at higher levels of $CO_2$ concentration.

#### 25.3.2.2 Impact on Maize Yield

CERES-maize model was used to study the impact of climate change on maize production for two cultivars (Ganga Safed-2 and GM-3) commonly grown in the state.

Effects of Temperatures, Solar Radiation and $CO_2$ Concentration

Results on effects of minimum and maximum temperatures, solar radiation and $CO_2$ concentration on simulated grain yield of maize (Table 25.4) revealed that as the maximum temperature increases the yield decrease and vise versa. In case of increase or decrease of minimum temperature yield was found to increase, however, there is drastic decrease in yield if minimum temperature falls by more than 3°C. Thus the minimum and maximum temperature influences the maize crop differently. Higher solar radiation receipt was found to increase the yield of maize while lower radiation may have adverse effect. Higher $CO_2$ concentration was found to have favourable effect on maize yield. Doubling of $CO_2$ may increase its yield by 8–9% (Table 25.4).

Combined Effect of Temperature and Radiation

The combined effect of minimum and maximum temperature revealed that if both temperatures are increased or decreased by more than 1°C, maize yield was found to decrease (Table 25.5). If the increase in temperature is accompanied by increase in solar radiation the favourable effect was noticed only up to two units of increment in the parameters. Otherwise the negative effect was observed either by increasing the parameters by more than two units or decreasing them (Table 25.6).

**Table 25.4** Effect of maximum and minimum temperature, solar radiation and $CO_2$ concentration maize cultivars

| | Simulated grain yield (kg ha$^{-1}$) | | % Change in yield | |
|---|---|---|---|---|
| Parameters | Ganga Safed-2 | GM-3 | Ganga Safed-2 | GM-3 |
| MaxT (°C) | | | | |
| 3 | 3,518 | 3,444 | −4.3 | −4.3 |
| 2 | 3,658 | 3,499 | −0.5 | −2.8 |
| 1 | 3,717 | 3,552 | 1.1 | −1.3 |
| −1 | 3,776 | 3,697 | 2.7 | 2.8 |
| −2 | 3,868 | 3,708 | 5.3 | 3.1 |
| −3 | 3,927 | 3,773 | 6.9 | 4.9 |
| MinT (°C) | | | | |
| 3 | 3,785 | 3,615 | 3.0 | 0.5 |
| 2 | 3,856 | 3,687 | 4.9 | 2.5 |
| 1 | 3,999 | 3,631 | 8.8 | 0.9 |
| −1 | 3,767 | 3,688 | 2.5 | 2.5 |
| −2 | 3,697 | 3,620 | 0.6 | 0.6 |
| −3 | 3,537 | 3,418 | −3.8 | −5.0 |
| Solar radiation (MJ m$^{-2}$day$^{-1}$) | | | | |
| 3 | 3,862 | 3,778 | 5.1 | 5.0 |
| 2 | 3,794 | 3,714 | 3.2 | 3.2 |
| 1 | 3,977 | 3,892 | 8.2 | 8.2 |
| −1 | 3,510 | 3,373 | −4.5 | −6.3 |
| −2 | 3,284 | 3,217 | −10.6 | −10.6 |
| −3 | 3,013 | 2,954 | −18.0 | −17.9 |
| $CO_2$ concentration (base value 330 ppm) | | | | |
| 440 | 3,781 | 3,701 | 2.9 | 2.9 |
| 550 | 3,873 | 3,790 | 5.4 | 5.3 |
| 660 | 3,993 | 3,907 | 8.7 | 8.6 |

**Table 25.5** Combined effect of maximum and minimum temperature for maize cultivars

| | Simulated grain yield (kg ha$^{-1}$) | | % Change in yield | |
|---|---|---|---|---|
| MaxT and MinT (°C) | Ganga Safed-2 | GM-3 | Ganga Safed-2 | GM-3 |
| 3 | 3,528 | 3,369 | −4.0 | −6.4 |
| 2 | 3,665 | 3,587 | −0.3 | −0.3 |
| 1 | 3,677 | 3,604 | 0.1 | 0.2 |
| −1 | 3,798 | 3,661 | 3.3 | 1.8 |
| −2 | 3,529 | 3,454 | −4.0 | −4.0 |
| −3 | 3,351 | 3,279 | −8.8 | −8.9 |

## 25.4 Conclusions

Gujarat being western-most state of India and having long seacoast has high variability in terms of biophysical parameters. Extreme arid climate to sub-humid climates are experienced in the state. The distribution of cropping systems is determined largely by the climatic gradient and distribution of soils. The temporal

**Table 25.6** Combined effect of temperature and solar radiation maize cultivars

| MaxT and MinT (°C) and SAR (MJ $m^{-2}d^{-1}$) | Simulated grain yield (kg $ha^{-1}$) | | % Change from base yield | |
|---|---|---|---|---|
| | Ganga Safed-2 | GM-3 | Ganga Safed-2 | GM-3 |
| 3 | 3,630 | 3,552 | −1.2 | −1.3 |
| 2 | 3,903 | 3,725 | 6.2 | 3.5 |
| 1 | 3,908 | 3,832 | 6.3 | 6.5 |
| −1 | 3,600 | 3,578 | −2.0 | −0.6 |
| −2 | 3,420 | 3,349 | −6.9 | −6.9 |
| −3 | 3,243 | 3,136 | −11.8 | −12.8 |

variability in rainfall indicated variable trend in different regions of the state. In middle Gujarat increasing trend is observed in rainfall as well as maximum and minimum temperatures during different seasons. Impact of climate change study revealed that increase in temperature significantly reduced the wheat yield while decrease in temperature increased the yield. The effect of maximum temperature on yield was more than that of minimum temperature. The higher radiation receipt and lower radiation receipt caused decrease in yield under optimal condition whereas, negative effect was seen under sub-optimal condition due to either increase or decreasing radiation. The combined effect of temperature and solar radiation were very marginal at the lower side of yield. More or less similar effects with less magnitude were observed for maize crop also.

## References

Anonymous (2007) Determination of spatial irrigation requirement and production potentials for major crops over Narmada canal command areas using crop models and GIS. Project completion report (2004-2007), Department of Agricultural Meteorology, BA College of Agriculture, AAU, Anand, pp 62

IPCC (2007) Climate change 2007: the physical science basis, fourth assessment report

Pandey V, Shekh AM, Parmar RS (1999) Occurrence of droughts and floods over Gujarat. J Agrometeorol 1(2):177–181

Pandey V, Patel HR, Patel VJ (2007) Impact assessment of climate change on wheat yield in Gujarat using CERES-wheat model. J Agrometeorol 9(2):149–157

Patel HR (2004) Simulation modeling of wheat (cv. GW-496) yield using CERES-wheat model in varied environmental ad moisture regimes of middle Gujarat agro-climatic region. Ph.D. thesis submitted to the Anand Agricultural University, Anand

Patel VJ, Patel HR, Pandey V (2007) Evaluation of CERES-wheat model for estimation of wheat yield in middle Gujarat. Asian J Environ Sci 2(1&2):89–93

# Chapter 26
# Climate Change Adaptation and Mitigation for Drought-Prone Areas in India

**R.P. Samui and M.V. Kamble**

**Abstract** Climate change is expected to bring more intense and more frequent extreme weather events including droughts and floods in India. The 2002 drought is an indicator of the coping ranges of key sectors such as agriculture and water management. It was devastating for many people and sectors, and posed considerable adaptation challenges. To enhance adaptation and promote sustainable development, strategic planning, assessment of natural resources, technological change and innovation are required to increase productivity, with sustainable economic growth that preserves finite natural resources. This study deals with current adaptation at the local, regional, and national scales to improve our understanding of current adaptation processes and options in Indian agriculture, particularly under drought or drought like situations. It is designed to provide an estimate of current adaptive capacity and processes, and to help decrease vulnerability to future droughts and integrated water management planning for reducing vulnerability to water scarcity.

We concluded with listing many adaptive strategies including increased understanding of the status of current adaptation and therefore vulnerability to multi-year, nation-wide and severe droughts, identification of suitable, realistic and practical adaptations to drought, provision of information to aid in the planning and actions to address adaptation gaps and limitations and to improve adaptation processes and enhanced information for building adaptation scenarios as required for climate impact assessments.

R.P. Samui (✉) • M.V. Kamble
Agricultural Meteorology Division, India Meteorological Department, Pune, India
e-mail: rsamui@yahoo.com

S.D. Attri et al. (eds.), *Challenges and Opportunities in Agrometeorology*,
DOI 10.1007/978-3-642-19360-6_26, 

## Abbreviations

| | |
|---|---|
| AICRPDA | All India Coordinated Research Project on Dryland Agriculture |
| CWWG | Crop Weather Watch Group |
| DDP | Desert Development Programme |
| DRM | Disaster Risk Mitigation |
| ENSO | Combination of El Nino and Southern Oscillation Index |
| EOF | Empirical Orthogonal Function |
| EQUINOO | Equatorial Indian Ocean Oscillation |
| EQWIN | Equatorial zonal Wind Index |
| FASAL | Forecasting Agricultural output using Space, Agro-Meteorology and Land based observations |
| GDP | Gross Domestic Product |
| ICAR | Indian Council of Agricultural Research |
| IIT | Indian Institute of Technology |
| IMD | India Meteorological Department |
| INSAT | Indian National Satellite System |
| ISMR | Indian Summer Monsoon Rainfall |
| IWDP | Integrated Wastelands Development Programme |
| IWMI | International Water Management Institute |
| NADAMS | National Agricultural Drought Assessment and Monitoring System |
| NCFC | National Crop Forecasting Centre |
| NCMRWF | National Centre for Medium Range Weather Forecast |
| NDVI | Normalized Difference Vegetation Index |
| NGO | Non Government Organization |
| NNRMS | National Natural Resource Management System |
| NRSA | National Remote Sensing Agency |
| PRECIS | Providing Regional Climates for Impact Studies |
| SAC | Space Application Centre |
| SC-AS | Standing Committee on Agriculture and Soils |
| SPI | Standardized Precipitation Index |
| SWAT | Soil and Water Assessment Tool |
| UNDP | United Nations Development Program |

## 26.1 Introduction

India being an agrarian country its economy is extremely dependent on agriculture. In spite of growing industrialization, the economy of the Indian subcontinent still depends mostly upon the rainfed agricultural production. Rainfed farming occupies 68% of the cultivable area and hence, has a distinct place in agriculture. About 44% of the food grain produced in India is the contribution of rainfed farming, which supports almost 40% of the total population of the country. The only source of water for rainfed farming and the subsequent crop yield is totally dependent on

quantum of rainfall and its distribution pattern, performance of the crop under other biotic and abiotic stresses. These areas are highly prone to irregularities in monsoon such as late onset, long breaks and early withdrawal etc. and hence are vulnerable to droughts of different durations and magnitudes (Shaw et al. 2005). The projected changes in climate patterns over India include increase in surface temperature, variations in rainfall, increasing occurrence of extreme weather events like floods and droughts, rise in sea levels and impact on the Himalayan glaciers. Sectors of the Indian economy are most likely to be impacted by such changes in climate are those dependent on natural resources, namely agriculture, water and forestry. The likely impacts such as reduction in food production, water scarcity, loss of forest biomass and enhanced risk to human health are likely to add burden to the society.

India has a long drought history with 21 major drought years during the period 1901–2004. Drought has affected nearly 1,061 million people and killed 4.25 million people in India during 1900–2006 (Center for Research on Epidemiology of Disasters 2006). So some of the key actions like water and energy resource conservation measures, promotion of good agronomic practices, weather based farming decisions and awareness creation through social mobilization and awareness campaigns are necessary for sustainable development of the country.

## 26.2 Impact of Drought

Drought has several impacts like likelihood death of human and animals, loss of agricultural production, short-term reduction in GDP, imbalance in fiscal budget due to emergency allocations for relief, panic/disruption in lives of people, increasing likelihood of social unrest leading to violent conflicts, damage to natural resources base and environment, migration of people and livestock and slow down in development.

The 2002 drought in recent year ranks as one of the most severe in India's recorded history affecting 56% of the geographical area. 19% of area experienced 'moderate drought' and 10% area suffered from 'severe drought'. The lack of rain caused a 15% drop in total food grains and a 19% drop in rice production i.e., 31 million tons and 17 million tons respectively. The Indian Department of Agriculture estimated that the 2002 drought year resulted in a 3.2% decline in agricultural GDP, a $9-billion loss in agricultural income and the loss of a staggering 1.3 billion person-days in rural employment due to shrinkage of agricultural operations.

### *26.2.1 People and Livestock Affected by Drought 2002*

- Chhattisgarh: 10,252 villages in 12 of 16 districts, 9,400,000 people.
- Gujarat: 12,240 villages in 22 of 25 districts, 29,100,000 people and 107,00,000 cattle.
- Madhya Pradesh: 22,490 villages in 32 of 45 districts, 12,700,000 people and 8,570,000 cattle.

- Orissa: 15,000 villages in 28 of 30 districts, 11,900,000 people and 39,900,000 cattle.
- Rajasthan: 31,000 villages in 31 of 32 districts, 33,000,000 people and 39,900,000 cattle.
- Himachal Pradesh: 4,600,000 people and 88,000 ha of crop area in all 12 districts.
- Maharashtra: 20,000 villages in 26 of 35 districts, 45,500,000 people and 258,000 cattle.

In 2004, rainfall for the country as a whole was 87% of the LPA. It was declared as a meteorological drought rather than all India Drought year. Out of 36 meteorological sub-divisions, 23 sub-divisions received normal rainfall and 13 sub-divisions received deficient rainfall. Following Table 26.1 summarizes the severe/moderate drought conditions of different states in 2004.

Years during which the rainfall deficiency in Indian subcontinent from long term average was more than −10% and the percentage of area affected by drought conditions is shown Table 26.2.

**Table 26.1** Sub-divisions experienced severe/moderate drought condition

| Meteorological sub-division | % departure of rainfall |
|---|---|
| Himachal Pradesh | −45 |
| Punjab | −44 |
| West Rajasthan | −40 |
| West Uttar Pradesh | −36 |
| Vidarbha | −31 |
| Telangana | −27 |

**Table 26.2** Percentage rainfall departure and area affected by drought

| Year | Rainfall % departure | % area affected by drought |
|---|---|---|
| 1901 | −13 | 27 |
| 1904 | −12 | 32 |
| 1905 | −17 | 36 |
| 1911 | −15 | 42 |
| 1918 | −25 | 69 |
| 1920 | −17 | 39 |
| 1941 | −13 | 34 |
| 1951 | −19 | 34 |
| 1965 | −18 | 30 |
| 1966 | −13 | 21 |
| 1972 | −24 | 42 |
| 1974 | −12 | 29 |
| 1979 | −19 | 23 |
| 1982 | −15 | 27 |
| 1986 | −13 | 25 |
| 1987 | −19 | 43 |
| 2002 | −19 | 29 |
| 2004 | −13 | 18 |

## 26.3 Empirical Orthogonal Function (EOF) Analysis of Rainfall and Its Teleconnection with ENSO and Other Features

There is a large spatial variability in the Indian summer monsoon rainfall (ISMR) (Rasmusson and Carpenter 1983; Pant and Kumar 1997). As mentioned by Parthasarathy (1984), the summer monsoon rainfall is highly correlated between some adjacent subdivisions in northwestern, central and peninsular India. It is therefore necessary to do empirical orthogonal function EOF analysis of the Indian summer monsoon rainfall to have a better idea about spatial distribution (Fig. 26.1).

One of the major reasons for these droughts has been a strong link with the El Nino Southern Oscillation (ENSO) patterns (Gadgil et al. 2003). For example, the country faced 10 drought years out of 22 during the ENSO period of 1965–87 while 3 drought years during 1921–64 during non ENSO period (Department of Agriculture and Co-operation 2004). In recent decades, a weakening relationship between the Indian monsoon and ENSO phenomenon was also suggested (Kumar et al. 1999). Thus it is a fact that the Indian monsoon system, its agricultural sector and droughts are very much linked to the regional and global climate system and hence are very much vulnerable to the changes in the climate both at regional and global scales (Fig. 26.2).

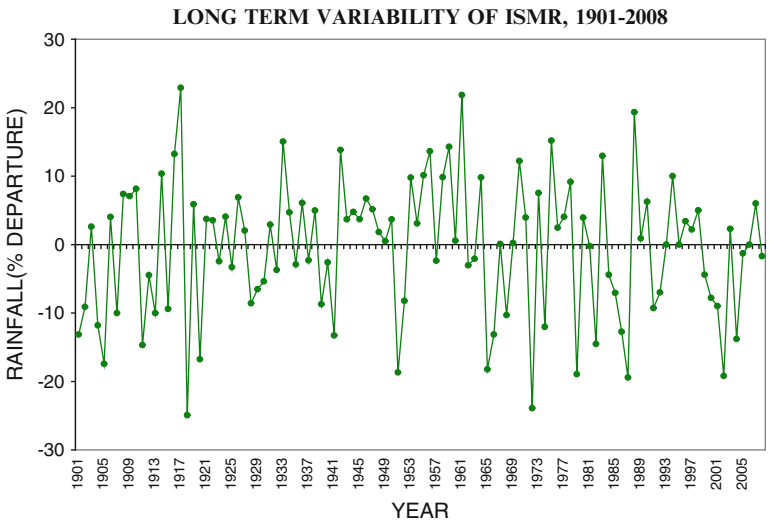


**Fig. 26.1** Long term Variability of ISMR, 1901–2008

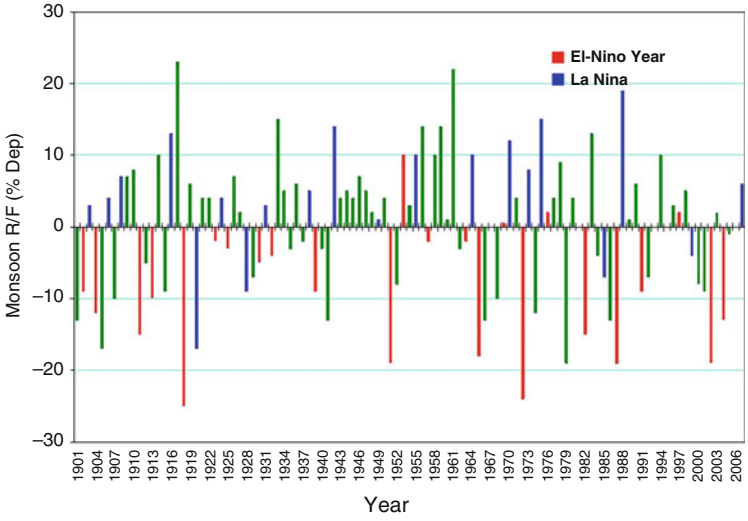


**Fig. 26.2** Variability in El-Nino and La Nina Years (1901–2008)

### *26.3.1 ENSO Effect on ISMR*

Studies have shown that there is an increased influence of drought occurrence during El Nino and of excess rainfall during La Nina. ENSO index is defined as the negative of the Nino 3.4 SST anomaly so that positive values of the ENSO index imply a phase of ENSO favourable for the monsoon. El Niño's are associated with ENSO index less than −1.0 and La Nina with ENSO index greater than 0. It is seen that when the ENSO index is favourable (>0.6), there is no droughts and when it is unfavourable (<−0.8) there are no excess rain in the monsoon season. But the experiences in 1997 and 2002 suggested that the link with ENSO had yet to be properly understood. Gadgil et al. (2007) showed that in addition to ENSO, the phase of the Equatorial Indian Ocean Oscillation (EQUINOO) which is considered to be the atmospheric component of the Indian Ocean Dipole/Zonal Mode makes a significant contribution to the interannual variation of ISMR. She further showed that there is a strong relationship between the extremes of ISMR and a composite index of ENSO and EQUINOO with all the droughts characterized by low values of this index and all excess monsoon seasons, high values. It is seen that when EQUINOO is favourable (EQWIN is >0.2), there are no droughts and when it is unfavourable (EQWIN <−0.8) there are no excess rain in the monsoon season. In the monsoon season of 2002, although the El Nino is weaker than 1997, EQUINOO was also unfavourable and a severe drought occurred. Thus with EQUINOO we can explain not only the droughts that occurred in the absence of El Nino but also excess rainfall seasons in which ENSO was unfavourable. In recent study, Kumar et al. (2005) suggested that El Nino events with the warmest SST anomalies in the central equatorial Pacific are more effective in focusing drought-producing subsidence

over India than events with the warmest SST patterns resulting from linear combinations of the first two leading patterns of tropical Pacific SST variability. It is seen that the El Nino monsoon relationship depends on the nature of evolution of El Nino in the seasons prior to the summer season. Incorporation of predictors associated with EQUINOO along with those associated with ENSO may improve predictions. It is possible to derive useful information with EQWIN and ENSO indices about nonoccurrence of extremes (either deficit or excess rainfall) for July and August together. More studies are required to assess whether it is possible to predict the EQUINOO for any part of the season and also the impact on the Indian rainfall in that part of the season for a given (predicted) ENSO state.

## 26.4 Climate Change Vulnerability of India

The global climate change is characterized by increase in surface temperatures by $0.6 \pm 0.2°C$ over the twentieth century with a projected rise in the range of 1–3.5°C by 2100 (Houghton et al. 2001). There has been agreement that the global climate change would modify the hydrological cycle hence increasing the possibility of droughts and floods globally though with uneven distribution of impacts over the continents (McCarthy et al. 2001). The study of the country indicates an increase in the temperature of 0.57°C per 100 years (Kumar et al. 1994; Singh et al. 2001). The climatic projection studies indicated a general increase in temperatures in the order of 3–6°C over the base period average with more warming in the northern parts than the southern parts of the country (Lal et al. 1995; Lonergan 1998; The Energy Resource Institute 2001). At the regional level, extreme summer rainfall events were observed in northwest India during recent decades (Singh and Sontakke 2002). Roy and Balling (2004) have computed the extreme daily precipitation indices in India and found upward trend in 114 weather stations and downward trend in 61 weather stations across India. The climate models predicted a change in precipitation by 5–25% over India by the end of the century with more reductions in the wintertime rainfall than the summer monsoon (Lal et al. 2001b). Changes in annual mean surface air temperature (°C) and rainfall (%) for 2071–2100 relative to baseline (1961–1990) are shown in Fig. 26.3a, b (Kumar et al. 2006).

Studies by (Lal et al. 2001b) also suggested increased variability in the onset of monsoons with implications on sowing time for the farmers in future. The high resolution ($50 \times 50$ km) climate prediction experiments involving state-of-art regional climate modeling system called PRECIS (Providing Regional Climates for Impact Studies) developed by the Hadley Center for Climate Prediction and Research revealed possibilities of increased rainfall and temperatures in global warming scenarios (Kumar et al. 2006). According to the experiments west central India showed maximum increase in rainfall with extreme precipitations in Western Ghats and northwestern peninsular India. Projections using Soil and Water Assessment Tool (SWAT) water balance model and HadRM2 indicated droughts and floods in climate change scenario (Gosain et al. 2006). The studies indicated acute

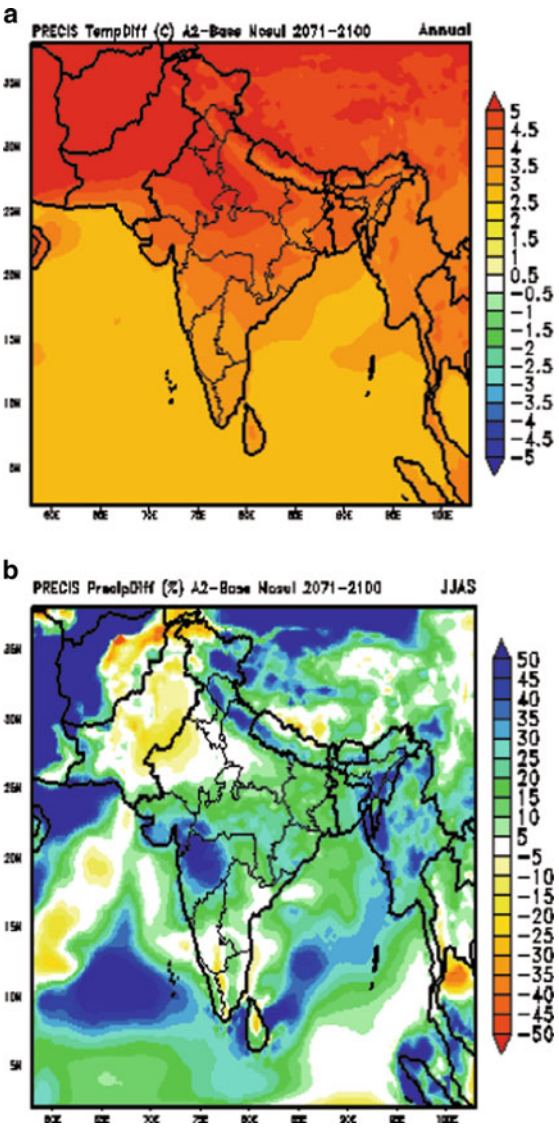


**Fig. 26.3** **(a)** Changes in annual mean surface air temperature (0 C) for 2071–2100 relative to baseline (1961–1990). **(b)** Changes in rainfall (%) for the period 2071–2100 relative to baseline (1961–1990)

water scarcity conditions in the river basins of Luni, Mahi, Pennar Sabarmati and Tapi and severe flood conditions in the river basins of Godavari, Brahmani and Mahanadi.

Thus, the most notable climate change implications for the drought vulnerable India would be the enhanced preparedness with due emphasis to the community based preparedness planning, reviewing the existing monsoon, drought prediction methodologies and establishing drought monitoring and early warning systems in association with a matching preparedness at the input level. The adaptation to

climate change will be carried out in various forms, including technological innovations, changes in arable land, changes in irrigation, etc. The changes in arable lands, due not only to the needs of agricultural production following population increase but also to climate change, are expected to be another form of adaptation. As the global climate has a tendency towards warming, a significant change in the irrigation of agricultural crops is expected.

## 26.5 Adaptation

Adaptation refers to change in a system in response to some force or perturbation such as climate change (Smithers and Smit 1997; Smit et al. 2000). Adaptation is important in climate change in two ways – in reducing the impacts of the future climate change and in understanding the options for such adaptations to climate changes. Within climate change adaptation community, there is a common assertion that if we could cope better with the present climate risks, possibly we could significantly reduce the impacts of future climate change (Thomalla et al. 2006). In absence of reliable climate predictions, adaptation strategies would vary from region to region at the scales that make them useful for policy level planning. The emphasis is on identifying no-regret adaptation options those would reduce current vulnerabilities while mainstreaming the adaptation in the long run. For India no regret adaptation strategies that should emphasize are:

### *26.5.1 Building Local Capacity for Drought Preparedness and Mitigation*

Involvement of communities in disaster management planning enables local governments and disaster management personnel to gain better understanding on the vulnerabilities of the communities (Mileti 1999; Pearce 2003). Currently India lacks such community based drought preparedness planning at village, district and region levels. The Disaster Risk Mitigation (DRM) program, a recent collaborative initiative between Government of India and United Nations Development Program (UNDP) can serve as a starting point for the country (National Institute of Disaster Management 2006). The Parliament of India has also passed The Disaster Management Act in 2005.

In order to involve village communities in the implementation of watershed projects under all the area development programmes namely, Integrated Wastelands Development Programme (IWDP), Drought Prone Areas Programme (DPAP) and Desert Development Programme (DDP), the Guidelines for Watershed Development were adopted and subsequently revised by the Government. In this endeavour many Governments and NGOs are working in different levels for

implementation of water conservation awareness programs. Better co-ordination among the organization on water conservation techniques and drought management strategies would help to provide education on different scientific aspects including cultural perspectives of water resources.

### *26.5.2 Enhancing Capacities of Local Governments*

The National Natural Resource Management System (NNRMS) along with a standing Committee on Agriculture and Soils (SC-AS) have been set up to monitor the progress of remote sensing applications to natural resources management in the country. Recent efforts to combat drought through policies formulated by governmental agencies include crop weather watch groups (CWWG) at the national and state level, food security through buffer stocks, priority to the most seriously affected areas for "food for work"/National Rural Employment, Project and other programs, high priority to food production in the most favourable/irrigated areas as compensatory programs, optimum input use, rural godowns to avoid crash sales and crop insurance schemes.

Most recently, sincere efforts are being made to develop areas on the basis of watersheds. The space-based National Agricultural Drought Assessment and Monitoring System (NADAMS), which has been operational since 1989 under India's Department of Agriculture, provides scientific information at the district level for most of the states and sub-district levels in a few states. Forecasting Agricultural output using Space, Agro-Meteorology and Land based observations (FASAL) is now also being implemented through co-operation and collaboration of SAC, Ahmedabad, IMD through State Agricultural Universities, ICAR institutions, IITs, etc.

## 26.6 Development of Skill for Drought Prediction, Monitoring, Mitigation and Communication

The long-range and extended range weather forecast particularly the summer monsoon rainfall forecast across Indian states is among the toughest task because of the complex nature of the atmosphere in the tropics. Therefore, India needs to look forward at its monsoon prediction techniques and methodologies and needs to develop method that is validated for its specific needs, particularly agricultural risk management and operational activities. A shift from empirical to dynamic models has already been started to enhance the forecasting skill (Roy Bhowmik and Durai 2008). The country has also planned to enhance the data processing facilities that utilize the large data already collected by INSAT satellites and also from other satellites those will be launched soon. There is also a need to integrate the

climatic forecasts and climate risk management with other aspects of infrastructure and input supply such as drinking water, fodder, seeds and fertilizers. Institutions, disciplines and people are to be brought together so that appropriate management decisions could be made from the available forecasts for reliable drought preparedness in India.

### *26.6.1 Drought Monitoring*

The drought monitoring system in India in the form inter-departmental exchange of data and information is being done by CWWG. The Southwest Asia Drought Monitor developed by the International Water Management Institute (IWMI), which currently covers only the western India, Afghanistan and Pakistan, can be a good beginning (Thenkabail et al. 2004). This monitor provides drought information at the regional, district/provincial and pixel level (currently 0.5 × 0.5 m) and helps local administrators to monitor and mitigate the drought impacts. Karnataka state has established a special Drought Monitoring Centre for monitoring state level drought onset conditions in order that the state administration plans in advance of the crisis. The centre monitors rainfall, water reservoir levels and other relevant parameters on daily basis in the rainy season. It has to be replicated in all other drought prone states too.

Important features of drought monitoring, declaration and management are summarized below:

- A multilevel institutionalized monitoring and early warning system both during normal and drought years and impact analyses for future guidance constitute the bedrock of the current comprehensive process-based management.
- The constitutional, legal and institutional framework of monitoring, declaration and management is undergoing rapid evolution for internalizing emerging technological and economic opportunities.
- Better governance need to be the key factor as it has reduced poverty to 15.28% in the frequently drought-affected State of Rajasthan as compared to 47.15% in the high rainfall state of Orissa and 42.6% in the least drought-affected State of Bihar.
- Different states have their own systems of drought management. A typical system consists of the Relief or Revenue Minister, Crop Weather Watch Group, Relief Commissioner, District Collector, Block Development Officer, and rainfall monitoring at Tehsil Mandal level and village Panchayats (elected representatives).
- When droughts are severe like that of 2002, special task forces at the central level and additional mechanisms at the state level reinforce the regular system of monitoring and management.
- Weather monitoring and forecasts of the India Meteorological Department (observed rainfall deficiency recorded at tehsil/district/state level and rainfall

prediction) would indicate limited water flow or water availability in major reservoirs and help recommendations of the Crop Weather Water Group trigger the process of drought declaration.
- Drought declaration after estimation of agricultural losses is the sole responsibility of States whereas the central government facilitates monitoring and management.
- Immediately after the receipt of declaration memoranda from states, central teams are constituted by the Central Relief Commissioner to verify the claims made by the state agencies.
- In the 2002 droughts, certain codes of estimating losses were waived off by the National Calamity Management Committee due to failure of rains in July itself, with a 51% deficit in rainfall in July and the inability to sow the crops.
- Impact of drought on crops, inputs support, energy availability, market responses, water availability, physical infrastructure, livestock, fodder availability and employment, etc., are monitored by the Central/State Relief Commissioners, and special groups/task forces.
- Estimations of sustained losses are, in general, inadequate for quantifying damages to perennial crops, Orchards, trees, livestock fertility, wildlife, groundwater resources, biodiversity and aquaculture.
- The scope of estimating losses may be expanded to secondary and tertiary-level ripple effects on nonfarm livelihood opportunities, especially for the resource-poor population.
- High-resolution spectral libraries and remote sensing censors are evolving to improve precision and real timeliness of forewarning systems and estimation of losses.
- Long-term monitoring and evaluation of groundwater resources and their potential for drought mitigation should be prioritized.
- Impact monitoring and documentation of each drought are important to learn lessons for devising future strategies and process refinement.
- A global force of oceanic and terrestrial systems determines rainfall of a country. This calls for unrestricted sharing of data, experience and knowledge among the neighboring countries.
- India has adequate experience in managing medium and severe droughts. This could be shared with neighboring countries having similar agro-ecologies, socioeconomic conditions and livelihood opportunities.
- India has created sufficient number of institutions, training materials, guides and manuals for capacity building and they may be quite useful for neighbouring countries.

### *26.6.2 Mitigation of Drought*

Generally, there are always some areas which are not affected by drought while some other areas may be reeling under drought. The major issues need to be

addressed in this connection are research and information technology based efforts to make a reliable assessment on the likely impact of drought, availability of resources such as credit, fertilizers, pesticides and power for increasing the production, organisation of buffer stocks of food grains and fodder to cope up with the likely/anticipated shortages and providing economic relief through creation of durable assets which will cope up with future drought rather than extending subsidies.

Agriculture is the most affected activity, which in turn affects the livelihood of the majority of population in India. Thus strategic planning for the rainfed agriculture becomes the major thrust area of drought management.

### *26.6.3 Drought Management*

Drought management is an integral and key factor in sustainable agriculture. Farmers should be encouraged to develop a range of flexible contingency plans that protect the soil, climate, and vegetation to resist the temptation of over extracting these limited resources, particularly under drought. Drought management procedures include community nurseries at points where water is available, early transplantation at right opportunity, sowing of alternate crops/varieties, ratooning or thinning of crops based on available soil water and forecast rainfall, soil mulching if the break in the monsoon is very brief, weed control, in situ water harvesting and/or run-off recycling, broad beds and furrows, graded border strips, inter-row and inter-plot water harvesting systems, intercropping systems for areas where the growing season is generally 20–30 weeks, alternate land use systems, development of agriculture on the basis of the watershed approach, alley cropping, agro-horticultural systems, water resources development through watershed approaches, treatment of lands with soil conservation measures and using forage as horticultural production.

During drought year, supply of drinking water to remote places becomes the cause of concern. This could be solved by targeting potential groundwater sites for taking up emergency well digging by using high resolution Landsat/IRS data. Several new technologies like the remote sensing, geographical information system and the information & communication are being employed for forecasting, mitigation and governance of drought relief measures. Indices like Normalized Difference Vegetation Index (NDVI), Standardized Precipitation Index (SPI), etc. are sensitive to the changes in vegetation affected by moisture stress. The vegetation index maps are prepared by the National Remote Sensing Agency (NRSA) are available for monitoring agricultural drought. An integrated (water, agricultural, land, fodder resources and socioeconomic database) study using data from IRS satellite, Census integrate and prescribe appropriate land use, fodder and water management practices.

## 26.7 Water Management Strategies

Conceptually, there are two ways of fighting drought. Replacing/reducing rain-fed agriculture and animal husbandry by industry and services as contributors to our economy. This is almost an impossible task as 75% of India's population is dependent on agriculture-related occupations for their livelihood. The other alternative is to manage drought by improved water management and crop management by monitoring and mitigating its effects by creating livelihood/income generation alternatives.

### *26.7.1 Some Techniques for Increasing Available Water Supply in Drought Prone Regions*

The methods can be listed under two main headings, namely.

#### 26.7.1.1 Water Development and Management Practices

Methods of harvesting involves: reshaping the soil surface, treatment of catchments, chemical treatments, use of Brackish water, underground water recharge, waterproof membranes, water storage, sand dams, small weirs, off-stream storage and storage below ground level using percolation tank.

#### 26.7.1.2 Water Conservation Measures

The conservation method involves evaluation of water quantity and quality from new sources, inventory water bank contracts to find new water supplies for drought-stricken areas and by improving the accuracy of seasonal runoff and water supply forecasts. It can be established by stronger economic incentives for private investment in water conservation, voluntary water conservation, implementation of water metering and leak detection programs and by reducing consumptive use by changing the type of water application system. The water-saving measures for urban areas include modifying rate structure to influence consumer water use by increasing rates during summer months, imposing excess-use charges during times of water shortage, modifying plumbing system by distributing water-saving kits, including replacement showerheads and flow restrictors changing plumbing standards, reducing water-system losses by reducing water main-leak-detection survey teams followed by water main repair or replacement, starting a meter-replacement program, recycling filter plant backwash water and recharging groundwater supplies. Water-conservation programmes should be conducted to educate the public and of school children, including special emphasis during times of water shortage.

The water-saving measures for farms include use of accurate land leveling, installation of return-flow systems, using line canals or installing piping to control seepage, use of sprinkler and drip irrigation systems, scheduling irrigation by demand, using soil-moisture monitoring and deep pre-irrigation during periods when surplus water is available, improving tillage practices and by growing drought- or salinity-tolerant crops.

Water supply can be increased by issuing emergency permits for water use, providing pumps and pipes for distribution, inventory self-supplied industrial water users for possible use of their supplies for emergency public water supplies and by establishing water banks for voluntary sale, transfer, or exchange of water.

## 26.8 Enhanced Operational Preparedness

In case of monsoon failure in the midseason the standing crops suffer and may be lost due to drought. In that case, short duration alternative crop seeds should be sown and satisfactory crop could be obtained in many parts of the country.

Economic Development is possible by providing incentives for farm and business diversification, promoting off-farm industry to diversify wage-earning strategies and by enhancing information flow between bankers, farmers/ranchers, businesses, and government agencies.

On health and nutrition point of view, it is necessary to establish food subsidy programs for drought-affected individuals, to conduct public information campaigns on the health dangers of drought (e.g., heat stress, low flow of water, fire risk, deteriorated water quality, etc.).

Government, NGOs and media participation in the drought management programme can be achieved by establishing linkage between authorities as shown in the flow chart (Fig. 26.4). Media personnel need to be in constant touch for different drought issues. This should also include media personnel's participation in drought planning and they also need to be updated about new conditions and plans.

## 26.9 Summary of Features of EWS in India

Early Warning System plays an important role in risk management of drought. India Meteorological Department (IMD), National Centre for Medium Range Weather Forecast (NCMRWF), National Agricultural Drought Assessment and Monitoring System (NADAMS) and All India Coordinated Research Project on Dryland Agriculture (AICRPDA) provide drought early warning management advisories at different crop growth stages depending on the drought situation and forecast weather (including medium range). Based on the information provided by the National Crop Forecasting Centre (NCFC), the Crop Weather Watch Group (CWWG) and other agencies act as shown in the flowchart.

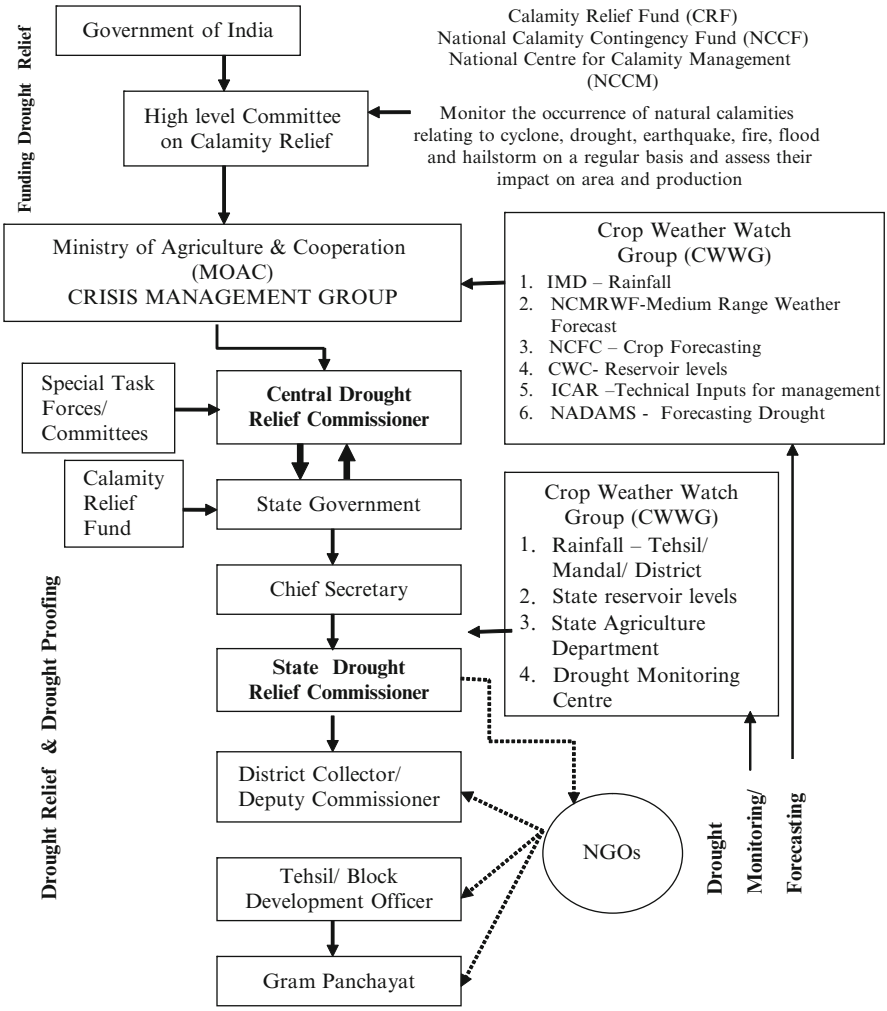


**Fig. 26.4** Flow chart of drought management program

The existing limitations in dealing with uncertainties can be effectively dealt with if an integrated assessment of climate change impacts on biophysical, environmental and socioeconomic aspects be carried out by down scaling the outputs from the global and regional simulation models, which would enhance the utility of climate change prediction research for regional policy planning (Mall et al. 2006). Technical Assistance for advising people on potential sources of water, additional training to natural resource personnel, adopting water conservation measures, conducting workshops on various drought topics, including crop survival during drought, design and implementation of water rationing programs, awareness programme for optional use of water for irrigators and urban water suppliers,

creating low-interest loan and aid programs for agriculture constructing a drought information center and dissemination of real-time weather data and weather forecast evaluating capacities to withstand losses associated with drought such as incomes, assets, credit flexibility and decision-making processes, subsidy, loan, and welfare program applicability and the effect of government programs and policies is very much needed.

## 26.10 Conclusion

The study focuses on strategies used for decision making. The probabilities of drought occurrence as well as drought prediction using ENSO or any other indices would form the baseline information for mitigation and adaptation. Decision support system for estimating losses to crops, orchards, trees, grasslands, biodiversity, livestock, fisheries, groundwater resources, etc. would be useful for different vulnerable regions and livelihood opportunities. Non-rainfall-dependent income from nonagricultural occupations (handicrafts, mining, etc.) in vulnerable areas is an indigenous coping strategy for drought monitoring and resilient drought proofing could be a sound strategy of mitigation. Banks for food, water, fodder, feed and seeds of short-duration drought-tolerant crops/varieties for contingence cropping may be set up in vulnerable areas. Drought-mitigation strategies may be built upon the traditional systems of drought management/coping mechanisms. Our approach involves participatory research with active collaboration of an interdisciplinary group of scientists with farmers, so that the problems are addressed with the modern tools and datasets that are available. With such approach, the recent advances in sciences can be harnessed for identifying appropriate farmer-acceptable strategies for achieving sustained high production in highly variable drought prone regions.

**Acknowledgement** The authors express their sincere thanks to Prof. Sulochana Gadgil for her valuable suggestions and guidance during the course of the work. They are also thankful to Dr. D. S. Pai, Director, ADGM(R) office for his timely help in providing necessary information.

## References

Center for Research on Epidemiology of Disasters, (2006) India country profile of natural disasters. EM-DAT: the international disaster database. http://www.em-dat.net/disasters/Visualisation/profiles/countryprofile.php. Cited 6 Mar 2006

Department of Agriculture and Co-operation (2004) Drought, (2002) A report, Department of Agriculture and Co-operation, Ministry of Agriculture, New Delhi, p 190

Gadgil S, Vinaychandran PN, Francis PA (2003) Droughts of the Indian summer monsoon: role of clouds over the Indian Ocean. Curr Sci 85:1713–1719

Gadgil S, Rajeevan M, Francis PA (2007) Monsoon variability: links to major oscillations over the equatorial Pacific and Indian Oceans. Curr Sci 93(2):182–194

Gosain AK, Rao S, Basuray D (2006) Climate change impact assessment on hydrology of Indian river basins. Curr Sci 90(3):346–353

Houghton JT, Ding Y, Griggs DJ, Noguer M, Van der Linden PJ, Dai X, Maskell K, Johnson CA (2001) Climate change 2001: the scientific basis. Contribution of working group I to the third assessment report of IPCC. Inter governmental panel on Climate Change

Kumar RK, Kumar KK, Pant GB (1994) Diurnal asymmetry of surface temperature trends over India. Geophys Res Lett 21:677–680

Kumar KK, Rajagopalan B, Cane MA (1999) On the weakening relationship between the Indian monsoon and ENSO. Science 284:2156–2159

Kumar KK, Hoerling M, Rajagopalan B (2005) Advancing Indian monsoon rainfall predictions. Geophys Res Lett 32:1–4

Kumar RK, Sahai AK, Kumar KK, Patwardhan SK, Mishra PK, Revadekar JV, Kamala K, Pant GB (2006) High resolution climate change scenarios for India for the 21st century. Curr Sci 90(3):334–345

Lal M, Cubasch U, Voss R, Waszkewitz J (1995) Effect of transient increase in greenhouse gases and sulphate aerosols on monsoon climate. Curr Sci 69(9):752–763

Lal M, Nozawa T, Emori S, Harasawa H, Takahashi K, Kimoto M, Abe-Ouchi A, Nkajima T, Takemura T, Numaguti A (2001b) Future climate change: implications for Indian summer monsoon and its variability. Curr Sci 81:1196–1207

Lonergan S (1998) Climate warming and India In: Dinar A, Mendelsohn R, Evenson R et al (eds) Measuring the impact of climate change on Indian Agriculture. World Bank Technical paper No. 402, Washington, DC

Mall RK, Singh R, Gupta A, Srinivasan G, Rathore LS (2006) Impact of climate change on Indian agriculture: a review. Clim Change 78:445–478

McCarthy JJ, Canziani OF, Leary NA, Dokken DJ, White KS (2001) Climate change 2001: impacts, adaptation and vulnerability: contribution of working group II to the third assessment

Mileti DS (1999) Disasters by design. A reassessment of natural hazards in the United States. John Henry Press, Washington, DC

National Institute of Disaster Management (2006) National disaster risk management program. Mid-term review report, National Institute of Disaster Management, Ministry of Home Affairs, Government of India, India

Pant GB, Kumar R (1997) Climates of South Asia. Int J Climatol 18(5):581–582

Parthasarathy A (1984) Fluctuations in all-India summer monsoon rainfall during 1871–1978. Clim Change 6:287–301

Pearce L (2003) Disaster management and community planning and public participation: how to achieve sustainable hazard mitigation? Nat Hazards 28(2–3):211–228

Rasmusson EM, Carpenter TH (1983) The relationship between eastern equatorial pacific sea surface temperatures and rainfall over India and Sri Lanka, American meteorological society. Mon Weather Rev 111:517–528

Roy Bhowmik SK, Durai VR (2008) Multi-model ensemble forecasting of rainfall over Indian monsoon region. Atmosfera 21(3):225–239

Roy SS, Balling RC (2004) Trends in extreme daily precipitation indices in India. Int J Climatol 24:457–466

Shaw R, Prabhakar SVRK, Fuieda A (2005) Community level climate change adaptation and policy issues: a case study from Gujarat, India. Graduate School of Global Environmental Studies. Kyoto University, Japan, p 59

Singh N, Sontakke NA (2002) On climatic fluctuations and environmental changes of the Indo-Gangetic plains. India Clim Change 52:287–313

Singh RS, Narain P, Sharma KD (2001) Climate changes in Luni river basin of arid western Rajasthan (India). Vayu Mandal 31(1–4):103–106

Smit B, Burton I, Klein RJT, Wandel J (2000) An anatomy of adaptation to climate change and variability. Clim Change 45(1):223–251

Smithers J, Smit B (1997) Human adaptation to climatic variability and change. Glob Environ Change 7(2):129–146

The Energy Resource Institute (2001) India's first national communication to UNFCCC. The Energy Resource Institute, New Delhi

Thenkabail PS, Gamage MSDN, Smakhtin VU (2004) The use of remote sensing data for drought assessment and monitoring in south west Asia. Research report 85, International Water Management Institute, Sri Lanka

Thomalla F, Downing T, Spanger Segried E, Han G, Rockstrom J (2006) Reducing hazard vulnerability: towards a common approach between disaster risk reduction and climate adaptation. Disaster 30(1):39–48

# Chapter 27
# Climate Change in Relation with Productivity of Rice and Wheat in Tarai Region of Uttarakhand

**H.S. Kushwaha**

**Abstract** The rice-wheat cropping system is a very important and popular cropping system being followed in the tarai area of Uttarakhand. The area, characterized by shallow water table and moist soil regime, lies within a narrow east-west strip of 8–25 km wide, on an outwash plain, gently slopping (<1%) southwards below the Bhabar tract along the foot hills of the Himalayas. The entire area is dissected by a number of small streams originating as springs from the junctions of Bhabar and tarai belts. In India, about 10.0 million hectare area is under rice-wheat cropping system and of this 4.8 m ha falls in the tarai area of Uttarakhand. The sowing of wheat after rice is being followed since about more than five decades after bringing the area under crop cultivation since its deforestation in 1950. In rice-wheat cropping system a complete recommended set of agronomic practices is followed including timely control of pests and diseases, proper integrated nutrient management, application of balanced fertilizers and crop residue management, recommended tillage practices after harvesting of rice crop and control of weed flora over a time period under different conditions and crop stages. In-spites of these the yield of wheat after rice in the area has declined by about 20–30% after the green revolution. It was thought that this decline in tend may follow the change in climatic conditions specially the air temperature and the rainfall pattern in the area. Crop productivity can be affected by climate change in two ways, one directly due to changes in climatic variables mainly temperature and precipitation and indirectly through changes in soil, distribution and frequency of infestation by insects, diseases or weeds.

In the present investigation, the productivity and sustainability of rice-wheat cropping system has been evaluated by analyzing the impacts of temperature and rainfall over past 45 years on yields of rice and wheat crops recorded at G.B. Pant University of Agriculture & Technology, Pantnagar (29° N latitude,

H.S. Kushwaha (✉)
Department of Soil Science, College of Agriculture, G. B. Pant University of Agriculture & Technology, Pantnagar, Uttarakhand 263145, India
e-mail: kushwahahs@yahoo.co.in

S.D. Attri et al. (eds.), *Challenges and Opportunities in Agrometeorology*,
DOI 10.1007/978-3-642-19360-6_27, 

79° 30′E longitude and altitude 243.84 m amsl) located in tarai and bhabar agro-climatic zone of Uttarakhand. The rice yields for 45 kharif wet seasons from 1961 to 2005 and wheat yields from rabi seasons of 1961–1962 to 2005–2006 was collected from the Pantnagar University Farm where these crops were grown using all standard & recommended agronomic & plant protection practices to maximize crop yields. The maximum and minimum temperatures as well as rainfall data of the same duration were collected from meteorological observatory situated within the University Campus. Five year averages of the yields and climatic variables were worked out from 1961 to 2005 and then the changes in yields and rainfall and temperature change trends were calculated and finally, the simple regression equation of the type as well as curvilinear regression analysis (Ezekiel and Fox 1959) were employed to develop regression equations between yields of rice and wheat with changes in climatic variables using statistical programs.

The following curvilinear regression equation for change in yield of rice as a function of change in rainfall and maximum, minimum and mean air temperatures during the kharif season was developed:

$$Y = 6.344 - 1.02X_1 + 3.45X_2 - 0.0157X_3 - 4.073X_4, R^2 = 0.712$$

This shows that in this area about 71.2% variations in rice yields are due to variations in south-west monsoon rainfall and temperatures. However, for wheat in rabi season, following regression equation between change in wheat yield and climatic variables was obtained:

$$Y = 12.767 - 1.080X_1 + 0.261X_2 + 1.917X_3 + 1.632X_4, R^2 = 0.924$$

This indicates that in this area about 92.4% variations in wheat yields are due to variations in winter rainfall and temperatures.

Results of this studies showed that there has been a gradual increase in mean seasonal air temperature. The average seasonal change in maximum temperature and minimum temperature was found to be are 0.4°C and 0.2°C, respectively during kharif wet season. However, the rainfall variability is within 10–30% during kharif season (from June to October) over last 45 years at tarai & bhabar agroclimatic-zone of Uttarakhand. There have been changes in rice yields as well. The Rice yields were found to increase over the years due to introduction of high yielding varieties and adoption of improved cultivation technology and irrigation facilities in last two decades. Data also showed that the years in which rainfall is very high, the rice yields are low due to more incidences of diseases in crop in the area.

Results of analysis for rabi seasons from 1961–62 to 2005–06 over last 45 years showed that the average seasonal change in maximum temperature and minimum temperature were 0.4°C and 0.4°C, respectively, and rainfall variability is within 8–40%. However, the wheat yields have also been found to change depending upon the rainfall distribution and rainfall variability except some variations. Results also indicate that in years in which winter rainfall was excessive, and then wheat yields

were found to decline may be due to lodging and insect problems. However, in years of low winter rains, there has been response of irrigation in maximizing wheat production in the area. It has also been observed that in years in which mean monthly air temperature in the month of March is 1–2°C below the normal value, there has been delay in wheat maturity by 7–10 days and an increase in wheat yield is by 4–6 quintal per ha have been observed more compare to other years.

As a conclusion it can be said that in this irrigated area, the effective beginning and end of rice growing season is determined by temperatures and rainfall distribution. For getting maximum yields it is necessary that the rice must be planted at the time i.e. in last week of June where optimum temperature conditions are met and since then the flowering will reach the date before night temperature falls below 20°C. The results further showed that, over the years in wheat for each degree rise in air temperature and lack of winter rains, there has been reduction in yields by 5–10% in timely and late sown wheat. However, there has been reduction in yields by 10–20% in early and late planted rice due to early withdrawn of monsoon and decrease in air temperature in the month of October. So in general, it can be said that there has been impacts of climatic variability on rice and wheat crops grown even using standard agronomic practices and control measures. Early rise in air temperature in the month of March due to lack of winter rains adversely affects the wheat yields in many years in the area. This type of study will be of immense use for other location as well, if the long range weather forecast for important climatic variables such as rainfall and temperature are available well in advance, the productivity of rice and wheat can be assessed for that location and it will promote in deciding the optimum sowing dates of Rice and also of wheat after rice and will help in deciding irrigation schedules & for taking control measures for maximizing their production.

## 27.1 Introduction

In India, wheat is grown in 24.2 m ha area and out of this 50–70% wheat is taken in rice-wheat rotation. Rice – wheat cropping system occupies first place in area (around 11 m ha), and production (more than 150 million tonnes) in India (India 2002). Nearly 25% of the total rice area of the country is grown in rotation with wheat (Sen and Sharma 2002) and it is the backbone of country's food security with yield potential of 8.12 t $ha^{-1}$ $year^{-1}$ (Singh and Singh 1996; Bhandari et al. 1992). The productivity of wheat in this rotation is very low due to many factors. Some of the problems in rice-wheat rotation for the cultivation of wheat crop are firstly due to the delayed wheat sowing (temperature gets reduced) as the harvesting of rice generally gets prolonged till the end of November and secondly due to the nature of puddled soil which develops large clods on ploughing which cannot be managed by ordinary implements etc. Increasing nitrogen level mitigates the deleterious effect of puddling and flooding on wheat yield. Additional 60 kg N $ha^{-1}$ applied to hasten the decomposition of rice stables at ploughing over normal management was found

suitable. The rice-wheat cropping system is a very important and popular cropping system being following in the tarai area of Uttarakhand. The area, characterized by high water table and moist soil regime, lies with a narrow east-west strip of 8–25 km wide, on an outwash plain, gently slopping (<1%) southwards below the Bhabar tract along the foot hills of the Himalayas. The entire area is dissected by a number of small streams originating as springs from the junctions of Bhabar and tarai belts. In India, about 4.8 m ha million hectare area cultivated under rice-wheat cropping system falls in tarai belt of Uttarakhand. The sowing of wheat after rice is being followed since about more than three decades after bringing the area under crop cultivation since its deforestation in 1950. In the study area, a complete recommended set of standard agronomic practices is followed including timely control of pests and diseases, proper integrated nutrient management, application of balanced fertilizers and crop residue management, recommended tillage practices after harvesting of rice and control of weed flora over a time period under different conditions and crop stages for in rice-wheat cropping system. In-spites of these, the yield of wheat after rice in the area has declined by about 20–30% after the green revolution. It was thought that this decline in tend may follow the change in climatic conditions specially the air temperature and the rainfall in the area.

Therefore, in the present investigation this region has been selected for evaluating the productivity and sustainability of rice-wheat cropping system by analyzing the climatic conditions over past 45 years and correlates them with the yields of rice and wheat. Detailed analysis of monthly temperatures were carried out to determine the effective and critical temperature ranges for wheat and rice for this region for maximizing their yields.

## 27.2 Material and Methods

The present investigations were carried out at G. B. Pant University of Agriculture & Technology, Pantnagar (29° N Lat., 79° 30′ E Long. and altitude 243.84 m amsl), Uttarakhand. The area called tarai, lies in the foothills of Himalayas. The climate of the reason is humid sub-tropical with severe cold (lowest minimum temperature 2.0 ± 1.5) during winter and hot (highest maximum temperature 43.0 ± 1.0) during summer. The average annual rainfall of the region is 1433.4 mm of which 90% rainfall is received during south – west monsoon season from mid June to end of September. The soils of tarai are mainly sandy loam to clay loam, coarse to fine texture having good moisture storage capacity, highly productive, associated with shallow to deep water table conditions and are classified as Mollisols. The physical and chemical properties of the soil are described by Deshpande et al. (1971). The rice yield data for 45 years from kharif season of 1961 to 2005 and wheat yield data from rabi season of 1961–1962 to 2005–2006 was collected from the Pantnagar University Farm, where standard agronomic practices were followed for raising these crops. The meteorological data was collected from meteorological observatory of the University located within the University Campus. The simple regression

equation as well as curvilinear regression analysis (Ezekiel and Fox 1959) was employed to develop regression equations between change in yields of Rice and Wheat with changes in climatic variables specially the seasonal rainfall, number of rainy days and maximum, minimum and average temperatures using statistical programs. Five year averages on these weather variables were also correlated with average yields to study the trend of variation in yields of Rice during kharif season (June to October) & for Wheat during Rabi season (November to April) over 45 years for Tarai & Bhabar agroclimate zone of Uttarakhand.

1. The simple regression equation was used with the help of statistical program which is as follow:

$$Y = m + a\ X$$

   Where Y = Yield of crop (kg/ha),
   X = Weather parameter, for which regression equation is developed m & a are the constants.
2. The curvilinear regression analysis (Ezekiel and Fox 1959) employed to develop regression equations was

$$Y = a + f_1(X_1) + f_2(X_2) + f_3(X_3) + f_4(X_4)$$

   Where, Y = Yield of crop, kg/ha for Rice or Wheat,
   $X_1$ = Rainfall (mm), $X_2$ = Maximum Temperature (°C)
   $X_3$ = Minimum Temperature (°C), $X_4$ = Average Temperature (°C)

## 27.3 Results and Discussion

Five years' average data of rainfall, number of rainy days, maximum and minimum temperatures weather variables for crop growing seasons for rice (June to October), and for wheat (November to April) and the rice and wheat yield for 45 years i.e., from 1961–62 to 2005–06 were analyzed. The 5 year average seasonal weather variables viz. rainfall (mm), average number of rainy days, maximum and minimum temperatures (°C), during rice and wheat growing seasons over past 45 years from 1961 to 2006 of study area are shown in Figs. 27.1 and 27.2, respectively. The average seasonal change in maximum temperature and minimum temperature was found to be are 0.4°C and 0.2°C, respectively during kharif season (Fig. 27.1). However during rabi season from 1961–1965 to 2001–2005, the average seasonal change in maximum temperature and minimum temperature were 0.4°C and 0.4°C, respectively (Fig. 27.2). Two statistical techniques viz. linear and curvilinear regression techniques were employed in assessing the impacts of climate change on Rice & Wheat yields:

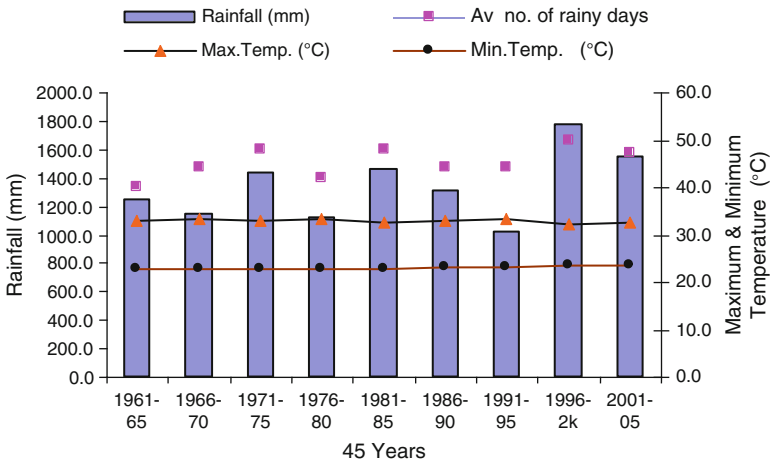


**Fig. 27.1** Five years' average seasonal variations in rainfall (mm), average number of rainy days, maximum and minimum temperatures (°C) for 45 years during Kharif season (June, 1961 to October, 2005) at Pantnagar

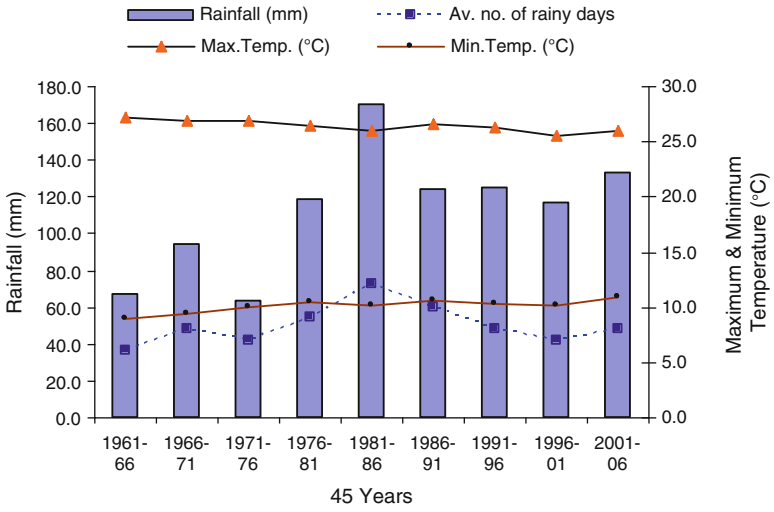


**Fig. 27.2** Five years' average seasonal variations in rainfall (mm), average number of rainy days, maximum and minimum temperatures (°C) for 45 years during Rabi season (November, 1961–1962 to April, 2005–2006) at Pantnagar

### *27.3.1 Impact of Climate Change on Rice Yield*

The following linear regression equations were developed between rice yields and rainfall, number of rainy days, maximum & minimum temperatures are given below:

(a) Effect of rainfall distribution on rice yield
The linear regression equation obtained for rainfall distribution on rice yield was

$$Y = 4096.07 - 0.1380\ X$$

The coefficient of determination ($R^2$) obtained was 0.0026.

(b) Effect of number of rainy days distribution on rice yield:

$$Y = 3156.75 + 16.699\ X$$

The coefficient of determination ($R^2$) obtained was 0.0124.

(c) Effect of maximum temperature distribution on rice yield:
The linear regression equation for maximum temperature thus obtained is given below:

$$Y = 16555.86 - 385.51\ X$$

The coefficient of determination ($R^2$) obtained was 0.0429.

(d) Effect of minimum temperature distribution on rice yield:
The linear regression equation for minimum temperature thus obtained is given below:

$$Y = -24279.1 + 1231.13\ X$$

The coefficient of determination ($R^2$) obtained was 0.2089.

The impact of 5 years average variations of rainfall on rice yield is shown in Fig. 27.3a and that of average number of rainy days in Fig. 27.3b. The trend clearly indicates that there has been effect of seasonal rainfall on rice yields but its distributionhas significantly contributed towards the yields. In general years in which rainfall is sufficient to meet the water requirement of rice, more yields have been observed. However, heavy rainfall at the end of the season has adversely affected the rice yields except some variations. Number of rainy days has also contributed in the same manner (Fig. 27.3b).

### *27.3.2 Impact of Climate Change on Wheat Yield*

The following linear regression equations were developed between wheat yields and rainfall, number of rainy days, maximum & minimum temperatures are given below:

(a) Effect of rainfall distribution on wheat yield
The linear regression equation obtained for rainfall for wheat was

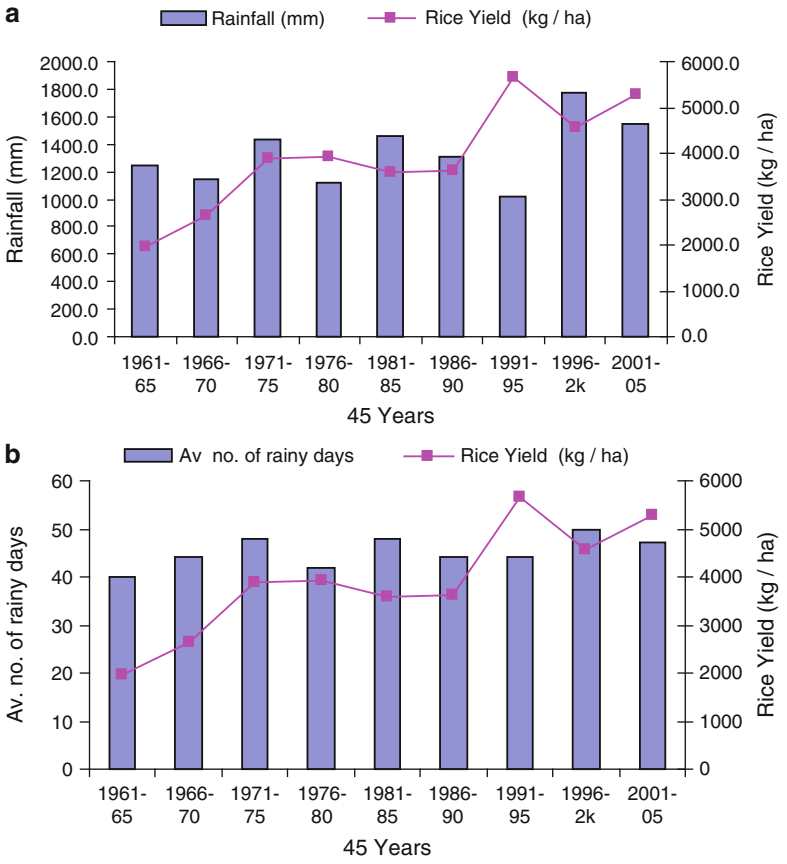


**Fig. 27.3** (**a**) Five years' average variations in rice yield (kg/ha) and rainfall (mm) for 45 years from 1961 to 2005 at Pantnagar (**b**) 5 years' average variations in rice yield (kg/ha) and average number of rainy days for 45 years from 1961 to 2005 at Pantnagar

$$Y = 2865.49 + 1.591\ X$$

The coefficient of determination ($R^2$) obtained was 0.0103.

(b) Effect of number of rainy days distribution on wheat yield:
The linear regression equation obtained for number of rainy days distribution on wheat yield was

$$Y = 3034.19 + 1.222\ X$$

The coefficient of determination ($R^2$) obtained was 0.0314.

(c) Effect of maximum temperature distribution on wheat yield
The linear regression equation obtained for maximum temperature for wheat was

$$Y = 13460.97 - 395.19\ X$$

The coefficient of determination ($R^2$) obtained was 0.1547.

(d) Effect of minimum temperature distribution on wheat yield
The linear regression equation obtained for minimum temperature for wheat was

$$Y = -1551.41 + 456.44\ X$$

The coefficient of determination ($R^2$) obtained was 0.1616.

The impact of 5 years average variations of rainfall on wheat yield is shown in Fig. 27.4a and that of average number of rainy days in Fig. 27.4b. The data indicates that there has been effect of rainfall during winter season resulting due to western disturbances on wheat yields. Some years in which rainfall is well distributed during the season at intervals coinciding with the growth stage of the crop, there is increase in wheat yields. Under low rainfall conditions response of irrigation has been observed to optimized wheat yields. Under heavy rain conditions decline in yield has been observed (170.1 mm rainfall, 2617 kg $ha^{-1}$ yield) as shown in Fig. 27.4a. A similar trend was observed on average number of rainy days affecting wheat yields (Fig. 27.4b).

### *27.3.3 Effect of Climate Change on Change in Rice Yields*

The study was made to assess the change in rainfall, maximum, minimum and average temperatures on change in rice yields for over 45 years from kharif 1961 to 2005 seasons. The following curvilinear regression equation for rice was developed

$$Y = 6.344 - 1.02X_1 + 3.45X_2 - 0.0157X_3 - 4.073X_4, R^2 = 0.712$$

This shows that in this area about 71% (coefficient of regression, $R^2 = 0.712$) variations in rice yield and were due to variations in south-west monsoon rainfall and temperature conditions prevailed during kharif season.

The graphical representation between changes in rainfall and average number of rainy days on rice yield are given in Fig. 27.5, while the effect due to changes in maximum and minimum temperature is given in Fig. 27.6. It is evident from the analysis that there was maximum positive increase in rice yield (2,037 kg $ha^{-1}$) during the year 1986–1990 to 1991–1995 (F) except during 1991–1995 to 1996–2000 (G, 1,090 kg $ha^{-1}$, Fig. 27.5), where there was a decrease in yield due to heavy rainfall. It may be due to flower dropping or lodging of the crop in the time of maturity. Figure 27.6 clearly indicates that almost there was no significant change in minimum temperature (0.2°C), during the kharif season; however the maximum temperature indicated influence on change in rice yields. Highest

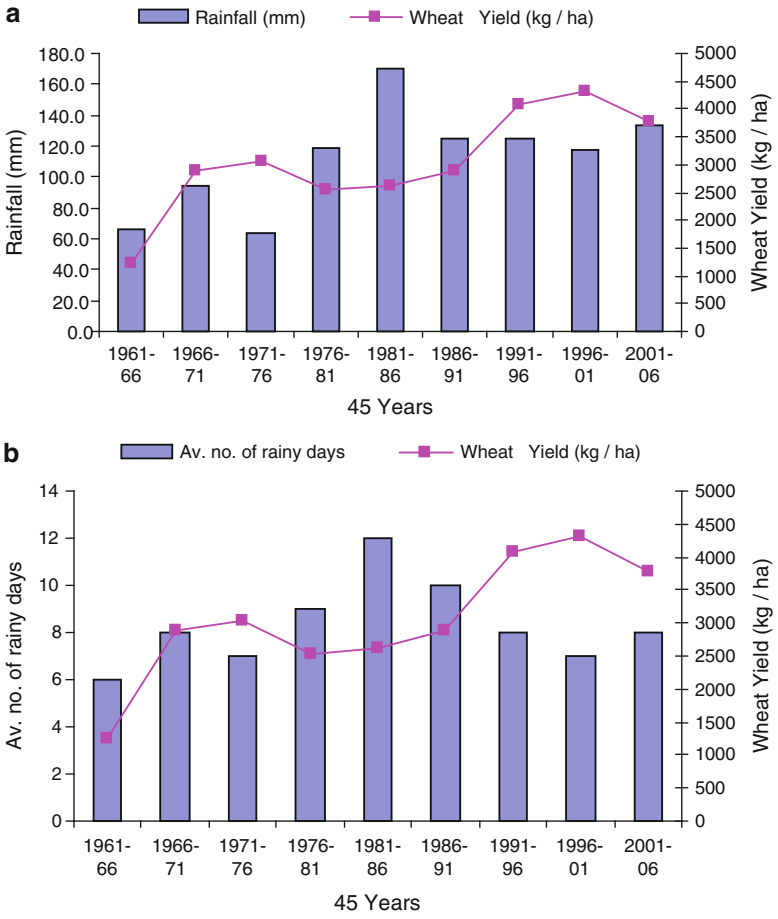


**Fig. 27.4** (**a**) Five years' average variations in wheat yield (kg/ha) and rainfall (mm) for 45 years from 1961–1962 to 2005–2006 at Pantnagar (**b**) 5 years' average variations in wheat yield (kg/ha) and average number of rainy days for 45 years from 1961–1962 to 2005–2006 at Pantnagar

decrease in rice yield (1,090 kg $ha^{-1}$) was observed during 1991–1995 to 1996–2000 (G), as a result of decrease in maximum temperature (−1.2°C) during this period, followed by 1976–1980 to 1981–1985 (−0.6°C). This is slightly contrary to the findings reported by Sinha and Swaminathan (1991) in which a 2°C increase in mean air temperature could decrease rice yield by about 0.75 t/ha in the high yield areas.

| | | | |
|---|---|---|---|
| A | 1961–1965 to 1966–1970 | B | 1966–1970 to 1971–1975 |
| C | 1971–1975 to 1976–1980 | D | 1976–1980 to 1981–1985 |
| E | 1981–1985 to 1986–1990 | F | 1986–1990 to 1991–1995 |
| G | 1991–1995 to 1996–2000 | H | 1996–2000 to 2001–2005 |

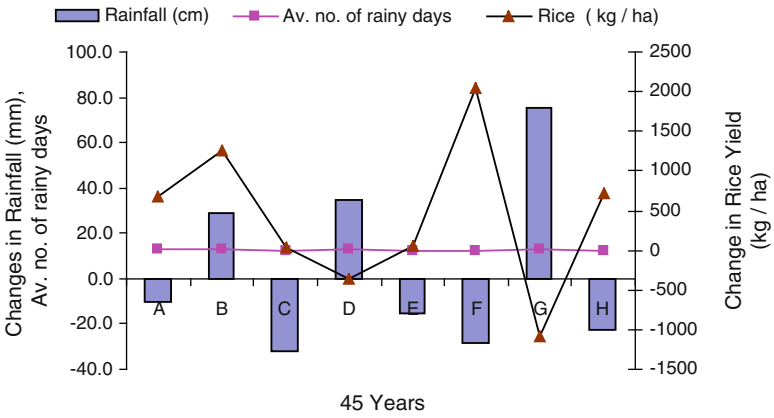


**Fig. 27.5** Change in rice yield vs changes in rainfall (mm) and average number of rainy days for 45 years from 1961 to 2005 at Pantnagar

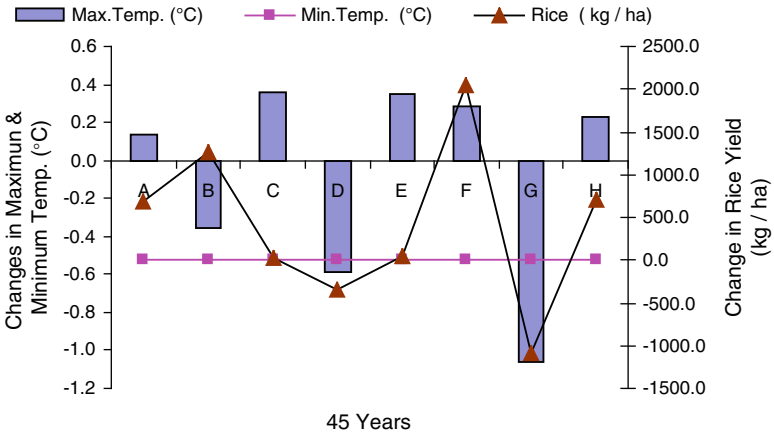


**Fig. 27.6** Change in rice yield vs changes in maximum & minimum temperatures (°C) for 45 years from 1961 to 2005 at Pantnagar

### *27.3.4 Effect of Climate Change on Change in Wheat Yields*

During rabi season (November and April), the impact of change in rainfall, maximum, minimum and average temperatures on change in wheat yields for over 45 years from rabi 1961–1962 to 2005–2006 seasons was assessed. The following curvilinear regression equation for wheat was developed

$$Y = 12.767 - 1.080X_1 + 0.261X_2 + 1.917X_3 + 1.632X_4, R^2 = 0.924$$

This shows that in this area about 92.4% (coefficient of regression, R2 = 0.924) variations in wheat yields were due to variations in winter rains and favorable temperature conditions prevailing during the rabi season in the area.

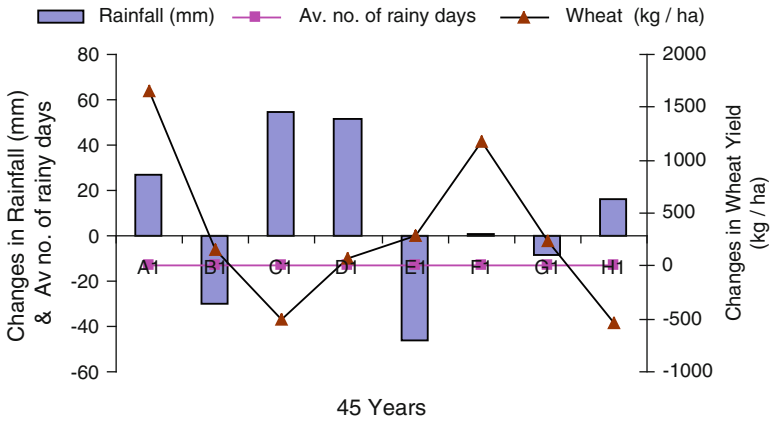


**Fig. 27.7** Change in wheat yield vs changes in rainfall (mm) and average number of rainy days for 45 years from 1961–1962 to 2005–2006 at Pantnagar

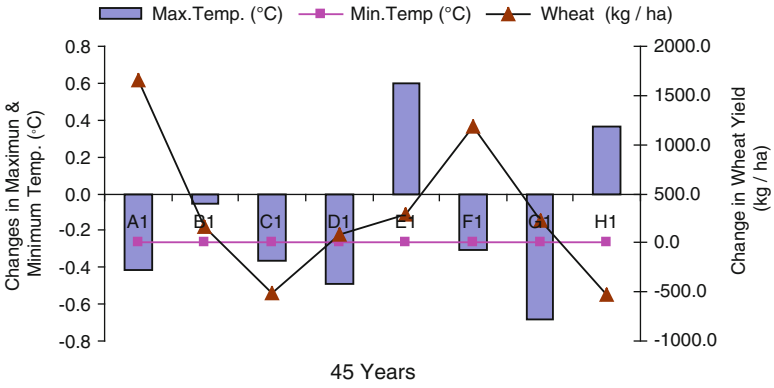


**Fig. 27.8** Change in wheat yield vs change in maximum and minimum temperatures (°C) for 45 years from 1961–1962 to 2005–2006 at Pantnagar

The graphical representation between changes in rainfall and average number of rainy days on wheat yield are given in Fig. 27.7, while the effect due to changes in maximum and minimum temperatures is given in Fig. 27.8. It is evident from the analysis that there was maximum positive increase in wheat yield (1182.2 kg $ha^{-1}$) during the years 1986–1991 to 1991–1996 ($F_1$) except during 1971–1976 to 1976–1981. A significant decrease in yield observed during 1971–76 to 1976–1981 (C1, 509 kg $ha^{-1}$) and 1996–2001 to 2001–2006 (H1, 535 kg $ha^{-1}$, Fig. 27.7) due to high rainfall during flowering to maturity stage. Figure 27.8 clearly indicates that almost there was no significant change in minimum temperature (0.4° C), during the rabi season, however, the changes in maximum temperature influenced wheat yields. Highest decrease in wheat yield (535 kg $ha^{-1}$) was observed during 1996–2001 to 2001–2006 (H1), as a result of increase in maximum

temperature (0.4°C) during this period, followed by 1981–1986 to 1986–1991 (0.6°C, 280.8 kg $ha^{-1}$). This agrees with the findings reported by Sinha and Swaminathan (1991), where a 0.5°C increase in winter temperature would reduce wheat crop duration by seven days and reduce yield by 0.45 tonnes per hectare. Wheat yield was also found to decreased with decrease in temperature during 1971–1976 to 1976–1981 (C1, −0.4°C, 509 kg $ha^{-1}$). However, an increase in winter temperature of 0.5°C would thereby translate into a 10% reduction in wheat production in the high yield states of Punjab (Sinha and Swaminathan 1991).

| | | | |
|---|---|---|---|
| A1 | 1961–1966 to 1966–1971 | B1 | 1966–1971 to 1971–1976 |
| C1 | 1971–1976 to 1976–1981 | D1 | 1976–1981 to 1981–1986 |
| E1 | 1981–1986 to 1986–1991 | F1 | 1986–1991 to 1991–1996 |
| G1 | 1991–1996 to 1996–2001 | H1 | 1996–2001 to 2001–2006 |

## 27.4 Conclusion

1. The effective beginning and end of rice growing season is determined by temperatures and rainfall distribution and for getting maximum yields, it is necessary that the rice must be planted at the time i.e. in last week of June where optimum temperature conditions are met.
2. During past decade, in tarai area, the amount of total rainfall during rainy season has increased (average 1,433.4 mm) but the number of rainy days have decreased. However, the increase in maximum and minimum temperatures over past 45 years during kharif s is 0.4°C and 0.4°C, while during rabi season this increase is 0.4°C and 0.4°C, respectively.
3. There was maximum positive increase in rice yield (2,037 kg $ha^{-1}$) during the year 1986–1990 to 1991–1995 (F) except during 1991–1995 to 1996–2000 (G, 1,090 kg $ha^{-1}$, Fig. 27.5), where there was a decrease in yield due to heavy rainfall. It may be due to flower dropping or lodging of the crop in the time of maturity.
4. Highest decrease in rice yield (1,090 kg $ha^{-1}$) was observed during 1991–1995 to 1996–2000 (G), as a result of decrease in maximum temperature (−1.2°C) during this period, followed by 1976–1980 to 1981–1985 (−0.6°C).
5. The results further showed that, over the years in wheat for each degree rise in air temperature and lack of winter rains, there has been reduction in yields by 5–10% in timely and late sown wheat, while there has been reduction in yields by 10–20% in early and late planted rice due to early withdrawn of monsoon and decrease in air temperature in the month of October.
6. A significant decrease in wheat yield observed during 1971–1976 to 1976–1981 (C1, 509 kg $ha^{-1}$) and 1996–2001 to 2001–2006 (H1, 535 kg $ha^{-1}$, Fig. 27.7) due to high rainfall during flowering and maturity stage of wheat crop.

7. Highest decrease in wheat yield (535 kg $ha^{-1}$) was observed during 1996–2001 to 2001–2006 (H1), as a result of increase in maximum temperature (0.4°C) during this period, followed by 1981–1986 to 1986–1991 (0.6°C, 280.8 kg $ha^{-1}$). However wheat yield was also found to decrease by decrease in temperature during 1971–1976 to 1976–1981 (C1, −0.4°C, 509 kg $ha^{-1}$).

So in general, it can be concluded that there has been impacts of climatic variability in yields of rice and wheat crops and their productivity also depends upon the use of high yielding varieties, follow of standard agronomic practices and control measures. This type of study will be of immense use for a location, if the long range weather forecast for important climatic variables such as rainfall and temperature are available well in advance, the productivity of rice and wheat can be assessed and forecast for that location and it will promote in deciding the optimum sowing dates of wheat and rice as well as in scheduling the irrigation and for taking control measures for maximizing their production.

## References

Bhandari AL, Sood A, Sharma KL, Rana DS (1992) Integrated nutrient management in rice – wheat system. J Ind Soc Soil Sci 40:742–747

Deshpande SB, Fehrembacher JB, Ray BW (1971) Mollisols of Tarai region soils of Uttar Pradesh., Northern India. 2. Genesis and classification. Geoderma 6(3):195–201

Ezekiel M, Fox KA (1959) Methods of correlation and regression analysis, John Wiley Sons, New York, pp 204–248

India (2002) Ministry of Information and Broadcasting Government of India, New Delhi, pp 373

Sen A, Sharma SN (2002) Zero tillage: rice – wheat cropping system increases wheat production. Indian Farming 52(6):3–6

Singh PK, Singh Y (1996) Effect of reduced tillage on soil physical properties, root growth and grain yield in rice – wheat system. Ind J Agric Res 30(3–4):179–185

Sinha SK, Swaminathan MS (1991) Deforestation, climate change and sustainable nutrients security; a case study of India. Clim Change 19:201–209

# Chapter 28
# Estimation of Wheat Productivity Under Changing Climate in Plains Zones of Chhattisgarh Using Crop Simulation Model

**S.R. Patel, S. Tabasum, A.S. Nain, R. Singh, and A.S.R.A.S. Sastri**

**Abstract** The productivity of wheat is marginal in Eastern Central India and slight decrease may turn cultivation of wheat unviable due to low returns. Thus, it is inevitable to test the performance of wheat crop in the future climate change scenario. Simulation model, with its complete ability to simulate the soil-plant-atmospheric system, offers an ideal tool to analyse response of wheat to changing climatic conditions. Crop simulation model not only saves the precise time but also the huge cost of experimentation. Keeping in mind the implications of climate change on agriculture CERES-Wheat crop simulation model was calibrated and validated in Chhattisgarh conditions and wheat response was simulated in projected increased temperature scenarios. To have an idea of the effect of changing climate on wheat productivity, crop simulation model, CERES-Wheat has been used to simulate the effect of global warming on wheat production. The results showed that anthesis, physiological maturity, biomass, grains per ear & grain yield were highly sensitive to change in temperature. The biomass and grain yield decreased at varying degree ranging from 7% to 44% in case of biomass and from 10% to 48% in case of grain yield, when the temperature was increased in the range of 1–3°C. When temperature was decreased up to 3°C, the increasing trends in the biomass and grain yield were observed to the tune of 20–80% and 19–79%, respectively.

## 28.1 Introduction

Wheat (Triticum sp.) is the most important grain crop both in regard to its antiquity and its use as a source of human food. Wheat serves as a staple food for about one billion people in as many as 43 countries of the world. So it is the most widely

S.R. Patel (✉) • S. Tabasum • A.S. Nain • R. Singh • A.S.R.A.S. Sastri
Department of Agrometeorology, Indira Gandhi Krishi Vishwavidyalya, Raipur 492006 (C.G.), India
e-mail: srpatelsr@yahoo.com

S.D. Attri et al. (eds.), *Challenges and Opportunities in Agrometeorology*,
DOI 10.1007/978-3-642-19360-6_28, 

cultivated food crop of the world. Three main species commonly grown in the world including India are the common wheat (*Triticum aestivum*), the macaroni or durum wheat (T. durum) and the emmer wheat (*T. dicoccum*) out of these species maximum area is under T. *aestium*. In India, more than 80% of the total wheat area is under this species whereas the area under macaroni and emmer wheat is only 12% and 1%, respectively. As wheat is one of the most important staple food crops in India, is grown under diverse set of agroclimatic conditions. It is grown over an area of 25.6 million ha with an average productivity of 2,578 kg $ha^{-1}$ (Anon. 2004), which contributes to about 25% of the total food grain production in the country. It is grown from 15 to 32°N and from 72 to 92°E and from sea level to about 3,000 m above sea level. In Chhattisgarh, wheat is grown over 0.125 million ha with an average productivity of 1,050 kg $ha^{-1}$. In this state it is mostly grown under irrigated condition in rice based cropping system.

In recent times, simulation modelling has become one of the most powerful tools for analyzing interactions in the soil – plant atmosphere system. Simulation models of agricultural system are quantitative tools based on scientific knowledge that can evaluate the effect of climatic, adaphic, hydrologic and agronomic factors on crop growth and yield. Crop growth simulation models, thus, play a vital role in bringing out the specific relationships between weather conditions and productivity and provide capabilities for transferring agriculture production from sites of origin to new location (Ramakrishna 1990). These dynamic models not only help in understanding the climate-crop interaction and the process that contribute to the growth and yield of crops but also assist in evaluating the potentials of various soil and crop management options (Hoogenboom et al. 1997) and form an important component in systems approach research (Ritchie 1986; Ritchie and Algarswamy 1989; Ramakrishna et al. 1994 and Ramakrishna et al. 1997).

Simulation modelling is being increasingly recognized as cost-effective and efficient way of synthesizing knowledge of agricultural environment systems and applying this knowledge to solve practical problems. Crop simulation modelling has great importance in agriculture related studies. Crop modelling is the best tool to analyze the complex soil-plant-atmospheric system and optimize the agriculture practices for maximum output. Crop modelling not only saves the precise time but also the huge cost of experimentation. Crop simulation modelling based studies are increasing in India; however, not much study has been carried out in Chhattisgarh so far. Keeping the importance of simulation modelling and its applicability, the present investigation was carried out.

## 28.2 Methodology

The present research work was carried out in the Department of Agrometeorology, Indira Gandhi Agricultural University, Raipur situated at 21°15' N latitude, 81°36' E longitude and at an altitude of 289.56 m from the mean sea level. The climate of Raipur is hot and sub humid. The mean annual rainfall is about

1,200 mm, of which 85% rainfall is received during monsoon months i.e. June to September. Maximum and minimum temperature ranges between 17.0°C to 45.2°C and 8.0°C to 22.0°C during the year. The soil of the experimental field was sandy loam in texture, locally known as "Matasi" belonging to the "Inceptisol" group, with a bulk density of 1.38 $gm^{-3}$, and field capacity of 17%). The soil was near neutral in reaction and had low phosphorus and medium nitrogen and potassium content.

DSSAT (Decision Support System for Agro-technology Transfer) was designed for researchers to easily create "experiments" to simulate the soil-plant-atmospheric system on computers. The outcomes of the complex interactions between various agricultural practices, soil and weather conditions are simulated to suggest appropriate solutions to site-specific problems. DSSAT relies heavily on simulation crop models to predict the performance of crops for making a wide range of decisions. The CERES (Crop Environment REsource Synthesis) family of crop models is used in DSSAT to predict the performance of six grain crops (Wheat, rice, maize, sorghum, pearl millet and barley). All six of these models are designed to use a minimum set of soil, weather, genetic and management information.

The CERES-wheat model simulates crop growth with a daily time step from sowing to maturity based on physiological processes that describe the crops response to soil and aerial environmental conditions. Phase development is quantified according to plants physiological age in CERES, the crop growth submodels treat leaf area development, dry matter production, assimilate partitioning and tiller growth and development. The model describes plant development into five stages excluding the extra stages in the model for pre sowing simulation of the soil water balance and grain dry-down to harvest. The main driving force is the temperature from sowing to physiological maturity while during stage I (emergence to terminal spikelet), vernalization, photoperiod and phylochron also influence the rate of development. Number of leaves are computed in first two stages as a function of air temperature and a cultivar specific phyllochron interval. The daily potential dry matter production (PCARB) is dependent on photosynthetically active radiation (PAR) and its interpretation, where PAR is set equal to 0.5 solRAD (daily total solar radiation). The daily potential dry matters production (PCARB g plant-1) is:

$$\text{PCARB} = \frac{7.5^{*} \times \text{PAR}^{0.6}[1 - \text{Exp}\,(0.85^{*}\,\text{LAI})]}{\text{Plants}}$$

Daily weather data collected at the Agro-meteorological observatory of Agrometeorology department, Indira Gandhi Agricultural University, Raipur (Chhattisgarh) were used. Daily weather data for CERES–wheat model includes parameters of temperature (°C) (maximum and minimum), rainfall (mm) and solar radiation (MJ $m^{-2}$ $day^{-1}$).

A regression equation relating solar radiation received on a horizontal surface at a particular time and place to clear day solar radiation and sunshine ratio as

proposed by Angstrom (1924) was used for computation of solar radiation, using the following equation

$$S = Sa^{*}[a + b^{*}(n/N)]$$

Where,

a and b are empirical coefficients. Angstrom proposed values 0.25 and 0.75, respectively, S = estimated solar radiation on ground surface (MJ $m^{-2}$ $day^{-1}$) and Sa = extra terrestrial solar radiation received on horizontal surface at the top the of atmosphere (MJ $m^{-2}$ $day^{-1}$)

Soil input data for CERES model includes, soil texture, soil local classification, soil family SCS system, soil depth (m), colour (moist), Aledo (fraction), Evaporation limit (cm), Drainage rate (fraction $day^{-1}$), Runoff curve number, mineralization factor (0–1 scale), photosynthesis factor (0–1), pH in buffer, determination method, amount (%) and determination method of nitrogen, phosphorus and potassium.

Crop genetic coefficients used in CERES-wheat model include P1V, P1D, P5, G1, G2, G3 and PHINT. First three genetic coefficients P1V, P1D and P5 are related to development aspect and the remaining three G1, G2 and G3 to the growth aspect of crop. GENCALC software developed by (Hunt et al. 1993) was used to develop genetic coefficients of wheat varieties Kanchan, Bilasa, Arpa and GW-273. GENCALC software requires the initial values of all genetic coefficients to start with. Then software start simulating treatment and find the best match based on least square error method. Phenological coefficients, which determine the development of crops, are estimated first, followed by the growth coefficients. The coefficients value of "low latitude spring wheat" cultivars defined in CERES model were used to initiate the GENCALC.

CERES – wheat model incorporated in DSSAT 3.5 was run for calibration and validation of wheat varieties Kanchan, Bilasa, Arpa and GW-273 at Raipur district. The calibration was done using the experimental field observed crop data of the season 2002–2003 and the validation was done using the crop data of 2003–2004.

Sensitivity analysis was performed to measure the responsiveness of crop to change in temperature. The maximum and minimum temperatures of the year 2002–2003 of the Raipur district during the full growing season were first increased by 1°C, 2°C and 3°C and the model was run to estimate the crop response and then the maximum and minimum temperature of the above said years were decreased by 1°C, 2°C and 3°C during the full growing season and the model was used to simulate the effect of change in temperature on growth and development in Raipur district.

A regression model was developed for the prediction of yield by using the fortnightly average of weather data and wheat yield (1980–2004) for the months from November to April. In order to find out the relationship between yield of wheat and weather parameters (Tmax, Tmin, Rainfall and sunshine hours) correlation matrix developed using following formula

$$r(x, y) = \frac{Cov(x, y)}{\sqrt{Var(x).\ Var(y)}}$$

Where,
r (x, y) = correlation coefficients between combination x & y
Var (x) = variance of x combination
Var (y) = variance of y combination

The weather parameters, which show high correlation with the yield were used to develop the model in the SPSS software. Forward steps wise selection method providing probability limit of 0.15 for accepting the important weather parameters for model development was adopted.

Thus the model constructed was

$$Y = a + b_1x_1 + b_{2X2} + \ - - - - nx_n$$

Where,
Y = yield (kg/ha), x1, x2, xn = weather parameters, a = intercept and b = slope

## 28.3 Results and Discussion

CERES-Wheat model a part of DSSAT 3.5 shell was calibrated using the data on weather parameters, crop biometric parameters and management practices. The data of the cropping year 2002–2003 were used for calibration studies. In this crop season the four cultivars (Kanchan, Bilasa, Arpa and Gw-273) of wheat crop were sown on four dates of sowing (20th November, 5th December, 20th December and 4th January). The Genetic coefficients were determined for the all four wheat varieties. GENCALC software package integrated with DSSAT 3.5 was used to develop the genetic coefficients. Hunt approach (Hunt et al. 1993), which implies the development of phenological coefficients (P1V, P1D, P5, PHINT) first, and then production coefficients (G1, G2, G3), was used to determine the coefficients of all four cultivars. The GENCALC software start running the simulation model on initially provided values of genetic coefficients and checks the range of values to find out the best suitable match using least square error method. Model compares observed and simulated growth and development parameters of crop. A close collaboration of biometric parameters is achieved in order to establish the genetic coefficients. A comparison of the simulated crop parameters with observed crop parameters was carried out. Observed and simulated values of phenological events (Anthesis, Physiological maturity), biomass dynamics (biomass at anthesis, biomass at harvest maturity, LAI stalk at harvest maturity), yield attributes (grain yield, number of grain/$m^2$, grain weight) and harvest Index were compared using different statistics techniques such as Root Mean Square Errors (RMSE), Coefficient of Determination (R2), Mean, and simple deviations. The results of calibration of CERES-Wheat model for physiological maturity and grain yield are being discussed below:

## 28.3.1 Calibration of CERES-Wheat Model

### 28.3.1.1 Phenological Maturity

Two major crop phenological stages viz. anthesis and physiological maturity were compared. The deviations between simulated and observed anthesis duration were 3 to +7 days (average +5 days), 0 to +3 days (average +2.25 days) +2 to +4 days (average +3.25 days) and +2 to +3 days (average +2.5 days) for Kanchan, Bilasa, Arpa and GW-273, respectively. The RMSE (Root Mean Square Error) obtained between the actual and predicted anthesis was 5.20, 2.60, 3.35 and 2.55 days for the average anthesis days of 68.5, 69.3, 69 and 71 for Kanchan, Bilasa, Arpa, and GW-273 respectively. The R2 obtained was 0.94 for Kanchan, 0.65 for Bilasa, 0.97 for Arpa and 0.99 for GW-273, GW-273 is highly significant at 1% probability level, Kanchan and Arpa are highly significant at 5% probability level while, Bilasa is not statistically significant but RMSE was within the expectable limit. Simulated and observed anthesis days after sowing are plotted in Fig. 28.1. A very close collaboration between observed and simulated anthesis dates was noticed in GW-273 followed by Bilasa, Arpa and Kanchan. The anthesis dates were over-estimated by slight difference; however, R2 values suggest that the pattern of anthesis dates could be well captured.

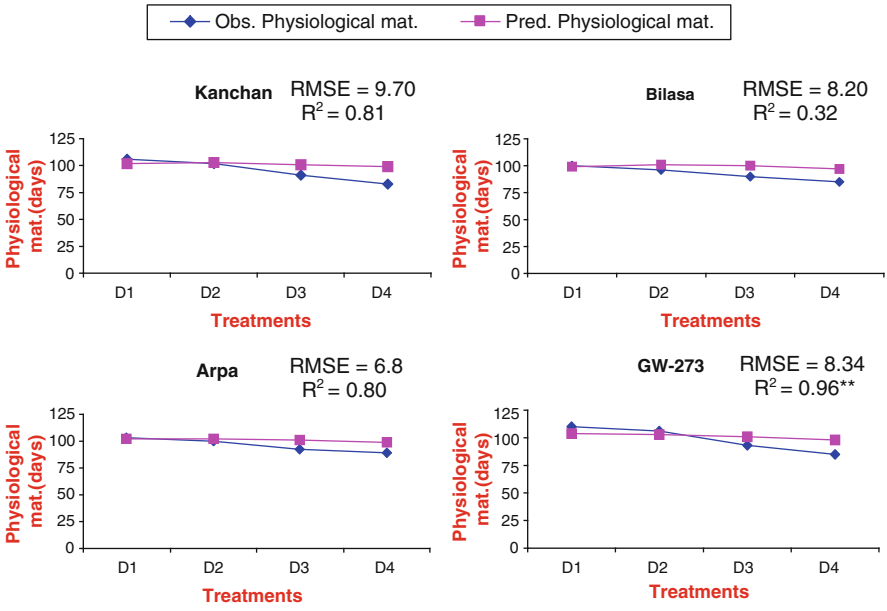


**Fig. 28.1** Comparison between observed and predicted physiological maturity. D1 – 1st sowing date (20th November) D2 – 2nd sowing date (5th December) D3 – 3rd sowing date (20th December) D4 – 4th sowing date (4th January)

Crop phenological stages play a great role in defining crop growth duration, biomass partitioning and finally crop production. As far as the prediction of physiological maturity dates were concerned, the deviation varied with in the range of −4 to +10 days (average +7.75 days) for Kanchan, −1 to +10 days (average +7 days) for Bilasa, −1 to +10 days (average +5.5 days) for Arpa and −6 to +13 days (average +7.5 days) for GW-273. The RMSE (Root Mean Square Error) was 9.7 days for average physiological maturity of 95.5 days for Kanchan, 8.2 days for average physiological maturity of 92.8 days for Bilasa, 6.82 days for average physiological maturity of 96 days for Arpa and 8.34 days for average physiological maturity of 98.5 days for GW-273. Coefficients of determination (R2) between observed and simulated physiological maturity were 0.82, 0.32, 0.80, and 0.96 for Kanchan, Bilasa, Arpa and GW-273, respectively, Gw-273 is statistically significant at 5% probability level while Kanchan, Bilasa, and Arpa are not statistically significant but RMSE was within the expectable limit. The patterns of simulated and observed physiological maturity dates have been depicted through Fig. 28.1. The graphs show that the genetic coefficients, which govern the physiological maturity in CERES-Wheat model (P5) developed by GENCALC software, over-predicted the physiological maturity of various wheat cultivars, however coefficient of determination values suggest that the variation in physiological maturity arising due the varying dates of sowing could be very well captured.

#### 28.3.1.2 Grain Yield

The grain yield is the main entity of the crop and is the prime concern for the model for forecasting acceptably. The analysis of predicted and measured grain yields of all the four cultivars (Kanchan, Bilasa, Arpa and Gw-273) was carried out and yields have been presented in Fig. 28.2. The grain yield predicted by the model and observed in the field deviates from −0.62 to +0.70 t $ha^{-1}$ (average 0.4 t $ha^{-1}$) for Kanchan, +0.09 to +0.79 t $ha^{-1}$ (average +0.35) for Bilasa, −0.61 to +0.68 (average +0.55) for Arpa and −0.61 to 0.13 t $ha^{-1}$ (average −0.32) for GW-273. The RMSE obtained between the observed and predicted grain yield were 0.48, 0.44, 0.58, 0.40 t $ha^{-1}$ for the average grain yield of 2.99, 2.50, 2.77 and 3.09 for Kanchan, Bilasa, Arpa and GW-273, respectively. The R2 obtained was 0.75, 0.89, 0.36 and 0.72 for Kanchan Bilasa, Arpa and GW-273, respectively. The statistical analysis suggests that simulated yields and observed yield are in very close collaboration ($P \leq 0.05$) except Arpa not only in terms of the yield levels but also the pattern of yield in different treatments.

The results indicate that the model is able to predict phenology, Biomass, yield and yield attributes of the crop cultivars (Kanchan, Bilasa, Arpa and GW-273) for various treatments with fairly good accuracy. The LAI predicted by the model does not reveal the satisfactory results, in all the cultivars for various treatments due the obvious reason of different method of LAI calculation. Other simulated crop parameters showed good agreement with the observed parameters except slight bias in the simulation of phonological stages. Results are in agreement with those

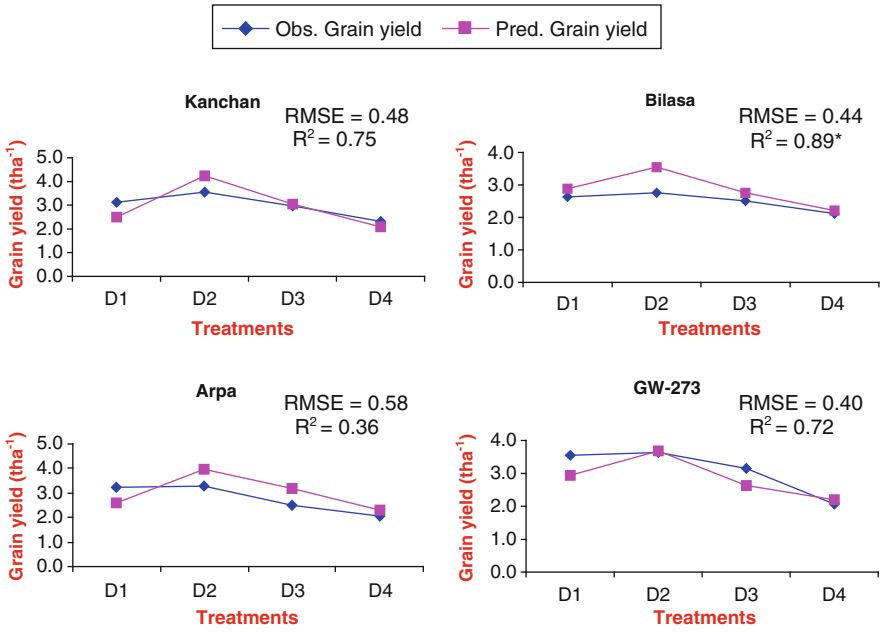


**Fig. 28.2** Comparison between observed and predicted grain yield. D1 – 1st sowing date (20th November) D2 – 2nd sowing date (5th December) D3 – 3rd sowing date (20th December) D4 – 4th sowing date (4th January)

obtained by (Chipanshi et al. 1997), who simulated the wheat yields of three locations in Saskatchewan from current and historical weather data using the CERES-wheat model.

## *28.3.2 Validation of CERES-Wheat Model*

The validation of CERES wheat model was done using the observed field data in the year 2003–04. Four wheat cultivars (Kanchan, Arpa, Bilasa and GW-273) with different treatments were used for validation study. Predicted above ground biomass, leaf area index, and yield and yield attributes were compared with actual observed values.

### 28.3.2.1 Phenological Observations

The field observed and model predicted anthesis (first flower) showed the deviation from −2 to +2 days (average ± 1.33 days) −2 to +3 days (average ± 1.67 days), −1 to +2 days (average ± 0.67 days) and 0–2 days (average +0.83 days), for Kanchan, Bilasa, Arpa and GW-273 respectively. The RMSE obtained between

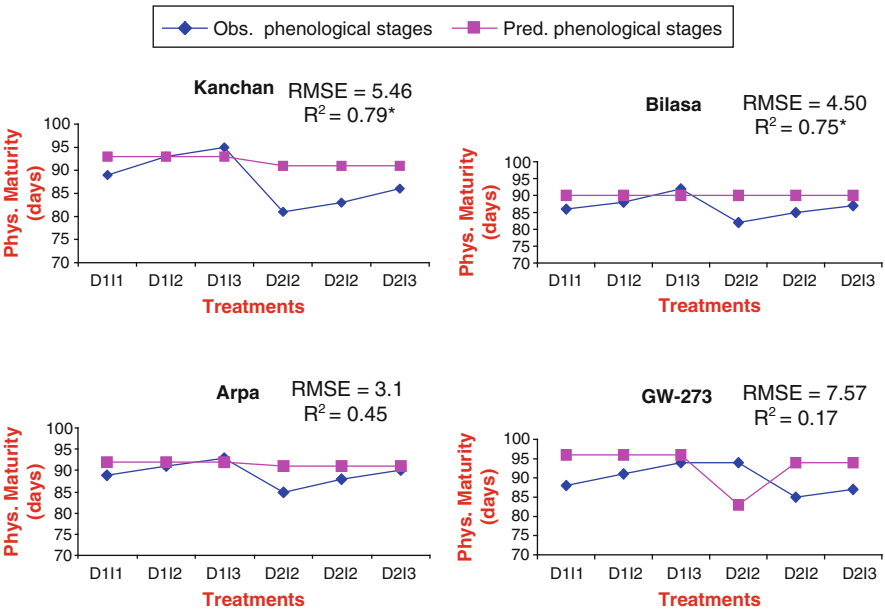


**Fig. 28.3** Comparison between observed and predicted physiological maturity. D1 – 1st sowing date (20th December) D2 – 2nd sowing date (30th December) I1 – 1st irrigation I2 – 2nd irrigation I3 – 3rd irrigation

observed and predicted anthesis was 1.53, 1.83, and 1.02 and 1.2 for the average anthesis of 60.5, 61, 62.5 and 62.6 days for Kanchan, Bilasa, Arpa and GW-273 respectively. The R2 (coefficient of determination) observed was 0.86 for Kanchan, 0.85 for Bilasa, 0.71 for Arpa and 0.82 for GW-273. Kanchan and Bilasa are statistically significant at 1% level, while Arpa and GW-273 are significant at 5%. The physiological maturity dates showed the difference of −2 to +10 days (average +4.83 days), −2 to +8 days (average +4 days), −1 to +6 (average +2.5 days) and +2 to −11 (average +7 days) for Kanchan, Bilasa, Arpa and GW-273. The RMSE and R2 obtained between observed and predicted phenology were 5.46 days for the average physiological maturity of 87.8 days and R2 0.79 for Kanchan, 4.5 days for the average physiological maturity of 86.7 days and R2 0.75 for Bilasa, 3.1 days for the average physiological maturity of 89.3 days and R2 0.45 for Arpa and 7.57 days for the average physiological maturity of 89.8 days and R2 0.17 for GW-273 respectively (Fig. 28.3).

### 28.3.2.2 Grain Yield

The difference between the predicted and measured grain yield ranges from −0.51 to +0.25 t $ha^{-1}$ (average −0.37 t $ha^{-1}$) in Kanchan with RMSE 0.36 t $ha^{-1}$ for the

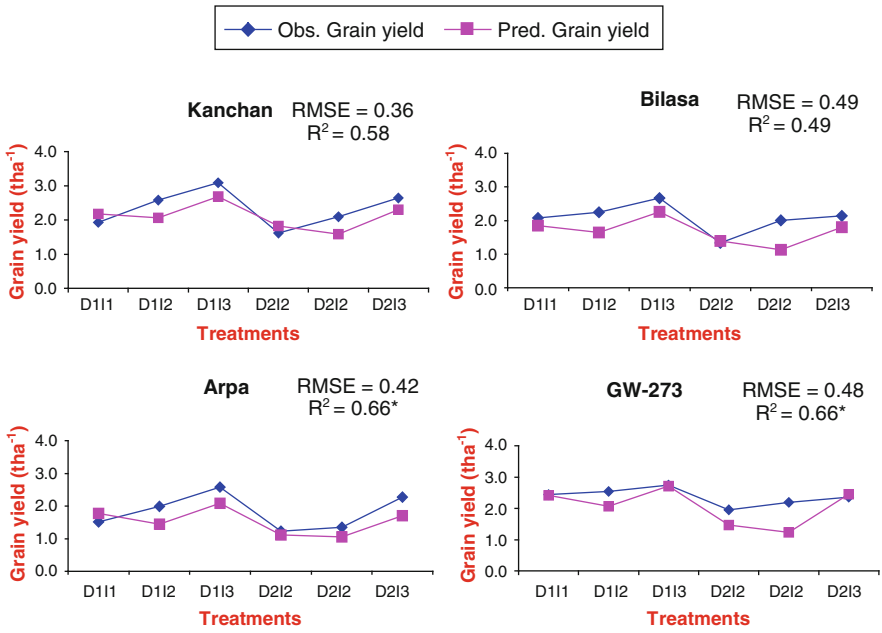


**Fig. 28.4** Comparison between observed and predicted grain yield. D1 – 1st sowing date (20th December) D2 – 2nd sowing date (30th December) I1 – 1st irrigation I2 – 2nd irrigation I3 – 3rd irrigation

average grain yield of 2.33 t ha$^{-1}$, −0.88 to +0.1 t ha$^{-1}$ (average −0.42 t ha$^{-1}$) in Bilasa with RMSE 0.49 t ha$^{-1}$ for the average grain yield of 2.08 t ha$^{-1}$, −0.57 to + 0.26 t ha$^{-1}$ (average −0.38 t ha$^{-1}$) in Arpa with RMSE 0.42 t ha$^{-1}$ for the average grain yield of 1.83 t ha$^{-1}$ and −0.96 to +0.08 t ha$^{-1}$ (average −0.35 t ha$^{-1}$) with RMSE 0.48 t ha$^{-1}$ for the average grain yield of 2.38 t ha$^{-1}$. The R2 obtained between the observed and predicted grain yield were 0.58, 0.49, 0.66 and 0.66 for Kanchan, Bilasa, Arpa and GW-273 respectively. Arpa and GW-273 are significant at 5% except Kanchan and Bilasa.

The above results indicated that the model predicted the phonological events and grain yield in cultivars, Kanchan, Bilasa, Arpa and GW-273. CERES-wheat model was also validated for cultivars WH 592 and HD 2329 at Jaipur and Ludhiana (Attri et al. 2001). Simulated phonology and yield were found to be in good agreement with the observed ones (Fig. 28.4).

### *28.3.3 Sensitivity Analysis of CERES-Wheat Model*

The sensitivity analysis is an important step to be able to use the simulation model, which explains that what would be impact of change in input on growth and development of plant. It also explains that what will happen if the inputs are out

of the range of data used in calibration and validation. The sensitivity analysis is done mainly for three reasons: (1) to know the sensitivity of model for unit change in input, (2) to know the effect of various management practices and (3) to know the possible effect of future climatic scenarios. In present study sensitivity analysis has been carried out in different temperature scenarios, which are addition in daily temperature by 1°C, 2°C and 3°C and subtraction of temperature by 1°C, 2°C and 3°C. Results of the sensitivity analysis are shown in Table 28.1. The grain yield, biomass at anthesis, biomass at harvest maturity, and grains per year were highly affected by change in temperature in all four cultivars (Kanchan, Bilasa, Arpa, and GW-273) of wheat in various treatments.

#### 28.3.3.1 Physiological Maturity

When the temperature was increased by 1°C the mean decrease in physiological maturity duration was observed −0.75, −0.25, −1 and −1 days, in Kanchan,

**Table 28.1** The effect of climate change on wheat in Chhattisgarh

| Cultivars | Climate change scenarios (°C) | Physiological maturity (days) | | | Grain yield (t/ha) | | |
|---|---|---|---|---|---|---|---|
| | | Present | Climate change | Deviation | Present | Climate change | Deviation |
| Warming environment | | | | | | | |
| Kanchan | +1 | 101.25 | 100.50 | −0.75 | 2.97 | 2.69 | −0.29 |
| Bilasa | +1 | 99.25 | 99.00 | −0.25 | 2.85 | 2.21 | −0.64 |
| Arpa | +1 | 101.00 | 100.50 | −0.50 | 3.01 | 2.34 | −0.67 |
| GW-273 | +1 | 101.50 | 100.50 | −1.00 | 2.86 | 2.52 | −0.34 |
| Kanchan | +2 | 101.25 | 99.50 | −1.75 | 2.97 | 2.00 | −0.98 |
| Bilasa | +2 | 99.25 | 98.00 | −1.25 | 2.85 | 1.90 | −0.96 |
| Arpa | +2 | 101.00 | 100.50 | −0.50 | 3.02 | 1.97 | −1.05 |
| GW-273 | +2 | 101.50 | 100.00 | −1.50 | 2.86 | 2.20 | −0.66 |
| Kanchan | +3 | 101.25 | 99.50 | −1.75 | 2.97 | 1.55 | −1.42 |
| Bilasa | +3 | 99.25 | 98.00 | −1.25 | 2.85 | 1.53 | −1.32 |
| Arpa | +3 | 101.00 | 100.25 | −0.75 | 3.01 | 1.58 | −1.44 |
| GW-273 | +3 | 101.50 | 99.75 | −1.75 | 2.86 | 1.50 | −1.35 |
| Cooling environment | | | | | | | |
| Kanchan | −1 | 101.25 | 101.75 | 0.50 | 2.97 | 4.03 | 1.05 |
| Bilasa | −1 | 99.25 | 100.25 | 1.00 | 2.85 | 3.40 | 0.55 |
| Arpa | −1 | 101.00 | 101.75 | 0.75 | 3.01 | 3.85 | 0.84 |
| GW-273 | −1 | 101.50 | 102.50 | 1.00 | 2.86 | 4.03 | 1.17 |
| Kanchan | −2 | 101.25 | 102.75 | 1.50 | 2.97 | 4.22 | 1.25 |
| Bilasa | −2 | 99.25 | 101.25 | 2.00 | 2.85 | 3.77 | 0.92 |
| Arpa | −2 | 101.00 | 102.75 | 1.75 | 3.01 | 4.53 | 1.51 |
| GW-273 | −2 | 101.50 | 103.00 | 1.50 | 2.86 | 4.55 | 1.69 |
| Kanchan | −3 | 101.25 | 103.50 | 2.25 | 2.97 | 4.99 | 2.01 |
| Bilasa | −3 | 99.25 | 102.00 | 2.75 | 2.85 | 4.40 | 1.55 |
| Arpa | −3 | 101.00 | 104.25 | 3.25 | 3.01 | 4.82 | 1.81 |
| GW-273 | −3 | 101.50 | 103.75 | 2.25 | 2.86 | 5.12 | 2.26 |

Bilasa, Arpa and GW-273, respectively. The highest decrease was found in Arpa and GW-273 in treatment D1 in both varieties (sowing on 20th November), while the lowest difference was observed in Bilasa in treatments D1 D2 and D4 (sowing on 20th November 5th and 4th December, respectively). The increase in temperature by 2°C, the mean reduction was observed −1.75, −1.25, −1 and −1.5 days in Kanchan, Bilasa, Arpa and GW-273, respectively. The highest decrease was observed in Kanchan in treatments D1 and D2 (sowing on 20th November and 5th December), while the lowest decrease was observed in Arpa in treatment D3 (sowing on 20th December). The increase in the temperature by 3°C, the mean decrease observed was −1.75, −1, −1.25 and −1.75 in Kanchan, Bilasa, Arpa and GW-273. The highest difference was observed in Kanchan and GW-273 in treatment D2 in both varieties (sowing on 5th December), while the lowest difference was observed in Bilasa in treatment D4 (sowing on 4th January).

When the temperature was reduced by 1°C the mean increase in the physiological maturity was obtained 0.5, 1, 0.75 and 1 days in Kanchan, Bilasa, Arpa and GW-273. The highest increase was observed in cultivars Bilasa and GW-273 in treatment D1 (sowing on 20th November) and the lowest increase was observed in Kanchan in treatments D2 and D4 (sowing on 5th December and 4th January, respectively). The decrease in temperature by 2°C increases the mean physiological maturity by 1.5, 2, 1.75 and 1.5 days in Kanchan, Bilasa, Arpa and GW-273, respectively. The highest increase was observed in Bilasa in treatment D1 (sowing on 20th November) and the lowest increase was in Arpa in treatment D3 and D4 (sowing on 20th December and 4th January, respectively). The reduction in temperature by 3°C increases the physiological maturity by 2.25, 2.75, 3.25 and 2.25 days in Kanchan, Bilasa, Arpa and GW-273, respectively. The highest increase was in the cultivar Arpa in D1 treatment (sowing on 20th November), while the lowest increase was in GW-273 and Kanchan in D3 and D4 treatments (sowing on 20th December and 4th January, respectively).

#### 28.3.3.2 Grain Yield

The mean difference between the normal and simulated grain yield when temperature was increased by 1°C were −0.43, −0.64, −0.79 and −0.34 t $ha^{-1}$ in the cultivars Kanchan, Bilasa, Arpa and GW-273, respectively. The highest difference was obtained in Arpa in treatment D2 (sowing on 5th December) and the lowest in GW-273 in the treatment D1 (sowing on 20th November). When, the temperature was increased by 2°C, the deviation was −0.98, −0.95, −1.05 and −0.66 t $ha^{-1}$ in Kanchan, Bilasa, Arpa and GW-273, respectively. The highest deviation was observed in Arpa in treatment D2 (sowing on 5th December) and the lowest deviation in GW-273 in treatment D1 (sowing on 20th November). The increase in temperature by 3°C decreased the grain yield by −1.42, −1.32, −1.44 and −1.35 t $ha^{-1}$ in Kanchan, Bilasa, Arpa and GW-273, respectively. The highest decrease was observed in Arpa in treatment D2 (sowing on 5th December) and the

lowest in Bilasa in treatment D1 (sowing on 20th November). The decrease in the temperature by 1°C increased the average grain yield in Kanchan, Bilasa, Arpa and GW-273 by 1.1, 0.55, 0.84 and 1.17 t $ha^{-1}$. The highest increase was obtained in GW-273 in D3 treatment (sowing on 20th December) and the lowest in Bilasa in D3 treatment (sowing on 20th December). The 2°C decrease in temperature increased the yield by 1.25, 0.92, 1.51 and 1.69 t $ha^{-1}$ in Kanchan, Bilasa, Arpa and GW-273, respectively. The cultivar GW-273 showed highest increase in treatment D3 (sowing on 20th December), while Bilasa showed lowest increase in treatment D4 (sowing on 4th January). The 3°C decrease in temperature increased the grain yield by 2.01, 1.55, 1.81 and 2.26 t $ha^{-1}$ in Kanchan, Bilasa, Arpa and GW-273, respectively. The highest increase was found in GW-273 in D1 treatment (sowing on 20th November) and the lowest in Bilasa in treatment D2 (sowing on 5th December).

### *28.3.4 Analysis of Crop-Weather Relationship*

Empirical – statistical model use samples of yield and weather data from an area to estimate coefficients by regression technique. The 48 correlation coefficients were found out between yield and fortnightly average of weather parameters (maximum temperature, minimum temperature, rainfall and sunshine hours), shown in Table 28.2. The yield data of spring wheat and meteorological data during the crop season (Nov. April) were collected from 1980 to 2004. From first fort night of November to 2nd fortnight of April the correlation coefficients were non-significant, during first fortnight of November the minimum temperature show high correlation (0.21) with yield. In second fortnight of November the maximum temperature and sunshine hours show high positive correlation (0.3 and 0.2 respectively) while the rainfall show negative high correlation (0.2). During 2nd fortnight of December the rainfall show high correlation (−0.3) but negative. During second fortnight of

**Table 28.2** Correlation Matrix of Yield and Weather Parameters

| Duration | T. max. | T. min. | Rainfall | S.S. hrs |
|---|---|---|---|---|
| FFN-Nov | 0.04 | 0.21 | 0.01 | −0.14 |
| SFN-Nov | 0.3 | 0.1 | −0.2 | 0.2 |
| FFN-Dec | 0.1 | 0.1 | 0.0 | −0.1 |
| SFN-Dec | 0.1 | −0.1 | −0.3 | −0.1 |
| FFN-Jan | 0.1 | 0.1 | 0.0 | −0.1 |
| SFN-Jan | −0.2 | −0.3 | −0.1 | 0.1 |
| FFN-Feb | 0.1 | −0.2 | −0.4 | 0.3 |
| SFN-Feb | 0.3 | 0.0 | −0.2 | 0.2 |
| FFN-Mar | 0.1 | 0.2 | 0.1 | 0.0 |
| SFN-Mar | −0.3 | 0.3 | 0.3 | 0.0 |
| FFN-Apr | −0.2 | −0.1 | 0.1 | 0.0 |
| SFN-Apr | −0.2 | −0.1 | 0.0 | −0.2 |

*FFN*: First fortnight, *SFN*: Second fortnight, *Tmax*: Maximum temperature, *Tmin*: Minimum temperature, *S.S.hrs*: Sunshine hours

January the maximum and minimum temperature show negative high correlation (−0.2 and –0.3 respectively). During first fortnight of February the minimum temperature show negative high correlation (−0.2) and the sunshine hrs show positive high correlation (0.3). During second fortnight of February maximum temperature and sunshine hours show positive high correlation (0.3 and 0.2 respectively), while rainfall show negative high correlation (−0.2). During first fortnight of March the maximum temperature shows high correlation (0.2). During second fortnight of March the minimum temperature and rainfall show positive high correlation (0.3 and 0.3 respectively) and the maximum temperature show negative high correlation (−0.3). During first fortnight of April the maximum temperature shows negative high correlation. In the second fortnight of April the maximum temperature and sunshine hours show negative high correlation (−0.2 and −0.2, respectively).

### 28.3.5 *Development of Weather Based Model for Wheat Yield Forecasting*

These sensitive weather parameters, which show high correlation coefficients, were selected as factors for working out the regression equation. The minimum temperature of first fortnight of February, the maximum temperature of second fortnight of March, minimum temperature of second fortnight of March and the sunshine hours of second fortnight of April, were selected for developing the model. The regression equation obtained is given below:

$$\begin{aligned} Y = {} & 3.291 + (-1.591) \times \text{TminFFF} + (-3.790) \times \text{TmaxSFM} \\ & + (3.197) \times \text{TminSFM} + (2.010) \times \text{S.ShrsSFA} \end{aligned}$$

Where,

Y = predicted yield

Tmax SFM – The mean maximum temperature during the first fortnight of March.

Tmin FFF – Mean minimum temperature during the first fortnight of February.

Tmin SFM – Is the mean minimum temperature during the second fortnight of March.

S.Shrs SFA – The mean sunshine hours during second fortnight of April.

Coefficient of determination R2 of 0.54 was obtained.

The actual and estimated yield for different years has been obtained. Estimated yields showed good agreement with observed yields of the district except in year 1983, 1999 and 2001. The RMSE between observed and predicted wheat yields is 163.2 kg $ha^{-1}$ (Fig. 28.5). The above results revealed that weather parameters (maximum and minimum temperature, rainfall and sunshine hours) show non-significant correlation with yield. The model developed for the yield prediction predicts the yield successfully the predicted yields showed good agreement

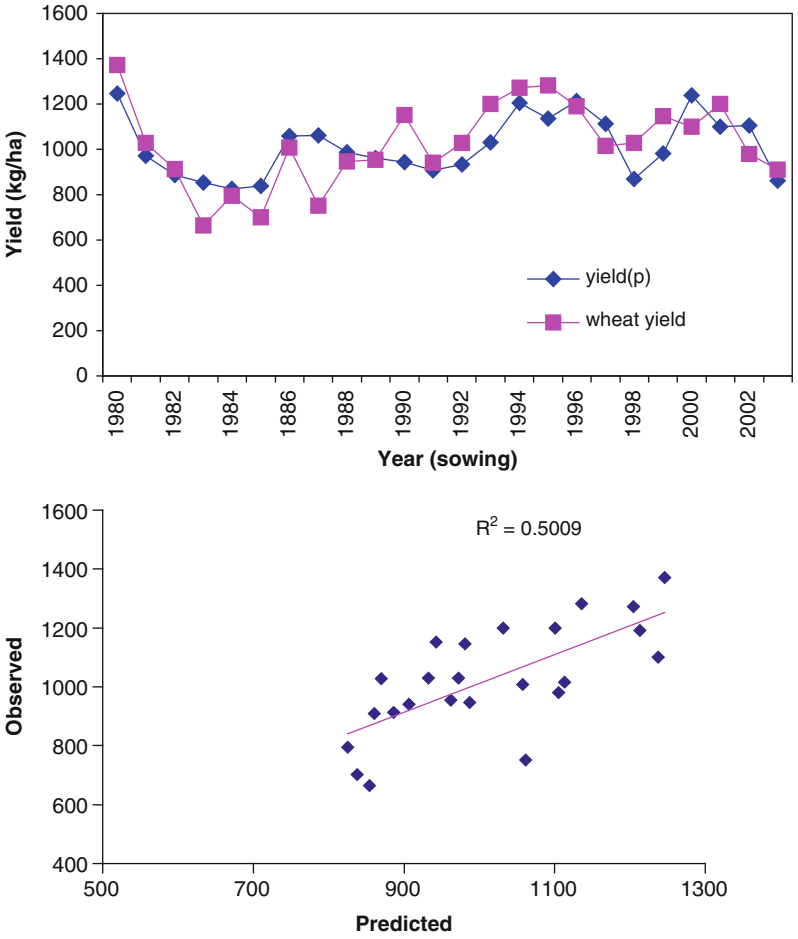


**Fig. 28.5** Comparison of grain yield predicted by regression model with observed yield (1980–2003)

with the observed yields. Mall and Gupta (2000) used empirical statistical model for predicting the wheat yield using the crop yield as dependent variable and weather factors as independent variables. The model forecast the wheat yield successfully.

## References

Angstorm A (1924) Solar and terrestrial radiation. Q J Roy Meteorol Soc 50:121–126
Anonymous (2004) Agricultural statistics. Ministry of Agriculture, Government of India.
Attri SD, Singh KK, Kaushik A, Rathore LS (2001) Evaluation of dynamic simulation model for wheat genotypes under diverse environments in India. Mausam 52(3):561–566

Chipanshi AC, Ripley EA, Lawford RG (1997) Early prediction of spring wheat yields in Saskatchewan from current and historical weather data using the CERES-wheat model. Agric For Meteorol 84:223–232

Hoogenboom G, Georgiev G, Singh U (1997) Performance of the CERES rice model for three locations in the asian region. START Rep. 2. Ed Michale Monton, Anne Phelan and Hasan Virjji. Report on START/WCRP/IGBP/GCTE workshop , Bogor, Indonesia, 19–22 Feb 1997 pp 43–41

Hunt LA, Pararajasingham S, Jones JW, Hoogenboom G, Imamura DT, Ogosgi RM (1993) GENCAL software to facilitate the use of crop models to analyze field experiments. Agron J 85:1090–1094

Mall RK, Gupta BRD (2000) Wheat yield forecast models based on meteorological parameters. J Agrometeorol 2(1):83–87

Ramakrishna YS (1990) Crop growth models–CERES millet. Paper presented at crop growth modeling workshop at CASAM, Pune India, 4–6 Oct 1990, p 55

Ramakrishna YS, Joshi NC, Rao AS, Singh HP (1994) Performance of modified CERES millet model under arid and semi-arid conditions

Ramakrishna YS, Vijaya Kumar P, Rao GGSN (1997) CERES-millet presented at Training Workshop on Crop growth modeling at CASAM, 6 Oct, pp 7

Ritchie JT (1986) The CERES – MAIZE model, p 3-6. In: CA Jones and JR Kinry (Eds.) CERES-Maize Texas A & M Univ. Press, Texas, pp 194

Ritchie JT, Algarswamy G (1989) Simulation of sorghum and pearl millet phenology. ICRISAT Bulletin No. 12: 24–26.

# Chapter 29
# Impact of Climate Change on the Grape Productivity in the Southern Coast of the Crimea

**S. Korsakova**

**Abstract** Peculiarities of climate changes in the Southern coast of Crimea (Ukraine) in the conditions of global warming have been shown in this work. The influence of climate changes over the productivity of grape which has been cultivating in the Southern coast of Crimea has been researched. The main agro-climatic phenomena which decrease grape's productivity have been determined. Possible positive and negative consequences of climate changes influence over the grape's productivity in Southern coast of Crimea have been determined. Recommendations on the measures of the adaptation in the viticulture practice in the connection with the global warming have been given.

## 29.1 Introduction

The weather is the second factor after the vine rod which influences on the grape's productivity and this factor is very changeable. All other factors including climate are more or less settled and they are known beforehand. As the result the yield of one or another years destroyed by the weather changes.

Without enough quantity of rainfalls and warmth the grape cannot to ripe. Redundancy of both factors can worsen grape and wine quality. Separate weather phenomena – hail or frosts – influence not mostly on quality but on the quantity of grape, sometimes they decrease yield in tenth. The real horror for vine-grower is frosts in the end of spring when the buds are especially vulnerable. The same thing can be told about hail but luckily as a rule it concerns only small areas. Strong storm cannot only injure the yield but it can also beat the buds and even damage the wood of the vine rod which will influence the next year yield.

S. Korsakova (✉)
Center for Hydrometeorology of the Autonomous Republic of the Crimea, Agrometeorological Station of the Ukraine, State Committee for Hydrometeorology, Nikitskij Sad, Yalta, Ukraine
e-mail: korsakova@i.ua

S.D. Attri et al. (eds.), *Challenges and Opportunities in Agrometeorology*,
DOI 10.1007/978-3-642-19360-6_29, 

Viticulture – is one of the perspective and profitable branches on the territory of the Crimea (Southern region of the Ukraine). An important role in the economics of this region plays viticulture on the Southern coast of the Crimean peninsula. Particularly here the most costly kinds of grape are planted. They are used for making famous vines such as "Pino-Gry," "Tokaj," "Muscat white Livadia," "Muscat white Red Stone," honored with two cups "Gran Pry" Solar (1996).

Region of the Southern coast of the Crimea is characterized by moderate warm Mediterranean type of climate with the predominance of autumn-winter precipitation and drought summer period Loginov (1976). The mean annual air temperature is 12.4°C, the middle air temperature in January is 3.1°C, in July – 23.2°C, total rainfall is 589 mm. Cold part of the year is differed with the alternation of short time periods of slight frosty, dry weather and warm rainy days sometimes with strong winds. In this period sudden raises of air temperature up to 16–18°C are observed Fursa et al. (2006).

## 29.2 Data and Methodology

For researches influence of climate changes on the grape productivity data at agrometeorological station "Nikitskij Sad" have been used in the present study: air temperature and rainfall for 78 years (1930–2007); dates of the active grape vegetation and mass sugars' concentration in grape berries kind Pinot Gris for 18 years (1991–2008); the main agroclimatic phenomena which are lowering grape productivity in the Southern coast of Crimea for 48 years (1961–2008). For analysis dynamics of the average grape yield in the Southern coast of Crimea using data of National industrial-agrarian society "Massandra" during the last 52 years (1956–2007).

## 29.3 Results and Discussion

The most important factors which influence the climate of wine-making region are air temperature and quantity of rainfall. According to the analysis of data about the annual air temperature and total rainfall which are presented in Fig. 29.1 (period 1930–2007 years), in the present time climate changes in the Southern coast of Crimea can be characterized as warming which is accompanied by some increasing of rainfalls quantity. The most active warming begins in the end of 70–80s and it lasts till now. In the year course of the air temperature warming is strongly expressed both in cold and warm year periods. The speed of warming is increasing during the last years. During the period 2001–2007 the main growth of the air temperature, in the comparison with the standard climatic norm (average meaning over 30-years period 1961–1990, which had been

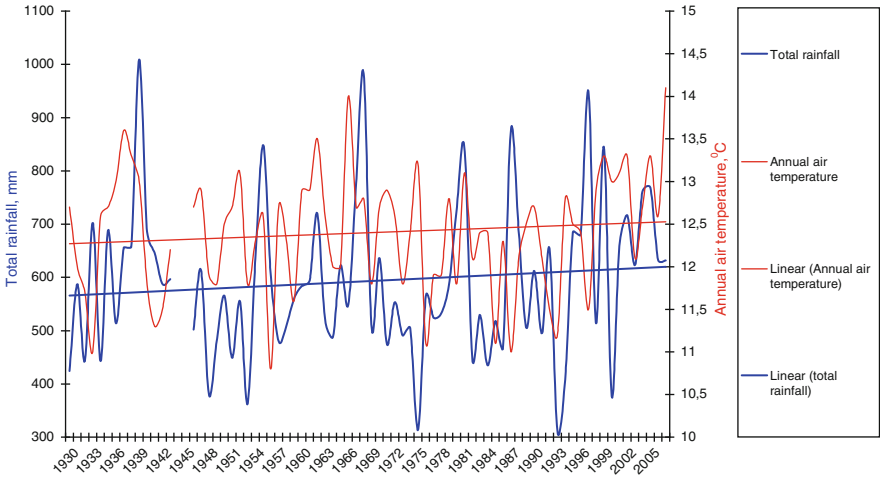


**Fig. 29.1** The dynamics of annual air temperature and total rainfall in the Southern coast of Crimea

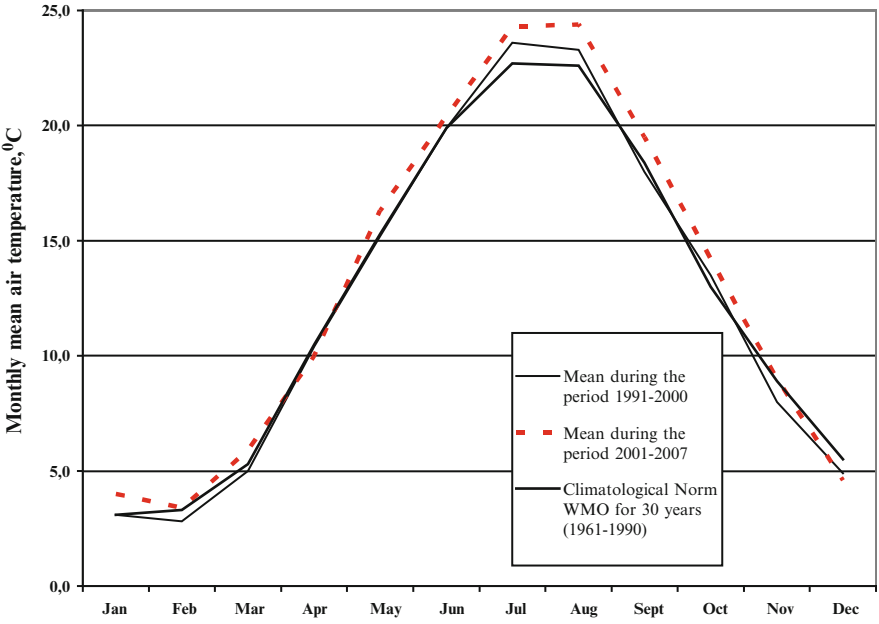


**Fig. 29.2** Annual course of air temperature in the Southern coast of Crimea

adopted by World Meteorological Organization) took place in January, May, July-August, at an average 0.9–1.8°C (Fig. 29.2, Table 29.1). At the same time the air temperature in April became lower on 0.5°C and on 1.1°C in December.

**Table 29.1** Monthly mean and annual air temperature (degree Celsius) in the Southern coast of Crimea

| Period | Jan | Feb | Mar | Apr | May | Jun | Jul | Aug | Sep | Oct | Nov | Dec | Annual |
|---|---|---|---|---|---|---|---|---|---|---|---|---|---|
| 1961–1990 | 3.1 | 2.8 | 5.0 | 10.4 | 15.2 | 19.9 | 23.6 | 23.3 | 18.0 | 13.5 | 8.0 | 4.9 | 12.3 |
| 1991–2000 | 4.0 | 3.4 | 5.9 | 10.0 | 16.3 | 20.4 | 24.3 | 24.4 | 19.5 | 14.2 | 9.0 | 4.6 | 13.0 |
| 2001–2007 | 3.1 | 3.3 | 5.3 | 10.5 | 15.3 | 19.9 | 22.7 | 22.6 | 18.4 | 13.0 | 8.9 | 5.5 | 12.4 |

Because of the lower temperature régime of December and in some years of November grape plants receive necessary sum of lower temperatures. Frequent and deep thaws in January during the last years when maximum air temperatures are grow up to 12...16°C favor to the quiescence breaking of grape buds. Such changes in wintering conditions bring to the negative consequences – lowering of plants' frost resistance (as the example it can be given January 2006, when after the sharp lowering of minimum air temperatures in the Southern coast of Crimea up to −12°C to −15°C wintering eyes on some grounds were damaged on 25–30% that leaded to the yield lowering). Before 2006 cold winters predominate in theSouthern coast of Crimea during the periods from 1930 till 1956 and from 1964 till 1976. In those winters minimal air temperature fell down to −10°C to −15°C. From 1977 till 2005 warm winters had been observed over the whole Crimea. Minimal air temperature in the Southern coast of Crimea in that period didn't fall down lower than −3°C to −9°C and only in the separate years it fell down to −10°C. The winter of 2006 has showed that possibility of extremely cold periods, months and seasons is still present. As in the XX so in the beginning of the twenty-first century extremely cold winter can be noticed once in 10–15 years.

Changes of temperature regime which had been given earlier lead to the further time changes in nature complexes development. After 1997 year (with the exception of 2003) almost every year the earlier development of spring processes (buds' swelling and opening in some fruit trees, spring growth of some ether-bearing plants and so on) has been noticed in the Southern coast of Crimea. In the separate years, for example in 2007, stable transition over 5°C to the side of the lowering was practically absent. At the same time, as we can see from the Table 29.2, in the connection with cool weather in April (the air temperature in April in 2001–2007 in the comparison with 1991–2000 lowered on 0.4°C) dates of the active grape vegetation beginning had changed considerably less that is pointed on the increasing of the period between the dates of transition over 5°C and 10°C in spring. Low temperature regime of April during the last years favored to the formation of the greater number inflorescences on the shrubs. But in the background of the global warming of climate on the territory of the Crimea such peculiarity as long late frosts has been noticed. The influence of climatic changes over the increasing of number and recurrence of frosts is mostly depended by the great positive anomalies of the air temperature during the period which precedes the spring frosts. Such anomalies scientists explain with the disturbance of zonal air mass transfer and intensive cold comings from arctic latitudes in winter which became

**Table 29.2** Mean dates of the active grape vegetation (grape kind Pinot Gris) in the Southern coast of Crimea

| Period | Flow of sap (exudation) | The swelling of the buds | Bud bursting | Flowering date | Physiological ripeness | Leaf fall |
|---|---|---|---|---|---|---|
| 1991–2000 | 29 Mar | 07 Apr | 24 Apr | 15 Jun | 16 Sep | 06 Nov |
| 2001–2008 | 24 Mar | 10 Apr | 20 Apr | 12 Jun | 07 Sep | 17 Nov |

more frequent during the last years. So, in 1999 after the mass inflorescences' formation, firstly since 1930 there were frosts with the intensity −1°C to −4°C all over the territory of the Crimea with the exception of Big Yalta region. Frosts brought great damage to the vineyards of the Crimea: regions at the mountains bottoms were especially damaged. Even in Alushta region 12 ha of the vineyards had been damaged by frosts on 40%, and about 4 ha – on 80–100%. In 2004 in the Southern coast of Crimea up to 30–40% of open grape buds were damaged with frosts. According to experts' estimations it will be preserved the tendency of the more intensive air temperatures rise in March and preservation and even some lowering of the air temperatures in April that will increase the possibility of late spring frosts.

As we can see in the Fig. 29.2, during the period from 2001 till 2007 the average months' air temperatures in May, July, August and September were particularly higher than in previous decennials on the coast. And 2007 was the warmest year in the whole period of observations in the Nikitsky Botanical Gardens since 1930. In summer period recurrence and length of high air temperatures (higher than 25°C and 30°C) and length of the periods with such high temperatures has particularly increased. At the same time absolute maximums hadn't been often exceeded. High temperature regime during the last years favors to the earlier grape ripening. As you can see from the Table 29.2, the average date of the whole ripening of grape kind Pinot Gris in the last 8 years was 9 days earlier in the comparison with the previous 10 years' period. September was particularly warm during the last 8 years, almost 1.5°C higher than during the previous 10 years' period 1991–2000. In the Southern coast of Crimea intensive accumulation of mass sugars' concentration in the berries of technical grape kinds which are used for preparing of high quality dessert wines has been noticed in September. On the Fig. 29.3 it has been shown the sums of active air temperatures higher than 10°C in the region of Nikitsky Botanical Gardens (the Southern coast of Crimea) on the 31$^{st}$ of October during 1930–2007 years. Analysis of heat-providing has shown that whether many years average sum of the active air temperatures higher then 10°C over 78-years period was near 3645°C, the average sum of the air temperatures in the period 2001–2007 has reached 3860°C. The higher temperature is the higher mass sugars' concentration in grape berries is. It has been known that for grape ripening daily average air temperatures higher than 18–20°C are needed. The more sums of active air temperatures higher than 18–20°C has been accumulated the earlier grape ripens and the higher mass sugars' concentration is and the larger quantity of high quality chateau wines are made of it. However not

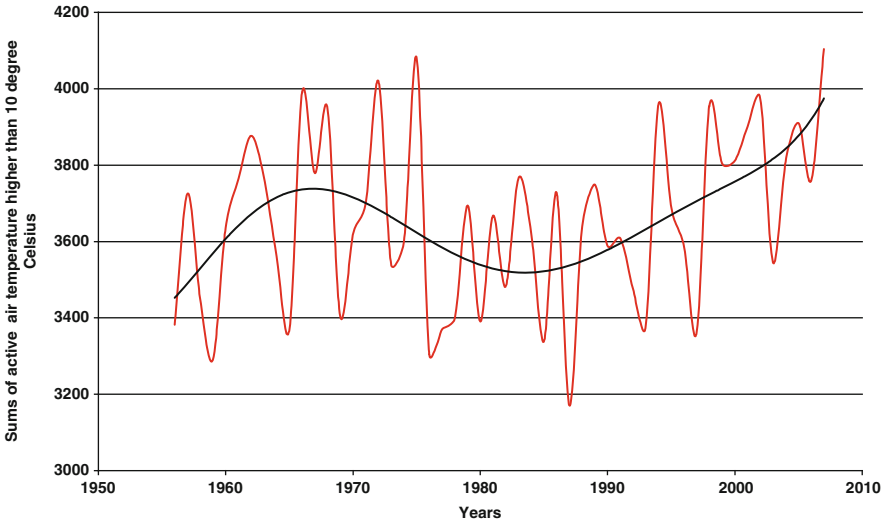


**Fig. 29.3** The sums of active air temperatures higher than 10°C in the Southern coast of Crimea on the 31st of October

only warmth but water is also needed by the vine rod. If the rod hadn't enough water it has so called "water stress" and it gives small berries with thicker skin. In spite of this fact leads to the yield lowering it let to make wines with bright bouquet and color. But the result of severe drought which stops the process of ripening is inharmonious wines. At the same time if it is strong rains before the crop gathering especially after the period of rather drought weather grape berries can quickly ripen and concentration of sugars, acids and other flavoring substances can become lower. As the example in the Fig. 29.4 variability of mass sugars' concentration in grape berries kind Pinot Gris at the time of crop gathering over the last 18 years has been shown. An observing ground is situated in the central part of the Southern coast of Crimea on the height 160–180 m over the sea level. It doesn't have watering that's why weather conditions had the main influence on the mass sugars' concentration on that ground year by year. For heat-providing characteristics of the ripening period for each year the sums of the active air temperatures higher than 20°C in the period from July 20th till October 10th and also the sums of rainfalls during the period of active grape vegetation – from April till October has been given in the diagram. As we can see in the Fig. 29.4 during the period from 1991 till 2008 years the lowest values of mass sugars' concentration in grape berries kind Pinot Gris – 19.8 and 20.3 g/dm3 had been noticed in 1993 and 1997 years. In those years the lowest heat-providing of the ripening period had been noticed, the sums of active temperatures higher than 20°C hadn't been more than 1111–1229°C. In 1993 conditions for sugars' accumulation in grape berries were very unfavorable: in the background of lower temperature regime a very severe drought has been noticed. From the end of July

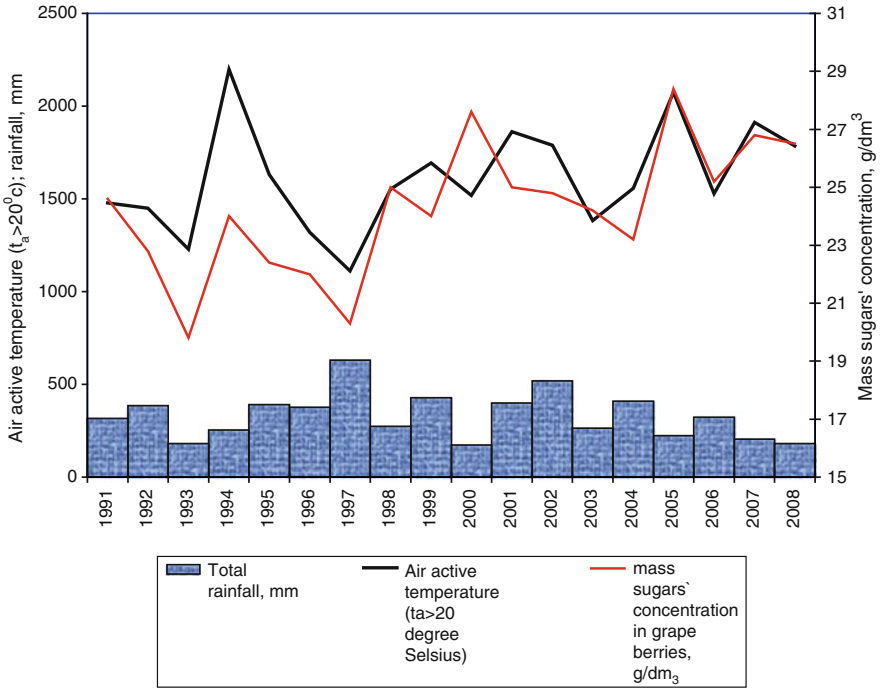


**Fig. 29.4** Variability of mass sugars' concentration in grape berries kind pinot gris at the time of crop gathering

to the end of September reserves of productive moisture in 1 m soil layer were practically absent. In such conditions the delay of grape gathering would lead only to the great lost of crop, that's why the farms of the Southern coast of Crimea gathered grape which was not technically ripened. In the contrast to 1993 in 1997 during the grape ripening on the Southern coast of Crimea very strong downpours have been noticed in the background of the lower temperature regime and low intensity of sugars' accumulation. After such downpours grape berries began to rot. The highest values of mass sugars' concentration – 27.6, 28.4 and 26.8 g/dm$^3$ have been noticed in 2000, 2005 and 2007 years. Those years were characterized by high heat-providing. The sums of active air temperatures higher than 20°C in the ripening period in 2000, 2005 and 2007 years were up to 1518, 2074 and 1914°C; from April till October sums of rainfalls were 173–222 mm under the norm 263 mm, and in the period of berries growth and in the beginning of ripening drought has been noticed. Correlation of mass sugars' concentration in grape berries with the air temperature and rainfalls in the conditions of the Southern coast of Crimea has been shown in the Fig. 29.5. It's needed been noticed that in the years with high heat-providing vine rod suffers from temperature and water stress if there are dry winds in the background of the air-soil drought in the

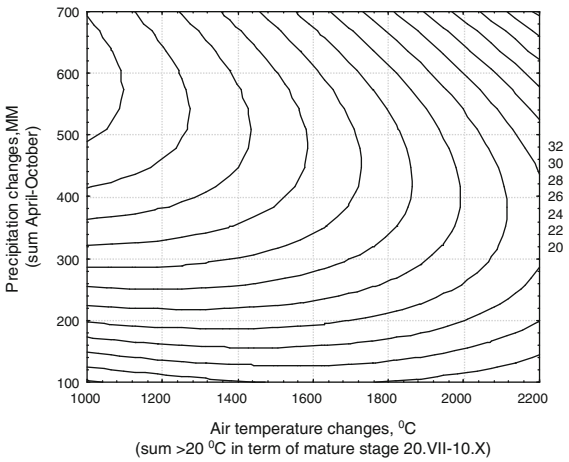


**Fig. 29.5** Correlation of mass sugars' concentration in grape berries with the air temperature and rainfalls in the conditions of the Southern coast of Crimea

Southern coast of Crimea. Such picture has been noticed in the hot dry summer 2007 when after dry winds the process of grape berries ripening was stopped and the process of sugars' accumulation was better on the watering grounds.

In the common wetting regime it has been noticed valuable increasing of the rainfalls on the territory of the Southern coast of Crimea during the last years that is undoubtedly positive. According to many years average data in 1930–2007 years in the area of agrometeorological station "Nikitsky Sad" the total rainfalls were 589 mm. During 2001–2007 years the mean total rainfalls were 630 mm. In the year course of the precipitation which is shown in the Fig. 29.6 general tendency of rainfalls' increasing in January – March (on 20–28%), in July (on 20%) and in September – October (on 39–59%) and their valuable decreasing in May, June and August has been observed. Rainfalls decreasing in the background of high summer temperatures leads to the increasing of drought phenomena number which makes crop capacity lower. So in spite of high inflorescences formation in spring 2007 strong drying of grape berries has been noticed because of strong winds and dry winds in July – August. That led to the valuable yield losses on the dry valleys.

Dynamics of the average grape yield on the Southern coast of Crimea according to the data of National industrial-agrarian society "Massandra" during the last 52 years have been shown in the Fig. 29.7. Making an analysis of yield dynamics over 1956–2007 years one can see its particular growth during the last years. If the average yield in the farms had been 3.7 t/ha during the whole period, then during the last 7 years it has grown up to 4.9 t/ha. Such growth has been favored by the introduction of high yield kinds, agrotechniques' improving and widening of watering vineyards. But even in the background of intensive agrotechnique real productivity is strongly depends of weather conditions of the year. Under strong drought yield can fall down to 1.6–1.9 t/ha (1971). Under good moisture-providing and optimal environmental conditions for spring differentiation of inflorescences

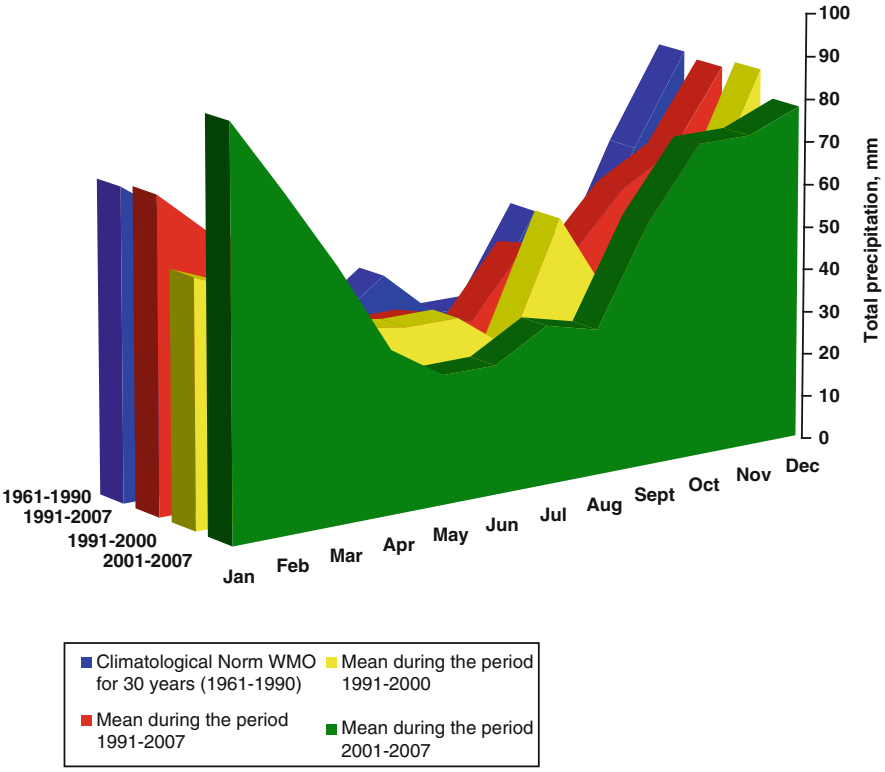


**Fig. 29.6** The year course of the precipitation in the Southern coast of Crimea

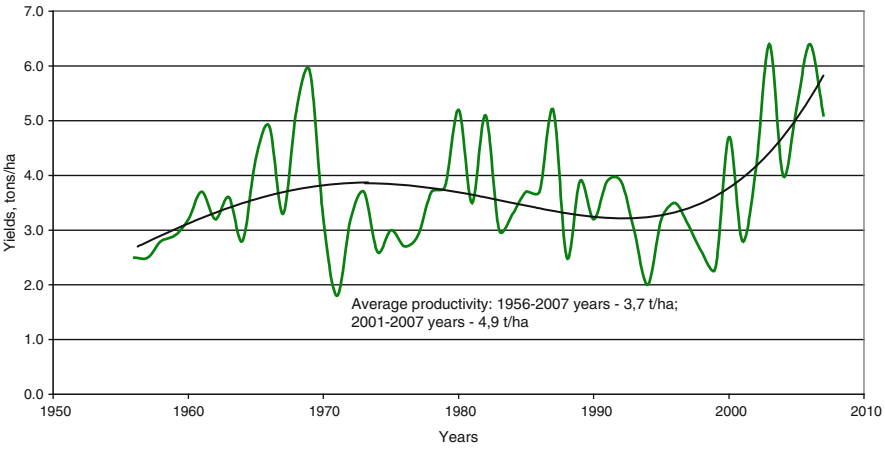


**Fig. 29.7** Dynamics of the average grape yield in the Southern coast of Crimea

average grape yield in different farms can reach 6.4 t/ha. For example in 2003 and 2006 unusually high yield – 5.9–6.9 t/ha was gathered. And those is for all that in 2006 partial damages by frost in winter and by hail in summer have been noticed on some grounds that made the yield lower.

One of the negative climate changes reveals all over Ukraine and particularly in the Crimea is the increasing of frequency and intensity of extreme events which brings terrible losses to the farms in the Southern coast of Crimea. Extreme events in 1991–2008 were very unusual – it has been noticed such events which can be noticed once in 50 and 100 years. It has been firstly settled extreme events which reach criteria of elemental during untypical seasons. So in May 1999 in the Southern coast of Crimea firstly from 1930 there has been noticed unusually strong north-western wind the speed of which reaches 32–34 m/s in Yalta-Alushta. Stormy wind strongly damaged leaves, young shoots and inflorescences of grape. In May 2008 this phenomenon repeated. Because of strong drought in 1994 in the central part of the Southern coast of Crimea the lowest grape crop since 1935 has been gathered. After strong rains on 24th September 1996 and 14th September 2002 grape berries began to crack and to rot. On 29th August 2006 during the downfall large hail with diameter 25 mm with some hail-stones up to 30 mm in diameter has been noticed. Up to 20% of grape clusters have been damaged with hail.

In the world practice two types of reactions over the climatic influence are used: limitation and adaptation. Limitation strategy is directed to the preventing and delay of hothouse gas concentration in the atmosphere. The politics of hothouse gas emissions limitations (Kiotsky protocol) has already brought to some stabilization of the process, but it principally can't prevent climate changes. Strategy of adaptations is needed in calculation both negative and positive effects of climate changes. With this aim it has been built diagrams of main agroclimatic phenomena distribution which are lowering grape productivity in the Southern coast of Crimea over the standard 30-years period 1961–1990 and also over the next 18-years period 1991–2008 and over the last 8 years (2001–2008). Diagrams are given in the Fig. 29.8a, b. The most valuable negative influences over the grape yield in the Southern coast of Crimea are drought, strong rains and low air temperatures during the ripening period, unfavorable weather conditions during the periods of inflorescences differentiation in spring and flowering, damages with low temperatures in winter and spring frosts, hail, strong wind, and also fungous diseases. Analysis of the diagrams shows that among the given characteristics the main grape yield losses in the Southern coast of Crimea are noticed because of droughts. And the number of drought phenomena increases. If during the period since 1961 till 1990 years the part of yield losses because of drought phenomena was 28%, then during the last years this index has increased up to 32%. At the same time considerable increasing of the air temperature in July, August and September had positive influence over the grape yield. Losses because of strong downfalls and berries' rotting decreased to 15% after 1991 year, and because of low air temperatures during mass sugars' concentration accumulation to 10% after 2001 year. During the last years rainfalls increasing in March and more cool weather in April delayed buds' opening and favor to the greater

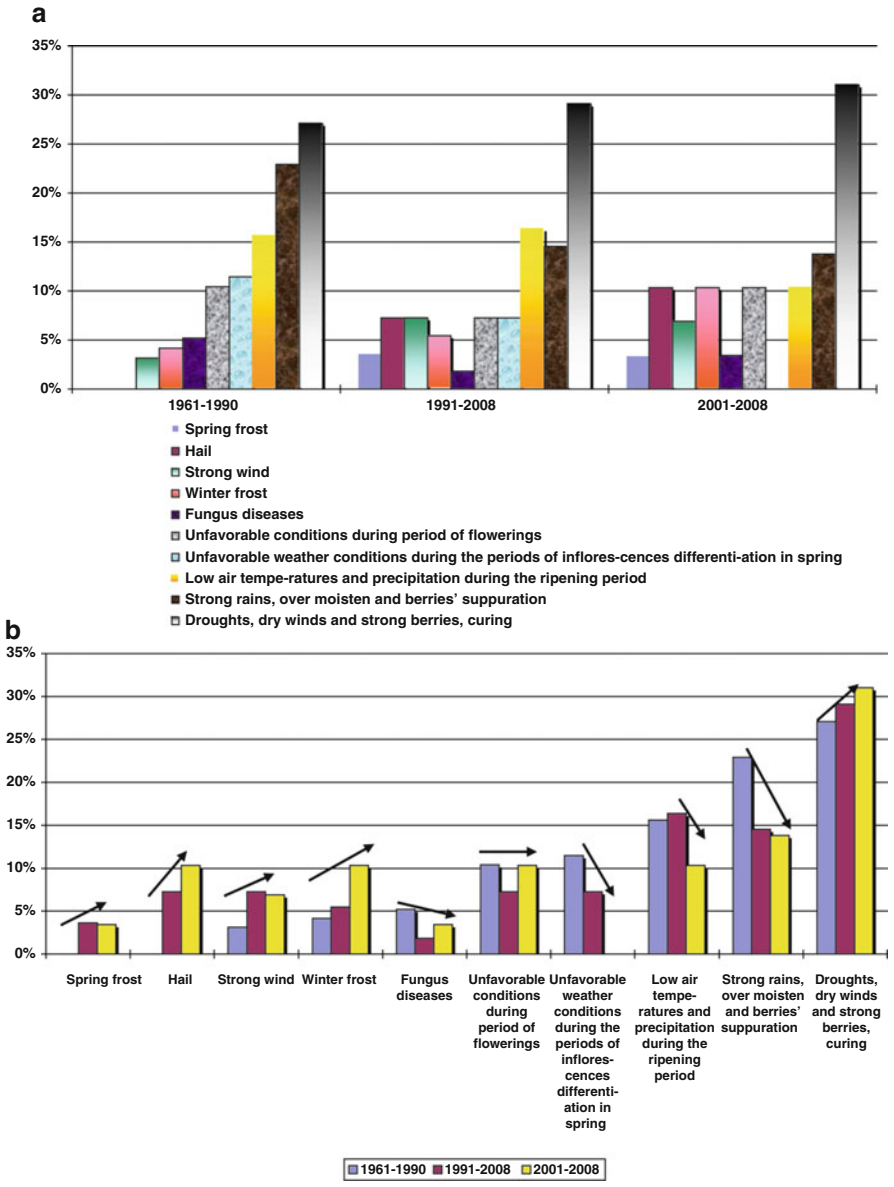


**Fig. 29.8** (**a** and **b**) The main agroclimatic phenomena distribution which are lowering grape productivity in the Southern coast of Crimea

number inflorescences formation. Though because of earlier spring processes and lowering of the air temperatures level in April it has been determined grape damages with late spring frosts in the Southern coast of Crimea.

## 29.4 Conclusions

Thus warming in the Southern coast of Crimea will have as positive though negative influence over the grape productivity in the nearest time.

*Possible positive consequences*:

- rainfalls‘ increasing in January – March and cool weather in April are favorable for greater number inflorescences formation;
- yield increasing;
- mass sugars‘ concentration increasing;
- earlier technical ripening;
- absence of early autumn frosts;
- decreasing of yield losses because of over moisture during the ripening;
- increasing of vegetative period length.

*Possible negative consequences*:

- late spring frosts;
- yield losses because of droughts and dry winds;
- successful winter spending of pests and weeds;
- soils‘ hardening;
- spreading of pests and diseases from other regions;
- increasing of frequency and intensity of extreme events number;
- decreasing of plants‘ winter resistance;
- not all grape kinds which are used today can be adopted to the production of particular wines with traditional quality;
- increasing of vegetative activity and vine rods‘ yield in the detriment of yield quality.

Measures for adaptation in the connection with global warming in the Southern coast of Crimea are:

- selection of optimal kinds which corresponds to the new conditions;
- maximal increasing of watering grape areas, particularly drop watering;
- optimal distribution of vineyards in cross relief conditions;
- development of new agricultural methods which are corresponded to the maximal moisture preservation in soil;
- using of new remedies for vineyards protection from pests, diseases and weeds;
- new agroclimatological zoning;
- development of droughts insurance system.

## References

Fursa DI, Korsakova SP, Fursa VP, Ivanchenko VI (2006) Agroclimatic resources of the Southern coast of Crimea in Big Yalta region, and their assessment in relation to grapes. Institute for Vine and Wine “Magarach”, Yalta

Loginov KT (1976) The agro-climatic hand book of Ukraine. Gidrometeoizdat, Leningrad

Solar “Massandra”. (1996) Classified publication-Fund, Massandra

# Chapter 30
# The Impact of Extreme Weather Events on Agriculture in the United States

**Raymond P. Motha**

**Abstract** The United States has sustained over 90 weather-related disasters in the past 30 years in which overall damages exceeded $1 billion. The total normalized losses for the 90-plus events exceeded $700 billion. Droughts, floods, hurricanes, severe storms, heat waves, freezes, and wildfires pose serious challenges for farmers and the agribusiness community. Socio-economic costs of some of these natural disasters are far-reaching and long-lasting. The enduring changes in climate, water supply, and soil moisture necessitate mitigation measures and adaptation strategies to cope with these changes in order to develop effective long-term risk management plans. The preparedness strategies should include alternatives to current agricultural management schemes in certain regions.

## 30.1 Introduction

While agriculture in the United States continues to achieve enhanced productivity, it is also experiencing greater variability in crop yields and associated farm income in recent decades. The increased yield variability is, in part, directly related to increases in extreme weather events during critical growth phases of crop development. Pests and diseases can also cause significant crop damage, which is indirectly related to climate conditions. Pest and disease occurrences often coincide with extreme weather events and with anomalous weather conditions. Agriculture is highly sensitive to climate variability and weather extremes, such as prolonged drought, floods, severe storms, heat waves, and untimely freezes. Thus, in the U.S., while agricultural production may benefit from the projected warmer climate in

R.P. Motha (✉)
U.S. Department of Agriculture, Office of the Chief Economist, World Agricultural Outlook Board, 1400 Independence Avenue, Room 4441 South Building, Washington, DC 20250-3812, USA
e-mail: rmotha@oce.usda.gov

S.D. Attri et al. (eds.), *Challenges and Opportunities in Agrometeorology*,
DOI 10.1007/978-3-642-19360-6_30, 

northern crop areas, the increased weather extremes across all growing areas will likely have an adverse effect on yield potential.

## 30.2 Weather Disasters and Agricultural Impacts

Weather disasters cause billions of dollars of damage and considerable loss of life in the United States. Every year, droughts, floods, heat waves, severe storms, wildfires, or other weather disasters caused deaths, destruction, and significant agricultural losses in various regions across the United States. During the last several decades, there has been an increasing frequency and severity of extreme weather events (Riebau and Fox 2005). Extreme weather events can have severe detrimental effects on crop yield, and therefore, agricultural production. Most crops are sensitive to direct effects of high temperature, decreased precipitation, flooding, and untimely freezes during critical growth phases. Other effects on crops are indirect, through influences on soil processes, nutrient dynamics, and pest organisms.

### *30.2.1 U.S. Droughts*

The economic impact of drought in the United States has been estimated at about $6–8 billion annually (FEMA 1995). On average, over the last 110 years, 10–20% of the United States experiences moderate to extreme drought annually, based on averaging over 5-year periods using the Palmer Drought Index. The 1980 drought/heat wave in the Midwest resulted in 10,000 human deaths and an estimated $55 billion in agricultural losses. In 1988, another prolonged summer drought/heat wave led to 7,500 deaths and over $70 billion in agricultural losses.

The severe drought of 1988 in the U.S. Midwest, accompanied by higher than normal temperatures, began early in the spring and continued throughout most of the summer. It spread to the central and southeastern parts of the nation, affecting agriculture, water resources, transportation, tourism, and the environment. Crop yields dropped by approximately 37% and required a $3-billion Congressional bailout for farmers (Wilhite et al. 2005).

Crop pests were also affected, with outbreaks of two-spotted spider mites damaging soybeans throughout the entire Midwest region. The damage occurred during the critical flowering, pod development, and pod filling growth stages. Approximately 3.2 million hectares were sprayed with insecticides to control the mites across the region, and estimated losses to Ohio farmers were $15–$20 million (Rosenzweig et al. 2001)

The drought led to decreased flows in the Ohio and lower half of the Mississippi Rivers by the end of May, restricting barge movement, and extending salt water intrusion from the Gulf of Mexico 105 miles up the Mississippi River, past New Orleans.

### 30.2.2 U.S. Flooding

Studies have examined trends in wet periods, finding that there is an increase in the area experiencing severe moisture surplus since about 1970 (Karl et al. 1995; Easterling et al. 2000). Population and infrastructure continues to increase in areas that are vulnerable to extremes such as flooding, and severe storm damage.

In 1993, Midwest flooding caused 48 deaths and $30 billion in damages. Flooding in the summer months of 1993 affected 41,400 square kilometers of farmland, with Nebraska, Iowa, and Michigan hardest hit. In July, the Mississippi River flood crest at St. Louis, Missouri broke the previous record. Over 4,451,000 hectares of crops were damaged, with losses of over $3 billion. Excess water presents a particularly severe problem for Iowa's low-lying soils, and increased pathogen outbreaks. Emergency measures cost over $222 million.

The flood of 1993 generated a strong pulse of nitrates and other nutrients and farming chemicals into the Mississippi River and Gulf of Mexico. The runoff of nutrients may have contributed to the doubling of the Gulf's "Dead Zone" in 1993, following the flood (Rosenzweig et al. 2001). In 2009, record flooding occurred in the upper Midwest causing the Red River to overflow its banks, and setting record annual peak flow values. The Red River crested over 6.95 m above flood stage, a new record.

Precipitation is crucial for agriculture and irrigation reserves during the growing season and for replenishment of urban water supplies throughout the year in the eastern two-thirds of the United States. In the western Rocky Mountain region, winter snowfall is essential to build mountain snowpack for the western U.S. Melting snow in the spring and summer months supply over 70% of the water supply to both agriculture and urban center in the West (NRCS 2008). Excessive spring rainfall and rapid snowmelt may cause severe flash flood hazard, which can quickly endanger both life and property. Insufficient winter snowfall can cause river systems to carry insufficient water supplies to meet the demands for both agriculture and urban population reserves.

### 30.2.3 U.S. Hurricanes

Hurricanes are one of the most physically destructive and economically disruptive extreme events that impact the United States. In addition to the torrential downpours and destructive winds associated with hurricanes, storm surges, and salt water intrusion into freshwater river systems are serious consequences.

In 2005, Hurricane Katrina caused over $130 billion in property damage and over 1800 deaths. The nation was made painfully aware of the damages possible from extreme storm events when hurricanes Katrina and Rita struck. A total of 233,099 square kilometers was declared a federal was declared a Federal disaster area following Hurricane Katrina, covering four states and 23 coastal counties.

80% of the city of New Orleans was flooded. More than 350,000 homes were destroyed and another 46,000 seriously damaged.

Hurricane Katrina killed or severely damaged 320 million large trees across over two million hectares of forest in the southern United States. Furthermore, coastal fisheries (e.g., oyster beds, shrimp) and harvesting infrastructure (e.g. boats, processing, and storage facilities) were also severely damaged. The storm surges exceeded over 25 ft where Katrina hit the Louisiana coast. The storm hit New Orleans, causing a portion of its levee system to fail. The economic damage caused by Hurricane Katrina exceeded $133 billion, making this extreme event the most destructive natural disaster to affect the United States in its history (Lott et al. 2008).

In September 1999, Hurricane Floyd, though not an overly powerful storm when it made landfall in eastern North Carolina, dumped copious amounts of rain leading to major flooding and 77 deaths. However, storm runoff created a major pollution event due to flooding of sewage treatment facilities, farms, farm waste lagoons, and chemical and petroleum storage facilities. The flooding caused the deaths of millions of farm animals (Easterling et al. 2000).

### *30.2.4 El Nino/La Nina of 1997–1998*

In late 1997, the tropical Pacific experienced the development of a major El Nino event, rivaling the strength of the 1982–83 El Nino. In the U.S., the El Nino was associated with several severe weather events, with heavy rain events on the West Coast from November 1997 to March 1998. In the summer of 1998, there were extremely high temperatures in Texas and Oklahoma, causing severe heat stress among the elderly population and damaging crops. These conditions spread across the South to the Carolinas. In the Southeast, there was El Nino related flooding throughout the winter and spring, while in Florida, summer dryness triggered forest fires. However, despite these regional El Nino effects, there was little impact on U.S. agriculture nationally. Wheat yields were at a record high, with the highest production since 1990; corn and soybean production was also the highest on record.

The abrupt April 1998 La Nina ushered in another year of extremes. The U.S. experiences a particularly warm winter, with January rains (rather than snow) interrupted by a cold snap, resulting in a crippling ice storm in the Northeast. The decreased winter snowpack and spring runoff exacerbated the spring and summer drought throughout the U.S. Atlantic states, severely affecting agricultural production. The second driest April-July period on record began in 1998 and intensified during 1999, inflicting the driest growing season in 105 years on the Northeast. A total of 109 million people and an estimated 918,960 farms suffered some drought in 1999. The 1998–99 drought in the U.S. resulted in reduced commodity receipts (from 1998) by an estimated $1.29 billion. Estimated net farm income losses, including yield losses, increased expenses and insurance indemnities, totaled $1.35 billion, approximately 3% of 1999 U.S. net farm income.

Then, Hurricane Floyd (September 1999) flooded coastal regions in North Carolina and New Jersey. North Carolina was also hit by Hurricane Dennis and Hurricane Irene, causing prolonged flooding and increasing the risk of fungal infections to agriculture and human health.

## 30.3 Food Production Vulnerability to Weather Events

### *30.3.1 Crop Responses*

Precipitation, the primary source of soil moisture, is probably the most important factor determining the productivity of crops. Interannual precipitation variability is a major cause of variation in crop yields and yield quality.

Drought stress and heat stress frequently occur simultaneously, exacerbating one another. They are often accompanied by high solar irradiance and high winds. Under drought stress, the crop's stomata close, reducing transpiration and, consequently, raising plant temperatures. Flowering, pollination, and grain-filling of most grain crops are especially sensitive to water stress. By reducing vegetative cover, droughts exacerbate wind and water erosion, thus affecting future crop productivity.

Excessively wet years may cause yield declines due to waterlogging and increased pest infestations. High soil moisture in humid areas can also hinder field operations. Intense bursts of rainfall may damage younger plants, promote ripening-grain lodging in standing crops, and cause soil erosion. Episodes of high relative humidity, frost, and hail can affect yield and quality of fruits and vegetables. And, the costs of drying corn are higher under wetter climate regimes.

Greater precipitation (if not excessive) during the growing season tends to increase yields. Corn yields decline with warmer temperatures due to acceleration of the crop's development, especially during the grain-filling period.

The extent of any crop damage depends on the duration of stress and the developmental stage of a particular crop. Crop yields are most vulnerable to adverse weather conditions, especially extreme temperatures and excess or deficit precipitation, during critical developmental stages such as seedling and reproductive development stages.

A general outline of stress indicators by growth stage is summarized below.

### *30.3.2 Juvenile Stages*

Soil temperature higher than 35°C (95°F) causes seedling death in soybeans. Air temperature above 30°C (86°F) for more than 8 h can reverse vernalization in wheat. Saturation of soil increases the risk of seedling diseases, especially at air

temperatures above 32°C (89.6°F). Flooding causes seedling death in corn and soybean; the combination of flooding with high temperature accelerates death.

### *30.3.3 Reproductive Stages*

Air temperatures higher than 36°C (96.8°F) cause pollen to lose viability in corn and reduce grain yield in post-blooming soybeans. Soil temperature higher than 20°C (68°F) depresses potato bulking. Soil moisture deficits are very detrimental to corn – 4 days of soil moisture stress reduces yields up to 50% – and other grain crops. Grain crops are also highly vulnerable to flooding. A spring freeze in April 2007 in the eastern U.S. affected 11 states and caused $2 billion in agricultural losses to field and horticultural crops.

### *30.3.4 Mature Stages*

Soil saturation causes long-term problems related to rot and fungal development and increased damage by diseases (e.g., crazy top and common smut in corn). Water deficits increase aflatoxin concentration in corn.

### *30.3.5 All Stages*

Extremely high air temperatures (>45°C; 113°F) persisting for at least 30 min directly damage crop leaves in most environments; even lower temperatures (35–40°C; 95–104°F) can be damaging if maintained for longer periods.

The United States is responsible for about 40% of the world's corn supply and nearly 70% of the total global exports (USDA/WAOB). U.S. corn yields have steadily increased since the 1950's. However, the annual growth rate in yields (i.e., relative percentage gain in annual yields) has steadily declined since the 1960's (Kucharik and Ramankutty 2005). Moreover, corn yield variability has escalated since 1950 in the United States (Naylor et al. 1997; Reilly et al. 2003).

## 30.4 Regional Impacts of Climate Extremes in the Future

### *30.4.1 Western United States*

Major climate change models predict winter snowpack in the western U.S. will decline in the twenty-first Century and snowmelt will occur earlier, resulting in greater runoff. The demand for water is rising in the region. Ground-water

withdrawals have increased significantly in recent years in many Western states both for irrigation agriculture and for increasing urban demand for water throughout the region.

Consequently, water shortages will force farmers in the region to fallow their lands. The estimated economy-wide loss for the Central Valley region of California is expected to reach up to $6 billion annually during the driest years. Decreased supplies of water are expected to significantly diminish the value of farmland in California. The value of wine production in California is $3.2 billion, which may be compromised, as grape quality will likely diminish with higher temperatures. The decline in dairy cow productivity is directly correlated with higher temperatures, as well. A loss is expected in this industry in California as well.

Forestry in the Pacific Northwest is expected to be greatly impacted as increased incidence of fire is expected. Increases in spring and summer temperatures and earlier melting of snowpacks have contributed to the six-fold spike in the area of forest burned since 1986, compared with the 1970–1986 period. Moreover, the average duration of fires increased from 7.5 to 37.1 days since 1986. In 1987, 486,000 ha of forest burned throughout the U.S., the first time since 1919 that more than 400,000 ha burned in 1 year. As a result of similar fires in 1988, 1994, and 1996, and a record 866,000 h fire in 2000, fire suppression costs increased significantly. A 50 percent increase in the number of hectares burned is expected by 2020, and a 100% increase by 2040.

Agriculture in the Pacific Northwest may benefit from a longer growing season, but these benefits may be offset by higher maximum temperatures and water shortages. Expected annual crop losses from water shortages are projected to rise from $13 million at present to $79 million by mid-Century.

### *30.4.2 Great Plains*

The agricultural sector in the region contributes $22.5 billion annually in market value of products – 35% of which is attributed to crops and the rest to livestock. The consumptive demand for water for crops (especially grass and alfalfa) may increase by 50% by 2090, straining water resources in the region. Farmers who plant corn in the Great Plains will likely experience declines in yields, while wheat yields may increase. Adaptation, especially at the farm level, will be essential for limiting losses due to changing climatic conditions (Scheraga and Grambsch 1998).

The Southern and Plains regions may experience a decline in productivity totaling as much as 70% for soybeans and 10–50% for wheat; although crops in other areas may temporarily increase their yields.

An additional burden on the agricultural sector may be an increased resilience of insects to pesticides. Pesticide use and the associated costs are estimated to increase by 10–20 % for corn; 5–5% for potatoes; 2–5% for cotton and soybeans; and 15% for wheat.

Higher incidences of severe weather events are likely to cause major damage to the region's infrastructure. For example, a 1999 outbreak of tornadoes in the Great Plains caused $1.16 billion in damages and 54 deaths; and an extreme flooding event in 1998 in southeast Texas inflicted $1.16 billion in damages and caused 31 deaths.

### *30.4.3 Midwest*

A big concern in the region is drought-like conditions resulting from rising temperatures, which increase evaporation and contribute to decreases in soil moisture and reductions in lake and river levels. Forestry is an integral part of the economic structure in the Midwest. Over 90% of forestland is used for commercial forestry, resulting in economic activity valued at $4.6 billion. The sector employs 200,000 people and produces $27 billion in forest products. Potentially negative impacts are expected to the $5.7 billion dairy industry, since milk production is temperature-sensitive and is reduced once temperatures advance beyond a certain threshold. The agriculture sector also may experience losses similar to the 1988 drought, which cut production of grain by 31% and production of corn by 45%.

### *30.4.4 Southeast*

With warmer weather and warmer water in the Atlantic and the Gulf of Mexico, the region may experience an increased frequency and intensity of storms, seal level rise, and the loss of important agricultural areas, crops, and timber species. In addition to coastal infrastructure, forests, agriculture and fisheries, water quality and energy may be subject to notable change and damages as well.

Forestry is a major economic sector in the Southeast. The state of South Carolina boasts 60% forest cover and forestry is, after tourism, the second largest economic sector. Given the diversity of species and environmental conditions, short- to medium-term impacts on forests are uncertain. Sea level rise resulting in salt water intrusion may damage forests, particularly in southern Florida and Louisiana. Higher temperatures, decreased soil moisture, and more frequent fires may stress forest ecosystems and ultimately lead to a conversion from forest to savannah and grassland. However, some species may see, at least temporarily, increases in productivity and forested acreage due to a longer growing season, $CO_2$ fertilization, and a switch from stressed to more acclimated species.

As increased storm frequency and intensity impacts coastal infrastructure, they may also reduce water quality and harm fish populations. Fish and shellfish are at risk in warmer waters and when exposed to increased pollution following major storm events. Much of this pollution will come from stronger storms stressing water management systems and causing sewer systems to overflow, as well as increased nutrient runoff from agricultural lands.

## 30.5 Expected Changes in Extreme Climate Events in the Twenty-First Century

The following observed changes in U.S. extreme events can be summarized, as well as the likelihood that the changes ill continue through the twenty-first Century. First, over most land areas, the last 10 years had lower frequency of severe cold outbreaks than any other 10-year period with this trend very likely to continue. Second, more frequent hot days and nights are observed over most of the country. Third, more frequent heat waves are most pronounced over the northwestern two-thirds of the nation, and this trend is very likely to continue. Fourth, more frequent and intense heavy downpours, with a higher proportion of heavy precipitation events, are expected over many areas of the U.S. 50 increases in area affected by regional drought are likely to expand.

Finally, likely increases in intense hurricanes are expected in the Atlantic Ocean linked directly to increasing sea surface temperatures.

## 30.6 Measures to Improve Our Understanding of Climate Extremes and Preparedness Strategies for Long-Term Planning

Drawing on the material presented in this report, there are opportunities to define highest priority areas for rapid and substantial progress in improving understanding of weather and climate extremes and developing adaptation strategies for agriculture to cope with both short-term climate variability and extreme events to longer-term changing climate. These include:

1. The continued development and maintenance of high quality climate observing systems to improve our ability to monitor and detect future changes in weather and climate extremes;
2. Efforts to digitize, homogenize, and analyze long-term data observations analyses to improve our confidence in detecting past changes in climate extremes;
3. Weather observing systems adhering to standards of observation consistent with the needs of both the climate and the weather research communities to improve our ability to detect observed changes in climate extremes;
4. Extended reconstructions of past climate using weather models initialized with homogenous surface observations to help improve our understanding of strong extratropical cyclones and other aspects of climate variability;
5. The creation of annually-resolved, regional-scale reconstructions of the climate for long-term historical records to help improve our understanding of very long-term regional climate variability;
6. Improvements in our understanding of the mechanisms that govern hurricane intensity would lead to better short and long-term predictive capabilities;

7. More extensive access to high temporal resolution data (daily, hourly) from climate model simulations both of the past and for the future to allow for improved understanding of potential changes in weather and climate extremes;
8. Enhanced communication between the climate science community and those who make climate-sensitive decisions to strengthen our understanding of climate extremes and their impacts;
9. A reliable database that links weather and climate extremes with their impacts, including damages and costs under changing socioeconomic conditions, to help our understanding of these events;
10. Preparedness is the key to proactive agricultural risk management planning measures;
11. Preparedness plans for weather and climate extreme events need to develop and incorporate comprehensive insurance and financial strategies into their overall long-term plans;
12. Crop insurance is an important risk management option;
13. A safety net of emergency relief should be maintained to emphasize sound stewardship of natural resources;
14. The combination of preparedness programs and emergency response measures needs to be coordinated in an effective, efficient, and customer-oriented manner;
15. The long-term strategy is threefold: (i) preparedness to improve the effectiveness of response and recovery, such as through establishment of early-warning systems; (ii) mitigation measures to reduce the impact of extreme events or natural disasters prior to their occurrence; and, (iii) adaptation strategies to prepare for and cope with the potential impacts of extreme events or natural disasters.
16. Weather and climate knowledge should be incorporated into planning and management decisions for agricultural production.
17. Sustainable, optimized production levels can be achieved through the effective use of weather and climate information, while maintaining environmental integrity and minimizing the degradation of soil, nutrients, and water resource bases.
18. Finally, technology (fertilizers, new seed varieties, farming practices) should aid production, but not harm there resource bases in the long run.

## References

Easterling DR, Evans JL, Groisman PYa, Karl TR, Kunkel KE, Ambenje P (2000) Observed variability and trends in extreme climate events: a brief review. Bull Am Meteorol Soc 81:417–425

FEMA (1995) National mitigation strategy. Federal Emergency Management Agency, Washington, DC

Karl TR, Knight RW, Easterling DR, Quayle RC (1995) Trends in U.S. climate during the twentieth century. Consequences – the nature and implications of environmental change. Symp US Global Change Res Inform Office 1(1/Spring):3–12

Kucharik CJ, Ramankutty N (2005) Trends and variability in US corn yields over the twentieth century. Earth Interact 9(1):1–29

Lott N, Ross T, Houston T, Smith A, Shein K (2008) NOAA, National Environmental Satellite, Data, and Information Service (NESDIS), National Climatic Data Center (NCDC). Billion dollar weather disasters 1980–2008. Available online at: http://222.ncdc.noaa.gov/oa/reports/billionz.html

Naylor R, Falcon W, Zavaleta E (1997) Variability and growth in grain yields, 1950–94: does the record point ot greater instability? Popul Dev Rev 23(1):41–58

NRCS (2008) Snow surveys and water supply forecasting: agricultural information bulletin 536, National Resources Conservation Service, USDA

Reilly J, Tubiello F, McCarl B, Abler D, Darwin R, Fuglie K, Hollinger S, Izaurralde C, Jagtap S, Jones J, Learns L, Ojima D, Paul E, Paustian K, Riha S, Rosenberg N, Rosenzweig C (2003) US agriculture and climate change: new results. Clim Change 57:43–69

Riebau AR, Fox DG (2005) Damage assessment of agrometeorological relevance from natural disaster: economic and social consequences. In: Sivakumar MVK, Motha RP, Das HP (eds) Natural disasters and extreme events in agriculture-impacts and mitigation. Springer, Dordrecht, pp 119–136

Rosenzweig C, Iglesias A, Yang XB, Epstein PR, Chivian E (2001) Climate change and extreme weather events – implications for food production, plant diseases, and pests. Glob Change Hum Health 2(2):90–104

Scheraga JD, Grambsch AE (1998) Risks, opportunities, and adaptation to climate change. Clim Res 10:85–95

Wilhite DA, Svoboda MD, Hayes MJ (2005) Monitoring drought in the United States: status and trends. In: Boker VK, Cracknell AP, Heathcoe RL (eds) Monitoring and predicting agricultural drought – a global study. Oxford University Press, New York, pp 121–131

# Chapter 31
# Inter-Annual Variation of Fog, Mist, Haze and Smoke at Amritsar and Its Impact on Agricultural Production

**Jagadish Singh and R.K. Giri**

**Abstract** Fog, mist, haze and smoke are low visibility phenomena witnessed in the Amritsar district of Punjab during cold season from November to February. The impact of meteorological data of Rajasansi Airport, Amritsar for 27 seasons for the period 1981–2007 for main Rabi crops wheat and potato for Amritsar district were analyzed. It has been observed that wheat yield increased appreciably during the season 1999–2000 to 2001–2002 when the departures from LPA ranged between +22% and +26% which could be attributed to the cooling produced by excessive fog reducing the temperature near the ground surface. It can also be seen that during the recent five seasons (1998–1999 to 2002–2003) the departures of potato yield from LPA were negative and fog durations were positive. Therefore, it can be inferred that the potato yield decreases with increase in Fog activity. The correlation coefficients computed for wheat yield and low visibility phenomena like, fog (F), mist (M), haze/smoke (H/S) and combination of the three are found to be 0.53, 0.51, 0.29 respectively. When computed for the combined durations of F & M only, it comes out to be 0.65. This shows that the wheat yield is largely affected by the composite effect of F & M. This could be explained with the physical linkage between the wheat yield and low visibility phenomena occurring during cold season.

## 31.1 Introduction

Agriculture is the main primary constituent of Indian economy and backbone of the nation. Punjab state in India occupies 1.5% of the geographical area of the country and produces two-third food grains annually. Amritsar city is one of the cities of the

J. Singh (✉)
Mausam Apartments, West Enclave, Pitampura, Delhi 110 034, India

R.K. Giri
Meteorological Office, India Meteorological Department, Lodi Road, New Delhi 110 003, India
e-mail: rkgiri_ccs@rediffmail.com

S.D. Attri et al. (eds.), *Challenges and Opportunities in Agrometeorology*,
DOI 10.1007/978-3-642-19360-6_31, 

Punjab state in India and famous for spiritual, culture and agricultural production. Amritsar, which literally means a pool of nectar, lies 20 km east of the Indo-Pakistan border, is the Punjab state's second largest town. It experiences climatic conditions owing to its location. By mid – summer, the temperature becomes exceedingly hot while winters are marked by freezing cold chilliness. Temperature usually ranges between 30°C and 46°C in summers and between 0°C and 17°C in winters. The wheat–paddy cropping pattern is largely responsible for declining ground water table in Punjab and secondly, that the wheat–paddy cropping system is becoming unsustainable over time as the yield levels of these two major crops are stagnating (Sarkar et al. 2009). Out of all the Rabi crops, wheat and potato are the major crops in Amritsar district. The yield of these crops are depends on the low visibility weather phenomena, like fog, mist, smoke and haze over the area. Due to the rapid changes in the cropping pattern and urbanization the productivity of the wheat and rice crops also affected. Most of the time horizontal visibility is less than 3 km during December and January and affect the economy and agriculture productivity. The area of Amritsar, which is mostly plain, experiences radiation fog with visibility less than 1 km. It normally occurs after the passage of Western Disturbances when clear nights, moist and calm conditions prevail in the district. Mist (visibility 1–2 km), Haze & smoke (visibility 2–3 km) are generally seen when fog is lifted with increase in wind speed and insolation under moist conditions of the atmosphere. These two phenomena occur due to insufficient cooling and moisture availability. With the increase of air pollution in the district in recent years frequency and intensity of fog, mist, haze & smoke are increasing at the alarming rate thereby affecting aviation, rail and road transports, human health and agriculture production adversely. In the projected climate change scenario, the work done by Yadav et al. 1987, shows that the increased temperature will lead to forced maturity and poor harvest index due to limited water supply and water stress during grain filling period may result decline of grain yield. The technology trend in Fig. 31.1 shows the increasing nature of wheat yield from 1980–1981 to 2006–2007.

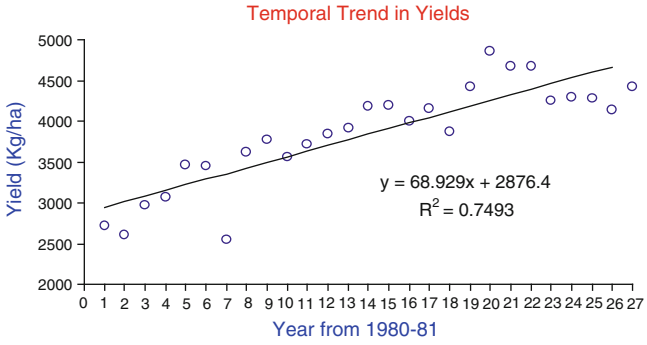


**Fig. 31.1** Variability of wheat yield of Amritsar, Punjab, India

## 31.2 Data and Methodology

In this study authors used two types of data, one is meteorological data and other is crop yield data. The meteorological data of fog, mist, haze, smoke for the duration of 1981–1982 to 2007–2008 is taken from current weather records of Raja Sansi Airport, Amritsar and the crop yield data is taken from state department of agriculture, Punjab from 1980–1981 to 2006–2007. The methodology used in this paper is graphically explained in the Fig. 31.2a, b. The yield LPA and low visibility phenomena normal departures regression analysis (Fig. 31.2a). The cooling produced during the foggy days by the obstruction of insolation will affect the rabi crops (mainly wheat and potato) productivity, which is shown in Fig. 31.2b.

## 31.3 Result and Discussion

The present study based on 27 years (1981–2007) data related to the impact of low visibility weather phenomena, like fog, mist, haze & smoke on the wheat and potato yield which are the main rabi crops of the winter season (November-February) for Amritsar district, Punjab, India. The normal is calculated for fog, mist and haze/smoke based on 27 years of the data. The normal seasonal value of fog, mist, haze/smoke and combined (fog, mist, haze/smoke) duration are 227.5, 438.0, 829.4 and 1495.0 h respectively. The percentage duration of fog, mist, haze/smoke and combined are 7.9%, 15.2%, 28.8% and 51.9% respectively. It is therefore shows that the weather phenomena which reduce horizontal visibility to 3.0 km or less have percentage duration 51.9%. The number of foggy days increases from 1981 to 2007 may be due to increase in air pollution over the district. Table 31.1, b show the normal number of foggy days (NFD) and wheat yield. The value of NFD is 44 and when the number of foggy days are more than 44 then wheat yield increases from long period average (LPA) and decreases as the number of days are less then 44. In this study LPA is 27 years. Out of 27 seasons under study there are 11 seasons which have positive departures and 16 seasons which have negative departures from normal. Inter-annual variation of fog, mist, haze & smoke and combined (fog, mist, haze/smoke) duration from normal with polynomial trend fitted in the graphs are given in Figs. 31.3–31.6. The graphical analysis of low visibility phenomena events (fog, mist, smoke/haze) departures with wheat yield departures for Amritsar district are shown in Figs. 31.7–31.11. The maximum wheat yield during the season 1999–2000 is fairly matching with the departures of fog, mist and haze/smoke from normal. The increase in yield in the season 2000–2001 and 2006–2007 are in conformity with the increase in fog, mist and haze/smoke. Wheat yield is found to correlate positively with the durations of weather phenomena associated with low horizontal visibility. The correlation coefficients computed for F, M, H/S and combination of the three are found to be 0.53, 0.51, 0.29 respectively. When computed for the combined durations of F & M only, it comes out to be 0.65. This shows that the wheat yield is largely

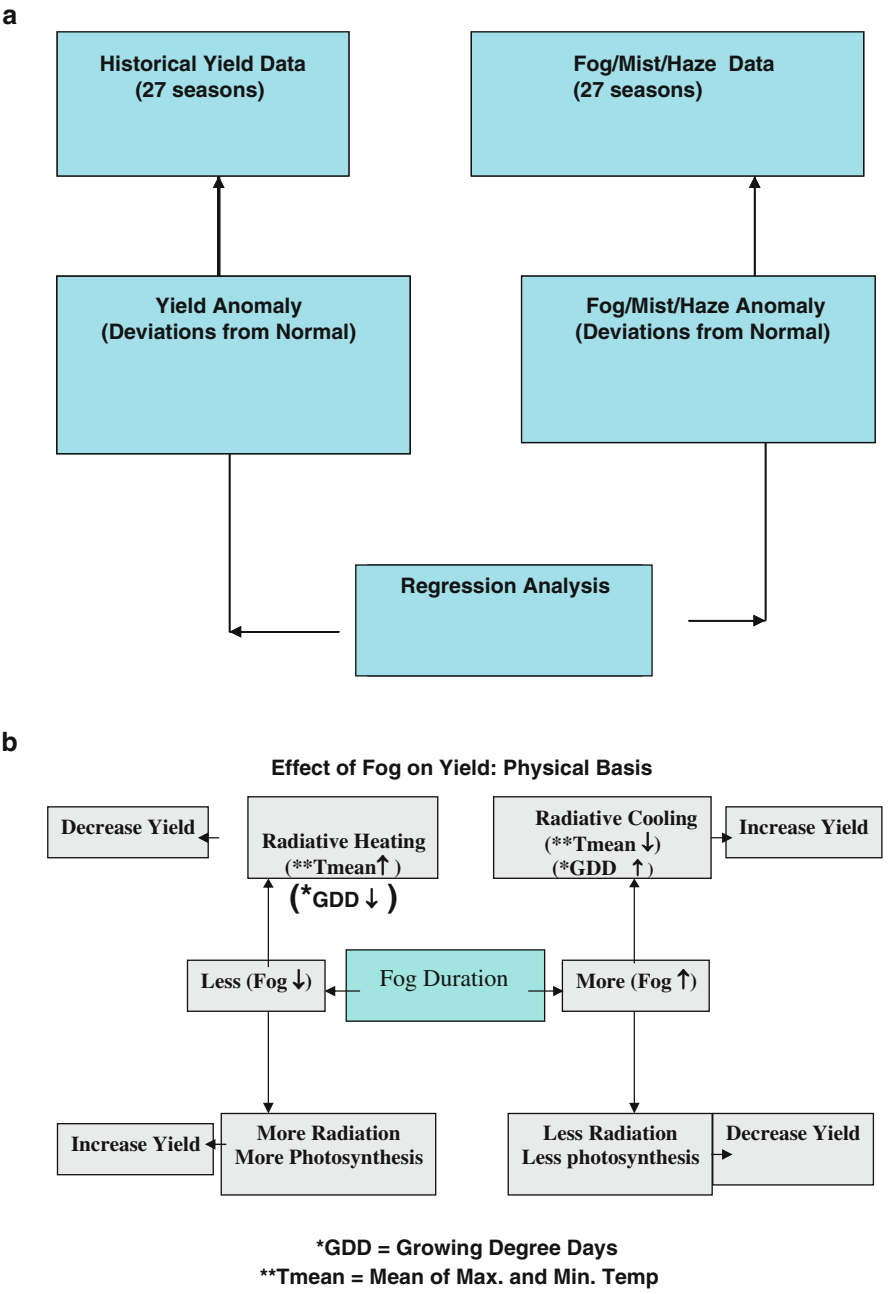


**Fig. 31.2** (**a**) Methodology of wheat yield and duration of low visibility phenomena. (**b**) Effect of fog on wheat yield (physical basis)

**Table 31.1** Wheat yield in Amritsar district and number of seasonal foggy days

| S. No. | Season | Wheat yield (kg/ha) | Percentage departure from LPA | No of foggy days | Percentage departure from NFD Normal |
|---|---|---|---|---|---|
| (a) Cases when number of foggy days are more then 44 | | | | | |
| 1 | 2006–2007 | 4,429 | +15.3 | 56 | +27 |
| 2 | 2004–2005 | 4,276 | +11.3 | 51 | +16 |
| 3 | 2003–2004 | 4,296 | +11.8 | 55 | +25 |
| 4 | 2002–2003 | 4,250 | +10.6 | 51 | +16 |
| 5 | 2000–2001 | 4,682 | +21.9 | 49 | +11 |
| 6 | 1999–2000 | 4,855 | +26.4 | 59 | +34 |
| 7 | 1998–1999 | 4,427 | +15.2 | 62 | +64 |
| 8 | 1997–1998 | 3,876 | +0.9 | 52 | +18 |
| 9 | 1996–1997 | 4,149 | +8.0 | 48 | +9 |
| 10 | 1995–1996 | 3,993 | +3.9 | 52 | +18 |
| 11 | 1992–1993 | 3,919 | +2.0 | 52 | +18 |
| (b) Cases when the number of foggy days are less then 44 | | | | | |
| 1 | 1981–1982 | 2,612 | −32.0 | 37 | −16 |
| 2 | 1982–1983 | 2,971 | −22.7 | 29 | −34 |
| 3 | 1983–1984 | 3,076 | −19.9 | 29 | −34 |
| 4 | 1984–1985 | 3,471 | −9.6 | 12 | −73 |
| 5 | 1985–1986 | 3,445 | −10.3 | 40 | −9 |
| 6 | 1987–1988 | 3,614 | −5.9 | 40 | −9 |
| 7 | 1990–1991 | 3,717 | −3.2 | 37 | −16 |

NFD = Number of foggy days

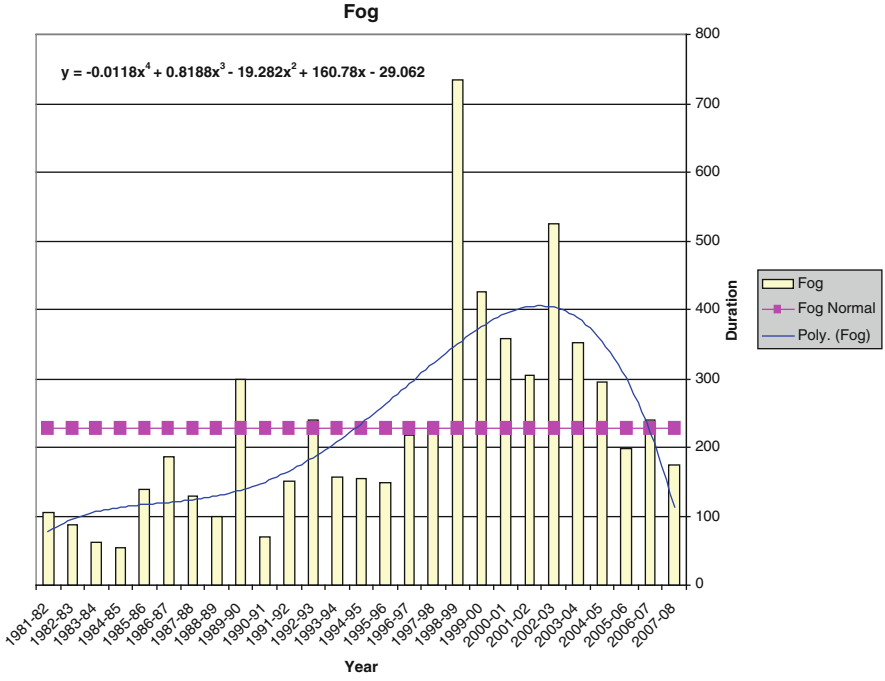


**Fig. 31.3** Inter-annual variation of fog over Amritsar, Punjab, India

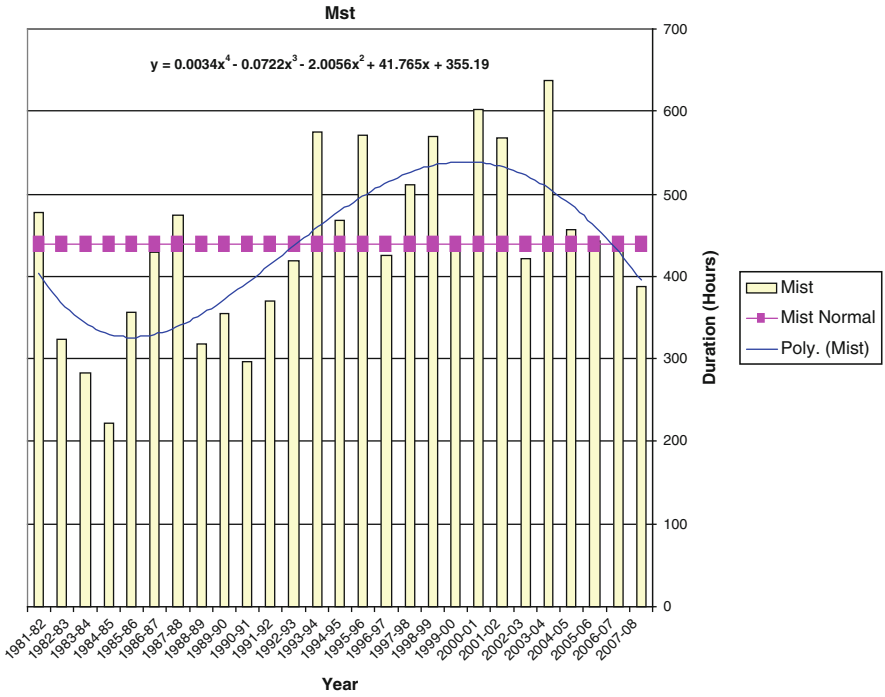


**Fig. 31.4** Inter-annual variation of mist over Amritsar, Punjab, India

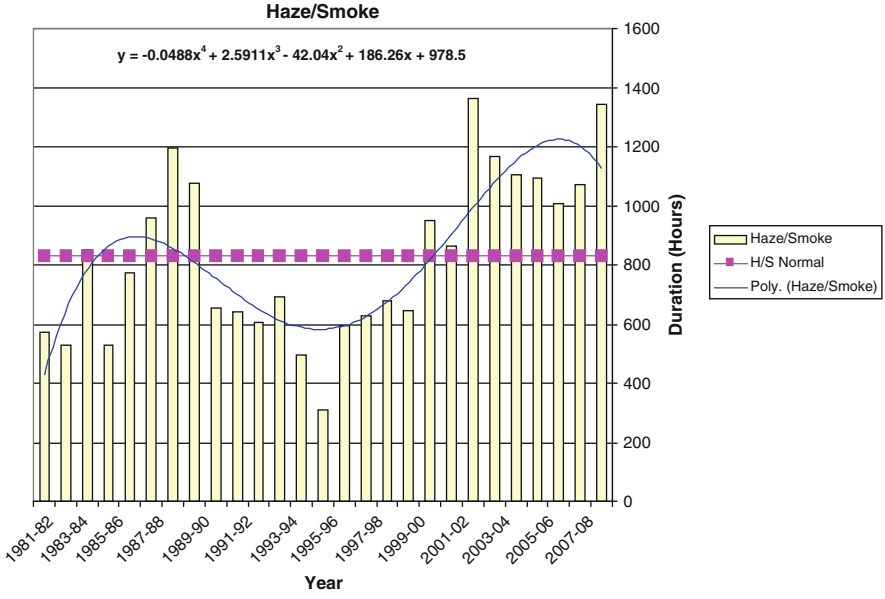


**Fig. 31.5** Inter-annual variation of haze/smoke over Amritsar, Punjab, India

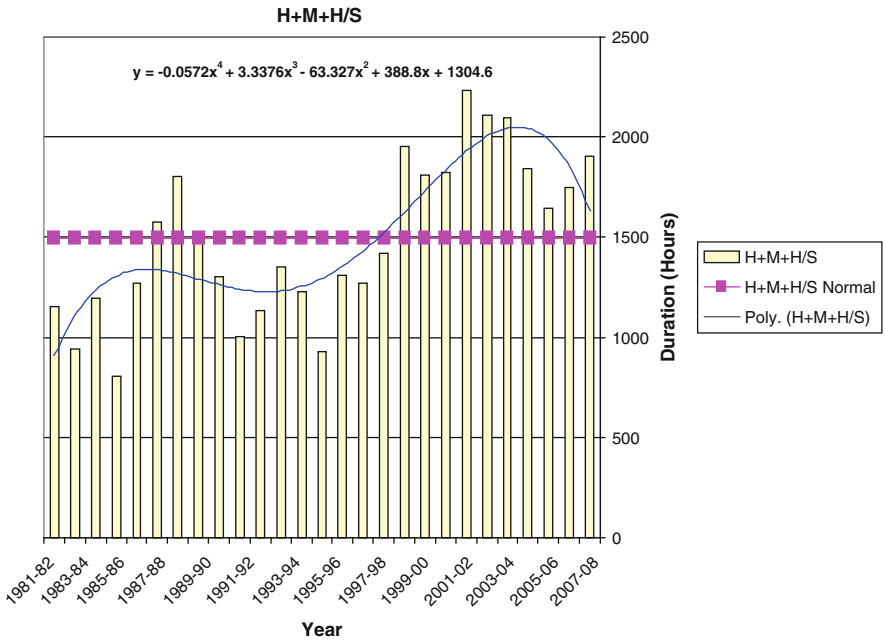


**Fig. 31.6** Inter-annual variation of haze + mist + haze/smoke over Amritsar, Punjab, India

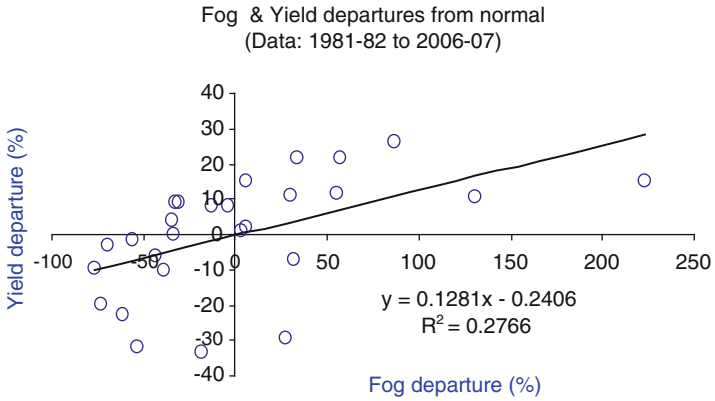


**Fig. 31.7** Fog and wheat yield departure from normal for Amritsar, Punjab, India

affected by the composite effect of F & M. This could be explained with the physical linkage between the wheat yield and low visibility phenomena occurring during cold season. The obstruction of solar radiation by long durarion F & M in reaching the ground causes lowering of temperature beneath the phenomena and thus the cooling of the areas having the wheat crop results into its long life and thereby increasing the yield. The inter-annual wheat yield departures with the duration anomalies of low

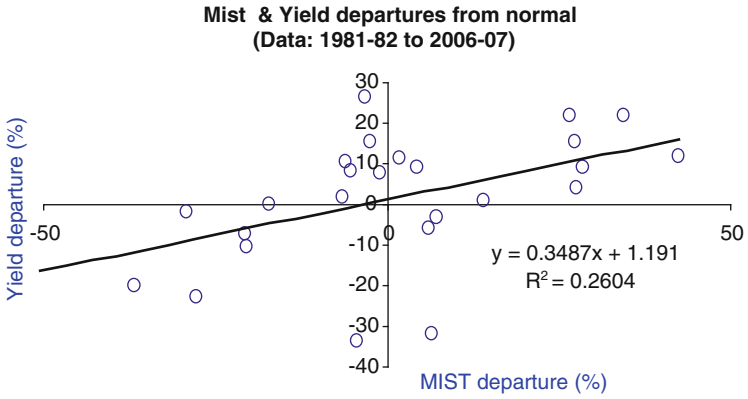


**Fig. 31.8** Mist and wheat yield departure from normal for Amritsar, Punjab, India

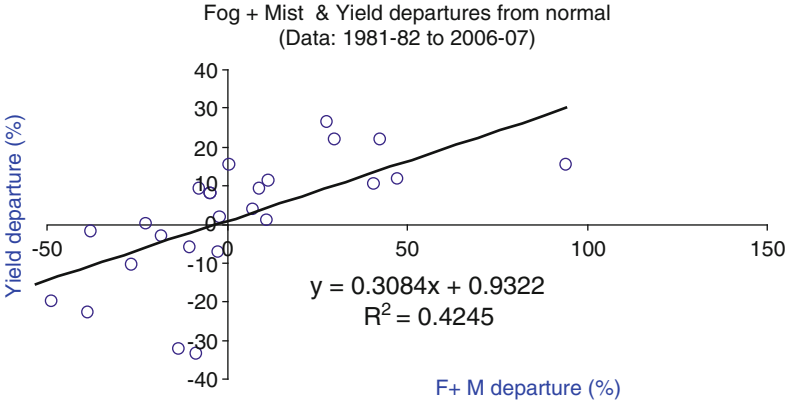


**Fig. 31.9** Fog + mist and wheat yield departure from normal for Amritsar, Punjab, India

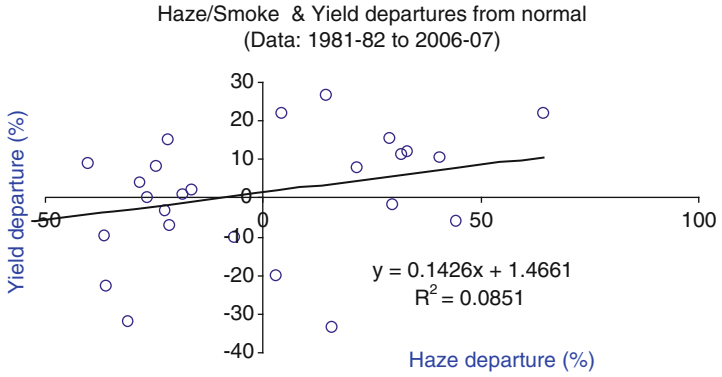


**Fig. 31.10** Haze/smoke and wheat yield departure from normal for Amritsar, Punjab, India

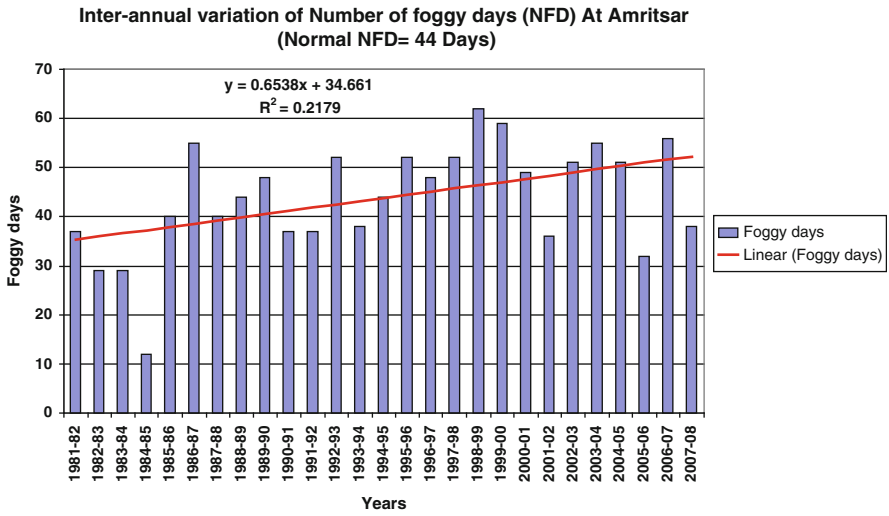


**Fig. 31.11** Inter-annual variation of number of foggy days for Amritsar, Punjab, India

**Table 31.2** Relation of inter-annual wheat yield departures with the duration anomalies of fog, mist, haze/smoke and their combination

| S. No. | Season | Percentage departure of wheat yield from LPA | Percentage departure of fog from normal | Percentage departure of mist from normal | Percentage departure of (haze/ smoke) from normal | Percentage departure of (Fog + Mist + Haze/Smoke) from normal |
|---|---|---|---|---|---|---|
| (a) | | | | | | |
| 1 | 2006–2007 | +15.3 | +5.5 | −0.2 | +28.9 | +16.8 |
| 2 | 2005–2006 | +7.9 | −12.8 | +1.1 | +21.5 | +10.3 |
| 3 | 2004–2005 | +11.3 | +30.1 | +4.0 | +31.8 | +23.4 |
| 4 | 2003–2004 | +11.8 | +55.1 | +45.5 | +33.1 | +40.1 |
| 5 | 2002–2003 | +10.6 | +130.5 | −3.9 | +40.5 | +41.2 |
| 6 | 2001–2002 | +21.9 | +34.0 | +29.6 | +64.3 | +49.5 |
| 7 | 2000–2001 | +21.9 | +57.1 | +37.4 | +4.2 | +22.0 |
| 8 | 1999–2000 | +26.4 | +87.0 | −1.0 | +14.4 | +20.9 |
| 9 | 1998–1999 | +15.2 | +223.2 | +30.1 | −22.0 | +30.6 |
| 10 | 1997–1998 | +0.9 | +3.3 | +16.7 | −18.3 | −4.8 |
| 11 | 1992–1993 | +2.0 | +5.7 | −4.5 | −16.6 | −9.6 |
| (b) | | | | | | |
| 1 | 1981–1982 | −32.0 | −53.6 | +9.0 | −31.0 | −22.7 |
| 2 | 1982–1983 | −22.7 | −61.3 | −26.1 | −36.0 | −37.0 |
| 3 | 1983–1984 | −19.9 | −73.0 | −35.4 | +2.9 | −19.9 |
| 4 | 1984–1985 | −9.6 | −76.7 | −49.3 | −36.3 | −46.3 |
| 5 | 1985–1986 | −10.3 | −39.1 | −18.7 | −6.7 | −15.2 |
| 6 | 1986–1987 | −33.6 | −18.0 | −2.3 | +15.8 | +5.4 |
| 7 | 1987–1988 | −5.9 | −43.7 | +8.3 | +44.4 | +22.4 |
| 8 | 1988–1989 | −1.8 | −56.1 | −27.6 | +29.7 | −0.1 |
| 9 | 1989–1990 | −7.3 | +31.8 | −18.8 | −21.3 | −12.5 |
| 10 | 1990–1991 | −3.2 | −69.5 | −32.5 | −22.6 | −32.6 |

**Table 31.3** Variation of potato yield and fog activity in Amritsar district, Punjab, India

| S. No. | Season | Potato yield (kg/ha) | Percentage departure of potato yield from LPA | Fog duration (Hours) | Percentage departure of fog duration from LPA |
|---|---|---|---|---|---|
| 1 | 2003–2004 | 22,872 | +16.6 | 353.0 | +41.9 |
| 2 | 2002–2003 | 18,534 | −05.5 | 524.5 | +110.8 |
| 3 | 2001–2002 | 17,070 | −12.9 | 305.0 | +22.6 |
| 4 | 2000–2001 | 18,278 | −06.8 | 357.5 | +43.7 |
| 5 | 1999–2000 | 19,500 | −00.6 | 425.5 | +71.0 |
| 6 | 1998–1999 | 17,809 | −09.2 | 735.5 | +195.6 |

visibility phenomena are given in Table 31.2. The increase of wheat yield is with closely related to the positive departures of low visibility phenomena. Table 31.3 shows for potato yield with the duration of fog and it is negatively related with the duration of fog. It shows that the cooling which is normally produced by the obstruction of insolation is not favorable for potato production.

## 31.4 Conclusions

The conclusions of the above study is given below:

1. Seasonal fog duration increased from approx. 100 h in early eighties to approx. 400 h in 2000–2004 with reduction as much as 200 h in present winter seasons.
2. There is a decreasing tendency in case of fog and mist durations in the past few years (5 years) in contrast to haze and smoke in corresponding years.
3. It was observed that increase in Fog and Mist durations resulted in increase in yield of wheat crop. This was due to reduction in the surface temperature caused by radiative cooling due to obstruction in solar radiation which was found conducive to vegetative growth of wheat.
4. Variability in the Haze and Smoke was found relatively less correlated with wheat yield as compared to Combined Fog and Mist Conditions.
5. Number of foggy days increased slowly from 1981–2007 probably due to increase in air pollution and seasonal departures of wheat yield from LPA are in conformity with the departures of number of foggy days.
6. The Maximum Wheat Yield during the season 1999–2000 is fairly matching with the departures of Fog, Mist and Haze/Smoke from normal. The increase in Yield in the season 2000–2001 and 2006–2007 are in conformity with the increase in Fog, Mist and Haze/smoke.
7. Duration of Fog, Mist and Haze/Smoke at Amritsar during the season is nearly 52% this shows that the low visibility phenomena which reduce the visibility to 3 km or less play better role in cooling the atmosphere near the ground and helping crop productivity to grow.

The correlation coefficients computed for wheat yield and low visibility phenomena like, fog (F), mist (M), haze/smoke (H/S) and combination of the three are found to be 0.53, 0.51, 0.29 respectively.

## References

Sarkar A, Sucharitta S, Animesh K (2009) Rice–wheat cropping cycle in Punjab: a comparative analysis of sustainability status in different irrigation systems. Environ Dev Sustain 11(4) 751–763

Yadav SK, Singh DP, Singh PS, Kumar A (1987) Diurnal pattern of photosynthesis, evapotranspiration and water use efficiency of barley under field conditions. Indian J Plant Physiol 30:233–238

# Chapter 32
# Impact of Drought and Flood on Indian Food Grain Production

**Ajay Singh, Vinayak S. Phadke, and Anand Patwardhan**

**Abstract** Agriculture provides livelihood to almost three fourth of population of India. Indian agriculture is highly dependent on spatial and temporal distribution of rainfall. Climate extremes such as drought and flood affect agriculture severely. An account of impact of climate extremes viz. drought and flood, on Indian food grain production has been presented in this paper. There are temporal fluctuations in food grain production and area under the food grain. In secular terms, both of them increased up to mid-eighties. After mid-eighties there is decline in the area of food grain while maintaining an increase in production of food grain suggesting the improvement in agricultural technology and policy. There is more temporal fluctuation in the production of food grain than the area under food grain. The analysis reveals that impact of drought on Indian agriculture is more than that of flood. Rabi food grain production depicts better adaptability to drought than Kharif food grain production mostly due to better access to irrigation infrastructure. Among the various food crops analysed all except jowar can effectively face flood events. Wheat and jowar perform relatively better during drought events. Rice is most sensitive crop to the extreme climate events. Since rice is staple food in the subcontinent, management of rice productions against climate extremes needs special attention for food security and sustainability.

A. Singh (✉) • A. Patwardhan
Shailesh J. Mehta School of Management, Indian Institute of Technology Bombay, Powai, Mumbai 400076, MH, India
e-mail: ajayvisen@yahoo.co.in; anand@iitb.ac.in

V.S. Phadke
2/17 Dnyanayog Society, Vazira Naka, Lokmanya Tilak Road, Borivli (W), Mumbai 400091, MH, India
e-mail: vinayakphadke@hotmail.com

S.D. Attri et al. (eds.), *Challenges and Opportunities in Agrometeorology*,
DOI 10.1007/978-3-642-19360-6_32, 

## 32.1 Introduction

In developing countries, agriculture is the primary contributor to the nation's economy. Agriculture and allied activities are the single largest constituent of Indian economy, contributing almost 17% of the total Gross Domestic Product (GDP) in the year 2008–2009 (CIA 2009). Agriculture exports accounts for 13–18% of total annual exports of the country (Ministry of Finance 2002). However, given that 62% of the cropped area is still dependent on rainfall (MoEF 2002), Indian agriculture continues to be fundamentally dependent on weather. The Indian summer monsoon circulation influences more than 60% of world's population (Webster et al. 1998) due to its large-scale impact on agriculture, water resources, power generation and overall economy (Mooley et al. 1981; Mooley and Parthasarathy 1983; Parthasarathy et al. 1988). There is strong relationship between agricultural performance and climate; subsequently there will be significant loss in net revenue due to global warming (Kavi Kumar and Parikh 2001). Crop production in India is significantly influenced by monsoon and some of its potential predictors (Krishna Kumar et al. 2004).

About 80% of the total rainfall over the Indian sub-continent occurs during only 4 months (June–September), as a result of the southwest monsoon which is vital to India's agriculture (Parthasarathy et al. 1992). While drought is a recurring problem in some areas of India, floods cause a severe damage to livelihood and agriculture in other areas; one third of the average flood prone area in the country constitutes agricultural land (IPCC 1995). The contribution of agriculture to the Gross Domestic Product (GDP) has decreased substantially since independence and led to the expectation that the impact of the monsoon on the economy would have also decreased. However, a study of the variation of the GDP and the monsoon has revealed that the impact of severe droughts on GDP has remained between 2% and 5% of GDP throughout (Gadgil and Gadgil 2006).

The paper is organised as follows. Next section deals with data and analysis carried out in the study. Subsequent section describes the results and discussion, finally conclusions has been drawn.

## 32.2 Data and Analysis

The major cropping seasons in India are Kharif and Rabi. The Kharif season crops (rice, sorghum, maize, pigeonpea and blackgram) are grown during the summer monsoon (June–September) period and harvested in the autumn or early winter months. The Kharif crop production is >50% of the total annual food grain production and constitutes the principal source of food supply. The Rabi cropping (wheat and chickpea) season starts after the summer monsoon and continues up to the spring or early summer months. The rainfall, which occurs towards the end of the summer monsoon, provides soil moisture for the Rabi crop, which is sown in the

post-monsoon season. Therefore, the summer monsoon is mainly responsible for both Kharif and Rabi food grain production in India (Parthasarathy et al. 1988). A small region in the extreme of peninsular India also benefits from the northeast monsoon (October–December) rainfall for Rabi food grain production.

The annual production of total food grains and area under it over the country for the agricultural years (1 June–31 May) has been downloaded from www.indiastat.com. The total food grains consist of (a) cereals (rice, wheat, jowar, bajra, maize and barley) and (b) pulses (chickpea, pigeonpea, greengram and blackgram). The cereals form the core staple food, and pulses are the protein supplement for the large vegetarian population. All India Summer Monsoon Rainfall (AISMR) series has been downloaded from Indian Institute of Tropical Meteorology, Pune web page (http://www.tropmet.res.in). This rainfall data have been used to derive the extreme years of monsoon rainfall, i.e., drought and flood. The year is considered a drought year if the rainfall is less than the mean of AISMR minus standard deviation of it. Flood year is the one when rainfall is greater than the mean plus one standard deviation of AISMR. Normal years fall in the range of mean plus and minus one standard deviation of AISMR. Regression analysis of the production and area figures has been performed to get trend in the variable. Moving average of these variables has been calculated to have long term fluctuations.

To get an idea about the fluctuation in production in respect to maximum production a characteristic of production data has been hypothesised as production loss. Production loss has been calculated from the following methodology:

1. National level production time series has been considered. The production of all the food grain crops is taken together for 54 years from 1950 to 2003.
2. For each year Y, the maximum production value Pm in the 7-year interval from Y-3 to Y + 3 is to be noted.
3. The difference between the production P of year Y and Pm is computed and expressed as a percentage "loss"; i.e., (Pm-P)/Pm $\times$ 100%.

The approach assumes that no marked technological progress took place during the 7 year period. Similar analysis is carried out for change in planted area. Correlation coefficients between production data and rainfall have been calculated to know the extent of association between them.

## 32.3 Results and Discussion

### *32.3.1 Trends in Food Grain Production and Planted Area*

There has been rise in food grain production from about 50 million tonnes in 1950 to about 175 million tonnes in 2003. This is primarily due to increase in area under food grain production and improvement in agricultural technology and policy.

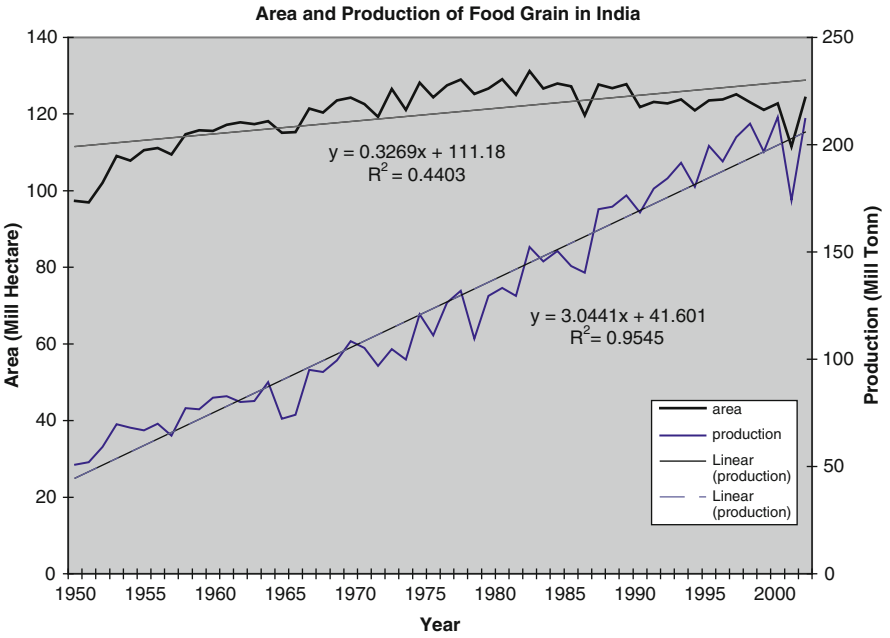


**Fig. 32.1** Area and production of food grain in India

There is sharp fall in some years followed by rise (Fig. 32.1). These sharp falls in the production are accounted for by bad monsoon.

The regression line shows a marked increasing trend in the production of food grains (Fig. 32.1). All the production points however are not on trend line and this is easily explicable. Generally, between 1950 and 1965 one finds positive residuals followed by negative residuals till late 1980s and then again positive residual till 2002. The year 2003 shows negative residual. The negative residuals in middle period are despite rise in production compared to the first period suggesting the failure of this period to raise the production at the expected rate. This is in spite of the fact that planted area has increased over this time and there was a tremendous improvement in agricultural technology, this period saw the success of green revolution. This is due to the fact that in the beginning green revolution was attempted only in pockets, which had an advantage in terms of fertile soils and assured availability of water. This process later got extended to other areas, as green revolution was slowly defused from the earlier cores to the other areas. There is overall increase in area under food grain production from 1950 to 2003 (Fig. 32.1). There has been a peak in early 1980s since then there is decline in the area under food grain crop. Some years have experienced sharp falls in the area, which is accounted for bad monsoon conditions.

After early 1980s, there is fall in the area under food grain production. This is due to many factors including encroachment of agricultural area by the cities,

switching over to crops other than food grains; there is also a shift from extensive to intensive farming. The linear trend line shows a slight increase in the area under food grain production (Fig. 32.1). Between 1950 and 1960, there are negative residuals followed by positive residuals till late 1980s and then again negative residuals till 2003. The observed increase in planted area is due to green revolution between 1960s and late 1980s.

### *32.3.2 Decline in Food Grain Production and Planted Area*

It is evident that percent loss of food grain production varies from 0 to about 25% (Fig. 32.2). Loss in area under food grains varies from 0 to about 7% (Fig. 32.2). This shows that production undergoes larger fluctuation than that in area. This is primarily due to the fact that the former is an ex post phenomenon while the latter is ex ante. The farmer is not in a position to take a decision to reduce the area under cultivation and production is left to subsequent behaviour of monsoon rain, other factors remaining the same. It is not only the reduction in area that affects production but also lowering of productivity due to failure of monsoon rain.

A comparison of the loss in area and production shows that there is a general coincidence between losses in the two (Fig. 32.2). However, it is not perfect as indicated by the value of r (Table 32.1). One finds that area comes to normal earlier compared to production. In fact, there are years when the loss in area decreases but

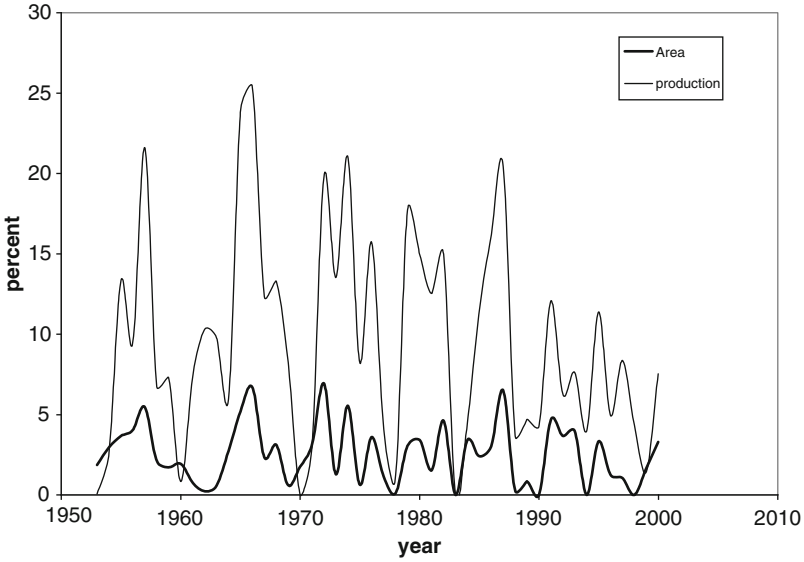


**Fig. 32.2** Percent loss of the area and production of food grain crop in India

**Table 32.1** Correlation matrix for production, area and AISMR variables

| | Loss in area (%) | Area residuals | Loss in production (%) | Production residuals | AISMR (cm) | Departure in AISMR |
|---|---|---|---|---|---|---|
| Loss in area (%) | 1.00 | | | | | |
| Area residuals | −0.54 | 1.00 | | | | |
| Loss in production (%) | 0.73 | −0.23 | 1.00 | | | |
| Production residuals | −0.58 | −0.16 | −0.82 | 1.00 | | |
| AISMR (cm) | −0.68 | 0.21 | −0.71 | 0.74 | 1.00 | |
| Departure in AISMR | −0.70 | 0.22 | −0.72 | 0.75 | 0.99 | 1.00 |

loss in production increases (e.g. 1962), although this could be attributable to the factors cited above.

The percent loss in food grain production in India is negatively related with AISMR, this is confirmed quantitatively by value of $r = -0.71$ (Table 32.1). This is quite explicable as failure of rains is related to failure in production. Therefore, the higher values of AISMR go with the lower values for percent loss in food grain production and vice versa.

The percentage loss in planted area under food grains is also negatively related with AISMR and is confirmed quantitatively by $r = -0.68$ (Table 32.1). This is quite explicable as failure of rains is related to failure of the farmer in planting the intended area. The same trend is indicated when production and area losses are regressed against departure of AISMR from the average for the period 1961–90 and one finds slight improvement in the values of r (Table 32.1). This suggests that area and production are more related to departure in rainfall rather than rainfall amount by itself.

### *32.3.3 Impact at National Scale*

In India, drought is very significant extreme climate event and persistent climatic problem. In the last decade, losses from drought events significantly increased. In recent years, increased losses from droughts suggest growing societal vulnerability to drought.

India is the most flood affected country in the world after Bangladesh. India accounted for one-fifth of the global death count due to floods from the 1960s to the 1980s (CSE 1991); over 30 million people were displaced annually. The flood affected area rose from an average of 6.4 million hectares a year in the 1950s to nine million hectares a year in the 1980s. The annual flood affected population has risen from 16 million in the 1950s to 53 million in the 1980s. Annual flood damages increased nearly 40 times from an average of Rs.60 crore a year during the 1950s to Rs. 2,307 crore a year during the 1980s. Some of this increase is definitely the result of inflation and increasing population, encroachment of the flood plains and investment in agriculture as well as other activities in the flood plains.

**Table 32.2** Drought, flood and normal years in India

| Drought year | Flood year | Normal year |
|---|---|---|
| 1951 | 1956 | 1950 |
| 1965 | 1959 | 1952 |
| 1966 | 1961 | 1953 |
| 1968 | 1970 | 1954 |
| 1972 | 1975 | 1955 |
| 1974 | 1983 | 1957 |
| 1979 | 1988 | 1958 |
| 1982 | 1994 | 1960 |
| 1985 | | 1962 |
| 1986 | | 1963 |
| 1987 | | 1964 |
| | | 1967 |
| | | 1969 |
| | | 1971 |
| | | 1973 |
| | | 1976 |
| | | 1977 |
| | | 1978 |
| | | 1980 |
| | | 1981 |
| | | 1984 |
| | | 1989 |
| | | 1990 |
| | | 1991 |
| | | 1992 |
| | | 1993 |
| | | 1995 |
| | | 1996 |
| | | 1997 |

Using AISMR data from 1950 to 1997, the flood, normal and drought years were identified (Table 32.2). These flood and drought years exactly match with the surplus and deficient monsoon years characterised in a study by Raju et al. (2002) which is based on all India summer monsoon seasonal rainfall (Parthasarathy et al. 1994). Among the 48 years, flood and drought years number 8 and 11 respectively. Rest of the years are normal years. Positive relationship between AISMR anomalies and Indian food grain production anomalies ($r = 0.3$) was significant at 10% level. During drought year, total food grain production decreased from that of the previous year up to 24% in 9 out of 11 events. During flood year, only 2 out of 8 events have reported decrease in total food grain production in India. The remaining 6 flood years have witnessed increase in the food grain production. Maximum gain in the production (18%) has occurred in a flood year of 1975, which is preceded by a drought year of 1974. This is obvious because while drought affects all the regions, from those getting high rainfall amounts to those getting

scanty amount, adversely, the floods adversely affect only the regions with high rainfall amount; the regions with scanty rains are benefited during the flood years.

From the above analysis it can be concluded that during drought year, total food grain production decreases and during flood year, the production increases, when compared to that of the previous year. This suggests that during flood events, food grain crops show more adaptive capacity than during drought events. Maximum increment in food grain production has occurred in the situation when a flood year is preceded by a drought year. This is partly due to drop in the preceding drought year; thus drop in total food grain production in the drought year enhances the increment in the total food grain production in flood year.

The extreme events have differential impacts on food grain production during the different cropping seasons, viz., Kharif and Rabi. Positive correlation coefficient ($r = 0.40$) has been found between Kharif food grain production anomaly and AISMR anomaly, which is significant at 5% level. During flood year Kharif food grain production has increased from the previous year, on an average by about 18%. All flood events have noticed increment in Kharif food grain production over that of the previous year (Table 32.3). During flood events maximum increase in Kharif food grain production (28%) has been found in the year 1988 which is preceded by a drought year of 1987. During the drought years, on the other hand, Kharif food grain production has increased only in one event (1985) out of nine; the remaining eight events have recorded decrease in production from that of the previous year. During drought events, on an average, Kharif food grain production decreases from that of previous year by about 8%. During drought events, maximum decline of 19% in the Kharif food grain production has been found in the year 1979. Thus, it is evident that Kharif food grain production during flood year has better adaptive capacity than during drought year.

**Table 32.3** Impact of flood and drought events on Kharif and Rabi production of food grains

| S. No. | Flood year | Drought year | Trend in Kharif production (%) | Trend in Rabi production (%) |
|---|---|---|---|---|
| 1 | 1970 | | 10.54 | 6.33 |
| 2 | 1975 | | 25.03 | 15.74 |
| 3 | 1983 | | 27.65 | 5.90 |
| 4 | 1988 | | 28.27 | 12.90 |
| 5 | 1994 | | 0.67 | 7.83 |
| 6 | | 1966 | NA | NA |
| 7 | | 1968 | −1.96 | 0.44 |
| 8 | | 1972 | −6.91 | −8.99 |
| 9 | | 1974 | −12.88 | 10.59 |
| 10 | | 1979 | −18.99 | −13.69 |
| 11 | | 1982 | −11.94 | 10.57 |
| 12 | | 1985 | 0.86 | 6.83 |
| 13 | | 1986 | −5.92 | −3.02 |
| 14 | | 1987 | −7.03 | 4.07 |

A positive correlation (r = 0.21) between Rabi food grain production anomaly and AISMR anomaly is not statistically significant. All flood events have noticed the increment in Rabi food grain production from that of the previous year and this averages to about 9%. Maximum increment in Rabi food grain production during a flood event has occurred in the year 1975 (about 15%). Impact of drought events on the Rabi food grain production is mixed. Three out of eight drought events have shown decrease in Rabi food grain production from that of the previous year while the remaining five drought events have depicted an increase. The increment in Rabi food grain production during five drought events mentioned above averages to about 7%. Maximum increment in Rabi food grain production during these events has occurred in the year 1974 (about 10%). The decline in Rabi food grain production during three drought events mentioned above averages to about 9%. Maximum decrease in Rabi food grain production during these events has occurred in the year 1979 (about 13%).

Thus, it is evident that Rabi food grain production has better adaptive capacity to drought than Kharif food grain production. It reflects on the fact that Rabi food grain crops have a better access to irrigation facility than Kharif crops which are more dependent on monsoon rainfall. Moreover, it is noteworthy that Rabi crops are grown keeping in mind lower availability of water and are less water intensive. Further, the drought during the Kharif season is 'unanticipated' while that during Rabi season is 'known' and farmer is, therefore, more careful in the choice of crops.

The impact of climatic extremes on individual food grain crops has been studied because of the variable adaptive capacity of these crops to the extremes. Impact on major food crops such as rice, wheat, bajra, barley, jowar, maize and pulses have been analysed. A summary has been provided for the impact of climate extremes on the production of different crops (Tables 32.4 and 32.5).

During all the eight flood events, the rice production has increased from that of the previous year by an average of about 11%. Maximum increment of about 27% has been noticed in the year 1983, which is preceded by a drought year in the record. During drought years, 8 events out of 11 have experienced a decrease in rice production from that of the previous year by about 6% on an average; the remaining three are characterised by a marginal increment. Maximum decrease in rice production (22%) from previous year has occurred during year 1965. This is the year showing second maximum negative anomaly in AISMR.

**Table 32.4** Proportion of extreme event years showing impact on production of different crops

| | Flood events | | Drought events | |
|---|---|---|---|---|
| Crop | Increase (%) | Decrease (%) | Increase (%) | Decrease (%) |
| Rice | 100.00 | 0.00 | 27.28 | 72.72 |
| Wheat | 100.00 | 0.00 | 54.54 | 45.56 |
| Bajra | 75.00 | 25.00 | 18.18 | 81.82 |
| Barley | 87.50 | 12.50 | 18.18 | 81.82 |
| Jowar | 25.00 | 75.00 | 54.55 | 45.45 |
| Maize | 87.50 | 12.50 | 45.45 | 54.55 |
| All pulses | 75.00 | 25.00 | 36.36 | 63.64 |

**Table 32.5** Impact of climatic extremes on production of different crops

| | | | Trend in production of crops (%) | | | | | | |
|---|---|---|---|---|---|---|---|---|---|
| S. No. | Flood year | Drought year | Rice | Wheat | Bajra | Barley | Jowar | Maize | All Pulses |
| 1 | 1956 | | 5.4 | 7.3 | −16.3 | 1.7 | 8.9 | 18.5 | 4.6 |
| 2 | 1959 | | 2.7 | 3.6 | −9.8 | 0.9 | −5.0 | 17.6 | −10.3 |
| 3 | 1961 | | 3.1 | 9.7 | 11.3 | 11.7 | −18.1 | 5.6 | −7.4 |
| 4 | 1970 | | 4.4 | 18.6 | 50.7 | 2.5 | −16.6 | 32.1 | 1.1 |
| 5 | 1975 | | 23.1 | 19.7 | 75.5 | 1.8 | −8.7 | 30.6 | 30.1 |
| 6 | 1983 | | 27.5 | 6.3 | 50.5 | −1.8 | 10.9 | 20.9 | 8.7 |
| 7 | 1988 | | 24.0 | 17.2 | 135.8 | 8.1 | −16.6 | 43.9 | 26.4 |
| 8 | 1994 | | 1.9 | 9.9 | 44.1 | 31.5 | −21.4 | −7.5 | 5.5 |
| 9 | | 1951 | 3.5 | −4.3 | −9.6 | −0.5 | 10.5 | 20.2 | 0.1 |
| 10 | | 1965 | −22.2 | −15.2 | −17.0 | −5.5 | −21.7 | 3.4 | −20.0 |
| 11 | | 1966 | −0.5 | 9.5 | 19.2 | −1.4 | 21.6 | 1.5 | −16.0 |
| 12 | | 1968 | 5.7 | 12.8 | −26.8 | −30.8 | −2.5 | −9.1 | −13.9 |
| 13 | | 1972 | −8.9 | −6.3 | −26.1 | −7.7 | −9.7 | 25.3 | −10.6 |
| 14 | | 1974 | −10.1 | 10.7 | −56.5 | 32.2 | 14.4 | −4.1 | 0.1 |
| 15 | | 1979 | −21.3 | −10.4 | −29.1 | −24.2 | 1.8 | −9.7 | −29.6 |
| 16 | | 1982 | −11.5 | 14.3 | −7.4 | −6.3 | −10.9 | −5.1 | 3.0 |
| 17 | | 1985 | 9.4 | 6.8 | −39.5 | 26.1 | −10.5 | −21.3 | 11.7 |
| 18 | | 1986 | −5.1 | −5.8 | 23.2 | −14.9 | −9.9 | 14.3 | −12.4 |
| 19 | | 1987 | −6.1 | 4.2 | −26.8 | −4.6 | 32.8 | −24.6 | −6.4 |

All the eight flood events have recorded an increment in wheat production from that of the previous year by an average of about 11%. Maximum increment of about 20% is noticed in year 1975, which is preceded by a drought year of 1974. The loss in wheat production in preceding drought year has enhanced the gain in production in following flood year. During drought events, wheat production has shown a mixed scenario. Out of 11 drought events, five have recorded a decrease in wheat production while six are characterised by an increase. Over all, one observes an average of about 1% increase in the wheat production from that of the previous year during drought events. The increment in wheat production during six drought events mentioned above averages to about 10%. Maximum increment in wheat production during these events has occurred in the year 1982 (about 14%). This is explained in terms of maturation effects where extension of green revolution has played a significant role. The decline in wheat production during five drought events mentioned above averages to about 8%. Maximum decrease in wheat production during these events has occurred in the year 1965 (about 15%). This is again the result of second maximum anomaly in AISMR. Moreover, in mid-1960s, the crop was not as much protected against drought by providing irrigation coverage as in later years.

Production of bajra has increased during six flood events and decreased during two such events. The dominant trend is thus towards an increase. On an average bajra production has increased by about 43% from that of the previous year and maximum increment is found to be about 135% in year 1988. As indicated earlier, this year is preceded by a drought year of 1987. Maximum decrease in bajra

production during flood year, on the other hand, is only 16% reported in the year 1956. Drought events have revealed a decrease in bajra production in nine cases while an increase in only two cases. The impact of drought on bajra production is thus negative with an average decrease in production of 18%. The decline in bajra production during nine drought events mentioned above, averages to about 27%. Maximum decrease in bajra production during these events has occurred in the year 1974 (about 56%). The increment in bajra production during two drought events mentioned above, averages to about 21%. Maximum increment in bajra production during these events has occurred in the year 1986 (about 23%). This can only be explained in terms of the prevailing drought and the farmer has gone in for a drought resistant crop of bajra.

In the case of barley, during seven out of eight flood events the production has shown an increase; only in one event one observes a decrease in the production. The impact is thus positive leading to an average increase in production of about 7%. A maximum increase of about 32% has occurred in the year 1994. During drought events, on the other hand, only 2 out of 11 events have recorded an increase in barley production; nine drought events have revealed a decrease in barley production. The dominant trend is thus for a decrease with an average decrease of 3%. The decline in barley production during nine drought events mentioned above, averages to about 11%. Maximum decrease in barley production during these events has occurred in the year 1968 (about 31%). The increment in barley production during two drought events mentioned above, averages to about 29%. Maximum increment in barley production during these events has occurred in the year 1974 (about 32%). This can only be explained in terms of the prevailing drought and the farmer has gone in for a drought resistant crop of barley.

During flood events, in six out of eight cases one notices a decrease in jowar production; remaining two flood events have experienced an increase. The dominant trend is thus towards a decrease. The decline in jowar production, during six flood events mentioned above, averages to about 14%. Maximum decrease in jowar production during these events has occurred in the year 1994 (about 21%). The increment in jowar production during two flood events mentioned above, averages to about 10%. Maximum increment during these events has occurred in the year 1983 (about 11%); this is probably because 1982 was a drought year. Jowar thus responds negatively to flood events and this is easily explicable considering that its water requirements are limited. Jowar production has shown a mixed response to drought events. Six out of 11 drought events are characterised by a decrease in jowar production; remaining five drought events, on the other hand, have shown an increase. On an average only about 1% increase has been noticed in jowar production during drought events. Maximum decrease in production of 22%, from that of the previous year, has been observed in year 1965. The average increase, on the other hand, is 16%, although maximum increase of 33% has occurred in the year 1987. This shows that jowar is not completely immune to drought, but its performance is not as bad as that during the flood years.

During flood events, only one out of eight cases is characterised by a decrease in maize production compared to that of the previous year; remaining seven events

have experienced an increase. An average of 20% increase in maize production has been observed during flood events. Maximum increase of about 44% has occurred in year 1988. Flood years seem to favour maize as it is a water loving crop. During drought events, maize production reveals a mixed scenario. Six out of 11 drought events have noticed a decrease in maize production, from that of the previous year; remaining five events have revealed an increase. A decrease by 1%, on an average, has been noticed during drought events. Maximum decrease of 25% in maize production is observed in year 1987. While the average increase in maize production is 13% a maximum increase of about 25% has been recorded in the year 1972. It is noteworthy that 2 years prior to 1972 were also drought years and this increase is illusory; it has been made possible because of a considerable fall in the previous year.

Two out of eight flood events have shown a decrease in production, from that of the previous year, of all pulses taken together; remaining six flood events have shown an increase. On an average, about 7% increment has been noticed in production of all pulses. Maximum increment of about 30%, from that of the previous year, has been observed in the year 1975. Higher rainfall seems to favour production of pulses, which is a Kharif crop. During drought events, 7 out of 11 cases have noticed decrease in production of all pulses taken together; remaining four cases have depicted an increase. On an average, during drought events, a decrease of about 9% in production of all pulses has been observed. Maximum decrement of about 30% has been observed in the year 1979.

## 32.4 Conclusions

From the foregoing analysis it is clear that both area and production of food grains have shown fluctuations from year to year. In secular terms, both of them increased up to mid-eighties; this shows emphasis on extension till that time; increase in production was at least partly related to increase in area. Thereafter, while area under food grains declined production continued to increase suggesting improvement in technology and policy. Decline in planted area and production shows periodicity. Fluctuation in area is less compared to that in production as the climatic extremes cannot be anticipated at the time of plantation but they show their impact at the time of harvest.

In general it is concluded that Indian agriculture is more vulnerable to drought than flood. Rabi food grain production shows better adaptability to drought than Kharif food grain production and this is primarily because Rabi crops have better access to irrigation infrastructure. Among the various food crops analysed all except jowar can effectively face flood events. Almost all of them cannot do so during the drought events. Wheat and jowar perform relatively better during drought events; the former is a Rabi crop while the latter is grown in both the seasons. Moreover, both of them are less water intensive. Since impact of drought is more than flood, its proper and effective management for minimising the effect on

Indian agriculture is needed more promptly. Kharif crops are more vulnerable than Rabi crops, adequate planning for minimising the impact of climate extremes is essential. Rice is one of the important staple foods which occupies major portion of Indian diet, is most sensitive to climate extremes, and draws better planning, management for its production to meet future demand. Enhancement of irrigation facility, forecasting of climate extremes well in time and technological development for suitable variety of crops to minimise the negative impacts of these extremes are required for food security and sustainable development.

**Acknowledgement** The present work has been possible due to financial support through project PGRDFI95052.

## References

Central Intelligence Agency (CIA) (2009) Economy of India. https://www.cia.gov/library/publications/the-world-factbook/geos/in.html#Econ

Centre for Science and Environment, New Delhi (CSE) (1991) State of India's environment: a citizen's report 3: floods, flood plains and environmental myths

Gadgil Sulochana, Gadgil Siddhartha (2006) The Indian monsoon, GDP and agriculture. Econ Pol Wkly XLI:4887–4895

Intergovernmental Panel on Climate Change (IPCC) (1995) The regional impacts of climate change, an assessment of vulnerability. Cambridge University Press, Cambridge

Kavi Kumar KS, Parikh J (2001) Indian agriculture and climate sensitivity. Glob Environ Change 11:147–154

Krishna Kumar K, Rupa Kumar K, Ashrit RG, Deshpande NR, Hansen JW (2004) Climate impacts on Indian agriculture. Int J Climatol 24:1375–1393

Ministry of Environment and Forests (MoEF) (2002) Agenda 21: an assessment, New Delhi. Ministry of Environment and Forests, Government of India

Ministry of Finance (2002) Economic survey 2001–2002, New Delhi. Ministry of Finance, Economic Division, Government of India

Mooley DA, Parthasarathy B (1983) Indian summer monsoon and El Niño. Pure Appl Geophys 121:339–342

Mooley DA, Parthasarathy B, Sontakke NA, Munot AA (1981) Annual rainwater over India, its variability and impact on the economy. J Climatol 1:167–186

Parthasarathy B, Munot AA, Kothawale DR (1988) Regression model for estimation of Indian food grain production from summer monsoon rainfall. Agric For Meteorol 42:167–182

Parthasarathy B, Rupa Kumar K, Munot AA (1992) Forecast of rainy season foodgrain production based on monsoon rainfall. Indian J Agric Sci 62:1–8

Parthasarathy B, Munot AA, Kothawale DR (1994) All India monthly and seasonal rainfall series 1871–1993. Theor Appl Climatol 45:217–224

Raju PVS, Mohanty UC, Rao PLS, Bhatla R (2002) The contrasting features of Asian summer monsoon during surplus and deficient rainfall over India. Int J Climatol 22:1897–1914

Webster PJ, Magana VO, Palmer TN, Shukla J, Tomas RA, Yanai M, Yasunari T (1998) Monsoons: processes, predictability, and the prospects for prediction. J Geophys Res 103:14451–14510

# Chapter 33
# Chinese Extreme Climate Events and Agricultural Meteorological Services

**Chen Huailiang, Zhang Hongwei, and Xue Changying**

**Abstract** The thesis comprehensively discusses the types of Chinese extreme climate disasters as well as their influence on agriculture, forestry and stock-breeding. With the worsening of green house effect, extreme climate events happen more frequently in more types, with the loss increasing, which greatly restrains Chinese economic development. On the basis of different types of meteorological disasters and their damages to agriculture, forestry and stockbreeding, Chinese local meteorological departments have undertaken overall, multi-level and multi-field services with excellent effects. At the last part of the thesis, new thoughts on future services are proposed to solve problems in agricultural meteorological services of extreme climate events at present.

## 33.1 Preface

In the past decades, the disasters caused by natural disasters have killed over 600,000 people and affected over 2.4 billion people in the world, most of whom are in developing countries (Qin 2008). Serious natural disasters usually create severe destructions, which push hundreds of thousands of people into poverty, reduce the prevention against natural disasters and cause vicious circle. According to the statistics of WMO, the loss of meteorological disasters from 1980 to 2005 in the world account for 75% of the total loss caused by natural disasters (Sciences and Technology Daily 2009). With the development of economy and society, the economic loss caused by meteorological disasters is increasing. With the worsening of global warming, more serious extreme climate disasters are happening more frequently and earlier (Zhang et al. 1991; Comprehensive Disaster Research

C. Huailiang (✉) • Z. Hongwei • X. Changying
Henan Institute of Meteorological Sciences, 110 Jinshuilu Rd., Zhengzhou, Henan 450003, P. R. China
e-mail: chenhl@cams.cma.gov.cn; xxqxjzhw1966@163.com; xuecy9@163.com

S.D. Attri et al. (eds.), *Challenges and Opportunities in Agrometeorology*,
DOI 10.1007/978-3-642-19360-6_33, 

Group 2004). Due to the complicated landform conditions and other elements, China, in particular, suffers from much more extreme climate events than other countries, and has been one of the countries with most serious meteorological disaster damages. The thesis introduces three aspects of Chinese extreme climate events, influence of extreme climate onto economy and the agricultural meteorological services against extreme climate by Chinese local meteorological departments, and proposes the ideas and suggestions for the meteorological services against extreme climate events in the future.

## 33.2 Brief Introduction of Extreme Climate Events in China

Various meteorological disasters usually affect 50 million hectares of farmlands in each year in China, added with the serious meteorological disasters including typhoon, storm, drought, high temperature, sand storm and thunder which influence 400 million people. According to the statistics from 1990 to 2006, the Mainland of China had to suffer 185.9 billion direct economic loss due to meteorological disasters each year in the past 17 years, which was 2.8% of the total GDP on average. Meanwhile, meteorological disasters always lead to other disasters like flood, geological disaster, sea disaster, biological disaster and forest and grassland fire, which all greatly threaten national economic construction, biological construction and living and property security.

Meteorological disasters have been occurring more frequently and seriously since the 1970s, greatly threatening food production safety as well as food productivity in China (Yang et al. 2007; Wang et al. 2006).

Meteorological disaster is over 70% (over 80% according to the data of WMO) of the total natural disasters, and agricultural meteorological disaster takes 60% of total meteorological disasters. The pressure caused by environment worsening, resource exhaustion and population explosion has been increasing, demonstrated by the acceleration of economic loss by meteorological disasters especially in the recent 10 years.

### *33.2.1 Drought*

As the most serious agricultural meteorological disaster in China, drought causes 62% of the total loss by various meteorological disasters (Wang et al. 2006; Liu et al. 2003). Drought refers to the phenomenon of water unbalance of crops due to external environmental elements like long-term little rain or great reduction of precipitation which leads to slow growth, withering, shattering, drying, death, output reduction and even harvestless ness of crops. According to the traditions and characteristics of agricultural production as well as the appearance seasons of drought, China divides drought into spring drought, summer drought and autumn

drought. Spring drought happens mainly in the Yellow River and Huaihe River watershed during March to May, when temperature rises quickly, air humidity is relatively low and soil moisture loses rapidly; summer drought occurs during Jul. and Aug. when the temperature in China reaches the highest level, evaporation undergoes quickly and crops are in prosperous growth period, so it usually causes relatively serious damages. Autumn drought happens during slight heat to autumnal equinox, when north China suffers from little rain which greatly influences the irrigation and sowing of crops. The Yangtze River watershed, area between Yangtze River and Huaihe River and area in the south of Yangtze River mainly suffer from summer drought, added with autumn drought sometimes. Agricultural drought, with most serious effect on Chinese food production and highest occurrence frequency, enjoys the following characteristics:

Drought occurs all over the country with great unbalance. The area suffering from drought in the Yellow River and Huai River watershed covers around 50% of the total disaster area in each year. In addition, the middle and lower reach of the Yangtze River is also one of the areas suffering serious drought. In disaster area of the two areas takes over 60% of the total disaster area in China. The six provinces and autonomous regions including Inner Mongolia, Heilongjiang, Hebei, Shandong, Henan and Jilin are the most serious disaster areas with over 1.5 million hectares on average for each; the 7 provinces including Henan, Shanxi, Shaanxi, Liaoning, Gansu, Anhui and Hubei are relative serious disaster area with 1–1.5 million hectares on average for each.

Drought happens frequently and lasts for a long time. In China, regional drought happens every year. As far as drought duration is concerned, many areas suffer from continuous spring-summer drought or summer-autumn drought, and even spring-summer-autumn drought. In some areas like the Yangtze River watershed, drought happens together with high temperature, which worsens drought. Consistent and large-scale drought usually cause great damages to national economy, especially agriculture. From 1978 to 2006, China had to suffer 210.85 million hectares of drought area on average in each year. From 1949, several severe drought years including 1959, 1960, 1961, 1972, 1978, 1997, 1999, 2000 and 2001 had been seen. In 1997, the drought area was 33.51 million hectares, including 20.01 million hectares influenced by drought and 3.958 million hectares harvestless, 47.6 million tons of crops was reduced. The drought in 1997 occurs in the areas in the north of the Yangtze River, especially the Yellow River and Huai River area, north China, northeast China and northwest China, most of where suffered 50–70 days and even over 100 days of continuous drought; the most serious flow break in history even happened in the lower reach of Yellow River. In 2000, China suffered from a nationwide drought, with over 20 provinces, autonomous regions and municipalities experiencing serious drought; the north Yangtze River area suffered from large-scale, long-term and severe spring-summer drought from February to July, with north China and eastern northwest China enduring drought for half a year. The drought in 2000 affected 405.4 million hectares of area, which was the highest since 1949. Among the disaster area, 26.78 million hectares was influenced by drought and 8 million hectares harvestless; 60 billion tons of crops was reduced, added with

51 billion loss of economic crop. Generally speaking, the drought of 2000 is the most serious drought disaster year since 1949.

### *33.2.2 Storm and Flood*

Most precipitation of happens in summer in most regions of China with obvious seasonal characteristics, so that flood disaster occurs frequently, growing into another important meteorological disaster affecting crop output (24% output reduction) (Liu et al. 2003; Xin and Xu 2007). Most floods are caused by continuous storm and extreme storm, submerging or destroying crops and reducing output or leading to failure of harvests. Most flood areas are concentrated in southeastern China, especially the Yangtze River watershed and Yellow-Huaihe River watershed. The annual average flood disaster area of China from 1978 to 2006 is 8.682 million hectares. The 1990s witnesses the most serious flood disaster since 1949 (Table 33.1), with the annual average flood area of 15.314 million hectares and affected area of 8.722 million hectares. Among the 10 years, the year of 1991 suffered from the most serious flood disaster since 1949, with total flood area of 24.596 million hectares, affected area of 14.614 million hectares, coverage of 24 provinces, autonomous regions and municipalities, especially 8 provinces like Anhui, Jiangsu, Hubei and Henan and the direct economic loss of ¥7.7908 million. The great flood of 1998 also affected as many as 29 provinces, autonomous regions and municipalities especially Jiangxi, Hunan, Hubei, Heilongjiang, Inner Mongolia and Jilin.

Storm flood disaster mainly occurs in the areas of middle and lower reaches of the Yangtze River, central China, north China and northeast China. On average, China had to suffer from 9.43 million hectares of storm flood disaster area each year from 1950 to 2005 (Fig. 33.1). Since the 1990s, China has been suffering much more serious storm flood disaster than the normal year, with the flood disaster frequency increasing obviously in the Yangtze River and Huaihe River watershed. For example, the great flood in the Yangtze River, Songhuajiang River and Nenjiang River watersheds in 1998 led to ¥299.8 billion direct economic loss; the

**Table 33.1** Proportion of economic loss by meteorological disasters in Chinese GDP during 1991 and 2000

| Year | 1991 | 1992 | 1993 | 1994 | 1995 | 1996 | 1997 | 1998 | 1999 | 2000 |
|---|---|---|---|---|---|---|---|---|---|---|
| Absolute economic loss by meteorological disasters (100 million) | 1,214 | 855 | 994 | 1,875 | 1,865 | 2,824 | 1,966 | 2,977 | 1,970 | 2,416 |
| Proportion of economic loss by meteorological disasters in Chinese GDP (%) | 5.62 | 3.21 | 2.87 | 4.01 | 3.19 | 4.16 | 2.64 | 3.80 | 2.40 | 2.70 |

**Fig. 33.1** The flood caused by the great storm of 75.8 in Henan destroyed the dam of the Banqiao reservoir

great storm of 75.8 in Henan made the highest daily precipitation record of the Mainland of China which was 1,060 mm, with the precipitation of 830 mm within 6 h in Linzhuang of Banqiao Reservoir which was the center of the storm (the original record was 782 mm of Pennsylvania, U.S.) (Truth of Dam break for the Worlds Largest Reservoir 2009).

### *33.2.3 Severe Convective Weather (Thunder, Hailstone and Tornado)*

Thunder strikes over 1,000 people in China every year, with over 50% of them killed. The economic loss caused by thunder is estimated to be ¥5–10 billion. Hailstone affects 1.73 million hectares and even 4 million hectares of disaster area per year, with about ¥1 billion economic loss (Liu et al. 2003; Xin and Xu 2007). China also suffers from around 100 tornados every year on average, added with frequent storms and gales, causing very severe loss to agricultural production, transportation, electricity, and property security. For example, in 2005, the severe convective weather like gale, hailstone and tornado killed 645 people, affected 3.29 million farmlands and produced ¥15.3 billion direct economic loss. In Beijing, 87,666 individuals suffered from hails on 31st May 2005 , with direct economic loss of ¥48,155,000. At the end of spring and beginning of summer, thunder happens to nearly each province, autonomous region or municipality of China. For instance, in the night of Jun. 3rd, 2009, severe convective weather happened to Shangqiu city,

Henan, killing 18 people, injured 46 people seriously, affected 62 towns severely and caused ¥258 million direct economic loss to agriculture (China News 2009a, b).

### *33.2.4 Sand Storm*

North China suffers from frequent sand storm, which is the common severe convective weather in northwest China and northern north China. Due to aggravated desertification and ecological deterioration, 2, 4,000 villages have disappeared till now. In recent years, China has to be confronted with ¥54 billion direct economic loss in every year due to sand storm, which is 3 times more than the financial income of northwestern 5 provinces and autonomous regions of China in 1996 (Liu et al. 2003; Xin and Xu 2007; Cheng et al. 2007; Tang 2007). Sand storm, especially severe sand storm, causes great damages. With the growth of population and social demand as well as social and economic development, the damages caused by sand storm are increasing. For example, it was estimated that 330,000 t sand fell in Beijing on Apr. 17th, 2006 (Xinhua 2009a, b, c, d).

### *33.2.5 Low Temperature Damage (Cold Wave, Frost and Cold Dew Winter)*

China usually has to suffer from 3 to 4 cold waves each year, with some areas affected by low temperature in Heilongjiang, Jilin, Liaoning, Inner Mongolia, Ningxia and Hebei in summer, in the Yangtze River watershed and south China in autumn, and in south Yangtze River area and south China in winter. Frost mainly happens in northwest China, north China, east China and central south China. Cold dew wind mainly happens in southern China, which produces 20–30% empty grain rate of late double season rice (30–50% and 70% empty grain rate in severe years) greatly reducing output (Liu et al. 2003; Xin and Xu 2007; Cheng et al. 2007; Tang 2007). In the late 10 days of April of 2002, 43 counties and cities of Shandong suffered severe frost which widely affected fruit tree, mulberry sapling, tobacco leaf, winter wheat and vegetable, with the disaster farmland of 510,000 ha and ¥6.4 billion direct economic loss.

### *33.2.6 Heavy Fog and Dust Haze*

Heavy fog usually occurs in Huaihe River watershed, south China, north China and northeast China, especially in Szechwan Basin and Yangtze River watershed. Heavy fog always causes severe influence on transportation and power transmission

(Xin and Xu 2007; Cheng et al. 2007; Tang 2007). For instance, from Dec. 1st to 2nd in 2002, over 100 flights and about 10,000 passengers were delayed in Beijing Capital Airport (China News 2009a, b).

In recent years, dust haze has been more and more serious in the large cities like Guangzhou and Beijing. In every autumn, the visibility of the cities decreases greatly, added with worsening traffic jam and increasingly breaking-out of diseases like respiratory tract infection. In 2007, the dust haze days of Zhujiang Delta surpassed 100 days, and the average dust haze days of Guangdong Province reached 75.7 on average, which was much more than the common level. The year of 2007 has the most dust haze days in the past 59 years since 1949, which breaks the record (Nanfang Daily 2009).

### *33.2.7 High Temperature and Dry Hot Wind*

High temperature disorders the heat balance of human body, with heatstroke rate increasing greatly. In 2003, southern China suffered heat waves and was susceptible to continuous high temperature. There were 12 continual days that were over 40°, with maximum high temperature of 43.2° on 32nd August in Lishui City, Zhejiang Province, which was the highest in the history. High temperature also intensifies drought, leading reservoir dry-up and water interception. Dry hot wind happens in the Hexi corridor of Gansu, Tulufan Basin, Shaanxi, Ningxia, Shandong, Henan, Hebei, Anhui, Shanxi, north Jiangsu, etc. in each year, which causes serious agricultural loss (Liu et al. 2003; Xin and Xu 2007; Cheng et al. 2007; Tang 2007; Chen et al. 2006).

### *33.2.8 Continuous Rain*

Continuous rain refers to relatively long-term cloudy and rainy period with short-term sunlight and high soil moisture which influence the growth or harvest of crops. For example, the continuous rain in 2005 autumn of Henan (Wang et al. 2009) caused farmland submergence, failure of drying harvested crop and sowing of winter wheat, output reduction or failure of harvests, and direct agricultural economic loss of ¥1.73 billion (Liu et al. 2003; Xin and Xu 2007; Cheng et al. 2007; Tang 2007; Chen et al. 2006).

### *33.2.9 Snow Disaster, Ice Rain*

Snow disasters, seen in northeast China, Xinjiang, Inner Mongolia, Gansu, Qinghai and Yunnan, cause great damages to the production and living of grazing land.

Moreover, it also blocks traffic, communication and power transmission. From March 2nd to 5th, 2007, a strong extra-tropical cyclone brought the severest storm and snow since 1951 to Liaoning, Jilin, Heilongjiang, Shandong, etc., which greatly affected the civil aviation, road and railway transportation, power transmission, agricultural facilities and livings of northeast China, producing direct economic loss about ¥14.13 billion to the 8 provinces, autonomous regions and municipalities (Liu et al. 2003; Xin and Xu 2007; Cheng et al. 2007; Tang 2007). The snow and ice rain from January to February of 2008 in south China, which was wide, strong and consistent, caused severe damages to the crop production of China, including 14,317,700 $hm^2$ disaster-affected area, 7,375,300 $hm^2$ disaster area and 1,971,100 $hm^2$ area with harvest failures; Hunan was the province with severest damages among the 20 provinces, autonomous regions and municipalities, and the crops including rapeseed plant, winter vegetables, canopy, orange and tea suffered from the greatest damages (Liu et al. 2008).

### *33.2.10 Forest Fire*

Forest fire refers to the artificial fire which loses control and spreads freely in forest, causing certain damages and loss to forest, ecological system and human beings. Forest fire is sudden, destructive and difficult to be stopped.

Forest fire occurs frequently in spring and autumn in north China, winter and spring in south China and 1–2 months after the rainy spell in early summer in the Yangtze River watershed. The fire prevention period of the Great and Lesser Hingan Mountains and the Changbai Mountain is spring and autumn. For example, forest fire usually occurs during Mar. and Jun. and Sep and Nov. in the Great and Lesser Hingan Mountains under most circumstances, with April, May and October as the most frequent fire disaster months.

Since 1950, China has been suffering 13,067 forest fires on average in each year, with disaster-affected forest area of 653,019 ha and casualties of 580. During 1950 and 1988, China had to suffer 15,932 forest fires on average in each year, with disaster-affected forest area of 947,238 ha and casualties of 788 (678 injuries and 110 deaths). After 1988, the average number of fire disasters in each year of China was reduced to 7,623, with disaster-affected forest area of 94,002 ha and casualties of 196 (142 injuries and 54 deaths). Compared with the situation before 1988, the figures were reduced by 52.2%, 90.1% and 75.3% respectively. The most typical fire disaster happened to the Great Hingan Mountain in May of 1987, causing ¥6.913 billion economic loss.

### *33.2.11 Acid Rain*

Acid rain refers to the precipitation with its pH value less than 5.6. $H_2SO_4$ and $HNO_3$ are the two main components in acid rain, which are produced by fossil fuel

including coal, petroleum, $SO_2$ and nitrogen oxides in tail gas. Acid rain is able to acidify fresh water lakes, affecting the survival of fishes and diversification of water bodies, and change the physicochemical nature of soil, reducing soil fertility. As far as forest is concerned, acid rain does not only change the physiological tissues of trees and plants, but also reduce the insect resistance ability of the forest. What's more, acid rain also destroys marble architectures, stone statues and metal materials, and damages human organs like respiratory tract and cutis and mucous membrane (Liu et al. 2003; Xin and Xu 2007; Cheng et al. 2007; Tang 2007).

## 33.3 The Extreme Climate Weather Trend and Effects on Chinese National Economy

In recent years, extreme climate events and their damages have been increasing in the world. According to the statistics related, the serious meteorological disasters in the 1990s are five times more than that in the 1950s in the world (Liu 2009). Frequent extreme climate events are closely related with the background of global warming. As demonstrated by the analysis and simulation of scientists with advanced computers, climate warming leads to the growth of many extreme climate events. For example, it is probable to witness increasing hot waves in almost each continent, extreme precipitation amount and frequency in many areas, and even the frequency of strong typhoon, though common typhoon frequency does not grow obviously.

In the recent 20 years, China has also been witnessing global warming. Before the 1980s, the average surface temperature of China fluctuates slightly, while the temperature keeps increasing rapidly after the 1980s. Under the general background of global warming, China begins to witness more extreme precipitation events, with the average extreme precipitation intensity and amount growing, especially in the 1990s. Since late 1990s, China has been suffering more frequent drought events. For instance, the great drought in north China in 1997, followed by the abnormal droughts from 1999 to 2002, the severest drought since 1951 in Sichuan and Chongqing in summer caused by consistent little rain, and the drought from the spring of 2003 to the winter of 2004 in south China. Though typhoon does not increase, it comes stronger and more concentrative. For instance, Rananim of 2004 and Damrey of 2005 are the strong typhoons ever seen in history, and the record has been broken soon in each of the past 3 years (Liu 2009). According to statistics, typhoons have caused direct economic loss of ¥24.6 Billion and 570 deaths averagely in China (Li and Chen 2007).

Under the circumstances of climate warming, the world has been in a period of frequent extreme climate events, and China is possibly going to be faced with extremer and more frequent abnormal climate events (Figs. 33.2–33.7).

From the 1990s, China has to suffer over ¥100 billion economic loss (3–6% of total GDP (Summer Davas forum 2009) in each year due to meteorological disasters

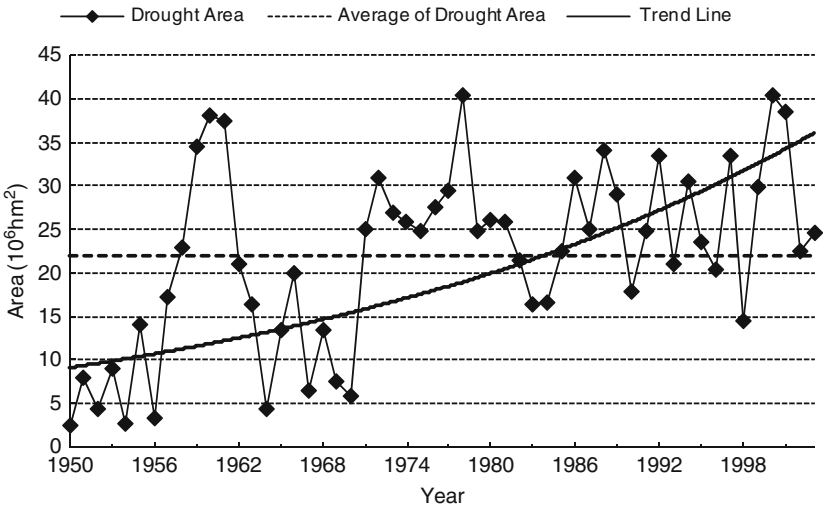


**Fig. 33.2** Time sequence of drought-affected area of China from 1950 to 2003

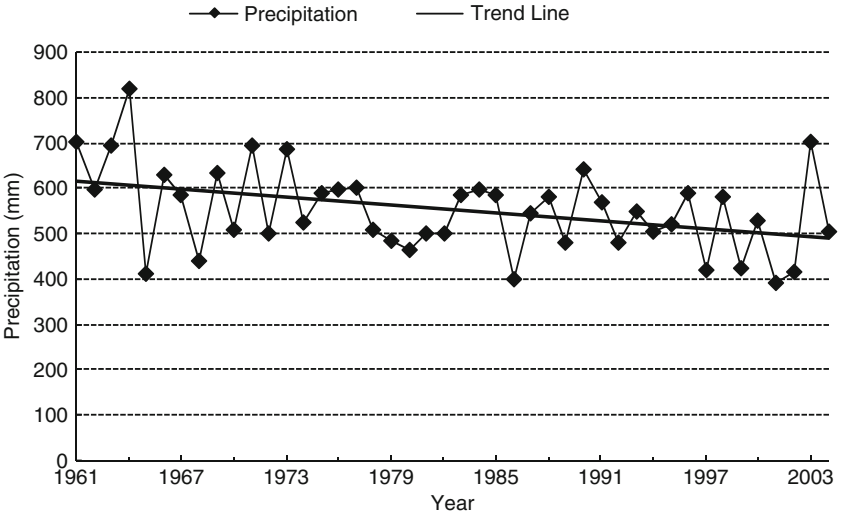


**Fig. 33.3** Time sequence of annual precipitation of agricultural area of north China from 1961 to 2003

(see Table 33.1 and Fig. 33.8), food output reduction of 10–20 billion kg and thousands of casualties (Xinhua 2009). In addition, the loss of secondary disasters to ecology, environment, society, culture and economy caused by the meteorological disasters is unable to be estimated. The extreme climate events, due to their

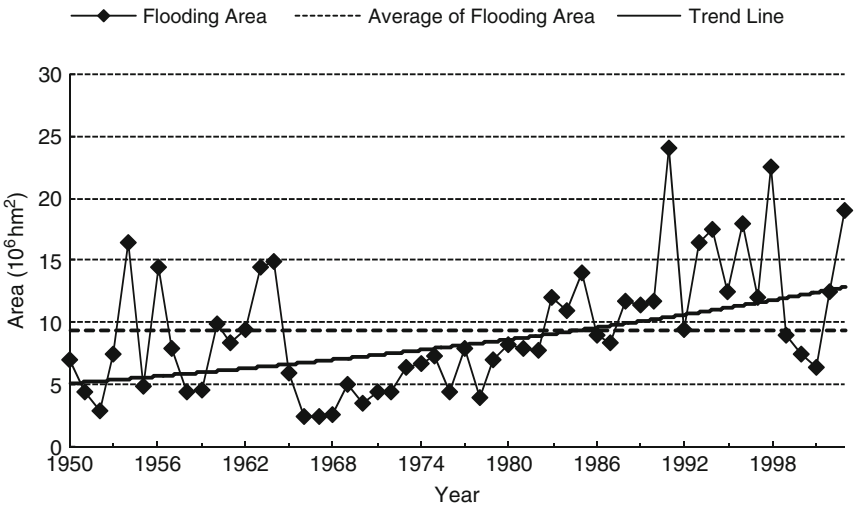


**Fig. 33.4** Time sequence of flood-affected crop area of China from 1950 to 2003

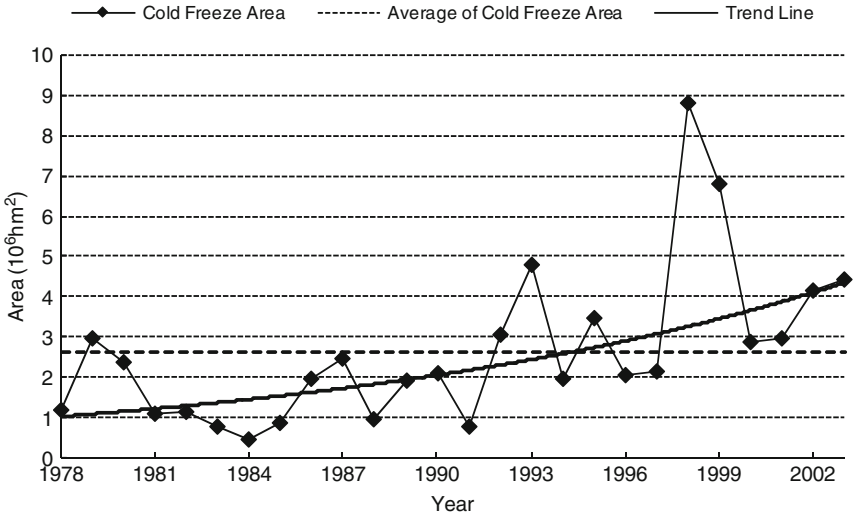


**Fig. 33.5** Time sequence of frost-affected area of agricultural area of China from 1978 to 2003

characteristics, usually cause different degrees of effects on different industries, and thus affect the development of Chinese national economy.

Climate changes will reduce the yield of most crops. It is estimated that Chinese crop yield is going to be reduced by 5–10% in 2030, with the yield of three main crops including rice, wheat and corn decreasing (Fig. 33.9).

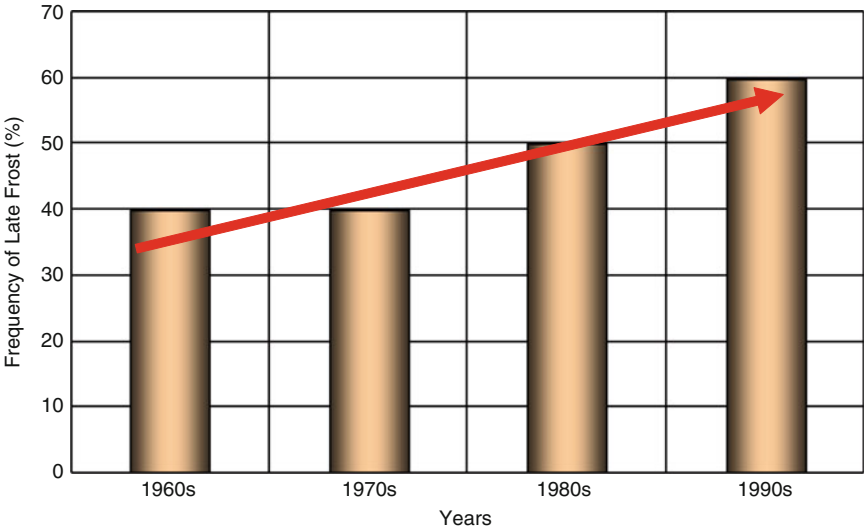


**Fig. 33.6** Time sequence of late frost frequency of China in different years in the twentieth century

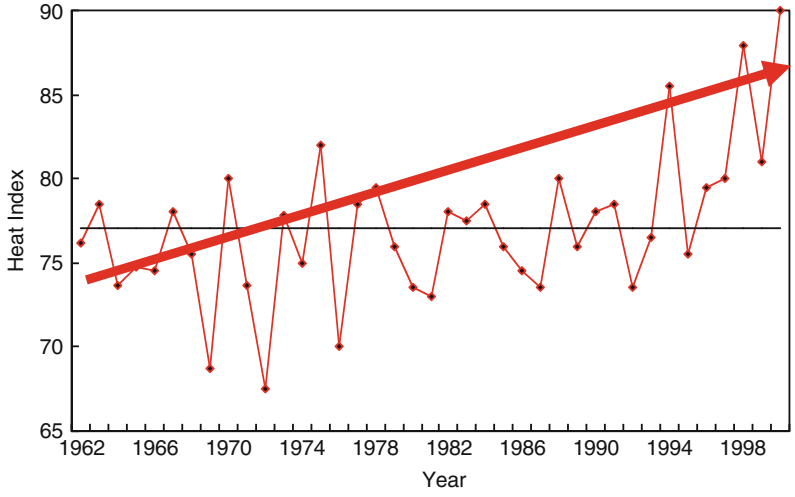


**Fig. 33.7** Time sequence of Chinese heat index from 1961 to 2000

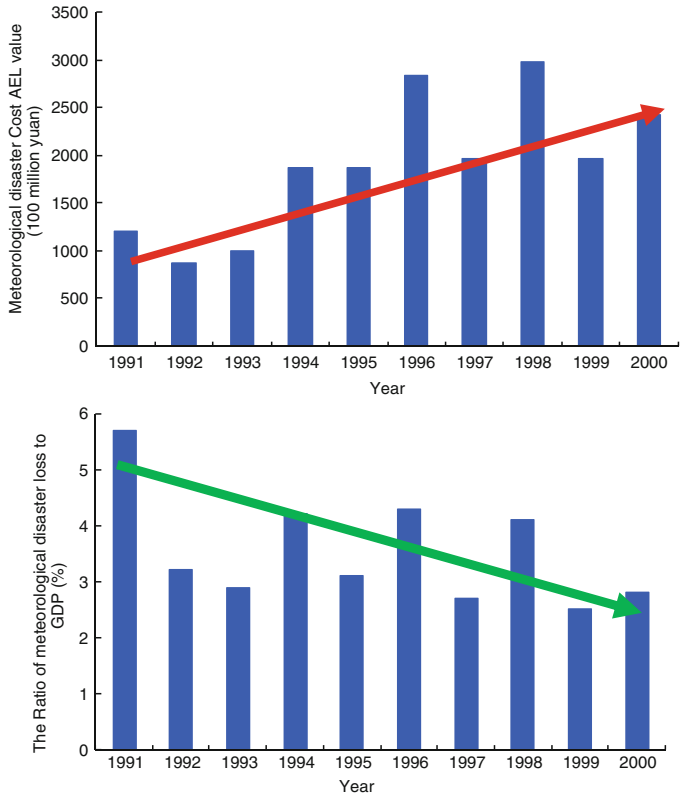


**Fig. 33.8** Figure of proportion of economic loss by meteorological disasters in Chinese GDP during 1991 and 2000

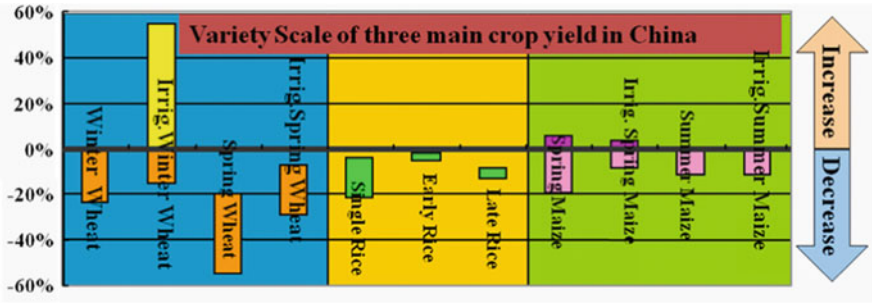


**Fig. 33.9** Effects of climate change on the yield of Chinese three main crops

## 33.4 Agricultural Meteorological Services of Chinese Local Meteorological Departments Against Extreme Climate Events

The elements of different extreme climate events, climate backgrounds, geological conditions, service targets and characters of agriculture, forestry and stockbreeding decide the diversification, time uncertainty and comprehensive measures of Chinese agricultural meteorological services against extreme climate events. Chinese local meteorological departments have released different services for different extreme climate events and service targets. The services mainly consist of the monitoring, forecasting, warning, risk analysis, effect assessment, comprehensive prevention and control for extreme climate events such as (i)drought and flood; (ii) extreme high/low temperature and frost; (iii) extreme convective climates like heavy rain, storm and hailstone; (iv) strong wind, gale, typhoon, dry hot wind and cold dew wind; (v) snow disaster; (vi) fire disaster; (vii) sand storm; (viii) other environmental disasters like blue algae and red tide.

The suddenness of extreme climate events decides non-periodic agricultural meteorological service as the main service characteristics of Chinese local meteorological departments, and thus the diversification and flexibility of agricultural meteorological service products. Meanwhile, periodical agricultural meteorological service products are the main service measures like soil moisture monitoring report, drought monitoring report and 10-day (monthly or weekly) of agricultural meteorological report. The terms of periodical agricultural meteorological service products are divided into month, 10-day, week and day. Chinese local meteorological departments, according to the meteorological disaster types and service targets, mainly undertake the following types of services.

### *33.4.1 Agricultural Meteorological Services for Disaster Prevention and Mitigation*

#### 33.4.1.1 Meteorological Disaster Monitoring and Warning Analysis

The services of meteorological disaster monitoring and warning analysis on drought, typhoon, storm, high temperature, gale, snow, hailstone, sand storm, heavy fog, low temperature, frost and thunder are undertaken, such as the Grid Soil Moisture and Drought Forecasting System of Henan (Agricultural Meteorological Research office 2009). Meanwhile, the monitoring forecasting services for secondary and derived disasters like flood, torrent, storm tide, landslide, debris flow, forest (grassland) fire and desertification are also undertaken. Services like disaster monitoring forecasting, pre-assessment, effect evaluation, prevention measures and countermeasure suggestions are also provided in time before the disasters, services including timely monitoring forecasting and tracking evaluation are provided during the

disasters, and services including after-disaster conclusion, historical comparison analysis and overall disaster evaluation are provided after the disasters.

#### 33.4.1.2 Releasing of Meteorological Disaster Forecasting Information

The sudden meteorological disaster forecasting information releasing system is established, with the releasing contents and forms regularized; the cooperation with the main media is strengthened to monitor the information releasing of each medium, adding, inter-cut, supplement or revise the related information directing against the key disastrous weather changing process; the meteorological disaster forecasting information releasing system are improved gradually, strengthening the facility construction in the areas with weak information communication, and improving the satellite digital audio broadcasting system of meteorological forecasting information in rural areas in recent years; the disaster broadcasting system via mobile phone in communities in urban areas is developed; and the sea broadcasting station providing meteorological forecasting information is developed (Xinhna Net 2009).

#### 33.4.1.3 Meteorological Disaster Risk Evaluation

Meteorological disaster risk evaluation business is developed according to the meteorological disaster survey. The evaluation modes for meteorological disaster danger, disaster bearing fragility, disaster loss degree, risk index and risk class are established; GIS-based database for meteorological disaster risk evaluation is established; the division maps of meteorological disaster risk including the division difference map of meteorological disaster risk distribution, the meteorological disaster risk-time sequence map of meteorological disaster risk degree changing with time and the meteorological disaster risk map of time and space meteorological disaster changing rules are worked out; countermeasures against meteorological disaster risks for avoiding and reducing meteorological risk, protecting or transferring the effect of meteorological disaster risk on human groups, and resolving risks through risk transfer and risk sharing (such as policy insurance) are formulated (Wang et al. 2005; Luo 2007; Liu 2008).

#### 33.4.1.4 Meteorological Disaster Effect Evaluation

The pre-disaster evaluation business for meteorological disaster is undertaken, realizing prediction evaluation on the location, time, scale and damage degree of disasters before the occurrence and providing evidence for the formulation of disaster reduction plan; the meteorological disaster tracking evaluation business is set up, realizing evaluation on the process and developing trend of the meteorological disasters and providing evidences for the governments and society to understand

the disaster and organize disaster prevention and mitigation; the after-meteorological disaster evaluation business is started, realizing overall evaluation on the disaster type, intensity, time, location, casualty, economic loss and disaster prevention and mitigation measures through comprehensive investigation after the disaster (Luo 2007; Liu 2008).

#### 33.4.1.5 Meteorological Disaster Information Collection, Report and Evaluation

The meteorological disaster investigation and collection network in province, city and county is established and the meteorological disaster information collection hotline is also opened; the direct meteorological disaster report system is improved, shortening the disaster information collection period (Guo et al. 2009); the sport investigation and evaluation system for meteorological disaster is also set up, investigating, analyzing and evaluating the meteorological reasons causing disasters, and making the latest information available through spot investigation; disaster information discussion is undertaken against key meteorological disasters; and nationwide disaster information sharing is realized, promoting the collection, analysis and handling capability on meteorological disaster information.

#### 33.4.1.6 Meteorological Disaster Survey

The nationwide meteorological disaster survey is undertaken to classify Chinese meteorology and related disastrous divisions, basically grasping the distribution, target, loss, intensity, frequency, vulnerable area, reoccurring position, forming element, disaster prevention and weak link (Application Service office 2009).

#### 33.4.1.7 Emergency Response to Meteorological Disaster

The national and local disaster response plans are established; the instruction on starting or ending the related meteorological disaster response plan is released in time according to the meteorological disaster warning information, including the first key meteorological disaster response plan in Hebei (Xinhua 2009); the emergency exercise is undertaken periodically, strengthening the dynamic management on emergency plan, revising and renewing the plan in time; the meteorological response linking mechanisms with the departments of water resource, civil affairs, traffic, earthquake, power, aviation and military are established, together with the regular meeting system across multiple departments, the meteorological disaster response management team among each department, and the mobile phone information forecasting releasing stage among the meteorological disaster emergency headers of each department, which promote the mobile emergency insurance ability

and the establishment of emergency mobile meteorological stations and disastrous climate live broadcasting system.

#### 33.4.1.8 Construction of Meteorological Disaster Prevention Team

The meteorological disaster prevention team covering rural and urban areas is established. Each assistant and meteorological information assistant is responsible for receiving and spreading meteorological disaster warning information, reporting real disastrous climate information to the local meteorological department, and taking part in the formulation of local meteorological disaster prevention plan and publication of meteorological disaster prevention, emergency disposal, investigation and evaluation. The meteorological information assistant training is undertaken periodically, such as the establishment of meteorological disaster volunteer team of Taiyuan, Shanxi (Taiyuan Meteorological Bureau 2008), which greatly promotes the local meteorological disaster prevention works. The establishment of military-civil integrated emergency rescue team is promoted to take part in the emergency rescue work with social groups, enterprises and volunteer.

#### 33.4.1.9 Scientific Propaganda for Meteorological Disaster Prevention

The propaganda of meteorological prevention knowledge is undertaken together with related departments and units with various carriers to promote the disaster prevention awareness of the whole society, strengthen the construction of rural and urban meteorological education base, and organize straightaway TV film, calendar, card and handbook on meteorological prevention; the education and propaganda in schools, countryside and key disaster areas are strengthened, including the propaganda of culture, science and technology and hygiene on disaster prevention into the scientific propaganda activity to promote the disaster prevention awareness and disaster evasion ability of the society; the related scientific explanation and instruction works shall be well done directing against some special natural phenomenon, promoting the recognition of the public to various meteorological disasters. The World Meteorological Day (23rd of March) of each year shall be the best moment to propagandize meteorological knowledge.

### *33.4.2 Agricultural Meteorological Services Against Climate Changes*

Climate change has aroused wide attention in the world, for it will have positive or negative effect on agricultural production. Agriculture enjoys a special position in China, which provides basic supplies for over 1.3 billion population. However, the

natural disasters caused by climate change, together with population growth and water resource insufficiency, will probably make Chinese agriculture more fragile. Climate change will present three serious problems for Chinese agricultural production in the future: (i) increasing instability of agricultural production and fluctuating crop yield; (ii) changes of agricultural production pattern and structure; and (iii) changes of agricultural production condition and increasing agricultural cost and investment. Generally speaking, climate change will cause unbearable, irreversible and consistent serious effect on Chinese agriculture. Therefore, further and comprehensive researches must be undertaken on the effect of climate change on Chinese agriculture and appropriate measures must be proposed. Chinese local meteorological departments thus have undertaken the following services:

#### 33.4.2.1 Undertaking Refined Agricultural Climate Division

The 3rd national refined agricultural climate resource division shall be started and deepened. The comprehensive division of refined agricultural climate resource with km differentiation rate shall be finished generally, the special division of refined agricultural climate resource with 100 m differentiation rate for single crop, special agriculture, facility agriculture, forestry, stockbreeding and fishing shall be finished, and the refined agricultural climate resource division with 100 m differentiation rate for hill and mountainous areas shall be completed. Characteristic dynamic division of refined agricultural climate resource and timely evaluation business shall be developed gradually, which provide not only evaluation analysis report and evidence for long-term agricultural production structure and crop pattern, but also reference for the decision-making of local agricultural production pattern and advantageous species.

Refined agricultural climate resource division is mainly undertaken by the national and provincial units periodically (before the starting of each year or each production period). On the basis of two-level division above, the business units in cities and counties, directing against the local characteristic agriculture, facility agriculture, forestry, stockbreeding and fishing, especially the complicated agricultural climate types in hill and mountainous areas, non-periodic refined agricultural climate resource division and evaluation shall be undertaken according to the demands.

#### 33.4.2.2 Undertaking the Analysis on the Effects and Adaptability of Climate Changes on Agriculture

The analysis on the effects and adaptability of climate changes on agriculture shall be strengthened. The analysis on the effect of historical climate changes on agricultural production, the effect evaluation of future climate changes on agricultural production, effect prediction under different climate, and the long-term adaptability of agricultural production as well as the countermeasures against climate changes shall be

undertaken according to the elements of temperature, precipitation, $CO_2$ density and extreme climate events, so that the business products like the Effect and Adaptability Evaluation Report of Climate Changes on Agriculture are presented, which are materials for the evaluation report of IPCC and the National Evaluation Report on Climate Changes of China.

The national business departments are responsible for carrying on the effect and adaptability analysis of climate changes on agriculture, starting from one or several staple rice, cotton and oil crops to the influences of climate changes on agriculture, forestry, stockbreeding and fishing, and the sensibility, fragility and adaptability analyses of agriculture to climate changes. One or several local programs can be selected for further researches in some provincial business units if necessary.

#### 33.4.2.3 Undertaking Agricultural Climate Demonstrability and ADM

Agricultural climate demonstrability shall be undertaken and ADM suggestions shall be raised. Directing against local agricultural engineering construction and governmental decision-making, the analysis and evaluation of climate adaptability, risk and possible effect shall be undertaken on the selection of planting base construction, planting system adjustment, new species introduction, key farming and cultivation, and the development and planning of disaster prevention measures, and characteristic agriculture, facility agriculture, forestry, stockbreeding and finishing, providing the special report of agricultural climate demonstrability and the report of decision-making consultation.

According to the demands of local agricultural engineering construction and governmental decision-making, the demonstrability of agricultural climate and ADM shall be fulfilled by the national, provincial, city and county meteorological departments according to the Law of the Peoples Republic of China on Meteorological Services and the other management regulations.

### *33.4.3 Meteorological Services in Rural Reform and Development*

#### 33.4.3.1 Strengthening Public Meteorological Service Ability in Rural Area

The prevention of meteorological disasters and secondary disasters including torrent, landslide, debris flow, thunder and gale in rural areas has been strengthened. The releasing system of meteorological disaster forecasting information in rural area is improved to establish a multi-channel meteorological service information communication stage, aiming at solving the bottleneck problems like the last 1 km limitation for information release. Meanwhile, the rural economic information network host by the government, undertaken by the departments and assisted by agricultural departments has been developed on the basis of the meteorological information system, promoting the construction of rural and information service

stations. The rural meteorological disaster emergency management system shall be established and improved gradually. For instance, the new mechanism for meteorological disaster forecasting of Hubei Province of government dominance, department linking and public participation has been established to prevent meteorological disasters (China Meteorological Administration 2009a, b, c).

#### 33.4.3.2 Strengthening the Construction of Agricultural Disaster Prevention and Mitigation System

Agricultural meteorological disaster monitoring, forecasting, warning and evaluation shall be strengthened, focusing on the research and development of quantitative analysis and evaluation technologies for agricultural meteorological disaster on agricultural production and activities; agricultural meteorological disaster information system shall be developed gradually to further promote the service ability for agricultural disaster prevention and mitigation directing against key agricultural activities and detailed agricultural productions. In order to meet the requirements of each links of modern agricultural production and the growth of crops, the meteorological forecasting for key agricultural activities and key agricultural insect diseases shall be undertaken, aiming at providing information for insect disease prevention and mitigation like disease scale, time, target and prevention measures, which effectively serves the development of issue of agriculture, farmer and rural area (Xie et al. 2008; China Meteorological Administration 2009a, b, c).

#### 33.4.3.3 Promoting the Meteorological Service Ability on National Food Security Insurance

Various agricultural weather forecasts including agricultural disaster forecast shall be promoted gradually to enhance the ability to go after profits and avoid disadvantages for agricultural production. The service ability construction of artificial effect on weather shall be strengthened to provide effective services for drought resistance and water resource addition of agriculture (Li 2009). The monitoring of extreme climate events, climate trend prediction and agricultural climate prediction shall be strengthened, too to provide effective decision-making services for scientific planning of annual agricultural production of the agricultural production departments. The food yield meteorological forecasting business shall be enhanced and improved, the dynamic monitoring forecasting of Chinese crop yield shall be undertaken, and the meteorological evaluation and forecasting services on crop yields shall be provided. The following information such as crop growth, quantitative evaluation of meteorological effect on crop yield, dynamic meteorological prediction information on crop yield, different crop planning area, total yield area as well as yield growth/reduction percentage shall be provided. The forecasting services on several agricultural product yield of rice, cotton and oil shall be undertaken, and the service on the yields of

foreign main crops related with Chinese crop export and import shall be developed (Yi 2007; Anon. 2009).

#### 33.4.3.4 Meteorological Services on Stockbreeding, Forestry and Fishing Being Strengthened

The meteorological services for stockbreeding, forestry, fishing, aquiculture, ecological tourism and food storage shall be developed appropriately facing grand agriculture. Meteorological services for characteristic agriculture, facility agriculture and precision agriculture have been undertaken to provide pros and cons analysis, countermeasures and suggestions for characteristic agriculture, facility agriculture and precision agriculture according to the relations between meteorological conditions and characteristic agriculture, facility agriculture and precision agriculture, and highly-qualified and highly-efficient agricultural meteorological control technologies (China Meteorological News 2009; Chen 2009). The comprehensive monitoring evaluation business for ecological meteorology, especially meteorological monitoring evaluation on key ecological environmental problems is developed (The Central People's Government of P.R. China 2009). The forest and grassland fire forecasting services and meteorological poverty alleviation development have been strengthened and the promotion, modeling and consultation of applicable agricultural meteorological technologies have been undertaken, enhancing the self-development ability of the poverty-stricken areas.

## 33.5 Thoughts on Future Agricultural Meteorological Services Against Extreme Climate Events of China

1. The spatio-temporal distribution of monitoring stations for extreme climate events as well as their automation level shall be promoted to enhance overall atmosphere detection capability. We shall accelerate the construction of surface meteorological monitoring network and the modern meteorological business systems like meteorological satellite remote sensing, climate radar monitoring, automatic meteorological observation station (network), geographical information system, advanced computer, artificial rain addition with antiaircraft gun and radar examination; carry out olid, dynamic and high-resolution monitoring of climate system in larger scope to improve correctness and accuracy of weather and climate forecast; strengthen meteorological science research and technical development, promote automatic meteorological monitoring and science & technology service, and increase service achievement.
2. In order to promote the accuracy and instantaneity of meteorological services, the forecasting and releasing system for extreme weather events shall be considered in prior in decision-making. At present, the forecasting ability for extreme

climate events of China has been greatly lagged behind by the advanced countries and it can not meet national disaster prevention and mitigation demands, especially the ability of quantitatively forecasting strong convective weather such as sudden disaster climate and storm is lagging in particular. The technical system of weather forecast is imperfect, and technical forecasting route and system adaptable to the demand of modern climate forecasting business and refined meteorological service have not been established completely yet. Therefore, the improvement shall be undertaken focusing on the problems of sustainable development of figure forecast, professional forecasting business and technical system construction. We shall accelerate innovating atmosphere detection equipment, improve monitoring density, promote construction of meteorological satellite detection and new generation meteorological Doppler radar network, speed up special observatory business and develop whole-course rolling modified refined weather forecast with fixed time, fixed point and fixed quantity. At the same time, we shall actively promote weather forecast and extreme weather warning information releasing channels. Cooperated with Ministry of Information Industry, we make efforts to realize releasing of warning information "the last kilometer" in the countryside, so that meteorological information can be heard in the areas, especially the remote area, rural area and mountainous area where traditional communication technique cannot reach.

3. Quantitative and dynamic evaluation modes of extreme climate events are seriously insufficient. At present, most of evaluation modes are focused on after-disaster evaluation and quantitative and dynamic evaluation modes the value quantitative and dynamic evaluation modes shall be developed as soon as possible. Due to the complicity of effect evaluation of meteorological disaster on agriculture, no matured and practical quantitative dynamic evaluation method has been developed in modern agricultural meteorological business. Crop model is able to have value simulation to the key growth process and its environmental relations with meteorology and soil, so that the relations between crop growth and environmental elements can be descried quantitatively from the angle of mechanically. In the near future, it is the main development direction for quantitative evaluation of disasters to adopt crop model for quantitative disaster evaluation and operation.
4. At present, the warning signal based on weather conditions nearly does not consider the elements of agriculture. Some agricultural meteorological disasters like dry hot wind are not extreme climate events, and some have several differences from meteorological disasters, such as difference between agricultural meteorological drought and meteorological drought. Now, there is no warning information releasing standard of agricultural meteorological disasters, so it is urgent to establish special disaster warning releasing standard and mechanism based on characteristics of agricultural meteorological disasters.
5. Exploring and developing the risk evaluation business of agricultural meteorological disasters, actively taking part in policy agricultural insurance, agricultural re-insurance and risk management of extreme disasters. Under the background of climate changes, the frequency and intensity of Chinese

agricultural meteorological disaster are increasing, which cause more serious damages to agricultural production and greatly affect the income of farmers, production activeness of agricultural production, agricultural sustainable development and rural stability. The great effect of agricultural disaster on agricultural production asks for the establishment of a scientific and effective agricultural disaster insurance mechanism. However, Chinese agricultural disaster insurance is relatively lagged behind at present, with agricultural insurance developing slowly, either undertaken by authorities' financial relief or farmers themselves, so it is urgent to develop the agricultural disaster insurance mechanism.

## References

Agricultural Meteorological Research Office (2009) Henan Provincial Institute of Meteorological Sciences. Technical Conclusion of Soil Moisture Forecasting Business Service System of Henan [R], Zhengzhou

Anonymous author (2009) National crop yield forecasting and agricultural meteorological disaster influence evaluation conference of 2007 held in Yinchuan. (2007-8-27) [2009-6-9]. http://www.wsqx.cn/qxxw/gnqx/200708/1162.html

Application Service Office (2009) National climate centre: national meteorological disaster survey conference held in Beijing, (2008-05-14) [2009-6-5]. http://ncc.cma.gov.cn/Website/ index.php?ChannelID = 2&NewsID = 3126

Chen W (2009) Characteristic meteorological service assisting characteristic agriculture – auton omous meteorological stations in vegetable greenhouse. [2009-6-9]. http://www.db-nw.com/jszx/view.aspx?id=37668

Chen H, Zhang X, Deng W et al (2006) Analysis and zoning of agrometeorological disasters risk for wheat growing. J Nat Disasters 15(1):135–143

Cheng Z, Zhao Z, Jin H et al (2007) The climatic change to the Ju county agriculture meteorology disaster influence and countermeasure [J]. Chin Agric Sci Bull 23(8):540–543

China News (2009) Strong convective weather in Shangqiu, Henan killing 16 and injuring 46. (2009-06-04) [2009-6-5]. http://auto.chinanews.com.cn/gn/news/2009/06-04/1721028.shtml

China News (2009) Heavy fog delays over 100 flights in Beijing Capital Airport, China News: (2002-12-3) [2009-6-5]. http://www.chinanews.com.cn/2002-12-03/26/249704.html

China Meteorological Administration (2009) Hubei:new warning mechanism of government dominance, department linking and social participation. (2009-1-5) [2009-6-9]. http://www.cma.gov.cn/ztbd/2009jzh/gdld/200901/t20090105_24701.html

China Meteorological Administration (2009) Anniversary plan of agricultural meteorological service of Guangdong Meteorological Administration issued and fulfilled. (2009-4-9) [2009-6-9]. http://www.cma.gov.cn/ztbd/agri/yw/200904/t20090407_30972.html

China Meteorological News (2009) Gansu characteristic agricultural meteorological service bringing benefits to agriculture, farmer and rural area. (2009-3-12) [2009-6-9]. http://www.cma.gov.cn/ztbd/agri/jlpt/200903/t20090312_29082.html

Comprehensive Disaster Research Group by the State Plan Commission and State Economy & Trade Commission under the Leadership of MOST (2004) The atlas of Chinese major natural disasters and society [M]. Guangdong Science &Technology Press, Guangzhou

Guo J, Luo B, Zhang X (2009) China meteorologic disasters reporting system. (2008-10-15) [2009-6-5]. http://www.5icte.com/cms/ ti!view.jspa?cstaID = CG2008008257

Li C (2009) Anti-drought, rain addition, hailstone prevention and air water resource development-50th anniversary record of Jinlin artificial raining history [J]. Econ Vis 2009(1):32–33

Li L, Chen W (2007) Disaster emergency management and comprehensive mitigation of disasters [M]. Peking University Press, Beijing
Liu R (2008) Winter wheat drought assessment operational service system for Henan province[D]. Nan Jing: Nanjing University of Information Science and Technology, 2008
Liu Y (2009) Why extreme climate events happen frequently? (2006-8-24) [2009-6-5]. http://news.eastday.com/eastday/node81741/node81762/node156858/u1a2273461.html
Liu L, Sha Y, Bai Y (2003) Regional distribution of main agrometeorological disasters and disaster mitigation strategies in China[J]. J Nat Disasters 12(2):91–97
Liu B, Li M, Huo Z et al (2008) Effect of low temperature, rain, snow, frost and hailstone disasters on planting industry[J]. Chin J Agrometeorol 29(2):242–246
Luo P (2007) Risk assessment and decision of drought hazard based on GIS in Chongqing City[J]. Chin J Agrometeorol 28(1):100–104
Nanfang Daily (2009) Guangdong dust haze days breaking record in 2007. (2008-01-16) [2009-6-5]. http://unn.people.com.cn/GB/14748/6781028.html
Qin D (2008) Major meteorological disasters impacting on China and their development situation [J]. China Emerg Rescue 2008(06):4–6
Science and Technology Daily (2009) Disaster prevention and mitigation: meteorological warning cannot be neglected. (2006-10-31) [2009-6-3]. http://web.nuist.edu.cn/xb/news/36/2006103181240.htm
Summer Davos Forum (2009) Statistical data of GNP and GDP over the years of 1978–2005. (2007-7-29) [2009-6-5]. http://www.livebaby.cn/blog/u/WorldEconomic/ archives/2007/china-gdp-1978-2005.html
Taiyuan Meteorological Bureau (2008) Notice on establishing volunteer team for meteorological disaster. Bingqi No. 2008 [48]
Tang R (2007) Major agricultural meteorological disasters and research progress of the disasters [J]. J Anhui Agric Sci 35(29):9353–9362
The Central People's Government of P.R. China (2009) Bi Baogui introducing the works including China ecological meteorological monitoring and evaluation.(2007-3-1) [2009-6-9]. http://202.123.110.3/wszb/zhibo20/content_538467.htm
Truth of Dam-break for the World's Largest Reservoir (2009) About 75.8 Dam-break of Zhumadian Reservoir (2008-1-4) [2009-5-28]. http://www.360doc.com/content/ 080104/ 14/25966_ 944978.html
Wang S, Huo Z, Li S et al (2005) Risk regionalization of winter wheat loss caused by drought in North of china [J]. Crop Sci 31(3):267–274
Wang J, Shi P, Wang P et al (2006) Spatial-temporal pattern of natural disasters in China[M]. Science Press, Beijing
Wang Jifang, Chang Jun, Gu Wanlong (2009) Climate impact assessment of Henan in 2005. (2006-1-24) [2009-6-5]. http://jz.hnnw.net/zyt/qhpj/05hn.html
Xie J, Ying S, Cong X (2008) The whole-year service scheme and operational system development of agrometeorology[J]. J Anhui Agric Sci 36(32):14241–14242
Xin J, Xu X (2007) The main meteorological calamity and countermeasures of China[J]. Catastrophology 22(3):85–89
Xinhua Net (2009a) Strong sand storm attacking North China, (2006-4-19) [2009-6-5]. http://news.xinhuanet.com/politics/2006-04/19/content_4444861.htm
Xinhua Net (2009b) Over ¥100 billion economic loss for China due to meteorological disaster in each year. (2007-6-19) [2009-6-5]. http://news1.cnfol.com/070619/197,1800,170373, 00.shtml
Xinhua Net (2009c) China Meteorological Administration: informing the public of the sudden disaster information timely. (2009-7-6-7) [2009-6-9]. http://news.xinhuanet.com/newscenter/2009-06/07/content_11504379.htm
Xinhua Net (2009d) Hebei presenting the first key meteorological disaster emergency plan. (2009-1-9) [2009-6-9]. http://www.law-star.com/cacnew/200901/225028990.htm

Yang S, Zhang M, Yang Y (2007) Agriculture meteorological disaster analysis of China in recent 10 years [J]. Acta Agricult Jiangxi 19(7):106–108

Yi D (2007) Research and application of agricultural yield forecast technique in China[J]. Arid Meteorol 25(2):13–16

Zhang Y, He W, Li S (1991) An outline of China agricultural meteorological disasters[M]. Meteorological Publishing House, Beijing (in Chinese)

# Chapter 34
# Comparison of Sensible Heat Flux as Measured by Surface Layer Scintillometer and Eddy Covariance Methods Under Different Atmospheric Stability Conditions

**G.O. Odhiambo and M.J. Savage**

**Abstract** Surface fluxes of sensible heat and latent energy are important in many atmospheric processes and can be measured with reasonable accuracy over homogeneous surfaces. Direct measurements of turbulent fluxes such as sensible heat and latent energy, which are components of the shortened energy balance, are usually achieved by the eddy covariance (EC) method, which is considered the standard method for sensible heat and latent energy flux measurement and basically involves the use of single-point measurements from EC instruments mounted on a mast. However, the application of the EC method is often problematic. In this paper, results of the EC and surface layer scintillometer (SLS) estimations of sensible heat flux for different atmospheric stability conditions, namely, unstable, and near-neutral atmospheric stability conditions are presented. The aim of the study was to assess sensible heat flux measurements obtained by SLS, which relies on Monin-Obukhov Similarity Theory (MOST) and therefore assumes stationarity and homogeneity of the surface where measurements are taken with those obtained using the EC method for different stability conditions and different times (seasons) of the year. Statistical analysis of the data reveals a seasonal trend in the sensible heat flux, $F_h$ comparisons between the two measurement methods. There seems to be better agreement in the measurements obtained by the two methods, as noted by higher correlation coefficients and t-values, obtained in warm summer period from November to December during unstable atmospheric conditions while lower agreement in the values are recorded in the cold months of June and August. Also noted is a slight bias in the SLS measurement of $F_h$ compared to the EC measurements.

G.O. Odhiambo (✉)
Department of Geography and Urban Planning, College of Humanities and Social Sciences, United Arab Emirates University, P. O. Box 17771, Al Ain, United Arab Emirates
e-mail: godhiambo@uaeu.ac.ae

M.J. Savage
SPAC Research Unit, Agrometeorology Discipline, School of Environmental Sciences, University of KwaZulu-Natal, P/Bag X01, Scottsville 3209, Pietermaritzburg, Republic of South Africa

S.D. Attri et al. (eds.), *Challenges and Opportunities in Agrometeorology*,
DOI 10.1007/978-3-642-19360-6_34, 

The bias in SLS $F_h$ measurements is noticed for unstable atmospheric conditions whereas the EC method seems to record slightly greater values when the atmospheric condition is near-neutral. However the agreement between the $F_h$ values measured by the two measurement methods is still good. The agreement is even more remarkable considering that the EC method is a point measurement method depending on the covariance between $w$ and sonic temperature $T$ whereas the SLS method is an areal-averaging method that depends on MOST and therefore also on $z-d$. The inner scale length $l_o$ values measured by the SLS method are larger in the evening and night-time when the atmospheric condition is stable than during the daytime when the atmosphere is mainly unstable. This can be attributed to greater turbulent mixing during the unstable atmospheric condition compared to low turbulent mixing when the atmosphere is mainly stable. As for the agreement in the sensible heat flux values measured by the EC and SLS methods, there is no distinct or consistent pattern. Vegetation height also seems to slightly influence the agreement in the $F_h$ measurements obtained by the two methods (EC and SLS) as is noticed from the slope values. In general, the slope values approach 1 with increasing vegetation height for both unstable and near-neutral atmospheric conditions, although there are exceptions especially for the month of November.

## 34.1 Introduction

Surface fluxes of sensible heat and latent energy are important in many atmospheric processes and can be measured with reasonable accuracy over homogeneous surfaces. Direct measurements of turbulent fluxes such as sensible heat and latent energy, which are components of the shortened energy balance, are usually achieved by the eddy covariance (EC) method, which is considered the standard method for sensible heat and latent energy flux measurement and basically involves the use of single-point measurements from EC instruments mounted on a mast. However, the application of the EC method is often problematic. The necessary sensors for wind speed, air temperature and humidity must respond very quickly and at the same time must not show noticeable drift. This makes them delicate, expensive and in many cases difficult to calibrate. However more serious is the fact that flow distortions by the sensor, mast, etc., as well as horizontal misalignments often cause significant errors (Wyngaard 1981).

In addition, there are statistical problems due to the fact that temporal co-spectra, measured at a fixed local sensor extend to very low frequencies. To achieve acceptable significance often demands averaging periods of tens of minutes (Hill 1997; Thiermann and Grassl 1992; Anandakumar 1999). Such long averaging periods reduce the temporal resolution and conflict with the requirement of atmospheric stationarity within the averaging periods. The EC method for sensible heat flux measurement is also dependent on humidity through the speed of sound effect on the sonic-measured air temperature (Lumley and Panofsky 1964).

Turbulent fluxes play important roles in governing the transfer processes in the lower layers of the atmosphere and in fact are the basic parameters, which are

directly related to thermal and mechanical turbulence in the atmosphere and characterise the turbulence condition of the atmosphere in terms of 'atmospheric stability' (Daoo et al. 2004). Atmospheric stability, via $\zeta = (z-d)/L$, is one of the crucial parameters used as an input parameter in atmospheric dispersion or air quality models.

Scintillometry is a relatively new technique used for measuring turbulence fluxes such as sensible heat and momentum flux measurements within the surface and/or boundary layer of the atmosphere. The scintillometer method offers the ability to make path-averaged measurements of turbulent fluxes of sensible heat and momentum. It provide a different approach from the point measurement methods, such as Bowen ratio energy balance (BREB) and EC methods, to obtaining more spatially-representative sensible heat flux measurements over a given land surface. Because $F_h$ is derived from the line integral of the structure parameter of the refractive index, an average of $F_h$ is obtained over an area formed by the path-length of the beam of the scintillometer and an area in the upwind direction (de Bruin et al. 1995; Hill 1997).

Atmospheric stability characterises atmospheric turbulence quantitatively. Turbulence is an inherent property of the atmosphere which causes diffusion of such scalar quantities as sensible heat flux (Daoo et al. 2004). The extent of the diffusion depends on the intensity of atmospheric turbulence and hence it is related to atmospheric stability (Kanda et al. 2002). The atmospheric stability condition also partly influences the footprint for turbulence flux measurements. Sensible heat flux $F_h$ is related to the atmospheric stability and the scintillometer method provides direct measurement of $F_h$, is ideal for evaluating atmospheric stability through the measurement of the Obukhov length $L$.

In this study, results of the EC and surface layer scintillometer (SLS) estimations of sensible heat flux for different atmospheric stability conditions, namely, unstable, and near-neutral atmospheric stability conditions are presented. The aim of the study was to assess sensible heat flux measurements obtained by SLS, which relies on Monin-Obukhov Similarity Theory (MOST) and therefore assumes stationarity and homogeneity of the surface where measurements are taken with those obtained using the EC method for different stability conditions and different times (seasons) of the year. No published work (known to the author) has been carried out comparing EC measurements of sensible heat with measurements with the SLS ones, in terms of atmospheric stability. This work therefore attempts to fill this gap.

## 34.2 Theory

### *34.2.1 Scintillometry*

A scintillometer is an optical instrument that consists of a light/radiation source (transmitter) and a receiver. The receiver consists of a highly sensitive detector and a data acquisition system that can register the reduction in the intensity of

fluctuations of a beam after propagation through a turbulent medium from which the different meteorological parameters are deduced. Scintillometers have been widely used for measuring turbulent flux of sensible heat and momentum (e.g. Thiermann 1992; Thiermann and Grassl 1992; Green et al. 1994; de Bruin and Meijninger 2002; Hartogensis et al. 2002; Kanda et al. 2002). The use of the scintillometer method for the measurement of turbulent flux is based on the fact that the refractive index structure parameter $C_n^2$ ($m^{-2/3}$) measured directly by the scintillometer can be related to the structure function parameter of temperature $C_T^2$ ($K^2\ m^{-2/3}$) from which sensible heat flux $F_h$ ($W\ m^{-2}$) is derived. A beam is transmitted over a path and the fluctuations in the beam intensity at the receiver are analysed to give the variations in the refractive index along the path. Specifically, the turbulent intensity of the refractive index of air can be expressed by $C_n^2$ defined by Thiermann and Grassl (1992) as:

$$C_n^2 = \frac{n(r_1)^2 - n(r_2)^2}{r_{12}^{2/3}} \tag{34.1}$$

where $n(r)$ is the refractive index of air at location $r$ and the distance $r^{12}$ is between $r_1$ and $r_2$, the so called inner scale of turbulence (marks the transition between the inertial and viscous dissipation range of eddy sizes and is of the order of 5–10 mm) and the outer scale (dominant inhomogeneities which are of the order of the height of the beam above the surface).

The intensity fluctuations are caused by inhomogeneities in the refractive index of air, which are due to turbulent eddy motions along the scintillometer path. The transmitter emits a beam with a known wavelength. At a known horizontal distance from the beam source, the intensity fluctuations (expressed as $C_n^2$) at the receiver that are caused by the turbulent eddies are analysed. These eddy motions are generated by air temperature and atmospheric humidity fluctuations, and can be regarded as a collection of converging and diverging lenses focusing and defocusing the scintillometer beam. Because the measured variance of the logarithm of the signal intensity fluctuations is a measure of the turbulent behaviour of the atmosphere, it can indirectly be related to the transport of certain quantities such as sensible heat, latent energy and gases.

By emitting a beam with a specific wavelength through the atmosphere over a horizontal path, the intensity fluctuation can be observed at the receiver end. The intensity fluctuations are caused by turbulent temperature and humidity fluctuations and are expressed through $C_T^2$ and hence $F_h$. In the optical domain, $C_n^2$ mainly depends on temperature fluctuations in the atmosphere and only slightly on humidity fluctuations.

The distance between the transmitter and the receiver can range from tens of meters to tens of kilometers depending on the type of instrument. There are different types of scintillometers and the difference is mainly based on the size of the receiver aperture size compared to the Freznel zone (defined as, $F = \sqrt{\lambda L_{beam}}$ where $\lambda$ is the optical wavelength and $L_{beam}$ the path length), so that if the aperture

size is less than the Freznel zone, the scintillometer is classified as a small aperture scintillometer and the ones with larger aperture sizes greater than the Freznel zone are referred to as large aperture scintillometers. In this study, a surface layer (small aperture) scintillometer (SLS) (Scintec SLS40-A) which emits two parallel and differently polarised laser beams was used. This unit uses a class 3a type laser at a wavelength of 670 nm, a beam displacement distance of 2.7 mm and a detector diameter of 2.5 mm, which is a small aperture scintillometer.

### 34.2.2 Eddy Covariance

Swinbank (1951) proposed an 'eddy correlation', otherwise properly referred to as eddy covariance (EC) method to estimate vertical flux of heat and water vapour from a fully turbulent mean flow. The upward flux density of an entity is given by the covariance between the vertical wind speed and entity θ over a time interval:

$$F = \rho c_p \, \overline{covariance(w, \theta)} \tag{34.2}$$

where $F$ is the flux of the entity θ (in this case heat), $c_p$, specific heat capacity of dry air, ρ the air density and $w$ the vertical wind speed.

By definition the mean of a fluctuation should be zero (i.e. the positive and negative deviations from a mean should sum to 0), and so $\overline{w'} = 0$ (Arya 2001). Hence $w' = w - \overline{w}$ and $F = \rho \, c_p \overline{w' \, \theta'}$, where over bars represent component means and primes denote the instantaneous deviation from the mean (i.e. the effects from individual eddies).

The influence of sensor tilt or terrain irregularity can contaminate the computation of the flux by causing an apparent mean velocity (Finnigan et al. 2003). Often it is difficult to orient the vertical wind velocity sensors so that the mean vertical wind speed is zero, or at least nearly so; or find a perfectly flat experimental site. Rotation of the coordinate system of the three wind velocity components making the vertical and lateral velocity components equal zero is therefore necessary before proceeding with computation of turbulent fluxes (Turnipseed et al. 2003). Sensible heat flux is expressed as:

$$F = \rho \, c_p \overline{w' \, T'} \tag{34.3}$$

### 34.2.3 Atmospheric Stability and Obukhov Length

The Obukhov length, $L$, (m) is the height above the zero-plane displacement height $d$ at which free convection dominates over forced convection. Therefore the

**Table 34.1** Stability categories and stability parameter (Weiss 2002)

| Stratification | $\zeta = (z - d)/L$ |
|---|---|
| Stable | $\zeta > +0.05$ |
| Near-neutral | $-0.05 \leq \zeta \leq 0.05$ |
| Unstable | $\zeta < -0.05$ |

Obukhov length is a measure of the dynamic atmospheric stratification, with $L > 0$ for stable conditions and $L < 0$ for unstable conditions. Unstable conditions occur when part of the turbulence energy is generated by convection. Neutral conditions occur when the turbulence is generated by wind shear near the ground with convection providing no energy. Stable conditions occur when part of the turbulence energy is consumed by vertical motions. The turbulence persists in so far as the mechanical production equals the sum of consumptions (Weiss 2002).

The Obukhov length is calculated using:

$$L = \frac{T}{kg} . \frac{\rho c_p}{F_h} . u_*^3 \tag{34.4}$$

Monin and Obukhov (1954) where $T$ is the air temperature (K), $k = 0.4$ is von Karman's constant, $g$ the acceleration due to gravity, $F_h$ the sensible heat flux and $u_*$ is the friction velocity. The non-dimensional stability parameter $\zeta$ is calculated by dividing the measurement height relative to $d$ by $L : \zeta = (z - d)/L$. The calculated stability parameter is then used to divide data into the three atmospheric stability categories as shown in Table 34.1. In this study, data for two stability categories, namely unstable and near-neutral (mainly daytime data), were used in the analysis since the night-time (stable atmospheric condition) results are not always reliable for either methods (EC and SLS) due to mist and/or condensation of water on the sensors.

Statistical analysis of the sensible heat flux data obtained by the EC and SLS methods was then carried out for each of the stability categories to compare the performance and agreement in measurement for the two methods. Most of the published work involving use of the SLS is only for short periods and does not focus on the estimation of sensible heat by the EC and SLS under different atmospheric stability conditions (Table 34.1).

## 34.3 Experimental Details

Measurements of energy flux and weather variables were at a mixed grassland community site in Ashburton, Pietermaritzburg, South Africa. This was part of a research study using EC and SLS methods to estimate sensible heat and latent energy flux. The data analysed here resulted from measurements carried out from

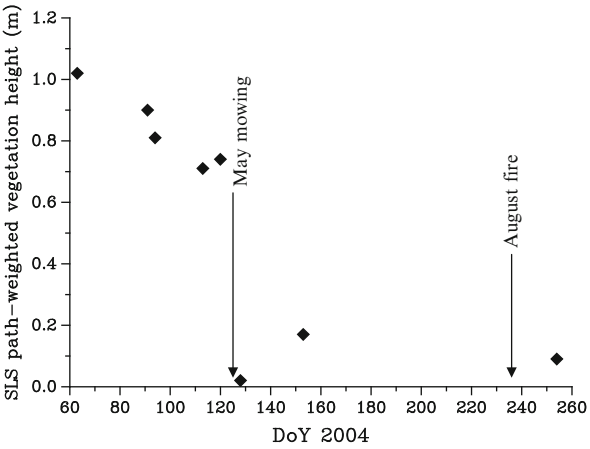


**Fig. 34.1** SLS beam path-weighted vegetation height. Between DoY 152 to 240, the vegetation height remained low

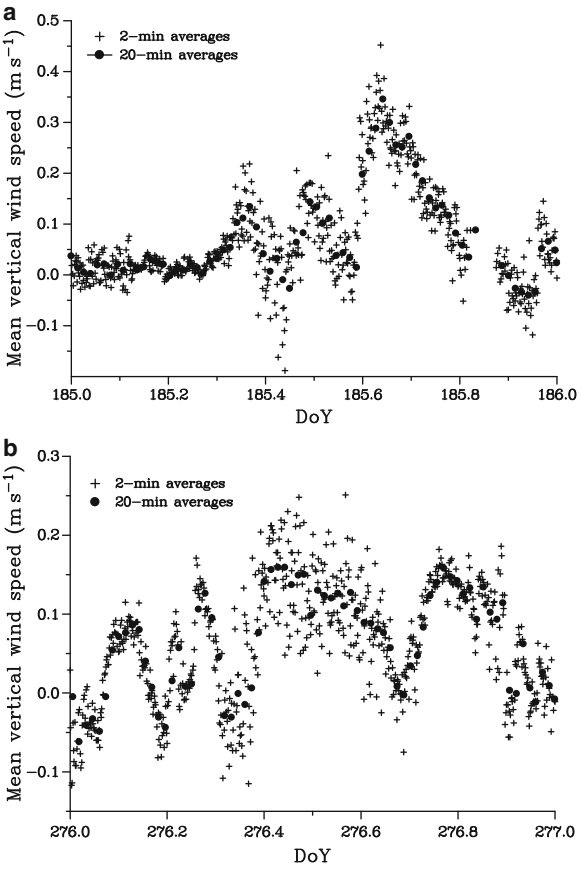


**Fig. 34.2** Two- and 20-min vertical wind speed obtained by EC for (**a**) DoY 185, and (**b**) DoY 276

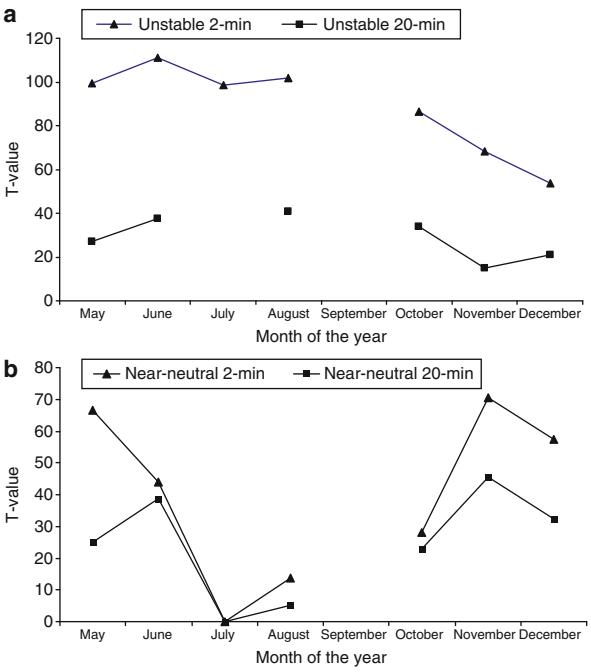


**Fig. 34.3** t-test values obtained from an analysis of $F_h$ measurements by the EC and SLS methods for the (**a**) unstable conditions, and (**b**) near-neutral conditions for the different months spanning different seasons

March to December 2004, spanning all the seasons in a year. Different methods were used for the determination of sensible heat flux namely: EC, SLS and an energy balance system for the determination of net irradiance and soil heat flux.

A dual-beam scintillometer (SLS40-A, Scintec Atmosphärenmessetechnik, Tübingen, Germany), operating at a frequency of 1 kHz, was set up at a height of about 1.68 m above the ground surface and the path length between the transmitter and receiver units was 101 m. The sensor height was referenced to the zero-plane displacement height $d \approx 2/3 \times h$ where $h$ is the vegetation height. Vegetation height along the beam-path was measured using a tape measure in metres.

The Scintec SLSRUN software together with the instrument makes online measurements of the refractive index structure parameter $\left(C_n^2\right)$, the structure function constant of temperature $\left(C_T^2\right)$ the inner scale length (lo, mm), the kinetic energy dissipation rate (ε, $m^2\ s^{-3}$), the sensible heat flux ($F_h$), and the Obukhov length ($L, m$). Two-minute averages of all the above parameters were stored on a computer for further analysis. Scintillometer data were rejected if lo was less than 2 mm and the percentage error free data less than 25%.

An EC system together with the energy balance system was installed approximately midway of the SLS path length and at a height of 2 m above the soil surface. A three-dimensional sonic anemometer (SWS-211/3 V, Applied Technologies, Boulder, Colorado, USA), was used as an EC system to measure the sensible heat

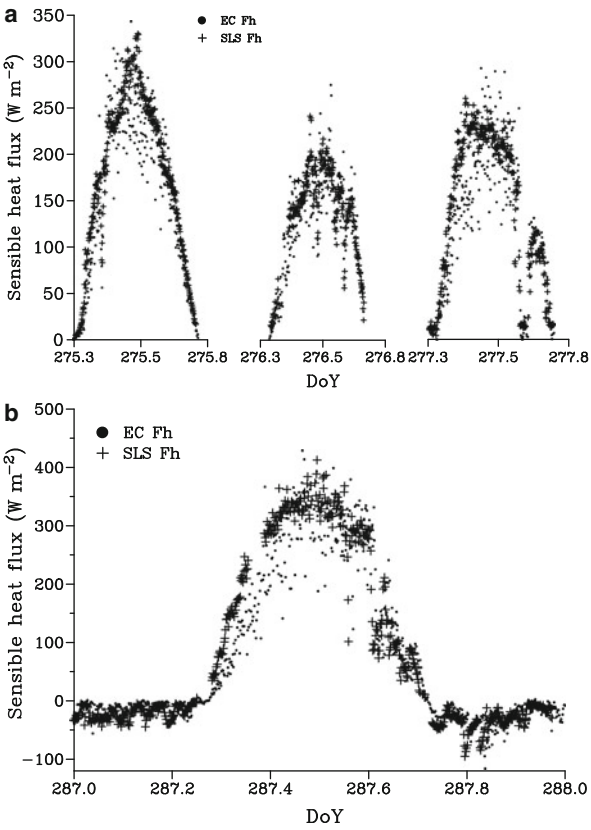


**Fig. 34.4** Examples of diurnal plot of 2-min sensible heat flux as measured by EC and SLS methods for (**a**) DoY 275 to 277, and (**b**) DoY 287

flux. Measurements of the three wind speed components and sonic temperature were performed every 0.1 s (frequency of 10 Hz) and 2-min turbulent fluxes were calculated from the covariance between vertical wind speed and sonic temperature using a 23X datalogger (Campbell Scientific, Logan, USA).

Net irradiance was measured at the site using a net radiometer (model Q*7.1, Radiation and Energy Balance Systems, (REBS), Seattle, Washington, USA). Soil heat flux was determined using soil heat flux plates (model HFT-3, REBS) buried at a depth of 0.08 m and a system of parallel thermocouples at 0.02 and 0.06 m used to calculate the soil heat flux stored above plates. The volumetric soil water content for the 0- to 0.06-m soil layer was measured using a frequency domain reflectometer (ThetaProbe, model ML2x, Delta-T Devices, Cambridge, UK).

Two-minute sensible heat flux data obtained using EC and SLS methods were then compared for the various stability categories as outlined in Table 34.1. Correlation analyses and t-tests were carried out to asses how the sensible heat flux values obtained by the EC and SLS methods compare for the different periods/seasons.

## 34.4 Results and Discussion

In this section, a comparison of the sensible heat flux measured by the EC and SLS methods for the unstable and near-neutral atmospheric stability conditions are presented and discussed. Brief discussions on the diurnal variations of $l_o$ as well as the influence of vegetation height on sensible heat flux measurements are also presented.

Only daytime sensible heat flux data were used in the analysis since the sensible heat flux measurements were mainly being used to estimate evaporation and this happens mainly during the day. The comparison of the EC and SLS methods, mainly performed to get an understanding about the performance of the SLS system with respect to the widely-used EC method, was therefore restricted to two atmospheric stability conditions, namely unstable and near-neutral as is already explained in Sect. 34.3. Real-time coordinate rotations for the EC measurements

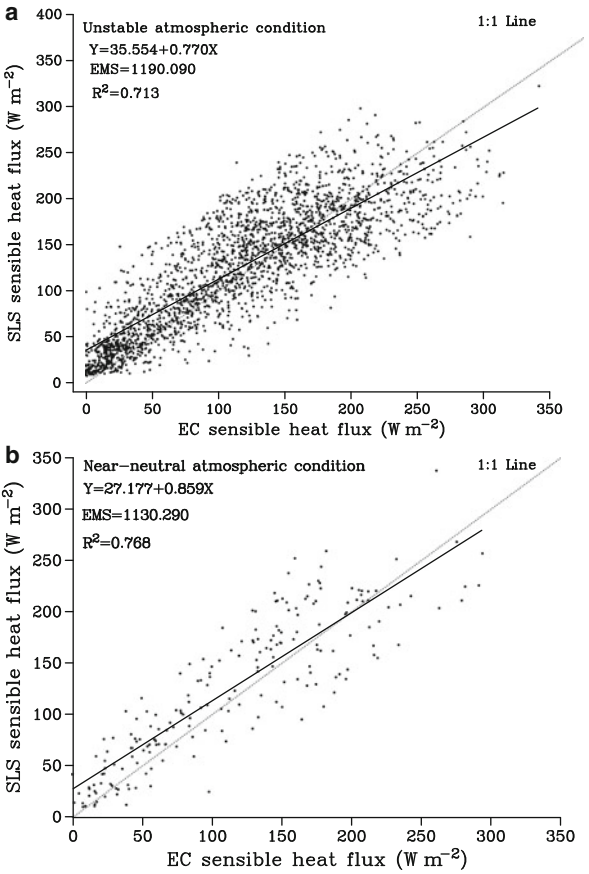


**Fig. 34.5** Correlation of EC and SLS 2-min sensible heat flux for (**a**) stability parameter $\zeta < -0.05$ (unstable), and (**b**) stability parameter $\zeta$ between $-0.05$ and 0.05 (near-neutral) for the month of May

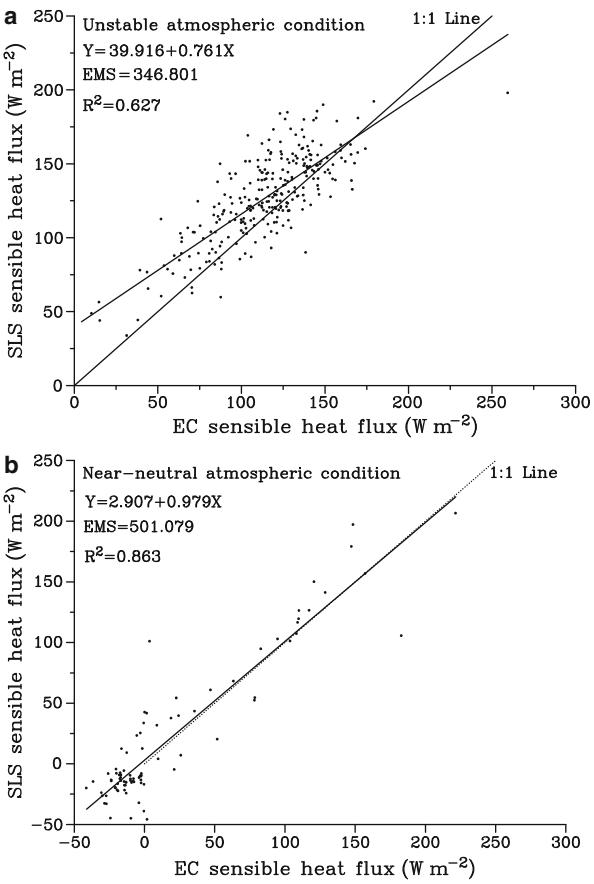


**Fig. 34.6** Correlation of EC and SLS 20-min sensible heat flux for (**a**) stability parameter $\zeta < -0.05$ (unstable), and (**b**) stability parameter $\zeta$ between $-0.05$ and 0.05 (near-neutral) for the month of May

of the three wind velocity components namely $u$, $v$ and $w$ was not done due to resource limitations.

The 23X datalogger used for storing the EC data at the research site could not store the raw data needed to do coordinate rotation and we also did not have a laptop permanently connected to the datalogger which could have been used for storing the raw data, and performing the necessary rotations.

Results for both 2- and 20-min averages of sensible heat flux measurements are presented. In some cases there were only a few data points for the time periods chosen. In most of these cases the problem was due to the missing friction velocity data from the EC method and hence the Obukhov length could not be calculated. The lack of $u_*$ data from the SLS measurements due to error in measurements for the coinciding periods also restricted the data that could be compared to the EC ones as well.

In Fig. 34.1, the path-weighted vegetation height is shown. The vegetation height varied with season and maintenance activities at the site such as mowing

which takes place in the months of May and August each year and burning which is carried out in mid-August. The weighted vegetation height at the site for the research period varied from 1.02 to 0.02 m. The effective measurement height of the SLS was 1.68 m.

The 20-min average data results in loss of a lot of data points and therefore only few data are available for analysis. A comparison of the 2- and 20-min averages of the vertical wind speed was therefore carried out to check if using 2-min data would be good enough for comparison with the SLS data. Example of plots of 2- and 20-min averages of the vertical wind speed ($\overline{w}$) measured by the EC method are shown in Fig. 34.2.

As is shown in Fig. 34.2, $\overline{w}$ deviates around 0 m s$^{-1}$, with the data points falling between −0.17 and 0.45 m s$^{-1}$ (Fig. 34.2a) (DoY 185, 2004) and for DoY 276, 2004, the $\overline{w}$ data range is between −0.12 and 0.26 m s$^{-1}$ (Fig. 34.2b). As can be seen from Fig. 34.2, both 2 and 20-min $\overline{w}$ averages deviate from 0 m s$^{-1}$ with the

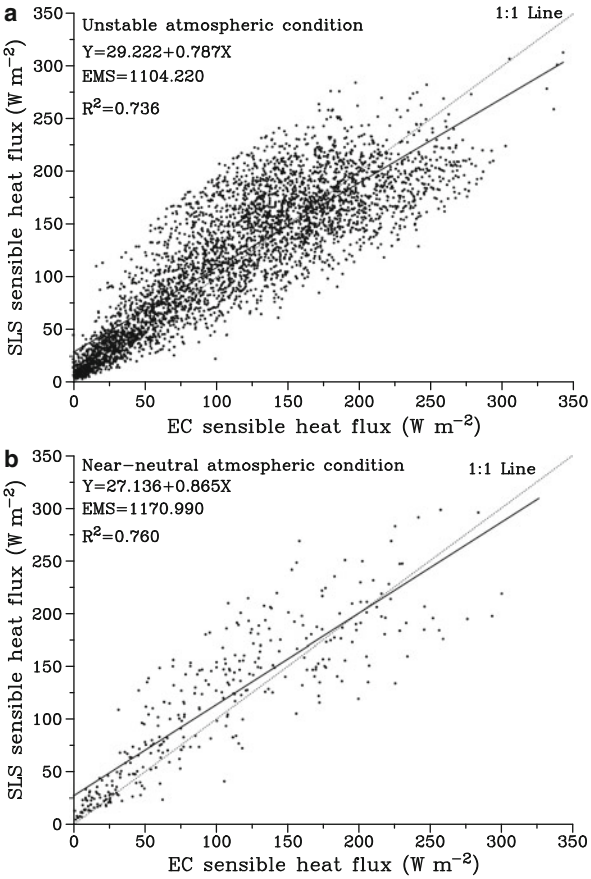


**Fig. 34.7** Correlation of EC and SLS 2-min sensible heat flux for (**a**) stability parameter $\zeta < -0.05$ (unstable), and (**b**) stability parameter $\zeta$ between −0.05 and 0.05 (near-neutral) for the month of June

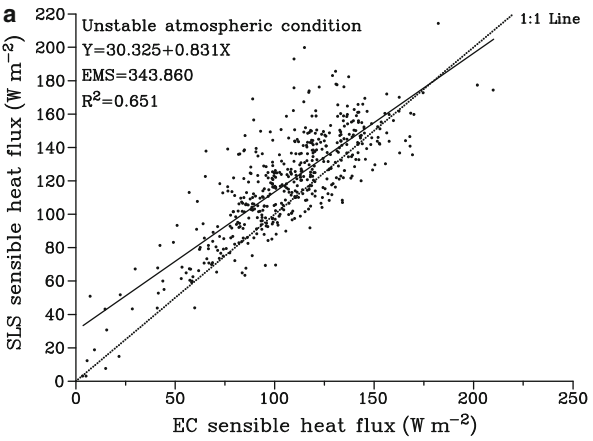


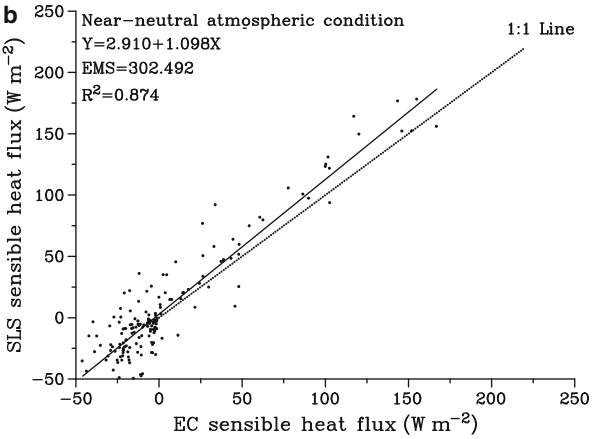


**Fig. 34.8** Correlation of EC and SLS 20-min sensible heat flux for (**a**) stability parameter $\zeta < -0.05$ (unstable), and (**b**) stability parameter $\zeta$ between $-0.05$ and 0.05 (near-neutral) for the month of June

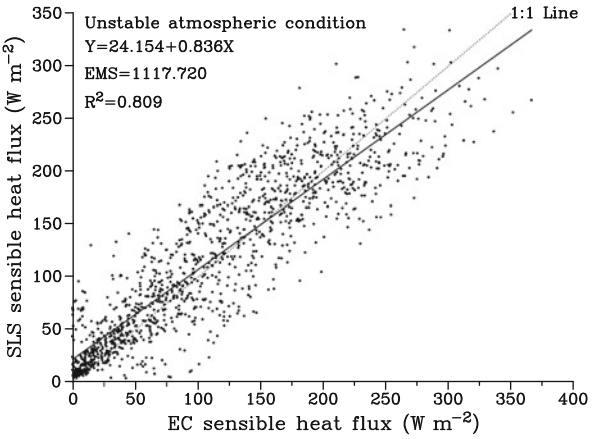


**Fig. 34.9** Correlation of EC and SLS 2-min sensible heat flux for stability parameter $\zeta < -0.05$ (unstable) for the month of July

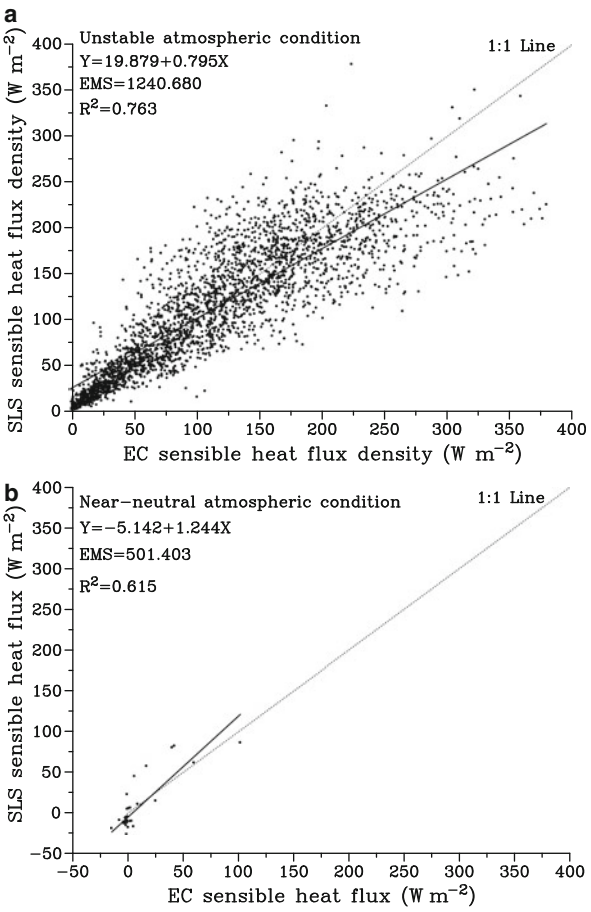


**Fig. 34.10** Correlation of EC and SLS 2-min sensible heat flux for (**a**) stability parameter $\zeta < -0.05$ (unstable), and (**b**) stability parameter $\zeta$ between $-0.05$ and 0.05 (near-neutral) for the month of August

same trend. Considering that some of the EC data are averaged out for 20-min averages, 2-min averages of EC data were used in the analysis.

In Fig. 34.3, the t-test values relating to differences between corresponding $F_h$ values as measured by EC and SLS methods under unstable conditions and near-neutral conditions spanning different seasons, are shown. Greater t-values were obtained for the unstable conditions, with the largest t-value being 110.97 obtained in the month of June.

Sensible heat flux measurement by the SLS was done within the inertial sublayer (beyond the transition layer) where MOST is valid. Linear regression analysis of the EC and SLS sensible heat flux data for the various atmospheric stability conditions as well as a t-test were used to evaluate how well corresponding values obtained by the two methods agree with each other are shown in Figs. 34.4–34.17.

In this study, 2-min averages of EC data were used in the analysis. The use of 2-min averages of sensible heat flux was based mainly on the fact that smoothening (or averaging out) of data occurs for 20-min averages of EC data whereas with 2-min average EC data, some data may be averaged out but there is still enough left from which 20-min averages are obtained. The 2-min averages of sensible heat from the SLS were then compared with the corresponding EC measurements.

A general comparison of the sensible heat flux measurements from the two methods (EC and SLS) show reasonably good agreement as shown both in the diurnal plots of sensible heat flux (Fig. 34.4) and the statistical analyses (Figs. 34.5–34.17). The EC values appear more scattered especially around midday when peak sensible heat values are recorded compared to the smoother variations of the sensible heat flux measured by the SLS.

The sensible heat flux values measured by the EC and SLS methods therefore appear more in agreement when the values are low as is the case from early morning hours until late morning and again after the midday peak as observed from the

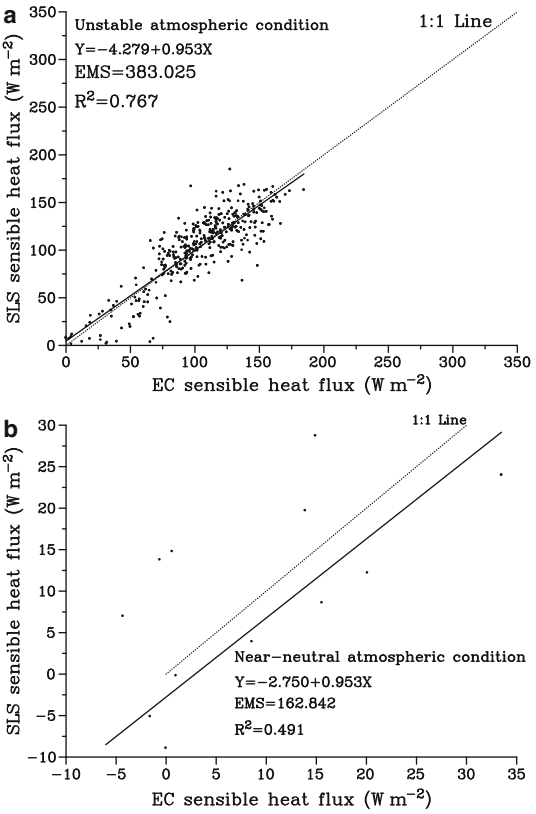


**Fig. 34.11** Correlation of EC and SLS 20-min sensible heat flux for (a) stability parameter $\zeta < -0.05$ (unstable), and (**b**) stability parameter $\zeta$ between $-0.05$ and 0.05 (near-neutral) for the month of August

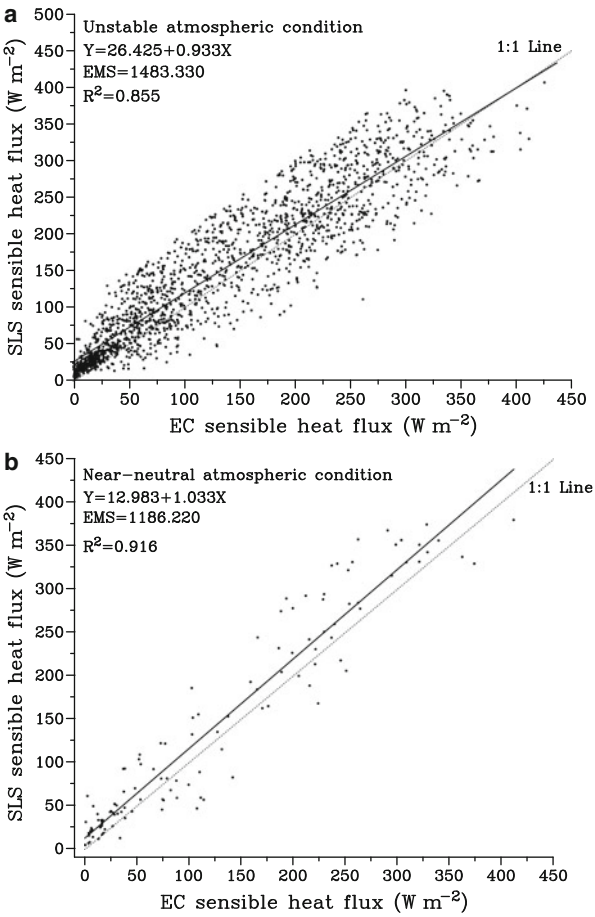


**Fig. 34.12** Correlation of EC and SLS 2-min sensible heat flux for (**a**) stability parameter $\zeta < -0.05$ (unstable), and (**b**) stability parameter $\zeta$ between $-0.05$ and 0.05 (near-neutral) for the month of October

diurnal plots as well as the regression curves where the data points appear more widely scattered around the line of best fit. There is a bias in the EC measurements as indicated by the slope values and deviation of the line of best fit from the 1:1 line (Table 34.2 and Fig. 34.3). The reason for the bias in EC measurements when the atmospheric stability condition is unstable is not known. For the unstable condition, there is a better agreement in $F_h$ values measured by EC and SLS, as denoted by greater $r^2$-values, in warm summer months of October to December while smaller $r^2$-values are obtained in colder months of June to August.

The comparison of the $F_h$ measurements by the two methods for the near-neutral atmospheric condition also show better agreement in the warm months of the year (September to December). In July and September there were very few data points since the missing friction velocity data from the EC system meant that Obukhov

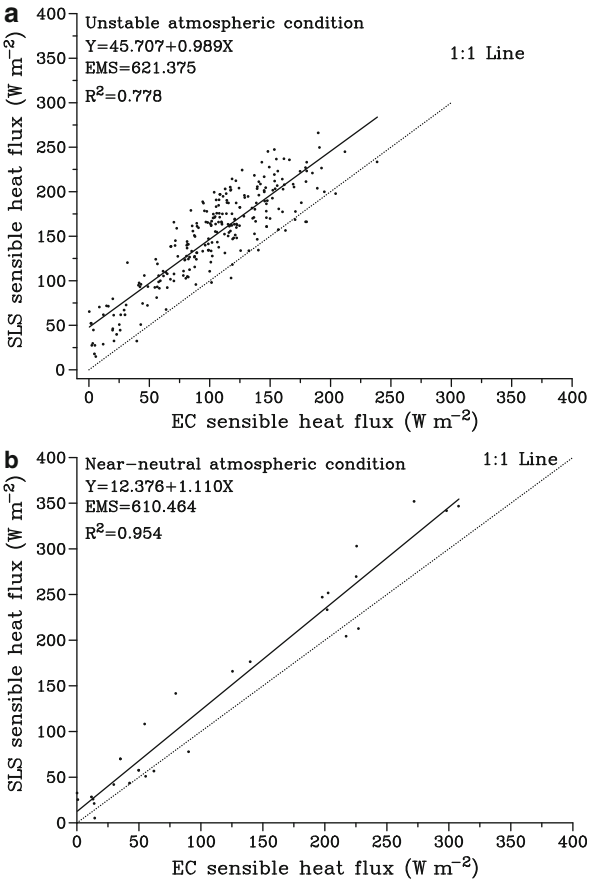


**Fig. 34.13** Correlation of EC and SLS 20-min sensible heat flux for (**a**) stability parameter $\zeta < -0.05$ (unstable), and (**b**) stability parameter $\zeta$ between $-0.05$ and 0.05 (near-neutral) for the month of October

length could not be calculated. The lack of $u_*$ data from the SLS measurements due to error in measurements for the coinciding periods also restricted the data that could be compared to the EC ones as well. This problem resulted in the reporting of only unstable condition data, for July and no comparison results for September.

There is a noticeable bias in the $F_h$ values with the SLS $F_h$ measurements greater than those measured by the EC method especially when the atmospheric condition is unstable while the EC method records slightly greater $F_h$ values when the atmosphere is near-neutral (Table 34.2 and Figs. 34.5–34.17). The bias can be observed from the regression slope as well as from the deviation of the line of best fit from 1:1 line (Figs. 34.5–34.17), although the reason for the bias is not known.

The better agreement between EC and SLS $F_h$ measurements during unstable atmospheric conditions could be explained by the fact that the increased turbulence during these periods causes greater mixing of the air and so the sensible heat flux is

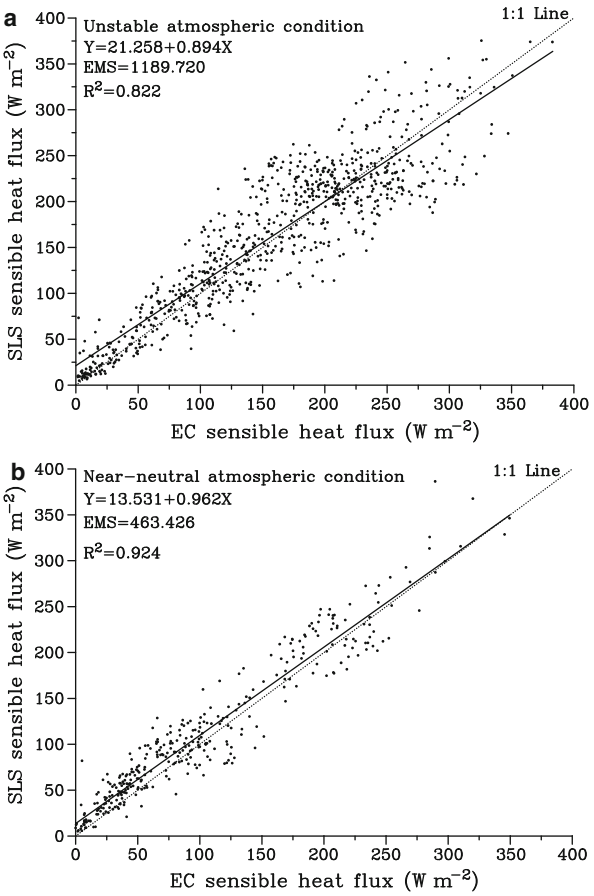


**Fig. 34.14** Correlation of EC and SLS 2-min sensible heat flux for (**a**) stability parameter $\zeta < -0.05$ (unstable), and (**b**) stability parameter $\zeta$ between $-0.05$ and 0.05 (near-neutral) for the month of November

almost uniform within the surface layer over a wider area so the SLS (giving a spatially-averaged sensible heat flux measurement) and EC (a point measurement method) measurements seem to agree well.

However, in spite of the slight bias sometimes noticed in the measurements and hence reduced correspondence in $F_h$ obtained by the two methods, the agreement in the $F_h$ obtained is generally good to excellent considering that the EC method represents a point-estimate of sensible heat flux and SLS a path-weighted estimate. The general agreement is also an indication of the correct choice of $z-d$ used for the SLS MOST calculations and that the MOST coefficients used resulted in accurate determination of sensible heat flux.

The comparison of EC- and SLS-measured sensible heat flux for a day when $l_o$ values (for part of the day) was around 2 mm (Fig. 34.18a) is also presented. On this particular day the correspondence between the EC- and SLS-measured sensible heat values was poorer as indicated by $R^2 = 0.741$, slope $= 0.896$. It can also be

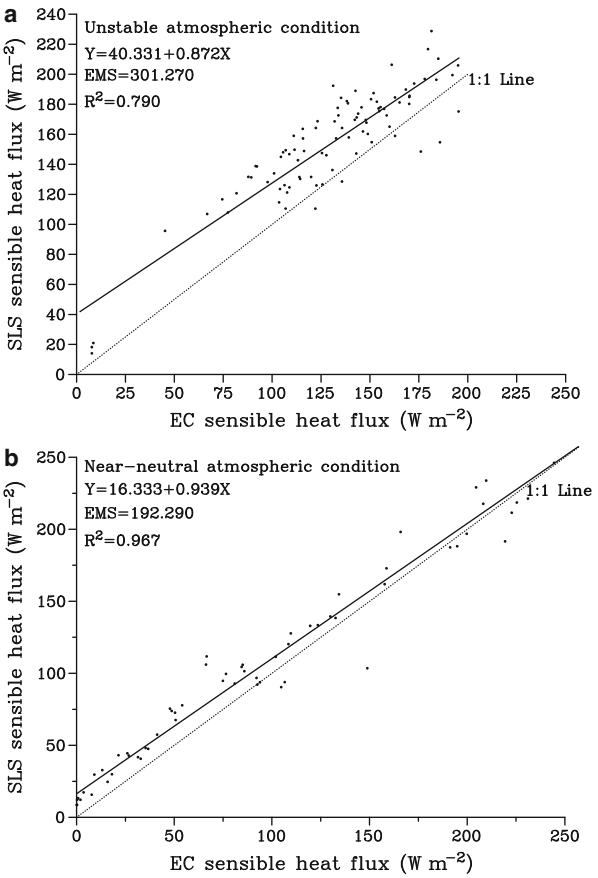


**Fig. 34.15** Correlation of EC and SLS 20-min sensible heat flux for (**a**) stability parameter $\zeta < -0.05$ (unstable), and (**b**) stability parameter $\zeta$ between $-0.05$ and 0.05 (near-neutral) for the month of November

noted from the diurnal plot of the EC and SLS sensible heat flux values for the same day (Fig. 34.18b) that for the period when $l_o$ is around 2 mm, the correspondence in the sensible heat values is less than for the period when $l_o$ values are greater than 2 mm. Around midday when $l_o$ approaches 2 mm, the sensible heat flux values measured by the EC and SLS methods appear more scattered. This can be attributed to high turbulent mixing during the unstable atmospheric condition compared to low turbulent mixing when the atmosphere is mainly stable.

Vegetation height also seems to slightly influence the agreement in the $F_h$ measurements obtained by the two methods (EC and SLS) as is noticed from the slope values (Table 34.2 and Figs. 34.5–34.17). However, this influence is not very consistent. For instance, for the 20-min $F_h$ values during the unstable atmospheric conditions, the slopes corresponding to 0.10 and 0.19 m vegetation height (short vegetation cover) are 0.953 and 0.989 respectively, which are greater than the slope values of 0.777 and 0.872 for vegetation heights of 0.43 and 0.46 m

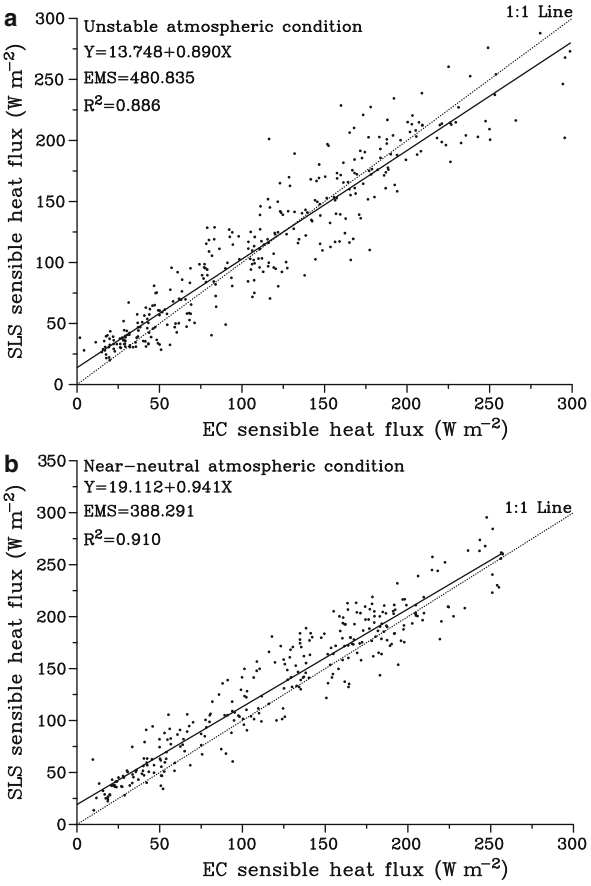


**Fig. 34.16** Correlation of EC and SLS 2-min sensible heat flux for (**a**) stability parameter $\zeta < -0.05$ (unstable), and (**b**) stability parameter $\zeta$ between $-0.05$ and 0.05 (near-neutral) for the month of December

(tall vegetation cover) respectively. On the other hand, for the 2-min averages under unstable atmospheric conditions, greater slope values are obtained for tall vegetation cover.

For vegetation heights of 0.43 and 0.46 m, slope values of 0.894 and 0.890 corresponding to tall vegetation height are obtained, whereas the slopes corresponding to shorter vegetation heights of 0.10 and 0.19 m are 0.836 and 0.795 respectively.

## 34.5 Conclusions

In this paper an analysis of the $F_h$ values measured by the two methods (EC and SLS) for different atmospheric stability conditions, unstable and near-neutral, was carried out. Also presented are the mean vertical wind speed plots as well as the

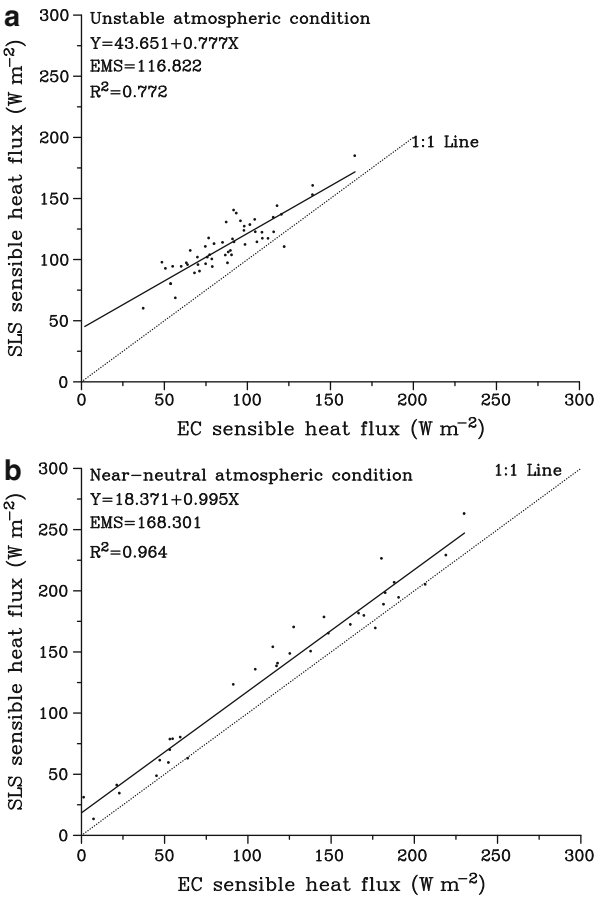


**Fig. 34.17** Correlation of EC and SLS 20-min sensible heat flux for (**a**) stability parameter $\zeta < -0.05$ (unstable), and (**b**) stability parameter $\zeta$ between $-0.05$ and 0.05 (near-neutral) for the month of December

path-weighted vegetation height. The mean vertical wind speed values measured by the EC method vary about 0 m $s^{-1}$ for most of the days, both for the 2- and 20-min averages. The 20-min averaging period results in data loss and therefore only few data were available for analysis. The 2-min average data used in the statistical analysis were good enough for comparison with the SLS data, resulting in reasonable results. The statistical analysis of the data reveals a seasonal trend in the $F_h$ comparisons between the two measurement methods. There seems to be a better agreement in the measurements obtained by the two methods, as noted by higher correlation coefficients and t-values, obtained in warm summer period from November to December during unstable atmospheric conditions while lower agreement in the values are recorded in the cold months of June and August.

Also noted is a slight bias in the SLS measurement of $F_h$ compared to the EC measurements. The bias in SLS $F_h$ measurements is noticed for unstable atmospheric conditions whereas the EC method seems to record slightly greater values

**Table 34.2** Results of correlation and t-test analysis of the sensible heat flux values obtained by SLS and EC methods for different stability conditions and different data-averaging periods. Also included in the table is the vegetation height $h_{canopy}$

| Month | Hcanopy (m)[a] | Stability condition | n | $R^2$ | t-Value | t-Table | Slope |
|---|---|---|---|---|---|---|---|
| May | 0.02 | Unstable 20-min | 278 | 0.627 | 27.202 | 1.969 | 0.761 |
| Jun | 0.17 | Unstable 20-min | 495 | 0.651 | 37.585 | 1.965 | 0.831 |
| Jul | – | Unstable 20-min | – | – | – | | – |
| Aug | 0.10 | Unstable 20-min | 390 | 0.767 | 40.807 | 1.966 | 0.953 |
| Oct | 0.19 | Unstable 20-min | 258 | 0.778 | 33.958 | 1.969 | 0.989 |
| Nov | 0.43 | Unstable 20-min | 54 | 0.772 | 15.102 | 2.007 | 0.777 |
| Dec | 0.46 | Unstable 20-min | 93 | 0.790 | 20.817 | 1.986 | 0.872 |
| May | 0.02 | Unstable 2-min | 2852 | 0.711 | 99.306 | 1.961 | 0.769 |
| Jun | 0.17 | Unstable 2-min | 3290 | 0.733 | 110.971 | 1.961 | 0.789 |
| Jul | 0.19 | Unstable 2-min | 1856 | 0.809 | 98.523 | 1.961 | 0.836 |
| Aug | 0.10 | Unstable 2-min | 2462 | 0.763 | 101.881 | 1.961 | 0.795 |
| Oct | 0.19 | Unstable 2-min | 1086 | 0.855 | 86.463 | 1.962 | 0.933 |
| Nov | 0.43 | Unstable 2-min | 829 | 0.822 | 68.162 | 1.963 | 0.894 |
| Dec | 0.46 | Unstable 2-min | 330 | 0.886 | 53.639 | 1.967 | 0.890 |
| May | 0.02 | Near-neutral 20-min | 88 | 0.863 | 25.055 | 1.988 | 0.979 |
| Jun | 0.17 | Near-neutral 20-min | 190 | 0.874 | 38.627 | 1.973 | 1.098 |
| Jul | – | Near-neutral 20-min | – | – | – | | – |
| Aug | 0.10 | Near-neutral 20-min | 15 | 0.491 | 5.054 | 2.160 | 0.952 |
| Oct | 0.19 | Near-neutral 20-min | 26 | 0.954 | 22.842 | 2.064 | 1.110 |
| Nov | 0.43 | Near-neutral 20-min | 70 | 0.967 | 45.394 | 1.995 | 0.939 |
| Dec | 0.46 | Near-neutral 20-min | 40 | 0.964 | 32.489 | 2.024 | 0.995 |
| May | 0.02 | Near-neutral 2-min | 1027 | 0.768 | 66.469 | 1.962 | 0.859 |
| Jun | 0.17 | Near-neutral 2-min | 463 | 0.760 | 43.827 | 1.965 | 0.865 |
| Jul | – | Near-neutral 2-min | – | – | – | | – |
| Aug | 0.10 | Near-neutral 2-min | 76 | 0.615 | 13.864 | 1.993 | 1.243 |
| Oct | 0.19 | Near-neutral 2-min | 68 | 0.916 | 28.031 | 1.997 | 1.033 |
| Nov | 0.43 | Near-neutral 2-min | 380 | 0.924 | 70.524 | 1.966 | 0.962 |
| Dec | 0.46 | Near-neutral 2-min | 300 | 0.910 | 57.542 | 1.968 | 0.941 |

[a]SLS measurement height for the SLS was 1.68 m. The EC method measurement height was 2 m

when the atmospheric condition is near-neutral. However the agreement between the $F_h$ values measured by the two measurement methods is still good. The agreement is even more remarkable considering that the EC method is a point measurement method depending on the covariance between $w$ and sonic temperature $T$ whereas the SLS method is an areal-averaging method that depends on MOST and therefore also on $z–d$.

The inner scale length $l_o$ values measured by the SLS method are larger in the evening and night-time when the atmospheric condition is stable than during the daytime when the atmosphere is mainly unstable. This can be attributed to greater turbulent mixing during the unstable atmospheric condition compared to low turbulent mixing when the atmosphere is mainly stable. As for the agreement in the sensible heat flux values measured by the EC and SLS methods, there is no distinct or consistent pattern. Vegetation height also seems to slightly influence the

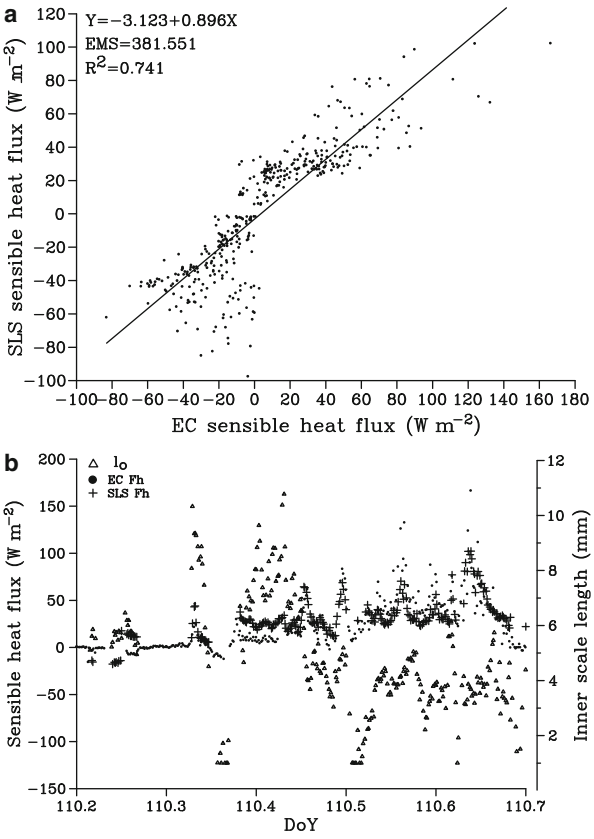


**Fig. 34.18** (**a**) Comparison of 2-min EC- and SLS-measured sensible heat flux, and (**b**) diurnal plot of the EC- and SLS-measured sensible heat flux for DoY 110. Also plotted is the diurnal variation of $l_o$ (*right-hand y-axis*)

agreement in the $F_h$ measurements obtained by the two methods (EC and SLS) as is noticed from the slope values (Table 34.2 and Figs. 34.5–34.17). In general, the slope values approach 1 with increasing vegetation height for both unstable and near-neutral atmospheric conditions, although there are exceptions especially for the month of November.

## References

Anandakumar K (1999) Sensible heat flux over a wheat canopy: optical scintillometer measurements and surface renewal analysis estimations. Agric For Meteorol 96:145–156

Arya SP (2001) Introduction to micrometeorology, 2nd edn. Academic, London, p 420

Daoo VJ, Panchal NS, Faby S, Raj VV (2004) Scintillometric measurements of daytime atmospheric turbulent heat and momentum fluxes and their application to atmospheric stability. Exp Therm Fluid Sci 28:337–345

de Bruin HAR, Meijninger WML (2002) Displaced-beam small aperture scintillometer test. Part I: the WINTEX data-set. Bound-Lay Meteorol 105:129–148

de Bruin HAR, van den Hurk BJJM, Kohsiek W (1995) The scintillometer method tested over a dry vineyard area. Bound-Lay Meteorol 76:25–40

Finnigan JJ, Clement R, Malhi Y, Leuning R, Cleugh HA (2003) A re-evaluation of long-term flux measurement techniques – part I: averaging and coordinate rotation. Bound-Lay Meteorol 107:1–48

Green AE, McAneney KJ, Astill MS (1994) Surface-layer scintillation measurements of daytime sensible heat and momentum fluxes. Bound-Lay Meteorol 68:357–373

Hartogensis OK, de Bruin HAR, van de Weil JH (2002) Displacement-beam small aperture scintillometer test. Part II: CASES-99 stable boundary-layer experiment. Bound-Lay Meteorol 105:149–176

Hill RJ (1997) Algorithm for obtaining atmospheric surface-layer fluxes from scintillation measurements. J Atmos Oceanic Technol 14:456–465

Kanda M, Moriwaki R, Roth M, Oke TR (2002) Area-averaged sensible heat flux and a new method to determine zero-plane displacement length over an urban surface using scintillometry. Bound-Lay Meteorol 105:177–193

Lumley JL, Panofsky HA (1964) The structure of atmospheric turbulence. Wiley, New York, p 239

Monin AS, Obukhov AM (1954) Basic laws of turbulent mixing in the atmosphere near the ground. Acad Nauk 24:163–187

Swinbank WC (1951) The measurement of vertical transfer of heat and water vapour by eddies in the lower atmosphere. J Meteorol 8(3):135–145

Thiermann V (1992) A displaced-beam scintillometer for line-averaged measurements of surface layer turbulence. Tenth symposium on turbulence and diffusion. American Meteorological Society, Portland

Thiermann V, Grassl H (1992) The measurement of turbulent surface-layer fluxes by use of bichromatic scintillation. Bound-Lay Meteorol 58:367–389

Turnipseed AA, Anderson DE, Blanken PD, Baugh WM, Monson RK (2003) Airflows and turbulent flux measurements in mountainous terrain part 1. Canopy and local effects. Agric For Meteorol 119:1–21

Weiss A (2002) Determination of thermal stratification and turbulence of the atmospheric surface layer over various types of terrain by optical scintillometry. Ph.D. Thesis. Swiss Federal Institute of Technology. Zurich, p 152

Wyngaard JC (1981) The effects of probe-induced flow distortion on atmospheric turbulence measurements. J Appl Meteorol 20:784–794

# Chapter 35
# Crop Water Satisfaction Analysis for Maize Trial Sites in Makhado During the 2007/2008 Season

**M.E. Moeletsi, N.S. Mpandeli, and E.A.R. Mellaart**

## 35.1 Introduction

High variability of rainfall together with high evaporative demand impact negatively on plant growth and yield in the dryland farming areas of Limpopo Province, South Africa. Water availability to crops is the main limiting factor for optimum crop production in most areas of the country, caused by varying seasonal rainfall. Although the total seasonal rainfall amount may be sufficient, its poor distribution throughout the season is often the cause of crop failure (Barron et al. 2003). Crop water requirements depend mainly on the nature and stage of growth of the crop as well as environmental factors such as soil and climate characteristics (Taha et al. 1982; Allen et al. 1998; Sharma 2006). Water deficit during the growing period develops when the crop water requirements are not realised to an extent where the plant growth and yield are affected (Doorenbos and Kassam 1979). For good management and utilization of limited water resources in semi-arid climates, it is important to estimate crop water requirements accurately (Jabloun and Sahli 2008). This paper presents a water satisfaction analysis for dryland maize fields in the Makhado Municipality of Limpopo Province during the 2007/2008 cropping season.

M.E. Moeletsi (✉) • N.S. Mpandeli
ARC-Institute for Soil, Climate and Water, Private Bag X79, Pretoria 0001, South Africa
e-mail: moeletsie@arc.agric.za; SMpandeli@deat.gov.za

E.A.R. Mellaart
EcoLink, P.O. Box 83, Karino 1204, South Africa
e-mail: mellaart.e@soft.co.za

S.D. Attri et al. (eds.), *Challenges and Opportunities in Agrometeorology*,
DOI 10.1007/978-3-642-19360-6_35, 

## 35.2 Materials and Methods

The simple water balance model incorporated in INSTAT software was used in the assessment of water requirements of maize for different hypothetical planting dates (INSTAT 2007) in three different trial sites in the Makhado Municipality (Table 35.1). To obtain the crop water requirements, crop coefficients (Kc) together with reference evapotranspiration (ETo) were used at different growth stages (Doorenbos and Pruitt 1977; Sharma 2006). The Water Requirement Satisfaction Index (WRSI) model was run using dekadal rainfall, evapotranspiration, soil water-holding capacity and crop coefficients as inputs. Dekadal rainfall was obtained from the observed rainfall at the trial sites while evapotranspiration was estimated using data from the nearest automatic weather stations which showed the highest correlation with daily rainfall. Soil water-holding capacity was obtained from the soil analysis results. With the sites showing less variation in evapotranspiration during the growing season, the crop coefficients were kept constant for all the hypothetical planting dates. The life-cycle was taken as 12 dekads/120 days because the maize variety (ZM423) that was planted at the trial sites takes 100–120 days to mature. The WRSI was determined from the onset of rains (3rd dekad of September 2007) to the 1st dekad of February 2008, representing 14 different planting dates. This was done to see how the WRSI will differ at different planting dates compared with the actual planting date of the 3rd dekad of November.

## 35.3 Result and Discussion

Dekadal rainfall recorded at the trial sites (Fig. 35.1) shows a clear onset of rains in the 3rd dekad of September 2007 with a great variation of rainfall from station to station. For the Mashamba trial site (Fig. 35.2), the WRSI ranged from 29 to 99% with the WRSI for the 2nd dekad of September to the 1st dekad of November being over 75%. Seasonal rainfall (cumulative rainfall for 12 dekads) at Mashamba decreased gradually with the first four planting dekads showing seasonal rainfall exceeding the crop water requirements (Fig. 35.2). In addition the number of water deficits of more than 10 mm increased gradually from early planted maize to late planted maize. At Makhitha (Fig. 35.3) the WRSI ranged from 17 to 75% with the highest indices of 65% and 75% being obtained in the 3rd dekad of September and 1st dekad of October 2007, respectively. Here it was only the first 2 dekads which accumulated seasonal rainfall exceeding the estimated crop water requirements.

**Table 35.1** Geographical information for the three trial sites

| Village | Lat | Long | Alt (m) |
|---|---|---|---|
| Mashamba | −23.232480 | 30.180150 | 595 |
| Tshivhuyuni | −23.211160 | 30.106360 | 622 |
| Makhitha | −23.048900 | 29.668920 | 843 |

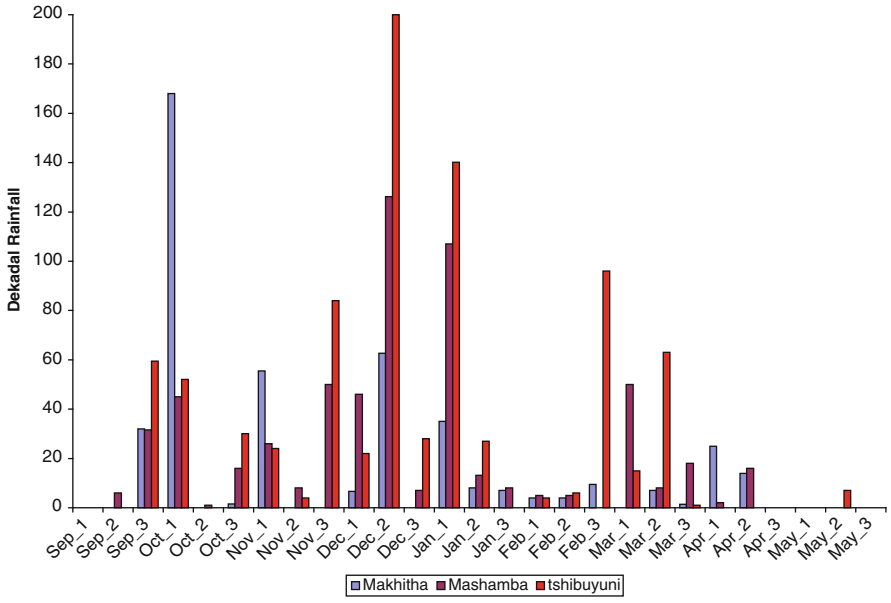


**Fig. 35.1** Dekadal rainfall for Makhitha, Mashamba and Tshivhuyuni from September 2007 to May 2008

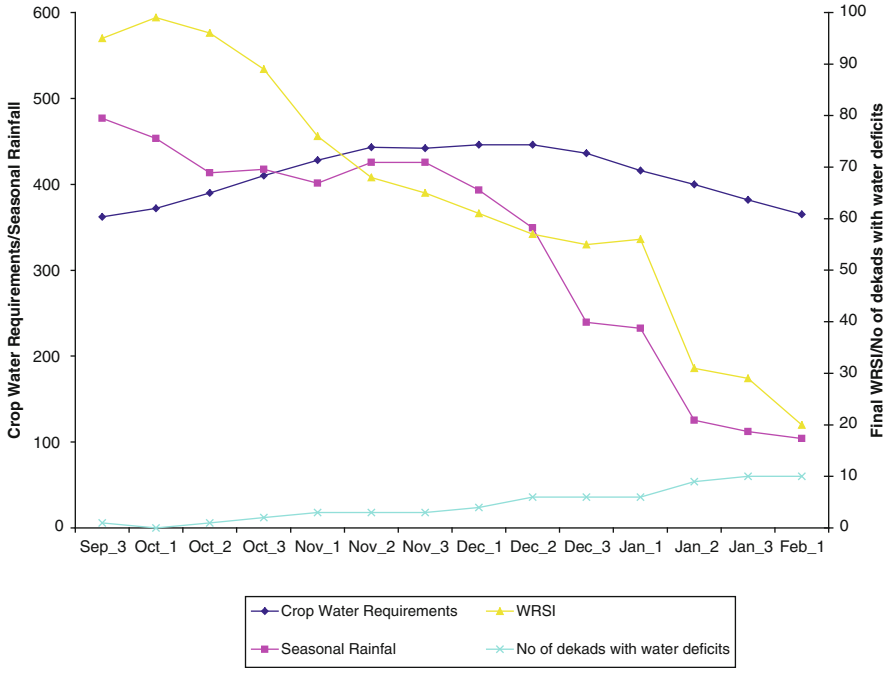


**Fig. 35.2** Mashamba crop water requirements, seasonal rainfall and water deficit dekads for different planting dekads

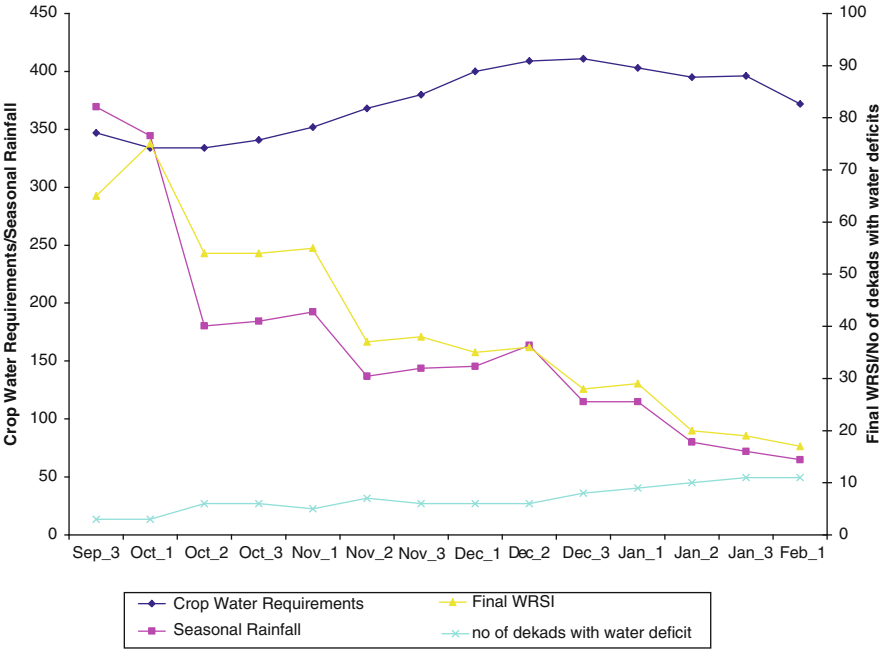


**Fig. 35.3** Makhitha crop water requirements, seasonal rainfall and water deficit dekads for different planting dekads

Water deficits of 10 mm or more were obtained in over 5 dekads for the 12 out of 14 planting dekads. At Tshivhuyuni (Fig. 35.4) the WRSI ranged from 51 to 97% with an index of over 75% from the 2nd dekad of September to the 1st dekad of November 2007. Seasonal rainfall for Tshivhuyuni exceeds the crop water requirements in 9 out of the 14 planting dekads while the water deficits of 10 mm or more showed a frequency exceeding 5 dekads in the last planting dekads. The actual planting dates were 22 November 2007 for both Makhitha and Mashamba and 17 January 2008 for Tshivhuyuni. The total water requirements up to maturity of the maize crop were 443, 368 and 400 mm for Mashamba, Makhitha and Tshivhuyuni, respectively, while the cumulative rainfall was 400, 475 and 212 mm, respectively. The WRSI values for Makhitha, Mashamba and Tshivhuyuni corresponding to their respective planting dates are 65.3%, 37.2% and 53.3%, respectively.

## 35.4 Conclusions

The results of the WRSI show that, in the 2007/2008 cropping season, early planting at all three trial sites would have resulted in better yields. This is supported by high seasonal rainfall and low frequency of dekads with water deficits exceeding

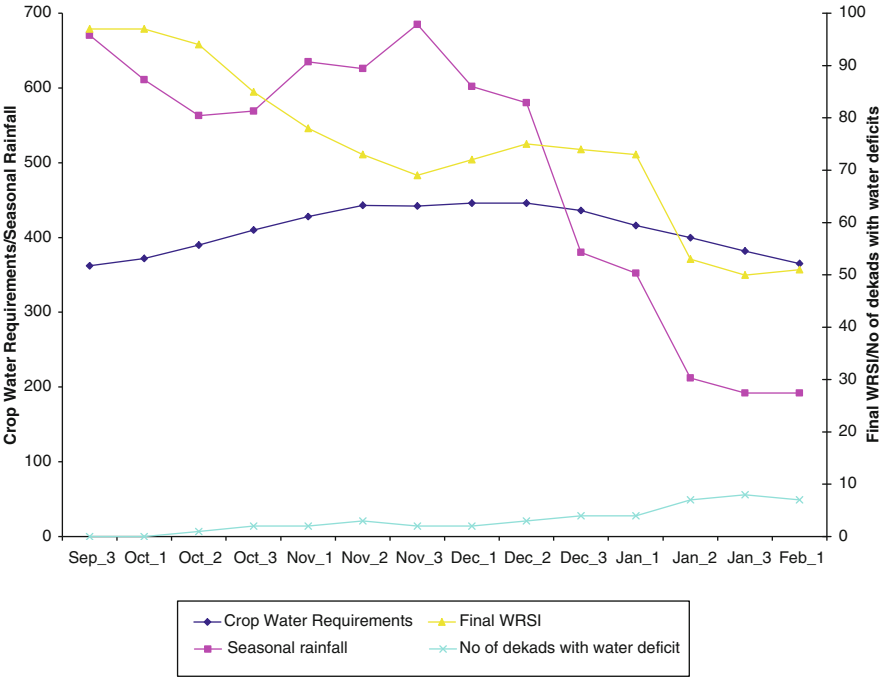


**Fig. 35.4** Tshivhuyuni crop water requirements, seasonal rainfall and water deficit dekads for different planting dekads

10 mm experienced in the months of September and October for Mashamba and Makhitha while at Tshivhuyuni the period extends to December. The WRSI at Mashamba and Tshivhuyuni was always higher than that obtained at Makhitha for all the planting dates, and thus maize was expected to perform better as evidenced by the yields of 3.1, 1.6 and 0.9 t/ha, respectively. Maize was expected to perform better in areas surrounding Tshivhuyuni and marginally at Mashamba, while at Makhitha it was expected to fail when using the WRSI. However, long-term analysis of the WRSI at these sites is crucial to determine the planting dates with the least water deficits to help farmers alleviate the impacts of drought.

**Acknowledgements** We thank the Government of France (through SADC) for funding the Response Farming project, as well as the Limpopo Provincial Department of Agriculture and all the farmers for their involvement in the project.

## References

Allen RG, Pereira LS, Raes D, Smith M (1998) Crop evapotranspiration: guidelines for computing crop water requirements. FAO irrigation and drainage paper 56. Rome, Italy

Barron J, Rockstrom J, Gichuki F, Hatibu N (2003) Dry spell analysis and maize yields for two semi-arid locations in east Africa. Agric For Meteorol 117:23–37

Doorenbos J, Kassam AH (1979) Yield response to water. FAO irrigation and drainage paper 33. Rome, Italy

Doorenbos J, Pruitt WM (1977) Guidelines for predicting crop water requirements. FAO irrigation and drainage paper 24. Rome, Italy

INSTAT (2007) Instat software. Available at http://www.ssc.rdg.ac.uk/software/download.html, Accessed on 23 July 2008

Jabloun M, Sahli A (2008) Evaluation of FAO-56 methodology for estimating reference evapotranspiration using limited climatic data application to Tunisia. Agric Water Manage 95: 707–715

Sharma BR (2006) Crop water requirements and water productivity: Concepts and practices. Available at http://www.waterandfood.org/gga/Lecture%20Material/BRSharma_CWR&WP.pdf, Accessed on 27 May 2008

Taha MA, Malik MNA, Chaudry FI, Makhdum MI (1982) Water requirements of cotton (Gossyium Hirsutum) sown on different dates in a monsoon climate. Agric For Meteorol 18: 209–217

# Chapter 36
# Prediction of Mungbean Phenology of Various Genotypes Under Varying Dates of Sowing Using Different Thermal Indices

**K. K. Gill, Guriqbal Singh, G. S. Bains, and Ritu**

**Abstract** A field experiment was conducted at Punjab Agricultural University farm during summer 2007. The experiment was carried out with four dates of sowings, four genotypes under split plot design with three replications. Phenology and thermal requirement of mungbean genotypes were studied under varying dates of sowing. Early sown crop (10th July) consumed more number of GDD, HTU and PTU to attain physiological maturity as compared to crop sown on 20th July and 30th July, which were at par with each other. While crop grown during 10th of August acquired lowest heat units hence resulted in low yield. Heat use efficiency was also characterized for production of biomass and seed yield. Among various mungbean genotypes viz. SML 668, ML 818, PAU 911 and ML 1299, the genotype ML-1299 resulted in higher HUE for both dry matter and seed yield as compared to other genotypes under study. Significant regression relationships were also worked out to obtain relationships for occurrence of different phenophases and HTU and PTU to predict mungbean phenology, DMA and seed yield. These three agroclimatic prediction models can be used to estimate crop growth and yields of mungbean.

## 36.1 Introduction

Mungbean is a short duration crop and is sensitive to photo thermal regimes. In recent years, dynamic crop simulation models are being used for predicting growth and yield of crops but these require large input data and are very complex to use.

K.K. Gill (✉) • G.S. Bains • Ritu
Department of Agricultural Meteorology, Punjab Agricultural University, Ludhiana, India
e-mail: kgill2002@gmail.com; waliadimpy@rediffmail.com

G. Singh
Department of Plant Breeding and Genetics, Punjab Agricultural University, Ludhiana, India
e-mail: singhguriqbal@rediffmail.com

S.D. Attri et al. (eds.), *Challenges and Opportunities in Agrometeorology*,
DOI 10.1007/978-3-642-19360-6_36, 

Therefore, simplified growth and yield prediction models, needing less input data, would be quite useful. Agroclimatic models based on thermal indices can meet these objectives. Temperature based agro-meteorological indices such as growing degree days (GDD) and heat use efficiency (HUE) can be quite useful in predicting growth and yield of crops. Growing degree days are based on the concept that real time to attain a phenological stage is linearly related to temperature in the range between base temperature ($T_b$) and optimum temperature (Monteith 1981). Attempts have been made to predict phenology (Hundal et al. 1997), leaf area index (Benbi 1994) and growth and yield (Hundal et al. 2001) of crops using thermal based indices. Thermal and photoperiodic conditions experienced by the crop during its life cycle play an important role in deciding the initiation and completion of different phenophases, growth and final yield. The application of agro-climatic indices provides a base for determining the effect of temperature and photoperiod on phonological behaviour of the crop. The total heat energy available to any crop is never completely converted to dry matter under even the most favorable agroclimatic conditions. Efficiency of conversion of heat energy into dry matter depends upon genetic factors, sowing time and crop type (Rao et al. 1999).

An attempt has been made to study the phenology of kharif sown mungbean genotypes in relation to energy summation indices such as growing degree days, heliothermal and photothermal units under variation in dates of sowing.

## 36.2 Material and Methods

The field experiment was conducted at Ludhiana (30°–54′ N and 75°–48′ E, 247 m above mean sea level), with mungbean genotypes 'SML 668', 'ML 818', 'PAU 911' and 'ML 1299' under four dates of sowing ($D_1$ = 10th July, $D_2$ = 20th July, $D_3$ = 30th July and $D_4$ = 10th August) during the summer season of 2007. The field experiment was conducted under split plot design comprising of four dates of sowing in main plots and four genotypes in sub plots with three replications during summer season. The crop was sown after a pre-sowing irrigation of 7 cm depth at a row spacing of 30 cm and plant-to-plant spacing was maintained at about 10 cm using 25 kg seed per hectare. A basal dose of 12.5 kg N as urea and 40 kg $P_2O_5$ as SSP was applied through urea (46% N) and single superphosphate (16% $P_2O_5$), respectively at the time of sowing. All other cultural practices were followed as per local recommendations. The phenological development of mungbean crop was recorded on the basis of visual observations. Meteorological data were recorded from Agro-Meteorological observatory situated near the experimental site.

Three agroclimatic indices, viz., growing degree-days (GDD), heliothermal units (HTU) and photothermal units (PTU), were calculated. The accumulated heat units for each day were calculated for different phonological stages as per the equation suggested by Nuttonson (1955) using base temperature of 10°C. Heliothermal units (HTU) are the product of growing degree days (GDD) and

corresponding actual sunshine hours for that day were computed on daily basis. Photothermal units (PTU) are the product of growing degree days and corresponding day length hours for that day were computed on daily basis. GDD, HTU and PTU were accumulated from the date of sowing to each date of sampling relative to a particular phenophase up to physiological maturity. Phenothermal index (PTI), the ratio of degree-days to the number of days between two phenological stages was calculated for all the phenophases.

Heat use efficiency (HUE) for seed yield was computed following as under:

HUE = Seed Yield/Accumulated heat units

## 36.3 Result and Discussion

In early sowing of the crop, higher agroclimatic indices (Growing degree-days, Heliothermal Units, Photothermal units) were required for the crop to attain maturity. However, as the sowing was delayed, comparatively lower agroclimatic indices were needed by mungbean to attain physiological maturity (Table 36.1). The crop sown on 10th July required more number of days for completion of all the phenological events as compared to late sown crops. First date of sowing resulted in accumulation of 1450 GDD, 11680 HTU and 18775 PTU to attain physiological maturity with a variability of 3.4%, 6.8% and 15.8% in second date of sowing,

**Table 36.1** Accumulated growing degree-days for different phenophases and heat use efficiency as influenced by varying dates of sowing

| Parameters | $D_1$ | $D_2$ | $D_3$ | $D_4$ |
|---|---|---|---|---|
| Accumulated heat units (°C day) | | | | |
| Emergence | 87 (3) | 88 (3) | 83 (3) | 86 (3) |
| Seedling | 103 (4) | 108 (4) | 101 (4) | 107 (4) |
| Vegetative phase | 663 (31) | 666 (31) | 597 (28) | 585 (28) |
| Flower bud appearance | 832 (39) | 768 (36) | 697 (33) | 644 (31) |
| Flower initiation | 851 (40) | 789 (37) | 717 (34) | 665 (32) |
| Pod formation | 934 (44) | 850 (40) | 777 (37) | 727 (35) |
| Completion of flowering | 1,135 (54) | 1,061 (51) | 868 (42) | 816 (41) |
| Completion of pod formation | 1,337 (65) | 1,288 (63) | 1,146 (57) | 1,010 (54) |
| Physiological maturity | 1,450 (73) | 1,400 (71) | 1,350 (68) | 1,210 (66) |
| Heat use efficiency (kg/ha/°C/day) at harvest | | | | |
| Dry matter | 2.30 | 2.00 | 2.43 | 1.28 |
| Seed yield | 0.72 | 0.73 | 0.76 | 0.57 |
| Dry matter heat use efficiency ($g/m^2$/°C/day) | | | | |
| 20 DAS | 0.025 | 0.024 | 0.021 | 0.020 |
| 40 DAS | 0.234 | 0.240 | 0.258 | 0.220 |
| 60 DAS | 0.275 | 0.289 | 0.299 | 0.234 |
| 70 DAS | 0.311 | 0.307 | 0.328 | 0.296 |

DAS – days after sowing, figures in parentheses indicate actual number of days taken to different phenophases

3.9%, 9.8% and 15.6% in third date of sowing and 3.6%, 8.3% and 18.8% in fourth date of sowing in comparison to first date of sowing, respectively (Table 36.1).

In general, earlier sown crop availed more growing degree-days and accumulated more dry matter and also resulted in higher grain yields compared to later sown crop irrespective of cultivar type. The July sown crop availed more accumulated growing degree days ranged between 1,350 and 1,450 to attain physiological maturity as compared to August sown crop. It was observed that highest grain yield for July sown crop were 1,047 kg/ha, 1,021 kg/ha and 1,028 kg/ha for first, second and third date of sowings, respectively as compared to August sown crop which was 699 kg/ha only. Heat-use efficiency (HUE) was computed to determine the grain or biomass yield per unit of growing degree-day for mungbean cultivars. In general, it was observed that grain yield HUE (2.30–2.43 kg/ha/°C day) and biomass yield HUE (0.72–0.76 kg/ha/°C day) was more in crop sown in July as compared to August sown crop. This may be attributed to the fact that in July sown crop more number of growing degree-days were utilized to attain maturity for which higher grain and biomass yields were recorded. Similar results have been reported by Rao et al. (1999) from Hisar in Haryana. There was a successive increase in HUE for dry matter at each periodical interval of observation up to maturity. Hence, under Punjab conditions GDD can be used as an agro-meteorological index for predicting yield of mungbean. Similarly, Hundal et al. (1997) reported earlier that AGDD could be used as an index to predict phenological development of wheat under Punjab conditions.

Significant variation in days taken to reach different phenophases, GDD, HTU and PTU was also observed within the mungbean genotypes. ML 1299 consumed lesser days and thermal time to attain physiological maturity as compared to ML 818 but closer to PAU 911and recorded higher DMA and seed yield as compared to other genotypes under study. Among genotypes ML 1,299 recorded highest yield 1,117 kg/ha followed by PAU 911 i.e., 1,015 kg/ha and ML 818 i.e., 913 kg/ha but lowest was in the case of SML 668 i.e. 750 kg/ha. This resulted in comparatively better HUE of ML 1299 for dry matter (2.32 kg/ha/°C/day) and seed yield (0.81 kg/ha/°C/day) over other genotypes (Table 36.2). The data further indicated that vegetative phase, flower bud appearance and flower initiation were slightly earlier in ML 1299 than in others except SML 668, however, the occurrence of later phenophases followed a reverse trend. This could be due to resource-induced competition for the earliness of phenological stages.

The phenothermal index for consecutive phenphases of mungbean genotypes for different sowing dates during the crop season was also computed and is presented in Table 36.3. The phenothermal index is expressed as degree-days per growth day (Sastry and Chakravarty 1982). It was also observed that the index gradually decreases from emergence to physiological maturity in all four dates of sowing being the highest at seedling and lowest during physiological maturity stages indicating a decrease in daily heat consumption toward maturity. The occurrence of phenological growth showed a linear relationship with accumulated HTU and PTU (Table 36.4) and could be used for predicting the phenology of mungbean cultivars. A positive and significant but low correlation was observed between

**Table 36.2** Accumulated growing degree-days for different phenophases and heat use efficiency as influenced by mungbean genotypes

| Parameters | SML 668 | ML 818 | PAU 911 | ML 1299 |
|---|---|---|---|---|
| Accumulated heat units (°C day) | | | | |
| Emergence | 65 (2) | 83 (3) | 83 (3) | 65 (2) |
| Seedling | 87 (3) | 103 (4) | 103 (4) | 87 (3) |
| Vegetative phase | 597 (28) | 658 (31) | 658 (31) | 637 (30) |
| Flower bud appearance | 658 (31) | 777 (37) | 757 (36) | 717 (34) |
| Flower initiation | 678 (32) | 796 (38) | 796 (38) | 737 (35) |
| Pod formation | 796 (38) | 835 (40) | 876 (42) | 876 (42) |
| Completion of flowering | 933 (45) | 987 (48) | 1,025 (50) | 1,044 (51) |
| Completion of pod formation | 1,120 (54) | 1,185 (59) | 1,202 (60) | 1,220 (61) |
| Physiological maturity | 1,302 (66) | 1,414 (73) | 1,366 (70) | 1,382 (71) |
| Heat use efficiency (kg/ha/°C/day) at harvest | | | | |
| Dry matter | 1.32 | 2.16 | 2.29 | 2.32 |
| Seed yield | 0.58 | 0.65 | 0.74 | 0.81 |
| Dry matter heat use efficiency ($g/m^2/°C/day$) | | | | |
| 20 DAS | 0.019 | 0.024 | 0.024 | 0.025 |
| 40 DAS | 0.204 | 0.221 | 0.259 | 0.265 |
| 60 DAS | 0.225 | 0.270 | 0.310 | 0.324 |
| 70 DAS | 0.274 | 0.305 | 0.348 | 0.386 |

DAS – days after sowing, figures in parentheses indicate actual number of days taken to different phenophases

**Table 36.3** Phenothermal index (°C days/day) for four mungbean cultivars sown on four different dates of sowing

| Parameters | Seed-ling | Vege-tative phase | Flower bud appearance | Flower initia-tion | Pod forma-tion | Completion of flowering | Completion of pod formation | Physiolo-gical maturity |
|---|---|---|---|---|---|---|---|---|
| Phenother-mal index | | | | | | | | |
| 10 July | 16.1 | 20.7 | 21.1 | 19.0 | 20.8 | 20.1 | 18.4 | 14.1 |
| 20 July | 20.0 | 20.7 | 20.4 | 21.0 | 20.3 | 19.2 | 18.9 | 14.0 |
| 30 July | 13.0 | 20.7 | 20.0 | 20.0 | 20.0 | 18.2 | 18.5 | 18.5 |
| 5 August | 21.0 | 19.9 | 19.7 | 21.0 | 20.7 | 14.8 | 14.9 | 16.7 |
| SML 668 | 22.0 | 20.4 | 20.3 | 20.0 | 19.7 | 19.6 | 20.8 | 15.2 |
| ML 818 | 10.0 | 20.6 | 19.8 | 19.0 | 19.5 | 19.0 | 18.0 | 16.4 |
| PAU 911 | 10.0 | 20.6 | 19.8 | 19.5 | 20.0 | 18.6 | 17.7 | 16.4 |
| ML 1299 | 22.0 | 20.4 | 20.0 | 20.0 | 19.9 | 18.7 | 17.6 | 16.2 |

accumulated heat units and seed yield (Table 36.5). Thus, heat units concept could be applied to predict different growth phases of the crop and can also be useful in the identification of thermo-tolerant genotypes. The regression relationships obtained between thermal based agro-meteorological indices and grain yield of mungbean can serve as important tools for forecasting yield. Similar work on developing agroclimatic models based on temperature, photoperiod and daylength

**Table 36.4** Prediction equations for mungbean phenology

| Phenophases | Heliothermal units | | Photothermal units | |
|---|---|---|---|---|
| | Regression equations | $R^2$ value | Regression equations | $R^2$ value |
| Vegetative phase | Y = 0.0035X + 7.45 | 0.94 | Y = 0.0022X + 9.02 | 0.92 |
| Flower bud appearance | Y = 0.0042X + 5.56 | 0.98 | Y = 0.0055X + 8.44 | 0.96 |
| Flower initiation | Y = 0.0023X + 4.52 | 0.91 | Y = 0.0030X + 6.50 | 0.94 |
| Pod formation | Y = 0.0083X + 14.20 | 0.94 | Y = 0.0071X + 5.95 | 0.92 |
| Completion of flowering | Y = 0.0051X + 8.05 | 0.92 | Y = 0.0043X + 9.69 | 0.90 |
| Completion of pod formation | Y = 0.0049X + 10.22 | 0.90 | Y = 0.0023X + 12.12 | 0.94 |
| Physiological maturity | Y = 0.0053X + 8.00 | 0.97 | Y = 0.0033X + 14.05 | 0.97 |

Y = Days of occurrence of phenophases; X = Thermal units; Significant at 5% level

**Table 36.5** Correlation between growing degree-days at different phenological stages and seed yield of mungbean

| Characters | Vege-tative phase | Flower bud appear-ance | Flower initia-tion | Pod forma-tion | Completion of flowering | Completion of pod formation | Physio-logical maturity | Seed yield |
|---|---|---|---|---|---|---|---|---|
| Vegetative phase | 1.00 | 0.510 | 0.477 | 0.436 | 0.514 | 0.323 | 0.289 | 0.121 |
| Flower bud appearance | | 1.00 | 0.415 | 0.422 | 0.440 | 0.366 | 0.333 | 0.130 |
| Flower initiation | | | 1.00 | 0.460 | 0.463 | 0.389 | 0.450 | 0.127 |
| Pod formation | | | | 1.00 | 0.510 | 0.444 | 0.468 | 0.150 |
| Completion of flowering | | | | | 1.00 | 0.398 | 0.495 | 0.145 |
| Completion of pod formation | | | | | | 1.00 | 0.502 | 0.199 |
| Physiological maturity | | | | | | | 1.00 | 0.214 |
| Seed yield | | | | | | | | 1.00 |

Seed yield Significant at 1% and other phonological stages at 5% level of significance

for wheat (Hundal et al. 1997), mustard (Hundal et al. 2003a) and soybean (Hundal et al. 2003b) have been reported under Punjab conditions.

## References

Benbi DK (1994) Prediction of leaf area indices and yields of wheat. J Agric Sci Camb 122:13–20

Hundal SS, Singh R, Dhaliwal LK (1997) Agro-climatic indices for predicting phenology of wheat (Triticum aestivum) in Punjab. Indian J Agric Sci 67(6):265–268

Hundal SS, Kaur Prabhjyot, Malikpuri SDS (2003a) Agroclimatic models for prediction of growth and yield of Indian mustard (Brassica junea). Indian J Agric Sci 73(3):142–144

Hundal SS, Singh H, Kaur Prabhjyot, Dhaliwal LK (2003b) Agroclimatic models for growth and yield of soybean (Glycine max). Indian J Agric Sci 73(12):668–670

Monteith JL (1981) Climatic variations and growth of crops. Quart J R Meteorol Soc 107:749–774
Nuttonson MY (1955) Wheat climate relationships and use of phenology in ascertaining the thermal and photothermal requirements of wheat. American Institute of Crop Ecology, Washington, DC, p 388
Rao VUM, Singh D, Singh R (1999) Heat use efficiency of winter crops in Haryana. J Agrometeorol 1(2):143–148
Sastry PSN, Chakravarty NVK (1982) Energy summation indices for wheat crop in India. Agric Meteorol 27:45–48
Whisler FD, Acock B, Baker DN, Fye RE, Hodges HF, Lambert JR, Lemmon HE, McKinion JM, Reddy VR (1986) Crop simulation models in agronomic systems. Advances Agron 40:141–208

# Chapter 37
# Effect of Thermal Regimes on Crop Growth, Development and Seed Yield of Chickpea (*Cicer Arietinum* L.)

**K.K. Agrawal, U.P.S. Bhadauria, and Sanjay Jain**

**Abstract** A field experiment was conducted during 2004–2005 and 2005–2006 in *Rabi* season with five varieties of three chickpea types with three replications in split-plot design. The crop was raised with all the recommended package of practice of Jabalpur region of Madhya Pradesh. Experimental results revealed that crop sown with first date of sowing taken highest days to attain maturity as compared to second and third date of sowing. Among all five varieties c.v. JGK-3 and JG-74 sown on dated 04 November (first date of sowing) taken longest duration to attain the harvest maturity. Higher temperatures during grain-filling stage decreased the dry matter accumulation and seed yield whereas higher temperature during vegetative phase was favorable for higher dry matter production. Variations in temperatures occurred due to natural seasonal variability at this location revealed that higher yield attributes and seed yield of 2243.5 $ha^{-1}$ in JGK-3 (Kabuli type) and 2205.1 kg $ha^{-1}$ in JG-74 (Desi type) was recorded with first and second sowing date during both the years.

## 37.1 Introduction

Chickpea (*Cicer arietinum* L.) is an important pulse crop occupies about 7.25 million hectare with a total production of 5.77 million tones which grown as rainfed in diverse agro-climatic condition in different parts of India. Madhya Pradesh is largest producer of chickpea with total output of 2.5 million tones and highest productivity 819 kg/ha. To achieve targeted production of 7.37 million tones by 2010 two prolonged strategies involving horizontal expansion through crop diversification and productivity enhancement through strategic research are

K.K. Agrawal (✉) • U.P.S. Bhadauria • S. Jain
Department of Physics and Agrometeorology, College of Agricultural Engineering, JNKVV, Jabalpur 482004, MP, India
e-mail: kkagrawal59@yahoo.co.in; upsb2007@rediffmail.com; genomics_san@hotmail.com

S.D. Attri et al. (eds.), *Challenges and Opportunities in Agrometeorology*,
DOI 10.1007/978-3-642-19360-6_37, 

enviable (Sakya et al. 2008). With the introduction of soybean as a major Kharif crop in the state sowing of chickpea is delayed which ultimately affecting the productivity of chickpea. Among the abiotic stresses water, nutritional and temperature, particularly high temperature stress during reproductive phase of crop are damaging when sowing of chickpea is delayed particularly under rainfed conditions (Kalra et al. 2008). The temperature is a predominant weather parameter that often determines the productivity levels of the crop. Higher temperature particularly during reproductive phase is a major constraint for maximizing productivity of chickpea in this region. Therefore present field study was carried out to understand the Effect of thermal regimes on crop growth, development and seed yield of chickpea.

## 37.2 Material and Methods

The field experiment was conducted during Rabi season of 2004–2005 at Research area of Department of Physics and Agrometeorology, College of Agricultural Engineering, Jawaharlal Nehru Krishi Vishwa Vidyalaya, Jabalpur, Madhya Pradesh. The treatments comprises of five varieties of three chickpea types viz., JGG-1 (Gulabi), JG-74 and JG-322 (Deshi), JGK-3 and JGK-1 (Kabuli) with three date of sowing (4th November, 19th November and 16th December) with three replications in split plot design. The soil of experimental plots was clay loam in texture. Chickpea crop raised with all the recommended package of practice of the region. Total rainfall received during the crop period was 134.2 mm in 10 rainy days spread over in month of November to March except December. Maximum temperature during crop season ranged between 30.2°C and 33.2°C and minimum temperature was in the range of 8.4–17.7. The observations related to growth and yield and yield attributing parameters were recorded at different stages.

## 37.3 Result and Discussion

### *37.3.1 Phenology and Accumulated Growing Degree Days*

Crop sown on 4th November took more days (129) as compared to 19th November (114 days) and 16th December (100 days). Crop sown on 4th November (D1) took longest duration to attain the maturity in all the varieties. As regards the different chickpea types differences was not significant to attain maturity, whereas highest number of days (116) was taken by Kabuli type than Deshi and Gulabi. Deshi and Gulabi type were taken almost similar days (113). Differences was non significant in durations between Gulabi and Deshi type under late sown conditions. Early planted crop sown on 04th November accumulated higher Growing Degree Days (GDD) and it was reduced as the crop sown after 4th November. The lowest number

**Table 37.1** No. of Days taken to attain Different Phenological Stage of Chickpea and Accumulated Growing Degree Days (GDD)

| Treatments | Stages | | | | | | | | | |
|---|---|---|---|---|---|---|---|---|---|---|
| | Flowering initiation | | 50% Flowering | | Pod initiation | | Physiological maturity | | Harvest maturity | |
| | Days | GDD | Days | GDD | Days | GDD | Days | GDD | Days | GDD |
| Sowing dates | | | | | | | | | | |
| 04 Nov, 2004 (D1) | 55 | 763 | 65 | 884 | 75 | 1,003 | 120 | 1,719 | 129 | 1,853 |
| 19 Nov, 2004 (D2) | 59 | 761 | 67 | 888 | 83 | 1,030 | 110 | 1,506 | 114 | 1,687 |
| 16 Dec, 2004 (D3) | 51 | 653 | 60 | 764 | 67 | 889 | 89 | 1,264 | 100 | 1,483 |
| Genotypes | | | | | | | | | | |
| Gulabi (JGG-1) — V1 | 71 | 923 | 77 | 1,021 | 85 | 1,122 | 106 | 1,473 | 113 | 1,636 |
| Deshi (JG 322) — V2 | 57 | 760 | 67 | 894 | 79 | 1,048 | 105 | 1,507 | 112 | 1,606 |
| Kabuli (JGK — 3) — V3 | 44 | 591 | 54 | 707 | 66 | 826 | 108 | 1,494 | 115 | 1,661 |
| Deshi (JG 74) — V4 | 58 | 763 | 68 | 898 | 79 | 1,048 | 105 | 1,510 | 113 | 1,661 |
| Kabuli (JGK-1) — V5 | 44 | 591 | 54 | 707 | 66 | 826 | 108 | 1,506 | 116 | 1,615 |

of GDD was accumulated with 16th December sown crop. Among the different chickpea types difference was not very prominent whereas highest GDD were with Kabuli than Deshi and Gulabi type. Thus, there was significant differences in genotype × time of planting interactions in the duration of different phenophases and total crop duration. This variation is very well reflected by the differences in the GDD accumulated by different varieties sown at different times. These differences in GDD accumulation had major influence on all yield attributes and crop productivity (Table 37.1).

### *37.3.2 Dry Matter, Yield and Yield Attributing Characters*

Results on dry matter yield, total no. of branches, pod weight (g), test weight, total number of pods and seed yield are presented in Table 37.2. The results show an overwhelming influence of timing of planting on biological and economic productivity of the crop. Highest seed yield was recorded with D1 followed by D2 and D3 sowing date. All other yield attributing characters were also higher under same sowing dates with compare to D3. This may be due to optimal photo thermal conditions under crop sown on D1 and D2. Lowest seed yield of 608.97 kg $ha^{-1}$ was recorded under the crop sown on 16, December (Table 37.3). This may be due to sub optimal thermal conditions in late sown crop suffering. Among different chickpea varieties highest seed yield of 2243.5 kg $ha^{-1}$ was noted with the desi variety JG-322 followed by 2147.4 kg $ha^{-1}$ in JG-74 of Deshi type and lowest seed yield was recorded in JGK-3 of Kabuli type (608.97 kg $ha^{-1}$). There were significant differences among different chickpea types in total GDD accumulation for different phases. Gulabi type accumulated maximum GDD followed by Deshi type and Kabuli type.

**Table 37.2** Dry matter yield (gm/plant) at different stages of Chickpea types planted under different date of sowing (average of 2 years data)

| | Sowing dates | | | | |
|---|---|---|---|---|---|
| Phenological stages | V1 | V2 | V3 | V4 | V5 |
| D1 | | | | | |
| Branching | 15.7 | 10.9 | 22.5 | 12.5 | 11.9 |
| Flowering | 68.4 | 61.0 | 60.9 | 28.8 | 39.1 |
| Podding | 142.0 | 164.3 | 131.5 | 92.1 | 64.5 |
| Maturity | 394.4 | 415.7 | 378.4 | 222.9 | 401.5 |
| D2 | | | | | |
| Branching | 13.67 | 18.53 | 29.87 | 14.87 | 16.13 |
| Flowering | 52.67 | 64.53 | 61.47 | 27.53 | 35.8 |
| Podding | 94.53 | 149.67 | 213.67 | 56.07 | 164.8 |
| Maturity | 292.7 | 320.23 | 295.6 | 402.9 | 346.23 |
| D3 | | | | | |
| Branching | 12.67 | 20.67 | 27.8 | 15.2 | 14.67 |
| Flowering | 37.47 | 53.53 | 53.6 | 28.0 | 27.07 |
| Podding | 138.6 | 135.47 | 154.53 | 49.33 | 61.13 |
| Maturity | 233.63 | 246.5 | 290.63 | 233.57 | 210.33 |

V1 –K- 1 (Kabuli), D1 – 04 Nov, 2004, D2 – 19 Nov, 2004, D3 – 16 Dec, 2004

**Table 37.3** Yield and yield attributing characters as influenced by different date of sowing

| Treatment | Total No. of branches (per sq m) | Total number of pods (per sq m) | Pod weight (g) | 1,000-Grain weight (g) | Seed yield (kg $ha^{-1}$) |
|---|---|---|---|---|---|
| 04th Nov, 2004 (D1) | | | | | |
| V1 – JGG-1 (Gulabi) | 85.00 | 985.67 | 214.83 | 164.47 | 1580.13 |
| V2 – JG- 74 (Desi) | 111.33 | 1024.33 | 220.50 | 162.13 | 2147.43 |
| V3 – JG- 322 (Desi) | 63.33 | 748.33 | 188.73 | 139.33 | 2243.59 |
| V4 – JGK- 3 (Kabuli) | 55.67 | 283.00 | 95.93 | 374.67 | 657.05 |
| V5 – JGK- 1 (Kabuli) | 75.33 | 575.00 | 215.37 | 301.03 | 1298.08 |
| 19th Nov, 2004 (D2) | | | | | |
| V1 – JGG-1 (Gulabi) | 116.67 | 985.33 | 174.07 | 149.67 | 1842.95 |
| V2 – JG- 74 (Desi) | 127.00 | 896.00 | 152.37 | 167.53 | 2205.13 |
| V3 – JG- 322 (Desi) | 115.00 | 833.00 | 166.67 | 140.47 | 2083.33 |
| V4 – JGK- 3 (Kabuli) | 50.00 | 516.00 | 253.37 | 303.07 | 685.90 |
| V5 – JGK- 1 (Kabuli) | 70.33 | 607.00 | 242.93 | 310.93 | 1169.87 |
| 16th Dec, 2004 (D3) | | | | | |
| V1 – JGG-1 (Gulabi) | 103.67 | 941.67 | 144.03 | 135.27 | 798.08 |
| V2 – JG- 74 (Desi) | 142.67 | 1074.67 | 195.43 | 153.00 | 1647.43 |
| V3 – JG- 322 (Desi) | 102.00 | 673.33 | 157.17 | 144.07 | 1378.20 |
| V4 – JGK- 3 (Kabuli) | 37.67 | 382.33 | 138.50 | 351.47 | 608.97 |
| V5 – JGK- 1 (Kabuli) | 50.67 | 476.33 | 154.90 | 317.63 | 450.00 |

It is clear from the experimental results that higher temperatures during grain-filling stage lowered the dry matter accumulation and yield under late and early and late planted chickpea crop. Timely planted crop also accumulated higher GDD. Different genotypes tried in this experiment differed in their responsiveness to temperature but these differences were more pronounced during reproductive phase. Kabuli type chickpea appear to be more sensitive to temperatures compared to Deshi and Gulabi type. Summerfield et al. 1984 and Roberts et al. 1985 also found sensitivity of chickpea to hot temperatures during reproductive phase. However, these differences lessened as sowing was delayed and as a consequence subsequent phases of different types took almost similar days to complete. There was not much difference up to flowering stage in dry matter production, however, differences became more pronounced during reproductive phase suggesting that due to higher temperatures during reproductive phase the dry matter accumulated was not translated into economic yield. Thus, higher temperatures interfere with the translocation of food for grain filling and as a result grain-filling is affected and results into smaller size of grains and ultimately reduced yields.

## 37.4 Conclusions

From the above finding it may be concluded that higher temperature during reproductive phase of chickpea is more detrimental for reduction of seed yield in semi arid condition of Madhya Pradesh hence, to overcome this problem there is need to develop varieties which can tolerate higher temperatures during grain-filling stage for this region.

## References

Kalra Naveen, Chakraborty D, Sharma Anil, Rai HK, Jolly Monika, Chander Subhas, Kumar Ramesh P, Bhadraray S, Barman D, Mittal RB, Lal Mohan, Sehgal Mukesh (2008) Effect of increasing temperature on yield of some winter crops in northwest India. Curr Sci 94(1):82–88

Roberts EH, Hadley P, Summerfield RJ (1985) Effects of temperature and photoperiod on flowering in chickpeas (Cicer arietinum L.). Ann Bot 55:881–892

Sakya MS, Patel MM, Singh VV (2008) Knowledge level of chickpea growers about chickpea production technology. Indian Res J Ext Educ 8(2&3):65–68

Summerfielda RJ, Hadleya P, Robertsa EH, Minchina FR, Rawsthornea S (1984) Sensitivity of chickpeas (Cicer arietinum) to hot temperatures during the reproductive period. Exp Agric 20:77–93, Cambridge University Press

# Chapter 38
# Stomatal Adaptation and Leaf Marker Accumulation Pattern from Altered Light Availability Regimes: A Field Study

**K. Ramesh, S. Raj Kumar, and Virendra Singh**

**Abstract** Understanding crop-weather relationship is an important aspect to maximize productivity from cultivated plants. Valeriana jatamansi is a understorey plant while bring under cultivation, needs to be studied for their stomatal behavior. The herb endows its origin from Himalayas and is widely distributed in altitude ranging from 1500 to 2600 amsl comprising Afghanistan, southwest China and Burma. In Himachal Pradesh, it occurs naturally as an under storey plant of forest areas. The forests are being destroyed due to the climatic changes occurring in nature. Also, being a shade loving crop, valeriana can also be grown in apple orchards. Therefore, an attempt has been made to study the effect of artificial shading on valeriana crop. The easurement of stomatal behaviour is fundamental to many aspects of plant research. In V. jatamansi, the adaxial surface is exposed to solar radiation. The number of stomata, epidermal cells, stomatal density and stomatal index were observed to be significantly higher under full light conditions. As there is increase in the light intensity, there is an increase in no of stomata, epidermal cells, stomatal index and stomatal density. The leaf valepotriate content was negatively correlated with the number of stomata, epidermal cells, stomatal index and stomatal density. This gives an opportunity for the grower to cultivate under specific growth conditions so that to produce crop with different oil constituents. It is necessary to study further the implications of these compounds in the development of the plants under the light stressed environments.

K. Ramesh (✉) • S.R. Kumar • V. Singh
Natural Plant Products & Biodiversity Divisions, Institute of Himalayan Bioresource Technology (CSIR), Palampur, HP 176061, India
e-mail: kramesh@iiss.ernet.in; ramechek@yahoo.co.in

S.D. Attri et al. (eds.), *Challenges and Opportunities in Agrometeorology*,
DOI 10.1007/978-3-642-19360-6_38, 

## 38.1 Introduction

Understanding crop-weather relationship is an important aspect to maximize productivity from cultivated plants. Season has a profound influence on quantity and quality of medicinal and aromatic plants through the pronounced effect of the various weather elements on crop establishment, growth and development. Among the weather elements, light plays a major role. *Valeriana jatamansi* (Indian Valerian) is a commercially important plant used as a sedative in Ayurvedic & Unani systems of medicines and is an understorey herb. Several microclimatic (e.g. light quality) and physiological (leaf transpiration and carbon gain) parameters change concurrently with light intensity within plant canopies (Combes et al. 2000). Light is an important physical factor, which influences the formation of primary and secondary metabolites (Rout et al. 2000). Pons et al. (2001) showed that a reduced Vapour Pressure Deficit partly mimicked the effects of shading on photosynthesis in bean leaves and so they suggested that the local rate of import of xylem sap and, in particular, the influx of cytokinins from roots to shoots play an important role in the perception of partial shading by plants.

*Valeriana jatamansi* Jones (syn. *V.wallichii* DC), a perennial rhizomatous herb belonging to family Valerianaceae, is known for its aromatic and medicinal importance. It is a natural source of the sedative tranquilizing valepotriates (Violon et al. 1983) and fragrant monoterpenoids and sesquiterpenoids (Bos et al. 1997). The total sedative activity has been attributed to the presence of oxygenated sesquiterpenoid constituents (Mathela et al. 2005).

The herb endows its origin from Himalayas and is widely distributed in altitude ranging from 1,500 to 2,600 amsl comprising Afghanistan, southwest China and Burma (Polunin and Stainton 1987). In Himachal Pradesh, it occurs naturally as an under storey plant of forest areas. The forests are being destroyed due to the climatic changes occurring in nature. Also, being a shade loving crop, valeriana can also be grown in apple orchards. Therefore, an attempt has been made to study the effect of artificial shading on valeriana crop.

The rhizomes and extracts made therefore are used in traditional medicines in Bhutan, India, and Nepal and in traditional Chinese and Tibetan medicine (Fratkin 1986; Yang 1996). The taxon has also been reported as being made into stick incense and sold in certain countries in the Middle East (Burbage 1981), while it has long been used to make a costly perfumed ointment, much valued in ancient times. The plant has been widely used for medicine and in perfumery for centuries in India. It is valued for its antispasmodic and stimulant properties and is therefore useful in the treatment of fits and heart palpitations and also to regulate constipation, urination, menstruation and digestion (Jain 1968)

In view of the above, a study was conducted during 2005–2007 to study the stomatal adaptation and accumulation of chemical compounds from altered light availability regimes.

## 38.2 Materials and Methods

Field experiments were conducted during 2005–2007 at the research farm of Institute of Himalayan Bioresource Technology, Palampur, India to study the stomatal adaptation and accumulation of chemical compounds. The experimental site was located at Latitude, 76°33′29″ East; Longitude, 32°6′20″ North; and on the elevation of 1,356 m amsl. Soil of the experimental farm was clay to loamy with pH 5.5. The treatments consisted of four shading levels (100% open, 25% shade, 50% shade and 75% shade) and flower spike pinching (pinched and unpinched) on Valeriana jatamansi. Good quality seeds were obtained from the elite lines available at Natural Plant Products division of Institute of Himalayan Bioresource Technology, Palampur. Seeds were sown in well prepared sand bed nurseries and 3 months old seedlings were planted in a well prepared field at a spacing of 45 × 45 cm. The treatments were imposed in a factorial randomized block design with pinching and shading as 2 factors. Pinching was done from 12th month (at the time of initiation of flower spike) at weekly intervals till cessation of flowering season. Stomatal observations were taken at 15 months after planting and leaf valepotriate at 17 and 18 months after planting. Plants were harvested at 18 months after transplanting.

## 38.3 Result and Discussion

The measurement of stomatal behaviour is fundamental to many aspects of plant research. In V. jatamansi, the adaxial surface is exposed to solar radiation. The number of stomata, epidermal cells, stomatal density and stomatal index were observed to be significantly higher under full light conditions. This is in conformity with the findings of Ticha (1985). He found that stomatal density and index generally decrease with decreasing light intensity.

As there is increase in the light intensity, there is an increase in no of stomata (Fig. 38.1), epidermal cells, stomatal index and stomatal density (Fig. 38.2). But the leaf valepotriate content was found to decrease. Our results are contradictory to Russowski et al. (2006) who stated that light is not an indispensable physical condition for valepotriate formation under tissue culture conditions. Thus the leaf valepotriate content was negatively correlated with the number of stomata, epidermal cells, stomatal index and stomatal density.

Secondary metabolism utilizes a limited number of metabolites available from primary metabolism in novel ways. Acetyl-coenzyme A, also known as activated acetic acid, is the biogenetic precursor of terpenes. The “isoprene pathway”, the precursor is mevalonic acid derived from acetyl-CoA. The subsequent products are constructed from “isoprene” units often with further biochemical manipulation (Bentley 1999). The function of isoprene is still controversial, and this compound may act to increase the tolerance of photosynthesis to high temperatures by stabilizing the thylakoid membranes (Sharkey et al. 2001) or by quenching reactive

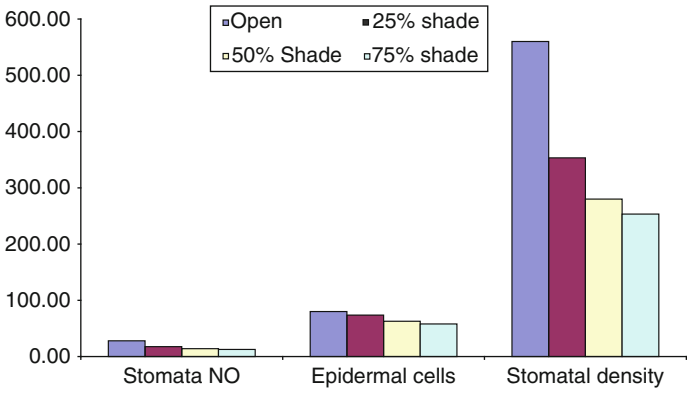


**Fig. 38.1** Effect of different shading levels on the stomata cells and epidermal cells

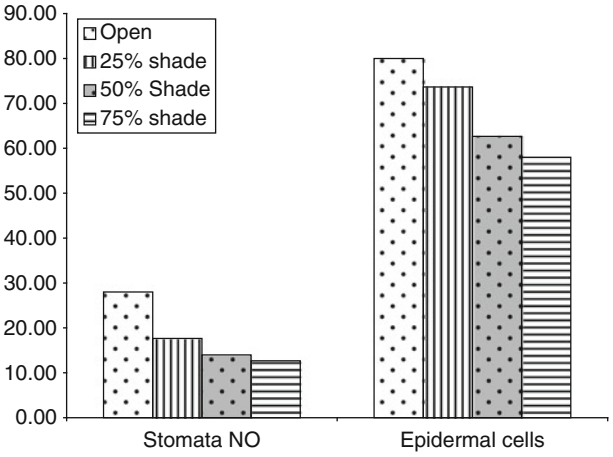


**Fig. 38.2** Effect of different shading levels on the stomata density

oxygen species (Loreto and Velikova 2001). The P-450 cytochrome oxidases are involved in numerous metabolic pathways (Schuler 1996). Not surprisingly, these enzymes have been found to be involved in many of the reactions of volatile biosynthesis (Dudareva et al. 2004). The level of the enzyme responsible for the final step of the biosynthesis of a particular volatile is not the only limiting factor. The target for the regulation of developmental production of volatile compounds also includes the level of supplied substrate in the cell (Dudareva et al. 2000). The graded shading might have interfered in the terpene production path way and as a result different compounds might have been formed. This gives an opportunity for the grower to cultivate under specific growth conditions so that to produce crop with different oil constituents. It is necessary to study further the implications of these compounds in the development of the plants under the light stressed environments (Ramesh 2010).

This study suggests that because of climate change if there is a shift in light and temperature regimes, different compounds may be obtained with varying concentrations which may open new avenues for industrial growth.

**Acknowledgement** The authors gratefully acknowledge the financial support of the Department of Science and Technology, Government of India. The authors thank The Director, IHBT for his constant encouragement for the work. The authors also thank Mr. Suresh Sood and Mr. Kuldeep S. Gill, Technical Assistants for the management of the experimental crop.

## References

Bentley R (1999) Secondary metabolite biosynthesis: the first century. Crit rev Biotechnol 19(1):1–40

Bos R, Woerdenbag JH, Hendriks H, Scheffer JJC (1997) Composition of essential oil from roots and rhizomes of Valeriana wallichii DC. Flavour Frag J 12:123–131

Burbage MB (1981) Report on a visit to Nepal: the medicinal plant trade in the Khardep area – a study of the development potential. Tropical Products Institute, London, UK. In: Anon. (1997). IUCN Analyses of Proposals to amend the CITES Appendices. Prepared by IUCN Species Survival Commission and the TRAFFIC Network for the Tenth Meeting of the Conference of the Parties to CITES. IUCN-The World Conservation Union, Gland, Switzerland

Combes D, Sinoquet H, Varlet-Grancher C (2000) Preliminary measurement and simulation of the spatial distribution of the morphogenetically active radiation (MAR) within an isolated tree canopy. Ann For Sci 57:497–511

Dudareva N, Murfitt LM, Mann CJ, Gorenstein N, Kolosova N, Kish CM, Bonham C, Wood K (2000) Developmental regulation of methylbenzoate biosynthesis and emission in snapdragon flowers. Plant Cell 12:949–961

Dudareva H, Pichersky E (2000) Biochemical and molecular genetic aspects of floral scents. Plant Physiol 122:627–633

Dudareva N, Pichersky E, Gershenzon J (2004) Biochemistry of plant volatiles. Plant Physiol 135:1893–1902

Fratkin J (1986) Chinese herbal patent formulas: a practical guide. Shya Publications, Boulder, USA. In: Anon., 1997. IUCN analyses of proposals to amend the CITES appendices. Prepared by IUCN Species Survival Commission and the TRAFFIC Network for the Tenth Meeting of the Conference of the Parties to CITES. IUCN. The World Conservation Union, Gland, Switzerland

Jain SK (1968) Medicinal plants. National Book Trust, New Delhi

Loreto F, Velikova V (2001) Isoprene produced by leaves protects the photosynthetic apparatus against ozone damage, quenches ozone products, and reduces lipid peroxidation of cellular membranes. Plant Physiol 127:1781–1787

Mathela CS, Chanotiya CS, Subhash SS, Anil KP, Pandey S (2005) Compositional diversity of terpenoids in the Himalayan Valeriana Genera. Chem Biodivers 2:1174–1182

Polunin O, Stainton A (1987) Concise flowers of the Himalaya. Oxford University Press, London

Pons TL, Jordi W, Kuiper D (2001) Acclimation of plants to light gradients in leaf canopies: evidence for a possible role for cytokinins transported in the transpiration stream. J Exp Bot 52:1563–1574

Ramesh K, Virendra Singh (2010) Environmental regulation of secondary metabolite accumulation in aromatic crops- a review. In: Gupta VK, Verma AK, Koul S (eds), Utilization and management of medicinal plants. Dayal Publishing House, New Delhi, pp. 32–47

Rout GR, Samantary S, Das P (2000) In vitro manipulation and propagation of medicinal plants. Biotechnol Adv 18:91–120

Russowski D, Maurmann N, Rech SB, Fett-Neto AG (2006) Role of light and medium composition on growth and valepotriate contents in Valeriana glechomifolia whole plant liquid cultures. Plant Cell Tissue Organ Cult 86:211–218

Schuler MA (1996) Plant cytochrome P-450 monooxygenases. Crit Rev Plant Sci 15:235–284

Sharkey TD, Chen XY, Yeh S (2001) Isoprene increases thermotolerance of fosmidomycin-fed leaves. Plant Physiol 125:2001–2006

Ticha I (1985) Ontogeny of leaf morphology and anatomy. In: Sestak Z (ed) Photosynthesis during leaf development. Kluwer, Dordrecht, pp 16–50

Violon C, Van CN, Vereruysse A (1983) Valepotriate content in different in vitro cultures of Valerianaceae. Pharm Week Bl Sci Ed 5:205–210

Yang YC (ed) (1996) Tibetan materia Medica. Qinghai People's Press, Qinghai

# Chapter 39
# Comparative Study of Diurnal Rate of Photosynthesis at Various Levels of Carbon Dioxide Concentration for Different Crops

**A. Kashyapi, Archana P. Hage, and R.P. Samui**

**Abstract** Crops capture solar energy and transform it into chemical energy by process of photosynthesis. Light energy is transformed into chemical energy, which, in turn is used for reduction of carbon dioxide to carbohydrates. With an extra supply of carbon dioxide both saturation light intensity and efficiency of light utilisation increases, which ultimately increases dry matter production. Crops with $C_4$ pathway show less response to increased carbon dioxide as compared to crops with $C_3$ pathway. Photosynthetic rate also fluctuates with diurnal variation of temperature. With this background an actual field experiment was conducted at adjacent plots of CAgMO (lat. 18° 32′, long. 73° 51′), Pune, with four crops *viz*., sunflower, soybean, mustard and jowar. All the crops were sown on 28 October 2003, in order to have better comparative study among the crops. Weekly observations were taken at 3 levels of carbon dioxide concentration *viz*., normal, 550 and 650 ppm by using LI 6400 portable photosynthatic system from 08 December 2003 to 19 January 2004 (i.e., from 42nd to 84th days after sowing or DAS). At each of the weekly intervals, observations were taken at 2 hourly intervals *viz*. 0800, 1,000, 1,200, 1,400 and 1,600 h IST to measure the rate of photosynthesis from which daily mean values were computed. Statistical analysis was carried out in Randomized Block Design (RBD) to find out critical differences in daily mean rate of photosynthesis at different levels of carbon dioxide concentration and various hours of observation, to identify statistically significant variation. The objective of the study was to quantify and compare mean rate of photosynthesis at various levels of carbon dioxide and at various hours of observation among different crops.

The paper discussed about how the rate of photosynthesis varied with levels of carbon dioxide and different hours of observation. Among the four crops studied during the study period, the rate of photosynthesis was the highest for sunflower

A. Kashyapi (✉) • A.P. Hage • R.P. Samui
Agricultural Meteorology Division, India Meteorological Department, Pune, India
e-mail: kashyapi_a@yahoo.co.in; rsamui@yahoo.com

S.D. Attri et al. (eds.), *Challenges and Opportunities in Agrometeorology*,
DOI 10.1007/978-3-642-19360-6_39, 

crop and the lowest for soybean crop. For all the crops studied, the rate of photosynthesis increased with levels of carbon dioxide at the earlier weekly observations. For sunflower crop, the rate of photosynthesis varied significantly between normal and 650 ppm $CO_2$ level, though the difference between 550 and 650 ppm levels were not significant up to 4th weekly observations (i.e., up to 63 DAS). Low critical difference values were observed at later weekly observations (i.e., after 70 DAS). For soybean, significant variation in rate of photosynthesis was observed up to 4th weekly observations (i.e., up to 63 DAS). However, in case of mustard, the rate of photosynthesis at various levels of $CO_2$ did not differ significantly at earlier weekly observations (i.e., up to 63 DAS), though low critical difference values were observed at later weekly observations (i.e., after 70 DAS). In case of jowar crop, rate of photosynthesis increased up to 3rd weekly observations (i.e., up to 56 DAS) and the critical difference values at normal and 550 ppm $CO_2$ level were almost significant. Similarly, the diurnal rate of photosynthesis showed that the values increased up to 1,200 or 1,400 h IST for the crops studied. The rate of photosynthesis mostly differs significantly between morning/evening observations and 1,200 or 1,400 h IST observations up to 4th weekly observations (i.e., up to 63 DAS), though critical difference values were less in later observations (i.e., after 77 DAS). In the present context of climate change scenario and its possible impact on crops, the study will be useful in predicting net assimilation.

## 39.1 Introduction

The dry matter of crops is produced through a process in which carbohydrates are synthesized from carbon dioxide in presence of solar energy. Several environmental factors which regulate rate of photosynthesis are solar radiation, environmental temperature, concentration of carbon dioxide in atmosphere, moisture status and turbulence. By diffusion, carbon dioxide is transported from atmosphere to the chloroplast of leaf. The concentration of carbon dioxide in atmosphere governs rate of the process. The local deficit of carbon dioxide may reduce photosynthetic rate by 10–20%; With an extra carbon dioxide level, both saturation light intensity and efficiency of light utilization increases, which increases dry matter production (Mavi 1994). For $C_4$ plants, the uptake of carbon dioxide stops at higher temperature (at 50°C or more) as compared to $C_3$ plants (at around 40°C). Hence, crops with $C_4$ pathway show less response to increased carbon dioxide as compared to crops with $C_3$ pathway. Nasser et al. (1982) indicated for corn, sugar beet, soybean and radish crops, that with an increase in carbon dioxide concentration from 350 to 675 μl/l, total dry matter increased in all species of plants, at all growth stages. High levels of carbon dioxide causes increase in net assimilation rate. Concentration of carbon dioxide in atmosphere is 0.03% by volume, which is not more than one-fourth the saturation level of carbon dioxide concentration for optimum photosynthesis. When crops are still

young the variation in concentration of carbon dioxide over the crop is very small, while the variation increases when the crop is actively synthesising (Mavi 1994). With this background an actual field experiment was conducted at adjacent plots of CAgMO (Central Agromet Observatory) with four crops at three levels of carbon dioxide concentration. The objective of the study was to quantify and compare mean rate of photosynthesis at various levels of carbon dioxide and at various hours of observation among different crops. In the present context of climate change scenario and its possible impact at increased carbon dioxide level on crops, the study will be useful in predicting net assimilation.

## 39.2 Methodology

The field experiment was conducted at adjacent plots of CAgMO (latitude 18° 32′, longitude 73° 51′), Pune, Maharashtra. Four crops were selected *viz*. sunflower, soybean, mustard, jowar and all the crops were sown on 28th October, 2003 (in order to have better comparative study among the crops). Weekly observations were taken at Three levels of carbon dioxide concentration *viz*. normal, 550 and 650 ppm by using portable photosynthetic system (LI 6400). The period of study was from 42nd to 84th days after sowing (DAS) i.e. from 8th December, 2003 to 19th January, 2004. At each of the weekly intervals, observations were taken at 2 hourly intervals *viz*. 0800, 1,000 1,200, 1,400 and 1,600 h IST from morning to evening. From daily rate of photosynthesis mean daily values were computed for each of the crops.

Statistical analysis was carried out in Randomized Block Design (RBD) involving 5 h of observation (with 4° of freedom i.e., df) and three levels of carbon dioxide concentration (with 2 df). ANOVA (analysis of variance) tables were formed for each of the weekly observations, for each crop and variance ratios were computed for conducting F-test, to determine level of significance at 5% and 1% level. When the variance ratios differed significantly, standard error differences ($SE_{diff}$) were computed to determine critical differences (C.D.) to identify statistically significant variation in the following way:

$$\text{C.D.} = \text{S.E.}_{\cdot\text{diff}} \times t_{(5\%\text{ with error df})}$$

The rate of photosynthesis under various levels of carbon dioxide concentration for each of the weekly observations for different crops are presented in Fig. 39.1a–d. The daily mean rate of photosynthesis at different levels of carbon dioxide concentration and daily mean rate of photosynthesis at different time with respective CD values are presented in Tables 39.1a, b–39.4a, b for all the four crops studied.

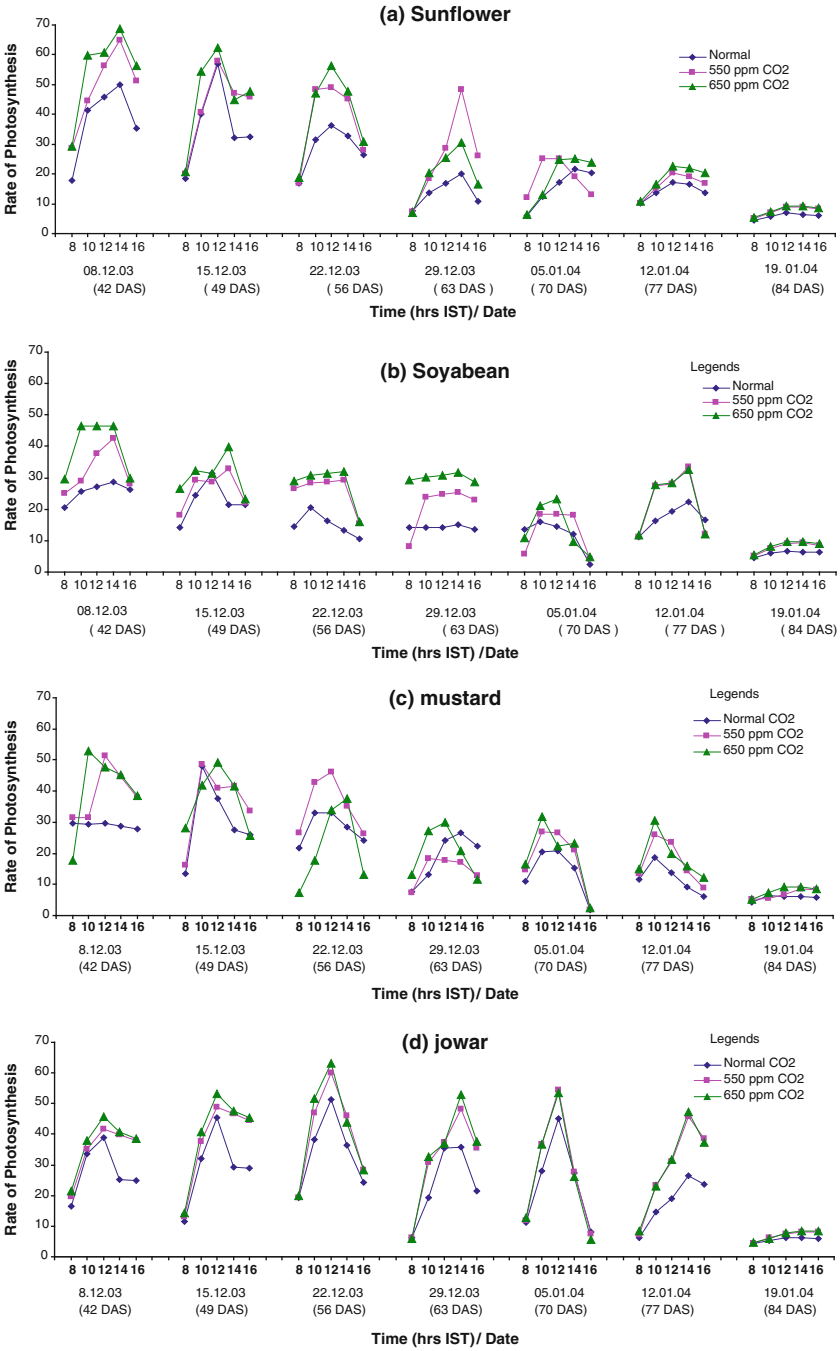


**Fig. 39.1** **(a–d)** Rate of photosynthesis (μ mole $CO_2$ $m^{-2}s^{-1}$) for different crops at various weekly observations at 2 hourly interval, under 3 levels of $CO_2$ concentration

## 39.3 Result and discussion

Figure 39.1a–d represents the rate of photosynthesis under various levels of carbon dioxide concentration for each of the weekly observations for four different crops *viz*. sunflower, soybean, mustard and jowar. Among the crops studied during the experimental period, the rate of photosynthesis was the highest for sunflower crop and the lowest for the soybean crop. The rate of photosynthesis increased with levels of carbon dioxide concentration at the earlier weekly observations.

**Table 39.1 (a)** Rate of photosynthesis at different levels of $CO_2$ concentration along with respective CD values for sunflower crop

| | Daily mean rate of photosynthesis (μ mole $CO_2$ $m^{-2}s^{-1}$) | | | |
|---|---|---|---|---|
| Date | N | 550 | 650 | CD value |
| 08.12.03 | 38.01 | 49.12 | 54.96 | 07.82 |
| 15.12.03 | 36.85 | 42.31 | 45.90 | 10.53 |
| 22.12.03 | 28.78 | 37.45 | 40.18 | 10.42 |
| 29.12.03 | 13.77 | 30.35 | 19.96 | 13.44 |
| 05.01.04 | 15.58 | 18.88 | 18.64 | NS |
| 12.01.04 | 14.24 | 16.36 | 18.42 | 02.81 |
| 19.01.04 | 05.89 | 07.66 | 08.05 | 0.97 |

NS: Not significant

**Table 39.1 (b)** Rate of photosynthesis at different time along with respective CD values for sunflower crop

| | Daily mean rate of photosynthesis (μ mole $CO_2$ $m^{-2}s^{-1}$) | | | | | |
|---|---|---|---|---|---|---|
| Date | 0800 | 1,000 | 1,200 | 1,400 | 1,600 | CD value |
| 08.12.03 | 25.20 | 48.67 | 54.21 | 61.17 | 47.56 | 05.53 |
| 15.12.03 | 19.63 | 45.01 | 59.02 | 41.33 | 42.0 | 07.45 |
| 22.12.03 | 17.50 | 42.36 | 47.24 | 41.81 | 28.42 | 07.37 |
| 29.12.03 | 07.35 | 17.38 | 23.59 | 32.92 | 17.82 | 09.50 |
| 05.01.04 | 8.13 | 16.82 | 22.40 | 22.02 | 19.11 | NS |
| 12.01.04 | 10.32 | 15.20 | 20.06 | 19.20 | 16.93 | 02.0 |
| 19.01.04 | 05.00 | 06.77 | 08.43 | 08.15 | 07.67 | 00.69 |

NS: Not significant

**Table 39.2 (a)** Rate of photosynthesis at different levels of $CO_2$ concentration along with respective CD values for soybean crop

| | Daily mean rate of photosynthesis (μ mole $CO_2$ $m^{-2}s^{-1}$) | | | |
|---|---|---|---|---|
| Date | N | 550 | 650 | CD value |
| 08.12.03 | 25.59 | 32.52 | 39.73 | 10.31 |
| 15.12.03 | 22.63 | 26.16 | 30.68 | 9.20 |
| 22.12.03 | 15.0 | 25.66 | 27.9 | 6.36 |
| 29.12.03 | 14.17 | 20.99 | 30.1 | 9.27 |
| 05.01.04 | 11.73 | 13.01 | 14.01 | NS |
| 12.01.04 | 17.13 | 22.5 | 22.44 | 9.38 |
| 19.01.04 | 05.94 | 07.86 | 08.33 | 01.45 |

NS: Not significant

**Table 39.2 (b)** Rate of photosynthesis at different time along with respective CD values for soybean crop

| | Daily mean rate of photosynthesis (μ mole $CO_2$ $m^{-2}s^{-1}$) | | | | | |
|---|---|---|---|---|---|---|
| Date | 0800 | 1,000 | 1,200 | 1,400 | 1,600 | CD value |
| 08.12.03 | 24.93 | 33.63 | 37.11 | 39.23 | 28.15 | 07.29 |
| 15.12.03 | 19.64 | 28.67 | 30.55 | 31.32 | 22.27 | 06.51 |
| 22.12.03 | 23.37 | 26.53 | 25.53 | 24.82 | 14.02 | 04.51 |
| 29.12.03 | 17.12 | 22.72 | 23.20 | 24.03 | 21.70 | 06.56 |
| 05.01.04 | 10.07 | 18.54 | 18.74 | 13.39 | 03.85 | NS |
| 12.01.04 | 11.37 | 23.78 | 25.30 | 29.48 | 13.53 | 06.65 |
| 19.01.04 | 05.01 | 07.13 | 08.43 | 08.44 | 07.89 | 01.03 |

NS: Not significant

**Table 39.3 (a)** Rate of photosynthesis at different levels of $CO_2$ concentration along with respective CD values for mustard crop

| | Daily mean rate of photosynthesis (μ mole $CO_2$ $m^{-2}s^{-1}$) | | | |
|---|---|---|---|---|
| Date | N | 550 | 650 | CD value |
| 08.12.03 | 29.08 | 39.36 | 40.43 | NS |
| 15.12.03 | 30.57 | 36.19 | 37.27 | 13.14 |
| 22.12.03 | 28.03 | 35.44 | 21.92 | 14.48 |
| 29.12.03 | 18.73 | 14.7 | 20.48 | NS |
| 05.01.04 | 13.88 | 18.21 | 19.35 | 05.81 |
| 12.01.04 | 11.91 | 17.18 | 18.76 | 05.14 |
| 19.01.04 | 05.72 | 06.87 | 07.96 | 02.1 |

NS: Not significant

**Table 39.3 (b)** Rate of photosynthesis at different time along with respective CD values for mustard crop

| | Daily mean rate of photosynthesis (μ mole $CO_2$ $m^{-2}s$) | | | | | |
|---|---|---|---|---|---|---|
| Date | 0800 | 1,000 | 1,200 | 1,400 | 1,600 | CD value |
| 08.12.03 | 26.22 | 37.90 | 42.95 | 39.53 | 34.86 | NS |
| 15.12.03 | 19.28 | 46.06 | 42.66 | 36.99 | 28.40 | 09.30 |
| 22.12.03 | 18.56 | 31.13 | 37.77 | 33.75 | 21.12 | 10.25 |
| 29.12.03 | 09.31 | 19.49 | 23.91 | 21.50 | 15.66 | NS |
| 05.01.04 | 14.15 | 26.32 | 23.28 | 19.88 | 02.10 | 04.11 |
| 12.01.04 | 13.35 | 25.05 | 19.09 | 13.20 | 09.07 | 03.64 |
| 19.01.04 | 04.86 | 06.45 | 07.38 | 07.98 | 07.59 | 01.49 |

NS: Not significant

For sunflower ($C_3$ crop) the rate of photosynthesis was high at 42 DAS, which decreased slowly up to 84 DAS (Fig. 39.1a). Daily mean rate of photosynthesis for each of the weekly observations was the highest at 650 ppm as compared to normal level of carbon dioxide concentration (Table 39.1a). The rate varied significantly between normal and 650 ppm carbon dioxide level, though the difference between 550 and 650 ppm levels were not significant. Low critical difference values were observed at later weekly observations (after 70 DAS). The diurnal variation in daily

**Table 39.4 (a)** Rate of photosynthesis at different levels of $CO_2$ concentration along with respective CD values for jowar crop

| | Daily mean rate of photosynthesis (μ mole $CO_2$ $m^{-2}s^{-1}$) | | | |
|---|---|---|---|---|
| Date | N | 550 | 650 | CD value |
| 08.12.03 | 27.76 | 34.86 | 36.9 | 07.73 |
| 15.12.03 | 29.43 | 38.14 | 40.28 | 09.06 |
| 22.12.03 | 33.94 | 40.11 | 41.41 | 06.75 |
| 29.12.03 | 23.65 | 31.63 | 33.25 | 10.05 |
| 05.01.04 | 23.87 | 27.66 | 26.91 | NS |
| 12.01.04 | 17.97 | 29.17 | 29.51 | 06.78 |
| 19.01.04 | 05.55 | 06.81 | 07.09 | 01.15 |

NS: Not significant

**Table 39.4 (b)** Rate of photosynthesis at different time along with respective CD values for jowar crop

| | Daily mean rate of photosynthesis (μ mole $CO_2$ $m^{-2}s^{-1}$) | | | | | |
|---|---|---|---|---|---|---|
| Date | 0800 | 1,000 | 1,200 | 1,400 | 1,600 | CD value |
| 08.12.03 | 19.19 | 35.57 | 42.03 | 35.24 | 33.84 | 05.47 |
| 15.12.03 | 12.99 | 36.88 | 49.12 | 41.19 | 39.57 | 06.41 |
| 22.12.03 | 19.54 | 45.68 | 58.19 | 42.07 | 26.94 | 04.77 |
| 29.12.03 | 06.13 | 27.61 | 36.67 | 45.70 | 31.43 | 07.12 |
| 05.01.04 | 11.88 | 33.80 | 50.94 | 27.06 | 7.05 | NS |
| 12.01.04 | 07.28 | 20.29 | 27.24 | 39.77 | 33.17 | 6.50 |
| 19.01.04 | 04.50 | 05.79 | 07.14 | 07.56 | 07.44 | 0.82 |

NS: Not significant

mean rate of photosynthesis (Table 39.1b) showed that the peak rate was recorded at 1,200 or 1,400 h IST for each of the weekly observations, which sometimes differed significantly as compared to the preceding or succeeding observations. The rate was low at morning or evening hours of observations.

For soybean ($C_3$ crop) the rate of photosynthesis was high at 42 DAS, which decreased slowly up to 84 DAS (Fig. 39.1b). Daily mean rate of photosynthesis for each of the weekly observations was the highest at 650 ppm (also differed significantly) as compared to normal level of carbon dioxide concentration (Table 39.2a), though the difference between 550 and 650 ppm levels were not significant (except observation recorded on 29th December, 2,003 was almost significant). The diurnal variation in daily mean rate of photosynthesis (Table 39.2b) showed the peak rate at 1,200 or 1,400 h IST, which differed significantly as compared to morning or evening hours of observations.

For mustard ($C_3$ crop) the rate of photosynthesis followed similar trend (was high at 42 DAS) like sunflower and soybean crops (Fig. 39.1c). However, the mean daily rate of photosynthesis at various levels of carbon dioxide concentration did not differ significantly up to 70 DAS (Table 39.3a). As the experiment started from 42 DAS and mustard is a short duration crop, the rate of photosynthesis did not differ significantly, though the trend like other crops was observed. The diurnal variation in daily mean rate of photosynthesis (Table 39.3b) showed the peak rate

mainly at 1,200 h IST and in some occasions at 1,000 h IST, which differed significantly as compared to morning or evening hours of observations.

For jowar ($C_4$ crop) the rate of photosynthesis was high at 49 and 56 DAS, which decreased slowly with the advancement of the crop growth (Fig. 39.1d). Daily mean rate of photosynthesis for each of the weekly observations was the highest at 650 ppm (also differed significantly) as compared to normal level of carbon dioxide concentration (Table 39.4a), though the difference between 550 and 650 ppm levels were not significant. The diurnal variation in daily mean rate of photosynthesis (Table 39.4b) showed the peak rate at 1,200 h IST mainly (for 5 weekly observations) and also at 1,400 h IST, which differed significantly as compared to preceding and succeeding observations as well as morning or evening observations.

Hence, among the four crops studied, enhancement of carbon dioxide concentration resulted significantly for three crops (except mustard) up to 550 ppm level as compared to normal, as 550 and 650 ppm levels did not differ significantly.

## 39.4 Conclusions

The study of diurnal rate of photosynthesis at various levels of carbon dioxide concentration for four different crops revealed the following conclusions:

(a) The rate of photosynthesis at early DAS was more, which decreased slowly at later DAS.
(b) The mean rate of photosynthesis for each of the weekly observations was the highest (and differed significantly) at 650 ppm as well as at 550 ppm levels as compared to normal carbon dioxide concentration.
(c) The difference in rate of photosynthesis between 550 and 650 ppm levels were not statistically significant, which indicated that optimum level of $CO_2$ enhancement for the crops studied was up to 550 ppm.
(d) The diurnal variation in rate photosynthesis recorded the peak at 1,200 or 1,400 h IST, which differed significantly as compared to morning or evening hours of observations.

## References

Mavi HS (1994) Introduction to agrometeorology. Oxford & IBH Publishing Co. Pvt. Ltd, New Delhi, pp 1–270

Nasser Sionit, Hellmers H, Strains BR (1982) Interaction of atmospheric $CO_2$ enrichment irradiance in plant growth. Agron J 74:721–724

# Chapter 40
# Effect of Weather Variability on Growth Characteristics of Brassica Crop

**Ananta Vashisth, N.V.K. Chakravarty, Goutam Bhagavati, and P.K. Sharma**

**Abstract** A field experiment was conducted at research farm of IARI, New Delhi with an aim to study the effect of weather variability on crop growth and seed yield. Three cultivars of Brassica were sown on three dates at an intervals of 15 days during 2007–2008 rabi season. The leaf area index, biomass, chlorophyll concentration index and aphid infestation were measured at different stages of crop growth. Study revealed that all the growth parameters were affected due to the change in the weather conditions. First sown crop experiences 2–3°C lower temperature as compared to late sown crop during maturity and more temperature during field emergence, vegetative and flowering. Because of more favorable weather conditions and less aphid infestation crop growth and seed yield were relatively more in the first sown crop as compared to late sown crop.

## 40.1 Introduction

Brassica is a major oilseed crop grown during rabi season. Weather variability causes substantial fluctuations in any crop production. Even under optimum conditions, variation in temperature influences the growth and development of the crop because most of the biological and physiological processes are known to be markedly affected by temperatures (Prasad 1989). Brassica being a cool season crop, 2–3°C higher temperature during pod formation and seed filling stage affects crop growth and yield significantly (Kar and Chakravarty 2000). Krishnamurthy and Bhatnagar (1998) reported that the time of sowing plays a key role in modifying the length of vegetative and reproductive phase in this crop. To mitigate the effects of weather variability, modification in sowing dates could be one option for optimizing the growth and seed yield. There have been a few studies both in

A. Vashisth (✉) • N.V.K. Chakravarty • G. Bhagavati • P.K. Sharma
Division of Agricultural Physics, Indian Agricultural Research Institute, New Delhi 110012, India
e-mail: anantavashisth@iari.res.in; nvkchak@iari.res.in

S.D. Attri et al. (eds.), *Challenges and Opportunities in Agrometeorology*,
DOI 10.1007/978-3-642-19360-6_40, 

India and elsewhere aimed to understand the nature and magnitude of grains and losses in yield of particular crops at selected sites under elevated atmospheric $CO_2$ conditions and associated climate change (Abrol et al. 1991; Sinha and Swaminathan 1991; Aggarwal and Sinha 1993; Lal et al. 1998). These studies have been mainly confined to cereal crops mainly wheat and rice. In this study an attempt has been made to assess the effect of weather variability and change on the productivity of Brassica crop.

## 40.2 Materials and Methods

Field experiments were conducted during 2007–2008 rabi season at research farm of IARI, New Delhi, India. The climate of the station is semiarid with dry hot summers and cold winters. Three varieties of *Brassica juncea* viz., Pusa Gold, Pusa Jaikisan (most popularly grown in north western parts of India) and BIO 169-96 (a pipe line variety) were sown on 16th, 30th October and 13th November 2007. The crops were raised following the standard recommended agronomic practices with three replications in a randomized block design (RBD). All growth parameters like leaf area index (LAI), Biomass, Chlorophyll content index (CCI), aphid infestation and weather parameters were taken at 10 days intervals. Number of days required to attain different phonological stages like field emergence, first flowering, 50% flowering, pod formation, maturity and harvesting were recorded.

### *40.2.1 Leaf Area Index (LAI)*

Three randomly selected plant samples (above ground) were taken and the leaf area was measured using leaf area meter (model LICOR-3100). The LAI was calculated with the following formula:

$$\text{LAI} = \text{Measured leaf area per plant}\left(\text{cm}^2\right)/\text{Ground area covered by the plant}\left(\text{cm}^2\right)$$

### *40.2.2 Biomass Production*

The samples collected for estimating leaf area index were utilized for assessing the biomass production. Plants samples were oven dried at 80°C for 48 h for constant weight in order to estimate the accumulation of dry matter in different plant parts.

### *40.2.3 Chlorophyll Concentration Index (CCI)*

Chlorophyll concentration index was measured using chlorophyll concentration meter. The CCM-200 takes non-destructive measurements of relative chlorophyll

concentration through optical analysis. Chlorophyll transmission is characteristically high in the near infrared range and very low in the red range because green plants absorb visible radiation for photosynthesis and transmit near infrared, which they do not use. The CCM-200 uses LEDs that emit specific wavelengths in the red and infrared ranges. The detector analyzes the ratio of the two wavelengths to determine chlorophyll concentration index (CCI). Chlorophyll concentration index (CCI) is defined as the ratio of transmission at 931–653 nm through a leaf.

### *40.2.4 Aphid Population*

Aphids from 10 cm tip portion of the central shoot of six randomly selected plants were counted. Among six randomly selected plants, two were chosen and tagged from second and third at one corner e. g. north, next two were selected from middle rows and last two plants were selected from the two rows at diagonally opposite corner leaving the border row.

### *40.2.5 Growing Degree Days (GDD)*

The summation of mean temperature above a base value represents the growing degree days or thermal time.

$$GDD = \sum (T_{\max} + T_{\min})/2 - T_b{}^{\circ}C$$

Where, $T_{max}$ and $T_{min}$ represent the daily maximum and minimum temperatures and $T_b$ is considered as 5°C following Morrison et al. (1990).

### *40.2.6 Seed Yield*

Plants from one square meter area each were cut above ground from three randomly selected places in each plot. After sufficient air drying, these samples were weighed. Thrashing was done separately and seed weight was recorded. The average seed yield was calculated.

### *40.2.7 Statistical Analysis*

The data was analysed using the software SPSS 10.0. The significant level of difference of all measured parameters was calculated. One way analysis of variance was carried out following a randomized complete block.

## 40.3 Result and Discussion

### *40.3.1 Weather During Rabi (2007–2008)*

#### 40.3.1.1 Temperature and Rainfall

The weekly mean maximum temperatures at sowing, crop establishment period, active vegetative and flowering were almost same except 2nd and 3rd week as that of the normal while during the reproductive stages of crop, the temperatures were higher than the normal. The minimum temperatures during the season were considerably lower than the normal values. From 48th standard week till 8th week the minimum temperature was lower than the normal except for 2nd and 3rd week (Fig. 40.1). During this period the temperature even touched lowest of −0.8°C on 2nd January and remained more or less near zero for over 9 days. The low temperature proved to be beneficial to mustard crop as it suppressed the aphid population dramatically, reducing the yield losses thus facilitating a good crop. The rainfall during this season was negligible. The relative humidity of morning was almost similar to the normal. The evening relative humidity is less during field emergence as well as pod formation and maturity. However it was more than normal for vegetative and flowering stages (Fig. 40.2). Evaporation was less than normal during vegetative and flowering stages, more for maturity and equal to normal for field emergence and pod formation. A bright sunshine hour was less than normal except 1 week during pod formation (Fig. 40.3).

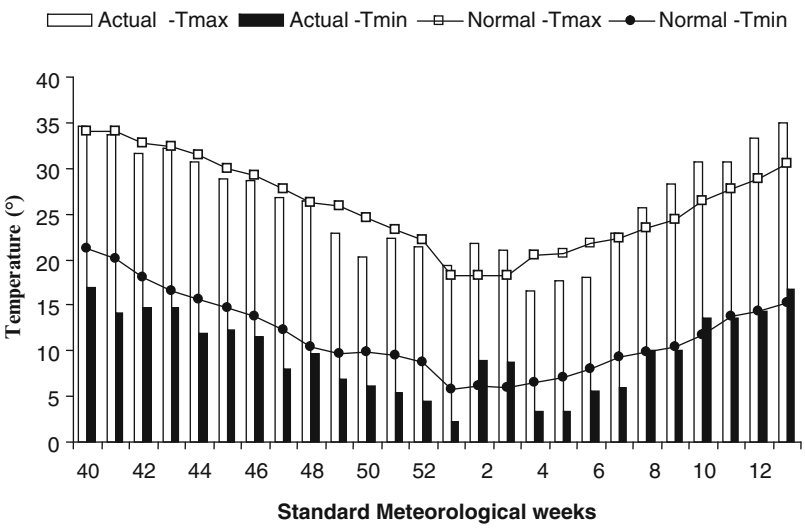


**Fig. 40.1** Maximum and minimum temperature during Rabi (2007–2008)

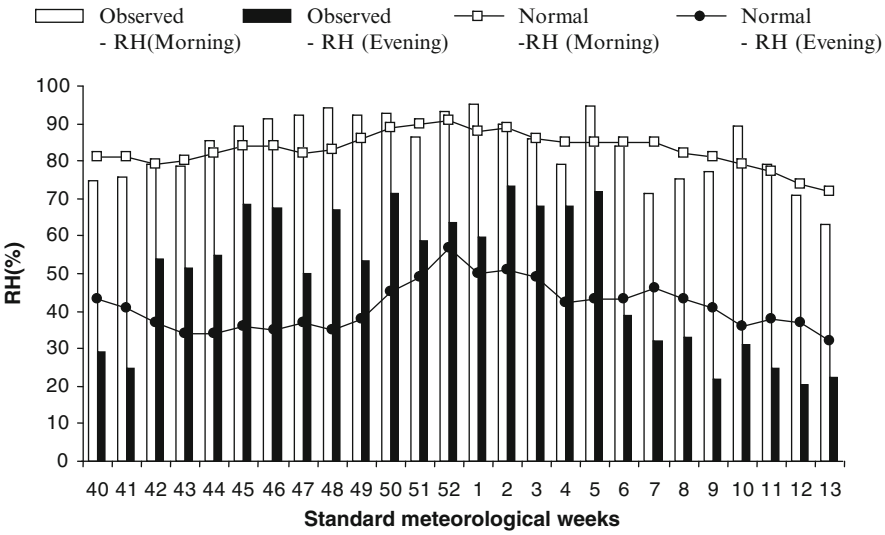


**Fig. 40.2** Relative humidity morning and evening during Rabi (2007–2008)

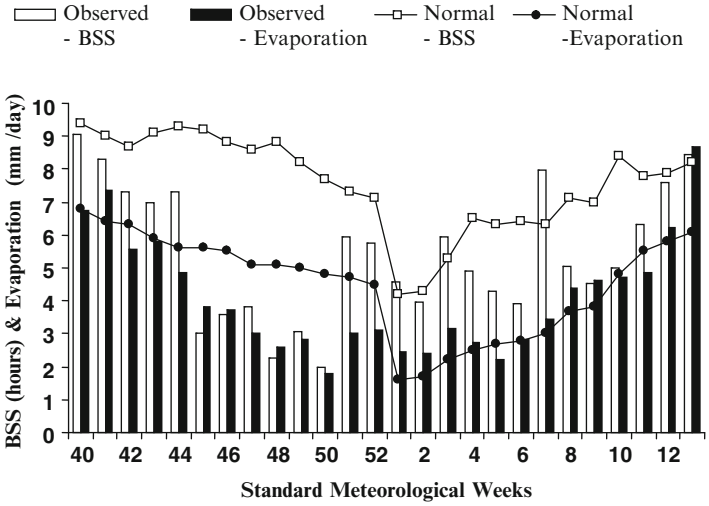


**Fig. 40.3** Bright sunshine hours and Evaporation during Rabi (2007–2008)

### 40.3.1.2 Variation in Temperatures During Different Phonological Stages of Brassica Sown at Different Dates

The weekly maximum and minimum temperature during germination for 1st sowing was 31.7°C and 14.8°C, for 2nd sowing it was 30.2°C and 11.8°C and for 3rd sowing it was 28.2°C and 10.6°C. Due to the less maximum, minimum and

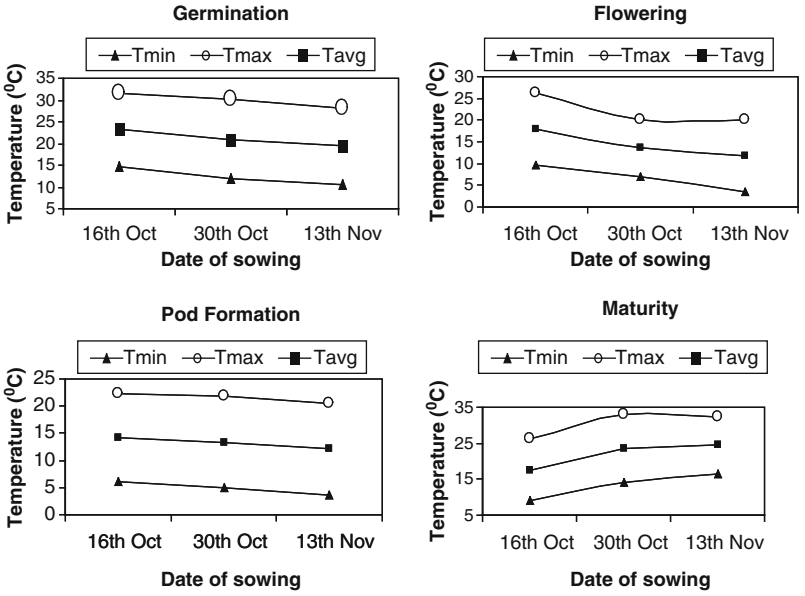


**Fig. 40.4** Variation in temperatures during different phonological stages of Brassica sown at different dates

average temperature, the germination rate was lower in 3rd sowing as compared to 1st and 2nd sowing. During flowering the weekly maximum and minimum temperature for 1st sowing was 26.3°C and 9.7°C, for 2nd sowing it was 20.2°C and 7.0°C and for 3rd sowing it was 20.0°C and 3.4°C. During pod formation the weekly maximum and minimum temperature for 1st sowing was 22.2°C and 6.0°C, for 2nd sowing it was 21.9°C and 4.9°C and for 3rd sowing it was 20.6°C and 3.5°C. During maturity the weekly maximum and minimum temperature for 1st sowing was 26.3°C and 9.1°C, for 2nd sowing it was 32.8°C and 14.0°C and for 3rd sowing it was 32.3°C and 16.5°C (Fig. 40.4). Due to the more maximum, minimum and average temperature during flowering and pod formation and less maximum, minimum and average temperature during maturity the yield was more in 1st sowing as compared to 2nd and 3rd sowing. Nanda et al. (1994) viewed that reduction in seed yield of Brassica species under late sown conditions might be attributed to increase in temperatures at the time of pod growth and seed filling stage, which reduced the dry matter accumulation into the seed and shortened the seed filling period.

### *40.3.2 Leaf Area Index*

It was observed that the leaf area index (LAI) was higher in BIO 169-96 by 38% and 18% than Pusa Jaikisan and Pusa Gold respectively. The first sown crop showed

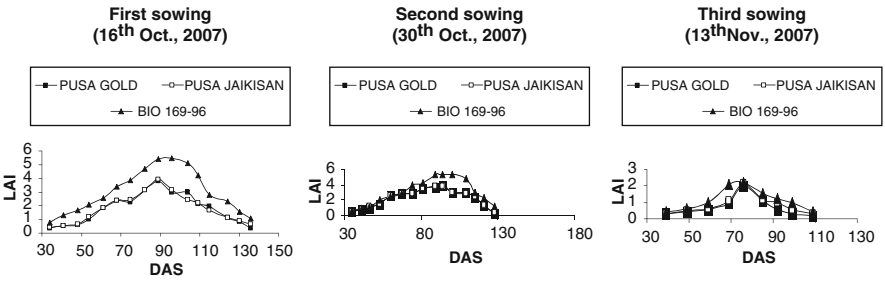


**Fig. 40.5** Leaf area index in different varieties of Brassica sown at different dates

40% and 24% higher LAI in Pusa Gold and BIO 169-96 than late sown crop. However there was no change in LAI in Pusa Jaikisan irrespective of date of sowing. . The peak leaf area index was highest in BIO 169-96 followed by Pusa Jaikisan and Pusa Gold in three respective sowings (Fig. 40.5). Leaf area index increased and reached a maximum around pod formation stage (45% flower to 85% podding stage) irrespective of weather conditions. Later, the leaf area index declined rapidly. Senescence and abscission coincided with onset of flowering and completed well before maturity. In all the three cultivars maximum leaf area index was attained in the first sowing. Kar and Chakravarty (2000) reported that LAI was lower in a season with higher temperature (2–3°C) during grain filling stages as compared to the season with relatively lower temperatures in the same period. Rao and Agarwal (1986) reported that, the maximum LAI was found at 90 DAS and thereafter declined towards maturity.

### *40.3.3 Biomass Production*

Biomass production in plant is the process of organic substance formation, product of photosynthesis. The timely accumulation of dry matter by the crop is important as it is followed by adequate translocation of assimilates to the sink resulting in higher yield. The variety BIO 169-96 produced higher biomass as compared to Pusa Jaikisan and Pusa Gold irrespective of sowing dates, which might be due to higher leaf area index and more proliferating characters. The biomass production was higher in early sown crop than late sown crop by 60% in BIO 169-96, 46% in Pusa Jaikisan and 58% in Pusa Gold. The reduction in the biomass production due to late sowing is in conformity with earlier findings of Kar and Chakravarty (2000).

### *40.3.4 Chlorophyll Concentration Index*

Chlorophyll concentration index was found to be 6% more in Pusa Gold as compared to Pusa Jaikisan and 12% more as compared to Bio-169-96.

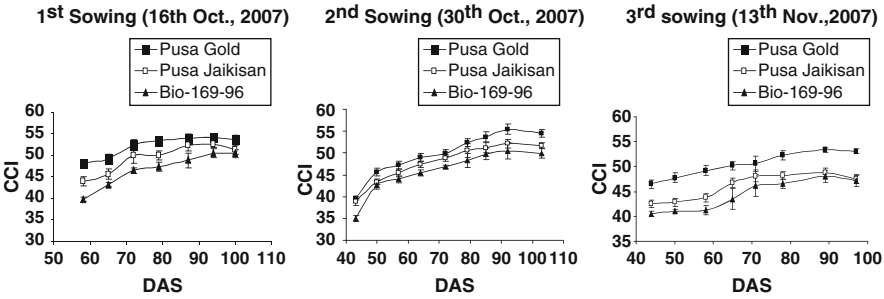


**Fig. 40.6** Chlorophyll concentration index in different varieties of Brassica sown at different dates

The chlorophyll concentration index was higher in early sown crop by 4% in Pusa Jaikisan and Pusa Gold than late sown crop (Fig. 40.6). However BIO-169-96 has marginal change with respect to date of sowing. CCI increased reached maximum during pod formation and thereafter decrease in all three varieties irrespective of weather conditions.

### *40.3.5 Validation of Aphid Forewarning Hypothesis*

The weather based aphid-forewarning hypothesis developed by Chakravarty and Gautam (2002) was validated with the aphid data taken during the mustard crop growth period. When the accumulated Growing Degree Days were lower, the peak population was higher. Before validating aphid forewarning hypothesis, physical impact of rain fall should be taken into consideration. The GDD based aphid for warning model was found to be valid for forewarning of aphids. This season, the peak aphid population was observed to be 300/10 cm main shoot. Collins and Leather (2001) from the controlled environment studies reported that nymphal development rate of aphid increased linearly with temperature and thermal requirement.

Aphid population was found to be more in Pusa Gold followed by BIO 169-96 and Pusa Jaikisan (Fig. 40.7). Also aphid infestation was more in late sowing. Patel et al. (2004) observed that the critical period of mustard exposure to aphids was found to be the 3rd week after aphid appearance when the crop was in flowering stage and hence the control measures have to be initiated before flowering. In present study the higher yield in first sown crop might be attributed to comparatively lower aphid population during crop growth and maximum time taken by the crop for its growth and development. These finding are in agreement with Verma et al. (1993). Rohilla et al. (1996) observed from field studies conducted in Haryana, that the pest incidence increased with an average temperature of about 13.7°C and a relative humidity 65% and decreased with temperature above 35°C.

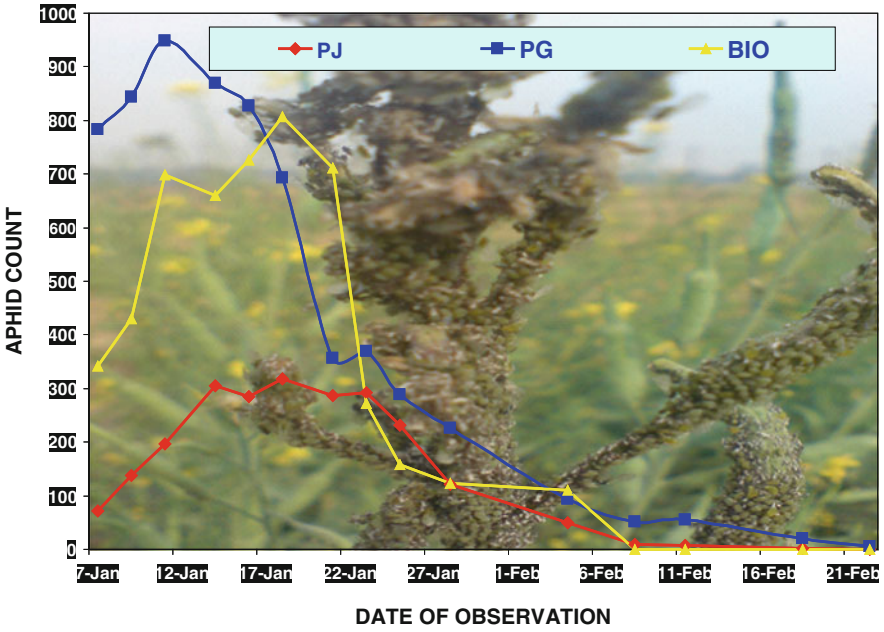


**Fig. 40.7** Aphid population in different varieties of Brassica

**Table 40.1** Seed Yield (q/ha) of different varieties of Brassica sown at different dates

| Varieties | Date of sowing (Mean ± SE) | | |
|---|---|---|---|
| | 16th Oct, 07 | 30th Oct, 07 | 13th Nov, 07 |
| Pusa Gold | 18.84 ± 0.058 | 16.4 ± 0.088 | 10.78 ± 0.062 |
| Pusa Jaikisan | 34.93 ± 0.035 | 24.75 ± 0.020 | 20.75 ± 0.05 |
| BIO-169-96 | 25.24 ± 0.058 | 20.63 ± 0.024 | 14.54 ± 0.052 |

### *40.3.6 Seed Yield*

The seed yield was found to be higher in Pusa Jaikisan followed by BIO169-96 and Pusa Gold in all three date of sowing. Early sown crop yielded higher 60% in Pusa Jaikisan, 15% in Pusa Gold and 22% in BIO 169-96 respectively than late sown crop. Pusa Jaikisan have 17% and 51% higher yield than BIO 169-96 and Pusa Gold (Table 40.1). Although BIO 169-96 had more LAI and Biomass as compared to Pusa Jaikisan but due to more aphid infestation in BIO 169-96 as compared to Pusa Jaikisan the seed yield was found to be less in BIO 169-96 then Pusa Jaikisan. The reduction in seed yield due to delay of sowing was also reported by Roy and Chakravarty 2002. Patel et al. (2004) reported that yield attributes and yield of mustard significantly decreased in delayed sowing even under protected conditions.

Thus it can be concluded that crop growth and seed yield were relatively higher in the first sown crop because of more congenial weather conditions and less aphid infestation during the entire crop growth period. Delay in sowing time reduces the

yield significantly. Since Pusa Gold was more susceptible to aphid infestation than Pusa Jaikisan and BIO 169-96, Pusa Gold can be used as trap crop to overcome the aphid infestation in other varieties and hence reduce the spray of insecticides.

## References

Abrol YP, Bagga AK, Chakravarty NVK, Wattal PN (1991) Impact of rice in temperature on the productivity of wheat in India. In: Abrol YP, Wattal PN, Gnaman A, Goyindjee, Ort DR, Teramuka AH (eds) Impact of global climate changes on photosynthesis and plant productivity. Oxford and IBH Publishing, New Delhi, pp 77–789

Aggarwal PK, Sinha SK (1993) Effect of probable increases in carbon dioxide and temperature on productivity of wheat in India. J Agric Meteorol 48(5):811–814

Chakravarty NVK, Gautam RD (2002) Forewarning Mustard Aphid. Published by Cooperating Centre for Mustard NATP-MMP-17 (Program 6), Division of Agricultural Physics, Indian Agricultural Research Institute, New Delhi, 63 p

Collins CM, Leather SR (2001) Effect of temperature on fecundity and development of giant willow aphid, Tuberolachnus salignus (Sternorrhyncha: Aphididae). Eur J Ent 98(2):177–182

Kar G, Chakravarty NVK (2000) Phenological stages and growth dynamics of Brassica as influenced by weather. J Agric Meteorol 2(1):39–46

Krishnamurthy L, Bhatnagar VB (1998) Growth analysis of rainfed mustard (Brassica juncea L.). Crop Res 15(1):43–53

Lal M, Singh KK, Rathore LS, Srinivasan G, Saseendran SA (1998) Vulnerability of rice and wheat yields in NW-India to future changes in climate. Agric Forest Meteorol 89:101–114

Morrison MJ, Mc. Vetty PBF, Scarth MJ (1990) Effect of altering plant density on growth characteristics of summer rape. Can J Plant Sci 70:139–149

Nanda R, Bhargava SC, Tomar DPS (1994) Rate and duration of siliqua and seed filling period and their relation to seed yield in Brassica spp. Indian J Agric Sci 64:227–232

Patel SR, Awasthi AK, Tomar RK (2004) Assessment of yield losses in mustard (Brassica juncea L.) due to mustard aphid (Lipaphis erysimi, Kalt.) under different thermal environment in eastern central India. Appl Eco Environ Res 2(1):1–15

Prasad R (1989) Response of Brassica species to thermal environment under Delhi conditions. Ph.D. thesis, Indian Agricultural Research Institute, New Delhi

Rao P, Agarwal SK (1986) Growth analysis of mustard as affected by soil moisture conservation practices and supplemental irrigation. Int Semin Water Manage Arid Semi-Arid Zones 27:434–437

Rohilla HR, Singh H, Yadava TP, Singh H (1996) Seasonal abundance of aphid pests on rapeseed-mustard crop in Haryana. Ann Agric Bio Res 1(1–2):75–78

Roy S, Chakravarty NVK (2002) Effect of variable weather conditions on leaf area, biomass and seed yield in Brassica spp. J Agric Phys 2(1):29–32

Sinha SK, Swaminathan MS (1991) Deforestation, climate change and sustainable nutrition security. Clim Change 16:33–45

Verma SN, Singh OP, And Nema KK (1993) Effect of dates of sowing on the incidence of mustard aphid and its parasites in Madhya Pradesh. Indian J Agric Res 27(2):76–80

# Chapter 41
# Agronomic Impacts of Climate Variability on Rice Production with Special Emphasis on Precipitation in South Western Plains of Uttarakhand

**S. K. Tripathi and B. Chintamanie**

**Abstract** Climate variability is a threat to food production. Weather aberrations and climatic fluctuations are the growing concern for their effects on agriculture have stimulated academic, public and policy-level interests on the analysis of the impacts of climate variability on agricultural production systems. Long-term climate variability influences sowing date, crop duration, crop yield, and other management practices adapted in rice production. Short-term weather episodes can also affect yield by inducing changes in temperature, potential evapotranspiration, and moisture availability. The degree of vulnerability of crops to climate variability depends mainly on the development stage of the crops at the time of weather aberration. The vulnerability and risk of crop production due to weather fluctuations and climate variability can be minimized if future weather variation could be precisely predicted and a suitable process-based ecophysiological crop yield forecasting model can be identified to produce real-time attack of insects pest and diseases of crop. Scientists and farmers must join efforts to further understand crop–climate relationships and formulate viable, locally adapted production technologies to sustain rice productivity against climate variability. This paper is presented to discuss the agronomic impacts of climate variability on rice production with special emphasis on rainfall in the Northern State of Uttarakhand.

## 41.1 Introduction

Rice is the most important cereal food crop of India. It occupies about 23.3% of gross cropped area of the country. It plays a vital role in the national food security. Rice contributes 43% of total food grain production and 46% of the total cereal

S.K. Tripathi (✉) • B. Chintamanie
Department of Water Resources Development and Management, Indian Institute of Technology Roorkee, Roorkee, India
e-mail: sankufwt@iitr.ernet.in

S.D. Attri et al. (eds.), *Challenges and Opportunities in Agrometeorology*,
DOI 10.1007/978-3-642-19360-6_41, © Springer-Verlag Berlin Heidelberg 2011

production of the country. Rice is the staple food of more than 60% of the world's population especially for most of the people of South-East Asia. Among the rice growing countries in the world, India has the largest area under rice crop and ranks second in production next to China.

Weather and climate have a direct influence on cropping systems and crop yield. Thus, weather fluctuations and climate variability play a significant role in crop growth and yield. Occurrence of abnormal weather conditions during the growing season or during critical development stages may hamper growth processes resulting in severe reduction in yield. This makes climate variability a threat to food security thus leading to serious social and economic implications (Hossain 1997). However, a clear understanding of the vulnerability of food crops as well as the agronomic impacts of climate variability enables one to implement adaptive strategies to mitigate its negative effects.

The concern on past, present and future weather aberrations, climate trends, and their effects on agriculture has continued to stimulate research as well as public and policy-level interests on the analysis of climate variability and agricultural productivity (IPCC 1996). It is well recognized that climate variability has a wide range of direct and indirect impacts on crop production. In the India, floods and droughts caused rice (Oryza sativa L.) production losses. Weather and climate affect plant growth and development, and the fluctuations and occurrences of climatic extremes particularly at critical crop growth stages may reduce yield significantly (Peng et al. 1996).

This paper presents the agronomic impacts of climate variability on rice production systems. These impacts are described based on the results of systems-based studies in the south western plains of Uttakhand. Key climate variables and measures of variability are examined with specific reference to rainfall. The analysis distinguishes the impacts of long-term weather variability and short-term weather episodes. Some adaptive strategies to climate variability to reduce vulnerability and risk are also presented. Suggestions and recommendations for an efficient and effective analysis of agronomic impacts of climate variability are also discussed.

## 41.2 Uttarakhand

The state of Uttarakhand lies in the eastern most part of the Western Himalaya within the vast east west expanse of the Himalayan range. Situated between 28°53′24″–31°27′50″ N latitudes and 77°34′27″–81°02′22″ E longitudes, it occupies an area of 53,483 km, which accounts for about 1.62% of the total area of the country (Fig. 41.1). The region is predominantly mountainous with exceptions in the South where plains areas occur along the foothills. The altitude ranges from 300 to 7,817 m (Nanda Devi peak). The climate of Uttarakhand varies from subtropical to alpine. It is relatively cool and humid compared to rest of the Western Himalaya. Except inner dry ranges, much of the state receives high precipitation during monsoon and heavy snow during winter at higher altitudes (>2,000 m).

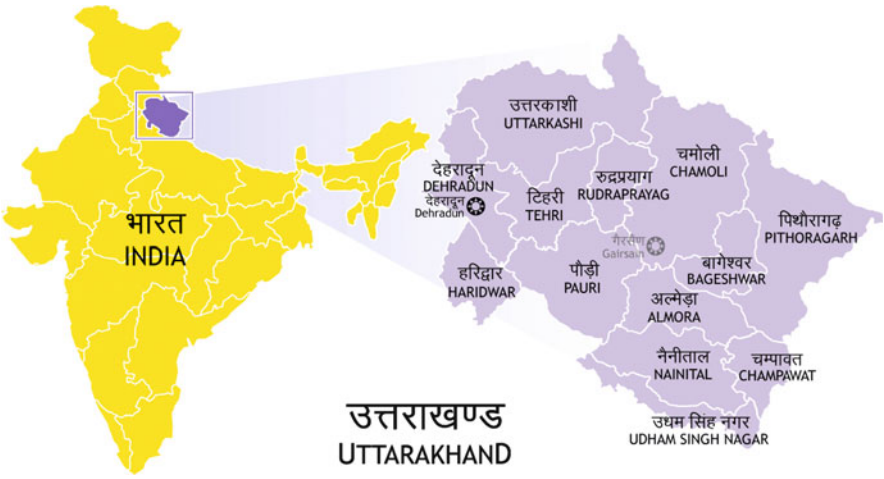


**Fig. 41.1** Map of Uttarakhand and its location in India

## 41.3 Soils of Uttarakhand

In Uttarakhand, there is a wide variation in soil type. It varies from the deep, alluvial and fertile soils of the terai tract to the down alluvium of the dun valleys; the thin fragile soil of the Siwalik Hills; the black soil of the temperate zones; and the arid bare soil of the inner dry valleys. There are several parameters that have significant bearing on the nature, composition, properties and distribution of the soils in Uttarakhand. These are the nature, composition, structure and texture of the parent rocks below the soil; the altitude at which the soils occurs; the process that had led to the formation of such soil type; the climatic conditions experienced in that locality; the nature and composition of vegetation on the soil; the use of the soil; the dominant process of erosion in the locality; disturbance of the soil by external agencies.

## 41.4 Crop Diversity in Uttarakhand

A study conducted by (Kuniyal 2003) show that there is low crop diversity in Uttarakhand. The derived levels of Index for Crop Diversity (Icd), ranging from 15.25 to 29.09, were separated into four levels of diversity, by quartiles. These are low (L), moderate low (ML), moderate high (MH) and high (H). The study showed that of the eight important crops grown, there are only two major crops, wheat (31.10%) and paddy (18.26%). This denotes a high degree of crop specialization and little diversity. In the Kumaun region also, out of the eight important crops, three/wheat (34.01%), paddy (28.80%) and sugarcane (23.59%)/occupy much of

the total cultivated area, which indicates less crop diversity and high specialization. The Icd for the region is 28.80 and falls in the low crop diversity level. Concerning the other districts, only two districts fall under the low (level (L) of crop diversity/ Chamoli (29.09) and Pithoragarh (27.10). On the other hand, two districts, Pauri (16.38) and Dehradun (15.25) have an (H) level of crop diversity.

## 41.5 Main Climatic Variables

The occurrence of weather episodes such as extremes characterized by maximum or minimum temperature, sequences of dry or wet days, and high winds may significantly affect crop growth and development which results in reduced crop yield. In Uttarakhand, monsoon currents, tropical and the inter-tropical convergence zone divide the year into wet and dry seasons. Many areas have rain from May to October, the peak amounts falling in August. During the dry months (February-April), rainfall is generally deficient. Climate variability can be readily observed from the fluctuations in rainfall, wind speed and direction, and temperature. Fluxes in rainfall volume below or above normal annual values may be experienced in areas affected by the anomaly. Similarly, shifts in temperature regimes in comparison with the temperature range for specific periods of the year and/or across several years also indicate climate variability. Inter-annual variability in wind speed and direction also reflect climate variability.

## 41.6 Effects of Long-Term Climate Variability

### *41.6.1 Sowing Date*

Climate variability affects timing of initiation of the cropping season which is determined largely by the start of the rainy season particularly in rainfed areas. For rice production in Uttaranchal land preparation starts as soon as the cumulative amount of rainfall for the last 20–30 days after April 1 reaches to about 150–200 mm. It is during this period that the soil accumulates enough moisture to support plant growth.

### *41.6.2 Crop Duration*

Weather and climate variability influence the initiation of the rice cropping season since it is often synchronized with the onset of the rainy season. The cropping calendar is often adjusted to coincide with the period with high probability of receiving adequate rainfall to support plant growth requirements. In Uttaranchal,

it is commonly observed that planting period, capable of sustaining effective rice production during the dry season, is narrower for most of the regions in Uttaranchal compared to the time frame available during the wet season. The narrower dry season planting period seeks to maximize the remaining moisture from the previous wet season rice cropping. Regions with more even year-round distribution of rainfall may also exhibit overlaps in rice planting and harvesting operations.

### *41.6.3 Crop Yield*

Crop yield is directly influenced by climate variability as exhibited in the time series data of Uttaranchal rice yields. Figure 41.2 illustrates rainfed rice productivity in the Uttaranchal (formerly UP) (1979–2007) as affected by Rainfall Variability. It shows how inter-annual rainfall variability can negatively influence yield of rice without any corresponding effect on the dry season cropping. This condition is due to the late onset and early termination and high and low intensity rain in the year.

### *41.6.4 Cropping Systems*

Cropping sequence/crop rotation of annual crops can be modified to adapt to climatic variability. This may also result in adjustments in scale of production often resulting in a decrease in area for crop production. The reduction in area cultivated is often a coping mechanism to reduce the impact associated with increased risk and uncertainty. Modification in choice of crops or cultivars to grow especially in areas accustomed to high crop diversification, and even changes in agronomic management practices including fertilizer use, irrigation, and control of pests and diseases are other adjustments resorted to in times of climate variability.

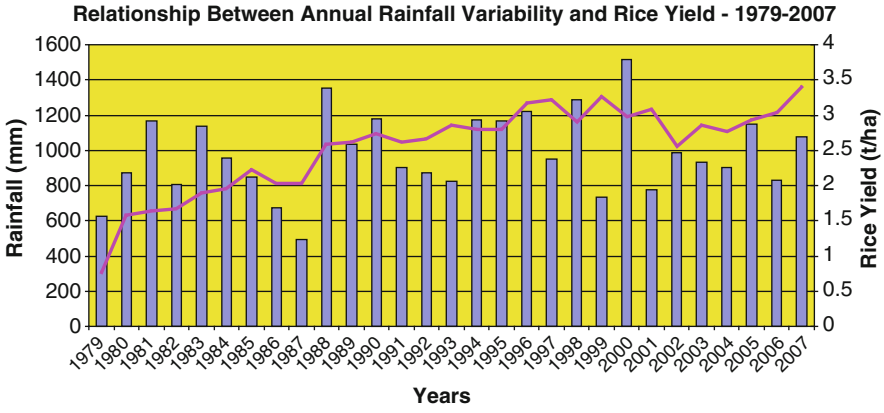


**Fig. 41.2** Inter-annual rainfall variability and rice yield in Uttarakhand

## 41.7 Impacts of Short-Term Weather Episodes

### *41.7.1 Changes in Temperature*

Crops have varying sensitivity to temperature. There are temperature threshold values beyond which crops become vulnerable to sharp temperature shifts. Satake and Yoshida (1978) reported that spikelet sterility in Indica rice varieties was induced when exposed to high temperature immediately before and during anthesis. The same study attributed the major causes of high temperature-induced sterility in rice to disturbance of pollen shedding and decreased viability of pollen grains. This resulted in decreased number of germinated pollen grains on the stigma. Thus, rice yield is expected to decrease during instances of high temperature during flowering. Similar results of induced sterility, reduced kernel quality, and decreased kernel dry weight in rice were reported by Tashiro and Tashiro when day/night temperature shifts from 27/22 to 36/31°C during the reproductive stage of plant development. "The presentation given in Figs. 41.3 and 41.4 shows the relationship between average temperature regimes (Minimum & Maximum) and average yield of rice in Uttarakhand."

### *41.7.2 Crop Water Requirements*

Occurrence of sequences of wet and dry periods can affect crop physiological processes that may prematurely hasten or retard crop growth and development. Prolonged periods of heavy rainfall (which may result in flooding) during initial crop development may abort crop growth, and may lead to significant yield reduction when the heavy rainfall events occur during the critical period of crop

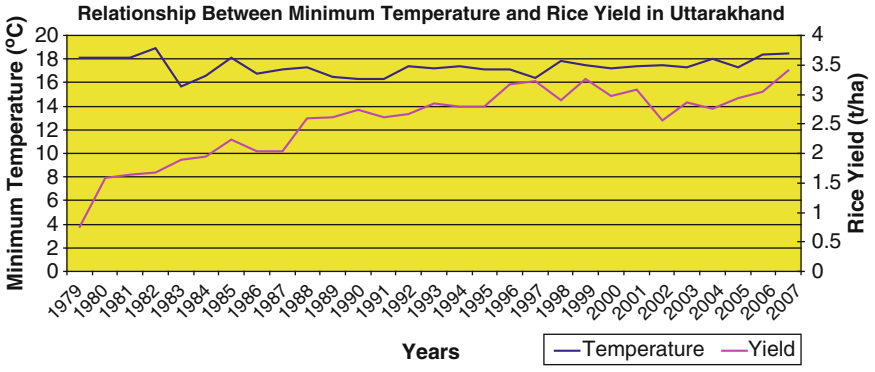


**Fig. 41.3** Relationship between minimum temperature and rice yield

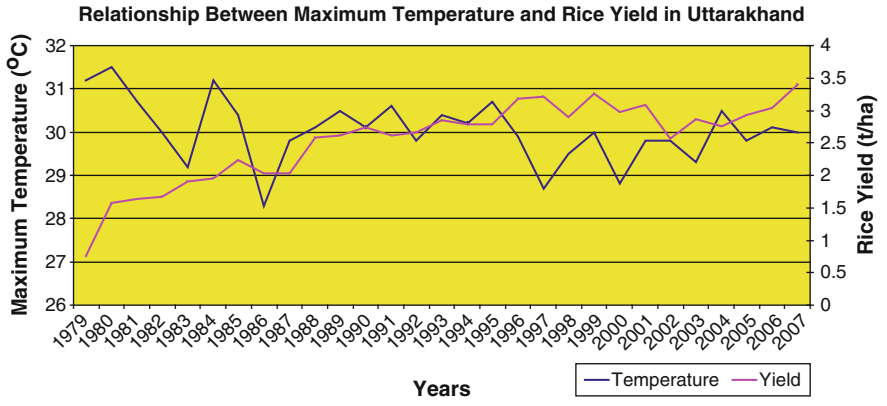


**Fig. 41.4** Relationship between maximum temperature and rice yield

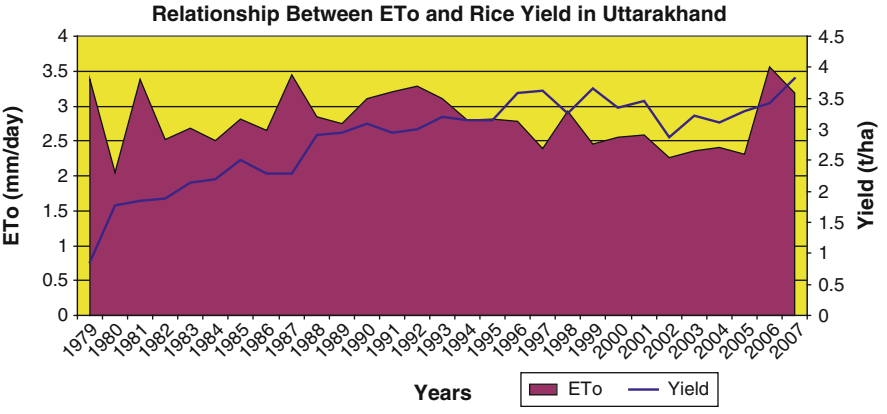


**Fig. 41.5** Relationship between ETo and rice yield

growth before harvesting. Effects of climate variability can also be seen in the difference in crop water requirements.

Crop water requirement is estimated by potential evapotranspiration (PET) which can be determined using the modified Penman equation (Schwab et al. 1993). Analysis of temporal distribution of mean annual PET values in Uttarakhand showed differences in average PET values during the reported period. Figure 41.5 show Relationship between ETo and Rice Yield. These differences determine what type of annual crops to grow or crop rotations to be followed as well as the timing of the initiation of the cropping season particularly for rainfed cropping systems to take advantage of rainfall needed to sustain crop growth.

From the graph it can be depicted that the period 1979–1985 were drier than the period 1985–2005 and therefore, during the period 1979–1985 crops would have

require more irrigation water than usual and may have resulted in the reduced yield. As a result, cropping sequence and schedule can be planned to take advantage of available soil moisture. Alternatively, planting can be delayed or adjusted depending on the sufficiency of accumulated rainfall.

### *41.7.3 Water Stress*

The variability of water supply in crops can cause negative effects to crop production. In rice, water stress at panicle initiation increased the proportion of unfilled grains and decreased 1,000-seed weight (Wopereis et al. 1996). Reduced availability of water at the vegetative stage resulted in reduced morphological and physiological measurements in rice. The affected morphological and physiological features include tiller number, leaf area index, apparent canopy photosynthetic rate, leaf nitrogen, shoot and root biomass, and root length density (Cruz et al. 1986). Varying degrees of water stress at different growth stages can result in a number of plant reactions that can also be variety-specific. In general, water stress during the vegetative stage will delay panicle initiation in rice, mild water stress at reproductive stage will extend panicle development by 10 days and reduce grain number. A severe water deficit during the same development stage will extend panicle development by 18–28 days, and reduce grain and panicle number (Lilley and Fukai 1994).

## 41.8 Weather Variability and Crop Yield Forecast

A process-based crop yield forecasting model can be developed which requires as input the historical weather variables (e.g. solar radiation, maximum temperature and minimum temperature, rainfall, etc.) observed up to the time the forecast is made (time of forecast), and the predicted weather variables from the point of forecast up to the time of harvest (Bouman et al. 1997). Using an adequate ecophysiological crop-forecasting model and a set of reliable predicted weather variables, real-time forecast of crop response and crop yield can be determined. At any given time period during crop development, measurable crop data and observed weather variables plus the predicted weather variables for lead times up to maturity or harvesting of the crop can serve as inputs to crop yield forecasting model. Figure 41.6, shows real-time forecast determined by the given the observed Rainfall and Evaporation. In the period 1979–1994 forecasted yields were higher than observed yields; this trend was reversed for the period 1994–2004. This showed that the time series model was not able to accurately predict yield. This may have been due to the lack of other information like soil, crop management data and the genetic coefficient data.

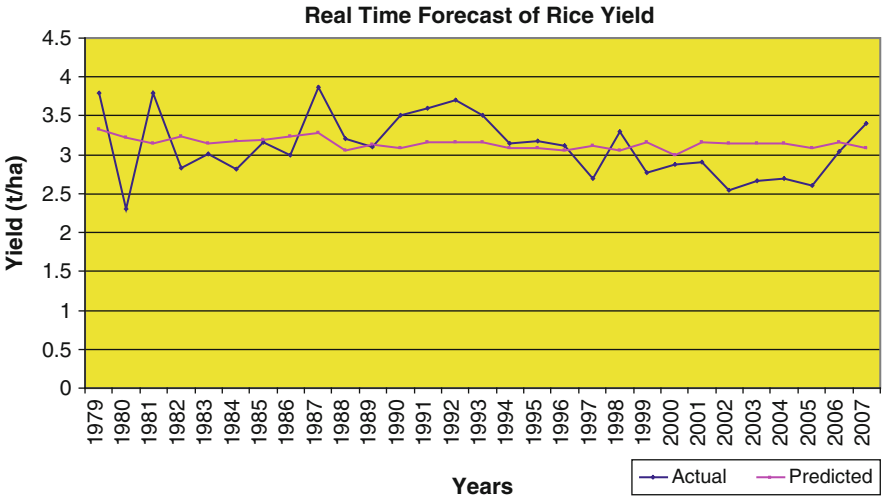


**Fig. 41.6** Actual and DSSAT predicted rice yield

In light of this we are currently evaluating the Effect of Climate Change on Rice Production using The Decision Support System for Agrotechnology Transfer (DSSAT). This model in cooperates soil data, crop management data, genetic coefficient data and weather data. It our hope that this model will be able to forecast rice yield more accurately, thus results can be used to make wise decisions in the Agricultural Sector.

## 41.9 Conclusions

The degree of vulnerability of crops to climate variability depends mainly on the development stage of the crops at the time of weather aberration. Even a slight change in temperature during a critical stage (e.g. flowering) may directly or indirectly result in significant reduction in crop yield. Climate variability also influences factors that may hamper crop growth. Incidence of pests and diseases may be hastened by the fluctuations in weather variables, such as temperature and rainfall patterns. Scientists and farmers must join efforts to further understand micro level crop–climate relationships to help them formulate viable, location-specific production technologies. Efficient and effective analysis of the agronomic impacts of climate variability requires a good understanding of the systems processes involved in crop growth and development and crop production which allows an objective assessment of the vulnerability of the production systems to exogenous climate variables. The inter-disciplinary, systems-based approach facilitates the understanding of the linkages and feedbacks among the system components.

## References

Bouman BAM, van Diepen CA, Vossen P, van der Wal T (1997) Simulation and systems analysis tools for crop yield forecasting. In: Teng PS et al (eds) Applications of systems approaches at the farm and regional levels, Vol. 1, IRRI and ICASA. Kluwer, Dordrecht, pp 325–340

Cruz RT, O'Toole JC, Dingkuhn M, Yambao EB, Thangaraj M, De Datta SK (1986) Shoot and root responses to water deficits in rainfed lowland rice. Aust J Plant Physiol 13:567–575

Hossain M (1997) Rice supply and demand in Asia: a socioeconomic and biophysical analysis. In: Teng PS, Kropff MJ, Ten Berge HFM, Dent JB, Lansigan FP, Van Laar HH (eds). Proceedings of the second international symposium on systems approaches for agricultural development. Vol 1: Applications of systems approaches at the farm and regional levels. International Rice Research Institute, Los Baños, pp 263–279

IPCC (1996) Houghton JT, Meira Filho LG, Callander BA, Harris N, Kattenberg A, Maskell K (eds), Climate change 1995: the science of climate change. Cambridge University Press, Cambridge, 572 pp

Kuniyal JC (2003) Regional imbalances and sustainable crop farming in the Uttaranchal Himalaya, India. Ecol Econ 46(3):419–435

Lilley JM, Fukai S (1994) Effect of timing and severity of water deficit on four diverse rice cultivars. III. Phenological development, crop growth, and yield. Field Crops Res 37:215–223

Peng S, Ingram KT, Neue HU, Ziska LH (eds) (1996) Climate change and rice. Springer/IRRI, Berlin/Los Banos, 374 pp

Satake T, Yoshida S (1978) High temperature-induced sterility in Indica rices at flowering. Jpn J Crop Sci 47(1):6–17

Schwab GO, Fangmeier DD, Elliot WD, Frevert RK (1993) Soil and water conservation engineering. Wiley, New York

Wopereis MC, Kropff MJ, Maligaya AR, Tuong TP (1996) Drought-stress responses of two lowland rice cultivars to soil and water status. Field Crops Res 46:21–39

# Chapter 42
# Selection of Suitable Planting Method and Nutrient Management Techniques for Reducing Methane Flux from Rice Fields

**Venkatesh Bharadwaj, A. K. Mishra, S. K. Singh, S. P. Pachauri, and P. P. Singh**

**Abstract** A field investigation was carried out during *kharif* season of 2004 at Crop Research Center, Pantnagar to know the effect of rice sowing and planting methods as well as nutrient management techniques on methane flux from rice fields. Performance of three planting methods viz., direct sowing, manual transplanting and transplanting by mat type rice transplanter and six nutrient management techniques viz., control, application of 100% NPK + Sulphur, 100% NPK + *Azotobacter*, 100% NPK + Farm Yard Manure (FYM), 100% NPK + wheat straw and vermicompost alone were assessed along with the control. The experiment was conducted in Split Plot Design (SPD) with 18 treatment combinations assigning planting methods as a main factor and nutrient management techniques as the sub factor. The experiment was replicated 3 times. On an average, direct sowing of rice recorded lowest methane flux (2.78 mg $m^{-2}$ $h^{-1}$) followed by transplanting with mat type rice transplanter (2.86 mg $m^{-2}$ $h^{-1}$) but manual transplanting recorded the highest methane flux i.e., 3.09 mg $m^{-2}$ $h^{-1}$. Among all the nutrient management techniques, application of vermicompost alone was found to be the most efficient measure for reducing methane flux (0.79 mg $m^{-2}$ $h^{-1}$) followed by control (1.26 mg $m^{-2}$ $h^{-1}$), Sulphur amendment (2.02 mg $m^{-2}$ $h^{-1}$), and *Azotobacter* (2.08 mg $m^{-2}$ $h^{-1}$). On the other hand, considerable higher methane flux was recoded in straw amendment (6.53 mg $m^{-2}$ $h^{-1}$) and FYM amendment (3.64 mg $m^{-2}$ $h^{-1}$). It was interesting to know that the combination of Vermicompost + direct sowing recorded the lowest methane flux (0.70 mg $m^{-2}$ $h^{-1}$) followed by Vermicompost + mat type rice transplanter (0.75 mg $m^{-2}$ $h^{-1}$) but it also reduced the grain yield of rice and can not be suggested. Further, the suitable treatment to achieve higher grain yield as well as reduced $CH_4$ flux was combination of 100% NPK + Sulphur + Direct Sowing

V. Bharadwaj (✉) • A.K. Mishra • S.K. Singh • S.P. Pachauri • P.P. Singh
Department of Agrometeorology, College of Agriculture, G.B. Pant University of Agriculture and Technology, U.S. Nagar, Pantnagar 263145, Uttarakhand, India
e-mail: dr.venkatbh@rediffmail.com

S.D. Attri et al. (eds.), *Challenges and Opportunities in Agrometeorology*,
DOI 10.1007/978-3-642-19360-6_42, 

followed by 100% NPK + Sulphur + mat type rice transplanter that gave 66.24 and 66.67 q $ha^{-1}$ rice grain yields with significantly lower i.e., 1.57 and 2.24 mg $m^{-2}$ $h^{-1}$ methane flux. These can be suggested to the farmers for reduced methane flux with higher grain yield.

## 42.1 Introduction

Methane ($CH_4$) is a strong greenhouse gas present in the atmosphere. Its concentration in the atmosphere is continuously increasing and reached up to 1,774 ppb in 2005 from a preindustrial value of about 715 ppb (IPCC 2007). It makes it important for mitigating methane emission to reduce the ill effects of climate change due to its strong ability to absorb infrared radiation combined with its relatively short lifetime in the atmosphere (10 years). It is further estimated that the total annual source strength of all methane emissions from anthropogenic origin lies around 550 Tg (Sass and Fisher 1994) out of which, the contribution from rice cultivation is estimated to range from 20 to 100 Tg $CH_4$ $year^{-1}$ with an average of 60 Tg $CH_4$ $year^{-1}$ (IPCC 1996).

India is an important rice producing country, comprising 28.6% of world rice cultivated area. There is a high possibility (about 70%) of increase in rice production during next 25 years to feed the growing human population (Dubey 2001). This will require additional fertilizer doses causing further increase in methane emission and therefore, the methane emission from rice cultivation may go up to 145 Tg $year^{-1}$ in the year 2025 as compared to 1990 level of 97 Tg $year^{-1}$ (Anastasi et al. 1992).

Although little information is available from field studies concerning cultural practices and methane emission from rice, it would appear to be feasible to reduce methane by short dry fallow or rotation with an upland crop to permit organic matter to be decomposed under aerobic conditions before subjecting the soil to anaerobic conditions for irrigated rice cultivation (Minami and Neue 1994). Additionally, numerous studies also have revealed the impact of chemical fertilizers on $CH_4$ emissions (Adhya et al. 2000; Sethunathan et al. 2000) which depends on rate, type and mode of fertilizer applications. Lindau (1994) reported decrease in $CH_4$ emission rate with the application of ammonium nitrate due to competitive inhibition of nitrate reduction in favour of methane production. Under field conditions, the application of sulphate based fertilizers such as $(NH_4)_2$ $SO_4$ and $CaSO_4$ have reduced $CH_4$ emission (Cai et al. 1997), while application of $K_2HPO_4$ enhanced the $CH_4$ emission (Adhya et al. 1998). It has also been found that application of straw increases $CH_4$ methane emission irrespective of soil type (Yagi and Minami 1990). There are numerous planting methods and nutrients management practices used in India for rice cultivation. Therefore, a field study was conducted to select the best planting method and nutrient management technique for reducing methane flux from rice fields.

## 42.2 Material and Methods

The experiment was conducted at Crop Research Centre, Govind Ballabh Pant University of Agriculture and Technology, Pantnagar, Uttarakhand (29°N latitude, 79.3°E longitude and 243.8 m above mean sea level) during *kharif* season of 2004. The centre is located in a narrow belt to the south from the foothills of Shiwalik range of Himalaya commonly called as *tarai* region. The climate of Pantnagar is humid sub-tropical with severe cold winter and hot summer. *Tarai* soils are silty loam in texture with good moisture storage capacity and are highly productive. According to USDA soil classification, the soil of experimental site has been placed under order – Mollisol, suborder – Udoll, great group – hapludoll, subgroup – aquic hapludoll, family – fine loamy mixed hyperthermic and series – Beni silty clay loam. The values of some of the specific soil parameters of the experimental site have been given in Table 42.1.

## 42.3 Layout and Treatments

The treatments consisted of three planting methods viz., direct sowing, manual transplanting and transplanting by mat type rice transplanter with the combination of six nutrient management techniques viz., application of 100% NPK + Sulphur, 100% NPK + *Azotobacter*, 100% NPK + Farm Yard Manure (FYM), 100% NPK + wheat straw and vermicompost alone. The treatment combinations comprised of $T_1$: Control with direct sowing, $T_2$: 100% NPK + Sulphur + Direct sowing, $T_3$: 100% NPK + *Azotobacter* + Direct Sowing, $T_4$: 100% NPK + FYM + Direct Sowing, $T_5$: 100% NPK + Straw + Direct Sowing; $T_6$: Vermicompost + Direct Sowing; $T_7$: Control + Manual transplanting; $T_8$: 100% NPK + Sulphur + Manual transplanting; $T_9$: 100% NPK + *Azotobacter* + Manual transplanting; $T_{10}$: 100% NPK + FYM + Manual transplanting; $T_{11}$: 100% NPK + Straw + Manual transplanting; $T_{12}$: Vermicompost + Manual transplanting; $T_{13}$: Control + Mat type rice transplanter; $T_{14}$: 100% NPK + Sulphur + Mat type rice transplanter; $T_{15}$: 100% NPK + *Azotobacter* + Mat type rice transplanter; $T_{16}$: 100% NPK + FYM + Mat type rice

**Table 42.1** Chemical characteristics of experimental site

| | Soil depth | |
|---|---|---|
| Soil Parameter | 0–15 cm | 15–30 cm |
| pH (1:2, soil : water) | 7.74 | 7.87 |
| Electrical Conductivity (dS $m^{-1}$) (1:2, soil : water) | 0.105 | 0.114 |
| Eh (1:2, soil : water; mV) | −0.059 | −0.070 |
| Organic Carbon (%) | 1.30 | 0.95 |
| Available Nitrogen (kg $h^{-1}$) | 181.8 | 106.62 |
| Available Phosphorus (kg $h^{-1}$) | 35.84 | 12.54 |
| Available Potassium (kg $h^{-1}$) | 241.9 | 156.8 |

transplanter; $T_{17}$: 100% NPK + Straw + Mat type rice transplanter and $T_{18}$: Vermicompost + Mat type rice transplanter. The experiment was conducted in Split plot design (SPD) with 18 treatment combinations and 3 replications. Planting method techniques were taken as a main factor, while nutrient management techniques were considered as a sub-factor. The net plot size for each treatment was 3 m × 2 m.

A fertile and well drained upland field near the source of irrigation was selected for nursery raising. Rice seeds (Var: Pant Dhan-4) were soaked for 24 h and seeds were used for sowing. The nursery was sown in a well prepared seedbed through puddling twice with peg type puddler at the seed rate of 30 kg $ha^{-1}$. The field for rice transplanting was prepared by disc harrowing thrice in the first and second week of June and later on puddling was done with the help of a peg type puddler before transplanting.

### 42.3.1 Sowing and Transplanting

Direct sowing of rice was done @ 60 kg $ha^{-1}$ after preparing field by disc harrowing thrice and levelling with a planker. Manual transplanting was done in the well puddled field where 23 days old rice seedlings were transplanted @ 2–3 seedlings per hill with a spacing of 20 cm × 10 cm. Mechanical transplanting of 23 days old rice seedlings was done with a self-propelled mat type rice transplanter that can transplant 8 rows of seedlings at a spacing of 23.8 cm × 12 cm in a well prepared puddled soil. In all the treatments, 50% of N, 100% P and K were applied and remaining 50% of nitrogen was applied in two split doses at tillering and panicle initiation stages.

### 42.3.2 Fertilizers and Organic Amendments Application

The organic manures viz., wheat straw, FYM and cowpea green manure were applied @ 10 t $ha^{-1}$ and vermicompost was applied @ 2 t $ha^{-1}$. Similarly *Azotobacter* was applied @ 500 g $ha^{-1}$. The recommended NPK doses for rice were given in the form of urea, single super phosphate (SSP) and muriate of potash (MOP), respectively. In those plots where sulphur was applied, NPK were given through Sulphur containing fertilizers like ammonium sulphate, single super phosphate (SSP), potassium sulphate and zinc sulphate.

### 42.3.3 Collection of Gas Sample

Gas samples from plots were collected by closed chamber technique (Hutchinson and Mosier 1981) using boxes, made up of acrylic sheets having

dimensions of 50 cm × 30 cm × 100 cm. An aluminum channel was pre-inserted in the field and water was filled in channel, whenever the chamber was placed for collecting the gas samples to make the set airtight. One mediflex three vent cannula (Eastern Medikit Ltd., India) was fitted at the top of chamber to collect gas samples. Three replicate gas samples were taken from each plot. To collect gas samples, the gas chamber was flushed several times and then gas samples at the interval of 0, 15 and 30 min were withdrawn with the help of 2 mL syringes.

### *42.3.4 Analysis of Gas Sample*

Methane concentration in the gas samples collected from rice field was estimated using Gas Chromatograph (Nucon 5765 series) attached to Flame Ionization Detector (FID) and Molecular Sieve stainless steel column. The standardization of method for the estimation of methane was done with various combinations of temperature for column, injector and detector and pressure of carries gas (Nitrogen) supporting gas (Zero air) and combustion gas (Hydrogen). Finally the temperature for column, injector and detector were kept at 90°C, 120°C and 120°C, respectively. The pressure of gases was kept as 4, 2 and 2 kg $cm^{-2}$ for nitrogen, zero air and hydrogen. The overall total pressure of gases was 8 kg $cm^{-2}$. The peak area was measured with microprocessor controlled Aimil integrator connected to computer. Pre calibrated standard of methane was used (Scott specialty gas standard). The area of Methane peak was used to calculate methane concentration against standard peaks.

### *42.3.5 Measurement and Calculation of Methane Flux*

Standard curves were made from the standard samples of known concentrations. Then gas samples of unknown concentrations were injected and the peak areas were noted. Using the peak area value and the standard, the concentration values were taken. To measure flux, the chamber was fixed at the experimental site and the change in concentration in the chamber so formed, with time, was determined by taking replicate gas samples from the chamber headspace by syringe and transported them to the laboratory for analysis.

Finally, the methane flux (F)from rice field was calculated as- $F = \frac{C_t - C_0}{t} \times H \times 42.857$ mg $m^{-2}$ $h^{-1}$ (Hutchinson and Mosier 1981) where $t$ is time (minute), $C_0$ is initial concentration (ppmv), $C_t$ is final concentration (ppmv) and $H$ is height of head space (m).

## 42.4 Results and Discussion

### *42.4.1 Effect of Sowing and Transplanting Methods on Methane Flux of Rice*

The methane flux from rice fields for different sowing and transplanting methods at different days after sowing (DAS) is being depicted in Fig. 42.1. During the entire crop growth period, highest methane flux was reported from manually transplanted rice except 65, 69 and 111 DAS. Direct seeded rice had shown its superiority in methane emission at 69 and 111 DAS. On the other hand, rice transplanted through mat type rice transplanter showed its peak methane flux at 65 DAS. On an average, manual transplanting of rice was found responsible for maximum methane flux (3.09 mg $m^{-2}h^{-1}$) followed by transplanting through mat type rice planter (2.86 mg $m^{-2}$ $h^{-1}$). Directsowing of rice has shown lowest methane flux on average basis i.e. 2.78 mg $m^{-2}$ $h^{-1}$. The similar findings have also been reported by other researches also (Duah et al. 1991; Corton et al. 2000) showing that transplanting of rice was more significant to the methane emission as comparison to direct sowing. Dubey (2001) also have suggested the use of direct seeding of paddy for minimizing production cost and $CH_4$ emission both.

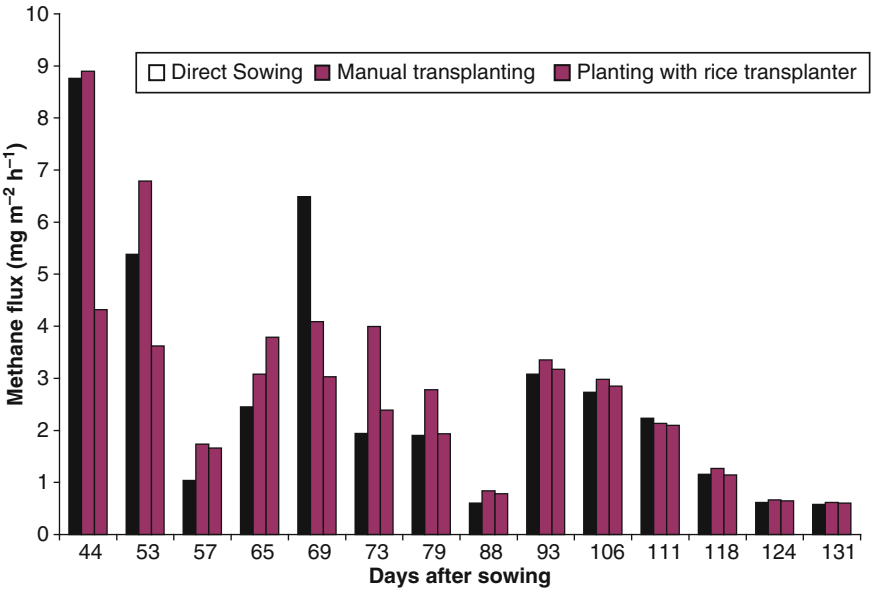


**Fig. 42.1** Methane flux (mg $m^{-2}$ $h^{-1}$) from rice fields in different sowing and plating methods at different days of sampling

### 42.4.2 *Effect of Nutrient Management Techniques on Methane Flux of Rice*

The effect of various nutrient management techniques on the methane production at different days of observation has been shown in Fig. 42.2. It is obvious from the graph that application of wheat straw increased the methane flux and it has recorded the highest methane flux among all other nutrient management techniques during all dates of observation except one single observation at 111 DAS, where it was closely surpassed by FYM amendment. Use of FYM amendment also recorded higher methane flux during the period of observation. On the other hand, the lowest methane flux was reported from vermicompost during entire crop growth period except few observations at 111 and 118 DAS, where lowest flux was recorded from control. Considering the growing season of the crop as a whole, the average methane flux from rice crop was found in the order of straw amendment (6.53 mg $m^{-2}$ $h^{-1}$) followed by FYM amendment (3.64 mg $m^{-2}$ $h^{-1}$) and *Azotobacter* (2.08 mg $m^{-2}$ $h^{-1}$). On the other hand, application of vermicompost alone was found to be the most efficient measure for reducing methane flux (0.79 mg $m^{-2}$ $h^{-1}$) followed by control (1.26 mg $m^{-2}$ $h^{-1}$) and use of Sulphur amendment (2.02 mg $m^{-2}$ $h^{-1}$). Increase in $CH_4$ flux with straw application was reported from many researches (Corton et al. 2000; Peng et al. 2008) and the reason for this may be explained on the basis of the fact that incorporation of straw selectively enhances the growth of *Methanosarcinaceae* and *Methanobacteriales* and suppresses

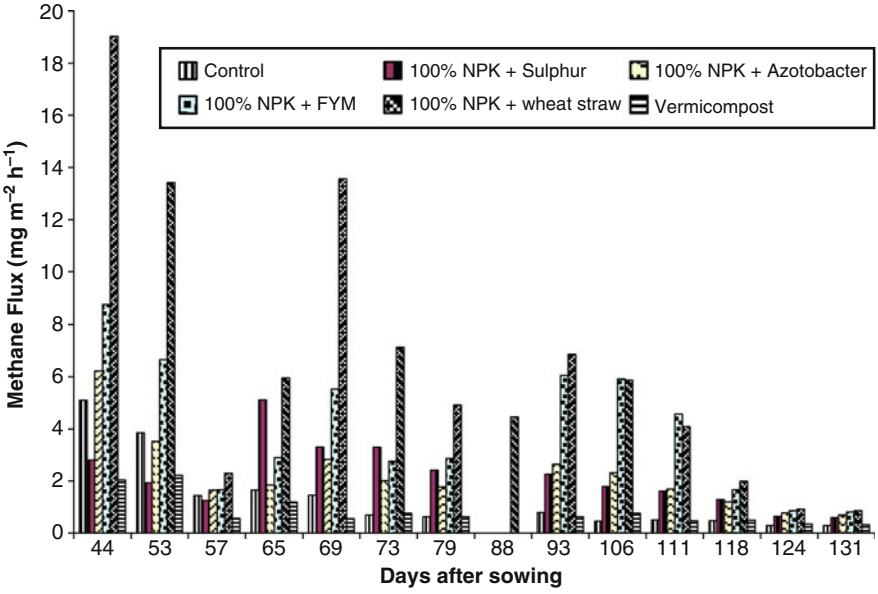


**Fig. 42.2** Methane flux (mg $m^{-2}$ $h^{-1}$) from rice fields in nutrient management techniques at different days of sampling

rice cluster I (RC-I) methanogens and *Methanomicrobiales* (Conrad and Klose 2006). Conversely, lowest methane flux values were found by application of vermicompost, control and Sulphur amendments. (Adhya et al. 2000) also found reduction in methane flux by replacement of green manures with compost. Lower methane fluxes with the application of sulphur (Corton et al. 1995; Ko and Kang 2000), ammonium sulphate (Schutz et al. 1989; Lindau et al. 1993) and gypsum (Denier et al. 1994) have also been reported from various parts of the globe. Hori et al. (1990) suggested that sulphate ions help to inhibit methane formation by activating sulphate reducers in soil which compete for the same substrates with methanogens and it may be a reason for lower methane flux in sulphur treated plots. Similarly, application of phosphorus already present in single superphosphate also helps to reduce $CH_4$ emission from rice (Li and Li 1999) resulting in decreased $CH_4$ emission from the plots treated with single superphosphate.

### *42.4.3 Effect of Treatments on Grain and Straw Yield*

A significant effect of different treatments was observed on grain yield and straw yield. Significantly higher grain and straw yields were recorded with the use of sulphur amendment followed by FYM, *Azotobacter* and straw amendments however the lowest values was found in control followed by application of vermicompost. Similar trends were recorded for straw yield of rice also (Table 42.2). Several researchers have concluded that the sulphur component of the fertilizer is responsible for increase in the rice plant growth, grain number and rice yield (Li and Li 1999; Sriramchandrasekhran et al. 2007). On the other hand, sowing and planting method

**Table 42.2** Grain and straw yield of rice as influenced by various treatments

| Treatments | Grain yield (q $h^{-1}$) | Straw yield (q $h^{-1}$) |
|---|---|---|
| Sowing and transplanting methods | | |
| Direct sowing | 54.27 | 89.14 |
| Manual transplanting | 55.86 | 91.36 |
| Transplanting by mat type rice transplanter | 54.83 | 90.43 |
| SEm± | 0.341 | 0.101 |
| CD (5%) | NS | 0.397 |
| Nutrient management techniques | | |
| control | 32.53 | 52.58 |
| 100% NPK + Sulphur | 67.49 | 111.95 |
| 100% NPK + Azotobacter | 60.61 | 100.98 |
| 100% NPK + Farm Yard Manure (FYM) | 63.37 | 104.00 |
| 100% NPK + wheat straw | 60.43 | 98.05 |
| vermicompost | 45.49 | 74.28 |
| SEm± | 0.630 | 0.667 |
| CD (5%) | 1.820 | 1.927 |

failed to show its significant role for grain yield of rice, however for straw yield, manual transplanting showed its superiority over other sowing methods.

## 42.5 Conclusion

The experiment was conducted with an objective of finding the best method of crop establishment which could effectively control methane emission without much reduction in rice grain yield. The study clearly indicated that combination of sowing and transplanting methods with nutrient management techniques may be one of the most promising measures to reduce methane emission from the rice fields. It was interesting to know from Fig. 42.3 that the combination of Vermicompost + direct sowing recorded the lowest methane flux (0.70 mg $m^{-2}$ $ha^{-1}$) followed by Vermicompost + mat type rice transplanter (0.75 mg $m^{-2}$ $ha^{-1}$) but it also reduced the grain and straw yield of rice and can not be suggested. Further, the suitable treatment to achieve higher grain and straw yield as well as reduced $CH_4$ flux was combination of 100% NPK + Sulphur + Direct Sowing followed by 100% NPK + Sulphur + mat type rice transplanter that gave 66.24 and 67.67 q $ha^{-1}$ rice grain yields, 110.58 and 111.60 q $ha^{-1}$ straw yields with significantly lower i.e., 1.57 and 2.24 mg $m^{-2}$ $ha^{-1}$ methane flux, respectively. These can be suggested to the farmers for reduced methane flux with higher grain yield of rice.

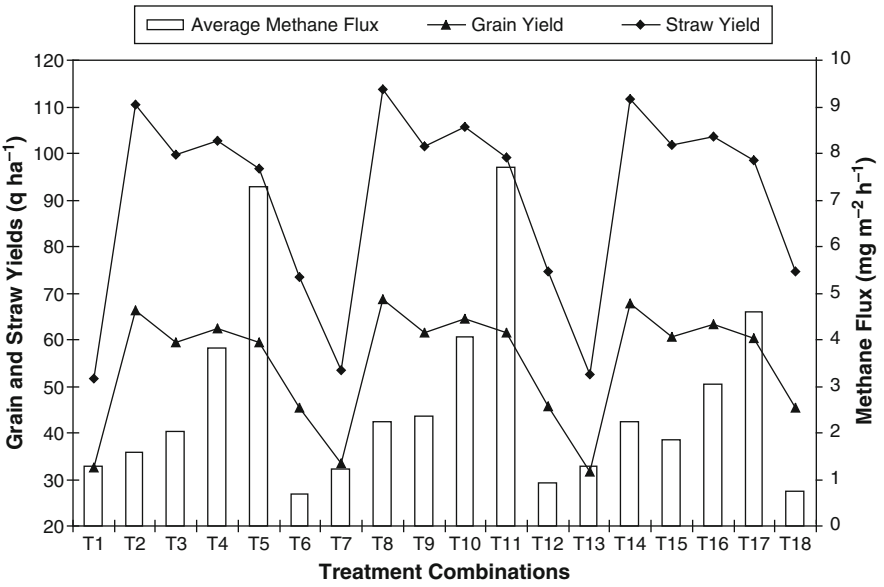


**Fig. 42.3** Average methane flux (mg $m^{-2}$ $h^{-1}$) during the crop growth period of rice with their corresponding grain and straw yields (q $ha^{-1}$)

## References

Adhya TK, Pattnaik P, Satpathy SN, Kumaraswamy S, Sethunathan N (1998) Influence of phosphorus application on methane emission and production in flooded paddy soils. Soil Biol Biochem 30:177–181

Adhya TK, Bharati K, Mohanty SR, Ramakrishnan B, Rao VR, Sethunathan N, Wassmann R (2000) Methane emission from rice fields at Cuttack India. Nutr Cycl Agroecosyst 58:95–105

Anastasi C, Dowding M, Simpson VJ (1992) Future CH4 emissions from rice production. J Geophys Res 97:7521–7525

Cai ZC, Xing H, Yan X, Xu H, Tsuruta HK, Yagi K, Minami K (1997) Methane and nitrous oxide emissions from rice paddy fields as affected by nitrogen fertilizers and water management. Plant Soil 196:7–14

Conrad R, Klose M (2006) Dynamics of the methanogenic archaeal community in anoxic rice soil upon addition of straw. Eur J Soil Sci 57:476–484

Corton TM, Majita JB, Pamplona RR, Asis CA Jr (1995) Methane emission from irrigated rice field: effect of nitrogen and sulphate fertilizers. Phil Rice Tech Bull 1(1):101–121

Corton TM, Bajita JB, Grospe FS, Pamplona RR, Asis CA Jr, Wassmann R, Lantin RS, Buendia LV (2000) Methane emission from irrigated and intensively managed rice fields in Central Luzon (Philippines). Nutr Cycl Agroecosyst 58:37–53

Denier van der Gon HAC, Neue HU (1994) Impact of gypsum application on the methane emission from a wetland rice field. Global Biogeochem Cycle 8:127–134

Dubey SK (2001) Methane emission and rice agriculture. Curr Sci 81:345–346

Duah BW, Lu WF, Chen W, Guo WM (1991) Evaluation of the effect of planted hybrid rice on methane emission from paddy yield. China Environ Sci 19(5):397–401

Hori K, Inubushi K, Matsumoto S, Wada H (1990) Competition for acetic acid between methane formation and sulfate reduction in the paddy soil. Jpn J Soil Sci Plant Nutr 61:572–578

Hutchinson GL, Mosier AR (1981) Improved soil cover method for measurement of Methane flux. Soil Sci Soc Am J 45:311–316

IPCC (1996) Climate change 1995: The scientific basis of climate change. XII summary for policy makers In: Houghton IT, Meira F, Callander LG, Harris BA, Kattenberg A, Maskell K (eds). Cambridge University Press, Cambridge, p 572

IPCC (2007) Climate change 2007: The physical science basis- summary for policymakers contribution of working group I to the fourth assessment report of the Intergovernmental Panel on Climate Change. IPCC secretariat, Geneva 2, Switzerland, 21 pp

Ko JY, Kang HW (2000) The effect of cultural practices on methane emission from rice field. Nutr Cycl Agroeco 58(1/3):311–314

Li Y, Li Y (1999) The characteristics of sulphur requirement and the effect of sulphur on yield and qualities of rice. Soil Fertil 1:24–26

Lindau CW, Bollich PK, DeLaune RD, Mosier AR, Bronson KF (1993) Methane mitigation in flooded Louisiana rice fields. Biol Fertil Soils 15:174–178

Lindau CW (1994) Methane emission from Louisiana rice fields amended with nitrogen fertilizers. Soil Biol Biochem 26:353–359

Minami K, Neue HU (1994) Rice paddies as a methane source. Climate Change 27:13–26

Peng J, Lu Z, Rui J, Lu Y (2008) Dynamics of the methanogenic archaeal community during plant residue decomposition in an anoxic rice field soil. Appl Environ Microbiol 74(9):2894–2901

Sass RL, Fisher FM Jr (1994) CH4 emission from paddy fields in the United States gulf coast area. In: Minami CK, Mosier A, Sass RL (eds) CH4 and N2O: Global emissions and controls from rice fields and other agricultural and industrial sources. NIAES Series 2, Tsukuba, pp 65–77

Sethunathan N, Kumaraswamy S, Rath AK, Ramakrishnan B, Satpathy SN, Adhya TK, Rao VR (2000) Methane production, oxidation and emission from Indian rice soils. Nutr Cycl Agroecosyst 58:377–388

Schutz H, Holzapfel-Pschorn A, Conrad R, Rennenberg H, Seiler WJ (1989) A 3-year continuous record on the influence of daytime, season, and fertilizer treatment on methane emission rates from an Italian rice paddy. J Geophys Res 94(D13):16405–16416

Sriramchandrasekhran MV, Bhavaneswari R, Ravichandran M (2007) Direct and residual effect of sulphur and organics on yield and S nutrition in rice-rice sequence. Ind J Crop Sci 2 (1):231–232

Yagi K, Minami K (1990) Effects of organic matter application on methane emission from Japanese paddy fields. In: Bouwmann AF (ed) Soil and greenhouse effects. Wiley, Chichester

# Chapter 43
# Operational Agrometeorological Strategies in Different Regions of the World

**M. V. K. Sivakumar**

**Abstract** The current financial crisis around the world is putting considerable stress on developing countries and countries in transition which are faced with the twin challenges of coping with the soaring food prices and the impacts of climate change on agriculture in the fragile economies of their countries. Agricultural sector is weather dependent and variations in weather and climate affect agricultural productivity. Concerns with the need for achieving greater efficiency in natural resource use while protecting the environment require that greater emphasis be placed on understanding and exploiting climatic resources for the benefit of agriculture and forestry. Hence there is now a growing recognition of the importance of operational agrometeorological services for the agricultural, livestock, forestry and fisheries sectors. These include services to help reduce the impact of natural disasters, including pests and diseases; early warning and monitoring systems; short- and medium-range weather forecasts; climate prediction/forecasting; and services to help reduce the contributions of agricultural production to global warming. Agrometeorological information plays a valuable part not only in making daily and seasonal farm management decisions but also in risk management and early warning systems. The ability to integrate information from interdisciplinary sources utilizing new computer-based technologies and telecommunications creates a great opportunity to enhance the role of agrometeorologists in many decision-making processes. This paper reviews the operational agrometeorological strategies in different regions of the world drawing on the different papers presented at the Inter-Regional Workshop on Strengthening Operational Agrometeorological Services at the National Level which was organized jointly by WMO, FAO, the United States Department of Agriculture (USDA) and the Philippines Atmospheric Geophysical and Astronomic Services Administration (PAGASA) in Manila, Philippines in March 2004. Perspectives on operational

M.V.K. Sivakumar
World Meteorological Organization, Geneva, Switzerland
e-mail: msivakumar@wmo.int

S.D. Attri et al. (eds.), *Challenges and Opportunities in Agrometeorology*,
DOI 10.1007/978-3-642-19360-6_43, 

agrometeorological services currently being provided at the national, regional and international level are reviewed and a critical review of strengthening operational agrometeorological services and needs from the agricultural sector are presented. Recommendations on addressing the priority issues are presented.

## 43.1 Introduction

The world has experienced unprecedented increases in population over the past few decades. In 2009, world population stood at 6.8 billion, up about 83 million from 2008. The world total is likely to reach seven billion in the latter half of 2011, with the bulk of growth in the world's poorest nations. The less developed countries of Africa, Asia, and Latin America and the Caribbean are projected to increase by just under 50% in the 41 years between 2009 and 2050, and the poorest of these are projected to double in population size over that period (PRB 2009).

India is the largest contributor to world population growth, accounting for 21% of the 78 million annual increment to the world. By 2016, the population of India (1.22 billion) is expected to be larger than the population of all the more developed countries combined. India will have a larger population than China by the year 2045 (1,496 millions).

More food and fibre will be required to feed and cloth these additional people and to increase the daily food uptake of the undernourished world wide. Global agricultural value added per capita has grown at an average rate of 0.4% per year in real terms since 1961. Latin America and South Asia have seen a small increase, while East Asia and the Pacific has more than doubled agricultural value added per capita over the last four decades. Sub-Saharan Africa is the only region in which per capita agricultural value added has not seen a sustained increase, with a declining trend on average for the period and considerable variation over time and across countries (FAO 2008).

According to FAO 2009 has been a devastating year for the world's hungry, marking a significant worsening of an already disappointing trend in global food security since 1996 (FAO 2009). The global economic slowdown, following on the heels of the food crisis in 2006–2008, has deprived an additional 100 million people of access to adequate food. For the first time since 1970, more than one billion people – about 100 million more than 2008 and around one sixth of all of humanity – are hungry and undernourished worldwide.

Demand for cereals will be essentially flat in the developed countries but will grow by about 40% in the developing countries – primarily as a result of population growth. Demand for meat will grow faster as people become richer – by 30% in the developed countries and by more than 160% in the developing countries (FAO 2010). Hence prices for agricultural commodities will remain 60–80% higher over the next decade than they were over the past decade, even after adjusting for inflation.

## 43.2 Growing Need for Operational Agrometeorological Services

The global agricultural scenario described above places a great deal of premium on our ability to continue to enhance productivity on a per hectare basis since the scope of extending cultivation to new areas is quite limited in scope. Given that rainfed agriculture continues to be the main mode of agricultural production, especially in the developing world, productivity enhancements per unit area in the rainfed ecosystems are a must. There is a need for a greater understanding of the effects of weather and climate variability on the rate of development, growth and yields of rainfed crops, and for improved methods of managing weather and climate risks in the rainfed ecosystems. Applications of agricultural meteorology are crucial in both these endeavours.

In much of the tropics, especially in the semi-arid tropics, farming systems are mainly rainfed and are affected by inter-annual as well as intra-seasonal climate variability. Farmers had to adapt to the range and frequency of shocks that climate variability brings and they have tried to use the available knowledge and information to develop their coping strategies. But the adoption of improved technologies is too slow, especially in Africa, to counteract the adverse effects of varying environmental conditions, and climate fluctuations continue to be the main factors that prevent a regular supply and availability of food, the key to food security.

Hence, there is now a growing recognition of the importance of operational agrometeorological services for the agricultural, livestock, forestry, and fishery sectors. These include:

- Services to help reduce the impact of natural disasters, including pests and diseases;
- Early warning and monitoring systems;
- Short- and medium-range weather forecasts;
- Climate prediction/forecasting; and,
- Services to help reduce the contributions of agricultural production to global warming.

The importance of each of these services is described below.

### *43.2.1 Services to Help Reduce the Impact of Natural Disasters, Including Pests and Diseases*

It largely goes undisputed that natural disasters have increased in number in recent decades. The charity group, Oxfam, in 2007 reported that disasters have quadrupled in the last two decades. The world suffered about 120 natural disasters per year in the early 1980s, and currently suffers about 500 per year. The number of people affected by extreme natural disasters has increased by almost 70% (from 174 million a year

between 1985 and 1994 to 254 million people a year between 1995 and 2004). Likewise, floods and wind-storms have increased from 60 events in 1980 to 240 a year in 2007, with flooding up six-fold. However, the number of geothermal events, such as earthquakes and volcanic eruptions, has barely changed. The economic cost associated with all natural disasters has increased 14-fold since the 1950s. World wide, annual economic costs related to natural disasters have been estimated at about $50–$100 billion.

Communities that are most exposed to risk from climate extremes and natural disasters and are potentially at risk from climate change, are those with limited access to technological resources and with limited development of infrastructure. Small farmers with limited means in most of the developing countries are at risk. The losses they suffer from the impact of natural disasters cannot be entirely eliminated, but timely and appropriate mitigation measures can certainly reduce the impacts. Planning, early warning, and well-prepared response strategies are the major tools for mitigating the losses. The longer in advance a warning can be given about potentially damaging conditions, the easier it will be to mitigate and reduce its impact. Operational agrometeorological services must recognize the need for such advance warnings to help the farming community and integrate them in the advisories that are issued.

For example, early information on El Niño episodes is now allowing advanced national planning, with considerable advantage in many sectors of the economy, such as in water resources management, tourism, and fisheries and agricultural production. In the case of the 1997–1998 El Niño event, advances in El Niño-related science and in monitoring the sea-surface temperatures in the Pacific Ocean, enabled scientists in the National Meteorological and Hydrological Services (NMHSs) to predict its formation longer in advance than all the previous events. With recent developments in communication technology, including the use of Internet, information on the El Niño was disseminated in a rapid and timely manner throughout the world. These enabled many governments to take appropriate measures, and stimulated international cooperation and integrated efforts to address the associated impacts. Similarly, the accuracy of tropical cyclone track forecasts and the timeliness of warnings have been steadily improving in the past few years.

The climatic factors affect the distribution, development, survival, behaviour, migration, reproduction, population dynamics and outbreaks of insect pests and diseases and their severity over a period can fluctuate according to climatic variation since climatic factors control the population growth rate of pathogens and insects. If climatic factors are not adverse enough to cause extinction, their populations can rise exponentially. To account for the impact of weather and climate variability on disease and pest incidence, information on agrometeorological variables such as relative humidity, maximum and minimum air temperature, soil temperature, total solar radiation, total rainfall and wind direction and wind speed is vital. Microclimate, a mixture of climatic factors (e.g. temperature, humidity, wind, and quantity of energy, etc.) near the ground, is the climate where plants and animals live and affects considerably the disease severity.

Agrometeorological information is needed to model the incidence of pests and diseases and for developing effective control strategies.

### 43.2.2 Early Warning and Monitoring Systems

The statistics of recorded disaster data (CRED 2005; IFRC 2005) show that over the period 1995–2004, nearly 6,000 disasters were recorded, accounting for about 900,000 dead, US$ 738 billion material losses and 2,500 million people affected. Improved early warning systems and better preparedness strategies hold the key to reducing the impact of natural disasters.

The expression 'early warning' is used in many fields to mean the provision of information on an emerging dangerous circumstance where that information can enable action in advance to reduce the risks involved (Basher 2006). ISDR (2004) defines early warning as 'the provision of timely and effective information, through identified institutions, that allows individuals exposed to a hazard to take action to avoid or reduce their risk and prepare for effective response'. To be effective and complete, an early warning system needs to comprise four interacting elements: (i) risk knowledge, (ii) monitoring and warning service, (iii) dissemination and communication and (iv) response capability (ISDR-PPEW 2005).

### 43.2.3 Short-Range and Medium-Range Weather Forecasting

There are increasing demands for timely and effective agrometeorological information for on-farm applications by farmers. Farmers need information on expected rainfall for planting and harvesting activities. Rainfall forecasts are also crucial for farmers to determine when and how to apply fertilizers. Agrometeorological information to assist in irrigation planning is very important to both the farming community as well as managers of water resources.

The importance of the type of weather information needed for a decision-making process depends upon the nature of the decision itself. For example, present weather and short-term forecasts are used in making daily operational decisions, while the analyses of past climate data are especially useful for planning decisions. Predictions of the potential for the incidence of diseases and pests are usually based on current and past weather conditions in a specific agricultural area and crop type.

Agricultural weather and climate data systems are necessary to expedite generation of products, analyses, and forecasts that affect agricultural cropping and management decisions, irrigation scheduling, commodity trading and markets, fire-weather management, and other preparedness for calamities, and ecosystem conservation and management. There is convincing evidence available from different parts of the world that judicious application of meteorological, climatological,

and hydrological knowledge and information, including long-range forecasts, greatly assists the agricultural community to develop and operate sustainable agricultural systems and increase production in an environmentally sustainable manner.

### *43.2.4 Climate Prediction/Forecasting for Agriculture*

One of the persistent demands of agriculturists is for reliable forecasts of seasonal climate information to make appropriate decisions as to which crops and cropping patterns should be chosen well ahead of the growing season to avoid undue risks. The past two decades have seen significant improvements in the forecasting of climate variability, based on advances in our understanding of ocean-atmosphere interactions. Such improvements permit the development of applications that predict climate at seasonal to interannual timescales, helping decision makers in the agricultural sector to deal more effectively with the effects of climate variability.

In several regions of the world, interpretation and delivery of the climate prediction information has been promoted more through the development of Regional Climate Outlook Forums-in which both meteorological services and agricultural end users participate-than through information availability on the Internet. Currently climate outlook forums are being held in different parts of the world on a regular basis to develop consensus climate forecasts. These regional climate assessments are based on consensus agreement between coupled ocean–atmosphere model forecasts, physically based statistical models, results of diagnosis analysis and published research on climate variability over the region and expert interpretation of this information in the context of the current situation (Berri 2000). Seasonal forecasts of precipitation are usually expressed in probabilistic terms.

### *43.2.5 Services to Help Reduce the Contributions of Agricultural Production to Global Warming*

The projected climate change and the attendant impacts on water resources and agriculture, especially in the arid and semi-arid tropical regions of the world, add additional layers of risk and uncertainty to an agricultural system that is already impacted by land degradation due to growing population pressures. Sub-Saharan Africa already under a lot of stress will also be impacted by stress induced by climate change and Africa as a whole will probably see 75–250 million people being affected by water stress by the year 2020 and that is round the corner.

Farmers have over centuries adopted cropping strategies, such as inter cropping and mixed cropping, that minimize the risk and ensure some degree of productivity even in poor years. Such strategies are based on their understanding of natural climatic variability, but the projected climate change is not factored into this understanding. Hence it is important to examine crop responses to a range of possible changes, especially in the nature, frequencies and sequences of extreme climatic changes. Issues such as sustainability or land productivity, changes in erosion, degradation and environmental quality also need careful consideration. Improved management strategies are necessary for coping with the projected global climatic change, especially in the arid and semi-arid tropical regions of the world.

## 43.3 Operational Agrometeorological Services and Limitations in Different Regions of the World

WMO, in collaboration with FAO, the United States Department of Agriculture (USDA) and the Philippines Atmospheric Geophysical and Astronomic Services Administration (PAGASA) organized an Inter-Regional Workshop on Strengthening Operational Agrometeorological Services at the National Level in Manila, Philippines in March 2004. A short summary of the operational agrometeorological services and their limitations presented at the workshop from different regions of the world (Motha et al. 2006) is given below.

### *43.3.1 Africa*

Abdalla and Tarakidzwa (2006) described the operational agrometeorological services in Africa based on the responses to a questionnaire designed by the World Meteorological Organization (WMO) Secretariat. Of the 54 countries in Africa, most Meteorological Services have independent agrometeorological units, some based in Agricultural Services. The major role of these units is to provide data on a real-time or historical basis and to make simple data analyses in addition to a routinely published bulletin. The units provide services for the agriculture, water and the environment sectors, and other related concerns.

A large majority of the countries issue regular agrometeorological bulletins and offer advisory services. Nearly half of the respondents mentioned that they issue early warning information valuable for strategic planning and efficient monitoring. More than 70% of the respondents indicated that they have an efficient role in assessing the impact of extreme events. Publications include mostly 10-day, monthly and annual bulletins, few weekly, daily data are provided for agricultural research. Only Mali and Tunisia acknowledged provision of services to help reduce

the contributions of agricultural production to global warming. It appears that studies targeted towards such services need some attention.

Inadequate data for agromet purposes due to low network density, uneven distribution of stations and limited communication facilities and lack of software is one of the major limitations for providing more effective operational services.

Abdalla and Tarakidzwa (2006) listed a variety of ideas on methods and tools of analysis to improve operational agrometeorological services at the national level based on the responses to the questionnaire and these include the following:

Improve and rehabilitate agrometeorological stations and introduce automatic stations;
Improve communication links and consider new facilities;
Provide training (short and long-term) and analytical tools (introduce and improve methodologies);
Update and strengthen information system and technology (computers, software, GIS technology, etc.);
Develop user-tailored products;
Enable monitoring and inspection;
Initiate roving seminars; and,
Improve bulletins and introduce automation of data collection, processing, and information transfer.

### *43.3.2 Asia*

Kamali et al. (2006) described the operational agrometeorological services in Asia based on the responses to questionnaire designed by the WMO Secretariat. Asia covers a vast expanse of the Indian Ocean and part of the Pacific Ocean and contains a large and diverse range of ecosystems, including desert, forests, rivers, lakes, and seas. The desert extends from east to west encompassing central and western Asia. Each country has a different climate regime. Over the long period of human occupation in the region, exploitation of natural resources, urbanization, industrialization, and economic development have led to land degradation and environmental pollution. Climate change and climate variations also represent future stress.

The first country in Asia that initiated agrometeorological operations was the Republic of Kazakhstan, which started its activities in 1922. Later, India in 1945, China in 1953, Vietnam in 1960, and Iran in 1978 joined this activity. The last country to begin a service was Bangladesh, which started its operations in 1986. Affiliation of agrometeorological departments in RA-II is very different. For instance, in Qatar and Bahrain, agrometeorological activities are conducted within the Ministry of Agriculture. However, in other countries like Japan and Vietnam, such operations are managed jointly by the Ministry of Agriculture and a meteorological organization. In Iran, the agrometeorological department is in the Iranian National Meteorological Service.

Most countries in Asia produce agrometeorological data and information such as 10-day or monthly and growth-season bulletins. Moreover, other countries produce various bulletins in different periods. For example, in the I.R. of Iran, all the climatic, phenological, biometrical, and soil data are produced in weekly, 10-day, monthly, and seasonal bulletins, and also specific reports are issued regularly. Agrometeorological weather forecasts are one of the most important items focused in these bulletins. In this context, short- and long-term forecasts bear particular importance in bulletins, which are widely applied by users. Short-term predictions are used in cultivating operations such as the suitable date for applying pesticides, irrigation, and date of planting in different short-term periods. Long-term predictions, provided based on statistical methods, are also issued by Bangladesh, Nepal, and Laos. These kinds of predictions lack agrometeorological forecasts and they suffice only for weather predictions with a lead-time of 48 h. In addition to weather predictions, some countries have agrometeorological forecasts that may include some piece of advice for operational agrometeorological services. It should be noted that sectorial requirements of some users upon request might be met through preparation of special bulletins giving the probability index in the forecast. Such special cases are among additional obligations of these services. The agrometeorological forecasts depend on the variety of vegetation and climate of each country.

All of the countries are trying to do more operational services for agriculture. Services such as early warning of weather disasters, untimely extremes, and plant pest and disease forecasting are the most frequent services reported. Early warnings, the most important operational service, are prepared in the form of notifications and announcements by NMSs in all the countries. These are given to the authorities in the agrometeorological division to adopt measures for mitigation of natural disaster impacts.

In most countries in Asia, there are shortcomings and limitations in the current methods and tools in the production and dissemination of agrometeorological sevices including data collection, data manipulation, analysis, evaluation/assessment, publishing, delivery and communication. Kamali et al. (2006) made the following recommendations to improve agrometeorological services:

- Developing agrometeorological forecasting centers
- Developing forest meteorology, predicting yield/biomass before planting
- Studying sand movement or desertification elements
- Using AMS for measuring climatic elements and soil moisture
- Measuring evapotranspiration
- Establishing the domestic infrastructure of a flux measurement network
- Developing agrometeorological models for crop growth and development and evaluate agromet environment using agromet advice model “AMBER”
- Integrating agrometeorological information services
- Collaborating with the World Agrometeorological Information System (WAMIS)

- Cooperating with the International Society of Agricultural Meteorology (INSAM)
- Strengthening agrometeorology networks including station density, fine equipment, and capacity building
- Providing more detailed agrometeorology information
- Developing the infrastructure of the information network to transfer agrometeorological information to farmers more easily and faster.

### *43.3.3 South America*

Velazco and Egana (2006) described the operational agrometeorological services in South America based on the responses to questionnaire designed by the WMO Secretariat. Twelve out of the 13 countries in South America have meteorological services, except French Guyana. A high percentage of agrometeorological services in South America are part of the national meteorological services and depend, to a great extent, on the financial resources provided by the government; however, there are also some countries like Paraguay and Venezuela with agrometeorological units in institutions that are independent from the national meteorological service. In the case of Paraguay, the Agriculture Research Directorate and Agrometeorological Program of the Ministry of Agriculture and Livestock is the institution that assumes the role of agrometeorological services. In the case of Venezuela, this role is assumed by the Agriculture Research Institute (INIA) and the Ministry of Environment (MARN).

The operational agrometeorological products provided by the National Meteorological and Hydrological Services in South America are mainly disseminated through regularly issued bulletins and agrometeorological announcements, such as daily forecasts and information on special events and warnings that in the specific case of Chile, refer to frost, forest fire, and vegetable diseases and pests. The last one mentioned was suspended after a decade of issuing warnings, due to the lack of information related to the insects caught in the farms where this activity occurred. Ninty percent of the services responding to the survey provide medium-term forecasts and 70% generate long-term outlooks.

Sixty percent of the countries consulted (Argentina, Brazil, Ecuador, Paraguay, Peru, Uruguay) generate services that contribute to natural disaster reduction. Thus, for example, concerning early warnings, the totality of the Services provides some form of aid to the agriculturist by means of warnings related to precipitation events (excessive rain, hail, and drought), conditions of wind outside the normal ranks, eruption of warm or cold air masses abnormally (frost, heat waves), etc. It is important to highlight that the Meteorological Services consider they are not providing specific products to help diminish global warming; which is related to the agricultural activities.

A high percentage of the services (70%) considered that the range of the information and the extension of the data series are not sufficient. The same

percentage considers that they have limitations and deficiencies in obtaining analytical tools. Eighty percent of the services estimate that they have deficiencies and limitations in the way they deliver agrometeorological services.

Velazco and Egana make the following recommendations to improve agrometeorological services in South America:

- Improve spatial resolution and adapt global models as tools for prognosis.
- Invest in the dissemination of meteorological tools applied to agriculture, oriented to the small and medium farmers.
- Implement the services modern tools that combine the different levels of information, besides the agrometeorological one, obtaining a global view that could be of help to the farmers and different levels of decision making in a country. (For example, the implementation of a geographical information system.)
- Implementation of radar use and satellite information.
- Carry out strategic associations with institutions that may need the agrometeorological products to be able to increase the agrometeorological stations network, maintain the existing ones, and develop competitive agrometeorological products.
- Implement a regional training program to include aspects related to climate modeling, interpretation of satellite imagery oriented to agriculture, geographical information systems, and handling of agrometeorological databases and analytical tools.
- Standardization of products, services, methods, and regional climatic and agroclimatic procedures.
- Carry out a program of regional exchange that will consider the transfer of methodologies and knowledge of the professionals of the different services, by means of seminars, workshops, or hands-on training.
- Carry out studies on climate variability and climate change and its impact on agriculture at a regional level.

### *43.3.4 North America and Caribbean*

Solano (2006) described the operational agrometeorological services in South America based on the responses to questionnaire designed by the WMO Secretariat. The 26 countries of North America, Central America, and the Caribbean include mountains, rainy areas, deserts, and tropical islands. With their associated variations in culture and biodiversity and the long period of human occupation, exploitation of natural resources, urbanization, industrialization, and economic development have led to land degradation and environmental pollution. Climate change and climate variations also represent future stress.

Of the 26 member countries, only 38% have independent agrometeorological services. About 77% of the countries issue regular agrometeorological bulletins, advisories and early warnings/alerts. Only 54% of the countries assess impacts of

extreme events and 54% of the countries undertake strategic studies of relevance. Some countries have early warning systems on forest fires and floods to farmers and conduct studies on climatic risks.

Solano (2006) made the following recommendations to improve agrometeorological services in North America and Caribbean:

- Introducing or improving agrometeorological monitoring services and early warnings and alerts to help reduce the agricultural impact of extreme events
- Improving observation networks and agrometeorological databases
- Training national meteorological and hydrological services technical staff and the extension-related agricultural sector
- Improving computer tools used to analyze agrometeorological data, for example, reference evapotranspiration estimation, soil water balance at the depth root, vegetation conditions; meteorological, hydrological, and agricultural drought; and potential forest fire danger
- Using agrometeorological models to evaluate existing and expected conditions on different agricultural sectors – crops, livestock, forest, pests, and diseases
- Creating capacity and apply operational GIS technology
- Using high-resolution satellite images [vegetal cover, Normalized Difference Vegetation Index (NDVI), soil humidity, etc.] in the operational agrometeorological services
- Create capacity in the agricultural meteorology specialty, either NMHSs or agrometeorological information users
- Identify funding sources and promote financial support to national agrometeorological services with users who guarantee to keep the agrometeorological services
- Create a National Technical Committee that promotes agrometeorological applications that meet the needs of the agricultural sector and coordinates this work among institutions and disciplines.

### *43.3.5 Southwest Pacific*

Boer et al. (2006) described the operational agrometeorological services in South America based on the responses to questionnaire designed by the WMO Secretariat. In the Southwest Pacific, in some cases, the agrometeorological services are provided by National Meteorological Services, while in some countries they are part of the National Agricultural Directorate or the Ministry of Environment. The major customers for the agrometeorological services are the Ministries of Agriculture, research institutes, agricultural industries, and national task forces dealing with climate. The services, which are mostly in the form of issuing regular bulletins or advisories, provide early warnings as appropriate and strategic studies. Only in the Philippines, services are provided to help reduce the contributions of agricultural production to global warming. In Indonesia, this type of service is provided by agricultural research agencies.

Among the limitations for the provisión of agrometeorological services are:

- Lack of staff with strong statistical /agrometeorological background
- Discontinuities/missing data
- Poor spatial coverage
- Low data quality
- Lack of skill for downscaling global forecasts to local scale
- Weak communication links with farmers

In order to strengthen operational agrometeorological services, most countries feel that the use of agricultural simulation modeling, GIS/remote sensing technologies, and downscaling techniques to localize the regional climate forecasts should be encouraged. Key factors for the success of operational agrometeorological services are improvement of climate station networks (particularly rainfall networks), timely transfer of local data to an analysis center, forecast delivery from data analysis center to users, ability to localize climate forecast information and assess the impact, and availability of an effective dissemination system. Conducting impact analysis, and designing adaptation strategies to variable climate, such as tailoring crop management to climate forecast, are necessary. Collaboration between NMHSs with other agencies in the country that may have such capacities should be enhanced. International research agencies should also open up free access to global climatic data such as Categorical Climate Forecasts (GCM) outputs and software.

### *43.3.6 Europe*

Dunkel and Marica (2006) described the operational agrometeorological services in South America based on the responses to questionnaire designed by the WMO Secretariat. Because there is no lack of food in Europe and overproduction exists, the national communities are generally not interested in a system that can promote the quantity of the food production. On the other hand, there is a very strict and difficult subsidization system (CAP) in the European Union that should be followed by farmers, and there is strict environmental protection which would minimize the environmental damage. Agricultural meteorology could be helpful in the optimization of the use of chemicals, herbicides, and irrigation water. From the point of view of the national and traditional organizations, agricultural meteorology is not in a favorable position because many activities of insurance and pesticide companies exist which have got their own agrometeorological services.

Of the 49 countries in Europe, 20 countries reported having operated an independent agrometeorological units, and only 13 countries responded having no independent unit. In a few cases, it was reported that few people deal with the agrometeorological service in the frame of other organizational units, mainly as a part of the commercial, forecast, or climate units. Agrometeorological bulletins are the traditional source of information in Europe, and many services disseminate

information through Internet. Of course many of the meteorological websites are not directly organized for agrometeorological purposes, but it can be assumed that every meteorological website can be used for agrometeorological goals.

Operational agrometeorological services provided include:

- Short- and medium-range forecasts
- Regular agrometeorological bulletins and advisories
- Early warning systems for weather hazards
- Advisories to reduce the impact of natural disasters

In order to improve operational agrometeorological services in Europe, Dunkel and Marica (2006) suggest that it is important to modernize the monitoring system, use GIS, build into the system as many tools of the remote sensing techniques as possible, and to upgrade the computer-based management. Application of agrometeorological models, the new dissemination system, the use of SMS, and the Internet as useful for disseminating information.

Dunkel and Marica (2006) also provided several useful examples of applications at the national level in a number of European countries.

## 43.4 Some Examples of Good Applications in Operational Agrometeorology

Several agencies around the world are successfully applying agrometeorological applications on an operational basis. Some examples of good applications are given below.

### *43.4.1 Joint Agricultural Weather Facility (JAWF) of United States Department of Agriculture (USDA)*

JAWF, established through an agreement between the Department of Commerce (DOC) and the United States Department of Agriculture (USDA), is operated by the USDA World Agricultural Outlook Board (WAOB) and the DOC National Oceanic and Atmospheric Administration (NOAA). The primary mission of the JAWF is to routinely collect global weather data and agricultural information to determine the impact of growing season weather conditions on crops and livestock production prospects. JAWF is located in USDA and is jointly staffed and operated by DOC/NOAA/NWS/Climate Prediction Center (CPC) and USDA/OCE/World Agricultural Outlook Board (WAOB).

JAWF consists of a team of NWS operational meteorologists and WAOB agricultural meteorologists that monitors global weather conditions and prepares real-time agricultural assessments (Puterbaugh et al. 1997; Motha and Heddinghaus 1986).

These assessments keep USDA commodity analysts, the Chief Economist, and the Secretary of Agriculture and top staff well informed of worldwide weather-related developments and their effects on crops and livestock. When integrated with economic analyses and information, these routine and special crop-weather assessments provide critical information to decision makers formulating crop production forecasts and trade policy. JAWF's primary mission is to monitor global weather and determine the potential impacts on agriculture. JAWF meteorologists rely heavily on weather and climate data from over 15,000 stations from international and U.S. sources. Consequently, one of JAWF's most critical tasks is to process large volumes of data in an efficient and timely manner, and to generate products and agricultural assessments that are meaningful to the user community (JAWF 1994).

For close to three decades, JAWF has developed techniques for the acquisition, processing, and archival of these data, creating a blend of "existing" and "newly-developed" methods and products used in agrometeorological data management and analysis. A database management system (DBMS) effectively handles large volumes of available information and allows full integration of data into other Windows-based packages (Puterbaugh et al. 1997). Products currently utilize Geographical Information System (GIS) techniques at JAWF, providing the agricultural meteorologists with additional tools to produce crop-weather assessments and enhancing analytical techniques. JAWF's assessments are the final product of a series of steps that include: (i) meteorological data acquisition and management, (ii) data processing, (iii) data analysis, and (iv) product and information dissemination.

### *43.4.2 US Drought Monitor*

The emergence of the U.S. Drought Monitor (Svoboda et al. 2002), established in 1999, was a major advancement in drought monitoring products. The Drought Monitor classifies drought severity into five categories. The category thresholds are determined from a number of indicators, or tools, blended with subjective interpretation. The United States Drought Monitor was developed as an operational tool for monitoring drought conditions, including aerial extent, severity, and type, around the country. The Drought Monitor has become a highly successful tool for assessing the development and duration of drought conditions. The USDA, DOC, and the National Drought Mitigation Center publish the drought map and text weekly and post them on the Internet (http://drought.unl.edu/dm). The product serves as an exemplary case of interagency cooperation. A major strength of the Drought Monitor is its inclusion of input from climate and water experts from around the country.

The Monitor requires a major collaborative effort to pull together the various sources of weather data and compile them in a single, comprehensive, operational, national report. The map not only delineates stages of drought but also specifies drought type when the impacts differ. For example, if severe drought affects

wildfire danger and water supplies, but is not in a significant agriculture area, then the map would depict W (water) and F (wildfire danger) only. If drought affected a major crop area, that area would be denoted with "A" for agriculture. The map also reflects forecast trends. If the forecast of drought is expected to intensify, a "+" is depicted in affected area. Similarly, if the forecast calls for rain to diminish drought conditions, a "-" is depicted in the affected area. No change in the drought classification forecast is depicted by no sign. The text of the Monitor provides a detailed discussion of the map.

The Drought Monitor itself is not an index, nor is it based on a single index, but rather is a composite product developed from a rich information stream, including climate indices, numerical models, and the input of regional and local experts around the country. These experts include regional and state climatologists, agricultural, and water resource managers, hydrologists, NWS field office employees, and others. The list of expert reviewers has grown to nearly 150. A Drought Monitor Workshop is held annually to allow all participants to meet and share ideas for improvement in the process and the product. The Drought Monitor authors must rely on a number of key and ancillary indicators from different agencies. The map fuses these indicators, using human expertise from across the United States, into an easy-to-read image presenting a current status of drought conditions. The Drought Monitor process is an evolving one as new, or better, indicators and information sources become available.

Lead responsibility for preparing the Drought Monitor rotates among nine authors from four agencies who sequentially take 2–3 week shifts as the product's lead author. Nationwide experts respond to the lead author's first draft when it arrives by Internet and through an e-mail list-server every Monday. An interactive process continues until the final product, both the map and text, are released on Thursday morning.

Classification of drought magnitude in the Drought Monitor is based on farm levels using a percentile approach. The percentiles are standardized for the year rather than for all times of the year at once. They are not meant to imply an average areal extent value for the United States at any given time. The categories include: D0 (abnormally dry), 21–30% change occurring in any given year at a given location; D1 (moderate drought), 11–20% chance; D2 (severe drought) 6–10% chance; D3 (extreme drought), 3–5% change; and D4 (exceptional drought), 2% or less change.

Classification of drought impact types is also included in the Drought Monitor. The categories include agriculture (crops, livestock, range and pastures), water (streamflow, snow pack, groundwater, reservoirs), and fire (wildfire – forest and range fires). Crop stress is often the earliest indicator of a developing drought situation because of the plants need for moisture and moderate temperatures during critical phases of development. On the other hand, hydrological impacts of a major drought often linger for months or even years after agricultural concerns disappear. Thus, it is essential to monitor the evolution of drought types as well as overall conditions.

### 43.4.3 Monitoring and Early Warning Systems for Potentially Dangerous Vegetation Fires in Cuba

According to the studies conducted by the Meteorological Institute Climate Center of Cuba, in the last three decades, the average air temperature has increased by 0.6°C, the presence of severe storms has increased (accompanied by strong winds and electric discharges), and the frequency and intensity of south winds and droughts has risen (Centella et al. 1997). All of these events contribute to a greater occurrence of vegetation fires. The general increase in temperatures has been accompanied by a reduction of annual total rainfall from 10% to 20% and an increase in the interannual variability from 5% to 10%. Another feature noted is diminishing rainfall in the rainy period (May–October) and increased rainfall in the drier period of the year (Lapinel et al. 1993).

Hence studies were conducted by Solano et al. (2006) in Cuba to develop an evaluation method that describes, using objective methods, the danger potential conditions of vegetation fires in an appropriate scale for an exploratory purpose and to apply the results obtained in the operational agrometeorological services and in the future generation of a database that allows developing new agrometeorological investigations and risk studies for vegetation fires. To evaluate the long-term danger potential conditions of vegetation fires, an index determined by Solano (2001) was used, modified to a five-values scale. To issue the early warnings alert on vegetation fires potential, the traditional agrometeorological prediction method was used. It was based on the vegetation, formed by inertia of agrometeorological conditions at the end of a 10-day period, and the dependence of the current inertia in the vegetation with regard to the present and past meteorological conditions.

The alert system has allowed Cuba National Body Keepers to keep its specialists informed about the danger conditions caused by weather and climate extremes; strengthen preventive activity and improve operational efficiency in fire monitoring surveillance; and more effectively combat forest fires. The early warning alerts make it possible to concentrate forces and resources on the more fire-prone danger areas; optimize the use of aviation resources used in observation, optimize specialized forces to combat these catastrophes; and inform the population about the potential hazard.

### 43.4.4 FAO Crop Monitoring and Yield Prediction

Most of the crop monitoring and forecasting methods are developed around the water balance calculated during the growing season and take into account the phenological development of the plant. The agrometeorological approach produces better results in semi-arid areas where the water deficit is the main factor limiting crop productivity.

FAO's monitoring of rainfed crops is based on the following principal tools (Bernardi and Gommes 2006):

- Use of real-time meteorological data;
- Use of crop-specific water balance models;
- Processing of real-time satellite images (mainly by NOAA, SPOT – Vegetation and Meteosat satellites);
- Use of spatial interpolation tools;
- Use of gridded surfaces of crop-related parameters derived, or not, from satellite images (e.g., soil water holding capacity, soil type, land cover, land use, crop area sample, etc.);
- Use of seasonal forecasts;
- Field sample surveys, mainly for harvest estimates.

These tools can be used for rapid qualitative evaluations of crop status (development, stage in the cycle, condition, etc.), which can become quantitative depending on the availability of additional information (agronomic data, statistics on yields, long-term time series, etc.) and providing the information is validated.

Starting in 1974, the Agrometeorology Unit of FAO has developed and continuously improved a crop-forecasting methodology with the aim of supplying updated information on crop conditions in sub-Saharan countries to FAO's Global Information and Early Warning System (GIEWS), and also to provide tools to the agrometeorological component of the various national Food Security Information and Early Warning Systems. The methodology aims to predict crop yields (tons/hectare) and production before the harvest actually takes place, typically a couple of months in advance (May or June for the Northern Hemisphere).

## 43.5 Conclusions

The diverse user community for agrometeorological services ranges from farmers to national and international planning agencies. The demand for information by the user community has increased dramatically due in part to the recognition of the importance of agroclimatic information for decision-making, in part to increased economic pressures, natural resource conservation, and environmental concerns, and in part to greater availability of technological resources. The agroclimatic information base is not only needed at the farm level for daily tactical decisions on planting, spraying and harvesting, but also for long-term strategic decisions at the national and international levels concerning marketing, global variability, and risk management.

One common theme that emerges clearly from the discussion on the requirements for agrometeorological services from an international perspective is the need for the provision of improved agrometeorological services, not just for enhancing agricultural productivity, but also for protecting the environment and biodiversity and coping with climate change. Preparedness strategies to cope with

the impact of the meteorological extreme events require better information and monitoring systems and effective early warning systems. There is also much emphasis on better dissemination and application of climate forecasts, in particular the El Niño/La Niña events, for increasing and sustaining agricultural productivity. Operational agrometeorological services should recognize the potential of working closely with departments and agencies involved in natural disaster preparedness and mitigation to provide quick and efficient help to the farming community. Remote sensing and GIS applications hold a lot of promise for improving operational agrometeorological services and more attention needs to be paid to enhancing such applications.

## References

Abdalla H, Tarakidzwa I (2006) Perspectives from Regional Association I (Africa). In: Motha RP, Sivakumar MVK, Bernardi M (eds) Strengthening operational agrometeorological services at the national level, pp 18–23. Proceedings of the inter-regional workshop, Manila, 22–26 March 2004. United States Department of Agriculture, Washington, DC; World Meteorological Organization, Geneva; Food and Agriculture Organization of the United Nations, Rome. Technical bulletin WAOB-2006-1 and AGM-9, WMO/TD No.1277

Basher R (2006) Global early warning systems for natural hazards: systematic and people-centered. Phil Trans R Soc A 364:2167–2182

Bernardi M, Gommes R (2006) Coordinating role of the Food and Agriculture Organization in developing tools and methods to support food-security activities in National Agrometeorological Services. In: Motha RP, Sivakumar MVK, Bernardi M (eds) Strengthening operational agrometeorological services at the national level, pp 114–124. Proceedings of the inter-regional workshop, Manila, 22–26 March 2004. United States Department of Agriculture, Washington, DC; World Meteorological Organization, Geneva; Food and Agriculture Organization of the United Nations, Rome. Technical bulletin WAOB-2006-1 and AGM-9, WMO/TD No.1277

Berri GJ (2000) Potential applications of climate forecast to water resources management in South America. In: Cunha GR, Haas JC, Berlato MA (eds) Applications of climate forecasting for better decision-making processes in agriculture. Embrapa Trigo, Passo Fundo, pp 149–158

Boer R, Hilario F, McGree S, Pajuelas B, Seng TL (2006) Perspectives from Regional Association V (South-West Pacific). In: Motha RP, Sivakumar MVK, Bernardi M (eds) Strengthening operational agrometeorological services at the national level, pp 69–80. Proceedings of the inter-regional workshop, Manila, 22–26 March 2004. United States Department of Agriculture, Washington, DC; World Meteorological Organization, Geneva; Food and Agriculture Organization of the United Nations, Rome. Technical bulletin WAOB-2006-1 and AGM-9, WMO/TD No.1277

Centella A, Naranjo L, Paz L, Cárdenas P, Lapinel B, Maritza Ballester R, Pérez AA, González C, Limia M, Sosa M (1997) Variaciones y cambios del Clima en Cuba. Informe Técnico Centro Nacional del Clima, Instituto de Meteorología, La Habana, p 58

CRED (2005) Data from EM-DAT, the OFDA/CRED International disaster database, www.em-dat.net, Centre for Research on the Epidemiology of Disasters (CRED), Universite´ Catholique de Louvain, Brussels (OFDA is the US Office of Foreign Disaster Assistance)

Dunkel Z, Marica A (2006) Perspectives from Regional Association VI (Europe). In: Motha RP, Sivakumar MVK, Bernardi M (eds) Strengthening operational agrometeorological services at the national level, pp 81–100. Proceedings of the inter-regional workshop, Manila, 22–26 March 2004. United States Department of Agriculture, Washington, DC; World

Meteorological Organization, Geneva; Food and Agriculture Organization of the United Nations, Rome. Technical bulletin WAOB-2006-1 and AGM-9, WMO/TD No.1277

FAO (2008) Current world fertilizer trends and outlook to 2011/12. Food and Agriculture Organization of the United Nations, Rome

FAO (2009) The state of food insecurity in the world 2009: economic crises – impacts and lessons learned. Food and Agriculture Organization of the United Nations, Rome

FAO (2010) Using agricultural growth to fight poverty. Note prepared by FAO for the OECD Committee for Agriculture. Food and Agriculture Organization of the United Nations, Rome

IFRC (2005) World disasters report 2005. (Disasters data prepared by the Centre for Research on the Epidemiology of Disasters from the EM-DAT database.) International Federation of Red Cross and Red Crescent Societies, Geneva

ISDR (2004) Terminology: basic terms of disaster risk reduction. http://www.unisdr.org/eng/library/lib-terminology-eng%20home.htm. Secretariat of the International Strategy for Disaster Reduction, Geneva

ISDR-PPEW (2005) ISDR platform for the promotion of early warning (PPEW), Bonn

JAWF (1994) Major world crop areas and climatic profiles. Joint Agricultural Weather Facility, Washington, DC: USDA, World Agricultural Outlook Board, Agricultural handbook No. 664, p 279

Kamali GA, Van Viet N, Rahimi M (2006) Perspectives from Regional Association II (Asia). In: Motha RP, Sivakumar MVK, Bernardi M (eds) Strengthening operational agrometeorological services at the national level, pp 24–33. Proceedings of the inter-regional workshop, Manila, 22–26 March 2004. United States Department of Agriculture, Washington, DC; World Meteorological Organization, Geneva; Food and Agriculture Organization of the United Nations, Rome. Technical bulletin WAOB-2006-1 and AGM-9, WMO/TD No.1277

Lapinel B, Rivero RE, Cutié V, Rivero RR, Varela N, Sardinas M (1993) Sistema Nacional de Vigilancia de la Sequía: Análisis del período 1931–1990. Informe Científico Técnico, Centro Meteorológico Provincial de Camagüey, Cuba, p 45

Motha RP, Heddinghaus TR (1986) The Joint Agricultural Weather Facility's operational assessment program. Bull Am Meteorol Soc 67:1114–1122

Motha R P, Sivakumar MVK, Bernardi M (eds) (2006) Strengthening operational agrometeorological services at the national level. Proceedings of the inter-regional workshop, Manila, 22–26 March 2004. United States Department of Agriculture, Washington, DC; World Meteorological Organization, Geneva; Food and Agriculture Organization of the United Nations, Rome. Technical bulletin WAOB-2006-1 and AGM-9, WMO/TD No.1277, pp 238

PRB (2009) 2009 world population datasheet. Population Reference Bureau, Washington, DC

Puterbaugh T, Stefanski R, Brusberg M (1997) The joint agricultural weather facility's operational procedures for processing and analyzing global crop and weather data. Proceedings of the 13th conference on interactive information and processing systems, American Meteorological Society, Long Beach, pp 46–49

Solano O (2001) Diseño de una estrategia para el combate de incendios forestales. Informe de consultoría sobre prevención de incendios forestales del Proyecto FAO TCP/CUB/0066(A). La Habana, p 77 (+24a)

Solano O (2006) Perspectives from Regional Association IV (North and Central America). In: Motha RP, Sivakumar MVK, Bernardi M (eds) Strengthening operational agrometeorological services at the national level, pp 54–68. Proceedings of the inter-regional workshop, Manila, 22–26 March 2004. United States Department of Agriculture, Washington, DC; World Meteorological Organization, Geneva; Food and Agriculture Organization of the United Nations, Rome. Technical bulletin WAOB-2006-1 and AGM-9, WMO/TD No.1277

Solano O, Vázquez R, Menéndez JA, Pérez E, Figueredo M (2006) Monitoring and early warning systems for potentially dangerous vegetation fires in Cuba. In: Motha RP, Sivakumar MVK, Bernardi M (eds) Strengthening operational agrometeorological services at the national level. Proceedings of the inter-regional workshop, Manila, 22–26 March 2004. United States Department of Agriculture, Washington, DC; World Meteorological Organization, Geneva; Food and

Agriculture Organization of the United Nations, Rome. Technical bulletin WAOB-2006-1 and AGM-9, WMO/TD No.1277

Svoboda M, LeComte D, Hayes M, Heim R, Gleason K, Angel J, Rippey B, Tinker R, Palecki M, Stooksbury D, Miskus D, Stephens S (2002) The drought monitor. Bull Am Meteorol Soc 83:1181–1190

Velazco CA, Egana M (2006) Perspectives from Regional Association III (South America). In: Motha RP, Sivakumar MVK, Bernardi M (eds) Strengthening operational agrometeorological services at the national level, pp 45–53. Proceedings of the inter-regional workshop, Manila, 22–26 March 2004. United States Department of Agriculture, Washington, DC; World Meteorological Organization, Geneva; Food and Agriculture Organization of the United Nations, Rome. Technical bulletin WAOB-2006-1 and AGM-9, WMO/TD No.1277

# Chapter 44
# Overview of the World Agrometeorological Information Service (WAMIS)

**Robert Stefanski**

**Abstract** Based on recommendations from an Inter-Regional Workshop on Improving Agrometeorological Bulletins in Barbados in October 2001, the World AgroMeteorological Information Service (WAMIS) website has been operational since December 2003. WAMIS is a dedicated web server that countries and organizations can place their agrometeorological bulletins and advisories. By providing a central location for agrometeorological information, users can quickly and easily evaluate the various bulletins and gain insight into improving their own bulletins. Also, these bulletins represent the expert knowledge of the individual countries and can be used to assess extreme events and disasters in a historical perspective especially when an archive of bulletins are present. Placement of agrometeorological bulletins on WAMIS also increases the visibility of the national meteorological/hydrological services (NHMS). The current issues facing the WAMIS project are increasing the use of the website by members and developing tools and resources applications.

## 44.1 Background

In October 2001, the World Meteorological Organization (WMO) along with the United States National Oceanic and Atmospheric Administration (NOAA) and the Caribbean Institute for Meteorology and Hydrology sponsored an Inter-Regional Workshop on Improving Agrometeorological Bulletins which was held in Barbados. The objectives of the workshop were to evaluate how the National Meteorological and Hydrological Services (NMHS) determine the contents and present information in their countries agrometeorological bulletins; identify shortcomings and limitations in the agrometeorological bulletin preparation; review

R. Stefanski
World Meteorological Organization, Geneva, Switzerland
e-mail: rstefanski@wmo.int

S.D. Attri et al. (eds.), *Challenges and Opportunities in Agrometeorology*,
DOI 10.1007/978-3-642-19360-6_44, 

the new methods and tools that can improve the content and presentation of information in agrometeorological bulletins and the timely dissemination of the bulletins to decision-makers; and formulate an effective training strategy to build the capacity of NMHSs to rapidily implement the improved systems of preparing and disseminating agrometeorological bulletins (Sivakumar 2002).

The purpose of the workshop was to assess the current status of agrometeorological bulletin preparation across the world and determine different methods to improve the contents of these bulletins to facilitate timely and efficient operational farming decision-making that relies on agrometeorological information. During the brainstorming sessions of the workshop the participants developed the concept of establishing an Internet server for all agrometeorological bulletins from various countries. The specific recommendation stated that a web server be created to share experiences in order to aid in the preparation of agrometeorological products and also to facilitate exchange of new ideas and that the new server should be in a location where all countries could routinely post their agrometeorological products. The view of the participants was that by having as many agrometeorological products and bulletins on one website, personnel from NMHSs could then readily compare, evaluate, and use these ideas to improve their own agrometeorological products and bulletins.

After this workshop, the Commission for Agricultural Meteorology (CAgM) of the WMO recognized the need for improved access to agrometeorological products by members and initiated a meeting to enhance the use of Internet technology. An Expert Group Meeting on Internet Applications for Agrometeorological Products was held in Washington, DC. in May 2002, organized jointly by NOAA, United States Department of Agriculture (USDA), and WMO. Based on the recommendations from this Expert Group meeting, the foundations of dedicated web server were created. Soon after the Expert Group Meeting, a project manager was assigned to the project with the initial task to develop an appropriate name and web address for the web server. After consultation with a group from the Washington meeting, the title of the World Agrometeotological Information Service (WAMIS) was agreed upon. The necessary steps were then taken to obtain the web address, www.wamis.org.

Since there were limited technical resources at the WMO to develop and maintain a dedicated web server for WAMIS, the technical aspects of website development and maintenance needed to be done by an outside contractor. Through the WMO bid selection process, the U.S. based web-hosting company INETU from Allentown, PA was chosen. During the autumn of 2003, INETU developed the website and logo with feedback from the WAMIS Project Manager and in December 2003, WAMIS officially went online with products from Peru and the US. Shortly thereafter, in January 2004, colleagues from Italy (http://wamis.bo.ibimet.cnr.it) developed a mirror site that copies the main website every day. Stefanski and Sivakumar (2006) provide more detail on these early developments of the WAMIS project.

The objective of WAMIS is to provide a dedicated web server on which countries and organizations can place their agrometeorological bulletins and advisories. Provision of such a central location for agrometeorological information,

enables users to quickly and easily evaluate the various bulletins and gain insight into improving their own bulletins. Also, these bulletins represent the expert knowledge of the individual countries and provide the possibility to assess extreme events and disasters in a historical perspective especially when an archive of bulletins are present. Placement of agrometeorological bulletins on WAMIS also increases the visibility of the NMHSs.

## 44.2 Current Status

As of the end of December 2009, there are products or links from 50 countries and organizations (see Fig. 44.1). The following describes these products and how they received by the project manager:

| | |
|---|---|
| Number of Web Links only | = 24 |
| Number of Actual Bulletins (PDF) | = 26 |
| Received by email | = 12 |
| Accessed by web | = 14 |
| Automatically uploaded | = 0 |


**Fig. 44.1** WAMIS home web page as of April 2010 (www.wamis.org)

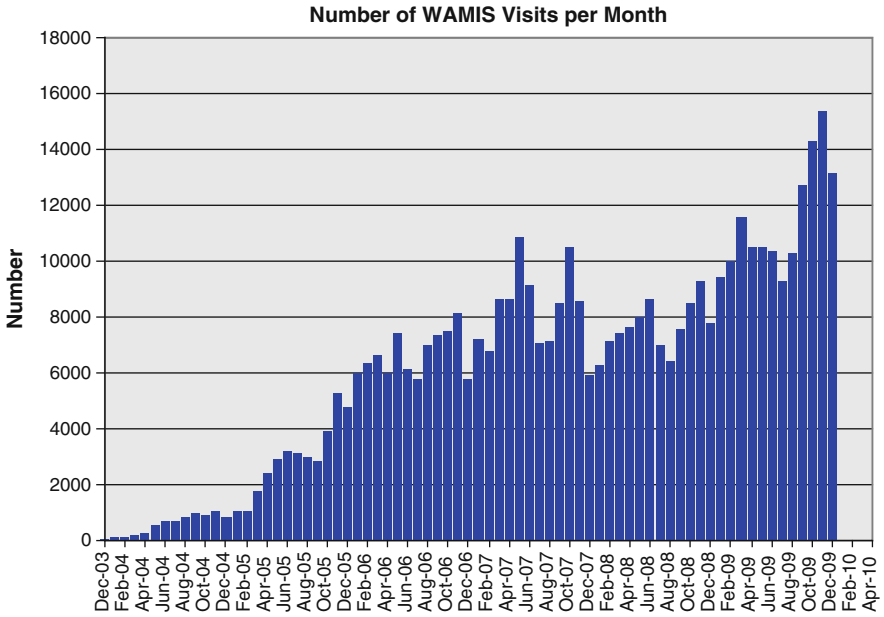


**Fig. 44.2** Number of monthly visits to the WAMIS web page since the inception of the website to December 2009

Just about half of the products on WAMIS are actual bulletins in PDF format while the remainder are only links to other websites. There have been over 450,000 visits since the inception of the website. During 2009, there has been on average of 11,400 visits per month (see Fig. 44.2).

The following is the current distribution by WMO region of bulletins and products from member countries.

| | |
|---|---|
| Region I (Africa) | = 16 |
| Region II (Asia) | = 5 |
| Region III (S. America) | = 7 |
| Region IV (N. & C. America) | = 8 |
| Region V (SW Pacific) | = 6 |
| Region VI (Europe) | = 8 |

There are 19 categories of Tools and Resources with over 77 links. The categories include:

| | | | |
|---|---|---|---|
| Climate forecasts | Forestry/fire | Observations | Remote sensing |
| Data management | GIS | Online training | Soil erosion |
| Dissemination | GRADS | Phenology | Statistics |
| Drought | Irrigation/drainage | Plant/animal Health | Weather/climate data |
| Feedback | Natural disasters | Rainfall monitoring | |

## 44.3 WAMIS Project

WAMIS is being used as file storage for the web pages of WMO's Agricultural Meteorology Programme and the Commission for Agricultural Meteorology. WAMIS stores PDF files from the WMO meetings and an archive of past CAgM reports and brochures for the WMO AGMP websites.

In October 2004, WMO organized an Expert Meeting on Meteorological Information for Locust Control in Geneva, Switzerland to discuss the response from NMHSs to the current Desert Locust plague. Representatives from the Food and Agriculture Organization, AGRHYMET, Italy, and India attended the meeting. One of the recommendations from this meeting was for NMHSs to Upload daily rainfall and temperature data to WAMIS and then allow National Locust Control Centres to view the data. This activity received the approval from the WMO Secretary-General and INETU developed the technical capability on WAMIS for this purpose. This capability became operational by the end of March 2005. The Locust Resource page still exits but the data uploading and viewing has been discontinued.

In 2009, WMO hired a web programming consultant to develop an online database of the National Progress Reports in Agrometeorology. This database is currently online at http://npr.wamis.org/ with the Reports based from 2002 to 2005. The results of the new Reports from 2006 to 2009 will also be put online before the 15th Session of CAgM in July 2010.

A CAgM Expert Team on Collection and Evaluation of Operational Agrometeorological Tools and Methodologies highlighted several tools and methodologies used by various agencies in different regions for agrometeorolgical applications. Based on the final report of the Expert Team, several of these links will be added to WAMIS before the CAgM-XV Session takes place in July 2010.

During the CAgM Management Group meeting in the Russian Federation in June 2008, there were discussions on how to improve the utility of WAMIS with new information technology. After the CAgM Management Group meeting, there were discussions at WMO Headquarters on how WMO Technical Commissions could contribute to the WMO Information System (WIS). Due to the active involvement of the Korean Meteorological Administration (KMA) in developing WAMIS and that KMA staff represents the CAgM in the Inter-Commission Coordination Group on the WMO Information System (ICG/WIS), it was decided to involve KMA in the development of a CAgM project to integrate WAMIS into the WIS. The first phase of this project is the development of an ISO compatible search engine on WAMIS, which would enable users to make searches on WAMIS via WIS. Through discussions with KMA and WMO, a WIS expert agreed to travel to the Republic of Korea in May 2009 to facilitate and provide guidance for this project. it was decided to provide the WIS-compliant search interface for WAMIS by implementing "GeoNetwork". GeoNetwork is free, open source, software written primarily in Java. Using some custom tools plus GeoNetwork facilities, KMA staff and the WIS expert created metadata for all of the links and

products accessible through WAMIS. Meanwhile, development and testing of the Geonetwork-based WAMIS metadata search and maintenance Web site continues.

## 44.4 Future Projects, Users and Issues

The future plans include to steadily increase the number bulletins and Tools and Resources on WAMIS. There are several information technologies and internet tools that have potential to aid the agrometeorological community. These include: web-based GIS tools, remote-sensing information, online crop model applications, XML standards for agrometeorological bulletins, downscaled model information (gridded evapotranspiration and soil moisture estimates), the use Numerical Weather Prediction information into agrometeorological models (crop, irrigation, pest/diseases), and online training and educational modules. During the Commission for Agricultural Meteorology (CAgM) Management Group meetings in Russia in 2008 and in Geneva in February 2010, it was decided that an expert meeting should be organized to review the status of WAMIS and to provide new ideas and guidance on the future development of WAMIS applications. This meeting will take place in April or May 2010 in the Republic of Korea. This expert meeting is considered to be a scoping or brainstorming meeting to identify any potential new information technology or internet tools that could be useful to the agrometeorological communities. Therefore, It is expected that some applications will be identified and draft project proposals be developed. A meeting report will be developed and the outcome of this meeting will be reported to the 15th Session of the Commission for Agricultural Meteorology in July 2010.

## References

Sivakumar MVK (ed) (2002) Improving agrometeorological bulletins. In: Proceedings of an inter-regional workshop held in Bridgetown, World Meteorological Organization, Geneva, 15–19 Oct 2001

Stefanski R, Sivakumar MVK (2006) World AgroMeteorological Information Service (WAMIS). Meteorol Appl (Suppl):49–53

# Chapter 45
# Analysis of Rainfall Variability and Characteristics of Rainfed Rice Condition in Eastern India

**P.K. Singh, L.S. Rathore, K.K. Singh, and B. Athiyaman**

**Abstract** The rainfall and crop data were analysis of Eastern India namely Orissa, West Bengal, Assam, Jharkhand, East Uttar Pradesh, East Madhya Pradesh, Chhattisgarh and Bihar. The rainfed rice is the main crop grown in this region. The greater part of the area in eastern Uttar Pradesh, Madhya Pradesh, Chhattisgarh, Bihar and Orissa where LGP vary from 19 to 24 weeks whereas it is only 17–18 weeks in the south western border of eastern Uttar Pradesh. It is observed that lowest productivity of less 5 q per ha in eastern Madhya Pradesh. In general, the rice yields are less than 10 q per ha in Chhattisgarh, Jharkhand, Orissa, north Bihar, western parts of Assam and northwestern portion of eastern Uttar Pradesh. The highest yield levels of 20–25 q per ha is seen in the middle parts of Uttar Pradesh and West Bengal. The productivity level remains at 10–15 q per ha in Orissa, Assam and eastern Uttar Pradesh.

It is generally observed that low productivity of 1 t/ha have been mostly observed in semi-arid to dry sub-humid type of climate with LGP varying 90–120 to 120–150 days. The highest productivity of 2–3 t/ha are recorded in hot sub-humid to humid regions of West Bengal where LGP vary from 150 to 200 days. The productivity was the order of 1–2 t/ha in hot sub-humid to humid regions of Assam, Orissa and West Bengal. Also the hot dry sub-humid climates in Uttar Pradesh and Bihar recorded the productivity of 1–2 t/ha.

P.K. Singh (✉) • L.S. Rathore • K.K. Singh
India Meteorological Department, Agromet Service Cell, Mausam Bhavan, New Delhi, India
e-mail: pksingh@ncmrwf.gov.in; pksingh66@gmail.com; lsrathore@ncmrwf.gov.in; kksingh2022@gmail.com

B. Athiyaman
India Meteorological Department, Agromet Service Cell, Mausam Bhavan, New Delhi, India
and
National Center for Medium Range Weather, Forecasting, Noida 201 307, India
e-mail: athiya@ncmrwf.gov.in

S.D. Attri et al. (eds.), *Challenges and Opportunities in Agrometeorology*,
DOI 10.1007/978-3-642-19360-6_45, 

## 45.1 Introduction

The rainfed agro-ecosystem occupies the major cropped areas in India. Out of the 142 Mha net sown area in the country, nearly two-thirds, i.e., 90 Mha is under rainfed agriculture. Nearly 67 Mha of rainfed area receive mean annual precipitation in range of 500–1,500 mm with high degree of variability leading to low productivity and stability of rainfed crops. Rainfed agro-ecosystem, which contributes to about 45% of agricultural production, is entirely at the mercy of the monsoon activity over the country and is beset with problems of mid-season drought and associated impacts on the crop productivity. Most of the regions in the rainfed agro-ecosystem experience moderate to severe drought conditions of prolonged nature once in 2–5 years. Apart from the prolonged drought, inadequate and erratic distribution of rainfall often exposes the plants to shortage of desired levels of moisture, and thus plant growth takes place under below optimum conditions (Raj and Dey 2004; Ramana Rao 1997).

As a result, the productivity levels remain low over the rainfed regions and hardly cross 1 t $ha^{-1}$ at most of the farmers' fields. The proper understanding and efficient utilization of the natural resources, especially of the weather, is, therefore, of great concern for improvement and sustainability of agriculture in the rainfed agro-ecosystem.

The rainfed agro-ecosystem covers the agro-ecological regions 3–10 (arid to sub-humid) i.e., including Assam, West Bengal, Orissa, Jharkhand, Bihar and Uttar Pradesh (Rajendra Prasad and Datar 1990). It also includes parts of humid and per humid regions of eastern and northeast India where crops are grown under rainfed conditions (Rao and Rajput 1996; Katyal et al. 1996b; Gangopadhyaya and Sarkar 1965). Although, substantial amount of rainfall is available which at times become excess hence because of flooding due to inadequate drainage. Hence, these regions are encountered with type of agri-management problems, which are entirely rainfed farm management different from in arid and semi-arid regions.

The rainfed agro-ecosystem is characterized by frequent moisture stress periods during the cropping season due to breaks in monsoon rains or early withdrawal of monsoon. The drought periods at times extend to more than 1 month and often occur during the later parts of the rainy season in August, extending into September and merging with the withdrawal of monsoon from the region (Srivastava et al. 1989).

## 45.2 Materials and Methods

The daily rainfall data and crop data were collected at eastern India namely Orissa, West Bengal, Assam, Bihar, Jharkhand, Eastern Uttar Pradesh, Eastern Madhya Pradesh and Chhattisgarh and analysis using computer program, computations of weekly averages, monthly and annual values has been worked out and also the probabilities of receiving different amounts of rainfall at weekly intervals have

been computed (Biswas 1982; Kulandaivelu 1984; Singh et al. 2008). The total crop season from germination of seedling to maturity is expected to be completed in 17 weeks. Out of which, the water requirements of crops in the last 2 weeks of maturity phase before harvesting is negligible. Hence, the rain dependent crop period of rainfed rice crop will be 15 weeks only (seedling 3 weeks, vegetative, reproductive and maturity 4 weeks each).

The weekly water requirements of rice crop under upland conditions up to the seedling stage (3 weeks) is assumed to be 100 mm while it is 50 mm per week for the rest of the weeks. Hence, the water need of the seasons (15 weeks) works out to be 700 mm. From the weekly rainfall amount at different probabilities (70, 60, 50 and 30%) of different stations spread over the study region, the rainfall at 60% (dependable precipitation) probability has been considered to compute the water availability at different growth stages as against the demand. Therefore, percentages of rainwater availability for different phenophases at each station have been worked out (Sastry 1976). Using spatial interpolation techniques in GIS, rainwater availability maps for all the growth stages, viz., seedling, vegetative, reproductive and maturity have been prepared (Kar and Verma 2005; ESRI 1998; Ramana Rao et al. 1993). Therefore, it is assumed that the season begins if the cumulative rainfall received over a period of three consecutive weeks is at least 100 mm and above.

To compute the annual and seasonal rainfall from the average weekly rainfall data at each station, total annual rainfall values (1–52 weeks), monsoon period (24–30 weeks) and post-monsoon period (40–48 weeks) have been computed for each station. The spatial distribution of seasonal (monsoon and post-monsoon) and annual rainfall maps has been prepared fusing GIS interpolation analysis (Kar and Verma 2005; Katyal et al. 1996b).

Thematic maps for all the basic parameters and the derivatives have been prepared using GIS package. The spatial variability maps of mean productivity and its changes over 30-year period for the entire study area have been prepared. Similar maps for each state have also been prepared.

## 45.3 Result and Discussion

### *45.3.1 Rainfall Pattern and Variability in Eastern India*

The rainfall is the most important parameter under tropical climate condition. Therefore, analysis of rainfall with respect to distribution in different seasons assumes greater significance. Maps showing the distribution of annual rainfall and in different seasons have been worked out and presented in Figs. 45.1–45.3, respectively. Similarly, rainfall maps for the same period have been prepared for 60% probability level, which is considered as dependable precipitation and are shown in Figs. 45.4–45.6.

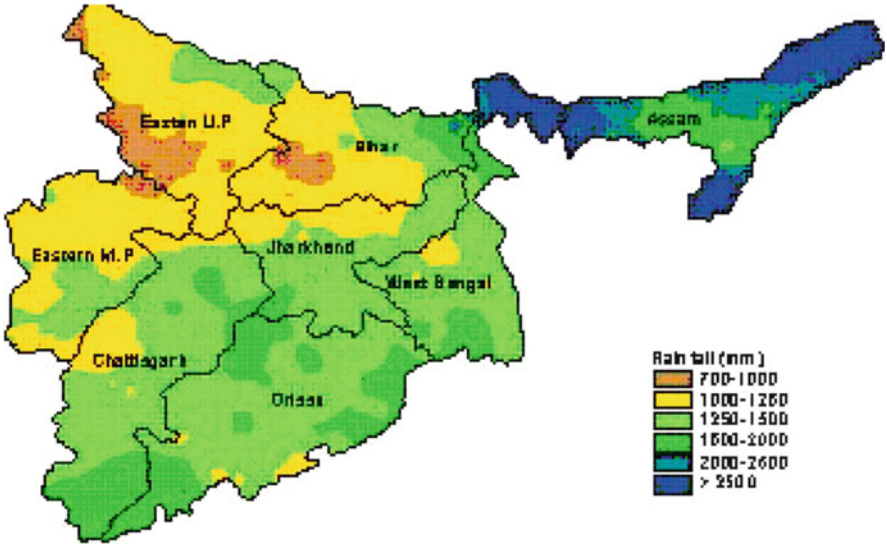


**Fig. 45.1** Average annual rainfall pattern in Eastern India

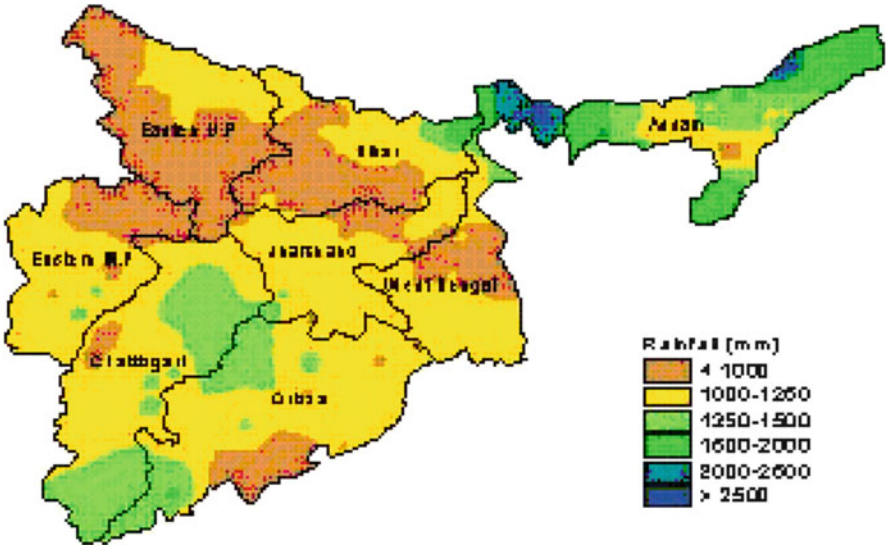


**Fig. 45.2** Average monsoon rainfall pattern in Eastern India

The average annual rainfall of the study area (Fig. 45.1) shows that the rainfall varies from 700 mm in the western parts of eastern Uttar Pradesh to greater than 2,500 mm per year in Assam. Greater part of the region comprising Chhattisgarh, Orissa, West Bengal, Bihar and Jharkhand receives a rainfall of about 1,250 mm per year. The monsoonal rainfall pattern (Fig. 45.2) indicated that except in eastern

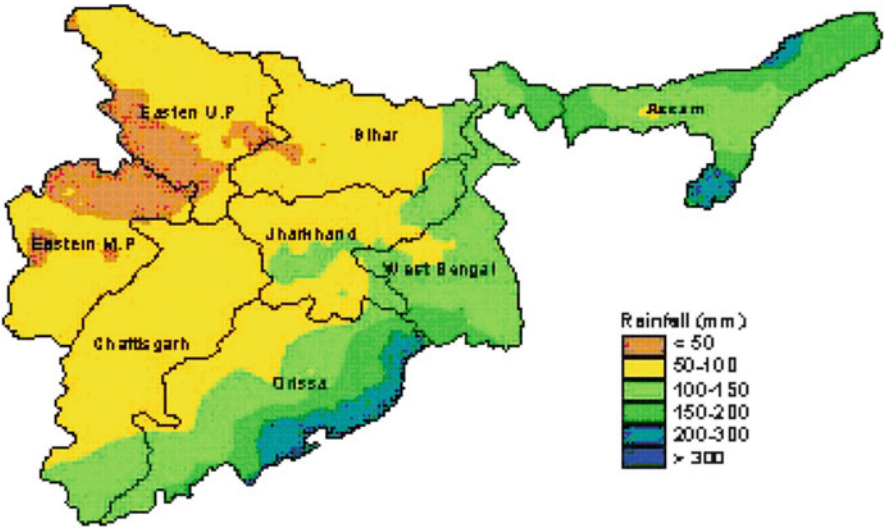


**Fig. 45.3** Average post monsoon rainfall pattern in Eastern India

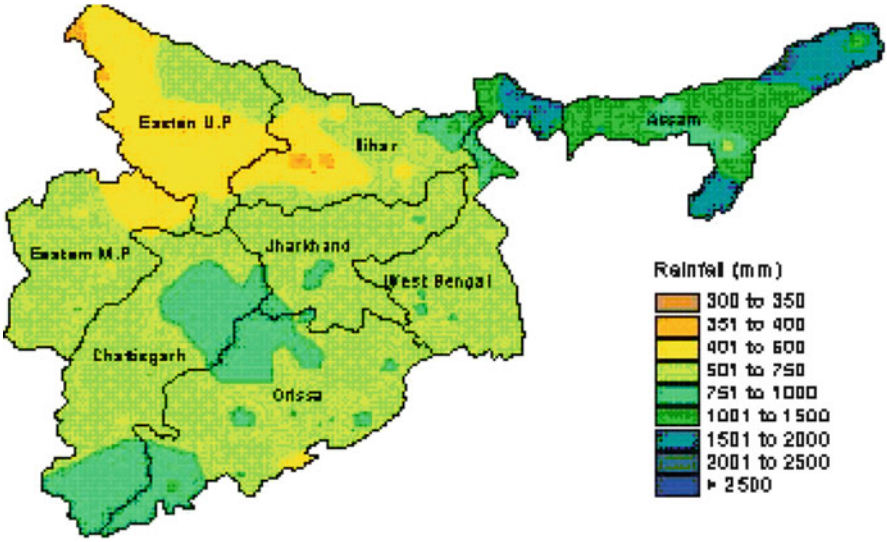


**Fig. 45.4** Annual rainfall (60% probability) pattern in Eastern India

Uttar Pradesh, Bihar, Jharkhand and West Bengal, coastal Orissa, the seasonal rainfall is above 1,000 mm. The highest rainfall is received in Assam. The quantum of post-monsoon rainfall is low (<100 mm) over greater parts of the region (Fig. 45.3). Few coastal districts in Orissa received the rainfall of about 200–300 mm due to occurrence of cyclones.

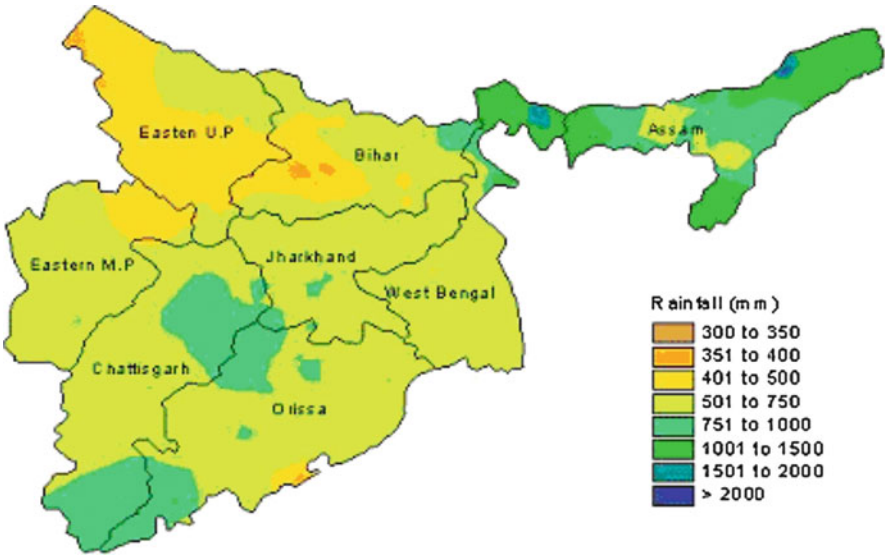


**Fig. 45.5** Monsoon rainfall (60% probability) pattern in Eastern India

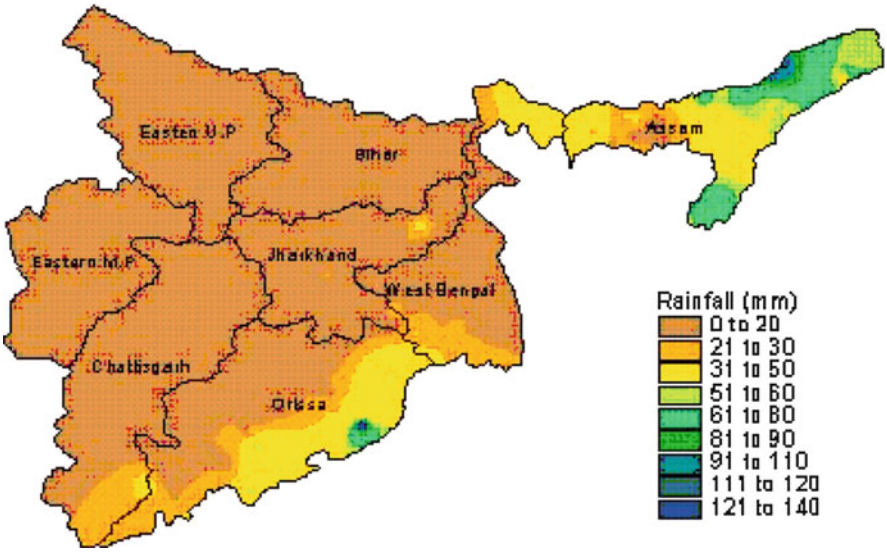


**Fig. 45.6** Post Monsoon rainfall (60% probability) pattern in Eastern India

### *45.3.2 Probability Pattern and Variability in Eastern India*

It is observed from the figures that annual rainfall of 60% probability (Fig. 45.4) as expected is higher towards north eastern region compared to western parts of the

study area. The greater part of the region is expected to have a rainfall amount of 500–750 mm. Majority of the area in eastern Uttar Pradesh, parts of Bihar and Madhya Pradesh can receive only about 500 mm of rain, which indicates that the failure of crop under rainfed conditions is not uncommon. Similarly, higher amounts of rainfall of 750–1,000 mm in forest areas of Chhattisgarh and Orissa can be seen as potential zones of higher productivity provided other conditions are conducive. Monsoon rainfall (Fig. 45.5) pattern follows the similar pattern as that of annual rainfall. However, some coastal districts in Orissa have recorded lower amounts of 400–500 mm indicating possible water stress condition. The post-monsoon season (October-November) rainfall scenario, Fig. 45.6 shows that except in the coastal districts of Orissa and parts of Assam, insignificant rainfall amount of less than 20 mm can only be possible in the entire region, which may not be contributing significantly for the crops growing in post-monsoon season.

### *45.3.3 Commencement Rainy Season Growing Pattern in Eastern India*

Knowledge on the commencement and end of growing season and its duration is useful for planning efficient cropping pattern and also to introduce new varieties matching with the length of growing period (LGP). From the MAI values obtained from water balance computations carried out for different stations spread over the study region, maps showing commencement and end of season (weeks) are given in Figs. 45.7 and 45.10. It is observed from the Fig. 45.7 that the commencement for

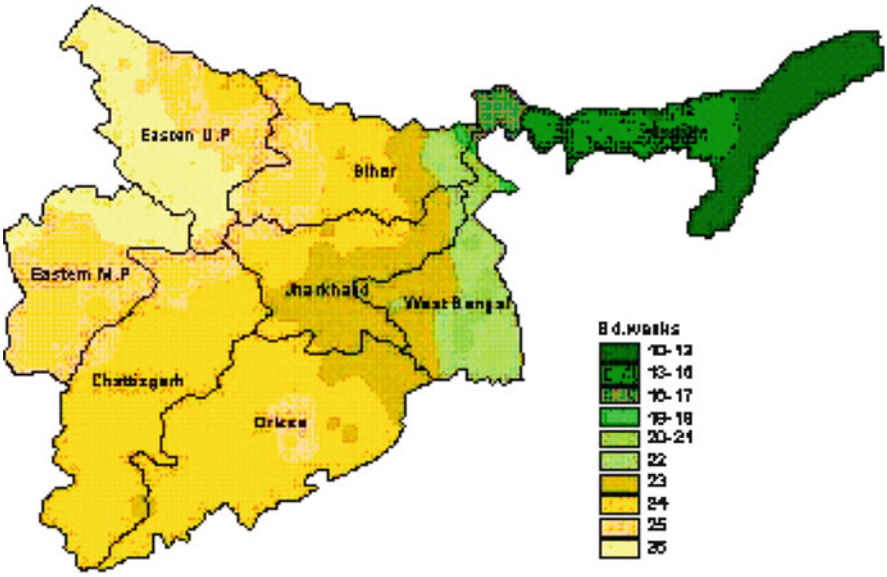


**Fig. 45.7** Commencement of growing period for rainfed rice in Eastern India

growing period starts as early as between 10 and 17 standard meteorological weeks in Assam and the adjoining areas. This is due to occurrence of rainfall during March due to northwest disturbances, which are largely isolated showers. These showers are useful for summer crops. The influence of such phenomena with occasional summer thundershowers is also seen in parts of West Bengal and in hilly regions of Indo-Gangetic Bengal up to 22nd week (end of May). In the 23rd week (1st week of June), Bihar, Jharkhand, West Bengal and northern Orissa are found to be conducive for commencement of the season. In general start of the season delays as one move towards west. Though greater Bihar, Uttar Pradesh, Madhya Pradesh and Orissa have conditions favorable for sowing by 24th week (mid-June), the extreme western part of the study region in Uttar Pradesh and eastern Madhya Pradesh will have a delayed start as the arrival of monsoon in to these regions is late compared to its neighboring areas in the eastern parts.

### *45.3.4 Cessation Rainy Season Growing Pattern in Eastern India*

The cessation of rainy season (Fig. 45.8) where AE/PE values less than 0.5 follows closely that of withdrawal of monsoon season. It is seen as early as by 42nd week (mid October) in the eastern parts of Uttar Pradesh and slowly moves towards east. By the beginning of November (45th week), the season ends from more than 50% of the area. The coastal parts of Orissa, West Bengal, the season ends by November

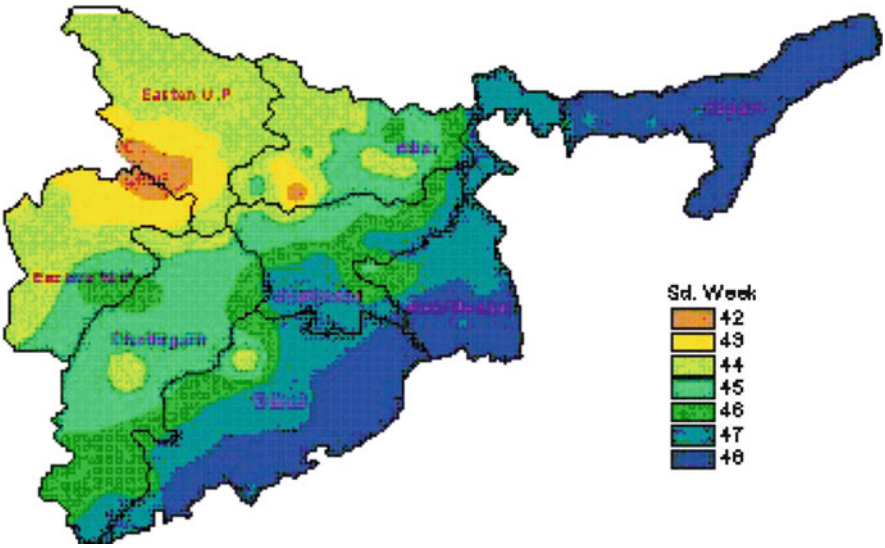


**Fig. 45.8** End of growing period for rainfed rice in Eastern India

(48th week). This is mostly due to the availability of residual moisture due to occurrence of cyclonic storms during October. In Assam too, the season ends by November due to extended period of rainy season.

### *45.3.5 Length of Growing Period (LGP) Pattern in Eastern India*

The difference between the commencement and cessation of growing season computes the average length of LGP at each station. The LGP map (Fig. 45.9) prepared from spatial interpolation techniques in GIS indicated that highest number of growing weeks of about 37–39 weeks are observed in the extreme eastern parts of Assam where double cropping is possible under rainfed conditions. It will be around 35–36 weeks in the western parts of Assam and adjoining West Bengal. Perhaps, here too, double cropping (summer+aman) is possible under rainfed conditions with supplemental irrigations at the critical crop growth stages. It varied between 25 and 30 weeks in coastal Orissa. Parts of Jharkhand, Bihar and West Bengal where one crop of long duration can be taken up successfully without subjecting to moisture stress. Greater part of the area in eastern Uttar Pradesh, Madhya Pradesh, Chhattisgarh, Bihar and Orissa where LGP vary from 19 to 24 weeks whereas it is only 17–18 weeks in the south western border of eastern Uttar Pradesh.

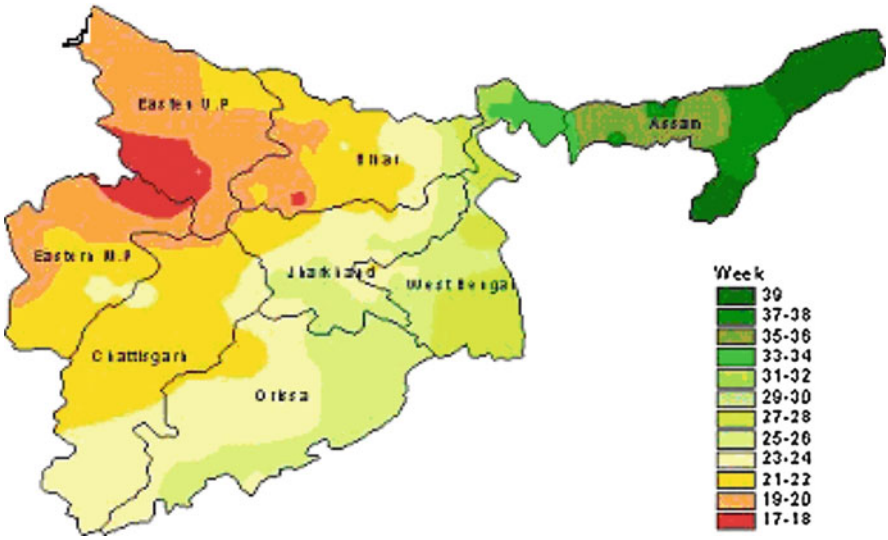


**Fig. 45.9** Length of growing period for rainfed rice in Eastern India

### 45.3.6 Rainwater Availability at Different Crop Growth Stages

In spite of the receipt of high rainfall of above 1,200 mm over the study area, which is expected to meet the water needs of the rice crop, the productivity under rainfed conditions is not satisfactory. The average yield works out to be around one tone per hectare. Therefore, to study the conditions leading to record such low productivity values, availability of dependable rainwater (rainfall at 60% probability) at different crop growth stages as against the demand has been worked out. The water requirement of rice under upland conditions is assumed to be 50 mm per week after initial establishment and the total water need worked out to be 700 mm.

Spatial maps showing the rainwater availability expressed as percentages of the water requirement at 60 probabilities for the entire crop growth period and at important growth stages, viz., vegetative, reproductive and maturity phases have been prepared and shown as Figs. 45.10–45.13, respectively. It is observed from the Fig. 45.10 that the rainwater satisfied the demand to an extent of about 100% over greater part of the study region. Even it exceeds more than 100% in some parts Chhattisgarh, Orissa and Jharkhand and the entire Assam. However, in some southern coastal parts of Orissa and entire eastern Uttar Pradesh, parts of Bihar and eastern Madhya Pradesh and in central parts of West Bengal, the rainwater could meet the demand up to 75%. These above conditions for the entire crop season appear to be satisfactory to record reasonably good yields of above 2 t/ha. As it is not so in reality, the rainwater maps prepared for different crop stages have been discussed as follows.

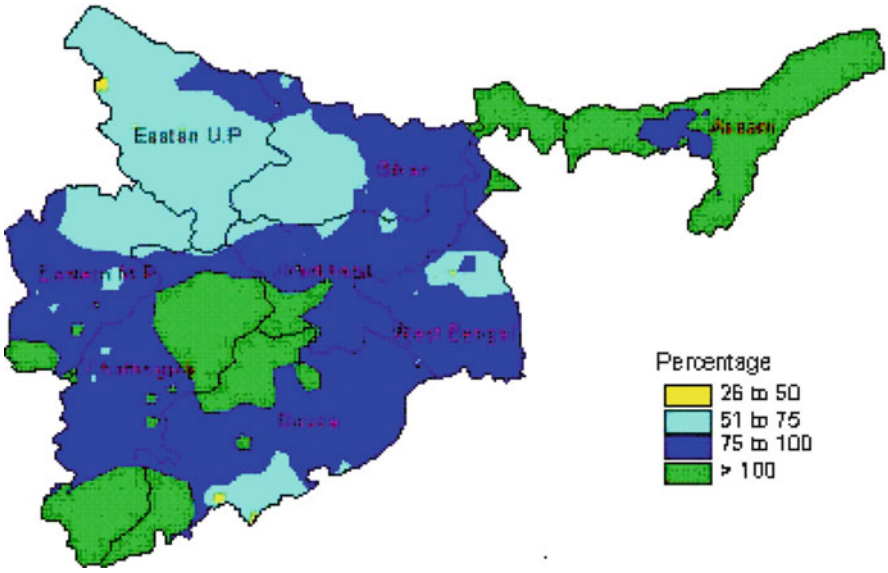


**Fig. 45.10** Rainwater availability (as percentage of requirement) at 60% probability during the total crop growth period for rainfed rice in Eastern India

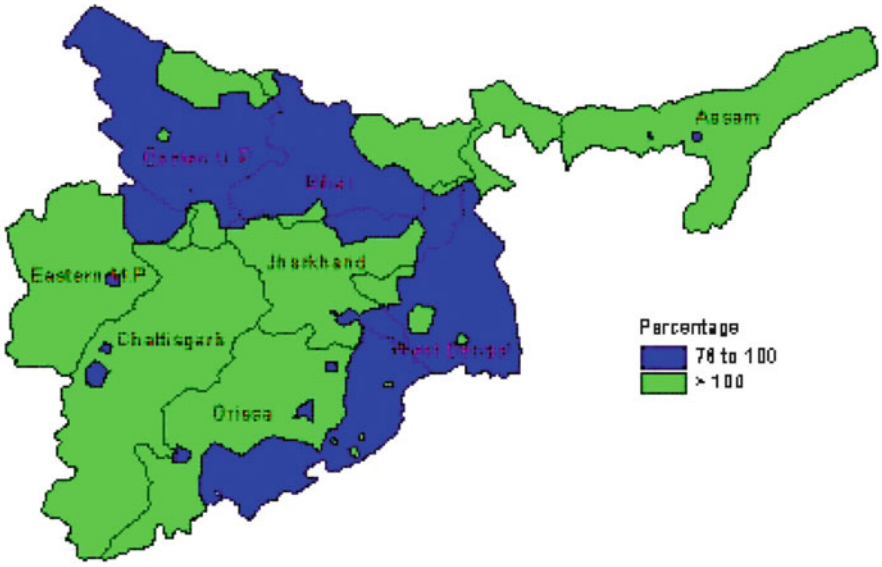


**Fig. 45.11** Rainwater availability (as percentage of requirement) at 60% probability during the vegetative period for rainfed rice in Eastern India

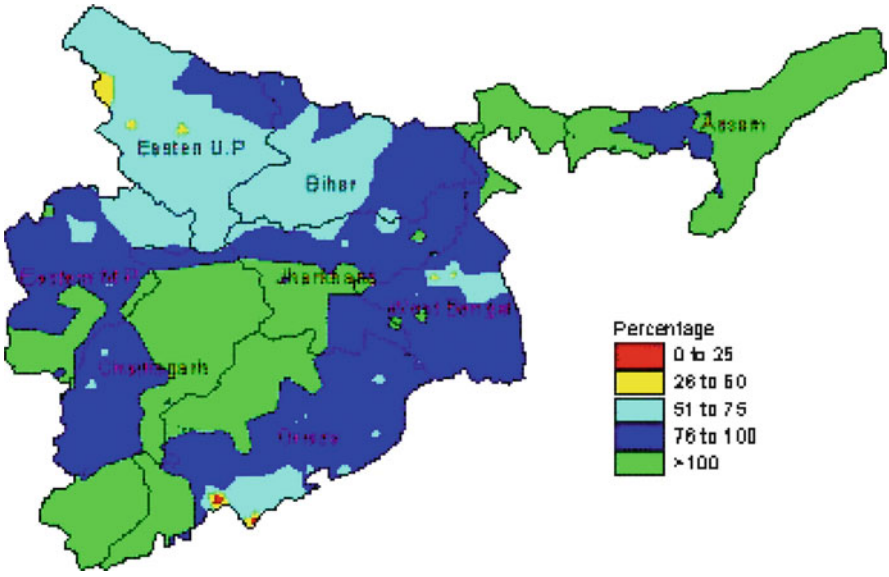


**Fig. 45.12** Rainwater availability (as percentage of requirement) at 60% probability during the reproductive period for rainfed rice in Eastern India

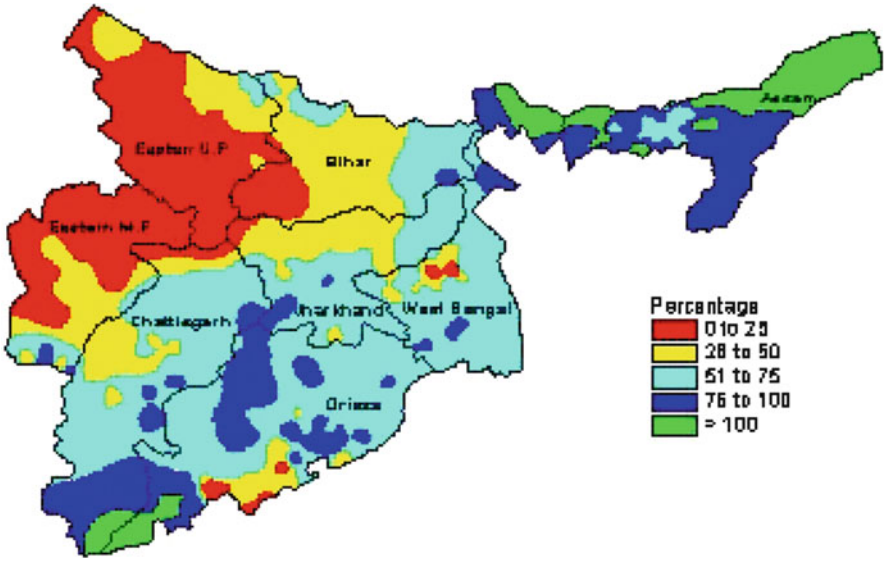


**Fig. 45.13** Rainwater availability (as percentage of requirement) at 50% probability during the maturity period for rainfed rice in Eastern India

The rainwater availability map at vegetative phase (Fig. 45.11) showed that the water availability is more than the demand in almost the entire region of the study area. It is 76–100% over eastern Bihar, parts of Jharkhand, West Bengal and coastal districts of Orissa. In general, the rainfall received at vegetative stage in the entire study region is sufficient to meet the crop water needs and is found to be not a limiting factor in the final yield. Figure 45.14 showing the rainwater availability at reproductive stage indicated that except in some parts of Uttar Pradesh, Bihar, northern parts of Madhya Pradesh, central parts of West Bengal and southern coastal districts of Orissa. The rainwater satisfies the entire water need of the crop (greater than 76%). However, in some small pockets in eastern Uttar Pradesh and in coastal Orissa, the rain availability is in between 26% and 50% indicating the initiation stress period. At maturity phase, (Fig. 45.13) which almost coincide with the withdrawal phase of monsoon indicating the lower water availability of rainwater (<25% of the demand) in the entire eastern Uttar Pradesh and small part of Bihar, half of part of eastern Madhya Pradesh.

Small portions in West Bengal and in Orissa too have possibility of having very low rainwater availability indicating severe water stress conditions. It is in between 26% and 50% in parts of Bihar and Chhattisgarh. Except in the Assam region, and in parts of forest regions in the southern portion of Chhattisgarh and in central Orissa, the water availability is in between 51% and 75%, indicating a strong possibility of water stress maturity phase. The above analysis has brought out clearly that water stress condition during maturity phase is found to be one of the major climate constraints in observing lower productivity in these regions.

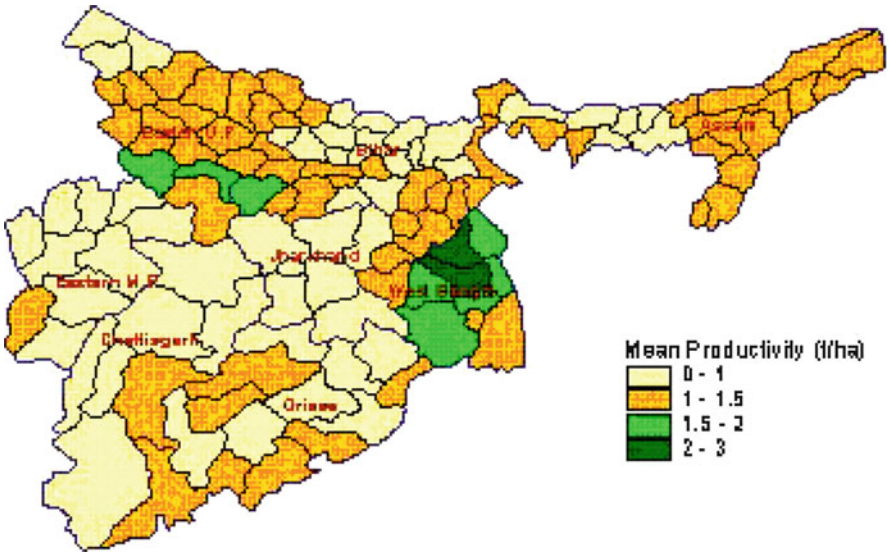


**Fig. 45.14** Mean Rice productivity in Eastern India

Probably better crop management strategies like advancing the sowing or transplanting and better fertilizer application and timely weeding may improve crop performance. Perhaps, raising nurseries wherever water resources are available and transplanting the seedlings immediately after rains will improve the rainwater use efficiency in these regions. The contributions of other climatic constraint, viz., and lower levels of radiation regime may also contribute significantly in recording lower yields.

### *45.3.7 Spatial Variability of Rice Productivity Pattern in Eastern India*

The spatial variability of mean rice productivity map has been generated using GIS and presented in Fig. 45.14. Also the percent changes in the productivity over the years have also been computed and map has been prepared and presented in Fig. 45.15. It is observed that lowest productivity of less 5 q per ha in eastern Madhya Pradesh. In general, the rice yields are less than 10 q per ha in Chhattisgarh, Jharkhand, Orissa, north Bihar, western parts of Assam and northwestern portion of eastern Uttar Pradesh. Highest yield levels of 20–25 q per ha is seen in the middle parts of Uttar Pradesh and West Bengal. The productivity level remains at 10–15 q per ha in Orissa, Assam and eastern Uttar Pradesh. The percent change in rice productivity (Fig. 45.15) over the period 1970–1998 in each district indicated that over the past 28 years period, about 50–100% increase in productivity has been

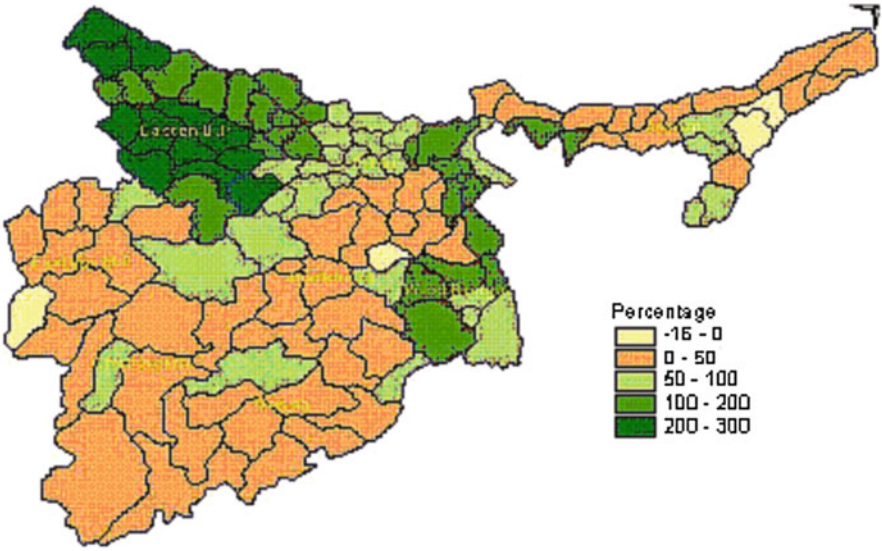


**Fig. 45.15** Change in Rice productivity from 1970 to 1998 over Eastern India

noticed in almost entire region except in parts of West Bengal and eastern Uttar Pradesh were spectacular increase in productivity of the order of 100–300% has been witnessed. This may largely be due to increased irrigation facility over the past few years and practicing better crop management techniques and use of high yielding varieties. It is surprising to notice that a few districts, *viz.,* Seoni, Dhanbad, Karbianglong and Golaghat in Madhya Pradesh, Jharkhand and Assam have shown negative growth rate.

### *45.3.8 Variability of Rice Crop Productivity in Different Agro-Ecological Regions*

In order to explain the variability of Rice crop productivity in terms of different agro-ecological regions, the productivity map has been superimposed on agro-ecological sub-regions map prepared by NBSS&LUP and presented in Fig. 45.16. Though it is difficult to interpret the variability of productivity on the agro-system basis, it is generally observed that low productivity of 1 t/ha have been mostly noticed in semi-arid to dry sub-humid type of climate with LGP varying 90–120 to 120–150 days. The highest productivity of 2–3 t/ha are recorded in hot sub-humid to humid regions of West Bengal where LGP vary from 150 to 200 days. The productivity was the order of 1–2 t/ha in hot sub-humid to humid regions of Assam, Orissa and West Bengal. Also the hot dry sub-humid climates in Uttar Pradesh and Bihar recorded the productivity of 1–2 t/ha. As the productivity data is being the combined data of both

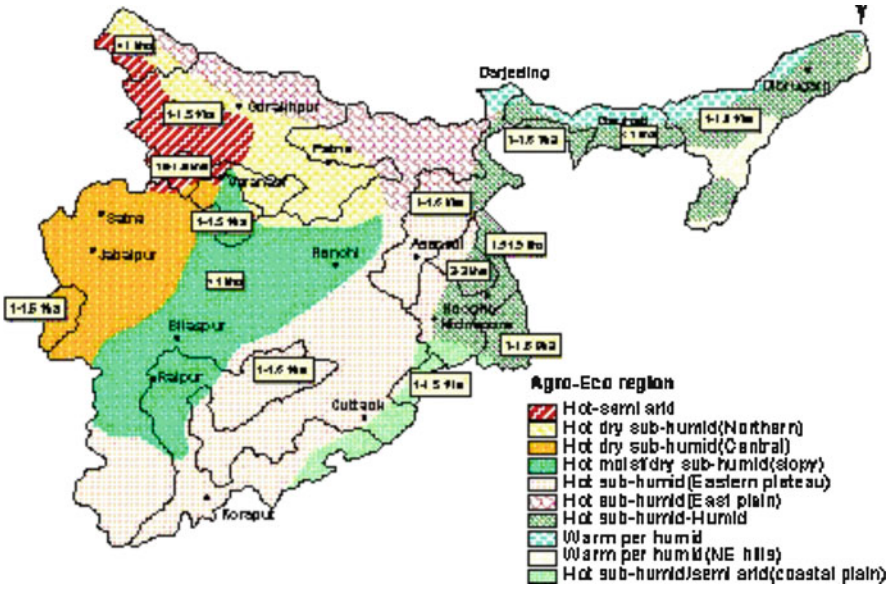


**Fig. 45.16** Mean Rice productivity (tfha) in different agro-eco regions of Eastern India (based on data for the period 1970–1998)

irrigated and rainfed, perhaps, the separation of irrigated crop yields from the original data sets may improve the interpretation in a better way.

## 45.4 Conclusions

Rainfall is the most important parameter under tropical climate condition. Therefore, analysis of rainfall with respect to distribution in different seasons assumes greater significance. The greater part of the region comprising Chhattisgarh, Orissa, West Bengal, Bihar and Jharkhand receives a rainfall of about 1,250 mm per year.

The knowledge on the commencement and end of growing season and its duration is useful for planning efficient cropping pattern and also to introduce new varieties matching with the length of growing period (LGP). It varied between 25 and 30 weeks in coastal Orissa. The parts of Jharkhand, Bihar and West Bengal where one crop of long duration can be taken up successfully without subjecting to moisture stress. The greater part of the area in eastern Uttar Pradesh, Madhya Pradesh, Chhattisgarh, Bihar and Orissa where LGP vary from 19 to 24 weeks whereas it is only 17–18 weeks in the south western border of eastern Uttar Pradesh.

It is observed that lowest productivity of less 5 q per ha in eastern Madhya Pradesh. In general, the rice yields are less than 10 q per ha in Chhattisgarh, Jharkhand, Orissa, north Bihar, western parts of Assam and northwestern portion

of eastern Uttar Pradesh. Highest yield levels of 20–25 q per ha is seen in the middle parts of Uttar Pradesh and West Bengal. The productivity level remains at 10–15 q per ha in Orissa, Assam and eastern Uttar Pradesh.

The percent change in rice productivity (Fig. 45.15) over the period 1970–1998 in each district indicated that over the past 28 years period, about 50–100% increase in productivity has been noticed in almost entire region except in parts of West Bengal and eastern Uttar Pradesh were spectacular increase in productivity of the order of 100–300% has been witnessed. This may largely be due to increased irrigation facility over the past few years and practicing better crop management techniques and use of high yielding varieties.

It is difficult to interpret the variability of productivity on the agro-system basis, it is generally observed that low productivity of 1 t/ha have been mostly noticed in semi-arid to dry sub-humid type of climate with LGP varying 90–120 to 120–150 days. The highest productivity of 2–3 t/ha are recorded in hot sub-humid to humid regions of West Bengal where LGP vary from 150 to 200 days. The productivity was the order of 1–2 t/ha in hot sub-humid to humid regions of Assam, Orissa and West Bengal. Also the hot dry sub-humid climates in Uttar Pradesh and Bihar recorded the productivity of 1–2 t/ha. As the productivity data is being the combined data of both irrigated and rainfed, perhaps, the separation of irrigated crop yields from the original data sets may improve the interpretation in a better way.

## References

Biswas BC (1982) Agroclimatic classification on the basis of moisture availability index and its application to the dry farming tract of Gujarat. Mausam 3(4):465–469

Environment System Research Institute (ESRI) (1998) Introduction to Arc view GIS. ESRI, Redlands

Gangopadhyaya M, Sarkar RP (1965) Influence of rainfall distribution on the yield of wheat crop. Agric Meteorol 2:331–350

Kar G, Verma HN (2005) GIS based crop water management analysis for Eastern Ghats and costal region. Indian J Soil Cons 33(1):1–7

Katyal JC Narayana Reddy M, Virmani SM (1996b) A case study on the spatial and temporal dynamic of area and productivity of sorghum and pigeonpea in India through GIS. The world Bank-NARP Report on Resource characterization of rainfed farming systems in peninsular India. CRIDA, India

Kulandaivelu R (1984) Probability analysis and its application in evolving cropping system for Coimbatore. Mausam 35(3):257–258

Prasad R, Datar SV (1990) Qualitative agroclimatic assessment of rainfed crops. Mausam 41(1):65–68

Raj S, Dey SK (2004) Spatial analysis of rainfall variability over the northeast with respect to rubber cultivation. J Agrometeorol 6(Spl. Issue 2004):52–57

Ramana Rao BV (1997) Agroecological based cropping strategies for topical rainfed areas in India. Lecture notes on training course on agrometeorology aspects of agricultural production. CRIDA, Hyderabad, Feb 1997

Ramana Rao BV, Katyal JC, Victor US, Srivastava NN, Vijaya Kumar P (1993) Rainfall variability and its impacts on crop yields at Hyderabad-An agroclimatic case study. Indian J Dryland Agric Res Dev 8(2):98–108

Rao GGSN Rajput RK (1996) Rice yields during kharif season as influenced by weather. In: Proceedings international symposium on water management in arid and semi arid zone, HAU, Hisar, pp 100–108

Sastry PSN (1976) Climate and crop planning with particular reference to the rainfall. In: Proceedings of the symposium on climate and rice, IRRI, pp 51–63

Singh PK, Rathore LS, Singh KK, Gupta AK, Baxla AK, Athiyaman B (2008) Rainfall probability analysis using markovchain model in Sabour region of Bihar. J Agrometeorol 10(2):213–217

Srivastava NN, Victor US, Ramana Rao BV (1989) Commencement of growing session and productivity of groundnut in Rajkot district. Mausam 40(4):399–402

# Index



S.D. Attri et al. (eds.), *Challenges and Opportunities in Agrometeorology*,
DOI 10.1007/978-3-642-19360-6, 